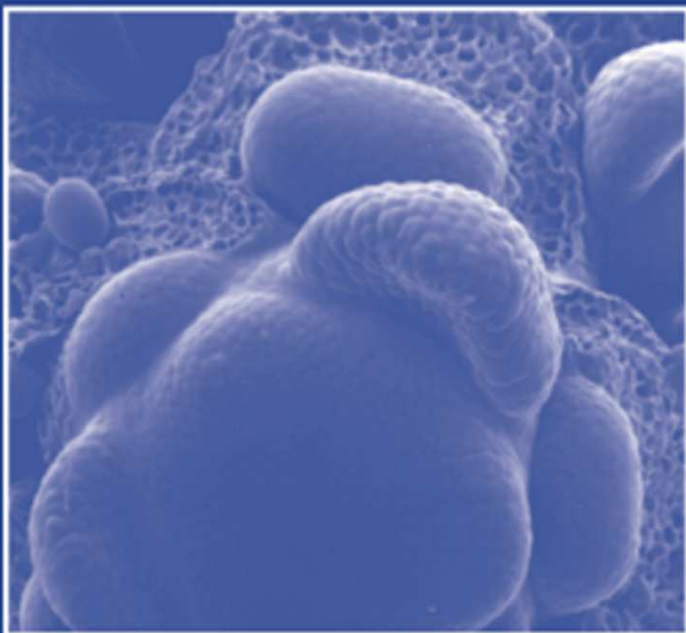


INTERNATIONAL  
REVIEW OF  
CYTOLOGY

A SURVEY OF CELL BIOLOGY

Edited by  
Kwang W. Jeon



Volume 208

ACADEMIC PRESS

International Review of  
**Cytology**

A Survey of  
**Cell Biology**

**VOLUME 208**

## SERIES EDITORS

<b>Geoffrey H. Bourne</b>	<b>1949–1988</b>
<b>James F. Danielli</b>	<b>1949–1984</b>
<b>Kwang W. Jeon</b>	<b>1967–</b>
<b>Martin Friedlander</b>	<b>1984–1992</b>
<b>Jonathan Jarvik</b>	<b>1993–1995</b>

## EDITORIAL ADVISORY BOARD

<b>Eve Ida Barak</b>	<b>Keith E. Mostov</b>
<b>Howard A. Bern</b>	<b>Andreas Oksche</b>
<b>Robert A. Bloodgood</b>	<b>Vladimir R. Pantić</b>
<b>Dean Bok</b>	<b>Jozef St. Schell</b>
<b>Laurence Etkin</b>	<b>Manfred Schliwa</b>
<b>Hiroo Fukuda</b>	<b>Robert A. Smith</b>
<b>Elizabeth D. Hay</b>	<b>Wilfred D. Stein</b>
<b>William R. Jeffrey</b>	<b>Ralph M. Steinman</b>
<b>Keith Latham</b>	<b>M. Tazawa</b>
<b>Anthony P. Mahowald</b>	<b>N. Tomilin</b>
<b>Bruce D. McKee</b>	<b>Robin Wright</b>
<b>M. Melkonian</b>	

International Review of  
**Cytology**

A Survey of  
**Cell Biology**

Edited by

**Kwang W. Jeon**

Department of Biochemistry  
University of Tennessee  
Knoxville, Tennessee

**VOLUME 208**



**ACADEMIC PRESS**

A Harcourt Science and Technology Company

San Diego San Francisco New York Boston London Sydney Tokyo

*Front cover photography:* Shoot apical inflorescence meristem of *Antirrhineum*. (See Chapter 3, Figure 1 for more details.)

This book is printed on acid-free paper. 

Copyright © 2001 by ACADEMIC PRESS

All Rights Reserved.

No part of this publication may be reproduced or transmitted in any form or by any means, electronic or mechanical, including photocopy, recording, or any information storage and retrieval system, without permission in writing from the Publisher.

The appearance of the code at the bottom of the first page of a chapter in this book indicates the Publisher's consent that copies of the chapter may be made for personal or internal use of specific clients. This consent is given on the condition, however, that the copier pay the stated per copy fee through the Copyright Clearance Center, Inc. (222 Rosewood Drive, Danvers, Massachusetts 01923), for copying beyond that permitted by Sections 107 or 108 of the U.S. Copyright Law. This consent does not extend to other kinds of copying, such as copying for general distribution, for advertising or promotional purposes, for creating new collective works, or for resale. Copy fees for pre-2001 chapters are as shown on the title pages. If no fee code appears on the title page, the copy fee is the same as for current chapters.  
0074-7696/01 \$35.00

Explicit permission from Academic Press is not required to reproduce a maximum of two figures or tables from an Academic Press chapter in another scientific or research publication provided that the material has not been credited to another source and that full credit to the Academic Press chapter is given.

**Academic Press**

*A Harcourt Science and Technology Company*

525 B Street, Suite 1900, San Diego, California 92101-4495, USA  
<http://www.academicpress.com>

**Academic Press**

Harcourt Place, 32 Jamestown Road, London NW1 7BY, UK

<http://www.academicpress.com>

International Standard Book Number: 0-12-364612-X

PRINTED IN THE UNITED STATES OF AMERICA

01 02 03 04 05 06 EB 9 8 7 6 5 4 3 2 1

# CONTENTS

Contributors .....	vii
--------------------	-----

## **Effects of Radiation Damage on Intestinal Morphology**

Katharine E. Carr

I. Introduction .....	1
II. Interpretation of Radiation-Induced Changes in Intestinal Structure .....	3
III. Effects of a Single Dose of Partial Body, Low-LET Irradiation .....	26
IV. Effects of a Single Dose of Unshielded, Low-LET Irradiation .....	53
V. Effects of a Fractionated Dose of Low-LET Radiation .....	70
VI. Factors Affecting Outcome and Summary for All Schedules .....	83
VII. Conclusions .....	98
References .....	101

## **Nonneuronal Cellular Prion Protein**

Jean-Guy Fournier

I. Introduction .....	121
II. The Prion Protein Gene and Protein Isoforms .....	123
III. Production and Subcellular Localization of Prion Proteins .....	131
IV. Functions of Cellular Prion Proteins .....	144
V. Concluding Remarks .....	149
References .....	150

**Cellular Basis of Shoot Apical Meristem Development**

Jan Traas and John H. Doonan

I. Introduction .....	161
II. Cellular Events during Morphogenesis .....	163
III. Meristem Organization .....	174
IV. Integration of Cells within the Meristem .....	183
V. Meristem Morphogenesis and Cellular Regulation .....	192
VI. Concluding Remarks.....	199
References .....	199

**Roles of Cytoskeletal and Junctional Plaque Proteins  
in Nuclear Signaling**

Stefan Hübner, David A. Jans, and Detler Drenckhahn

I. Introduction .....	207
II. Rules and Players Involved in Nuclear Transport.....	208
III. Roles of Plaque Proteins.....	214
IV. Nuclear Signaling by Nonjunctional Cytoskeletal Proteins .....	238
V. Concluding Remarks.....	247
References .....	249
Index.....	267

## CONTRIBUTORS

Numbers in parentheses indicate the pages on which the authors' contributions begin.

Katharine E. Carr (1), *The Queen's University of Belfast and MRC Radiation and Genome Stability Unit, Harwell, Didcot, Oxfordshire, United Kingdom*

John H. Doonan (161), *John Innes Centre, Norwich NR4 7UH, England*

Detler Drenckhahn (207), *Institut für Anatomie, Universität Würzburg, D-97070 Würzburg, Germany*

Jean-Guy Fournier (121), *Service de Neurovirologie, CEA-DSV/DRM, 92265 Fontenay aux Roses Cedex, France*

Stefan Hübner (207), *Institut für Anatomie, Universität Würzburg, D-97070 Würzburg, Germany*

David A. Jans (207), *Nuclear Signaling Laboratory, Division for Biochemistry and Molecular Biology, John Curtin School of Medical Research, Canberra, ACT 2601, Australia*

Jan Traas (161), *Laboratoire de Biologie Cellulaire, Institut National de la Recherche Agronomique, 78026 Versailles Cedex, France*

This Page Intentionally Left Blank

# Effects of Radiation Damage on Intestinal Morphology

Katharine E. Carr

The Queen's University of Belfast and MRC Radiation and Genome Stability Unit,  
Harwell, Didcot, Oxfordshire, United Kingdom

---

The current flow of papers on intestinal structure, radiation science, and intestinal radiation response is reflected in the contents of this review. Multiparameter findings and changes in compartments, cells, or subcellular structure all contribute to the overall profile of the response. The well-recognized changes in proliferation, vessels, and fibrogenesis are accompanied by alterations in other compartments, such as neuroendocrine or immune components of the intestinal wall. The responses at the molecular level, such as in levels of hormones, cytokines, or neurotransmitters, are of fundamental importance. The intestine responds to localized radiation, or to changes in other organs that influence its structure or function: some structural parameters respond differently to different radiation schedules. Apart from radiation conditions, factors affecting the outcome include the pathophysiology of the irradiated subject and accompanying treatment or intervention. More progress in understanding the overall responses is expected in the next few years.

**KEY WORDS:** Intestine, Radiation, Epithelium, Connective tissue, Muscle, Neuroendocrine. © 2001 Academic Press.

---

## I. Introduction

The first reference to radiation-damaged intestine appears in a clinical journal (Walsh, 1897), soon after the discovery of X rays, reporting a radiation worker complaining of symptoms after unshielded abdominal exposure. The author demonstrates substantial prescience in stating that "it is obvious that the subject is pregnant with future possibilities as it is instruct with present interest." Clinical

and environmental concerns are still uppermost in the minds of those working in the field. At therapeutic or high accidental dose levels, small intestinal tissues are much more radiosensitive than colon and rectum (Ming and Goldman, 1998), while at much lower, environmental exposures, large intestine is more at risk of late developing tumors. The side effects of abdominal irradiation include nausea, vomiting, diarrhea, bleeding, pain, obstruction, and increased bowel frequency (Cobb and Galland, 1990; Flickinger *et al.*, 1990). However, intestine transplanted to the oropharyngeal region, following excision of head and neck tumors, is comparatively radioresistant as far as its new function is concerned (Grasl *et al.*, 1991; Wei *et al.*, 1998).

Several books on the subject are available. The first takes a clinicopathologic approach (Galland and Spencer, 1990), covering radiology, clinical management, predisposing factors, and prevention, but with sections on history and tissue responses. Another book (Potten and Hendry, 1995) has a radiobiologic emphasis on changes in epithelial proliferation, differentiation, and regeneration, while also covering supportive tissues, ingested radionuclides, clinical aspects, and carcinogenesis. A third book (Dubois *et al.*, 1995) deals with emesis, motility, diarrhea, behavioral correlates of intestinal dysfunction, and relevance to tumors or transplantation.

Following an early report by Quastler (1956), subsequent reviews or articles cover epithelial responses and kinetics (Potten, 1990), apoptosis (Dewey *et al.*, 1995; Potten *et al.*, 1997b), motor abnormalities (Otterson and Summers, 1995), changes in the brain–gut axis (Kandasamy, 1995), comparative sensitivity of small and large intestine (Becciolini, 1987), and late effects (Hauer-Jensen, 1990; Coia *et al.*, 1995). Some articles cover general, clinical, or pathologic aspects (Busch, 1990; Touboul *et al.*, 1996; Wagner, 1996; Classen *et al.*, 1998) or describe the use of imaging techniques (Capps *et al.*, 1997). Others describe radiation effects alongside other topics, including nutrition (Thomson and Wild, 1997), gastrointestinal healing (Thornton and Barbul, 1997), and ischemia and inflammation (Panes and Granger, 1998). Topics of relevance such as radiation-induced vascular changes (Fajardo and Berthrong, 1988) or states producing free radicals (Parks *et al.*, 1983) are also described. Radioprotective approaches are either mechanistic (Gunter-Smith, 1995; Classen *et al.*, 1998), pharmacologic (Hanson, 1995; Weiss *et al.*, 1995), or nutritional (Srinivasan and Dubois, 1995). Interest in radiation-induced changes in multicellular organs such as intestine is strengthened by the development of space radiobiology (Conklin and Hagan, 1987).

This review is centered on morphologic effects of radiation on small and large intestine. It therefore concentrates on the interpretation of qualitative and quantitative descriptive data rather than on results from microcolony assay work, which has been extensively dealt with elsewhere (Cai *et al.*, 1997a). Section II gives brief descriptions of normal structure and the interaction of radiation with cells and tissues; the layout of subsequent sections on irradiated intestine is also described.

## **II. Interpretation of Radiation-Induced Changes in Intestinal Structure**

### **A. Intestinal Structure**

#### **1. General Structure**

Apart from histological and ultrastructural methods, many specialist techniques are used (Preedy and Watson, 1998) and baseline data must be regularly revised to take into account theoretical or technical improvements (Raja *et al.*, 1998). The small intestine mixes, absorbs, and partially desiccates the luminal contents (Phillips and Wingate, 1998), while storage, reabsorption, and intermittent propulsion are the major functions of the large intestine (Takahashi and Owyang, 1998). The layers of the wall are mucosa, submucosa, muscularis externa, and adventitia/serosa. Salivary glands, liver, and pancreas aid digestion; metabolism and sphincters control movement between different parts of the tract. Developmental and genetic studies cover organ-specific patterning, signaling pathways controlling epithelial–mesenchymal interactions, barriers to toxic insult, and cells controlling the activity of the wall (Montgomery *et al.*, 1999).

Villous protrusions increase the absorptive surface of small intestine (Fig. 1), but there are none in large intestine. Both have tubular crypts and epithelium, supported by the lamina propria connective tissue. Surface epithelial cells are mainly absorptive enterocytes and mucus-secreting goblet cells, while crypts contain undifferentiated, goblet, enteroendocrine, and Paneth cells, the latter only in small intestine. All derive from cryptal stem cells, for which substantial literature exists (Potten *et al.*, 1997a). They can be defined (Bach *et al.*, 2000) in functional terms as undifferentiated proliferative cells, with the capacity for self-maintenance, production of mucosal differentiated epithelial cell lineages, and postinjury regeneration. Each small intestinal crypt contains from four to six ultimate stem cells, not morphologically distinguishable, located in the proliferative zone just above the Paneth cells. A three-tiered stem cell hierarchy is deduced from postradiation data. If the ultimate stem cells are destroyed, the second and third tiers of more radioresistant daughter cells can maintain the crypt. In all, some 36 cells in each crypt have this regenerative capability. Stem cells have a cell cycle time of 24 hr in the mouse small intestine, dividing up to a thousand times in the animal's lifetime. The cell cycle time is a little longer in the mouse large intestine and substantially longer in humans.

After production in the cryptal proliferative zone, most differentiated epithelial cells migrate toward the luminal surface, where they are shed after several days. The scale of the process is remarkable; the mouse, for example, replaces the equivalent of its body weight in intestinal epithelial cells every 4 months. Cell loss by apoptosis also occurs (Potten, 1997; Potten *et al.*, 1997b) and is dealt with in the later section on epithelial response to injury. Recent papers describe the crypt–villus axis (Fig. 2); the role, in proliferation or growth, of cytokines,

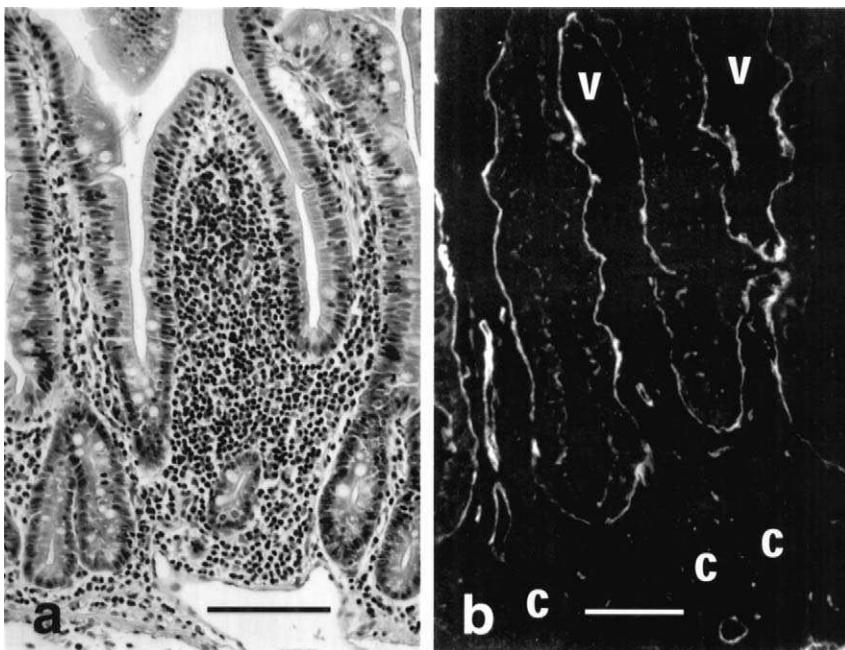


FIG. 1 (a) Light micrograph of human jejunal normal and lymphocyte-filled villi. The villus in the center is broader than surrounding classical villi, the lamina propria is packed with lymphocytes, and the epithelium contains a greater density of intraepithelial lymphocytes (H&E). Scale bar = 100  $\mu$ m. (b) Immunodetection of the  $\alpha_1$  chain of laminin in the adult small intestinal mucosa. Indirect immunofluorescence micrograph from a representative field of a cryosection of the ileum stained for the detection of the  $\alpha_1$  chain with the 4C7 antibody. The  $\alpha_1$  chain was found to be concentrated at the epithelial BM of villi (V). Crypts (C) are also labeled. Scale bar = 100  $\mu$ m. [Part (a) courtesy of G. Mayrhofer and W. B. Saunders Co., Orlando, FL, 32877, USA. Moghaddami, M., Cummins, A., and Mayrhofer, G. (1998). Lymphocyte-filled villi: Comparison with other lymphoid aggregations in the mucosa of the human small intestine. *Gastroenterology* **115**, 1414–1425, Fig. 1. Part (b) courtesy of J.-F. Beaulieu and Greenwich Medical Media Ltd., London. Bouatrouss, Y., Poisson, J., and Beaulieu, J.-F. (1998). Studying the basement membrane. In “Methods in Disease: Investigating the Gastrointestinal Tract.” (V. R. Preedy, and R. R. Watson, Eds.), pp. 191–200. Greenwich Medical Media Ltd., London, Fig. 17.1.]

dietary lectins, and  $H_1/H_2$  receptor antagonists (Thomson and Wild, 1997); stem cell dependence on signals from epithelial or mesenchymal neighbors; and clonal dispersion (Bjerknes and Cheng, 1999). Wong *et al.* (1999) highlight the gaps remaining in the knowledge base and emphasize the therapeutic potential of a better understanding of this complex system. Although the data from *in vitro* work on enterocytes are mostly based on a large intestine tumor line, small intestinal primary cultures and reliable cell lines (Beaulieu, 1999) now permit meaningful molecular studies (Brandsch *et al.*, 1998).

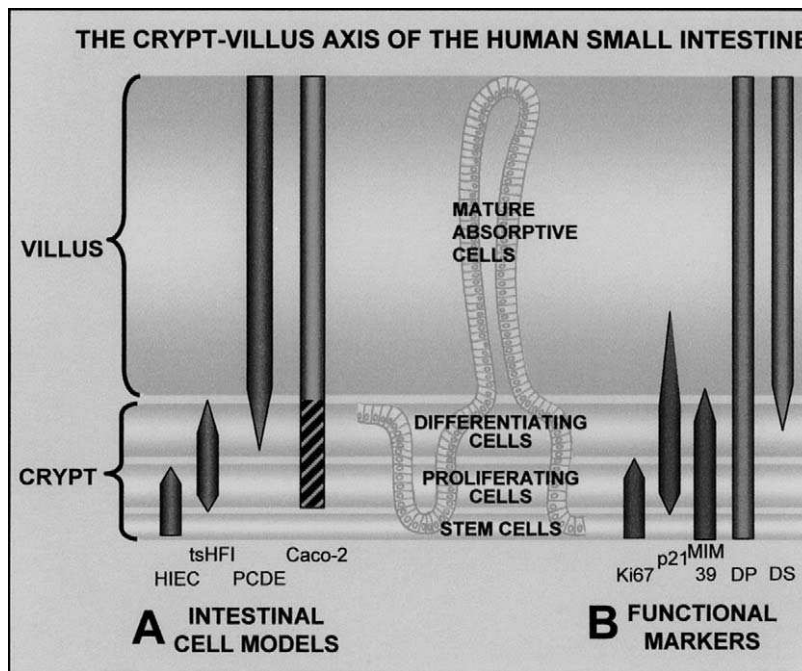


FIG. 2 Crypt-villus axis. This is the functional unit of the small intestine. In this rapidly renewing epithelium, the proliferating cells, which arise from the stem cells located at the bottom of the crypts, lose their ability to proliferate and start to differentiate in the upper third of the crypt, then migrate toward the tip of the villus before being exfoliated into the lumen. (A) Intestinal normal cell models that allow the recapitulation of the crypt-villus axis include the crypt-like proliferative cell line HIEC, the differentiating tsHFI cell line, and primary cultures of differentiated enterocytes (PCDE). The Caco-2 cell line, although of colon carcinoma origin, has been proven useful to the study of intestinal cell proliferation and differentiation. (B) Functional markers of intestinal cell state include the proliferating antigen Ki67, the cyclin-dependent kinase inhibitor p21/Waf-1/Cip1(p21), the crypt cell antigen MIM-1/39 (MIM39), the dipeptidases (DP) dipeptidylpeptidase IV and aminopeptidase N, and the disaccharidases (DS) lactase-phlorizin hydrolase and mature form of sucrase-isomaltase. [Courtesy of J.-F. Beaulieu. Reprinted from "Integrins and human intestinal cell functions," Jean-Francois Beaulieu (*Frontiers in Bioscience*, **4**, d310-d321, March 15, 1999), <http://www.bioscience.org/1999/v4/d/beaulieu/fulltext.htm> (PubMed#10077538), Fig. 2.]

Crypt fission provides a further mechanism for the expansion of the intestinal mucosal mass (St. Clair and Osborne, 1985; Totafurno *et al.*, 1987), which allows the orderly increase in mucosal surface accompanying body growth in infancy and childhood. The kinetics of crypt cell renewal and crypt fission are independently regulated (Park *et al.*, 1997), but are also in many respects interdependent, as in mucosal healing and repair. Disorders of crypt fission may mediate the effects of mutagens (Park *et al.*, 1995).

The epithelial basement membrane contains Type IV collagen, proteoglycans, laminin (Fig. 1), and nidogen/entactin, and interstitial matrix components tenascin and fibronectin, some of which have specific localization (Bouatrouss *et al.*, 1998). Basement membrane molecules (Orian-Rousseau *et al.*, 1996; Aumailley and Smyth, 1998) bind to integrins, contributing to adhesion (Beaulieu, 1999); activation of signaling pathways; and control of cell survival, cell cycle progression, or gene expression.

The lamina propria superficial reticular sheet (Toyoda *et al.*, 1997) contains pores through which lymphocytes, macrophages, and absorbed fat pass. The lamina propria, whose deep boundary is the thin muscularis mucosae, contains vessels, inflammatory and immune cells, smooth muscle cells, and nerves. The thicker submucosa contains larger vessels and nerves, including the submucosal (Meissner's) nerve plexus. Submucosal collagen, Types I, III, and V (Thornton and Barbul, 1997), is secreted by smooth muscle cells and fibroblasts. Tubular lymphatics join villous lacteals (Shimoda *et al.*, 1997) and lymphatic networks are seen in the submucosal and myenteric layers.

Alterations in the muscle tone and motility of the underlying muscularis externa (propria) may reflect the presence of dysfunction (Camilleri *et al.*, 1998). Differences are found in the distribution of actin types throughout chicken gastrointestinal tract (Yamamoto *et al.*, 1996). Both hormones and nerves can stimulate the contraction/relaxation cycle. Between the two muscle layers lie the myenteric (Auerbach's) nerve plexus profiles. Mature smooth muscle myocytes can dedifferentiate into proliferative myoblasts and isolated cells recapitulate some of their *in vivo* myogenic program (Brittingham *et al.*, 1998). Types of normal intestinal contractile activity, some of which change after radiation, include individual phasic contractions; organized groups of contractions, namely, migrating motor complexes; and ultrapropulsive contractions (Ottersson and Summers, 1995).

The outermost layer is either serosa or adventitia. Serosa is connective tissue covered by mesothelial cells, each with microvilli and a central single cilium. Pores may link subserosal lymphatic spaces with the peritoneal cavity (Michailova *et al.*, 1999). Adventitia lacks the mesothelial surface.

## 2. Intercellular Messengers

These messengers include hormones and cytokines and comprise a wide variety of extracellular signaling molecules. Hormones, or "regulatory peptides," are normally produced by specialized neuroendocrine cells, and gastrointestinal hormones can be divided into three groups or families (Gard, 1998). These are the gastrin/cholecystokinin (CCK) group; the secretin group, containing secretin, glucagon, vasoactive intestinal peptide (VIP), and glucose-dependent insulinotropic peptide; and the "other peptides" group, including somatostatin, motilin, substance P (SP), neuropeptides, and peptide YY (PYY). Cytokines are small regulatory peptides (Wang and Huang, 1998; Rang *et al.*, 1999), produced by many

cell types and important in control of immunity and inflammation. They include interleukins (ILs), monokines, chemokines, interferons, and colony-stimulating factors: growth factors are sometimes also included. They usually act over short distances as autocrine or paracrine signals and may produce cascades of triggers for cellular responses. The effects of peptides on the intestines are described by Thomson and Wild (1997) and Wingate and Phillips (1998), including some listed above and also serotonin, neuromedin, calcitonin gene-related peptide (CGRP), prolactin, growth hormone, and pancreatic polypeptide. These messenger substances contribute to the control of secretion, absorption, and motility and mediators of inflammation such as histamine and prostaglandins are also involved.

### 3. Individual Epithelial Cell Types

*a. Enterocytes (Absorptive Cells)* The importance of luminal biliary secretions, the glycocalyx, membrane trafficking, and signaling pathways controlling secretion is reviewed by Thomson and Wild (1997). Small intestinal enterocyte microvillous membranes have a high protein-to-lipid ratio and many integral membrane proteins, including hydrolases, transporters, and exchangers: the role of  $\text{Ca}^{2+}$  at these structures is also highlighted (Lange, 1999). Up-regulation of dipeptide transport activity may be influenced by specific amino acids and dipeptides (Shiraga *et al.*, 1999). The mucosal barrier is energy dependent (Gabe *et al.*, 1998) and affected by potassium channels (Lencer and Alper, 1999). Dysfunction here may be locally initiated (Osman *et al.*, 1998) and involve abnormal apical tight junctions (Schmitz *et al.*, 1999) or apoptosis (Sun *et al.*, 1998). Cytoskeletal elements include microfilaments, a terminal web, intermediate filaments, and microtubules. The movement of different proteins within enterocytes is regulated by actin and microtubule cytoskeletal networks and driven by “molecular motors” or mechanochemical enzymes (McNiven and Marlowe, 1999). There is migration-associated differentiation (Kasai *et al.*, 1997), possibly involving enterocyte–lymphocyte interactions. Enterocytes also present antigen to immune cells, secrete cytokines, express adhesion molecules, and release eicosanoids. They produce nitric oxide (NO) on exposure to pathogenic bacteria and several proinflammatory cytokines, including interleukin-8 (IL-8), tumor necrosis factor  $\alpha$  (TNF- $\alpha$ ), monocyte chemoattractant protein 1, granulocyte-macrophage colony-stimulating factor, and extractable nuclear antigen 78 (Hecht and Savkovic, 1997).

Duodenal villous enterocytes express enterokinase, converting trypsinogen to trypsin and activating digestive enzymes (Yuan *et al.*, 1998). Acid–base transporters in enterocytes (Ainsworth *et al.*, 1998) include an acid extruder, a base loader, and a base extruder.

Colonic microvilli have fewer digestive and uptake membrane proteins, more electrolyte uptake proteins, and a bicarbonate-chloride exchanger. Absorption may be a constitutive function of crypts, which could become secretory on signals from neighboring sources (Singh *et al.*, 1995). Water absorption from feces uses an

osmotic gradient (Dublineau *et al.*, 1998). Hydrolysis-induced increased intracellular levels of ceramide and sphingomyelin inhibit cell growth and induce apoptosis (Duan, 1998). Intracellular calcium mobilization by acetylcholine is initiated basally in isolated crypts and progresses toward the mucosal surface (Lindqvist *et al.*, 1998).

**b. Brunner's Glands** These proximal duodenal glands discharge glycoproteins and pepsinogen II into crypt lumina. Cytoplasmic membrane-related duodenase shows trypsin-like and chymotrypsin-like specificities (Zamalodchikova *et al.*, 1997). The role of Brunner's glands in the production of bicarbonate has been challenged, since the higher rate of bicarbonate secretion in proximal duodenum is apparently independent of their presence (Ainsworth *et al.*, 1995). They may reinforce the defensive activity of Paneth cells (Coutinho *et al.*, 1996).

**c. Goblet Cells** The mucous glycoprotein secreted by these cells, more sialomucin in small intestine mucin and more sulphomucin in large intestine, lubricates the mucosal surface and blocks bacterial binding sites. Garabedian *et al.* (1997) compare granule types in goblet cells, "intermediate" cells, and Paneth cells. Goblet cells also secrete trefoil peptides, which may produce a more viscous mucin by cross-linkage and may also encourage repair (Thomson and Wild, 1997).

**d. Endocrine Cells** These are part of the diffuse endocrine system and their function may overlap with that of central nervous system (CNS)-derived substances. The cells are often cryptal and, although regularly seen as abluminal with small basal granules, may have luminal microvillous tufts, with a possible sensory function. Nonspecific markers of neuroendocrine identity include neuron-specific enolase and chromogranin. The cells can be categorized more specifically by their hormone immunohistochemistry and granule ultrastructure. Secretion, motility, and sphincter control are regulated by peptides such as CCK, secretin, gastric inhibitory peptide, and motilin. Additional relevant neuropeptides are still being reported (Yazdani *et al.*, 1999). Somatostatin (growth hormone inhibitory factor) is involved in intestinal transport, in some species stimulates duodenal papillary muscle and nerves (Huang *et al.*, 1998) and contributes to short negative feedback loops.

**e. Paneth Cells** The role of these slowly renewing, basally situated cryptal cells has recently been reviewed (Lencer, 1998). They have mRNA for TNF, epidermal growth factor (EGF), and guanylin. Their large apical granules contain the bacteriolytic enzyme lysozyme, matrix metalloproteinase, and antimicrobial cryptdin peptides. They may contribute to mucosal defense, regulation of the cryptal bacterial microenvironment, regulation of salt and water transport, and the development of the crypt–villus unit. Several species do not have identifiable Paneth cells and transgenic mice survive for 180 days without them (Garabedian *et al.*, 1997), albeit in a pathogen-free environment.

#### 4. Gut Associated Lymphoid Tissue (GALT)

Nearly two-thirds of body lymphocytes are found in the intestine, where more than 70% of immunoglobulin is produced. GALT comprises small intestinal Peyer's patches, appendix, and solitary mucosal lymphoid follicles. Recently described additional lymphoid aggregates include submucosal isolated lymphoid follicles and jejunal lymphocyte-filled villi (Moghaddami *et al.*, 1998, Fig. 1). Mesenteric lymph nodes are sometimes also included as part of GALT.

Peyer's patches are covered by specialized follicle associated epithelium, containing microfold (M) cells, which may be derived from enterocytes (Kucharzik *et al.*, 1998). The patches are involved in antigen sampling and may allow entry of luminal material like bacteria or viruses. Deep to the epithelium are B lymphocytes, dendritic cells, and macrophages, which process and present antigen to T lymphocytes. The superficial reticular sheet of the lamina propria (Toyoda *et al.*, 1997) is particularly porous here, allowing easy passage of many lymphocytes.

There are many villous intraepithelial lymphocytes (IELs), predominantly memory cells, lying between the basolateral surfaces of epithelial cells. When stimulated, they demonstrate proliferative and cytotoxic activities. IL-15 is the most potent of the known cytokines for IELs (Ebert, 1998). There is evidence for "molecular cross-talk" between villous and cryptal IELs and epithelial cells (Kawabata *et al.*, 1998). The IELs in small intestine and colon have different expression of lymphocyte homing receptor, apparently due to the higher functional activity of the metalloproteinase sheddase in small intestine (Seibold *et al.*, 1998).

#### 5. Nerve Supply to the Intestines

**a. Components and Effector Pathways** The enteric nervous system (ENS) is sometimes described as a third subdivision of the autonomic nervous system, in addition to the sympathetic and parasympathetic divisions (Appenzeller and Oribe, 1997; Keast, 1999), or as a "mini-brain," providing integrative control over the final activity of the gut (Wood, 1998). The ENS comprises a neural network linking the intrinsic plexuses, the extrinsic ganglia, input from the CNS, and the intestine (Fig. 3).

The craniosacral parasympathetic outflow from the CNS synapses with ganglia in the intestinal plexuses; these (Balemba *et al.*, 1998) contain neuronal cell bodies, nerve fibers, and supporting Schwann cells. Postganglionic nerves contact effector structures in muscle and elsewhere. Both pre- and postganglionic nerves are cholinergic. The thoracolumbar sympathetic outflow makes cholinergic synapses in extrinsic (celiac, superior mesenteric, inferior mesenteric) ganglia. The noradrenergic postganglionic nerves contact structures such as parasympathetic and other cell bodies in the intestinal plexuses, where they reduce the firing of parasympathetic postganglionic nerves. In general, the parasympathetic system is excitatory to motor and secretory function, while the sympathetic is inhibitory,

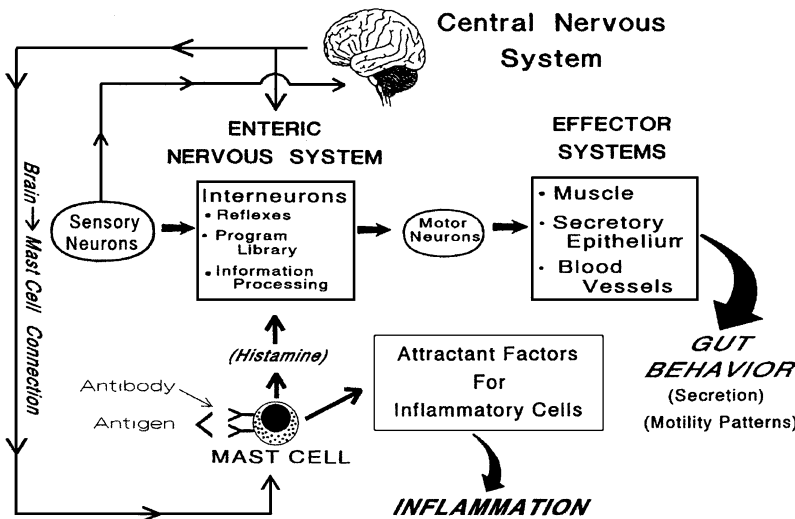


FIG. 3 Enteric nervous system. This behaves as an independent integrative nervous system, with functions like a “mini-brain.” It processes information derived from sensory neurons and inflammatory immune cells. Interneuronal processing involves reflex microcircuits and a library of programs responsible for stereotypic behaviors of the digestive tract. These include effects on systems that modulate motor, secretory, and circulatory function. Mast cells detect threatening antigens and release several paracrine mediators simultaneously. Some mediators alert the enteric nervous system while others act as attractants for the inflammatory response. The central nervous system signals the enteric nervous system by direct neural pathways and through brain–mast cell connections. [Courtesy of J. D. Wood. Reprinted from Wood, J. D. Enteric neuropathobiology. In “Functional Disorders of the Gut” (S. F. Phillips and D. L. Wingate, Eds.), pp. 19–42, 1998, by permission of the publisher Churchill Livingstone, Fig. 2.1.]

with opposite effects on sphincter control. The recently reviewed pelvic ganglia contain both parasympathetic and sympathetic components (Keast, 1999).

Acetylcholine and noradrenalin are thus the two main ENS neurotransmitters, but there are also nonadrenergic, noncholinergic neurotransmitters. These include ATP, VIP, NPY, SP, 5-HT,  $\gamma$ -aminobutyric acid, and dopamine. Also involved is nitric oxide (NO), synthesized from L-arginine by NO synthase (NOS). NOS activity and function are reviewed by Izzo *et al.* (1998) and Takahashi and Owyang (1998). Stimulation of the myenteric plexus releases NO, which mediates relaxation of intestinal smooth muscle, and inflammation, as in bacterial infection, can lead to expression of inducible nitric oxide synthase (iNOS) in macrophages, neutrophils, smooth muscle, and endothelium.

**b. Interface between Neurons and Smooth Muscle; Pacemaker Activity** The interstitial cells of Cajal (ICCs), found in intestinal plexuses, act as pacemakers for intestinal contraction (Fig. 4) and as intermediaries between the ENS and intestinal musculature (Huizinga *et al.*, 1997; Daniel *et al.*, 1998; Wingate and

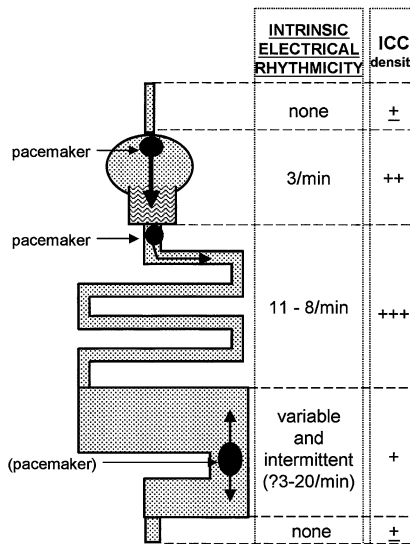


FIG. 4 Intrinsic electrical rhythmicity and interstitial cells of Cajal. Much controversy has surrounded the question of whether the regulation of gut function is “myogenic” or “neurogenic.” The key elements of the smooth muscle system are the pacemakers that confer rhythmicity; the pacemaking properties appear to be a function of the interstitial cells of Cajal (ICCs), and these cellular elements are found in the greatest numbers (right) where pacemaking and rhythmicity are prominent. [Courtesy of D. L. Wingate. Reprinted from Wingate, D. L. and Phillips, S. F. Functional anatomy and physiology, In “Functional Disorders of the Gut” (S. F. Phillips and D. L. Wingate, Eds.), pp. 3–18, 1998, by permission of the publisher Churchill Livingstone, Fig. 1.2, redrawn by the author.]

Phillips, 1998). These two functions may involve different groups of ICCs and they may also be important for sphincter function (Ward *et al.*, 1998). ICCs are linked into networks by their long processes and can be visualized with methylene blue or monoclonal Kit antibody ACK2, a membrane tyrosine kinase (Huizinga *et al.*, 1997). Their origin is mesenchymal and they have intermediate filaments, surface caveolae, a variable basal lamina, close or gap junction contacts with smooth muscle cells, and synapse-like contacts with nerve bundles. ICCs may amplify NO-mediated neural signals, generating “slow waves” and modulating phasic contractions and peristalsis. They may produce carbon monoxide, which could be a messenger between ICCs and smooth muscle (Miller *et al.*, 1998). Slow-wave controlled peristalsis is absent in mice lacking ICCs (Der-Silaphet *et al.*, 1998), but their role in motor dysfunction is still unclear.

**c. Other Aspects of the ENS** Secretomotor parasympathetic neurons stimulate cryptal secretory activity (Fig. 5) via acetylcholine and VIP, with arteriolar dilatation through collateral branches (Wood, 1998). Inhibitory signals include

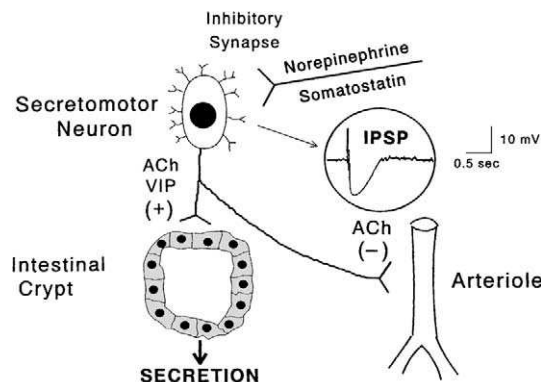


FIG. 5 Enteric secretomotor innervation. Intestinal crypts of Lieberkühn are innervated by secretomotor neurons, which are stimulated by the release of vasoactive intestinal peptide and acetylcholine. Simultaneously, axon collaterals to blood vessels dilate submucosal arterioles and increase mucosal blood flow. Secretomotor neurons receive inhibitory synaptic inputs from sympathetic postganglionic neurons (e.g., norepinephrine) and from other neurons in the enteric microcircuits (e.g., somatostatin). Activation of the inhibitory synaptic inputs evokes inhibitory postsynaptic potentials (IPSP) in secretomotor neurons. [Courtesy of J. D. Wood. Reprinted from Wood, J. D. Enteric neuropathobiology, In "Functional Disorders of the Gut" (S. F. Phillips and D. L. Wingate, Eds.), pp. 19–42, 1998, by permission of the publisher Churchill Livingstone, Fig. 2.3.]

sympathetic input, with noradrenalin and somatostatin as transmitters. There are also extrinsic and intrinsic sensory pathways, activated by muscle stretch or mucosal stimuli (Grider *et al.*, 1998), and information comes from mechanoreceptors, chemoreceptors, and thermoreceptors in the intestinal wall (Wood, 1998).

## 6. Factors Influencing Normal Structure and Function

These factors include diet, stress, and aging, all of which accompany irradiation. Intestinal pathology may be caused by radiation or be present as an underlying condition during it.

**a. Diet, Stress, and Aging** Certain components of food can cause villous desquamation, increases in secretion and motility, and triggering of nerve and peptide responses (Srinivasan and Dubois, 1995). Glutamine is highlighted for small intestine and dietary fiber for colon (Klurfeld, 1999). Stress can affect transit time, possibly by affecting pacemaker control (Muraoka *et al.*, 1998) and there may be input from the CNS via mast cell activation (Santos *et al.*, 1998). Aging can cause changes in glucose uptake (Thomson *et al.*, 1988) or the mesenteric extracellular matrix (Dutta *et al.*, 1995). A glycoxidation product may be used as a marker of oxidative stress in aging (Schleicher *et al.*, 1997). Possible changes in neural elements are also the subject of investigation (Johnson *et al.*, 1998).

**b. Gastrointestinal Disease Classification** Disorders of the gastrointestinal tract can be divided into six general groups: developmental; motor and mechanical; vascular; endocrine and metabolic; inflammatory; and neoplastic (Ming and Goldman, 1998). Mechanisms occurring in each of these six categories are relevant to the development of radiation damage, which is itself a form of physical injury.

Developmental disorders of the tract reflect its complex embryologic origins (Montgomery *et al.*, 1999). Motor and mechanical disorders may be complicated by vascular or inflammatory problems, immunologic responses, and tissue repair.

The inflammatory reaction involves vascular and cellular events; tissue necrosis and mucosal ulceration occur. The immunologic response includes progressive accumulation of lymphocytes, plasma cells, eosinophils, and macrophages. Tissue repair involves the formation of vascular granulation tissue, with fibroblast proliferation and collagen production. While inflammation, the immune response, and tissue repair may occur in combination, they are separately stimulated and regulated. Intestinal tissues are very sensitive to vascular and ischemic disorders. Short-term or mild hypoxia may produce only pain and disturbances in absorption or secretion, but persistent or severe hypoxia will cause necrosis and infarction. Endocrine and metabolic disorders include the effects of endocrine cell tumors and of disorders of other endocrine organs.

Metaplasia involves a change from one mature pattern of differentiation to another, often associated with chronic inflammation, which in turn may predispose to cancer. Dysplasia describes the morphologic abnormalities of cell growth and maturation occurring in benign tumors, various precancerous lesions, and malignancy. In neoplasia, a new, abnormal population is generated by genetic aberrations. Human tumors are more common in large than in small intestine. Benign tumors, such as polyps, project from, but do not invade, adjacent tissues. There are several studies of human colonic familial adenomatous polyposis and the multiple intestinal neoplasia (*Min*) mouse model (Moser *et al.*, 1990; Wasan *et al.*, 1998). Malignant tumors are “staged” by how far they have spread through or beyond the intestinal wall. Most important are colorectal adenocarcinomas, but there are also intestinal tumors of endocrine cell, lymphoid, and stromal origins. Gastrointestinal stromal tumors may originate from the interstitial cells of Cajal.

**c. Epithelial Responses to Injury** These responses include degeneration and cell death, regeneration, metaplasia, dysplasia, and neoplasia. Radiation may have any of these effects. In necrosis, widespread tissue death occurs, with associated inflammation. Individual cell death by apoptosis follows a recognized program, resulting in the phagocytosis of apoptotic cells by their neighbors, without an inflammatory response. Apoptosis is particularly relevant to radiation effects. A recent review describes its characteristic features (Fig. 6, Table I). These include genetic regulation, the role of p53 and the *bcl-2* gene family, adhesion molecules and cyclooxygenase, tumor susceptibility, and the profile of intestinal apoptosis, both spontaneous and induced by damage such as radiation (Potten *et al.*, 1997b).

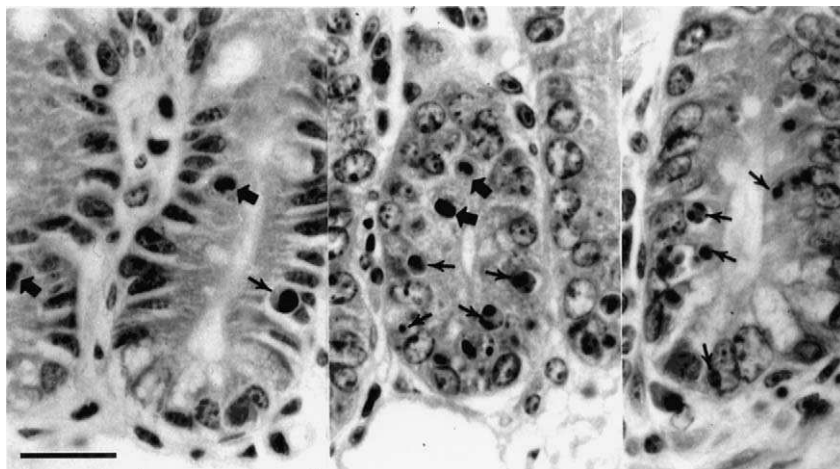


FIG. 6 Apoptosis. Longitudinal sections of small intestinal crypts in the mouse showing spontaneous apoptosis (left-hand panel) and radiation-induced apoptosis (middle and right-hand panels). Mitotic figures are indicated by large arrows and apoptotic figures by small arrows. The section is stained with haematoxylin and eosin and prepared from Carnoy's fixed material. Scale bar = 50  $\mu$ m. [Courtesy of C. S. Potten. Reproduced with permission from T. G. Cotter and S. J. Martin (Eds.) (1994), *(Techniques in Apoptosis, A User's Guide)*. Copyright Portland Press, p. 283.]

The complexity of the p53 pathway is itself reviewed (Prives and Hall, 1999). The regenerative capacity of intestinal stem cells after radiation exposure can be studied by the microcolony clonogenic stem cell assay of Withers and Elkind (1970). After radiation, small intestinal stem cells undergo p53-dependent apoptosis. Their threshold for apoptosis is lower than in the large intestine, which may be linked to the much lower frequency of cancer in the small intestine.

**d. Other Relevant Factors** Multiple organ dysfunction syndrome is a cause of death that may follow severe injury or infection. It may be linked to bacterial translocation (Nieuwenhuijzen *et al.*, 1996), which can be affected by radiation. Failure of the mucosal barrier allows passage of bacteria and endotoxins across the intestinal wall and on to other organs, such as lymph nodes and liver.

Wound healing is also relevant, because after tumor removal, surgical anastomoses may lie within the field of radiotherapy. Their strength depends initially on surgical clips or sutures, but as healing progresses, the bridging collagen fibers within the wound granulation tissue become stronger. This process differs from wound healing in skin (Thornton and Barbul, 1997) with respect to wound pH, microorganism populations, shear stress, and tissue oxygenation. There are also differences in collagen synthesis, collagenase activity, wound strength, and scar formation. The healing of anastomoses depends on both systemic and local factors, such as radiation and bacterial contamination, itself radiation sensitive.

TABLE I

Summary of the Observations and Conclusions Regarding Apoptosis in the Intestinal Epithelium and Their Likely Implications

	Observation	Conclusion	Consequences
Spontaneous apoptosis			
SI	AI at stem cell location approximately 10% Apoptosis is p53 independent	Apoptosis removes excess stem cells Apoptosis is part of stem cell homeostatic mechanism	Stable stem cell population leads to stable crypt
LI	Apoptosis is a very rare event, not concentrated at stem cell location Bcl-2 expressed in the stem cells Apoptosis increased in stem cells in Bcl-2 null mice	Occasional excess stem cells not removed Bcl-2 overrides stem cell homoeostatic process	Excess stem cells persist and numbers may increase with time Hyperplastic crypts
Damage-induced apoptosis			
SI	Cells at stem cell location exquisitely sensitive to damage Approximately 6 hypersensitive cells per crypt Damage p53 dependent	Very sensitive damage detection mechanism No attempt at repair Damaged cells efficiently removed	SI is protected against DNA damage (mutation) and carcinogenesis
LI	Lower levels than in SI Apoptosis distributed throughout the crypt Bcl-2 expressed in stem cells AI increased in stem cell position in Bcl-2 null mice	Damaged cells not removed Cell death prevented by Bcl-2	Damaged or unrepaired cells may persist as initiated cells, leading to higher risk of cancer Tumors arising in Bcl-2-expressing cells continue to express it, making them difficult to kill (chemoresistant)

Key: SI, small intestine; LI, large intestine; AI, apoptotic index.

Courtesy of C. S. Potten and AlphaMed Press. Potten, C. S., Wilson, J. W., and Booth, C. (1997). Regulation and significance of apoptosis in the stem cells of the gastrointestinal epithelium. *Stem Cells* **15**, 82–93, Fig. 6.

## B. Radiation

It has recently been commented that the current decade may be classified as a new “golden age” in radiation science (Alpen, 1998), similar in importance to the decade, beginning in 1895, when its foundations were laid by the discovery of X rays and radioactivity. Current research applies modern techniques in molecular biology and genetics to questions in radiobiology (Gordon and McMillan, 1997), which interest both clinicians and scientists (Peacock *et al.*, 1998; Stone *et al.*, 1998). There is a need for more “translational research” to address clinically relevant questions (Coleman and Harris, 1998). There is also a need to appreciate the intersubject variation in normal tissue responses (Peacock *et al.*, 1998) and possible contributions from nuclear medicine (Wagner, 1996).

This subsection sets out some basic information on radiation science and notes some recent advances, to allow intestinal responses to be put into context.

### 1. Characteristics of Radiation

Ionizing radiation is energy in the form of waves and/or moving particles. It is a source of physical injury to biologic tissue (Alpen, 1998; Ming and Goldman, 1998; Nias, 1998; Adams *et al.*, 1999), since the radiation carries sufficient energy to ionize molecules in the tissue, leading to damaging chemical reactions. Although there is public concern about radiation from artificial sources and about radiation accidents (Nenot, 1998), most exposure is natural background radiation (over 85%), while medical sources account for 14% (Nias, 1998).

Electromagnetic radiation includes, in order of increasing wavelength,  $\gamma$  rays, X rays, ultraviolet rays, visible light, infrared rays, and radiowaves. These are also sometimes described as consisting of packages of energy, or photons. Gamma rays, X rays, and some ultraviolet rays are ionizing radiations. Ionizing particulate radiation includes electrons, protons,  $\alpha$  particles, neutrons, and heavy charged ions, such as carbon, neon, argon, and iron ions. Radiation can be produced from the disintegration of radioactive elements, or by artificial means, such as in the formation of X rays, when high-energy beams of electrons strike matter, or when particles are accelerated to very high energies. Radioactive decay includes the emission of  $\alpha$  particles (positively charged helium nuclei),  $\beta$  rays (electrons),  $\gamma$  rays (electromagnetic radiation) and others such as Auger electrons. Electrons can be emitted, as described above, on interaction of radiation with matter, as  $\beta$  rays in radioactive decay or in therapeutic equipment. The effect of high-energy radiation may also be caused in part by the molecular interactions with the low-energy electrons associated with its tracks through biologic material (Michael and O'Neill, 2000).

The current S.I. unit of absorbed dose is the gray, representing the absorption of 1 joule of energy per kilogram of absorbing substance. It is the equivalent of

100 rads, the previously used unit. The S.I. unit of activity of a radioactive source is the becquerel (Bq), which is the activity of a radionuclide decaying at a rate of one spontaneous nuclear transition per second. This replaces the curie (Ci); 1 Ci =  $3.7 \times 10^{10}$  Bq.

## 2. Physical and Chemical Interactions with Radiation

Radiation affects different classes of substances in different ways: lipids are generally oxidized; nucleic acids show base damage, single- or double-strand breakage, or cross-linkage; proteins and carbohydrates may be degraded. These and other effects are due to the deposition of energy along the track of the radiation, the precise form of the interaction depending on the wavelength (photon energy) or the energy of the particle. Ultraviolet radiation causes excitation of orbital electrons, raising them to higher energy levels. At shorter wavelengths, for example, X rays and  $\gamma$  rays, ionization takes place and orbital electrons are ejected, generally with excess energy. The energy of electromagnetic radiation is important in determining the probabilities of the exact interactions involved. For photons below 0.1 MeV, the photoelectric effect is important, with the photon absorbed and emission of an electron and characteristic X-ray radiation. Between 1 and 5.0 MeV, Compton scattering of the photons is predominant: a variable amount of energy is transferred to an orbital electron, a recoil electron is produced, and the original photon continues on at lower energy. At energies above 1.02 MeV, the arrival of the photon at the target atom may lead to the production of an electron and positron pair.

The linear energy transfer (LET) is the rate at which energy is deposited per unit length of the track; electromagnetic radiation is described as low LET, and  $\alpha$  particles, neutrons, and heavy ion beams as high LET. Electrons can be regarded as being within the low-LET group. There is continuing work on the analysis of track structure (Nikjoo *et al.*, 1998), with increasing reference to effects caused by low doses and clustered damage. The interaction may cause damage by either direct or indirect action. In direct action, most strongly associated with high-LET radiation, biomolecules are damaged through excitation or ionization. In indirect action, greater for low-LET irradiation, free radicals are produced by radiation interacting with molecules such as water, present throughout biologic material: these cause destructive reactions with nearby sensitive molecular targets. The role of reactive oxygen species (ROS) produced endogenously or exogenously is important, with interactive effects on a range of subcellular features (Gamaley and Klyubin, 1999; Fig. 7). In the indirect effect, the hydroxyl radical causes the most damage (Michael and O'Neill, 2000). The secondary radicals produced by postirradiation amplification also include reactive nitrogen and sulphydryl species (Schmidt-Ullrich *et al.*, 2000). ROS may also have a regulatory role or be involved in signaling and their role in carcinogenesis is important (Marnett, 2000).

The level of oxygen present thus partly determines the tissue response to radiation or ROS. Well-oxygenated tissues will have additional oxygen available

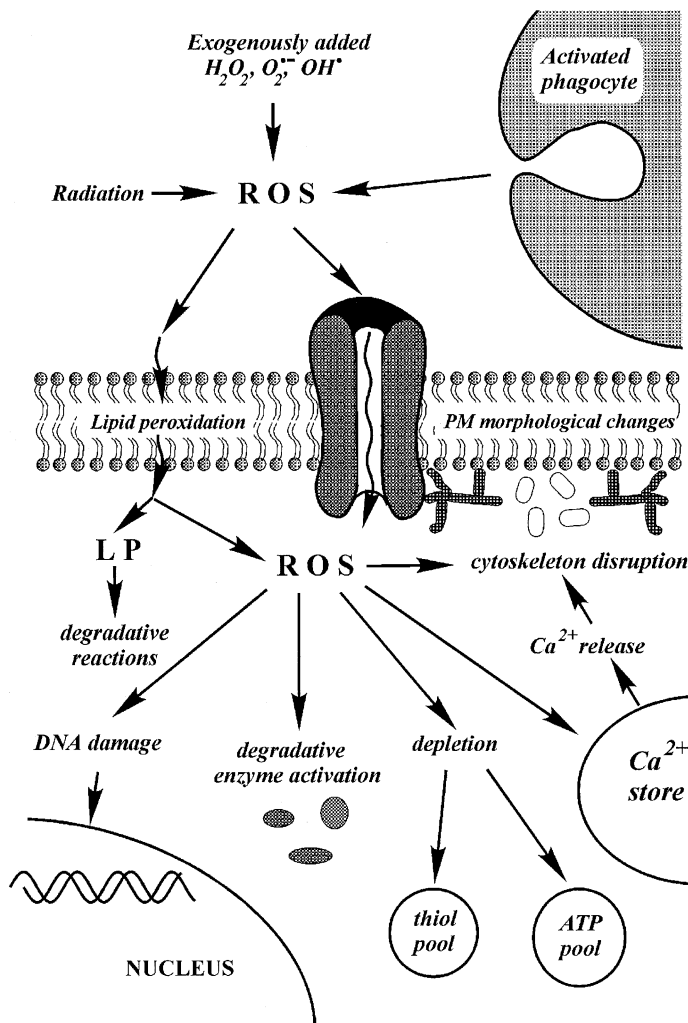


FIG. 7 Events that occur during cell injury under the effect of reactive oxygen species (ROS). PM, plasma membrane; LP, lipid peroxide. [Courtesy of I. A. Gamaley, I. V. Klyubin, and Academic Press, San Diego. Gamaley, I. A., and Klyubin, I. V. (1999). Roles of reactive oxygen species: Signaling and regulation of cellular functions. *Int. Rev. Cytol.* **188**, 203–255, Fig. 2.].

to disturb the equilibrium of radicals produced by water ionization or oxygen metabolism. More free radicals will be formed, with the likelihood of increased damage. Oxygen may also fix other organic radicals and prevent repair. Oxygen therefore acts as a radiation sensitizer and hypoxia as a protector. The situation is more complicated during wound healing, which is hampered by hypoxia. Other

radioprotective substances include sulphydryl-rich compounds, such as cysteine, glutathione, and thiophosphates, which rehydrogenate organic free radicals or those with affinity for electrons, thereby shifting the level of damage.

The physics of the interaction is over very quickly (Fig. 8), the chemistry of free radical reactions less so, the first structural biologic effects can be seen within minutes, while cell death and regeneration takes hours to days. For some of the morphologic changes described in this article, the timescale is hours to weeks for early effects and weeks to decades for late effects.

### 3. Cellular Interactions with Radiation

One of the principal sites for manifestations of radiation damage is the nucleus. However, radiation also interacts with other important cellular features (Coleman and Harris, 1998; Coleman, 2000; Fig. 9), such as plasma membrane receptors, and activates signaling pathways relating to cytoprotection and survival or cytotoxicity and apoptosis (Schmidt-Ullrich *et al.*, 2000). Other subcellular structures involved are endoplasmic reticulum and mitochondria. The signal transduction cascades in turn impinge on nuclear responses, implying a link between irradiation of the cytoplasm and the formation of mutations (Little, 2000). Damage to the nucleus includes effects on DNA at several levels and the production of various chromosomal abnormalities, visualized with fluorescence *in situ* hybridization painting (Tucker *et al.*, 1993; Finnon *et al.*, 1995; Griffin *et al.*, 1995). Whatever type of DNA damage is involved, it has an ultimate effect on protein synthesis.

Damage to DNA can be dealt with alongside consideration of the steps which the cell takes to recognize it and respond to it (Thacker, 1999; de Boer and Hoeijmakers, 2000; Lowndes and Murguia, 2000). Repair is dealt with by enzymes such as DNA glycosylases, endonucleases, polymerases, and ligases. Damage to a single DNA strand, either to a base or as a strand break, may be repaired by base excision repair (BER), with the undamaged strand used as a template. Alternatively, nucleotide excision repair may occur, in which a larger portion of the strand is removed and more enzymes are involved. Some damage results in base mismatches, which have to be removed by a specialized base excision pathway (mismatch repair pathway). Damage to both DNA strands involves enzymatic processing of the two broken ends, prior to repair by one of several pathways. One is homologous recombination repair (HRR), where an unbroken homolog is used as a template, before further cutting and rejoining. Another option, possibly used more often in humans, is nonhomologous end-joining, where simple ligase joining of the breaks occurs. Complex damage, caused by clusters of ionizations, may be repaired by a combination of different processes.

Fidelity of repair varies and mutations can occur, with BER and HRR having greater fidelity than the other pathways. Damage to DNA actively involved in transcription takes place particularly quickly. Repair genes involved in the repair of double-strand breaks are characterized and the importance of mismatch

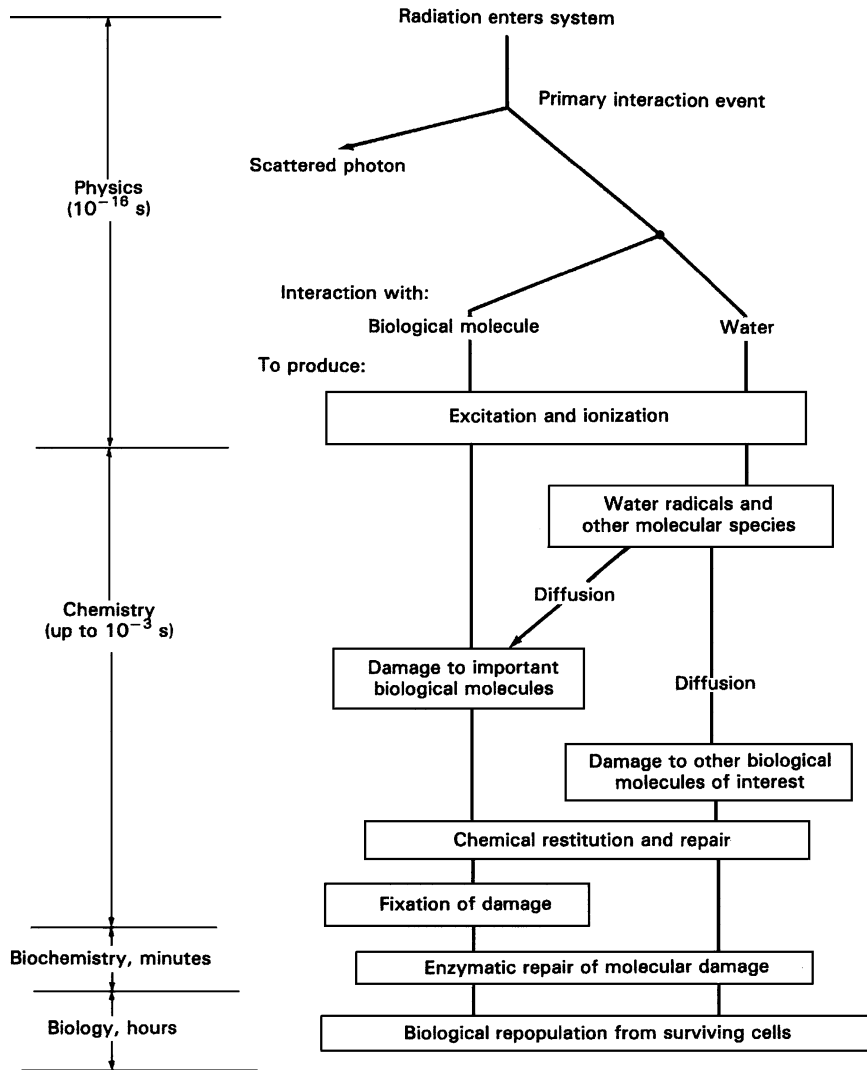


FIG. 8 A diagrammatic representation of the processes from energy transfer to final biological damage. [Courtesy of E. L. Alpen. Figure 4.1 from "Interaction of Radiation with Matter." In *Radiation Biophysics*, Second Edition, by Edward L. Alpen. Copyright 1998 by Academic Press, reproduced by permission of the publisher.]

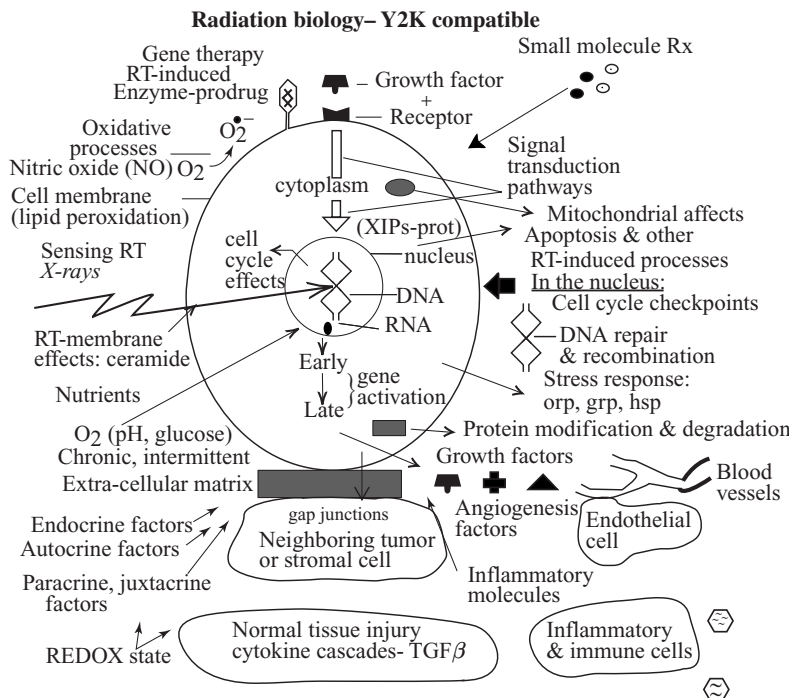


FIG. 9 Radiation biology in 2000—potential targets for translational research. For each of the pathways, detailed molecular and cellular knowledge is becoming available that will help explain the cellular phenotype and provide novel therapeutic targets. [Courtesy of C. N. Coleman and PRR Inc., New York. Coleman, C. N. Review of “Biological Basis of Radiation Sensitivity.” by Rosen, E. M., Fan, S., Goldberg, I. D., and Rockwell, S. *Oncology*, **14**, 757–761].

repair genes is recognized. There is also coordination with other cell activities, such as cell cycle checkpoints, which can be regarded as signal transduction pathways involved in “quality control” of the cell cycle and of DNA integrity (Diffley and Evan, 2000). These delay the cell’s entry to the next phase of the cycle until either DNA damage is repaired or the apoptotic process is triggered by pathways dependent on or alternatively independent of p53, both involving cytochrome *c* release from mitochondria (Lowe and Lin, 2000). If these checkpoint-driven processes fail, genomic instability can develop, whereby the progeny of irradiated cells, with delayed nonclonal mutations or aberrations in these nonirradiated descendants (Lorimore *et al.*, 1998; Wright, 1999), have an increased risk of malignant transformation (Carr, 2000). The various functions of p53 and other tumor suppressor genes include their categorization as “gatekeepers,” “caretakers,” or “landscapers” (Macleod, 2000). Factors covered include involvement in functions such as the control of  $\beta$ -catenin activity and in mismatch repair of genes involved in the development of tumors in human large intestine (Macleod, 2000).

#### 4. Tissue Interactions

Cells in tumors and normal tissues are not like isolated cells or cell culture monolayers, as used for some research. Each cell's microenvironment is important (Stone *et al.*, 1998; Diffley and Evan, 2000): the "bystander" effect points to the importance of communication between cells "hit" by radiation and their less obviously affected neighbors (Grosovsky, 1999). The microenvironment also includes the extracellular matrix, where, for example, metalloproteinases are important in activation of growth factors, cleavage of adhesion proteins, and production of genomic instability (Bergers and Coussins, 2000).

Radiation-induced proliferative changes in cultured cells are often measured, with emphasis on cell survival. The term "cell survival" is often used to imply retention of proliferative capacity, whereas cell "death" or "lethal damage" means its loss, rather than necessarily the actual death of the cell. Clonogenic assays measure the extent to which individual cells can proliferate to form colonies. This approach, based on counting plated microcolonies after irradiation, is adaptable to portray damage in cell populations that normally proliferate *in vivo*, such as intestinal crypts, for which a microcolony assay is used (Withers and Elkind, 1970; Potten *et al.*, 1981): varying crypt survival patterns are reported for different sites along the length of the intestine (Cai *et al.*, 1997a). After "sublethal damage" cells regain normal reproductive capacity after a short recovery period. This differs from "potentially lethal damage," where reproductive capacity is regained after time for recovery in the stationary phase. The radiation response may also be related to the type of functional subunit (FSU), defined structurally or functionally as "the largest unit of cells capable of being regenerated from a surviving clonogenic cell without loss of the specified function" (Withers *et al.*, 1988). Conversely, a tissue rescuing unit is the cell survival fraction related to one surviving clonogen per FSU. Different radiation volume outcomes are described for organs in parallel or in series. Examples of parallel organs include kidney, liver, and lung and examples of series FSUs are spinal cord and intestine; tumors are described by Fowler as the "ultimate parallel" organ (Peacock *et al.*, 1998).

#### 5. Delivery of Radiation

Radiation may be delivered to the whole body, or to part of the body (partial body), as a single dose, as several fractions, or via protracted or continuous delivery. It may be given by an external source (external radiotherapy, ERT), directly to an internal target as intraoperative radiotherapy (IORT; Touboul *et al.*, 1996), or through ingestion of radioactive material. Electrons, with short and tortuous tracks, are often delivered at operation, by IORT. Finally, light can be used to activate anticancer drugs exactly where they are needed, in photodynamic therapy.

### C. Analysis of Data on Morphology of Irradiated Intestine

#### 1. Variables

Variables influencing radiation-induced changes include species, site, radiation type, dose, and time of sampling. Other ways of varying the effect are dealt with in Section VI on factors influencing the outcome.

Species include mouse, rat, guinea pig, cat, dog, monkey, and human. Sites sampled include small and large intestine and related organs. Radiation type includes photons, particle beams, and radioactive emissions from ingested material.

Because a large range of doses is used, providing the details for each paper cited would interrupt the text flow. Doses are therefore classified into five broad groups (Table II), adapted from a three-group system for rat small intestine (Rubio and Jalnas, 1996). Although other authors use different dose bands, especially for other species (e.g., Potten, 1990), this standardization simplifies the text. The LD<sub>50</sub> values for several species are also noted in Table II.

Different time classifications include categorization into three phases (Hasleton *et al.*, 1985) or four stages (Hauer-Jensen *et al.*, 1983a; Wang *et al.*, 1999a). For textual organization, the current article uses two time frames, early and late, with 4 weeks as the cutoff point (Spitzer, 1995) and early manifestations given first in each subsection. For textual simplification, each time frame is further subdivided (Table III), using a composite of the phases described in the four papers cited above and in several others, including Eriksson *et al.* (1982) and Rubio and Jalnas (1996). On occasion, slightly different forms of wording are used.

Some studies use only one dose or time, while others collect information on dose- or time-dependent changes.

TABLE II  
Descriptors for Dose Ranges<sup>a</sup>

Descriptor	Dose range
Very low, lowest	<8 Gy
Low	8 to 13 Gy
Moderate	14 to 19 Gy
High	20 to 25 Gy
Very high, highest	>25 Gy

<sup>a</sup>These dose ranges exclude the lowest environmental levels. LD<sub>50</sub> for rat is 7.14 Gy, for mouse 6.40, and for monkey 6.00 (Nias, 1998).

TABLE III  
Descriptors for Time Ranges

Major time descriptor	Detailed time descriptor	Time range
Early	Within hours/soon after	<48 hr
Early	Within days/1 week	>48 hr but <7 days
Early	Around 2 weeks	7 days to <4 weeks
Early or late <sup>a</sup>	Around 1 month	48 hr to <3 months
Late	After several months	3 months to <9 months
Late	Around 1 year	9 months to <2 years
Late	After several years	2 years and later

<sup>a</sup>Data from this time period are classified as early or late depending on the overall balance of the protocol. If they form the final data set of an early protocol, which finishes around 1 month, they will be included with the rest of the early data. If they form the beginning of a late protocol, they will be classified as late.

## 2. Classification and Balance of Data

The text deals first with effects of single doses of commonly used low-LET radiation, such as X rays or  $\gamma$  rays (Sections III to V). Partial body data are addressed first (Section III). This avoids excessive interference from damage to other functionally interactive systems, such as the CNS, affected by nonshielded irradiation (Section IV). Splitting the dose into smaller fractions increases the total dose to tumor cells, but spares surrounding normal tissue (Section V).

Within these sections, the data are grouped according to structure affected; first, multiparameter studies and compartments, and then cell types, classified under epithelium, connective tissue, neuroendocrine, and muscle. Reports on small intestine are given first, with large intestine described thereafter; where the site differentiation is not clear, an account is given at the beginning. In the section on vascular changes, data on large vessels of supply are given first. Data are also grouped together by species and radiation conditions. When these are not explicitly described, the work is cited in Section I.

A brief review is given in Section VI of other factors influencing outcome. These include additional variations in radiation parameters, such as volume irradiated, LET, fractionation details, continuous irradiation, and ingestion of radioactive material. Factors relevant to the subject irradiated include underlying pathophysiology and other treatments given along with the radiation.

The volume and balance of data (Table IV) vary across radiation schedules, which are also studied with different types of factors affecting outcome (Section VI). It is difficult to compare information across schedules, because few aspects of the intestinal radiation response have information from more than one schedule. It is therefore seldom possible to separate clearly input from local as

TABLE IV  
Summary of Data Sets

Radiation delivery	Further detail	Radiation type	Species	Site sampled	Dose	Time
Single-dose partial body schedules (Section III)	Shielded, exteriorized, transplanted, isolated, IORT	Photons, electrons	Predominantly rodent, mainly rat A few results from pig, dog, cat, rabbit, and guinea pig Virtually no human data	Predominantly small intestine	Very low to very high	Mainly early
Unshielded radiation (Section IV)	Whole-body irradiation (Minority ingested effects in Section VI)	Mainly photons (Minority high LET in Section VI)	Predominantly rodent, mainly rat Also primate, pig, rabbit, cat, ferret (Minority environmental human data sets in Section VI)	Predominantly small intestine	Very low to very high	Predominantly early
Fractionated doses (Section V) A slightly smaller data pool than Sections III or IV	Usually partial body Details often scanty Mainly external, some intracavitory	Mainly photons, electrons	Majority human Also rodent, mainly rat (Minority pig, dog, guinea pig, mouse)	Majority small intestine	Cumulative dose high to very high Details often scanty	Many extend to late Details often scanty

Key: Predominantly, mainly, majority, and minority represent decreasing proportions of data pool.

opposed to whole-body effects or from single dose as opposed to different types of fractionated delivery.

### **3. Data Interpretation**

In addition to the difficulties involved in integrating the responses of the different cells and tissues present in the intestinal wall, there are also problems of interpretation specific to the cell type concerned. Data for enterocytes or goblet cells have to be taken in context with changes in villous shape, in small intestine, or variations in the tract diameter related to responses by smooth muscle. Secretory cells present an additional level of difficulty, since cell visibility at light microscope level may be altered by postirradiation granule release or by cell loss or damage. Therefore, complicated relationships can exist between apparent cell counts and levels of secretory material. These will be seen in alterations in amount or quality of luminal mucus or other products for goblet and Paneth cells or in hormone levels in blood or tissue for endocrine cells. A further complication, particularly for neuroendocrine cells, lies in the differences between total counts using a non-specific stain and numbers of subsets identified using specific techniques such as immunoreactivity, where there may, however, be thresholds below which cells will not be visible. There are also problems in comparing counts relating to different reference points. Many counts only reflect cell profiles, with section thickness and cell size also important if cell numbers are sought. Some data sets are also presented after normalization with respect to another population, giving results as proportions instead of raw data and leading to difficulties of interpretation, since each subpopulation may respond differently to the irradiation. Data expressed as cell profiles per unit length of tissue often do not take into account the extent of radiation-induced tissue shrinkage or collapse. Cell profiles per intestinal circumference may be more reliable. However, these data can also be affected by edema and changes in muscle status or compartment dimensions. These various points are all relevant during consideration of the data in Sections III to VI.

### **III. Effects of a Single Dose of Partial Body, Low-LET Irradiation**

The paucity of human data (Table IV) makes it difficult to extrapolate to human responses. Very few reports deal with both small and large intestine or with different sites within either, making it unrealistic to compare different organ or suborgan responses. Because the data for this section are predefined to refer to low LET, no further mention is made of radiation type, apart from some highlighting of IORT. Partial body irradiation is achieved by shielding nonabdominal tissues, exteriorization of intestinal segments or transplanting a segment to an easily irradiated site. Occasionally, the samples are irradiated isolated cells or tissue dissected from irradiated organs. Dose and time ranges are summarized in Table IV.

## A. Description and Integrative Summary of Responses

### 1. General Description

**a. Early** The lack of significant data sets on human tissues is accompanied by a similar deficiency in endoscopic findings. This highlights the value of endoscopic examination of animal small intestine, carried out within hours to days of treatment of dogs with low to moderate doses (Vigneulle *et al.*, 1990). There is dose-dependent edema, submucosal bleeding, and ulceration. Related symptoms, a few days after a low dose, include loss of appetite, emesis, and diarrhea, accompanied by bleeding (Summers *et al.*, 1991). They become more severe in the days thereafter.

There is a satisfactory number of data sets on rat small intestinal tissue, covering all but the shortest and very longest times after radiation and excluding also the effects of very low doses. Only days after a high dose, anorexia and weight loss occur (Sebes *et al.*, 1975), and after even the lowest range of doses, signs of reduced weight gain are seen (Keelan *et al.*, 1989). Two early data sets deal with the changes with time after doses in the high to very high range, with dose-dependent variation in the development of the lesions and subsequent regeneration (Osborne *et al.*, 1970; Sebes *et al.*, 1975). Within days, there is evidence of hyperemia and an acute inflammatory reaction, with shortened villi, flattened epithelial cells, and pyknotic nuclei. These changes are quickly followed by ulceration, severe crypt damage, necrosis at several levels, acute inflammation, incipient serosal fibrosis, and edema/hypertrophy of the main muscle layer. Within weeks, the prominent changes are ulceration, fibrosis, and continuing signs of an inflammatory reaction (Osborne *et al.*, 1970). At and after 1 month, there are signs of regeneration after appropriate doses, although damage is still also seen.

There is a substantially smaller database for general descriptions of early changes in large intestine. Endoscopy of rats from several days onward after moderate doses shows erythema, bleeding, excess mucus, and loss of submucosal vessels (Tamou and Trott, 1995). There is substantial improvement over a few weeks, although edema is still evident. High-dose irradiation of rat rectosigmoid region leads to rectal obstruction in almost all animals around 1 month after treatment (Trott *et al.*, 1986).

**b. Late** In the rat small intestine, there are signs of continuing damage, but also of regeneration (Sebes *et al.*, 1975). Mortality increases as dose rises from moderate through high and death is usually due to fibrosis-related obstruction (Hauer-Jensen *et al.*, 1983a). One of the serious late effects of moderate doses is the production of tumors, similar to adenocarcinoma and showing evidence of metastasis, from months to 1 year after treatment (Osborne *et al.*, 1963, 1970).

The small group of papers on rat large intestine covers a wide range of doses and times. Following the healing of early proctitis a few weeks after irradiation, chronic damage is produced thereafter by high doses. This manifests itself as decreased

defecation, colonic congestion, intestinal constriction, and fatal obstruction (Trott, 1984), or as weight loss, bleeding, and strictures (Geisinger *et al.*, 1990). The frequency of adenocarcinoma also increases as the very high dose rises further (Black *et al.*, 1980).

## 2. Multiparameter Studies—Methods

Closer examination reveals that morphologic changes occur in many of the different compartments, tissues, and cell types in the intestinal wall. One way of obtaining an overview of the complexity of the response is to review the work of the groups, which assess several parameters, since this often highlights changes in cell compartments or cell types that might otherwise be overlooked. These approaches often bring together the data for the different parameters into total scores, or compare the changes in different parameters. Most describe changes in small intestine, often in rat or mouse. The account that follows deals first with two systems of scoring, then with comparisons of parameter responses and concludes with a summary of the findings of these studies. Many of the parameters used are listed in Table V, which refers to some authors whose work is described in this subsection or used in the illustrations.

**a. Injury Score Approach** The first of the two main systems of scoring relies on the grading of pathologic changes seen in wax histology sections. The grades for the different parameters are summed to give a total empirical injury score. This rises as damage increases with, for example, dose (Eriksson *et al.*, 1982; Hauer-Jensen *et al.*, 1983a; Mulholland *et al.*, 1984; Vigneulle *et al.*, 1990; Solheim *et al.*, 1991; Summers *et al.*, 1991; Beyzadeoglu *et al.*, 1997; Richter *et al.*, 1997a). Some of these scoring systems for small intestine are developed from the work of Black *et al.* (1980) on late changes in large intestinal parameters.

Injury scoring is mainly based on data from irradiated rat small intestine. There is an early report by Forsberg *et al.* (1979), recording epithelial and stromal changes. Thereafter a multiparameter system is used by Hauer-Jensen *et al.* (1983a) to record changes in several structural parameters of the wall (Table V). These are macroscopic and histopathologic changes, the latter being mucosal alterations, epithelial atypia, serosal thickening, vascular sclerosis, fibrosis of the wall, lymph congestion, and ectopic glandular structures deep in the wall, termed ileitis cystica profunda.

The system is developed, named radiation injury score (RIS), and used by the group in an analysis of manifestations of radiation injury in periods spanning hours to several months after irradiation with very low to high doses. For example, the development of the RIS is correlated with other signs of radiation-induced change, such as the production of granulocyte marker protein (GMP) and fibrosis (Richter *et al.*, 1997a). It also provides a reference baseline for the changes in TGF- $\beta$ 1 gene expression and immunoreactivity (Hauer-Jensen *et al.*, 1998) and in

TABLE V

Examples of Parameters Used in Multiparameter Studies—Some Early Scoring Systems and Those Illustrated in This Review

	Investigators				
	Forsberg <i>et al.</i>	Hauer-Jensen <i>et al.</i>	K. E. Carr <i>et al.</i>	Rubio and Jalnas	Black <i>et al.</i>
Date of reference	1979	1983a	1992b	1996	1980
Part of intestine	Small	Small	Small	Small	Large
Structural integrity, score		E/L	E		
Mucosal height changes, villous blunting			E		
Cryptal changes				E	
Submucosal thickness, edema			E	E	
Muscle thickness			E	E	
(Sub)serosal thickness		E/L		E	
Nerve changes			E		
Ulcers		E/L		E	L
Ectopic glands		E/L		E	L
Necrosis				E	
Epithelial, enterocyte changes, adenoma	E-L	E/L	E	E	L
Mucous cells	E-L		E	E	
Endocrine cells			E		
Paneth cells			E	E	
Defensive cells			E	E	
Fibrosis	E-L	E/L		E	L
Vascular changes		E/L	E	E	L
Lymph congestion		E/L			

Key: E, immediate to 4 weeks; L, >4 weeks; E/L, both E and L; E-L, around 4 weeks.

the localization of the mannose 6-phosphate/insulin-like growth factor II receptor (Wang *et al.*, 1999a). Another group compares total scores with surface changes assessed by SEM and increases in the passage of absorbed contrast medium into serum and urine (Solheim *et al.*, 1991).

**b. Ratio Score Approach** The second approach uses glutaraldehyde-fixed thin resin sections to produce ratios of treated to control numbers of cellular profiles

per circumference, thus recording deviations from control levels. The model used is mouse, within hours and days of very low to high doses of radiation. The parameters used are classified according to the tissues of the body, epithelium, muscle, nerve, and connective tissue. Section areas of the tissues themselves are also measured and counts made of profiles of four epithelial and two connective tissue elements, muscle cell profiles in both layers of the muscularis externa and nerve plexus profiles (Table V). The areas and ratios for all parameters are then brought together to give a total analytical figure or morphological index (Carr *et al.*, 1992b). The index scores, unlike the injury scores, fall away from control levels as damage increases.

**c. Interparameter Comparisons** Data from multiparameter assessment of wax sections are also used specifically to classify the parameters (Table V) into dose/time- or time-dependent groups of changes (Rubio and Jalnas, 1996) in the time frame of days to weeks after low to high doses. Some other wax histology experiments are reported by Forsberg *et al.* (1979), Hauer-Jensen *et al.* (1983a), Vigneulle *et al.* (1990), Beyzadeoglu *et al.* (1997), and Wang *et al.* (1999a). Data from resin sections are also used for direct comparison at each dose/time point of the responses for different parameters, through statistical analysis of the percentage change of each parameter with respect to the relevant control population (Carr *et al.*, 1992b).

### 3. Multiparameter Results—Early

**a. Scores** The main group of data sets relates to rat small intestine in the time frame of hours to several months after very low to high doses of radiation. The total injury score reflects increasing damage as time passes from hours to weeks (Wang *et al.*, 1999a; Fig. 10), with the extent of the change dependent on dose, as are signs of recovery around 1 month (Solheim *et al.*, 1991). Comparison of scores from different systems shows that the damage increases with dose from very low upward (Richter *et al.*, 1997a; Hauer-Jensen *et al.*, 1998), with a suggestion of a plateau at moderate doses (Forsberg *et al.*, 1979).

These trends are confirmed by data from small intestine from other species, together covering a similar range of doses and times as the rat data sets, although with proportionally more information available hours after treatment and using the lowest doses. These ratio and injury score data sets show changes as early as a few hours after irradiation with low doses in mouse, with damage increasing during the next few days for both mouse (Carr *et al.*, 1992b; Fig. 10) and dog (Vigneulle *et al.*, 1990). The different total scores for sham and control groups are attributed to stress-related responses in enteroendocrine cells (Carr *et al.*, 1992b).

**b. Interparameter Differences** Some parameters feature in several of the main scoring systems (Table V), indicating that these are likely to be the changes most

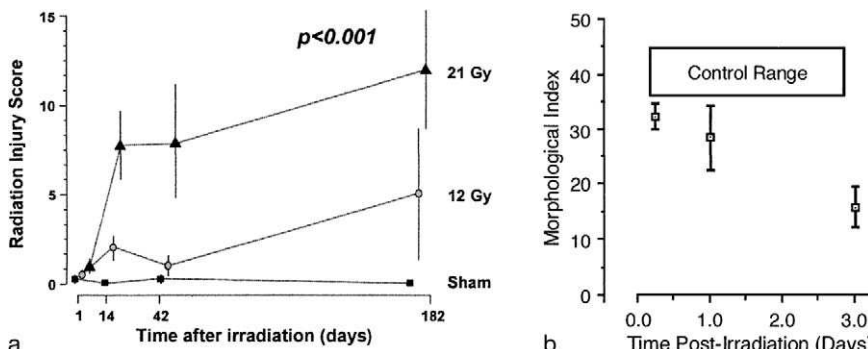


FIG. 10 (a) Time and dose dependence of histopathological changes (Radiation Injury Score) in sham-irradiated and irradiated intestine. (b) Total Morphological Index for time after treatment with 10-Gy X rays. The 3-day point stands out as clearly separate from the other groups. [Part (a) courtesy of M. Hauer-Jensen. Reprinted from *Radiotherapy and Oncology*, **50**, Wang, J., Richter, K. K., Sung, C.-C., and Hauer-Jensen, M. Upregulation and spatial shift in the localization of the mannose 6-phosphate/insulin-like growth factor II receptor during radiation enteropathy development in the rat, pp. 205–213. Copyright 1999, with permission from Elsevier Science, Fig. 2. Part (b) courtesy of Japan Radiation Research Society. Reprinted from Carr, K. E., Nelson, A. C., Hume, S. P., and McCullough, J. S. (1992). Characterisation through a data display of the different cellular responses in X-irradiated small intestine. *J. Radiat. Res.* **33**, 163–177, Fig. 3.]

often seen by observers scanning the whole organ. The most often used are epithelial and vascular changes, followed by ulceration and fibrosis. Least often used are changes in nerve, endocrine cells, and lymphatic vessels, although most of those parameters do show changes in some circumstances.

The main group of data sets from experiments using multiparameter scoring systems relates to rat small intestine, hours to months after very low to high doses of radiation. Days after treatment with moderate to high doses, the parameters most involved reflect mucosal changes (Solheim *et al.*, 1991). Weeks after irradiation across the same dose range, the most common features are ulceration, epithelial atypia, serosal thickening, and macroscopic changes (Hauer-Jensen *et al.*, 1983a). Similar data for this time point after a moderate dose are presented by another group who note the percentage of animals that demonstrate three grades of damage for different parameters (Beyzadeoglu *et al.*, 1997). The greatest extent and range of damage are seen in the development of epithelial atypia and ectopic glands. Ulceration and inflammation are most often seen only to a moderate extent, while fibrosis and vascular sclerosis are least well developed at this time point. Around 1 month after irradiation, using the dose range very low to high, variation of the dose alters the balance of damage related to goblet cells, ulceration, and fibrosis (Forsberg *et al.*, 1979).

A slightly different approach to the analysis of data from irradiated rats is taken by another group using moderate to high doses and examining the tissues from

hours to months after treatment (Rubio and Jalnas, 1996). Most parameters used are dose and time dependent. These include epithelial necrosis, ulceration, and ectopic glands (Fig. 11); decrease in goblet cells, Paneth cells, or mitotic figures; cryptal abscesses, structural changes, or clear cells; increased collagen deposition (Fig. 11) in submucosa, muscularis externa, or subserosa; and loss of intraepithelial or lamina propria lymphocytes. Time but not dose dependence is shown by racket-shaped surface epithelial cells, congested capillaries, and increased stromal round cells.

Similar data are obtained for mouse hours to days after very low to high doses (Carr *et al.*, 1992b). The vascular response seen within hours is replaced by epithelial changes in the following days, when endocrine cells respond at the very lowest dose, while goblet cells and enterocytes require at least moderate doses to elicit a significant response. Several parameters are also used for radiation injury to small intestine several hours to several days after irradiation of dogs with a low dose (Summers *et al.*, 1987). Mucosal atrophy, inflammation, and neutrophil numbers increase with time, although the scoring for eosinophils and mononuclear cells shows a different trend. Such changes as are seen in the muscularis externa accompany mucosal damage and no alterations are seen in the myenteric plexus, although substantial abnormalities are observed in myoelectric activity.

**c. Data Variation** Although there are no specific reports on variation within individual parameter responses, this can be deduced from several data sets. Rat small intestine, as before, contains the largest body of data. Beyzadeoglu *et al.* (1997), report that, weeks after a high dose, some parameters, such as ulceration, fibrosis, vascular sclerosis, and inflammation, vary from Grade I to II, while ectopic glands and epithelial atypia range from Grade I to III. A variation in the extent of responses is also reported by Solheim *et al.* (1991), particularly weeks after irradiation. A range of responses around 1 month after very low to high doses is described by Forsberg *et al.* (1979). Rubio and Jalnas (1996) report that, days to months after moderate to high doses of radiation, the percentage of animals showing a particular level of change varies for many parameters. The variation in response is confirmed in a recent study where morphologic changes are used as a baseline for reporting increased levels of neuropeptides after radiation (Hockerfelt *et al.*, 2000).

Variation in response is also reported for other species, such as irradiated mouse tissue, from an overshoot to 231% to a drop to 0.08% of the relevant control value, hours after very low doses (Carr *et al.*, 1992b). In the same data set, some parameters do change, but not to statistical significance. This indicates a large range of values in control or treated groups, confirming intersubject variation. The range of responses also varies in dog (Vigneulle *et al.*, 1990); not all animals are affected to the same extent within hours and days after irradiation with low to moderate doses.

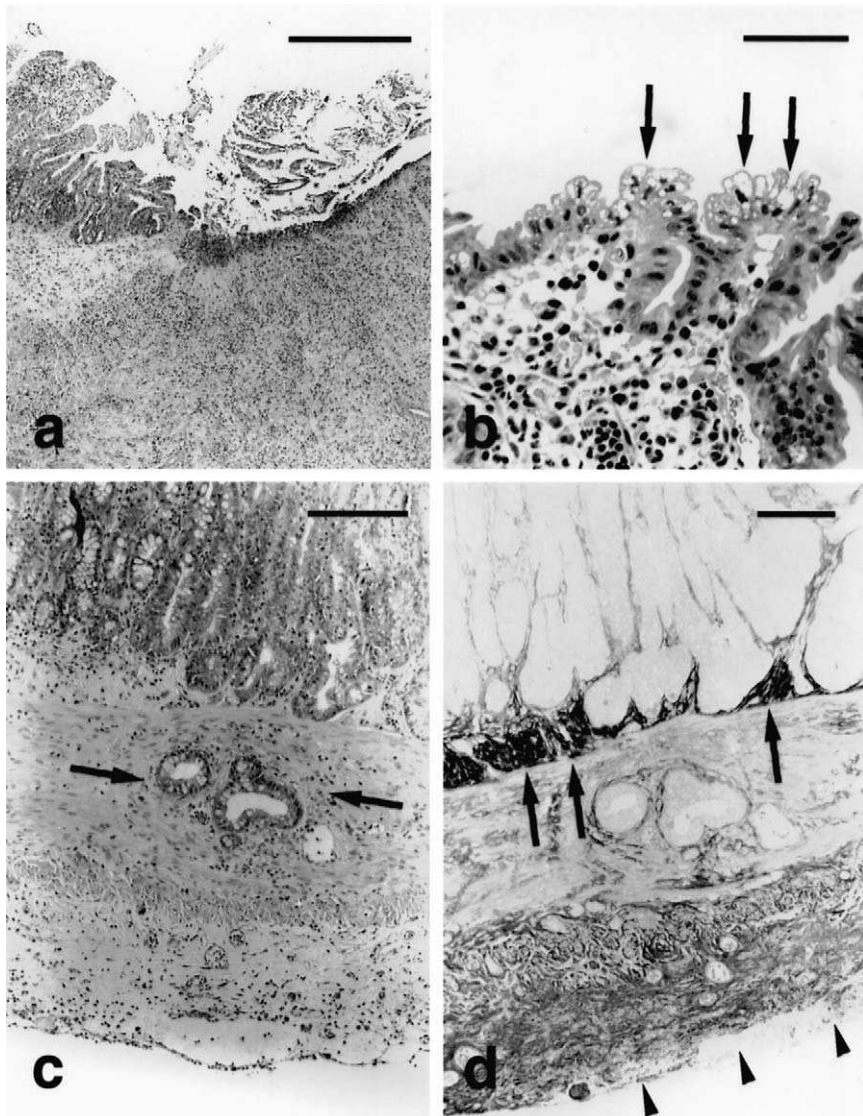


FIG. 11 Examples of parameters showing radiation-induced changes in small intestine. (a) Ulceration (right half of picture) in the small intestine of a rat 10 days after irradiation with 21 Gy (H&E). Scale bar = 1 mm. (b) Cell necrosis covering the villi of the small intestine of a Sprague-Dawley rat 3 days after irradiation with 21 Gy. Note pyknotic, vacuolated cells at arrows (H&E). Scale bar = 200  $\mu$ m. (c) Ectopic mucous glands in muscularis propria (at arrows) in the small intestine of rat irradiated 30 days with 21 Gy (H&E). Scale bar = 400  $\mu$ m. (d) Increased collagen in the submucosa (at arrows) and in the subserosa (at arrowheads) (Sirius stain). Scale bar = 400  $\mu$ m. [Courtesy of C. Rubio and Kluwer Academic/Plenum Publishers, 233 Spring Street, New York, NY 10013-1578. Rubio, C. A., and Jalnas, M. (1996). Dose-time-dependent histological changes following irradiation of the small intestine of rats. *Dig. Dis. Sci.* **41**, 392–401, Figs. 4, 1, 7, and 6, respectively.]

#### 4. Multiparameter Results—Late

The injury score rises as dose increases from low to high, months after treatment (Richter *et al.*, 1997a; Hauer-Jensen *et al.*, 1998; Wang *et al.*, 1999a). The parameters associated with late injury include vascular sclerosis, fibrosis, lymph congestion, and ectopic glands. The extent of these changes increases from a low level a few weeks after radiation, with a plateau several months later.

The scoring system used for the analysis of the data from cats, however, records the damage as decreasing from the worst score, days after irradiation, to a much lower figure months after moderate to high doses (Eriksson *et al.*, 1982). The discrepancy could be due to the fact that the Eriksson score uses proportionally fewer of the parameters described by Hauer-Jensen *et al.* (1983a) as late alterations. The parameters listed by Eriksson *et al.* (1982) as being particularly relevant to the late period are villous and cryptal abnormalities and fibrosis.

Injury scores for large intestine months to 1 year after treatment (Black *et al.*, 1980; Table V) tend to be higher at the later time, reflecting greater injury. The parameters contributing to this are fibrosis and atypical epithelial proliferation, the latter including the development of adenocarcinoma as its most serious manifestation.

### B. Changes in Intestinal Compartments

#### 1. Luminal

These are early changes. The few available data sets relate to a range of species, using very low to moderate doses and sampling hours to weeks after treatment. Bypass surgery (Mulholland *et al.*, 1984) allows comparison, days after a moderate dose, between intact guinea pig small intestinal segments in continuity with adjacent portions of the tract and other segments that are empty or contain bile only, or pancreatic juice and chyme together. The injury scores reflect damage that is increasingly greater than controls from empty through pancreatic group, bile group, in continuity group and intact group. There is a decrease in pancreatic secretion in pigs, hours after treatment with a very low to low dose, with recovery by several days later (Corring *et al.*, 1975). Alkaline pH gives some radioprotection in terms of rat mucosal thickness and height, but is less helpful with respect to villous goblet cells and crypt numbers (Delaney *et al.*, 1992). There is no effect on blood flow.

#### 2. Villous and Cryptal

*a. Early* There is a satisfactory database for villous shape and changes to villous and cryptal dimensions, almost entirely from mouse and rat studies of small intestine sampled hours to 1 month after very low to high doses. The results include

reports from SEM studies of mucosal surfaces, correlated directly or indirectly with histologic data.

The mouse data include empirically scored, SEM-derived, dose-dependent villous shape changes days after very low to high doses (Carr *et al.*, 1983). The villi change from control, erect structures through broader, shorter shapes to rudimentary undulations or a flat, avillous surface, with an accompanying reduction in likely absorptive capacity. Histologic study shows epithelial-stromal stripping (Wyatt *et al.*, 1987). In an investigation of postirradiation proliferation using uptake of radiolabeled recombinant urogastrone, villus to crypt feedback is highlighted as a possible regulatory factor (Saxena *et al.*, 1991). This is inferred from the relationship, days to weeks after a very low dose, between crypt cell production, crypt depth, and villous height. Comparisons of small and large intestinal crypt survival data are available for several days after irradiation, with low to moderate doses, of three groups of mice (Hendry *et al.*, 1997). These are wild-type, p53-null, and p53 heterozygous. It is deduced that the greater radioresistance in large intestine may be partly p53 related.

The rat database includes a report of the link between SEM imaging of villous collapse and histologic injury scores. A low score, reflecting minimal histologic damage, correlates with irregular villi and a high score with low to absent villi (Solheim *et al.*, 1991). The crypt–villus system is substantially reduced in height and organization days after irradiation with a low dose (Becciolini *et al.*, 1982a). The dose dependence of villous shape changes is confirmed by the fact that, although there is no change hours after a low dose (Thomson *et al.*, 1984), after a very high dose, the villous area is down to 87% of the control level while the cryptal area is decreased to 34% (Altmann, 1974). Within days, the villous figures are 55% and 20%, respectively, while the cryptal figures are 22% and 7% of control values. No variation is recorded for five different regions of small intestine (Altmann, 1974). However, differences in the extent of changes in villous shape and cryptal structure are reported for jejunum and ileum in a different model, days to 1 month after very much lower doses (Thomson *et al.*, 1984; Keelan *et al.*, 1986). Substantially more changes in villous parameters are seen in jejunal than in ileal samples, days to weeks after very low doses.

Villous height and crypts/mm also decrease in dogs hours to days after moderate doses (Vigneulle *et al.*, 1990) and villous collapse occur later in pigs than rodents (Chomette *et al.*, 1977).

The rat database also provides information at a more molecular level at various times after a range of doses. Expression of TGF- $\beta$ , particularly isoform 1, is increased in regenerating small intestinal crypt cells weeks after radiation with low to high doses (Wang *et al.*, 1998; Table VI). There is also strong cryptal immunoreactivity for mannose 6-phosphate/insulin-like growth factor-II (M6P/IGF-II) receptor (Fig. 12). It is thought that this is involved in TGF- $\beta$  activation (Wang *et al.*, 1999a). Changes in clusterin mRNA expression in small and large intestine are reported over a period of hours after irradiation with very low doses

TABLE VI

Expression of TGF- $\beta$  in Sham-Irradiated and Irradiated Intestine, 2 and 26 Weeks after Irradiation

	TGF- $\beta$ 1			TGF- $\beta$ 2			TGF- $\beta$ 3		
	Sham	2 weeks	26 weeks	Sham	2 weeks	26 weeks	Sham	2 weeks	26 weeks
Epithelium	++	+++	++	++	++	++	++	++	++
Neurons	+++	+++	+++	++	++	++	++	++	++
Smooth muscle	0	+++	+	0	++	0	0	++	0
Inflammatory cells	0	+++	+++	0	++	+	0	++	+
Fibroblasts	0	+++	+++	0	++	+	0	++	+
Endothelium	+	++	+++	0	++	+	0	++	+
Mesothelium	0	+++	++	0	++	0	0	++	0

Key: 0, negative; +, weakly positive; ++, positive; +++, strongly positive.

Courtesy of M. Hauer-Jensen and American Society of Investigative Pathology, 9650 Rockville Pike, Bethesda, MD 20814. Wang, J., Zhengh, H., Sung, C.-C., Richter, K.K., and Hauer-Jensen, M. (1998). Cellular sources of transforming growth factor- $\beta$  isoforms in early and chronic radiation enteropathy. *Am. J. Pathol.* **153**, 1531–1540, Table I.

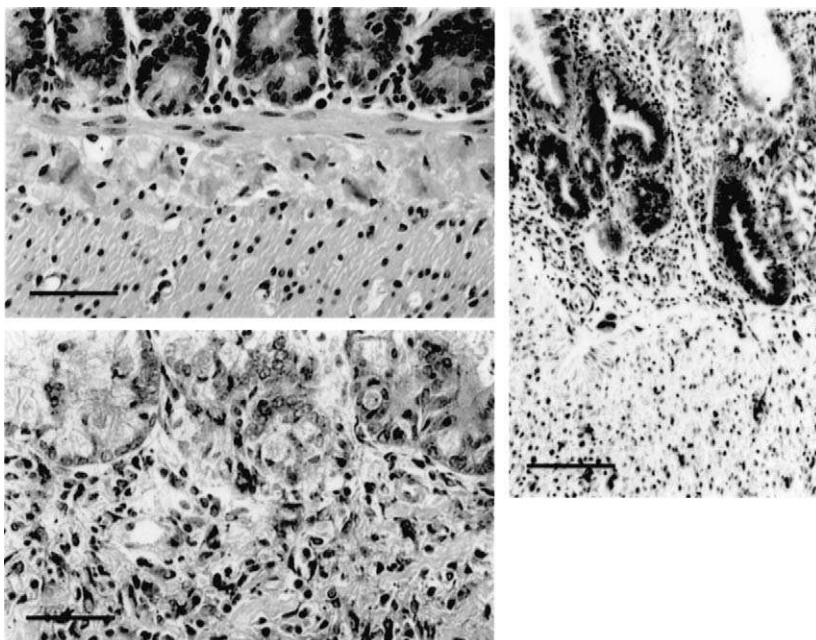


FIG. 12 Temporal and spatial shift in localization of M6P/IGF-II receptor immunoreactivity after irradiation. Reproduced from original color prints. (Top left panel) Sham irradiated intestine showed weak M6P/IGF-II receptor immunostaining mainly limited to crypt epithelium. Scale bar = 25  $\mu$ m. (Right panel) Two weeks after localized irradiation (21 Gy, single dose), regenerating epithelium exhibited strong immunoreactivity. Scale bar = 50  $\mu$ m. (Bottom left panel) At 26 weeks, epithelial immunoreactivity levels had returned to normal, whereas there was prominent staining of fibroblasts in fibrotic areas. Scale bar = 25  $\mu$ m. [Courtesy of M. Hauer-Jensen. Reprinted from *Radiotherapy and Oncology*, **50**, Wang, J., Richter, K. K., Sung, C.-C., and Hauer-Jensen, M. Upregulation and spatial shift in the localization of the mannose 6-phosphate/insulin-like growth factor II receptor during radiation enteropathy development in the rat, pp. 205–213. Copyright 1999, with permission from Elsevier Science, Fig. 3.]

(Arai *et al.*, 1996b). There is a brief decrease, followed by a rise and secondary decrease. This has the same time course as the incidence of apoptotic cells. However, clusterin expression is not restricted to apoptotic cells; it is associated with the Paneth cell zone in small intestine, but is more diffusely epithelial in large intestine (Fig. 13). Maximum expression appears 2 hr earlier in small than in large intestine, possibly related to the more effective removal by apoptosis of damaged cells in the former. The expression profile and timing could implicate clusterin in postapoptotic remodeling.

**b. Late** Similar dose and time ranges, namely, several months after low/moderate to high doses, are used to collect data from rat (Hauer-Jensen *et al.*, 1983a) and cat,

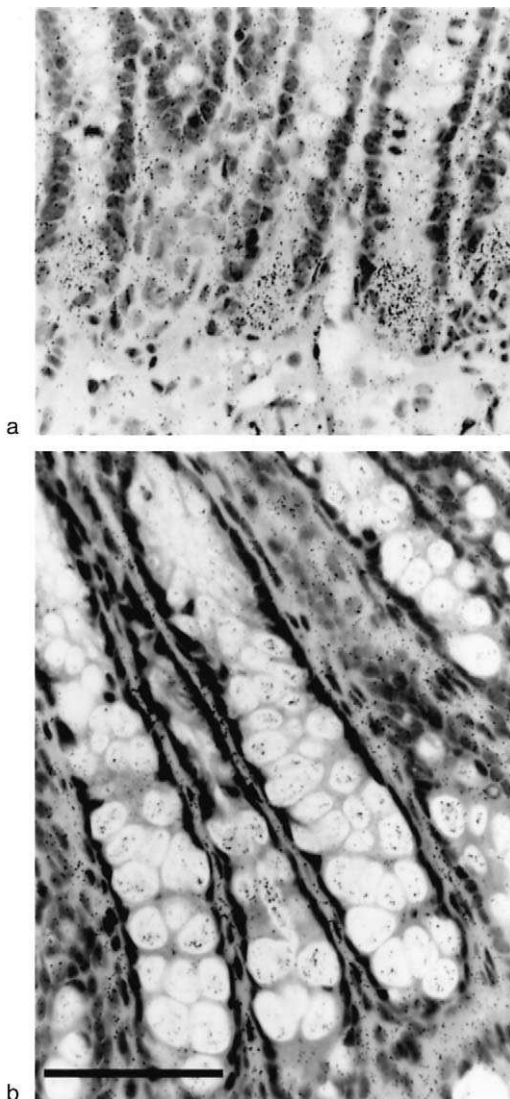


FIG. 13 (a) Bright-field micrograph showing the irradiated rat small intestine treated for *in situ* hybridization with clusterin antisense probe. Autoradiographic silver grains representing the signal for clusterin mRNA are densely accumulated over the Paneth cell region. (b) Similar micrograph of irradiated large intestine. Autoradiographic silver grains representing the signal for clusterin mRNA are diffusely distributed over the epithelial cells in the whole crypt and sparsely distributed over the lamina propria. Scale bar = 50  $\mu$ m. [Courtesy of T. Arai and Taylor and Francis Ltd., Rankine Road, Basingstoke, Hampshire, RG24, 8PR, <http://www.tandf.co.uk>. Arai, T., Kida, Y., Harmon, B. V., and Gobe, G. C. (1996). Expression and localization of clusterin mRNA in the small and large intestine of the irradiated rat: Its relationship with apoptosis. *Int. J. Radiat. Biol.* **69**, 547–553, Figs 3a and 4a, respectively.]

the latter at histologic (Eriksson *et al.*, 1982) and ultrastructural levels (Eriksson *et al.*, 1983). The radiation-induced alterations include cryptal abnormalities in both species and villous irregularities in cat.

### 3. Layers, Tissues, and Tissue Boundaries

**a. Early** The few reports of these fairly large-scale changes are restricted to small intestine, spread over several species, time spans, and doses. The details of changes in submucosa, muscularis externa, and subserosa are given by Rubio and Jalnas (1996). In cat, there is no overall thickening days to months after similar doses. However, this hides the fact that the mucosa shows early atrophic thinning, while the submucosa and external muscle layer are thicker at and beyond 1 month after treatment (Eriksson *et al.*, 1982). The mucosal change is not dose dependent, while the increases in the other layers are only seen with the high dose. With respect to changes at tissue interfaces, the thickening in the wall of the rat small intestine is accompanied by the presence of a pale gray serosa (Hauer-Jensen *et al.*, 1983a). *In situ* hybridization shows increases in expression of TGF- $\beta$  mRNA at the serosal mesothelial lining weeks after irradiation with low to high doses (Wang *et al.*, 1998; Fig. 14, Table VI). This is more marked for isoform 1 than for isoforms 2 and 3.

Changes at the mouse epithelial stromal interface include epithelial/stromal stripping several hours after low to moderate doses (Wyatt *et al.*, 1987). This is confirmed in rat several days later (Erbil *et al.*, 1998) and could be related to earlier subepithelial blebbing, accompanied by the presence of pale, acidophilic material in the space created by this (Buell and Harding, 1989).

**b. Late** In the papers quoted above for early changes, there is some dose dependence and species variation in late changes in thickness of the layers of the wall. However, in general, the mucosa becomes thinner, while the submucosa, muscularis externa, and subserosa become thicker. There is focal reduplication of the basal lamina at submucosal ectopic glands, which also herniate through the muscularis mucosae (Geisinger *et al.*, 1990). Several months after treatment with moderate to high doses, the level of expression of TGF- $\beta$ 1 for mesothelium, although decreased, is still higher than the control levels (Wang *et al.*, 1998; Table VI).

### 4. Disturbances of Cell Growth

These are late changes. The formation of adenocarcinoma as a subset of epithelial atypia is used as a parameter in some scoring systems for small and large intestine, respectively (Hauer-Jensen *et al.*, 1983a; Black *et al.*, 1980). The rat model is the basis for some further reports on the process of tumor formation. Some tumors are found in small intestine several months to 1 year after moderate to high doses, with the types listed as adenocarcinoma (Osborne *et al.*, 1963, Hauer-Jensen

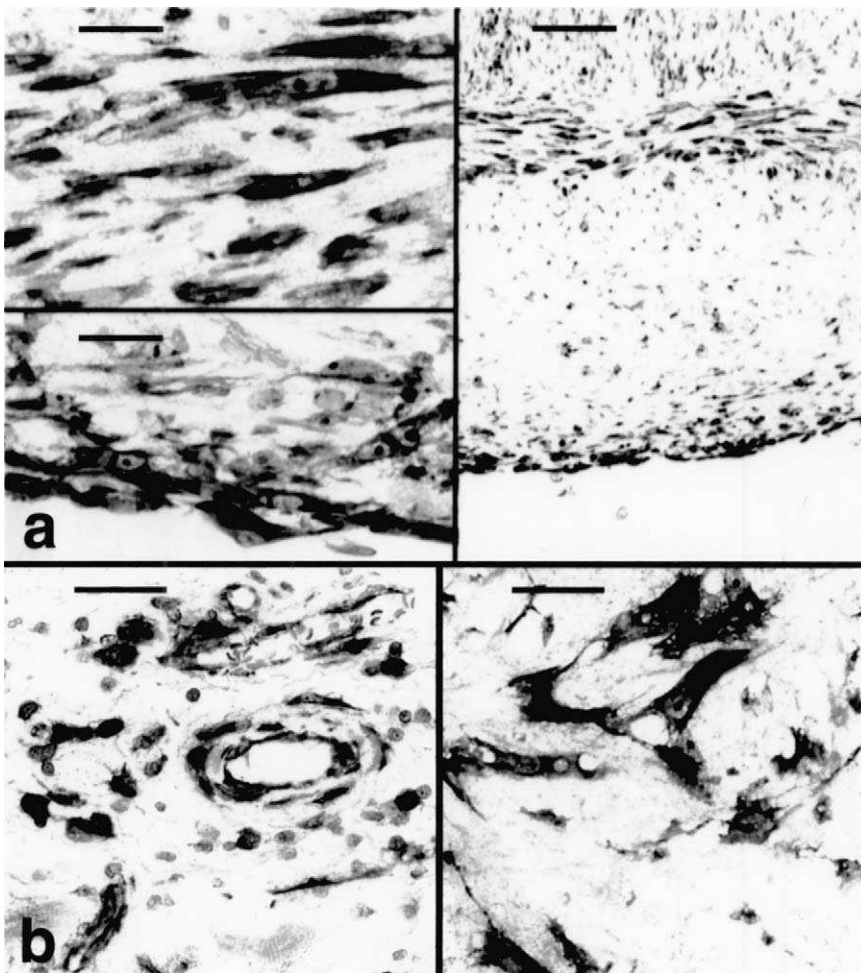


FIG. 14 *In situ* hybridization demonstrating TGF- $\beta$ 1 mRNA expression in irradiated intestine. Reproduced from original color prints. (a) Intestinal wall beneath a radiation-induced mucosal ulcer (right overview, scale bar = 100  $\mu$ m). Strong TGF- $\beta$ 1 expression in smooth muscle cells (left upper inset, scale bar = 25  $\mu$ m) and peritoneal mesothelium (left lower inset, scale bar = 25  $\mu$ m). Two weeks after 21-Gy single-dose irradiation. (b, left panel) TGF- $\beta$ 1 expression in vascular endothelial cells and perivascular cells. Twenty-six weeks after 21-Gy single-dose irradiation. Scale bar = 25  $\mu$ m. (b, right panel) Fibroblasts in fibrotic areas expressing TGF- $\beta$ 1 mRNA. Twenty-six weeks after 21-Gy single-dose irradiation. Scale bar = 25  $\mu$ m. [Courtesy of M. Hauer-Jensen and American Society of Investigative Pathology, 9650 Rockville Pike, Bethesda, MD 20814. Wang, J., Zheng, H., Sung, C.-C., Richter, K. K., and Hauer-Jensen, M. (1998). Cellular sources of transforming growth factor- $\beta$  isoforms in early and chronic radiation enteropathy. *Am. J. Pathol.* **153**, 1531–1540, Figs. 3C, 3D, and 3E.]

*et al.*, 1983a), angiofibroma or osteoid lesion (Sebes *et al.*, 1975). In large intestine, adenomas (Black *et al.*, 1980; Geisinger *et al.*, 1990) increase in number as the very high dose increases (Black *et al.*, 1980). An extraintestinal sarcoma is also reported (Geisinger *et al.*, 1990).

### C. Changes in Epithelial Cells

#### 1. Surface Epithelium, Enterocytes, and Glands

**a. Early** Apart from a report of mitotic arrest in human small intestine days after one fraction of a low dose (Wiernik and Plant, 1971), the data come mainly from rat samples hours to months after very low to moderate doses, with additional information from mouse, cat, dog, and pig. Most of the data refer to small intestine, with the few reports on large intestine describing similar changes.

The rat data include reports of cryptal enterocytes with degenerative cytoplasmic vacuoles, hours after irradiation with low doses (Buell and Harding, 1989). Within days of moderate to high doses, both villous and cryptal surface layers contain pale, swollen cells with pyknotic nuclei (Rubio and Jalnas, 1996). The number and length of ileal, but not jejunal microvilli, change days after a very low dose (Keelan *et al.*, 1986), as does brush border composition, perhaps contributing to altered passive permeability to lipid. A few weeks after treatment with a very low dose, microvillous blunting, swelling of mitochondria, and marked intercellular interdigitation of lateral membranes are seen (Thomson *et al.*, 1984). Different levels of patchy lesions are reported for jejunum and ileum, with structural and mitotic abnormalities.

In mice, villous enterocyte numbers decrease substantially days after irradiation with a low dose (Carr *et al.*, 1992b), a finding confirmed for duodenum, jejunum, and ileum (Ettarh *et al.*, 2000). In cats, intercellular separation is seen days after irradiation with moderate but not low doses, along with vacuolization and intermittent epithelial cell loss (Eriksson *et al.*, 1983). One month after treatment, only tissues from the highest dose groups still show damage, with irregular intercellular contacts and immature covering cells. In dogs, cryptal necrosis and collapse is followed by villous epithelial atypia or ulceration within days of low to high doses (Vigneulle *et al.*, 1990). In pigs, hours after a low dose, there is distention of rough endoplasmic reticulum, mitochondrial swelling, nuclear shrinkage, and prominent lysosomes (Chomette *et al.*, 1977). Vacuolization and necrosis are as described for rodents, but take longer to develop. Thereafter, the intercellular spaces are very marked.

The literature on uptake and translocation through the wall of the small intestine relies on rat data, whether the uptake is of contrast medium, bacteria, or organic macromolecules. The doses vary from very low to high, while the time span is from hours to months. Increased uptake of contrast medium is assessed by radiography or X ray fluorescence analysis. It is greater after high than moderate doses and

more obvious days than weeks after treatment (Solheim *et al.*, 1991). Uptake is compared with data from injury score and SEM techniques. No single variable is specifically responsible for the increased uptake. Absorption of glucose and proline shows a maximum decrease days after irradiation with very low and low doses, and a dose-dependent return toward control levels thereafter (Mohiuddin *et al.*, 1978). Bacterial translocation is increased days after low doses of radiation. This increase could be measured by lymph node colonization, directly (Blair *et al.*, 1996; Prieto *et al.* 1998) or using radioactive tracers (Chun *et al.*, 1997).

The literature on changes in enzyme activity and composition of the brush border is based on work from two groups, both using rat tissue, almost entirely on small intestine, in the time span from hours to 1 month after doses at the lower end of the range.

Hours to weeks after a very low dose, there is a gradual, sequential increase, reduction and recovery in the activity of brush border enzymes such as maltase, invertase, and lactase and leucine-amino-peptidase. Time course experiments for lactase show that the increase does not begin until 4–8 hr after irradiation (Becciolini *et al.*, 1975). This supports the concept of an increase in protein synthesis, rather than release of already available enzyme. It is also linked to radiation-induced changes in cells in the upper part of the crypt. Comparison of the activity of invertase, another brush border enzyme, with reduction in numbers of S-phase cryptal epithelial cells indicates that there is radiation-induced differentiation hours to days after treatment (Becciolini *et al.*, 1983a). However, extension of the work to time points up to 1 month shows a smaller differentiation compartment (Becciolini *et al.*, 1983b). Levels of lysosomal enzymes  $\beta$ -galactosidase and  $\beta$ -glucuronidase increase most at 36 and 48 hr, when morphologic changes are marked, but the responses of acid phosphatase and cathepsin D are less striking (Becciolini *et al.*, 1982b). The early increase in lysosomal enzyme activity after irradiation is related to cell damage, first in cryptal epithelial and then in stromal cells (Becciolini *et al.*, 1982b).

The second group of data concentrates more on lipid composition, although ileal but not jejunal increases are reported for alkaline phosphatase days to 1 month after very low doses (Keelan *et al.*, 1986). The uptake of cholesterol is unchanged, but there are alterations in the barrier to medium-chain fatty acids a few weeks after treatment, with minimal histologic and moderate ultrastructural changes at that point (Thomson *et al.*, 1984). In addition to this lack of correlation between structural and functional parameters, there are varying responses across jejunum, ileum, and colon and also with dose, time, and specific passively transported solute. There are also more ileal than jejunal changes in total free fatty acids and total phospholipids and in individual phospholipids at several time points from days to 1 month after treatment (Keelan *et al.*, 1986). These morphologic and compositional changes could contribute to the changes in passive permeability toward lipids.

**b. Late** The database for enterocytes is predominantly from small intestine, mainly rat, but with some additional information from cat and pig. The time frame

varies from several months to 1 year and the doses on the whole do not relate often to very low or very high doses. The smaller pool of data for large intestine is based on rat tissue.

With respect to rat small intestine, ulceration is one of the parameters used in injury scores (Hauer-Jensen *et al.*, 1983a). An individual score for ulceration, calculated several months after treatment, rises sharply within the range of moderate doses used (Scott *et al.*, 1995). The earlier increases in epithelial TGF- $\beta$ 1 and M6P/IGF-II receptor immunostaining are no longer present at this time (Wang *et al.*, 1998, 1999a). For low, but not very low doses, absorption of glucose and proline is decreased several months after irradiation, while the extent of the recovery, if any, between this late depletion and the earlier absorptive deficiencies is dose dependent within the range of low doses used (Mohiuddin *et al.*, 1978). The continuing absorption deficit is attributable to problems with transport across an increasingly fibrosed wall, rather than to mucosal dysfunction.

The cat data confirm the importance of dose, because several months after treatment, only the highest doses show residual irregularity in cell shape and immature microvilli (Eriksson *et al.*, 1983). Some scoring systems include ectopic glands (ileitis cystica profunda) in the small intestinal deeper layers. These are studied further by Rubio *et al.* (1983). They are more common several months after irradiation and are found in the submucosa and occasionally also in the muscularis externa. The lining cells vary from a surface epithelial type to nonpolarized cells with pleomorphic nuclei.

The pig data confirm impaired absorption several months after treatment with a very low dose and also note deficiencies in histochemical staining for brush border enzymes (Chomette *et al.*, 1977). Ultrastructurally, there is residual microvillous damage and epithelial cell separation.

In rat large intestine, fatal obstruction several months after a high dose is related to deep ulceration, extending to the muscularis externa, accompanied by subserosal fibrosis and vascular damage (Trott, 1984). The dilated cystic spaces of ectopic glands are also seen in proctitis cystica profunda 1 year after a high dose (Geisinger *et al.*, 1990). Epithelial abnormalities, inflammation, and fibrosis are reported and the fibroblastic-myocytic shell outside the basal lamina is not present in submucosal examples of the glands. The glands frequently herniate through gaps in the muscularis mucosae, the cells of which show ultrastructural abnormalities, including disruption of the myofilaments and basal lamina. These experimentally produced epithelial-lined submucosal spaces in rats, 1 year after irradiation, are similar to the rare human proctitis cystica profunda (Geisinger *et al.*, 1990).

## 2. Goblet Cells

*a. Early* Although there is a report of increased numbers of goblet cells in human subjects, moving from crypt up to villus, days after one low-dose fraction (Wiernik and Plant, 1971), most of the data are from rat small intestine. There is also

additional information from mouse, cat, and pig, overall spanning hours to 1 year after very low to high doses. There appears to be little consensus across the data sets. This may be because these cells, having a protective role, may be particularly responsive to dose and time. The situation is not simplified by the fact there is a particularly wide range of data collected. These include estimates of total goblet cell counts, cryptal counts, or villous counts; raw data numbers as opposed to epithelial proportions; and also qualitative textual notes.

The rat data for small intestine show sequential initial increase, decrease, and recovery from hours to 1 month after treatment in the lower dose ranges; there is some variation in the effect with time of day (Becciolini *et al.*, 1985). In contrast, no loss of cells in seen days to 1 month after low doses or 1 month after low to high doses (Rubio and Jalnas, 1996). The only change is goblet cell loss in just over half of the animals, days after moderate and high doses. This variation across animals is also reported for goblet cell scoring at about 1 month after treatment, except after very low doses, when they are less abundant (Forsberg *et al.*, 1979). Thomson *et al.* (1984), however, report focally increased cell numbers weeks after radiation with a very low dose.

The mouse small intestine data show a similar range of results. The numbers decrease hours after a low dose, but with a temporary increase toward control levels several days after treatment (Oberhausen, 1975). Data collected from resin instead of wax histology sections show no significant initial increase in total numbers until days after a low dose (Carr *et al.*, 1992b). The lack of a significant decrease days after a high dose could be due to interanimal variation or to radiation-induced damage to the granule release mechanism.

Finally, in pig after low-dose exposure, there is no mention of any change until weeks after radiation, when the lengthening crypts have additional mucosecretory cells and when goblet cells destined for the villous surface leave the crypts in groups (Chomette *et al.*, 1977). Ultrastructurally, however, apical granule fusion and apocrine-like secretion is reported several hours after treatment.

The changes are less marked for mouse large intestine hours to days after a low dose (Oberhausen, 1975). In dog large intestine, there is mucus depletion and lack of goblet cells, days after a low dose (Summers *et al.*, 1989).

**b. Late** Goblet cell depletion continues up to 1 month after irradiation of the rat small intestine with very low to low doses (Becciolini *et al.*, 1985).

### 3. Paneth Cells

**a. Early** The Paneth cell database is even smaller than for goblet cells, with a similar range of species and a similar variety of data sampling. In the rat, hours after a very low dose, *in situ* hybridization shows clusterin transcription localized to the Paneth cell region (Arai *et al.*, 1996b). Thereafter, a time-related pattern of cell loss after days and recovery by 1 month is seen, but only after moderate to

high doses (Rubio and Jalnas, 1996). In mice, Paneth cell depletion is confirmed, in duodenum, jejunum, and ileum, days after radiation with a low dose, but for only one of the two strains examined (Ettarh *et al.*, 2000; Carr *et al.*, 1992b). In pig, nuclear and lysosomal changes are reported several days after a low dose (Chomette *et al.*, 1977).

**b. Late** Paneth cell metaplasia is associated with submucosal ectopic glands in rat 1 year after a high dose (Geisinger *et al.*, 1990).

## D. Changes in Stroma/Connective Tissue

### 1. General: Fibers and Fibrogenesis

**a. Early** Although fibrosis is associated with late effects, increases in collagen deposition are also reported from days to 1 month after radiation with very low to high doses, mostly in rats, with additional information from dogs. The rat data show the increase to be dependent on time (Rubio and Jalnas, 1996). In the muscularis externa, there is clear dose dependence; no animals are involved after a low dose, but up to 75% after a high dose. The other two layers also show more deposition after moderate to high doses. Weeks after radiation with a high dose, TGF- $\beta$ 1 mRNA expression is more increased than isoforms 2 and 3 in fibroblasts and smooth muscle, both of which are involved in fibrogenesis (Wang *et al.*, 1998). TGF- $\beta$ 1 expression is increased in submucosal and subserosal regions, especially near mucosal ulceration and subserosal thickening (Fig. 14). There is also some association between fibrosis and M6P/IGF-II receptor positive cells after low to high doses (Wang *et al.*, 1999a). The linkage between fibrosis and ulceration is confirmed about 1 month after treatment with moderate to high doses (Forsberg *et al.*, 1979). The accompanying gradual increase in the content of hydroxyproline from very low to high doses, to a level more than 3 times the control value, is used as an assay for collagen and therefore for fibrosis.

**b. Late** The increase in thickness of the layers of the wall, often due to fibrosis, is dealt with in Section III.B.3.b. Further information on small intestinal fibrosis comes from data sets from rat tissue, which confirm some of the basic findings from irradiated cats. The time frame is from several months to 1 year after low to high doses. In rat, fibrosis is related to thickening of the wall and the deposition of broader, hyalinized collagen fibers (Hauer-Jensen *et al.*, 1983a) several months after treatment. At this time, the level of expression of TGF- $\beta$ 1 is maintained at that seen weeks after treatment (Wang *et al.*, 1998), while that for mesothelium, although decreased, is still higher than control levels. Extracellular matrix associated TGF- $\beta$ 1 immunoreactivity is still increased, while the expression and immunoreactivity for isoforms 2 and 3 are nearer to control levels. This increase

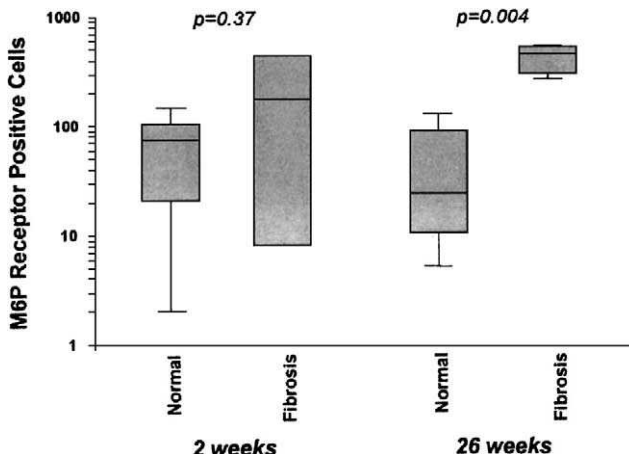


FIG. 15 Association between number of M6P/IGF-II receptor-positive cells in the intestinal wall and fibrosis (submucosal, serosal, or transmural) 2 weeks and 26 weeks after irradiation (data pooled across dose groups). [Courtesy of M. Hauer-Jensen. Reprinted from *Radiotherapy and Oncology*, **50**, Wang, J., Richter, K. K., Sung, C.-C., and Hauer-Jensen, M. Upregulation and spatial shift in the localization of the mannose 6-phosphate/insulin-like growth factor II receptor during radiation enteropathy development in the rat, pp. 205–213. Copyright 1999, with permission from Elsevier Science, Fig. 5.]

in immunoreactivity and radiation injury is preceded by an increase in TGF- $\beta$ 1 gene expression (Hauer-Jensen *et al.*, 1998). Immunoreactivity for the M6P/IGF-II receptor shifts from epithelial localization weeks after radiation with low to high doses, to fibroblasts in fibrotic areas months after treatment (Wang *et al.*, 1999a). There is a stronger association between the number of receptor positive cells and fibrosis several months after treatment than is the case some weeks after radiation (Fig. 15). Fibrosis is confirmed in cats several months after moderate to high doses (Eriksson *et al.*, 1982, 1983).

## 2. Cells of the Inflammatory and Immune Systems

**a. Early** Almost all of the data are from rat, mainly small intestine, examined days to several months after very low to high doses and mainly dealing with inflammatory rather than immune responses. Only one of these studies also covers large intestine. There is also some information from vessels draining the intestine hours after a high dose. The few additional data are from dog or pig small intestine.

In rats, more lymphocyte loss is evident days than weeks after treatment, particularly after moderate to high, rather than low, doses (Buell and Harding, 1989). Mucosal neutrophil granulocytes (PMNs), identified histochemically by their peroxidase granules, increase in number a few hours after irradiation, with return to control values over subsequent hours. This is more marked for the pericryptal than for the villous compartment and a similar overall pattern is seen in colon. The

increase in small intestinal GMP, measured in a noninvasive fecal assay, is at a maximum several days after radiation, more so after high than after low or very low doses (Richter *et al.*, 1997a). Animals with high GMP levels go on to develop fibrosis several months after treatment. The possible involvement of the NO pathway is shown by linking the increase in nitrite concentrations with radiation-induced increases in neutrophil numbers, measured by myeloperoxidase activity days after a low dose (Erbil *et al.*, 1998).

Leukocyte/endothelial relationships and vascular permeability are studied in rat mesenteric postcapillary venules hours after a high dose (Panes *et al.*, 1995). The significant increase in the number of rolling leukocytes and decrease in rolling velocity within a few hours after irradiation is followed, several hours later, by increased leukocyte adherence and emigration through the wall of the venules. Vascular permeability is then also increased, while the neutrophil count in peripheral blood is decreased. The leukocyte emigration may be responsible for the increased microvascular permeability, which could in turn leak through an epithelial layer with improperly functioning tight junctions, thereby contributing to luminal fluid volume and hence to diarrhea. Immunoneutralization using monoclonal antibodies points to involvement of both CD18, the common  $\beta$  subunit of the leukocyte adhesion glycoprotein CD11/CD18, and also of the endothelial cell adhesion molecule intercellular adhesion molecule (ICAM)-1, a counter receptor for  $\beta_2$  integrins. Endothelial surface P-selectin does not seem to be involved. Leukocyte activation and emigration into the perivascular tissues are also linked, several hours after irradiation, to a significant increase in mesenteric oxygen free radicals (Panes and Granger, 1996). These data contribute to the construction of a flowchart for this part of the radiation-induced response after partial body irradiation (Fig. 16).

Weeks after low to high doses, expression of TGF- $\beta$ 1 mRNA, and to a lesser extent TGF- $\beta$ 2 and 3, is increased in inflammatory cells (Wang *et al.*, 1998). Other signs of inflammation include a radiation-induced increase in mucosal ED-2 positive macrophages and IL-1 $\alpha$  positive cells, a few weeks, but not several hours, after irradiation, particularly with a high dose (Richter *et al.*, 1997a).

The importance of mast cells is indicated by the fact that mast-cell-deficient (Ws/Ws) mutant rats show a significantly higher injury score and more small intestinal mucosal injury than mast-cell-competent (+/+) littermates a few weeks after a high dose (Zheng *et al.*, 2000a; Fig. 17). The mast cell-deficient group also has significantly less smooth muscle proliferation and collagen deposition weeks after irradiation. However, there are no differences across the groups in the increase in TGF- $\beta$  mRNA or immunoreactivity. It was concluded that mast cells may be important in TGF- $\beta$  input to manifestations of radiation injury.

The small amount of information on dog responses describes signs of mucosal and submucosal inflammation, mainly the former, including mononuclear cells, neutrophils, and eosinophils (Summers *et al.*, 1991), days after a low dose. These morphologic changes are accompanied by alterations in myoelectric activity and

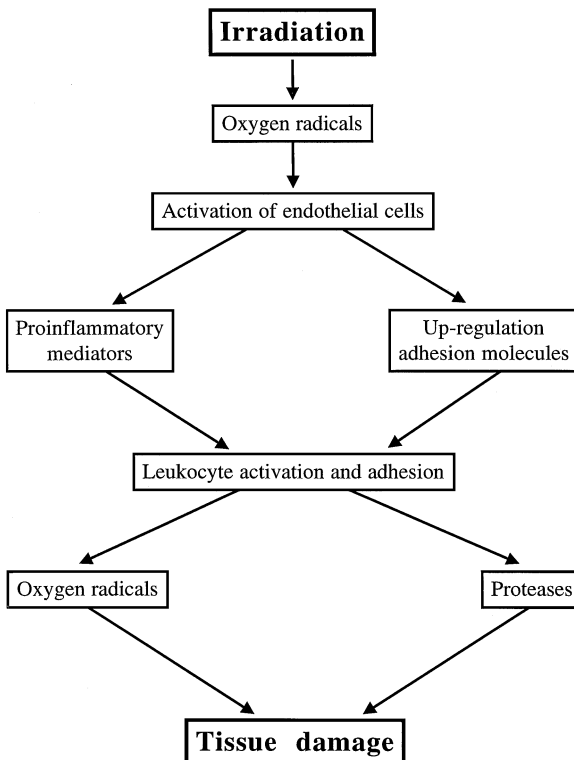


FIG. 16 Proposed chain of events that explains the leukocyte–endothelial cell adhesion and tissue damage caused by  $\gamma$  radiation. [Courtesy of D. N. Granger and W. B. Saunders, Orlando, FL, 32877, USA. Panes, J., and Granger, D. N. (1998). Leucocyte–endothelial cell interactions: Molecular mechanisms and implications in gastrointestinal disease. *Gastroenterology* **114**, 1066–1090, Fig. 6.]

increases in levels of prostaglandins  $\text{PGE}_2$ ,  $\text{PGF}_{2\alpha}$  and 6-keto- $\text{PGF}_{1\alpha}$ , within both vessels and the intestinal lumen. Lamina propria inflammatory cells, particularly macrophages, are highlighted as a potential source. Inflammation and edema are also seen in pig small intestine days after radiation with a low dose (Chomette *et al.*, 1977).

**b. Late** Several months after irradiation, expression of  $\text{TGF-}\beta$  in rat small intestine inflammatory cells is still increased for isoform 1, but not for isoforms 2 and 3, where the levels drop toward control values (Wang *et al.*, 1998). The reactivity here is presumably associated with  $\text{TGF-}\beta$ 's immunomodulatory role. At the same time point, mast-cell-competent rats contain more collagen and fibrosis in the intestinal wall and beneath the serosal layer than the mast-cell-deficient mutants, although there is no significant difference in their total injury scores (Zheng *et al.*, 2000a).

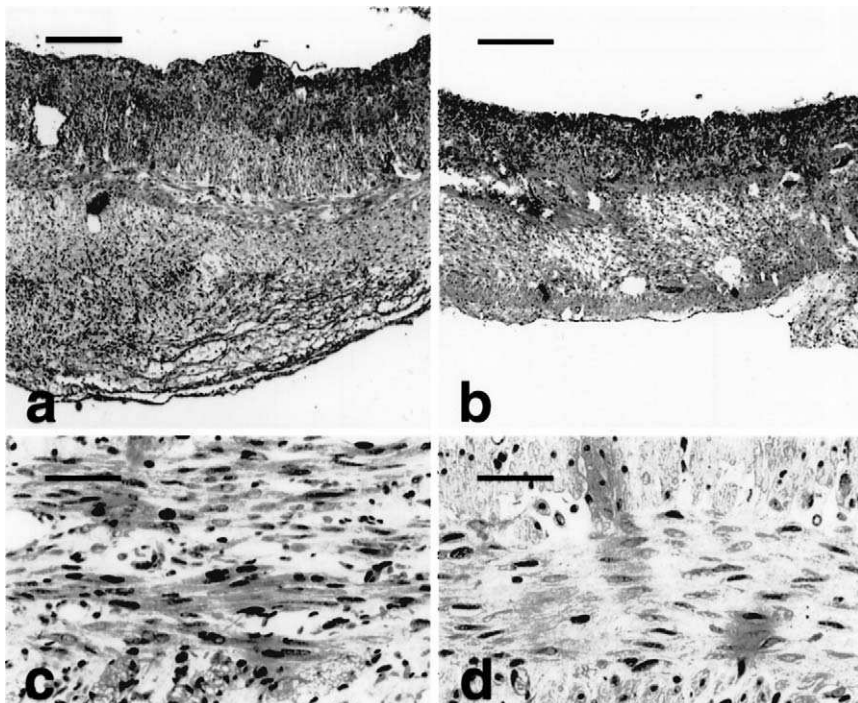


FIG. 17 Representative ulcerated areas in intestine from (a)  $+/+$  rats and (b) Ws/Ws rats, 2 weeks after 21-Gy single-dose irradiation. Difference in thickness is mainly due to minimal reactive subserosal thickening in the Ws/Ws specimen. H&E staining. Scale bar = 500  $\mu\text{m}$ . (c) PCNA-stained images from  $+/+$  and (d) Ws/Ws rats 2 weeks after 21-Gy single-dose irradiation, showing that the radiation-induced changes in smooth muscle are dependent on input from mast cells, missing from the Ws/Ws rats. Scale bar = 50  $\mu\text{m}$ . [Parts (a) and (b) courtesy of M. Hauer-Jensen and The Radiation Research Society. Zheng, H., Wang, J., and Hauer-Jensen, M. (2000). Role of mast cells in early and delayed radiation injury in rat intestine. *Radial. Res.* **153**, 533–539, Fig. 1. Parts (c) and (d) courtesy of M. Hauer-Jensen.]

### 3. Vascular Components

*a. Early* As for other structural features, there is a cluster of reports on rodent material, almost all rat, covering hours to 1 month after irradiation with very low to high doses. There is also a group of data from irradiated cat and rabbit. All describe vascular changes in small intestine, with only one also including large intestine and one on large vessels, which will be described first.

Within days, a very high dose of IORT produces positive immunohistochemical staining for TNF- $\alpha$  in rabbits, although the resolution does not permit differentiation between production of this cytokine within the smooth muscle cells or localization receptor-bound cytokine on the outer membrane of the cells (Kallfass *et al.*, 1996). The reactivity continues to rise throughout a further period of days, before

the addition of ERT at about 2 weeks (Section V.D.3). There are also TNF- $\alpha$  positive macrophages, seen days after treatment. Most are adventitial, although some are intraluminal or endothelial. This response decreases after a few weeks.

In rats, the PMN increases already described are accompanied by increases in tissue plasma volume in small and large intestine, several hours after irradiation with a low dose (Buell and Harding, 1989). This is linked to increased microvascular permeability, vasodilatation, edema, and epithelial basal blebbing. After low, moderate, and high doses, capillary dilatation and congestion are more marked days after treatment than 1 month (Rubio and Jalnas, 1996). A few weeks after irradiation with low to high doses, there is increased endothelial expression of all three isoforms of TGF- $\beta$  (Wang *et al.*, 1998; Table VI).

These rat data are reinforced by results from resin histology and TEM on mouse tissue. Coincidental with an increase in identifiable profiles of submucosal arterioles several hours after irradiation with a low dose (Carr *et al.*, 1992b), villous cross sections show capillary dilatation, with less prominence of endothelial fenestrae (Abbas *et al.*, 1990b). Hours later, the constricted capillaries are thick and irregular, with luminal cytoplasmic processes, nuclear changes and plasma-like granular material within widened perivascular spaces. A few days after treatment, there is a mixture of constriction and patency. Endothelial vacuoles and swollen mitochondria are found, along with structural features similar to those seen earlier.

The cat data relate to three studies from the same group, dealing with changes after treatment with low to high doses. Microangiography demonstrates reduced vascularity a few days after treatment (Eriksson, 1982). This is accompanied by a dose-dependent decrease in capillary filtration (Eriksson and Johnson, 1983). The same two studies show that, although there is marked regeneration of the vascular pattern 1 month after treatment with high or very high doses, capillary filtration is still compromised. Ultrastructural analysis of capillaries days after treatment shows no changes at the low dose used in the mouse work (Eriksson *et al.*, 1983), but moderate to high doses do lead to a similar picture, with endothelial vacuolization, swollen mitochondria, irregularity of the wall, and nuclear changes. About 1 month after treatment, moderate to high doses, particularly the latter, are needed to produce endothelial thickening, irregularity, and swelling. It is proposed that the decrease in capillary filtration days after treatment is related to endothelial damage, while the fact that this, although improved, had not returned to normal by 1 month, is linked to the increasing perivascular fibrosis.

There are few reports of changes in small intestinal lymphatic vessels, apart from a report of mild jejunal lymphangiectasia in a group of rats a few weeks after irradiation with a low dose (Thomson *et al.*, 1984).

**b. Late** With respect to changes in large vessels, the earlier increased TNF- $\alpha$  expression in rabbit medial smooth muscle continues in a dose-dependent fashion, several months after IORT (Kallfass *et al.*, 1996).

Much the same data pool is involved as for fibrogenesis. Vascular sclerosis, including thickening, hyalinization, and narrowing or blockage, is classified as a late

alteration (Hauer-Jensen *et al.*, 1983a). TGF- $\beta$ 1 levels, but not those of isoforms 2 and 3, are further increased, several months after treatment. This could lead to a reaction cycle, as the TGF- $\beta$ 1 down-regulates endothelial thrombomodulin, leading to a further release of TGF- $\beta$ .

The continuing vascular changes several months after treatment are also seen in pig after a low dose, with changes in the external laminae and perivascular collagen deposition (Chomette *et al.*, 1977). At the same time point, cat vessels display increasing capillary irregularity and endothelial thickening as the dose increases through the moderate to high range (Eriksson *et al.*, 1983). The continuing abnormal vascular pattern (Eriksson *et al.*, 1982) correlates with the lack of improvement in capillary filtration coefficient (Eriksson and Johnson, 1983), associated with perivascular fibrosis.

As for early change, there is little information on lymphatic vessels, apart from the classification of dilatation of lymphatic vessels or collections of lymph as a late alteration (Hauer-Jensen *et al.*, 1983a).

## E. Changes in Endocrine, Neural, and Muscle Components

### 1. Endocrine Cells

The few reports on endocrine cells describe early responses, all on mouse small intestine and all from one group. The resolution provided by glutaraldehyde-fixed resin sections allows the general endocrine population to be identified, but differentiation into subgroups is not possible. The increase in the apparent number of cell profiles per crypt visible several hours after anesthesia and handling during sham treatment (Wyatt *et al.*, 1987) is possibly due to stress-related granule release. After very low to high doses of radiation, the number of cell profiles per crypt in anesthetized duodenum decreases several hours and days after low to high doses, with dose dependence only at the latter time point (Wyatt *et al.*, 1987; Carr *et al.*, 1992b). Duodenum is more sensitive than jejunum and ileum (Ettarh *et al.*, 2000). The fact that the technique used only estimates changes in total endocrine cell profiles implies that the results can merely act as a pointer that stress is relevant and that it is important to carry out more specific tests to separate out the responses of each sub-population of cells. Some such data are now available for whole-body (Section IV.E) and fractionated radiation schedules (Section V.E).

### 2. Nerve

The few studies available are again at early time points. There are few reports of morphologic changes in nerve to coordinate with the occasional report of functional abnormalities, one of which shows brief contraction in isolated guinea pig small intestinal muscle minutes after a very high dose (Sprugel *et al.*, 1977). Blocking experiments implicate the postganglionic neuron and the interface between it

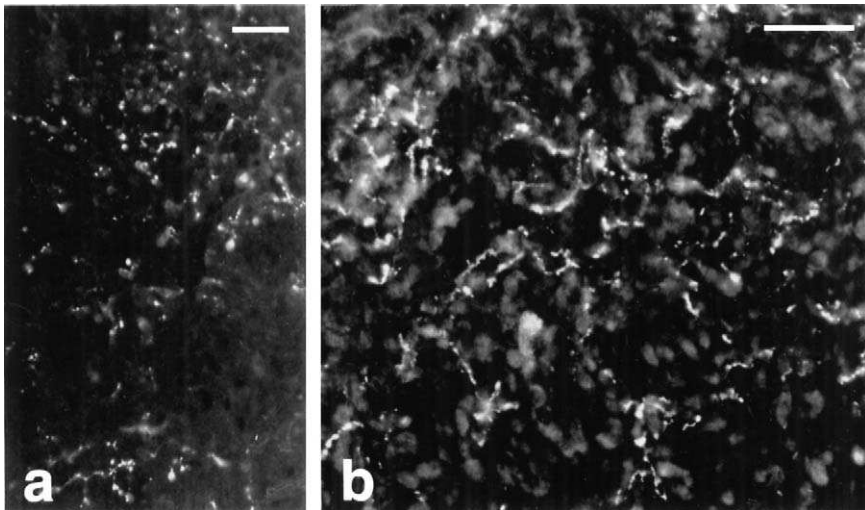


FIG. 18 (a) Rat duodenum after 30-Gy irradiation, showing the occurrence of a large number of VIP immunoreactive varicosities in irradiation-damaged mucosa. Scale bar = 30  $\mu$ m. (b) Irradiated mucosa (30 Gy) in a section stained for SP. A large number of SP-LI (like immunoreactivity) nerve fibers are seen in the granulation tissue in the damaged mucosa. Scale bar = 30  $\mu$ m. [Part (a) courtesy of S. Forsgren. Part (b) courtesy of S. Forsgren. Reprinted from *Peptides*, 21, 271–281. Hockerfelt, U., Franzen, L., Kjorell, U., and Forsgren, S. Parallel increase in substance P and VIP in rat duodenum in response to irradiation. Copyright 2000, with permission from Elsevier Science, Fig. 8.]

and the smooth muscle cell. Recent confirmation of neuronal involvement comes from a study describing increased radioimmunoassay levels for SP and VIP in rat small intestine several days after a very high dose (Hockerfelt *et al.*, 2000; Fig. 18). These results are supported by parallel immunohistochemistry, showing large numbers of VIP- and SP-immunoreactive nerve fibers in the mucosa and also in submucosal/myenteric plexus profiles. Distribution of immunoreactive fibers in the muscularis externa is not altered, but the extent of reactivity is increased. The reactivities are less marked in control specimens and in those irradiated with high, rather than very high doses. It may be that the increases in SP and VIP could act together, although in opposite directions, assisting in postirradiation initiation and/or regulation of the inflammatory process, the immune response, and the reorganization of the intestinal wall.

### 3. Muscle Layers

**a. Early** The sparse information available on changes in smooth muscle often relates to functional experiments or to the deposition of collagen within this layer. The database covers a wide range of doses and times. It is fairly evenly divided between rat and dog and there are more data on small than on large intestine.

Most of the structural information is from rat small intestine. The deposition of additional collagen increases from days to 1 month after treatment with moderate to high doses, particularly the latter (Rubio and Jahnas, 1996). TGF- $\beta$ , which has a likely role in fibrosis, is increased weeks after treatment with low to high doses, particularly for the levels of isoform 1 (Wang *et al.*, 1998). In the smooth muscle cells themselves, TEM shows some mitochondrial swelling and disrupted cristae hours after a moderate dose (Summers *et al.*, 1989). This correlates with increased levels of MnSOD, associated mainly with mitochondria, but not of Cu-ZnSOD, found in the cytosol. The increase in MnSOD could be due to mitochondrial damage and enzyme release or could reflect radiation-induced increase in the amount of the superoxide free radical, requiring dismutation to a nonradical species. Radiation with a high dose up-regulates protease-activated receptor 2 in muscle deep to intact mucosa and is associated with smooth muscle proliferation and deposition of collagen (Wang *et al.*, 2000b). There is also a shift in PAR-2 expression away from areas of severe injury.

The dog data confirm that alterations to the small intestine are minimal, despite changes in myoelectric activity extending from several hours to several days after a low dose (Summers *et al.*, 1987). There is, however, some vasodilatation in the muscle layer a few weeks after a low dose (Summers *et al.*, 1991).

The only abnormality in large intestine, detected using a similar protocol, is a thickening of the muscularis mucosae (Summers and Hayek, 1993).

**b. Late** Several months after irradiation with moderate to high doses, the high scores for fibrosis imply involvement of the muscularis externa (Hauer-Jensen *et al.*, 1983a). Levels of TGF- $\beta$ 1 expression in smooth muscle cells are still slightly raised, reflecting their continuing role in collagen deposition (Wang *et al.*, 1998). The cells of the muscularis mucosae associated with herniated large intestinal ectopic glands, produced 1 year after a high dose, show ultrastructural abnormalities, including disruption of the myofilaments and basal lamina (Geisinger *et al.*, 1990).

#### **IV. Effects of a Single Dose of Unshielded, Low-LET Irradiation**

The data sets have been dealt with as in Section III and are summarized in Table IV.

##### **A. Description and Integrative Summary of Responses**

The data here are entirely centered on early effects and are insufficient to subdivide. Text descriptions of whole-body radiation effects, even after very low doses, include immediate vomiting in pigs (Griffiths *et al.*, 1996) and frequent bowel

movements in ferrets (MacNaughton *et al.*, 1997) in the first half hour, followed by mucoid diarrhea for several hours. Several days later, the pigs are apathetic, eat less, and have a high temperature and decreased hematocrit and white cell count. Even 4–6 years later (Griffiths *et al.*, 1999), pigs weigh less and are leaner than their unirradiated counterparts.

For scoring, the whole-body data bank is also much smaller than that for partial body and relies on two studies on mouse small intestine. One, using an injury score approach based on parameters defined by Mulholland *et al.* (1984), shows that a low dose produces damage within hours, peaking within days and recovering thereafter (Yoon *et al.*, 1994). However, death follows several days after a moderate dose. The cell ratios score approach shows little total difference between sham and irradiated groups hours after a low dose, but there is substantial damage within a few days (Carr *et al.*, 1996). The parameters responsible for the change in total score are myenteric plexus; crypts; goblet cells, stromal cells, villous enterocytes; mitotic figures; and endocrine cells. Endocrine cells are significantly more depleted than crypt profiles, confirming that knowledge of the extent of radiation-induced crypt depletion does not necessarily give an understanding of the response of the different cryptal cell types. There is recovery by 1 week, with only crypts and villous stromal cells affected.

Some comparison is possible up to 3 days with the corresponding partial body results (Carr *et al.*, 1992b), although the protocols are not identical. In both, changes are seen in the vascular component hours after irradiation. The maximum damage days after irradiation with a low dose is substantially greater for the whole-body experiment, relating to larger decreases, particularly in endocrine cells, and also to responses in stromal and nerve compartments after whole-body but not partial irradiation. These could reflect intestinal changes secondary to damage in other sites, such as pituitary, lymphoid organs, or large nerves supplying the intestine.

## B. Changes in Intestinal Compartments

### 1. Luminal

The data all refer to the early response. The whole-body results are based on a more standard database than those for partial body, since they are almost all from rodent material, predominantly mouse, and register results in the early period after doses at the lower end of the dose range. All confirm that there are changes in this compartment.

There is a report of a relative increase in potentially damaging dihydroxylated bile acids in pigs several hours to days after a very low dose (Scanff *et al.*, 1997). In rats, indigenous filamentous microorganisms decrease in prominence, being replaced by short, rod-shaped microorganisms, several hours after both very low (sublethal) or low (lethal) doses (Porvaznik *et al.*, 1979). They progressively return days after the very low dose, but much less so after the low dose.

In mice after a low dose, the mucus covering, approximately 450  $\mu\text{m}$  thick, is progressively less complete within hours and days, and numbers of ileal facultatively anaerobic flora decrease (Walker *et al.*, 1985). The proportion of crypts containing parasites also rises several days after irradiation (K. E. Carr *et al.*, 1984). After a moderate dose, more surface debris and mucus are seen within hours and days, with more cellular debris, parasites, and microorganisms in the cryptal lumina (Indran *et al.*, 1991). Within days, the duodenal papilla is dilated and more prominent (Indran *et al.*, 1988), and appears to be closer to the gastroduodenal junction.

## 2. Villous and Cryptal

The data all describe the early response. The early whole-body database, like that for partial body schedules, is substantial and relies on rodent data, mostly mouse, and with a similar wide coverage of early time points and all dose ranges. Similar techniques are used, although with fewer molecular data sets.

The small pool of rat data confirms the use of SEM and light microscopy (LM) to record villous collapse and regeneration, over a period of days after a low dose (Anderson and Withers, 1973). LM is also used to demonstrate villous and cryptal shortening as signs of damage, using several doses in the very low range, and elongated villi are sometimes reported during recovery (Lewicki *et al.*, 1975). A fairly recent study uses a very low dose to report on intestinal kinetics in the period from hours to over a month after treatment (Becciolini *et al.*, 1996). In general, there is an initial decrease in epithelial cell numbers, labeling index, and mitotic index. This is followed by an increase, usually peaking a few days after irradiation. Thereafter, there is a decrease toward control levels. During recovery, there are more S-phase cells near the crypt–villus junction. The detailed shape of the response curve varies with parameter and, by comparison with earlier findings, with radiation conditions (Becciolini *et al.*, 1982a, 1983a, 1996).

The majority of mouse reports include some discussion of appropriate techniques. SEM alone is used to show villous collapse hours to days after moderate to high doses (Carr and Toner, 1972) and villous fusion and regeneration over a longer time scale after a low dose (Hamlet *et al.*, 1981; Carr *et al.*, 1982). Comparison of SEM and LM, days after irradiation, confirms the need for a low dose for the histologic microcolony assay method, while SEM reveals distorted villous tips after a very low dose (Hamlet *et al.*, 1976). Histologic description of the time course after a low dose shows substantial villous shortening within a few days and recovery over the subsequent week (Rufrok *et al.*, 1998a), but LM measurement of villous length is not as useful at very low doses as the microcolony technique (Rao and Fritz-Niggli, 1988). The method for SEM villous scoring is refined by the use of an acetate overlay on SEM montages, producing enhancement ratios for irradiated samples with respect to sham treated material (Indran *et al.*, 1991) and showing a change only 1 hr after a moderate dose. Correlative LM shows that the

increasing villous damage over the next few days is associated with underlying muscle damage.

An autoradiographic study of crypt squash cells in DNA synthesis (S) and mitosis (M), hours to several days after very low to low doses, reveals an underlying diurnal rhythm and a dose-related increase in the changes (Lesher and Lesher, 1970). Numbers of cells in S and M phases drop immediately, followed by overshoot and then a fluctuating recovery to the control situation. Other cryptal changes include the presence of dense bodies, disintegrating cells, and degeneration several hours after a very low to moderate dose (Indran *et al.*, 1991; Ruifrok *et al.*, 1998a).

Although changes in villous epithelial cell numbers lag 2 days behind the corresponding cryptal changes after very low and low doses (Ruifrok *et al.*, 1998a), there is good agreement in terms of proportional cell loss. Maximum cell loss/circumference decreases to 73% of control for both cryptal and villous cells after a very low dose and to 23% for cryptal and 16% for villous cells after a low dose. Expression of cryptal proliferation-stimulating factors TGF- $\alpha$ , EGF, and the EGF receptor (EGF-R) shows sequential increase, then decrease, days after both doses and there is a parallel response in TGF- $\alpha$  mRNA. Using transgenic mice, it is shown that villous enterocytes, although not themselves subject to radiation-induced apoptosis several hours after a very low/low dose, may re-enter the cell cycle and send signals, whereby the cryptal epithelium induces p53, with resultant apoptosis throughout the crypt (Coopersmith and Gordon, 1997). The usual resistance of villous epithelial cells to radiation may be related to their environment, possibly through integrin-related signals, rather than to their cell cycle arrest. Possible mechanisms for the villus–cryptal feedback are explored 1 week after a very low dose, using data on mitosis, apoptosis, cells per section and immunohistochemical staining for TGF- $\alpha$ , EGF, EGF-R, TGF- $\beta$ 1-3, and TGF- $\beta$ RI, and TGF- $\beta$ RII (Ruifrok *et al.*, 1997). The findings and sequence of events proposed include a decrease in cryptal cell numbers due to cell cycle block and apoptosis of damaged cells. There is also a reduction in TGF- $\beta$  levels, including those in the villi: this could reduce inhibition of crypt cell proliferation and increase production of TGF- $\alpha$  and EGF, with resultant cryptal proliferation. As the cryptal cell numbers and cryptal/villous TGF- $\beta$  increase, TGF- $\alpha$  would be inhibited and proliferation would decrease again.

Days after treatment, villous shape may be more sensitive to whole body than to partial body irradiation, after very low to moderate, but not high doses (Carr *et al.*, 1983), while this greater sensitivity is not seen in microcolony counts in similar conditions (Mason *et al.*, 1989).

### 3. Layers, Tissues, and Tissue Boundaries

**a. Early** The epithelial/stromal stripping seen after partial body irradiation is confirmed in rats after whole-body treatment a few days after very low or low

doses (Lewicki *et al.*, 1975; MacNaughton *et al.*, 1994). In mouse, although the basal lamina is often missing several days after a moderate/high dose (Carr *et al.*, 1985), no change is seen in basement membrane fibronectin over a similar time period after low and high doses (Berghem and Johanson, 1983).

**b. Late** In irradiated mouse jejunum and ileum, the response includes gaps between the base of epithelial cells and the basal lamina and contacts between enterocytes and stromal cells through basal lamina herniations (Fatemi *et al.*, 1985). Damage to the colon is less marked.

## C. Changes in Epithelial Cells

### 1. Surface Epithelium, Enterocytes, and Glands

**a. Early** The data bank on enterocytes is as substantial as that for partial body schedules. It relies equally heavily on mouse material, with important additional data from other species. There is, as before, a large predominance of data on small intestine. The time frames are mainly in the initial phase, hours to a few weeks, and the doses are at the lower end of the range.

With respect to purely structural information, there are two reports on rat small intestinal tissue. These describe degeneration, vacuolization, and cell depletion in cryptal and villous epithelial cells (Lewicki *et al.*, 1975; Abbas *et al.*, 1990a) hours to days after very low or moderate doses. Apart from these, most of the structural data are from studies on mouse small intestine, where there is confirmation of partial body effects in terms of epithelial damage (Fig. 19). With increasing dose, there is a downward trend in the number of villous enterocytes remaining several days after irradiation (Carr *et al.*, 1993, 1996; Brennan *et al.*, 1998), from 56% of control after a very low dose, through 35% for a low dose, to 19% after a moderate dose. Recovery to normal numbers is seen in the experiments for which the time of sampling extends sufficiently, to 1 week (Brennan *et al.*, 1998).

There is also a description of surface epithelial giant cells several days after a low dose (Carr *et al.*, 1981). They are 25–60  $\mu\text{m}$  in diameter and joined to the villus by a variable attachment zone. They can contain well over 10 irregular nuclear profiles per section profile, abnormal condensed chromatin patterns, many cytoplasmic vacuoles, lipid inclusions, and apical microvilli. Peg-like structures are also seen on individual enterocytes or at the edge of some giant cells (Carr *et al.*, 1982).

Other changes in irradiated mouse small intestine include uptake of *Campylobacter jejuni* in small intestine several hours after irradiation with a low dose and oral but not intraperitoneal challenge (Sosula *et al.*, 1988). Lipid uptake and transport also decline several days after a moderate dose (Hampton and Rosario, 1972), with ileum responding more quickly and to a greater extent than jejunum.

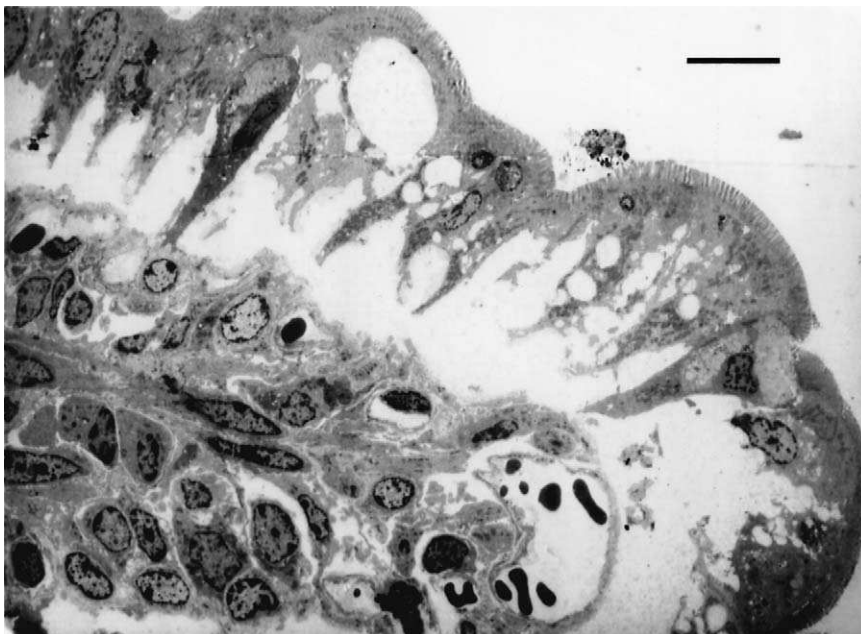


FIG. 19 Transmission electron micrograph of mouse intestinal villous tip 3 days after 10-Gy whole-body X irradiation. The epithelial cells are vacuolated and widely separated near the epithelial/stromal boundary and the apical capillary appears distended. Scale bar = 10  $\mu\text{m}$ . (Courtesy of H. Kamel.)

There is also increased permeability of tight junctions, demonstrated by identification of tracer in epithelial intercellular spaces and possibly related to changes in calcium content (Somosy *et al.*, 1993). The change is seen only 1 hr after irradiation and the extent of recovery over the next few hours is dependent on dose in the very low range. The importance of calcium is confirmed by the decrease of enterocyte lateral membrane  $\text{Ca}^{2+}$ -ATPase activity (Somosy *et al.*, 1994). This is seen a few hours after treatment and the extent of its persistence over subsequent hours is dose dependent. There is also a sequential increase, decrease, and recovery of mouse alkaline phosphatase activity in homogenized specimens from hours to several days after a very low dose, with jejunum showing a greater initial increase than duodenum or ileum (Kaur *et al.*, 1975). There is a similar pattern but different time frame for glucose-6-phosphatase activity, although the period concerned is slightly later and the ileal value has not recovered by the end of the observation time 10 days after treatment.

Further information linking structure with enzyme or functional data comes from work on irradiated rabbit or pig small intestine. Loss of rabbit villous enterocytes is linked to decreased uptake of alanine, an actively transported amino acid, several days after irradiation (Gunter-Smith, 1989), while a slightly earlier

decreased response to secretagogues is related to increased cryptal proliferation associated with less differentiation into potentially secretory cells. A decrease in alkaline phosphatase is also seen in rabbit small intestinal enterocytes in sectioned material, nearly 1 week after a low dose (Ciecura *et al.*, 1976), but there is no change in glucose-6-phosphatase, or in lysosomal enzymes. A few days after treatment, but not thereafter, there is less succinate dehydrogenase activity, mitochondrial numbers appear lower, and mitochondrial structure is abnormal. At the same time, cytoplasmic lactate dehydrogenase activity is decreased and there is subsequent prominence of polysomes and glycogen.

The pig data relate to changes in small intestinal membranes 1 week after a very low dose (Griffiths *et al.*, 1996). There is a reduction in activity of apically located enzymes sucrase and leucine aminopeptidase (LAP). A decrease is also reported in activity at the basolateral membranes. The decrease in Na, K-ATPase could affect uptake of nutrients and could itself be caused by the presence of free radicals, directly or indirectly through the inflammatory response. The other decreasing basolateral activity relates to adenylyl cyclase, involved in signal transduction of regulatory neurotransmitter/hormone signals. Further comment on this is given below in the section on neuroendocrine changes (Section IV.E.1).

More information on structural and functional changes comes from studies on rat tissues, some on small intestine, some on large and some on both. With respect to small intestine, the rat data show that, although ileal basal electrolyte transport *in vitro* does not change significantly over several hours after a low dose (MacNaughton *et al.*, 1994), conductance does increase. This implies less resistance to the applied short circuit current, possibly related to edema and subepithelial blistering and subsequent alterations in tight junction patency. The fact that tissue histamine and mast cell numbers are decreased, but the changes in SP and VIP fluorescence are minimal, is taken to mean that the radiation has decreased the response to a neural signal in which mast cells play a part.

Confirmation of the role of mast cells in the small intestinal response is obtained using ferret tissue (MacNaughton *et al.*, 1997), especially useful since this species develops diarrhea soon after irradiation, making it a good model for the human response. A very low dose produces a decrease in basal and electrical field stimulation stimulated short circuit current, with recovery within hours and overshoot within a few days. Although there is no significant change in villous height or cryptal depth, tight junction structure is not investigated. The changes are possibly related to neuroimmune effects, particularly involving mast cells, with no input from an inflammatory response.

A slightly lower dose than that used for rat ileum (MacNaughton *et al.*, 1994) is used to explore whether rat colon could increase its absorptive capacity to compensate for small intestinal problems (Dublineau *et al.*, 1998). Few morphologic changes are seen hours to days/weeks after this very low dose, apart from some early dilatation of the crypts. However, absorption of water,  $\text{Na}^+$ , and  $\text{Cl}^-$  shows a sequential decrease, and recovery and permeability data suggest that the link

between changes in absorption and tight junction dysfunction could be less important here than possible radiation-induced alterations in the pericryptal myofibroblast barrier. Secretion of  $K^+$  increases and remains high, possibly due to changes in GRP levels. Radiation with a low dose also leads to iNOS expression in ileum and colon and increased iNOS activity in the former in the period from a few hours to a few days (MacNaughton *et al.*, 1998). This suggests that NO derived in this way could be involved in small intestinal dysfunction, separate from any inflammatory response. The same theme is investigated for mouse large intestine, with a reduction in response to electrical field stimulated chloride secretion several days after a low dose (Freeman and MacNaughton, 2000). The levels of white blood cells are lower and there is no inflammatory response. There is also an increase of epithelial iNOS mRNA and nitrite/nitrate in irradiated specimens. Unirradiated colon shows little iNOS, whereas irradiated samples have immunoreactivity on the luminal aspect of the epithelium and, in some cases, also at the base of the crypts (Fig. 20). The importance of iNOS in the response is confirmed by the absence of the specific changes in iNOS-deficient as opposed to wild-type mice.

In a study of rat colon responses several hours to 1 week after very low and low doses, electrolyte transport and mast cell numbers are also described (Francois *et al.*, 1998). No histologic changes and no inflammatory infiltration are seen. However, mast cell numbers are decreased over the whole time period for both doses

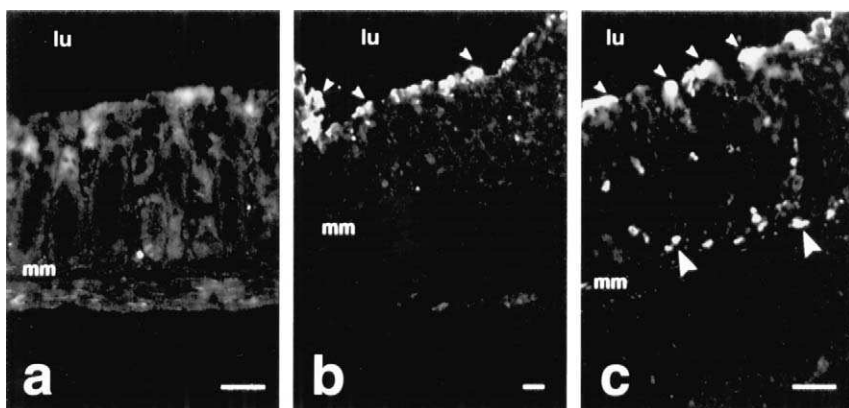


FIG. 20 iNOS immunoreactivity (iNOS-IR) in sections of colon taken from mice 3 days after either sham treatment (a) or exposure to 10-Gy  $\gamma$  radiation (b and c). Colon from sham-treated mouse shows almost no iNOS-IR. In contrast, colon from irradiated mouse shows iNOS-IR in epithelial cells on apical surface of the colon (small arrowheads) with immunoreactivity in a few scattered cells in lamina propria. In some cases, iNOS-IR was also observed in cells at base of the crypts (c, large arrowheads). lu, lumen; mm, muscularis mucosae. Scale bars = 50  $\mu$ m. [Courtesy of W. MacNaughton and The American Physiological Society, 9650 Rockville Pike, Bethesda, MD 20814. Freeman, S. L., and MacNaughton, W. K. (2000). Ionizing radiation induces iNOS-mediated epithelial dysfunction in the absence of an inflammatory response. *Am. J. Physiol.* **278**, G243–G250, Fig. 3.]

in proximal and distal colon. The response of both to electrical field stimulation is also decreased, particularly several days after treatment, with recovery by 1 week.

**b. Late.** One of the few studies of late effects is particularly useful in that it relates to monkey responses, in small intestine, 4–6 years after very low doses, although all animals are treated with atropine several hours before tissue collection (Griffiths *et al.*, 1999). Despite the long time lapse after irradiation, several changes are recorded. With respect to activity associated with apical epithelial membranes, small intestinal sucrase levels are increased, but LAP is not. Basolateral membrane changes include a small decrease in Na pump activity. This study is considered further in the section on neuroendocrine effects.

Another study of late effects comments first on signs of aging in unirradiated control mouse specimens. These changes include degeneration and additional lysosomes (Fatemi *et al.*, 1985). In irradiated jejunum and ileum, the response includes short stubby enterocyte microvilli, many vacuoles, and weakened intercellular attachments to neighboring cells.

## 2. Goblet Cells

**a. Early** The whole-body database is smaller than that for partial body, is all based on rodent material and all small intestine, and describes the earlier part of the time frame after very low to moderate doses.

With respect to rat data, several different techniques are used. Using freeze-fracture, TEM, and a luminal tracer, focal tight junction disruption and fragmentation are seen between goblet cells and their neighbors from several hours to several days after very low doses (Porvaznik, 1979). This is accompanied by leakiness of intercellular spaces to the tracer. Using wax histology to estimate cell numbers, there is sequential decrease, overshoot, and return to normal several hours to several weeks after a slightly higher range of very low doses (Lewicki *et al.*, 1975). The increase happens sooner in the cryptal region. Similar estimations are made on polystyrene sections of samples examined hours to over a month after a slightly lower dose (Becciolini *et al.*, 1997). The data show some similarities to the findings of Lewicki *et al.* (1975), although the timing of the minimum depletion is a little later and there is an initial rise in numbers before the decrease is seen. The goblet cell cytoplasm is more filled with secretory material soon after irradiation than it is later. The additional use of a goblet cell index, reflecting the ratio of goblet cells to total epithelial cells, allows for consideration of differential changes in differentiation. Further details are given in Section VI.B.3a, where the differences in groups irradiated at different times of the day are described.

The difference in the details of the responses between the Lewicki and Becciolini reports may be due to technique or to the lower dose used in the latter study. The significance of dose is also reflected in the mouse data. These show an overshoot in total goblet cell numbers days after a very low dose (Brennan *et al.*, 1998),

but a decrease to 34% and 22% after low (Carr *et al.*, 1996) and moderate (Carr *et al.*, 1993) doses, respectively. After very low doses, the percentage of the mucin perimeter exposed to the luminal surface increases (Brennan *et al.*, 1998), but there are no changes in the number of granules per cell profile.

**b. Late** The only description of late changes in goblet cells (Becciolini *et al.*, 1997) has already been covered, since the study does not extend much beyond the early points.

### 3. Paneth Cells

The data bank here relies entirely on results at early time points. The information available on this cell type is as scanty as for partial body schedules, with a similar scattering of comments in multiparameter papers. All the data are from rodent material, almost entirely from mouse, and cover the early time points after a very wide range of doses. In general, the data do not confirm the results from the partial body experiments.

The only report on rat Paneth cells describes enlargement and vacuolation several hours after irradiation (Lewicki *et al.*, 1975). The mouse data, unlike those for partial body schedules, show no significant Paneth cell loss hours to days after a very low dose (Brennan *et al.*, 1998) or days after low (Carr *et al.*, 1996) and moderate doses (Carr *et al.*, 1993). This lack of significant change may be due to variation within either the control or irradiated data sets, since the raw data do show depletion after the moderate dose. In ultrastructural terms, a low dose produces a significant decrease in granule numbers several hours after treatment (Brennan *et al.*, 1998). This is also the case for the ratio of granule diameter to core, several hours to several days after irradiation, when there are variations in the staining or cell shape and fewer granules after a moderate dose (Indran *et al.*, 1991). There is a series of changes a few days after a very high dose, including nuclear distortion, some mitochondrial damage, degenerative changes, and disappearance of the stages in granule formation, with disruption of endoplasmic reticulum and decrease of ribosome numbers (Hampton, 1966).

## D. Changes in Stroma/Connective Tissue

### 1. General: Fibers and Fibrogenesis

The data here refer only to early time points and are less detailed here than in the corresponding section on partial body effects. They all relate to rodents, mostly mouse, and are all from small intestine. The times tend to be early and the dose range is fairly wide.

The smaller group of rat data includes general descriptions of interstitial exudate, days after a very low dose, but no longer present thereafter (Lewicki *et al.*, 1975).

Mild edema is also seen hours to days after a low dose (MacNaughton *et al.*, 1994).

The stromal changes in mouse include the presence of prominent submucosal connective tissue days after a moderate dose (Indran *et al.*, 1991). Abnormalities are seen in stromal organization at different depths and in subepithelial fibroblasts, which contain pale, lipid-like inclusions (Carr *et al.*, 1985).

Significant decreases in total villous stromal cell numbers in several experiments show a trend toward greater depletion as dose increases and time after radiation passes (Brennan *et al.*, 1998; Carr *et al.*, 1993, 1996). The number drops to 29% of control levels days after a moderate dose, which also permits a subsequent trend toward recovery. The time of the earliest significant decrease appears to vary with mouse strain.

The significant decrease days after whole-body irradiation with a moderate dose (Carr *et al.*, 1996) is not seen after the corresponding partial body treatment (Carr *et al.*, 1992b).

## 2. Cells of the Inflammatory and Immune Systems

The data here refer only to the early time points. The amount available is similar to that on partial body effects, but providing more information on responses in the important GALT. Most of the data are from rat samples, although other species provide important information. The increasing amount of lymphoid tissue in more distal parts of the intestine is reflected in the relatively greater amount of data on irradiated large intestine. The times tend to be early and the doses at the lower end of the possible range.

The data on inflammatory cells are all from rat tissue. There are increased numbers of small intestinal mononuclear cells a few days after a very low dose (Lewicki *et al.*, 1975). This report also describes an increase in eosinophils at the same time, followed days later by a fall in their numbers. The latter decrease is confirmed, reported to be dose dependent after a slightly lower dose range and also to be followed by a return to normal values about 1 month after treatment (Sedgwick and Ferguson, 1994). However, unlike the situation for partial body treatment, neither myeloperoxidase-stained radiation-induced neutrophil influx nor increased 5-HT are seen hours to a few days after a low dose (MacNaughton *et al.*, 1994).

Mucosal mast cell numbers decrease in a dose-dependent way (Sedgwick and Ferguson, 1994). The cell depletion and diminished histamine levels are seen earlier than decreases in villous height and crypt depth (MacNaughton *et al.*, 1994). This implies that mast cells could be involved in the reduction in neurally evoked electrolyte transport and that nerve–mast cell interactions could be important. The epithelial increase in iNOS activity is separate from any inflammatory response, hours to a few days after a low dose (MacNaughton *et al.*, 1998).

In large intestine, eosinophil levels are still depressed about 1 month after irradiation, when the small intestinal levels have returned to normal, as described above,

while the mast cell response is similar in the two parts of the intestine (Sedgwick and Ferguson, 1994). The importance of mast cells in the response is confirmed in experiments showing that the decrease in the number of these cells and in histamine levels correlates with the onset of the decrease in electrolyte transport induced by electrical field stimulation (Francois *et al.*, 1998).

The data on the intestinal immune response come from several species, namely, mouse, rat, and chicken, with the emphasis shifting from mucosal changes to the more specialized part of GALT. In mouse, the number of small intestinal intraepithelial lymphocytes decreases several days after a low dose (K. E. Carr *et al.*, 1984), a trend confirmed in rat at the same time period and also earlier, but only for some of the very low doses used (Sedgwick and Ferguson, 1994). Further rat data, on Peyer's patches, also show depletion not only of intraepithelial lymphocytes in the follicle-associated epithelium, but also of lymphocytes within the patch and at the high endothelial venules (Chen *et al.*, 1995), days after a very low dose. Within a few weeks, the lymphocyte population has returned and by about 1 month after treatment, the size of the patches has also returned toward normal. There is some disagreement as to the role of the microenvironment, although its importance is accepted. Chen *et al.* (1995) report that the stromal microenvironment is unchanged, with continuing positive staining for dendritic follicular cells. Another paper, commenting on continuing lymphocyte depletion in Peyer's patches as opposed to other lymphoid organs, up to a few weeks after a similar dose, relates this to the epithelial microenvironment, including the change in its microbial colonization (Hale and McCarthy, 1984). Finally, in the chicken, lymphoid follicles in the bursa of Fabricius shrink and contain more pyknotic cells after a very low dose, peaking several hours after treatment and increasing with dose (Fig. 21). The pyknotic cells have characteristic features of apoptosis, such as shrinkage, chromatin condensation, and nuclear fragmentation, confirmed by gel electrophoresis (Arai *et al.*, 1996a).

### 3. Vascular Components

**a. Early** The pool of data for the whole-body response is similar in size to that for partial body treatment, but is entirely based on rodent material, mostly mouse, with both dose and time spread over a fairly wide range.

The techniques of resin casting and scanning microscopy are used to produce images depicting the three-dimensional changes in the villous capillary network. They show a reduction in the network a few days after very low to very high doses in mouse (Egawa and Ishioka, 1978) and greater tortuosity and apicobasal compression days after a low dose in rats (Abbas *et al.*, 1990a). The rat data also show dilatation or engorgement with red blood cells a few days after very low doses, findings that are not described in the next few days and weeks (Lewicki *et al.*, 1975). The dilatation several days after a low dose is estimated from resin sections to reflect an increase of 63% of the control figure (Abbas *et al.*, 1990a). This confirms the

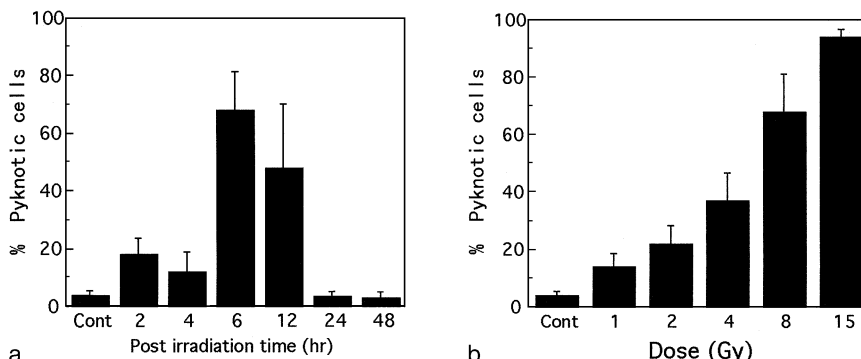


FIG. 21 Apoptosis in bursa of Fabricius. (a) Time course of induction of pyknotic cells in the chicken bursa of Fabricius after whole-body X irradiation of 8 Gy. Control: unirradiated chickens. Data are shown as mean  $\pm$  SD of 20 bursal follicles. (b) Dose response of induction of pyknotic cells in the chicken bursa of Fabricius at 6 hr after whole-body X irradiation. Control: unirradiated chickens. Data are shown as mean  $\pm$  SD of 20 bursal follicles. [Courtesy of S. Arai and Japanese Society of Veterinary Science, Rakunou-Kaikan Bld., 1-37-20 Yoyogi, Shibuya-ku, Tokyo 151-0053, Japan. Arai, S., Kowada, T., Takehana, K., Miyoshi, K., Nakanishi, Y. H., and Hayashi, M. (1996). Apoptosis in the chicken bursa of Fabricius induced by X-irradiation. *J. Vet. Med. Sci.* **58**, 1001–1006, Figs. 2 and 3.]

dilatation seen after partial body treatment and also the presence of prominent endothelial processes and signs of plasma leakage into the perivascular space.

The bulk of the mouse data confirms the presence of vascular dilatation, endothelial enlargement, thickening, disorientation, and irregularities days after moderate/high doses (Carr *et al.*, 1985; Indran *et al.*, 1991). There is clumping or splaying of endothelial flaps and thickening of the tunica media days after moderate/high doses (Carr *et al.*, 1985; Indran *et al.*, 1991). The apparent increase in the number of profiles of submucosal arterioles a few hours after a low dose (Carr *et al.*, 1996) confirms the finding for partial body effects (Carr *et al.*, 1992b), but is greater in the whole body group.

As for partial body schedules, there are few reports of changes in lymphatic vessels, although variable alterations in patency of mouse lacteals are described days after a moderate dose, during a study of lipid uptake (Hampton and Rosario, 1972).

**b. Late** Signs of aging in unirradiated specimens include thickening of capillary external laminae (Fatemi *et al.*, 1985). About 1 year after irradiation with a low dose, these are thick and folded in small and large intestine. The latter also sometimes shows degeneration of cells in vascular smooth muscle. In quantitative terms, capillary external laminae are thickened in jejunum and colon, but not in duodenum or ileum, while extensive multilayering of the external lamina is only seen in colon.

## E. Changes in Endocrine, Neural, and Muscle Components

### 1. Endocrine Cells

The endocrine and neural elements are dealt with separately, although there is overlap between the two groups in terms of substances involved and effects. Cross reference should therefore be made between the two subsections.

**a. Early** The whole-body data pool is substantially larger than that for partial body schedules. This provides useful information, which is, however, based on a more complicated situation, since many intestinal hormones also have a role in the CNS. That this is itself affected by radiation is shown by the radiation-induced increase of CCK in the rat hypothalamus (Kandasamy, 1998). This more complex response may explain the larger decrease in total endocrine cell profiles per circumference in mice after whole-body (Carr *et al.*, 1996) than after the comparable partial body exposure (Carr *et al.*, 1992b).

Most of the data on responses to whole-body radiation are based on rodent material, chiefly rat. They mainly refer to small intestine, but there are also a few on large intestine. There is a wide range of early time points, but most doses are in the very low range.

The small amount of mouse data includes a report (Carr *et al.*, 1993, 1996) of a dose-dependent fall in endocrine cell profiles per circumference several days after a low dose. There is recovery toward normal levels around 1 week after treatment. The cell profiles contain more granules than control cells, several days after a very low dose (Brennan *et al.*, 1998). Differential silver staining confirms the overall decrease in endocrine cell profiles (Kvetnoy *et al.*, 1996). Particularly after higher doses, the numbers continue to fall, from a few hours to several weeks after treatment. The decrease is also greater as dose rises from very low to high. It is postulated that the initial response includes serotonin release. In rats, a decrease in serotonin levels in intestinal tissues is seen within hours of a very low dose, with recovery toward control levels several days later (Penttila *et al.*, 1975). There is also irregularity in the borders of the individual endocrine cells and variable stain density a few days after treatment.

The rest of the rat data do not always confirm the decrease in cell profiles reported for partial body effects and also so far for whole-body effects. However, as noted earlier, it is important to differentiate between this parameter of endocrine change and alterations in specifically identified subsets of cell profiles, or in hormone levels in tissue or plasma.

Irradiation with very low doses causes SP levels to increase in plasma several hours to several days later (Esposito *et al.*, 1996). However, there is a decrease, hours to days after treatment, in small intestinal mucosal/submucosal tissue, but not in the muscularis layer. Radiation also alters gastrointestinal SP-specific binding sites, possibly contributing to the reported inflammation and contractility changes.

Further understanding of the role of SP can be gained by studying the effects of an appropriate blocking agent and its vehicle (Esposito *et al.*, 1998).

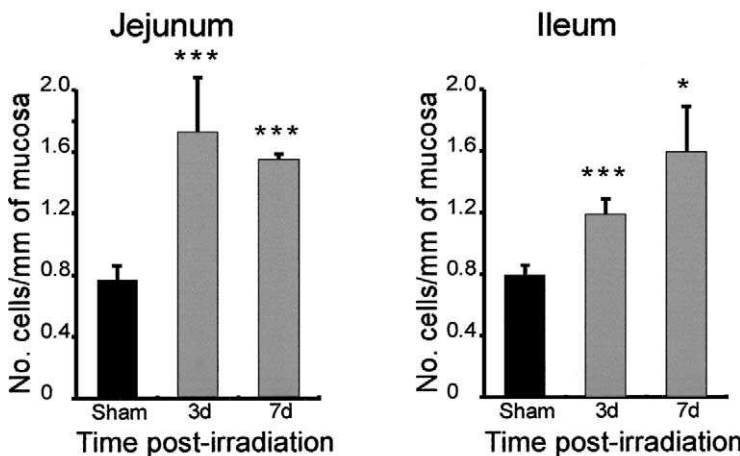
In a study of different parts of the tract, Lehy *et al.* (1998) report that plasma gastrin and acid secretion are increased from several days to 1 week after a very low dose. At the latter time, there is a decrease in the number per millimeter of mucosa of immunohistochemically identified small intestinal gastrin cell profiles, while the corresponding substance P cell profiles increase in ileum but not duodenum or jejunum. Neurotensin (NT) cell profiles increase in both jejunum and ileum at both time points, while enteroglucagon cell profiles are unchanged in ascending and descending colon several days after treatment, increasing at 1 week only for the latter (Fig. 22). Neurotensin is also studied in large intestine in similar radiation conditions (Linard *et al.*, 1997). Several days, but not 1 week, after treatment, there is an increase in plasma NT and NT-like immunoreactivity in cecum at both time points for mucosa and muscularis and for colon only in the latter layer. There is also an increase in the number of NT receptors in colonic muscle, which include an additional type of site. Irradiation also alters the contractile effect of NT on isolated colon muscle. In large intestine, increased  $K^+$  secretion over several days after a low dose (Dublineau *et al.*, 1998) may be related to increased plasma gastrin-releasing peptide (GRP), which could produce an increased inward short circuit current.

In the report already described on pig small intestinal membranes 1 week after a very low dose, the decrease in enzyme activities is accompanied by a decrease in VIP-stimulated adenylate cyclase activity and VIP-receptor affinity, but there is an increase in VIP receptor numbers (Griffiths *et al.*, 1996).

The overall picture is more informative than that gained from the partial body data. Hormones from all three groups are affected, with gastrin representing the gastrin/CCK group, VIP the secretin group, and substance P, NT and GRP the “other peptide” group. The functional outcomes are not always complementary and the changes could sometimes represent secondary outcomes. The high levels of GRP with the decreased levels of gastrin and the opposing signals on acid secretion and motility are examples of situations that need careful interpretation. As predicted, increases in circulating levels of a hormone are sometimes accompanied by decreased visibility of the corresponding intestinal cell profiles, although the relationship between the different assays of change may vary according to hormone type or postirradiation time.

**b. Late** Numbers of endocrine cells remain low 4 months after irradiation (Kvetnoy *et al.*, 1996). In the report mentioned earlier, on monkey 4–6 years after one of two very low doses (Griffiths *et al.*, 1999), VIP-stimulated short circuit current responses are reduced. Gastrin plasma levels also decrease, while NT levels are unchanged and SP levels increased only in the group exposed to the slightly higher dose. Plasma GRP levels show a dose-dependent increase.

## Neurotensin cells



## Enteroglucagon cells

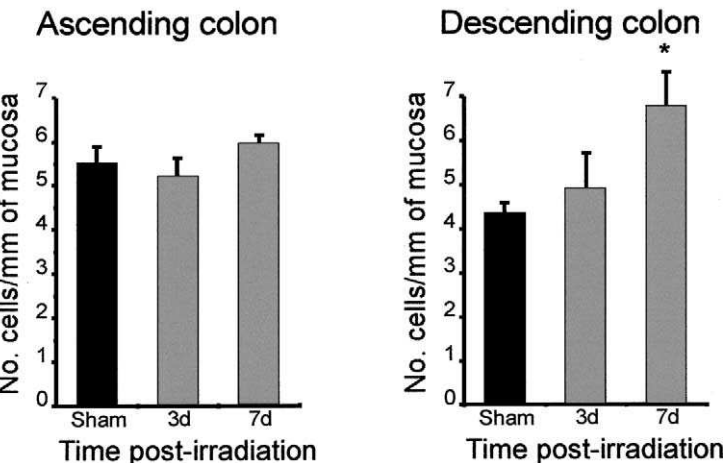


FIG. 22 Effect of whole-body exposure to 6-Gy gamma radiation on endocrine cells of the rat. Neurotensin cell density expressed as number of cells per mm of mucosa in the jejunal and ileal mucosae and enteroglucagon cell density in colonic mucosa. Each column represents the mean  $\pm$  SEM of 6–8 rats. \* $p < 0.05$  to  $p < 0.02$  versus shams; \*\*\* $p < 0.006$  to  $p < 0.002$  versus shams. [Courtesy of T. Lehy and Taylor and Francis Ltd., Rankine Road, Basingstoke, Hampshire, RG24, 8PR, <http://www.tandf.co.uk>. Lehy, T., Dessirier, V., Attoub, S., Bado, A., Griffiths, N. M., and Linard, C. (1998). Exposure to ionizing radiation modifies circulating gastrin levels and gastrointestinal endocrine cell densities in the rat. *Int. J. Radiat. Biol.* **73**, 331–340, Fig. 4.]

In tissue samples, no change is seen in SP for mucosa and muscularis in ileum and colon, while only ileal muscularis shows an increase for GRP. As for the early responses, there is contradictory evidence on, for example, acid secretion, which could be interpreted as compensatory hormone secretion or as residual damage.

## 2. Nerve

**a. Early** Although the literature on whole-body effects on nerve appears to be more substantial than that for partial body effects, some papers dealing with changes in neurally evoked electrolyte transport or epithelial iNOS expression are dealt with earlier. In the same way, other papers are explicit in their descriptions of muscle responses and are dealt with below. Those that remain are all rodent, both rat and mouse, at fairly early time points after doses in the lower part of the dose range.

They all cover small intestine, except for one paper on changes in innervation of different levels of branches of the rat superior mesenteric vessels (Zhang *et al.*, 1998). Here, the distribution of CGRP- and NPY-immunoreactive nerve fibers is not changed in the first few days after a very low dose. However, the densities of the fibers, as measured by a grid intersection counting method, do change. The greater increase in arterial CGRP than in neuropeptide YY (NPY) fibers at 1 day is thought to lead to vascular dilatation and increased blood flow. Thereafter, the combination of decreased CGRP and increased NPY reactivity could lead to vasoconstriction and reduction in blood flow.

The rat data on small intestine include a possible slight increase in mucosal VIP and SP immunoreactive staining density, possibly associated with "thicker" fibers (MacNaughton *et al.*, 1994), a few days after a low dose, confirming the findings for partial body effects. Another report records changes in enzyme levels, electrical parameters, and muscarinic receptors days to several weeks after a low dose (Lebrun *et al.*, 1998). It is concluded that the radiation produces a short-lived stimulation of cholinergic parasympathetic control of electrolyte transport and intestinal motility.

In mouse, some significant abnormalities, such as membrane whorls and dense bodies, are seen in the myenteric plexus within days of a moderate dose (Indran *et al.*, 1991). There is an increase in the apparent number of plexus profiles in the myenteric plexus several days after a low dose of whole-body irradiation (Carr *et al.*, 1996). This does not occur after the corresponding partial body treatment (Carr *et al.*, 1992b), possibly reflecting less swelling of the plexus components or in larger nerves supplying the intestine.

**b. Late** There is ultrastructural damage to some nerve processes and increased amounts of external lamina are seen around them in mice 1 year after a low dose (Fatemi *et al.*, 1985).

### 3. Muscle

**a. Early** The data bank here is a little larger than that for partial body effects. It relies on rodent material, with an additional paper on guinea pig. The data describe results at early time points after a wide range of doses. As indicated previously, there is overlap with earlier descriptions of changes in electrolyte transport or neuroendocrine control of muscular activity. There are reports of changes in both small and large intestine. A functional study of both, several hours after a low dose, links the radiation-induced changes in motility to increased sensitivity to cholinergic stimulation (Krantis *et al.*, 1996).

The mouse data refer entirely to small intestine. Several hours to a few days after moderate/high doses, muscle cells are patchily stained or fibrillar and the prominent intercellular gaps contain lamellated bodies (Carr *et al.*, 1985; Indran *et al.*, 1991). These are also seen within the cells, near mitochondria, which also show some damage: this echoes the changes seen after partial body irradiation in mitochondria and the associated MnSOD activity. In mechanistic terms, results from microscopy and electron paramagnetic resonance/spin trapping are correlated to infer that NO, involved in postirradiation changes in the contraction–relaxation cycle, moves from being intestinal in origin at day 2 to a macrophage/neutrophil source by days 3 and 4 (Steel-Goodwin and Carmichael, 1995).

In irradiated rat small intestine, the involvement of smooth muscle membrane SP binding sites a few days after a very low dose has already been noted (Esposito *et al.*, 1996). These more molecular results could relate to the ultrastructural membrane damage reported above for mouse. For rat large intestine, a link is proposed between contractile activity and neurotensin immunoreactivity and receptor binding, several days after a very low dose (Linard *et al.*, 1997).

In terms of comparison with partial body effects, it is noteworthy that little emphasis is placed in the whole-body data set on the deposition of additional collagen in the muscle layer.

**b. Late** One year after a low dose, there is ultrastructural damage to some smooth muscle cells (Fatemi *et al.*, 1985).

## V. Effects of a Fractionated Dose of Low-LET Radiation

The great majority of these studies is based on partial body shielded irradiation schedules. The data sets have been dealt with as in Section III and are summarized in Table IV. Because so much more information on the human response is available than for other schedules, the subsections often begin with a description of these data sets, with other information thereafter. Many of the clinical reports give no information as to radiation type, dose or time, apart from the fact that radiotherapy is used. Throughout the section, therefore, the details are seldom given, even when available. Many of these papers also contain little structural information,

concentrating instead on clinical findings. However, some of them, like multiparameter studies, highlight otherwise neglected areas. Although many papers apparently describe human responses, some of the references cited are based on animal experiments. A few papers on rat stomach have also been described, because they deal with experimentally induced intestinal metaplasia.

## A. Description and Integrative Summary of Responses

### 1. General Description

**a. Early** All of the reports refer to human responses, although, as noted above, some rely on a broader literature. Some papers describe changes to human small and large intestine. The key toxicities of irradiation are given as early diarrhea and late obstruction/fistula and bleeding (Spitzer, 1995). Incidences of radiation enteritis of 20–70% are cited (Classen *et al.*, 1998), with first symptoms appearing only hours after treatment. Modern imaging techniques visualize effects such as ulceration and thickening or edema of the wall (Capps *et al.*, 1997). Diarrhea is linked to abnormalities in absorption of bile salts and lactose, in bacterial populations and in motility (Classen *et al.*, 1998). Symptomatic relief is obtained with therapeutic agents aimed at these specific causal components, such as adsorbants of bile salts. Many subjects suffer acute small intestinal damage after irradiation for pelvic and abdominal tumors (Touboul *et al.*, 1996). During treatment (Touboul *et al.*, 1996), pain, nausea, malabsorption, and diarrhea occur. Some of the above responses are seen in rat small intestine, in particular obstruction and fistulas (Allgood *et al.*, 1996).

For large intestine, sigmoidoscopy shows edema during irradiation, erythema during and after treatment, and mucosal inflammation afterward (Haboubi *et al.*, 1988).

For humans and other species, changes in contractile activity, regulatory peptides, and cholinergic enzyme activity are important in the development of intestinal responses (Thomson and Wild, 1997).

**b. Late** A few papers cover human small and large intestine (Coia *et al.*, 1995). Between 9 and 10.5 months after radiotherapy, mild symptoms include tenesmus and rectal bleeding (Libotte *et al.*, 1995), while by 18 months, there are severe lesions such as obstruction and perforation. Images of strictures and fistulas are described (Capps *et al.*, 1997). Many morphologic changes are common to both small and large intestine; ulceration, perforation, gangrene and strictures are reported (Hasleton *et al.*, 1985). Rectal bleeding, although occurring at the same time as mild symptoms, is a serious complication (Libotte *et al.*, 1995). Tumor development is also reported in a small number of cases (Hasleton *et al.*, 1985).

With respect to human small intestine, clinical late effects are reported in 0.5–15% of cases, not necessarily following on from earlier symptoms (Touboul *et al.*, 1996). Delayed effects also include malabsorption, perforation, obstruction,

fibrosis, thickening of the wall, submucosal edema, strictures, gangrene, or hemorrhage (Taverner *et al.*, 1982; Lantz and Einhorn, 1984; Kalman *et al.*, 1995; Letschert, 1995; Wallace *et al.*, 1995; Touboul *et al.*, 1996). Some of these relate to structural abnormalities. These include mucosal atrophy, ulceration, abscesses, congestion, fibroblasts with long, densely stained nuclei, mucosal telangiectases, submucosal edema/vascularity, hyalinization of vessels, and hypertrophy of the muscularis mucosae. There have been reports of ileal hemorrhage (Taverner *et al.*, 1982) and of massive upper gastrointestinal bleeding caused by a duodenoaortic fistula (Kalman *et al.*, 1995).

With respect to human large intestine, images of fistulas and wall thickening are seen (Blomlie *et al.*, 1999). Colonic mucosal atrophy, bleeding telangiectases, and rectal bleeding are reported (Taverner *et al.*, 1982; Leborgne *et al.*, 1984). Radiation proctitis is associated with urgency or frequency of defecation or with incontinence (Kim *et al.*, 1998).

## 2. Multiparameter Results

**a. Early** For rat small intestine, the RIS is used to record changes following fractionated radiation schedules (Allgood *et al.*, 1996; Richter *et al.*, 1996): details are given in Section VI.A.4a. Increased vascularity, inflammatory cells, and a lymph node inflammatory reaction are seen 2 weeks after irradiation of pigs, while villous structure is abnormal and lymph follicle/nodal lymphocyte numbers are decreased (Borgstrom *et al.*, 1985). Scores indicate slight to marked damage. For human large intestine, most rectal damage during radiotherapy relates to epithelial nuclear changes or eosinophilic infiltration, whereas fibrosis is less common (Haboubi *et al.*, 1988). By 2 weeks after treatment, the estimated total score suggests less damage than is present during treatment.

**b. Late** For rat small intestine, the RIS system shows some increased damage several months after radiation, compared to sham groups and the early-irradiation group (Richter *et al.*, 1996). Dog small intestine, a few months after treatment, shows a substantial increase in histologic scores, particularly relating to damage to villi, epithelium, stroma, and vessels (Summers *et al.*, 1992).

For human large intestine, damage several months after treatment is greater than during radiotherapy or a few weeks after radiotherapy (Haboubi *et al.*, 1988). Most late damage involves cryptal disturbances, fibrosis, or eosinophilic infiltration.

## B. Changes in Intestinal Compartments

### 1. Villous and Cryptal

**a. Early** For small intestine, blockage of proliferation (Wiernik and Plant, 1971) and significant apoptosis are reported for human tissue (Touboul *et al.*, 1996).

Villous changes include collapse, atrophy, or loss in humans (Wartiovaara and Tarpila, 1977; N. D. Carr *et al.*, 1984), pigs (Borgstrom *et al.*, 1985), dogs (McArdle *et al.*, 1985) and mice (Carr *et al.*, 1979). Mice also occasionally display collared crypts, where the crypt opening is surrounded by a heaped-up ring of surface tissue. In rats, after an early reduction in the frequency of S-phase cells in the crypts, the proliferating zone extends upward and enzyme activity is affected (Becciolini *et al.*, 1983c).

For human large intestine, there is reduction in mucosal height (Hockerfelt *et al.*, 1999; Forsgren *et al.*, 2000) and immediate loss of rectal mitotic activity (Haboubi *et al.*, 1988). Different proportions of colonic crypts with discordant acetylation of sialoglycoproteins arise from radiation-related somatic stem cell mutation (Campbell *et al.*, 1994). The differences in numbers of clonogenic cells in three parts of mouse large intestine are explored using split-dose microcolony assay methods (Cai *et al.*, 1997b).

**b. Late** With respect to human small and large intestine, mitotic figures are increased and crypt abscesses are seen (Hasleton *et al.*, 1985). In small intestine, variable villous atrophy, fusion, and blunting are reported for humans (Wartiovaara and Tarpila, 1977; Taverner *et al.*, 1982; Kalman *et al.*, 1995), for dogs following IORT and external radiation (Ahmadu-Suka *et al.*, 1988; Summers *et al.*, 1992), and for mice (Dewit and Oussoren, 1987). Mice also show more macroscopic changes several months after radiotherapy than at earlier times. The changes include pallor, narrowing and rigidity of the wall, fibrotic adhesions, bleeding, and infarction (Dewit and Oussoren, 1987). Although crypt loss is reported for dogs after IORT (Ahmadu-Suka *et al.*, 1988), there is no significant shift in the mouse microcolony assay fractionated dose-response curve by comparison with the effect of single-dose or sham treatment (Dewit and Oussoren, 1987). Mitotic activity is increased.

In human large intestine, there is distortion or variation in crypt architecture, size, shape, or branching (Haboubi *et al.*, 1988).

## 2. Layers, Tissues, and Tissue Boundaries

**a. Early** For human small and large intestine, the mucosa is the layer most affected (Coia *et al.*, 1995). In human small intestine, there is some thickening of the basement membrane (Wartiovaara and Tarpila, 1977), and cell projections herniate through the basement membrane, contacting stromal cells, particularly in cryptal areas.

**b. Late** In human small and large intestine, the submucosa is the most affected layer (Coia *et al.*, 1995). Serosal perforation is accompanied by an acute inflammatory reaction (Hasleton *et al.*, 1985) and mesothelial cells show typical reactive changes, with prominent nuclei and voluminous cytoplasm. In human small

intestine, there are continuing basement membrane irregularities and gaps, allowing cryptal epithelial–stromal contact (Wartiovaara and Tarpila, 1977).

### 3. Disturbances of Cell Growth in Late Time Frame

**a. Tumors and Tumor Development** Approximately 3% of intestinal carcinoma in humans may be radiation induced, mostly associated with natural or accidental exposure and a minority due to cumulative medical exposure (Ming and Goldman, 1998).

For experimental radiation-induced changes in rat small intestine, obvious epithelial atypia, including adenocarcinoma, occurs several months after irradiation with two fractions (Hauer-Jensen *et al.*, 1983b). In experiments aimed at exploring the dose and fractionation schedules needed to produce intestinal metaplasia in rat stomach, as opposed to gastric cancer (Watanabe *et al.*, 1987), 11% of the animals develop adenocarcinoma in small intestine.

Carcinoma is reported in human large intestine in some cases (Hasleton *et al.*, 1985). In a group of seven patients, neither adenomatous remnants nor coexisting dysplasia are seen and the lesions are all moderately to well-differentiated carcinomas, with a substantial proportion of mucinous carcinomas (Minami *et al.*, 1998). An association is postulated between cancer development and radiation-induced aberrant glands.

**b. Other Radiation-Induced Disturbances** Intestinal metaplasia in the rat stomach, accompanied by the appearance of intestinal enzymes, follows doses smaller than those needed to produce tumors (Watanabe, 1978), although tumors are formed when an appropriate dose splitting schedule is used (Watanabe *et al.*, 1987). Metaplasia is not necessarily related to the presence of tumors and it is concluded that these two growth disorders develop independently.

## C. Changes in Epithelial Cells

### 1. Surface Epithelium, Enterocytes, and Glands

**a. Early** By the end of the second week of radiotherapy, the human small intestinal epithelial surface is reduced by about 40% (Touboul *et al.*, 1996). The larger total dose obtained by fractionated delivery results in a degenerative epithelium with loss of microvilli and cell separation; nucleolar changes; vacuolization of endoplasmic reticulum, with prominent polysomes; mitochondrial swelling; and many lysosomes (Wartiovaara and Tarpila, 1977). These changes reflect dysfunction in absorption, energy production, and intracellular catabolism and protein synthesis. Two weeks into radiotherapy, there is a temporarily increased permeability to cellobiose/mannitol (Carratu *et al.*, 1998), but this does not correlate with

acute symptoms, which are attributable instead to the combined effects of mucosal and motility disturbances and diarrhea associated with changes in absorption of fat and bile acids. In the rat, changes 2 weeks after irradiation include ulceration and epithelial atypia (Richter *et al.*, 1996). The correlation between mucosal barrier breakdown and early increase in TGF- $\beta$  immunoreactivity implies that the latter is important in the development of this abnormality. Most enzymes show the pattern of sequential increase, decrease, and return to normal values, as seen after single doses (Becciolini *et al.*, 1987), but with shorter and less marked impairment.

In irradiated human large intestine (Fig. 23), there is some ulceration and the epithelial cells are shorter than normal (Hockerfelt *et al.*, 1999; Forsgren *et al.*, 2000). They also show nuclear enlargement, alterations in chromatin patterns, and prominent nucleoli in both surface and cryptal epithelium (Haboubi *et al.*, 1988).

**b. Late** In human small and large intestine, the regenerating epithelial cells may be thinned or flattened (Hasleton *et al.*, 1985) and ulceration is reported (Hirschowitz and Rode, 1991). In small intestine, ulceration, mucosal atrophy (Richter *et al.*, 1997b), and increased epithelial–stromal contacts are seen (Wartiovaara and Tarpila, 1977).

In dog small intestine a few months after treatment, epithelial vacuolization and atypia and also crypt necrosis are seen (Summers *et al.*, 1992). After IORT, there is loss of villous epithelium and cryptal necrosis/hyperplasia (Ahmadu-Suka *et al.*, 1988). In rat small intestine, ulceration and epithelial atypia are reported several months after irradiation (Hauer-Jensen *et al.*, 1983b).

In human large intestine, many aspects of epithelial ultrastructure are normal, but some nuclear abnormalities are reported, along with changes in cytosol, cytoplasmic membranes, and organelles (Haboubi *et al.*, 1988).

## 2. Goblet Cells

**a. Early** For human small intestine, each fraction of radiation produces increased numbers of goblet cells, moving from crypt to villus (Wiernik and Plant, 1971).

For human large intestine, there is an increase in partially involved rectal crypts, with genetically controlled variation in the proportion of *O*-acetylated sialoglycoproteins (Campbell *et al.*, 1994). Mucus depletion during radiotherapy is reported (Haboubi *et al.*, 1988), as is an initial increase and subsequent decrease in the proportion of goblet cells (Ueno *et al.*, 1976). There is a significant decrease in the numbers of goblet cells in dog colon 2 weeks after irradiation (Otterson *et al.*, 1992).

**b. Late** The proportion of goblet cells in human large intestine increases about 1 month after irradiation, decreasing thereafter to a percentage slightly lower than that of unirradiated tissue (Ueno *et al.*, 1976). There is an increase in the numbers of wholly discordant crypts with respect to *O*-acetylation (Campbell *et al.*, 1994).

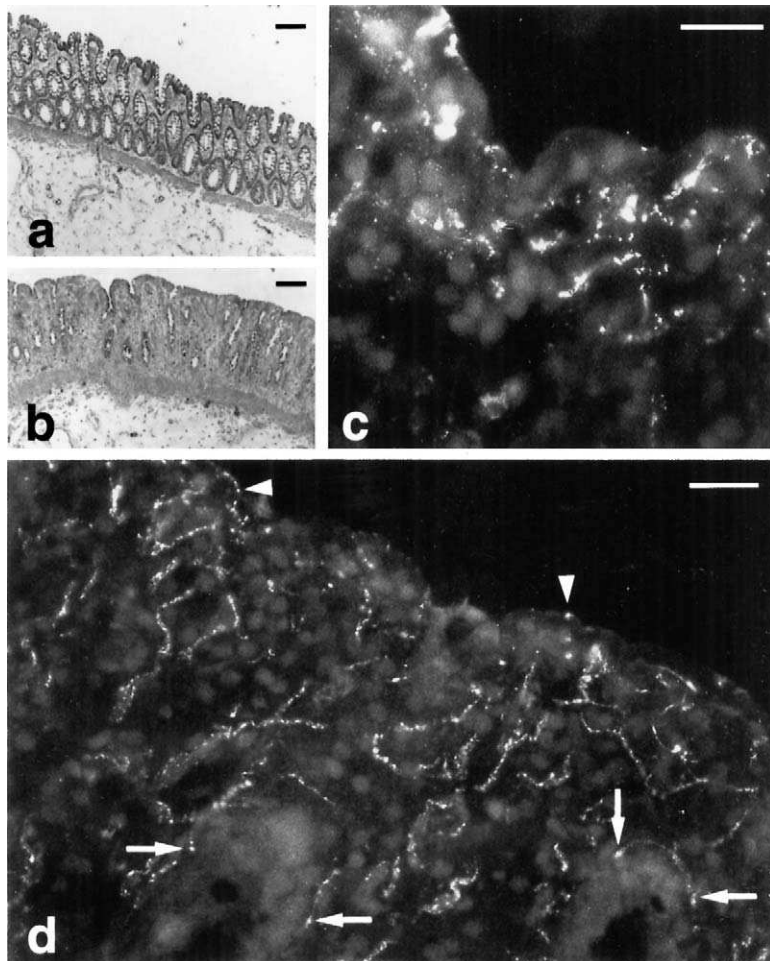


FIG. 23 (a) Normal and (b) irradiated human colonic mucosa in sections stained for morphology (NADH-TR activity). The mucosa in (b) is markedly affected by the radiotherapy, showing a relative increase in lamina propria, a relative decrease in epithelium and denudation. Scale bar = 200  $\mu$ m. (c) VIP immunoreaction after irradiation. The mucosa is facing the intestinal lumen. There are numerous VIP-immunoreactive fibers facing the intestinal lumen (above) and in relation to the cells in the lamina propria. Scale bar = 30  $\mu$ m. (d) Irradiation-damaged mucosa at high magnification in a section processed for SP. The surface epithelium has vanished (above). Immunoreactive varicose nerve fibers are numerous. Some of these abut epithelial crypts (arrows) and some face the intestinal lumen (arrowheads). Scale bar = 30  $\mu$ m. [Parts (a) and (b) courtesy of S. Forsgren. Part (c) courtesy of S. Forsgren and Kluwer Academic/Plenum Publishers, 233 Spring Street, New York, NY 10013-1578. Hockerfelt, U., Henriksson, R., Franzen, L., Norrgard, O., and Forsgren, S. (1999). Irradiation induces marked immunohistochemical expression of vasoactive intestinal peptide in colonic mucosa of man. *Dig. Dis. Sci.* **44**, 393–401, Fig. 16. (d) Courtesy of S. Forsgren. Reprinted from *Regulatory Peptides*, **88**, Forsgren, S., Hockerfelt, U., Norrgard, O., Henriksson, R., and Franzen, L. Pronounced substance P innervation in irradiation-induced enteropathy—a study on human colon, 1–13. Copyright (2000), with permission from Elsevier Science. Fig. 5.]

In dog small intestine a few months after treatment, fewer goblet cells are observed (Summers *et al.*, 1992).

### 3. Paneth Cells

With respect to late effects, Paneth cells are more prominent in some sections of human small intestine and even in large intestine (Hasleton *et al.*, 1985).

## D. Changes in Stroma/Connective Tissue

### 1. General: Fibers and Fibrogenesis

**a. Early** In human small intestine, fibroblasts contain prominent rough endoplasmic reticulum and vacuoles and some signs of pyknosis (Wartiovaara and Tarpila, 1977). Rat small intestine, a few weeks after radiation, shows a correlation between increased TGF- $\beta$  immunoreactivity and RIS, with particular reference to early morphologic alterations such as ulceration, epithelial atypia, and serosal thickening (Richter *et al.*, 1996).

In human large intestine, there appears to be more lamina propria relative to epithelium (Fig. 23): stromal hypertrophy is reported soon after radiotherapy (Ueno *et al.*, 1976). Lamina propria fibrosis also is reported in some patients during radiotherapy (Haboubi *et al.*, 1988).

**b. Late** In human small and large intestine, edema is seen in the stromal layers and around nerve plexuses (Hasleton *et al.*, 1985), as well as in small intestinal submucosa (Taverner *et al.*, 1982; Kalman *et al.*, 1995). After IORT, there is an apparent increase in the relative amount of lamina propria in dogs (Ahmad-Suka *et al.*, 1988). In human small and large intestine, the fibroblasts are abnormal (Hirschowitz and Rode, 1991), with marked cellular projections (Coia *et al.*, 1995). They contain large nuclei and prominent cytoplasm (Hasleton *et al.*, 1985).

In human small intestine, fibrosis and abnormal fibroblasts are also present (Kalman *et al.*, 1995; Richter *et al.*, 1997b). In dog small intestine a few months after treatment, there are abnormal submucosal fibroblasts and some deposition of collagen in the muscularis (Summers *et al.*, 1992). The remaining elevation in TGF- $\beta$  immunoreactivity in rats correlates with injury scores, particularly with respect to vascular sclerosis (Richter *et al.*, 1996). In human large intestine, there is diffuse hyalinization and marked collagen deposition in stromal layers (Haboubi *et al.*, 1988).

### 2. Cells of the Inflammatory and Immune Systems

**a. Early** In dog small intestine, 2 weeks after treatment, the inflammatory infiltrate in the lamina propria includes lymphocytes, plasma cells, and some

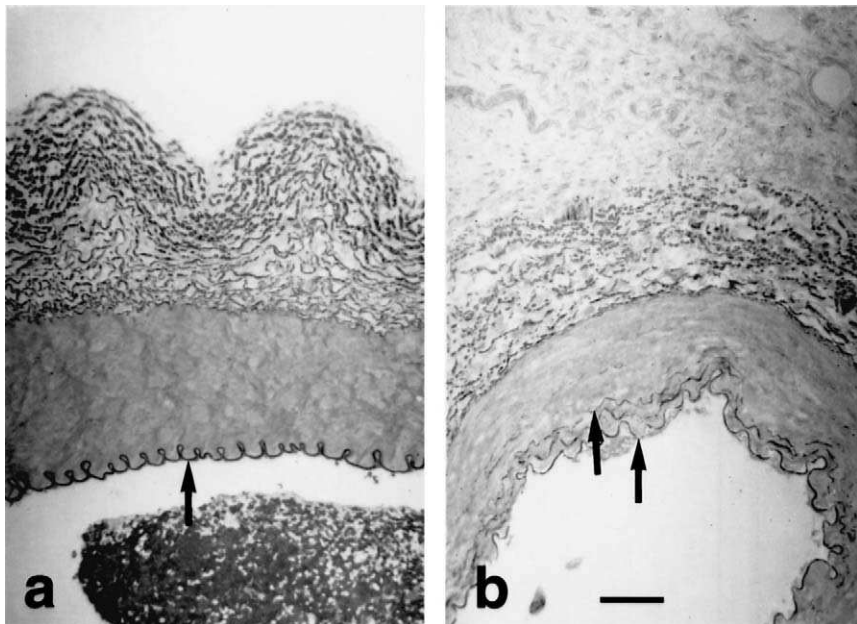


FIG. 24 Microphotographs of resorcin fuchsin staining of the inner elastic membrane in (a) an untreated control artery and (b) at 42 days after IORT, followed by ERT. The irradiated blood vessel shows disruption and fragmentation of the inner elastic membrane into multiple, disconnected layers. Scale bar = 100  $\mu$ m. [Courtesy of E. Kallfass and S. Schultz-Hector. Reprinted from *Radiotherapy and Oncology*, 39, Kallfass, E., Kramling, H.-J., and Schultz-Hector, S. Early inflammatory reaction of the rabbit coeliac artery, pp. 167–178. Copyright 1996, with permission from Elsevier Science, Figs. 3a and 3b.]

neutrophils, while the submucosa contains a number of lymphocytes (Otterson *et al.*, 1992). During radiotherapy of human large intestine, numerous mucosal eosinophils are seen, sometimes accompanied by eosinophilic abscesses (Haboubi *et al.*, 1988). The presence of leucocytes is also noted about 1 month after radiotherapy (Ueno *et al.*, 1976).

**b. Late** In human small and large intestine, there are reduced numbers of plasma cells, lymphocytes, and lymphoid aggregates; macrophages contain hemosiderin (Hasleton *et al.*, 1985). Regions of inflammation contain many eosinophils. In human large intestine, stromal leukocyte infiltration is reported (Ueno *et al.*, 1976). Eosinophils and eosinophilic abscesses are still seen several months to several years after radiotherapy (Haboubi *et al.*, 1988). SP receptor immunoreactive polymorphonuclear leucocytes are present in the mucosa (Forsgren *et al.*, 2000).

### 3. Vascular Components

**a. Early** Several changes are reported in the large vessels supplying the intestinal tract. Closest to the aorta, IORT-induced arteriosclerosis in the rabbit celiac artery supplying the upper intestine can be preceded by changes in the vessel wall within a few days (Kallfass *et al.*, 1996). These include invasion by TNF- $\alpha$ -positive macrophages, followed by strong expression of this proinflammatory vasoactive cytokine in medial smooth muscle and attendant damage to the elastic lamina (Fig. 24). In rats, ileal, but not jejunal or colonic, blood flow is increased several days after radiation (Wiseman *et al.*, 1996).

With specific reference to human small intestine, several vascular lesions are described, although some appear at later time points (Touboul *et al.*, 1996). The lesions include thrombosis and necrosis due to endothelial depletion, luminal narrowing by clones of surviving endothelial cells, and reduction in blood flow with relative ischemia. Lymphatic abnormalities are also reported within 2 weeks of treatment after high doses. No vascular changes are seen in human large intestine during radiotherapy (Haboubi *et al.*, 1988).

**b. Late** There is more information on late effects. A fatal radiation-induced fistula is described between human duodenum and aorta, along with several changes in the aorta itself (Kalman *et al.*, 1995), including atherosclerosis, fibrous thickenings, and medial/adventitial necrosis with inflammation. Some of the late responses of the rabbit celiac artery to IORT and ERT (Kallfass *et al.*, 1996) could contribute to the development of atherosclerosis, including luminal protrusions of smooth muscle cells between the endothelium and the internal elastic lamina, which is also disrupted. There is a decrease in the previously elevated levels of expression of TNF- $\alpha$  in medial smooth muscle and adventitial macrophages, but increased expression of collagen type I. Large elastic arteries in the human mesentery show intimal fibrosis, reduplication of the internal elastic lamina, proliferation of elastic tissue, and signs of inflammation and thrombosis or recanalization (Hasleton *et al.*, 1985). In vessels leading to the intestines and in those within the walls, there is significant thickening of the tunica media of intestinal vessels of various sizes, particularly arterial. For the intramural vessels, the amount of intimal fibrosis is also increased. Some of these changes are dose and time dependent (Hasleton *et al.*, 1985).

Also within the walls of human small and large intestine, contrast medium is used to relate vascular changes to gross lesions (N. D. Carr *et al.*, 1984). Strictures are associated with deep fibrosis, reduced vascularity, intimal arterial fibrosis, and capillary thrombosis. Perforations are associated with adjacent focal avascularity, necrosis, or thrombosis. Away from such serious lesions, the changes include reduced vascularity and intimal fibrosis. Abnormal villi contain ectatic vessels and fewer capillaries: patchy capillary ectasia is seen in the colon. The changes in small and large intestine are similar. There is also hyaline thickening of the vessel walls

and telangiectasis of vessels in the lamina propria (Hirschowitz and Rode, 1991). The submucosal changes are associated with hyalinized, thick walls, recanalized thrombi, and telangiectasia (Coia *et al.*, 1995).

In human small intestine, the changes recorded above under early effects (Toubul *et al.*, 1996) contribute to the development of chronic vascular insufficiency, characterized by hyalinization, fibrinoid degeneration, and collagenous fibrosis of vessel walls, leading to ischemia of the intestinal wall with its many resultant complications. There are reports of increased ileal submucosal vascularity, thick vessel walls, and telangiectasis (Taverner *et al.*, 1982). At the muscularis externa, there is vascular thickening, hyalinization, and loss of smooth muscle cells (Kalman *et al.*, 1995). There is vascular sclerosis, subendothelial fibrosis, vascular hyalinization, and luminal thrombosis (Richter *et al.*, 1997b). TGF- $\beta$  levels are increased, there are fewer thrombomodulin positive (+ve) vessels (Fig. 25), but there is no change in levels of endothelial von Willebrand factor. These conditions could promote thrombogenesis.

Some of these findings in human small intestine are confirmed in other species. A few months after irradiation, there is some sclerosis of dog submucosal vessels (Summers *et al.*, 1992) and several months after IORT, necrosis and degenerative alterations are seen in several submucosal blood vessels (Ahmadu-Suka *et al.*,

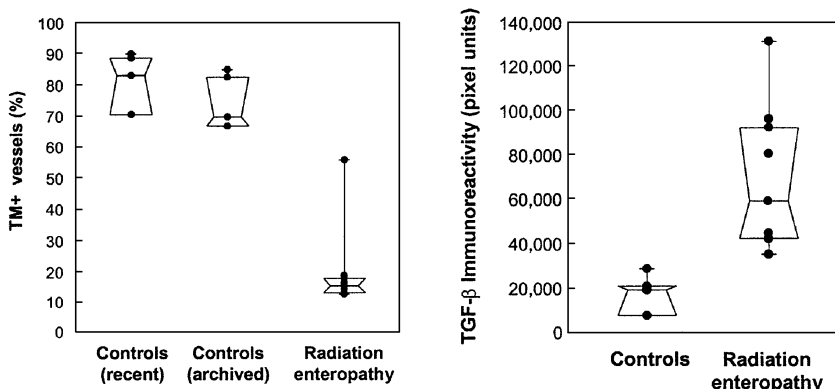


FIG. 25 (Left panel) Percent thrombomodulin positive (TM+) submucosal vessels in intestinal resection specimens from radiation enteropathy patients, recent control specimens (intestinal resection specimens from penetrating trauma victims), and archived control specimens. The difference between controls and radiation enteropathy patients is highly significant ( $p < 0.0001$ ). (Right panel) Extracellular matrix-associated TGF- $\beta$  immunoreactivity levels in intestinal resection specimens from radiation enteropathy patients and unirradiated control intestine. The difference between radiation enteropathy patients and controls is highly significant. ( $p = 0.002$ ). [Courtesy of M. Hauer-Jensen. Reprinted from *Radiotherapy and Oncology*, 44, Richter, K. K., Fink, L., M., Hughes, B. M., Sung, C.-C., and Hauer-Jensen, M. Is the loss of endothelial thrombomodulin involved in the mechanism of chronicity in late radiation enteropathy?, pp. 65–71. Copyright 1997, with permission from Elsevier Science, Figs. 4 and 6.]

1988). In rat samples several months after treatment, increased TGF- $\beta$  correlates with most morphologic changes, particularly vascular sclerosis (Richter *et al.*, 1996). This points to vascular input to the continuing radiation damage after the peak of mucosal damage and inflammation has passed. In rat terminal ileum, the early increase in blood flow is reversed to a decrease by about 1 month, is then greater than control values several months later, and returns to normal by 1 year (Wiseman *et al.*, 1996).

With respect to large intestine, the wall of the human rectum shows thickening and thrombosis (Ueno *et al.*, 1976). Focal ultrastructural damage includes vascular luminal fibrin deposits, endothelial degeneration, and fibrin-covered erosions (Haboubi *et al.*, 1988). Comparisons of responses by tumor and normal tissue are dealt with in Section VI.B.3.b (Richter *et al.*, 1998).

The mechanisms involved in human lymphedema (Humble, 1995), namely, increased tissue fluid, collagen deposition, inflammatory responses, fibrosis, and further vascular problems, can all contribute to the changes in irradiated intestinal tissue. The comments on edema in human small and large intestine (Hasleton *et al.*, 1985) imply malfunction of lymphatic capillaries. Although there can be a problem differentiating between blood and lymphatic vessels, particularly in edematous tissue, dilated submucosal and serosal lymphatics are reported (Hasleton *et al.*, 1985). In human small intestine, telangiectasis probably affects lymphatic vessels as well as blood vessels (Tavner *et al.*, 1982). In rat small intestine, lymph congestion is reported several months after radiation (Richter *et al.*, 1996).

## E. Changes in Endocrine, Neural, and Muscle Components

There is much overlap across these components. Endocrine and neural responses have been dealt with together, since some of the relevant papers use the term neuroendocrine for the cells affected.

### 1. Endocrine and Nerve

**a. Early** Shortly after the last fraction of a six-fraction schedule, altered motor activity in dog intestine is reported, along with various changes in levels of several neuroendocrine products in serum and in various parts of small and large intestine. These include increased VIP and SP and decreased motilin and peptide YY (PYY, Otterson *et al.*, 1995). There is also increased acetylcholinesterase activity in mucosal/submucosal samples, including neural elements. Several of these changes impinge on smooth muscle function, but, as for whole-body effects, it is difficult to appreciate the balance of the alterations to the signals received.

Two studies contribute further to the understanding of the early human colonic neuroendocrine response after fractionated schedules. Surgical specimens are available several days after radiotherapy (Hockerfelt *et al.*, 1999, Forsgren *et al.*,

2000; Fig. 23). Although no structural changes are seen in the main plexuses in the irradiated colon, there is increased VIP expression in ganglion cell bodies of the submucosal plexus and many mucosal nerve fibers show VIP immunoreactivity (Hockerfelt *et al.*, 1999). This could imply a role in the onset of diarrhea or in the inflammatory and regenerative responses. There is also marked SP-like immunoreactivity in nerve fibers in the lamina propria and in submucosal ganglion plexus profiles (Forsgren *et al.*, 2000). There is little indication of involvement by NPY and enkephalin or of CGRP related to sensory neurones. It is concluded that changes in levels of both VIP and SP are relevant for postradiation reorganization. The final balance of response can be difficult to interpret, since VIP and SP normally have opposite effects on the intestine, in terms of inhibition/excitation, and both are involved in responses from smooth muscle and inflammatory cells.

**b. Late** In a study of human small and large intestine, enteropathy (Pietroletti *et al.*, 1989) involves an increase in chromogranin-positive cells per unit length of muscularis mucosae in both sites. Neuroendocrine cells are also graded as present in the lamina propria, unlike the situation in unirradiated samples (Hirschowitz and Rode, 1991).

There are also reports of late nerve damage and nerve injury. In human small and large intestine, the edema around nerve plexuses (Hasleton *et al.*, 1985) can lead to dysfunction. There are increased numbers of nerves and nerve hyperplasia in the lamina propria of small and large intestine (Hirschowitz and Rode, 1991). In addition to the neuroendocrine cells reported above, structures similar to ganglion cell bodies are more common in the lamina propria than in the corresponding control samples. Swollen synaptic terminals are also identified by TEM. Because the regulatory peptides involved in gastrointestinal innervation include VIP, which can lead to diarrhea if overexpressed, it is possible that some radiation-induced symptoms may be associated with these changes. The possible significance of lamina propria complexes is also noted: these groupings of nerve bundles and ganglion, neuroendocrine, and Schwann cells may be involved in serotonin-linked onset of inflammation and pain.

In human small intestine, atypical ganglion cell bodies are seen in submucosal plexuses (Kalman *et al.*, 1995), while functional problems such as intestinal paralysis and obstruction are linked to nerve plexus lesions (Touboul *et al.*, 1996). Abnormal motility in small intestine can be linked to symptoms of radiation enteropathy, with manometry used as a helpful clinical test (Husebye *et al.*, 1994). In dog small intestine, possible involvement of the interstitial cells of Cajal is deduced from the changes in slow wave activity (Summers *et al.*, 1992).

## 2. Muscle

**a. Early** In dogs, a significant increase in large intestine contractile activity associated with diarrhea and cramps 2 weeks after treatment is accompanied by

some epithelial crowding, a significant decrease in goblet cell numbers, and the presence of an inflammatory infiltrate (Otterson *et al.*, 1992).

**b. Late** Anorectal manometry measurements indicate sensory and/or motor dysfunction in radiation proctitis patients (Kim *et al.*, 1998), with effects on reservoir capacity, sensory function, or the external anal sphincter muscle. Structural features implicated in sensory dysfunction include stretch receptors, cells and tissues of the afferent neural pathways or mucosal structures, with edema, bleeding, or vasodilatation as mediating biologic mechanisms. The corresponding structures involved in motor dysfunction include muscle cells of the internal or external sphincters, particularly the latter, or the vessels or nerve pathways supplying them.

In human small and large intestine, there are reports of atrophy or fibrosis of the muscularis externa (Hirschowitz and Rode, 1991). Patchy edema is seen between groups of muscle cells (Hasleton *et al.*, 1985). Lysis, necrosis, bleeding, inflammation, infarction, and replacement by fibrous tissue are also reported. Previous hemorrhage is indicated by the presence of hemosiderin-laden macrophages. Strictures are associated with fibrosis in the muscularis externa (N. D. Carr *et al.*, 1984).

In human small intestine, functional problems, such as intestinal paralysis and obstruction, are linked to smooth muscle degeneration as well as to the nerve plexus lesions described above (Touboul *et al.*, 1996). There may also be hypertrophy of the muscularis mucosae (Kalman *et al.*, 1995). In dog small intestine a few months after irradiation, the muscularis is thicker and there is collagen deposition (Summers *et al.*, 1992). This study concludes that the changes in myoelectric activity and in the cells involved in motility, such as muscle and nerve, are seen before the major tissue effects are noticeable.

## **VI. Factors Affecting Outcome and Summary for All Schedules**

This section first reviews the factors influencing outcome. There is so much material that only a selective account is given: scanty data sets are omitted and, for the sake of brevity, protocol details are often restricted. The data are categorized according to whether the factors concerned relate to radiation or the irradiated subject. Within each subsection, data are often clustered according to radiation schedule, although the inclusion of the additional factors makes it impractical to subdivide in a standard way across species, dose, and other parameters. For single-dose schedules, both partial body and unshielded, relevant factors mainly cover procedures used in addition to, or in comparison with, irradiation, often with the aim of probing the mechanisms involved. On the other hand, the factors affecting partial body fractionated schedules often relate to methods of delivering the radiation or to the health status and clinical care of the treated individual.

The section ends with a summary of the basic effects for all schedules, whether partial body, unshielded or fractionated, and with account taken of important additional factors influencing the final outcome.

## A. Radiation

### 1. Field/Volume Irradiated

For late effects after single/partial schedules, IORT of different fields produces different structural outcomes in dog small intestine years after irradiation: these affect mucosa, stroma, vessels, and muscle (Sindelar *et al.*, 1994). The significance of the volume irradiated is investigated by comparing the late outcome in rat large intestine after several irradiation schedules (Trott *et al.*, 1995). The volume irradiated is more directly related to functional disturbance, as seen by rectal obstruction, than it is to ulceration, highlighting the lack of a standard response, even in the same organ. Against the predictions of a probability model, there is a threshold length for mouse colorectal fibrosis, related to epithelial regeneration (Skwarchuk and Travis, 1998). The late increase in TNF- $\alpha$  expression in rabbit celiac artery is seen after IORT, but not after external irradiation (Kallfass *et al.*, 1996).

Moving on to general factors influencing fractionated low-LET effects, the theoretical likelihood of complications in “serial” organs such as intestine is reported by Fowler to rise with volume and then levels out (Peacock *et al.*, 1998). The relationship between volume irradiated and ensuing late complications is covered for human small and large intestine by Letschert (1995) and Gerard *et al.* (1995), respectively.

### 2. Shielding

For early effects in rat small intestine after partial/single schedules, distal rather than proximal shielding is the more effective and shielding one region influences the other (Vigneulle, 1995). There is greater villous collapse proximally and crypt depletion distally (Vriesendorp *et al.*, 1992) and endocrine involvement is also implicated in the outcome (Vigneulle *et al.*, 1989; Vriesendorp *et al.*, 1992). A different approach to shielding involves the production of varying patterns of “abscopal” mouse duodenal ulceration after irradiation of different thoracic fields (Michalowski *et al.*, 1983). The lesions are seen with SEM to consist mainly of low villi rather than epithelial discontinuities, as implied by the term “ulcer” (Carr *et al.*, 1986). SEM villous scores reflect the presence of increasing degrees of damage from days to 1 month after treatment with a moderate dose, although there is marked individual variation, particularly latterly. The areas covered by abnormal villi implicate variable damage to the pyloric sphincter as a cause, possibly due to radiation damage to the sympathetic nerve trunks or to the splanchnic nerves.

### 3. Radiation Type—LET

High-LET beams are often delivered to the whole body and it is important that this should also be the case for comparator low-LET schedules. Because high LET may produce more damage per unit dose, isoeffect doses with respect to a reference assay, such as the intestinal microcolony assay, are often used. This assay method is used to compare the effects of low- and high-LET radiation (Alpen *et al.*, 1980; Fukutsu *et al.*, 1997), with figures calculated for the relative biologic effectiveness of different high-LET schedules by comparison with the reference low-LET radiation type. High-LET beams often contain proportions of low-LET radiation and some authors describe the use of a combination of both (Benk *et al.*, 1993). Most, but not all, data relate to single-dose schedules and there is a range of doses and species, with mouse the most common, but dog and pig also featured.

**a. Neutrons** The data here refer to unshielded schedules, mostly small intestine, particularly mouse. There are also some data from pig and dog. There are more early than late results.

Early results include a decrease in pig bile flow hours after irradiation with a very low dose of a mixed neutron/ $\gamma$  beam (Scanff *et al.*, 1999). This rises thereafter, but falls again several days later. The bile composition also alters, with more harmful dihydroxylated bile acids present. There are more parasitized crypts in mouse small intestine days after a low dose of neutrons than after a moderate, crypt isoeffect dose of  $\gamma$  rays (K. E. Carr *et al.*, 1984).

There is also villous blunting in pigs (Scanff *et al.*, 1999) and mice (K. E. Carr *et al.*, 1984) and ectopic glands in pigs after neutron irradiation (Scanff *et al.*, 1999). Collared crypts (Carr *et al.*, 1990) and surface giant cells are a feature days after neutron irradiation (Carr *et al.*, 1981). Greater villous damage is seen than after the corresponding  $\gamma$  dose, using very low/low doses chosen to be radiobiologically equivalent in terms of crypt counting (Hamlet *et al.*, 1976).

Neutrons produce more total histologic damage hours after treatment, similar damage after several days, and less damage by about 1 week. However, ultrastructural examination of the neutron group reveals further damage, particularly 7 days after treatment (Carr *et al.*, 1992a). There are time-dependent epithelial changes in villous nuclei, microvilli, mitochondria, and inclusion bodies and in cryptal nuclei, microvilli, and cell separation. Enterocyte numbers decrease earlier after neutron than after X irradiation. Several days after irradiation with a very low dose of n/ $\gamma$  (1/1) or  $\gamma$  alone irradiation, there are similar changes in pig apical membrane enzymes, but greater changes in basolateral membrane enzyme activity (Griffiths *et al.*, 1996).

With respect to nonepithelial tissues, over a period of days after a very low dose of neutron irradiation, there are early decreases in mouse small intestinal stromal cell profiles (Carr *et al.*, 1996). There are also time-dependent stromal ultrastructural changes in cell separation, cytoplasmic vacuolization, and inclusion bodies, but edema and capillary endothelial changes do not increase with time (Carr *et al.*,

1992a). There is shrinkage of lymphoid follicles (Scanff *et al.*, 1999) and greater depletion of intraepithelial lymphocytes (K. E. Carr *et al.*, 1984). By comparison, low-LET damage includes vascular changes only hours after radiation, not present after neutron treatment (Carr *et al.*, 1991b, 1996). Using higher crypt isoeffect doses, inclusions in deep stromal cells are dense and lysosome-like after low-dose neutron treatment and pale and lipid-like after moderate/high dose  $\gamma$  irradiation (Carr *et al.*, 1985). Connective tissue fibroblasts and fibrils are irregular and disorganized in both groups, but there are differences in the relationships between red blood cells and endothelium.

There is earlier muscle loss and nerve damage after neutron irradiation (Carr *et al.*, 1996). Muscle vacuolization or rarification and myofilament degeneration increase with time, while dense bodies are seen in nerve twigs at 1 week. The villous shape changes relate best to subcellular muscle damage, confirming that neuromuscular input is important for villous shape (Carr *et al.*, 1992a). At higher doses, muscle cell separation is seen only in the higher dose  $\gamma$ -ray group, while many more dense bodies are seen in nerve twigs in the neutron group (Carr *et al.*, 1985). There are also greater changes in VIP receptor characteristics after n/ $\gamma$  than after  $\gamma$  irradiation (Griffiths *et al.*, 1996).

With respect to early results for rat large intestine, crypt disorganization and surface breakdown are seen several days after a very low dose of neutrons (Francois *et al.*, 1999). Recovery is seen about 1 week after treatment. There is also decreased water and sodium ion absorption and increased potassium ion secretion. The details of the changes suggest that they may be linked to epithelial and neural changes rather than to a decrease in the number of mast cells.

Several hours after a very low dose of 1.1/1 mixed field n/ $\gamma$ , there is a decrease in expression of rat colonic insoluble mucins (Joubert *et al.*, 1999). The greatest depletion occurs several days after treatment (Fig. 26). In the next few days, neutral and acid mucins reach control levels before acid sulphated mucins.

In terms of late effects, dog duodenum, examined several months to years after fractionated very high total doses of neutrons (Zook *et al.*, 1983), shows ulceration, bleeding, and fibrosis.

**b. Heavy Ion Beams** The effect of using a higher LET than neutrons is explored by single-dose unshielded irradiation of mice with beams of heavy ions, such as neon, iron, and niobium. In the early time period, small intestinal villous scores show more damage after a low dose of neon ion irradiation, than after a higher, crypt isoeffect X-irradiation dose (Carr *et al.*, 1987). Some higher LET particle beams such as iron produce collared crypts (Carr *et al.*, 1990; Fig. 27). However, the greater total cellular damage seen after this irradiation does not persist with even higher LET such as niobium, and nonepithelial damage declines (Carr *et al.*, 1994). After irradiation with low to moderate doses of niobium ion beams, there is early dose-dependent loss of crypts, endocrine cells, and mitotic figures, but the loss of enterocytes and goblet and Paneth cells does not depend on dose.

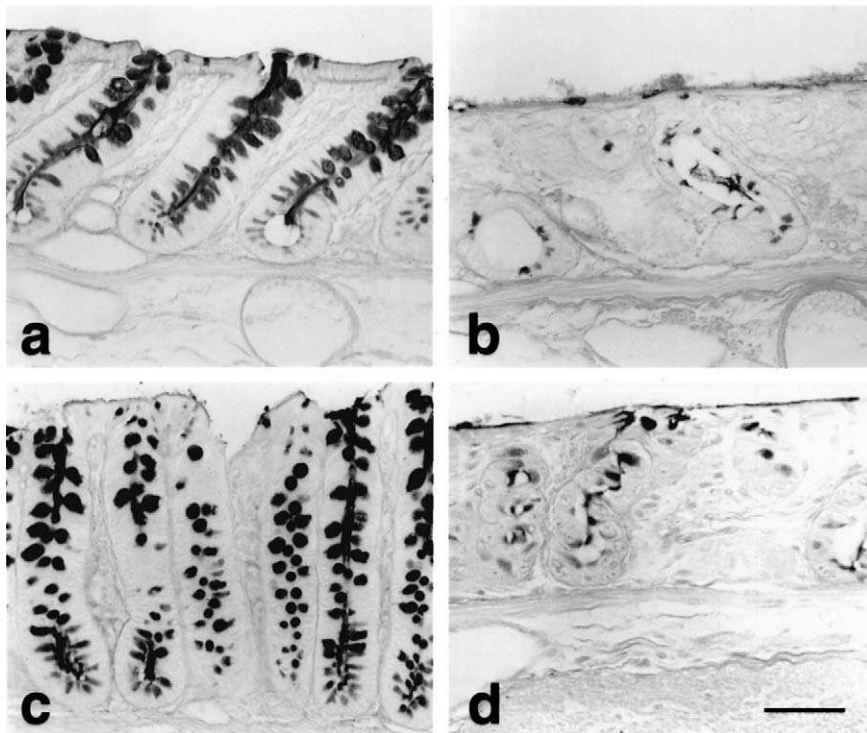


FIG. 26 Control rat distal colon stained with periodic acid Schiff (a) and high iron diamine (c). Micrographs (b) and (d) are the corresponding irradiated samples, 3 days after 6-Gy  $\gamma$ /neutron irradiation. Scale bar = 40  $\mu$ m. (Courtesy of C. Joubert, Institut de Protection et de Surete Nucleaire, France.).

One year after isodose irradiation of mice by a low dose of  $^{12}\text{C}$  or  $\gamma$  rays, the ultrastructural epithelial changes seen are similar, namely, enterocyte microvillus shortening and cytoplasmic vacuolization, loose intercellular junctions, and epithelial/mesenchymal contact through basal lamina herniations (Fatemi *et al.*, 1985). Paneth cell vacuolization is seen and the changes in large intestine are less marked. However, the vascular changes do differ across the two groups, with greater damage to vascular external laminae in the  $\gamma$ -irradiated group.

#### 4. Radiation, Time, and Dose

*a. Radiation Schedules* Many of these data sets refer to partial/single schedules. Different schedules do not always produce equivalent levels of early damage in mouse crypt counts and villous shape (Carr *et al.*, 1979). Three schedules produce

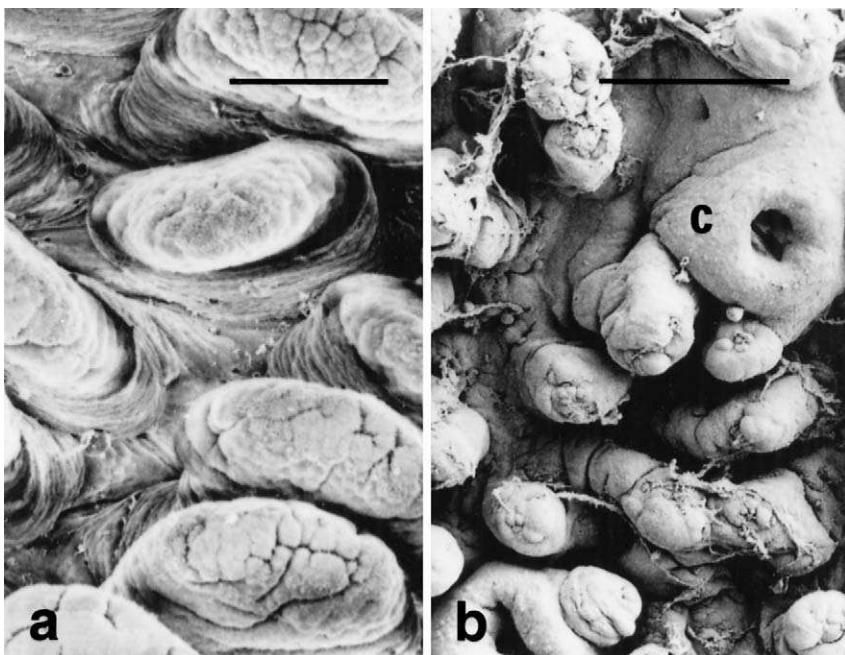


FIG. 27 Normal and irradiated crypts and villi. (a) Control jejunum, with villi and crypt mouths in the intervillous basin. Scale bar = 50  $\mu$ m. (b) One crypt of moderate size is seen beside a large collared crypt (c). A collared crypt nearby has a particularly large lumen. Iron 11 Gy, 5 days. Scale bar = 100  $\mu$ m. (Courtesy of B. Abbas.)

different levels of damage in pigs, classified as slight to moderate (Borgstrom *et al.*, 1985).

In rats, the fractionation schedule also affects the pattern of S-phase cell distribution (Becciolini *et al.*, 1983c, 1984) and the initial increase in goblet cell numbers (Becciolini *et al.*, 1985). Smaller daily fractions produce fewer ulcers and incidence rises with total dose (Scott *et al.*, 1995). Altering total dose and fraction schedule gives different mortality and radiation injury scores (Hauer-Jensen *et al.*, 1983b), particularly for mucosal ulceration and epithelial atypia. Macroscopic and microscopic injury is greater with shorter treatment time, both hours and weeks after irradiation (Hauer-Jensen *et al.*, 1988). A larger fraction produces a higher injury score and more fibrosis (Langberg *et al.*, 1996). Compressing the delivery time increases both early and late damage. Changes in arteriolar wall dimensions depend on fraction size, but not treatment time. The level of fibrosis correlates with ulcer incidence. The mucosal surface area affected increases with fraction size and compression of delivery time. Hours to months after concomitant boost fractionation (Allgood *et al.*, 1996), an early booster dose gives a higher injury score and decreases the cryptal labeling index, with more obstructions, fistulas, and

fibrosis. Intestinal complications and injury score also correlate with compression of delivery time and TGF- $\beta$  immunoreactivity (Richter *et al.*, 1996). Using a larger range of fractionation schedules, TGF- $\beta$  immunoreactivity and connective tissue mast cell hyperplasia are linked, suggesting that both are involved at a molecular level in the development of radiation injury (Richter *et al.*, 1997c).

There are so few reports of the morphologic effects of continuous irradiation that a separate section is not justified. Due to the accidental overexposure of a patient to a radioactive source broken in a catheter (Flynn *et al.*, 1995), continuous irradiation for several days with very high absorbed doses is reported, causing intestinal ulceration and lymphoid depletion, especially in Peyer's patches. There is also anorectal necrosis, with changes to vessels, stroma, and muscle. Exposure of mice to a very low dose of unshielded  $\gamma$  rays produces increasing levels of histologic small intestinal damage hours to days later (Brennan *et al.*, 1998). However, after protracted radiation with the same total dose over 25 days, both histologic and ultrastructural responses, some possibly adaptive, are seen hours after treatment finishes, decreasing in intensity over the next few days. The responses include changes in enterocytes, goblet and Paneth cells, and stroma.

With respect to late effects of fractionated schedules, the literature on fractionated radiotherapy of human subjects includes reference to correlation between incidence of complications and fractionation schedule (Ogino *et al.*, 1995), with a larger fraction dose increasing the incidence in humans (Deore *et al.*, 1993). In rats, splitting the dose into two as opposed to three fractions gives more small intestinal adenocarcinomas (Hauer-Jensen *et al.*, 1983b).

## 5. Ingested Radioactive Material

This type of exposure is by definition unshielded. There is continuing interest in the risks posed by environmental radionuclides (Harrison, 1995, 1998; Harrison and Stather, 1996) such as uranium (Taylor and Taylor, 1997) or radon (Sharma *et al.*, 1997). Exposure may be from background radiation, nuclear accidents, industrial plants, weapons testing, or medical use, and monitoring of effects is useful (Ropolo and Cesana, 1997). Radionuclides can also be accessed indirectly through the food chain (Hunt *et al.*, 1998; Fisk and Sanderson, 1999; Risica *et al.*, 1999; Sanchez *et al.*, 1999). Radionuclides vary in their uptake, distribution, kinetics, and retention profiles; models for estimating the associated doses and risks undergo regular review (Harrison, 1995; Harrison and Stather, 1996). Important radionuclide parameters include emission characteristics, half-life, and chemical properties, including similarities to substances normally dealt with by the body. Parameters relevant to the subject include age, transit time, and any underlying pathophysiology. The toxicity of radionuclides varies considerably, with differences of several orders of magnitude in dose per unit of activity ingested or inhaled. For example,  $^{3}\text{H}$  as tritiated water has weak  $\beta$  emission and short-term retention in the body and therefore low toxicity. On the other hand, polonium-210

and plutonium-237 are examples of  $\alpha$ -emitting nuclides with high toxicity (Harrison, 1995). Uptake by experimental animals (Sullivan *et al.*, 1987; Naylor *et al.*, 1993) or human volunteers (Giussani *et al.*, 1998) has been assessed. Most ingested particles are excreted by the gastrointestinal tract within days (Lang and Raunemaa, 1991). Radioactive iodine, as used in treatment of thyroid cancer, leads to a decrease in rat intestinal endocrine cell numbers hours to days after oral ingestion (Kvetnoy *et al.*, 1996). There are few morphologic data sets, although the Russian and Ukrainian literature has several descriptions of changes in small intestine of animal or human subjects exposed during the Chernobyl accident; English language abstracts of these can be retrieved electronically. Small intestinal changes reported include mucosal atrophy, metaplasia and dysplasia, abnormalities of proliferation or regeneration, inflammation, and disturbances in GALT. Ultrastructural effects include abnormalities in immune, epithelial, and stromal cells and changes in microvilli, organelles, and nuclei.

## B. Pathophysiology

### 1. Immune Status

Germ-free piglets 8 days after whole-body irradiation show increased jejunal sucrase activity, fewer absorptive vacuoles, and increased prominence of lysosomes and goblet cells (Kozakova *et al.*, 1994). There are more fibroblasts: fibrosis and vessel leakiness are also present, but no lymphocytes are seen and myeloid cells are scarcer. The longer renewal time in germ-free animals is associated with diminished signs of radiation damage.

### 2. Surgical Status or Physical Intervention

The effects of radiation on wound healing are important clinically, since surgical removal of a patient's tumor may be accompanied by radiotherapy, which can involve the surgical anastomoses. Surgery is seen as one of the treatments increasing the likelihood of complications after radiotherapy (Gerard *et al.*, 1995). Experimental surgically induced inflammatory features include fibrin clots, leukocyte and macrophage activity, and collagen synthesis (Biert *et al.*, 1998), all parameters affected by irradiation. Because of the risk of conflicting or complementary effects on fibrosis, several experimental studies of combined surgery and radiation are reported. Most, but not all, protocols use rat tissue and single/partial schedules. There are few other standard features, except within each research group: some use small intestine and some large, some irradiated before and others after surgery, and the parameters assessed differ. There is early rather than late decrease in wound strength in small intestine (Tepper *et al.*, 1983; Johnson *et al.*, 1995), but little consensus for large intestine (Biert *et al.*, 1993; Seifert *et al.*, 1995).

Minimal early and late morphologic changes are reported for small intestine (Tepper *et al.*, 1983), but there are also reports of late decreased capillary beds in small intestine (Jahson *et al.*, 1998). Although early changes in large intestine are only seen when hyperthermia is also used (Biert *et al.*, 1998), there are also reports of large intestinal accumulation of collagen and other matrix proteins and increases in gelatinolytic and collagenolytic enzymes (Seifert *et al.*, 1995, 1997). It is therefore likely that radiation does have a delaying effect, a conclusion reached in a review of gastrointestinal wound healing (Thornton and Barbul, 1997). The format of the anastomosis may also be important (Tepper *et al.*, 1983), while a further worrying possibility is the increase in radiation-induced tumors at the anastomoses (McCue *et al.*, 1995).

There are studies of the effects of other forms of surgical or physical intervention on the outcome of partial/single schedules on rats. These include reports of the radioprotective effects of pancreatic duct occlusion (Hauer-Jensen *et al.*, 1985) and hypoxia (Osborne *et al.*, 1970; Sebes *et al.*, 1975; Forsberg *et al.*, 1979).

With respect to fractionated doses, another form of physical intervention, with a direct clinical purpose, is the transplantation of intestinal grafts to provide a passage for swallowing and speech after surgical removal of neck tumors from patients, prior to radiotherapy. The grafts stand up well to the irradiation and are functionally useful as conduits, despite earlier villous blunting and later fibrosis (Grasl *et al.*, 1991; Wei *et al.*, 1998), similar to that seen after *in situ* irradiation.

### 3. Underlying Physiologic Variation or Pathology

**a. Time of Day of Irradiation** Although the time of day of delivery of treatment is in a sense related to the delivery of the radiation, it is fundamentally dependent on the physiologic variations in the intestine and is therefore dealt with here. The data are based on studies of rat small intestinal responses.

With respect to single-dose irradiation, the time of day of irradiation influences the extent of height loss, disorganization of the crypt–villus system, effectiveness of its recovery, and the distribution of S-phase cells (Becciolini *et al.*, 1982a, 1983a). There is more effective recovery of invertase activity in rats irradiated at the end of the dark period (Becciolini *et al.*, 1983b). The pattern of increase, decrease, and recovery is also dependent on the time of day of irradiation for brush border enzymes threlase, lactase, and alkaline phosphatase (Becciolini *et al.*, 1982c), but not for lysosomal enzymes (Becciolini *et al.*, 1982b).

Data are likewise available on the effects on responses to whole-body irradiation, confirming the importance of circadian rhythm for intestinal epithelial kinetics (Becciolini *et al.*, 1996): the detailed shape of the response curve varies with time of irradiation. The initial rise in goblet cell numbers (Fig. 28) is more marked in groups irradiated late in the day than in the other groups (Becciolini *et al.*, 1997). After a very low dose of irradiation, study of mouse parameters shows that the extent of apoptosis depends on the time of tissue sampling and duration

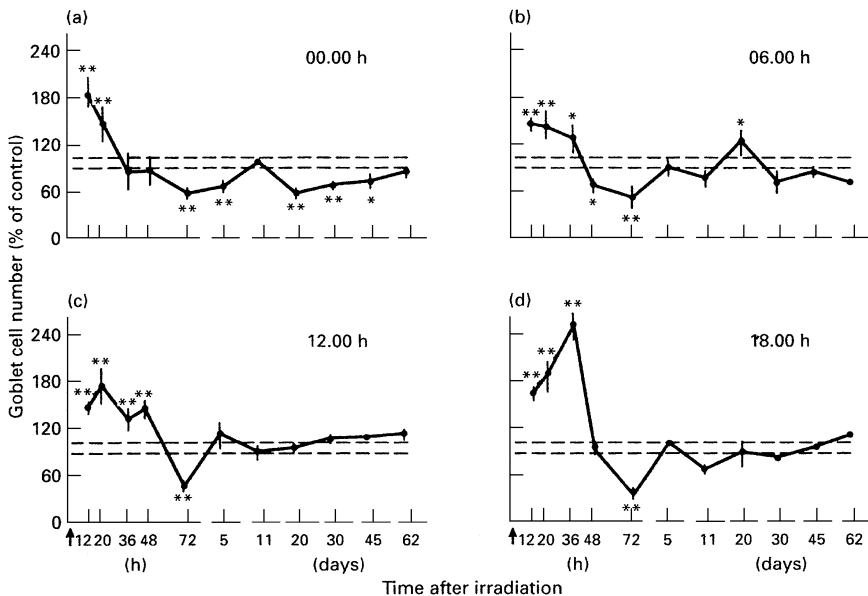


FIG. 28 Goblet cell number along the side of the crypt in groups of animals irradiated at four different times of the light/dark cycle; midnight (a), 0600 hr (b), midday (c), and 1800 hr (d). The mean values  $\pm$  SEM are shown expressed as a percentage of control values from animals sacrificed at the same time of the day. The limits of the mean standard error for the controls are shown as the dashed line. The arrow shows the time of irradiation. The first five time points are measured in hours and the last six in days. [Courtesy of A. Becciolini and Blackwell Science Ltd., Osney Mead, Oxford, OX2 OEL. Becciolini, A., Balzi, M., Fabbrica, D., and Potten, C. S. (1997). The effects of irradiation at different times of the day on rat intestinal goblet cells. *Cell Prolif.* **30**, 161–170, Fig. 2.]

between radiation and sampling (Rufrok *et al.*, 1998b). Mitotic index and crypt sensitivity also show some variation. Given the amount of data now being collected on radiation-induced changes in neuroendocrine cells, it is interesting that the influence of melatonin is proposed as a possible mechanism contributing to these variations.

**b. Underlying Pathology** With respect to fractionated schedules, in addition to the disadvantages of surgery, complications may be increased by obesity, chemotherapy, age, or emaciation (Gerard *et al.*, 1995; Touboul *et al.*, 1996). The theme of variation in response highlighted earlier is echoed in the description of patients with “constitutional” hypersensitivity to radiation, linked to possible genetic factors and leading to the need for further testing of varying degrees of sensitivity in cells such as fibroblasts (Touboul *et al.*, 1996). However, there are different accounts of possible overlap between radiation and collagen disease. Some authors list it as an indicator for care in constructing the radiotherapy schedule

(Gerard *et al.*, 1995) and others separate out rheumatoid arthritis (RA) as having no increased risk of late complications, unlike non-RA, which does (Morris and Powell, 1997).

Vascular pathology may also carry increased risk (Gerard *et al.*, 1995; Touboul *et al.*, 1996). Diabetes could therefore be expected to be relevant because of its effects on the vascular system, which is also affected by radiation and the same two groups report a risk of complications for these patients. Diabetes is also mentioned by another group, commenting on increased risk of radiation-induced intestinal and urinary complications in patients with this disease or hypertension (van Nagell *et al.*, 1979). They recommend assessing vascular competence by fundoscopic examination of the retina, since there is a correlation between vascular health there and in pelvic vessels. To balance these reports of increased complications in patients exposed to fractionated radiotherapy, there is one experimental study on streptozotocin-diabetic mice. Several days after a single low dose of partial body irradiation, jejunum, with more diabetic-induced changes than duodenum or ileum, has fewer radiation-associated changes, implying that diabetes gives a modicum of radioprotection (Ettarh *et al.*, 2000).

Despite its relevance, there has been little study of possible different responses by normal intestinal tissue as opposed to neighboring tumors. One study on human rectum describes changes in the endothelial surface protein thrombomodulin (TM), TGF- $\beta$ , and urokinase plasminogen activator (uPA) in patients treated with 5-fluorouracil and irradiation, the latter either 7 weeks (early group) or 12 months (late group) before surgical resection (Richter *et al.*, 1998). While down-regulation of TM is significant for normal tissue side effects, along with up-regulation of the fibrogenetic cytokine TGF- $\beta$ , the down-regulation of TM could also affect the response of the tumor. Unirradiated tumors have more TM+ve vessels, uPA+ve cells, and TGF- $\beta$  immunoreactivity than normal tissue. Radiation decreases the proportions of TM+ve vessels in both groups. Irradiation of tumors decreases the amount of uPA+ve cells and TGF- $\beta$  immunoreactivity. There are fewer TM+ve vessels in irradiated rectum from patients with recurrent tumors, but these could not be distinguished from primary tumors with respect to any of the three parameters used. The findings confirmed the role of endothelium in the development of rectal radiation damage.

## C. Treatment or Intervention

### **1. Medical Treatment**

Pharmacologic agents are selected to deal with the various symptomatic components of radiation enteritis in patients, such as changes in motility, malabsorption of bile salts, and bacterial changes (Classen *et al.*, 1998). Other treatments include hyperbaric oxygen for a range of radiation-induced late problems in patients

(Feldmeier *et al.*, 1996), improving vascularity by promoting endarterial neovascularization, and healing of hypoxic or necrotic tissues.

## 2. Diet and Dietary Supplements

Data are available on the effects of diet on single dose and also fractionated schedules, mostly the former, reporting on changes in rat small intestine and some other organs.

Most single-dose experiments use partial body schedules. A short-term diet rich in saturated fatty acids prevents early changes in brush border membrane lipid composition and uptake of some fatty acids (Thomson *et al.*, 1989a). Quicker recovery in absorptive function is also produced by using an elemental diet, decreasing mechanical abrasion and intraluminal toxicity (Mohiuddin and Kramer, 1978). Glutamine protects against changes in mucosal, villous, and mitotic parameters (Klimberg *et al.*, 1990) and bacterial uptake and translocation to lymph nodes (Klimberg *et al.*, 1990; Chun *et al.*, 1997), possibly due to its role in energy substrate provision for maintenance of the barrier function facilitated by tight junctions. Increased synthesis of glutathione also protects against the early radiation-induced high incidence of bacteria in lymph nodes, possibly by protecting against increases in levels of free radicals (Blair *et al.*, 1996).

Dietary or luminal administration of vitamin E, an antioxidant and free radical scavenger, leads to a reduced response in crypt numbers, mucosal thickness, and goblet cell numbers after irradiation (Felemovicius *et al.*, 1995). Vitamin A has a radioprotective effect on ulceration, vascular sclerosis, and fibrosis, but not on ectopic glands, atypical regeneration, or inflammatory processes (Beyzadeoglu *et al.*, 1997). Possible mechanisms for these effects center on its impact on epithelial differentiation and its fostering of wound healing through moderation of the inflammatory and immune responses and collagenesis. Effects of oral enprostil, a synthetic prostaglandin, are mixed, with some uptake profiles improved, but other damage parameters unaffected or even exacerbated (Keelan *et al.*, 1989; Thomson *et al.*, 1989b).

Fewer data are available from whole-body schedules. One describes diet-dependent variation in postirradiation anorexia and weight loss in rats (Bounous and Pageau, 1983). Another addresses the concern that glutamine, as well as protecting normal tissues, might make tumor cells more radioresistant. Gurbuz *et al.* (1998) therefore studied the effect of arginine, which aids wound healing, protects the immune system, and is a substrate for nitric oxide synthase. It protects some villous dimensions and mucus-secreting cells and decreases the number of bacterial colony-forming units in mesenteric lymph nodes, perhaps through a nitric oxide-dependent pathway or through its key role in macrophage function.

There are also few reports on the dietary moderation of the effects of fractionated schedules. An early account describes patient improvement in body weight and other general parameters (Bounous *et al.*, 1975). A glutamine enriched total

parenteral nutrition diet is used for a patient with intestinal fibrosis (Wicke *et al.*, 1996). Villous atrophy, epithelial loss, and microvillous shortening in irradiated dog small intestine are all substantially avoided by the use of an elemental diet (McArdle *et al.*, 1985), as are abnormal mitochondria and damaged endoplasmic reticulum. The basement membrane is intact, contributing to the continuing regularity of the villous epithelial sheet. Glutamine is reported to have no further effect on intestinal structure when added to elemental diets (McArdle, 1994), which, unsupplemented, assist the radioprotective activity of xanthine oxidase, superoxide dismutase, and glutathione dismutase. The discrepancy between this finding and that noted above for glutamine may be due to variations in protocol, species, radiation delivery, and parameter assessment.

### 3. Mechanistic Experiments

Many of these are based mainly on unshielded irradiation schedules and the data can be presented according to which tissue type they affect. With respect to changes in epithelial response, radiation is one of the models of mucositis (Farrell *et al.*, 1998) used to test the hypothesis that pretreatment with keratinocyte growth factor (KGF) could act as a radioprotectant, acting mainly on epithelial cells, either as a mitogen or specifically by stimulating production of mucus secreting cells (Khan *et al.*, 1997). Crypt survival, crypt depth, and villous height all show less damage in the KGF-treated groups (Farrell *et al.*, 1998). Radiation produces a reduction in responsiveness to secretion-promoting intervention, such as electrical field stimulation in rat ileum (MacNaughton *et al.*, 1994). A decrease in response to secretagogues forskolin and 5-HT is also seen in rat colon (Dublineau *et al.*, 1998).

Using intervention aimed at the immune system, the bacterial immunomodulator Nocardia delipidated cell mitogen produces more lymphocytes in unirradiated germ-free piglets and increased enzyme activity in the control group for both lactase and sucrase, but not after irradiation (Kozakova *et al.*, 1994). Morphologic improvements in the early radiation response are seen in enterocytes, goblet cells, lymphocytes, and stromal and myeloid cells. Inhibition of angiotensin I converting enzyme has some early protective effects on crypt counts and injury scores (Yoon *et al.*, 1994).

With respect to the neuromuscular response, Indran *et al.* (1991) test the hypothesis that radiation-induced changes in villous shape are influenced by damage in the smooth muscle layer by comparing the effects of irradiation and reserpine. This pharmacologic agent inhibits sympathetic neuronal function, allows overriding parasympathetic activity, contracts the muscle, and pulls the villous tips down via structural components running from the muscle layer to villous tips. The reserpine-treated villi are similar to those in irradiated groups, but show less damage. The timing of the villous collapse in the reserpine group coincides with the onset of parasympathetic dominance and it is concluded that the first two stages

of collapse are associated with changes in smooth muscle. Atropine, chosen to have the opposite effect, decreasing gastrointestinal motility through its action as a muscarinic antagonist of acetylcholine, provides radioprotection with respect to villous scores, muscle damage, and crypt depletion (Carr *et al.*, 1991a).

For partial/single irradiation of rats, the administration of growth hormone reduces radiation-induced bacterial translocation (Prieto *et al.*, 1998). The importance of TGF- $\beta$  and endothelial changes is confirmed by the results of administering an appropriate receptor protein and an inhibitor of platelet aggregation, respectively (Zheng *et al.*, 2000b; Wang *et al.*, 2000a). There are also some comments on moderation of the outcome of fractionated schedules. Radioprotective substances include those that minimize the effect of free radicals, such as superoxide dismutase or substances with a sulfhydryl grouping (Touboul *et al.*, 1996). Vasopressin injected into pigs gives different levels of radioprotection in several parameters, including villi, inflammation, and lymphoid tissue (Borgstrom *et al.*, 1985). The use of a synthetic somatostatin analog diminishes mucosal and other aspects of structural injury in rat small intestine, possibly through its influence on epithelial proliferation, motility, blood flow, and exocrine and endocrine secretions of the gastrointestinal system (Wang *et al.*, 1999b). The role of TGF- $\beta$  is again confirmed by the increased radiation injury after administration of an appropriate inducer (Hauer-Jensen *et al.*, 2000).

#### D. Summary of Changes of All Radiation Schedules

The scope of any review is dependent on the data available. Until recently, accounts of changes in the epithelial proliferative compartment form a large part of the literature, while other structures are more neglected, such as lymphatic vessels and serous membranes. Finally, the need to classify data according to so many radiation and biologic parameters, in order to make this review useful to radiation scientists as well as morphologists, makes it difficult to guarantee precision in every detail of protocols. Where necessary, original sources should be consulted. The current situation can be summarized by following the order used in the text so far.

Multiparameter or scoring methods for response to radiation injury are useful in interschedule comparisons, in pinpointing interindividual variations, and in identifying parameters needing further study, such as nerve or lymphatic vessels.

With respect to compartments, several aspects of the luminal zone may be relevant, including bile salts, pancreactic or other enzymes, pH and mucus, with attendant microorganisms. Luminal changes may affect microvilli, membrane enzyme activity, and tight junctions, which in turn may affect the absorption of nutrients and the uptake of bacteria. There is little information on the effects of fractionated irradiation on the luminal compartment. However, its possible importance is underlined by the good response to radiotherapy of intestinal tissues transplanted to the head and neck region, where the salivary luminal environment is less hostile than that of the intestine *in situ*.

In other compartments, reported changes include villous atrophy, cryptal epithelial mitotic arrest, epithelial degeneration, and alterations in S-phase profiles and villous-cryptal feedback loops. Signaling routes include cycling villous enterocytes and p53-related cryptal apoptosis, or cryptal clusterin and postapoptotic remodeling. The balance between cryptal proliferative and secretory functions is influenced by changes in the levels of TGF- $\beta$ , TGF- $\alpha$ , and EGF. The ongoing increases in TGF- $\beta$  and its activator are related to early mucosal injury and later fibrosis. Villous collapse involves not only the epithelium, but also vessels, stromal cells, and underlying muscle.

Other compartmental changes include ulceration; mucosal thinning; submucosal thickening due to edema and later fibrosis; and stromal, membrane, and SOD changes in the muscle layer. Some changes occur at interfaces between compartments or tissues. These include epithelial/stromal stripping, basal lamina gaps or reduplication, epithelial/stromal contacts, protrusion of ectopic glands through weakened muscularis mucosae, and damage to the pericryptal myoblast sheath. Neoplasia is the ultimate compartmental change; there remains debate about its relationship to earlier alterations.

The responses of individual cell types vary widely. Enterocyte changes include disturbance in water and ion movement and alterations in electrophysiologic responses, pointing to input from neural and mast cells. The involvement of iNOS confirms its role in abnormal as well as physiologic conditions. Although the changes in enterocytes are wide ranging, there is little disagreement about their general nature. This is not quite the case for other epithelial cells. However, from the data available, it can be concluded that goblet cells show particular sensitivity to the dose/time/delivery continuum and Paneth cells may respond differently to partial and whole-body treatment.

It is possible that more data are needed on the deposition of collagen after unshielded radiation. Other schedules show early as well as late collagen deposition and responses of collagenolytic and gelatinolytic enzymes, fibroblasts, TGF- $\beta$ , and mast cells. Inflammatory and vascular responses are also important and both leukocyte and endothelial adhesion molecules are involved in the cycle of ROS/TGF- $\beta$ /ROS production induced by local irradiation. Other early mechanisms involve TNF- $\alpha$ , TGF- $\beta$ , the coagulation mechanisms, and further cytokine up-regulation.

Many of the radiation-induced changes in smooth muscle are measured electrophysiologically and some of the few reported structural changes can be related to functional or mechanistic aberrations. These include abnormalities of myofilament organization and links between contractile activity and neurotensin levels. There is also cell membrane degeneration and involvement of membrane SP binding sites. Damage to mitochondria may be related to changing levels of MnSOD. Collagen deposition in the muscle layer is associated with increased TGF- $\beta$ .

Neuroendocrine cells respond to radiation, but there could be confusion between granule or cell depletion and raised serum or tissue levels of relevant hormones. All that can be said currently is that there is a response from all three main groups of enteroendocrine hormones, including gastrin, enteroglucagon, VIP, substance P, and

neurotensin, with complex effects on acid secretion, enzyme production, glucose and lipid balance, and smooth muscle activity. Some of these substances are also implicated in the changes in nervous tissue, including VIP and SP in the mucosa and plexuses; the outcome is again complicated. In addition, there are changes in CGRP and NPY innervation of mesenteric vessels. These changes in hormones or neurotransmitters are matched by other alterations involving molecular rather than histologic effects. Several enzyme systems are affected, including enterocyte brush border enzymes and proteases. Some cytokines contribute to several different aspects of the response and cytokine input is important in epithelial proliferation, secretion, inflammation, thrombogenesis, fibrogenesis, and radioprotection. Granulocyte marker protein is useful as a noninvasive marker.

Subcellular effects, apart from those at nuclei and microvilli, include changes in the lateral cell membranes, tight junctions, mitochondria and cytoplasmic membranes, filaments, and inclusions. In Section II.B.2, the general importance of ROS and other free radicals is stressed. The intestine is no exception and ROS are pinpointed as possible initiators of damage, for example, in leukocyte/endothelial adhesion changes. This is confirmed by increased levels of SOD during the radiation response and by the effectiveness of interventions to enhance the radioprotective activity of such enzymes.

The effects of irradiation appear, therefore, to be felt by cells in epithelium, muscle, nerve, and connective tissues and in all of the compartments examined.

## **VII. Conclusions**

The general conclusion is that the response of the intestine to irradiation is multifactorial, with all cells probably involved to some extent. Even cells with responses that have been little studied, such as the neuroendocrine components, show significant changes at both microscopic and molecular levels. Signals from cells such as these, or from noncellular structures such as epithelial and vascular basal laminae, could be important in developing the responses of their neighbors, even those known for some time to have a marked radiation response. Despite the fact that these new data sets are available, much still needs to be done.

The lacunae in the radiation literature include most interfaces and several collective structures. These include duodenal submucosal glands, mesothelial cells and the underlying serosal connective tissues, lymphatic vessels, lymphoid and neuroendocrine cells, and other possibly significant groupings, such as those of nerve elements with interstitial cells or neuroendocrine and other cell types. More work is also needed on the responses of several individual cell types, on extracellular structures, and on "cross-talk" around the intestinal component parts. Data are already available on the use of genetic manipulation to probe the responses of specific constituents, such as mast cells, or the relationships between compartments,

such as crypt and villous epithelium. More will be learned about the response to radiation by the extension of this work.

All radiation-induced abnormalities, whether currently well documented or requiring much further data, can only be appreciated if the corresponding normal situation is fully understood. As can be seen from Section II, work is currently being done on many normal intestinal constituents. Until such basic studies are complete, the understanding of the radiation response is likely to be imperfect. There may also be a need to update the radiation data whenever new results of significance are published on normal structure and function.

More information is also needed on the effects of stress, relevant to endocrine responses; of diet and its possible radioprotective effects; and on the links between radiation enteropathy and aging, necessary as a control for late effects. More data are also needed on the complex interactions between radiation and underlying pathology, or other clinical interventions such as transplantation or wound healing after surgery. Although it is known that germ-free status carries a measure of radioprotection, there is little information on the effects of immunologic impairment on the response to radiation.

When variations in the conditions of the irradiation are considered, there are also some neglected areas. Further work on the impact of different fractionation and combined schedules would undoubtedly be helpful. Few aspects of the response under several standard conditions are sufficiently understood; for example, using both partial and whole-body treatments. Such comparisons as are available suggest that schedule-related variations in responses by cells such as neutrophils and Paneth cells may depend on the extent of damage to other structures, such as the bone marrow and vessels or nerves supplying the intestine. Another area relating to radiation conditions concerns reports that low-LET radiation may produce more early vascular effects than high-LET schedules and that both total damage and nonepithelial injury peak at intermediate LET, decreasing as LET continues to rise. It also appears possible that radiation delivered very close to the intestinal wall, as in IORT, may produce a unique profile of response, as seen already in large vessels. Further systematic studies on these and related areas would be clinically and mechanistically helpful.

There is thus likely to be as much further movement toward a better understanding of the intestinal response to radiation in the near future as there has been in the recent past. There may even be further progress toward an appreciation of the way in which the individual changes and accompanying "cross-talk" combine to produce the final multiparameter response of the impaired organ. Further insight may be gained into the role of signaling molecules, such as hormones, neurotransmitters and substances such as NO and CO and into mechanisms for countering the effects of free radicals.

These aspects may need to be related to current topics of interest in radiobiology, where there are as yet, few available data on the relevance of genomic instability and the "bystander" effect to the response from entire organs. However, the fact that the intestine is a multiparameter organ with a variable response and not an

isolated cell preparation points to the importance of the microenvironment in any individual cell's response. Each cell's situation can be defined by several parameters. For example, an enterocyte usually has six or seven cellular neighbors able to influence it, either conventionally if themselves "unhit" by the radiation, or through the "bystander" effect if "hit." There could be a choice of around five options for the cellular makeup of the neighbors, including all neighbors being of the same enterocyte type, or five enterocytes plus another cell type, such as secretory, immune, or neuroendocrine. There are also two macro-interfaces, luminal and basal, each of which could have a variable response to radiation. When options are considered for influences on the cell from its neighbors, several hundred possibilities could arise. These would be made up of different combinations of "hit/unhit" and displaying genomic instability or not, although the extent of the latter would be related to the time between radiation and cell shedding. A substantial proportion of these options could be attributable to "bystander" effects. The situation would be complicated further by more than one hit per cell or the different circumstances of low- and high-LET schedules.

Other cell types could have a similarly large range of options, with the details being influenced by the relative balance of neighboring cells and interfaces. For all cell types, it would be important if a neighbor has a particularly radioprotective function, such as goblet or Paneth cells; is a dedicated information signaler, such as neuroendocrine cells; is part of a population with many subsets, such as endocrine or immune cells; or is affected by an underlying altered pathophysiologic state.

This large amount of potential variation in the microenvironment could explain the difficulty of obtaining a standard profile, at subcellular level, of the postirradiation changes in intestinal cell types. The fact that variation at the cellular level is much less marked could indicate the presence of a limited number of likely influences at this level for each cell type. It may be important to explore more thoroughly the causes of data variation within and across cell types in a multiparameter organ, instead of ignoring those aspects of the response that do not satisfy statistical testing. There may be a link between the very variability of the organ response and some of the current questions being asked about the importance of the microenvironment, genomic stability, and the "bystander" effect.

Given the large volume of data currently available, the involvement of most cell types in the integrated response, the preliminary burst of molecular data and the advances current in radiobiology, it is indeed "the best of times and the worst of times" to be reviewing this subject.

## Acknowledgments

I am grateful to Professor D. T. Goodhead, MRC Radiation and Genome Stability Unit, Harwell, and to Professor J. F. Morris, Department of Human Anatomy and Genetics, University of Oxford, for access to library and other unit and departmental facilities during a period of study leave. I am also grateful to those who have kindly provided illustrations or tabular material, to present and past collaborators for

their input to data and micrograph collections, and to Mr. Adrian Ford, MRC Harwell, and his colleagues for their expert photographic and computer contribution. Finally, I am indebted to colleagues at MRC Harwell, National Radiological Protection Board, the Universities of Oxford and Glasgow, and the Royal Hospitals Trust, Belfast, for valuable advice on the manuscript. Any remaining errors are my responsibility and I offer apologies to any author whose work has been omitted or inaccurately cited during the classification of data from such a diverse field.

## References

Abbas, B., Boyle, F. C., Wilson, D. J., Nelson, A. C., and Carr, K. E. (1990a). Radiation induced changes in the blood capillaries of rat duodenal villi: A corrosion cast, light and transmission electron microscopical study. *J. Submicrosc. Cytol. Pathol.* **22**, 63–70.

Abbas, B., Hume, S. P., McCullough, J. S., Wilson, D. J., Stewart, P. C., and Carr, K. E. (1990b). Early morphological changes in blood capillaries of mouse duodenal villi induced by X-irradiation. *J. Submicrosc. Cytol. Pathol.* **22**, 609–614.

Adams, G. E., Wilson, A., and Hamlet, R. (1999). Radiation toxicology. In "General and Applied Toxicology," 2nd ed. (B. Ballantyne, T. Marrs, and T. Syversen, Eds.), pp. 1683–1701. Macmillan Reference Ltd., London.

Ahmadu-Suka, F., Gillette, E. L., Withrow, S. J., Husted, P. W., Nelson, A. W., and Whiteman, C. E. (1988). Pathologic response of the pancreas and duodenum to experimental intraoperative irradiation. *Int. J. Radiat. Oncol. Biol. Phys.* **14**, 1197–1204.

Ainsworth, M. A., Koss, M. A., Hogan, D. L., and Isenberg, J. I. (1995). Higher proximal duodenal mucosal bicarbonate secretion is independent of Brunner's glands in rats and rabbits. *Gastroenterology* **109**, 1160–1166.

Ainsworth, M. A., Hogan, D. L., Rapier, R. C., Amelsberg, M., Dreilinger, A. D., and Isenberg, J. I. (1998). Acid/base transporters in human duodenal enterocytes. *Scand. J. Gastroenterol.* **33**, 1039–1046.

Allgood, J. W., Langberg, C. W., Sung, C.-C., and Hauer-Jensen, M. (1996). Timing of concomitant boost irradiation affects incidence and severity of intestinal complications. *Int. J. Radiat. Oncol. Biol. Phys.* **34**, 381–387.

Alpen, E. L. (1998). "Radiation Biophysics," 2nd ed. Academic Press, San Diego.

Alpen, E. L., Powers-Risius, P., and McDonald, M. (1980). Survival of intestinal crypt cells after exposure to high Z, high energy charged particles. *Radiat. Res.* **83**, 677–687.

Altmann, G. G. (1974). Changes in the mucosa of the small intestine following methotrexate administration or abdominal X-irradiation. *Am. J. Anat.* **140**, 263–280.

Anderson, J. H., and Withers, R. H. (1973). Scanning electron microscope studies of irradiated rat intestinal mucosa. *Scanning Electron Microsc.* **3**, 565–571.

Appenzeller, O., and Oribe, E. (1997). "The Autonomic Nervous System: An Introduction to Basic and Clinical Concepts," 5th ed. Elsevier Science B. V., Amsterdam.

Arai, S., Kowada, T., Takehana, K., Miyoshi, K., Nakanishi, Y. H., and Hayashi, M. (1996a). Apoptosis in the chicken bursa of Fabricius induced by X-irradiation. *J. Vet. Med. Sci.* **58**, 1001–1006.

Arai, T., Kida, Y., Harmon, B. V., and Gobe, G. C. (1996b). Expression and localization of clusterin mRNA in the small and large intestine of the irradiated rat: its relationship with apoptosis. *Int. J. Radiat. Biol.* **69**, 547–553.

Aumailley, M., and Smyth, N. (1998). The role of laminins in basement membrane function. *J. Anat.* **193**, 1–21.

Bach, S. P., Rencham, A. G., and Potten, C. S. (2000). Stem cells; The intestinal stem cell as a paradigm. *Carcinogenesis* **21**, 469–476.

Balemba, O. B., Grondahl, M. L., Mbassa, G. K., Semuguruka, W. D., Hay-Smith, A., Skadhauge, E., and Dantzer, V. (1998). The organisation of the enteric nervous system in the submucous and

mucous layers of the small intestine of the pig, stained by VIP and neurofilament protein immunohistochemistry. *J. Anat.* **192**, 257–267.

Beaulieu, J.-F. (1999). Integrins and human intestinal cell functions. *Front. Biosci.* **4**, D310–D321.

Becciolini, A. (1987). Relative radiosensitivities of the small and large intestine. *Adv. Radiat. Biol.* **12**, 83–128.

Becciolini, A., Cariaggi, P., and Gori, A. (1975). Behaviour of intestinal lactase after irradiation. *Strahlentherapie* **150**, 145–148.

Becciolini, A., Cremonini, D., Balzi, M., Fabbrica, D., and Cinotti, S. (1982a). Irradiation at different times of the day. Morphology and kinetics of the small intestine. *Acta Radiol. Oncol.* **21**, 169–175.

Becciolini, A., Giache, V., Lanini, A., Cremonini, D., and Drighi, E. (1982b). Modifications of small intestine lysosomal enzymes after irradiation at different times of the day. *Acta Radiol. Oncol.* **21**, 61–66.

Becciolini, A., Lanini, A., Giache, V., Balzi, M., and Bini, R. (1982c). Modifications in the brush border enzymes of the small intestine after irradiation at different times of the day. *Acta Radiol. Oncol.* **21**, 273–279.

Becciolini, A., Balzi, M., Cremonini, D., and Fabbrica, D. (1983a). S-phase cell distribution in the small intestine irradiated at different times of the day. I. Acute irradiation injury. *Acta Radiol. Oncol.* **22**, 305–313.

Becciolini, A., Balzi, M., Cremonini, D., and Fabbrica, D. (1983b). S-phase cell distribution in the small intestine irradiated at different times of the day. II. Recovery phase. *Acta Radiol. Oncol.* **22**, 337–344.

Becciolini, A., Cremonini, D., Fabbrica, D., and Balzi, M. (1983c). Modifications of S-phase cell distribution in the intestinal crypts after multiple daily fractionation. *Acta Radiol. Oncol.* **22**, 441–448.

Becciolini, A., Cremonini, D., Fabbrica, D., and Balzi, M. (1984). Qualitative and quantitative effects on the morphology of the small intestine after multiple daily fractionation. *Acta Radiol. Oncol.* **23**, 353–359.

Becciolini, A., Fabbrica, D., Cremonini, D., and Balzi, M. (1985). Quantitative changes in the goblet cells of the rat small intestine after irradiation. *Acta Radiol. Oncol.* **24**, 291–299.

Becciolini, A., Giache, V., Balzi, M., and Morrone, A. (1987). Brush border intestinal enzymes after multiple daily fractionation. *Radiat. Res.* **109**, 374–381.

Becciolini, A., Balzi, M., Fabbrica, D., and Potten, C. S. (1996). Cell kinetics in rat small intestine after exposure to 3 Gy of  $\gamma$ -rays at different times of the day. *Int. J. Radiat. Biol.* **70**, 281–288.

Becciolini, A., Balzi, M., Fabbrica, D., and Potten, C. S. (1997). The effects of irradiation at different times of the day on rat intestinal goblet cells. *Cell Prolif.* **30**, 161–170.

Ben, V. A., Adams, J. A., Shipley, W. U., Urie, M. M., McManus, P. L., Efird, J. T., Willett, C. G., and Goitein, M. (1993). Late rectal bleeding following combined X-ray and proton high dose irradiation for patients with stages T3–T4 prostate carcinoma. *Int. J. Radiat. Oncol. Biol. Phys.* **26**, 551–557.

Bergers, G., and Coussins, L. M. (2000). Extrinsic regulators of epithelial tumour progression: metalloproteinas. *Curr. Opin. Genet. Dev.* **10**, 120–127.

Berghem, L. E., and Johanson, K.-J. (1983). Effect of  $^{137}\text{Cs}$  gamma radiation on the fibronectin content in basement membrane of mouse small intestine. *Acta Radiol. Oncol.* **22**, 389–393.

Beyzadeoglu, M., Balkan, M., Demiriz, M., Tibet, H., Dirican, B., Oner, K., and Pak, Y. (1997). Protective effect of vitamin A on acute radiation injury in the small intestine. *Radiat. Med.* **15**, 1–5.

Biert, J., Wobbes, T., Hendriks, T., and Hoogenhout, J. (1993). Effect of irradiation on healing of newly made colonic anastomoses in the rat. *Int. J. Radiat. Oncol. Biol. Phys.* **27**, 1107–1112.

Biert, J., Siefert, W. F., Verhoffstad, A. A. J., Wobbes, T., de Man, B. M., Hoogenhout, J., and Hendriks, T. (1998). A semiquantitative histological analysis of repair of anastomoses in the rat colon after combined preoperative irradiation and local hyperthermia. *Radiat. Res.* **149**, 372–377.

Bjerknes, M., and Cheng, H. (1999). Clonal analysis of mouse intestinal epithelial progenitors. *Gastroenterology* **116**, 7–14.

Black, W. C., Gomez, L. S., Yuhas, J. M., and Kligerman, M. M. (1980). Quantitation of the late effects of X-radiation on the large intestine. *Cancer (N.Y.)* **45**, 444–451.

Blair, S. L., Rose, D. M., Sachar, S., and Burt, M. E. (1996). Oral L-2-oxo-4-thiazolidine reduces bacterial translocation after radiation in the Fischer rat. *J. Surg. Res.* **65**, 165–168.

Blomlie, V., Rofstad, E. K., Trope, C., and Lien, H. H. (1999). Critical soft tissues of the female pelvis: Serial MR imaging before, during, and after radiation therapy. *Radiology* **203**, 391–397.

Borgstrom, S., Aronsen, K. F., Augustsson, N.-E., Bjelkengren, G., Lindstrom, C., and Nylander, G. (1985). The protective effect of intra-arterial vasopressin injections on the small bowel during fractionated abdominal irradiation. A study in pigs. *Acta Radiol. Oncol.* **24**, 401–405.

Bouatrouss, Y., Poisson, J., and Beaulieu, J.-F. (1998). Studying the basement membrane. In “Methods in Disease: Investigating the Gastrointestinal Tract” (V. R. Preedy and R. R. Watson, Eds.), pp. 191–200. Greenwich Medical Media Ltd., London.

Bounous, G., and Pageau, R. (1983). Effect of dietary protein quality on the resistance of rats to total body radiation. *Strahlentherapie* **159**, 123–124.

Bounous, G., Le Bel, E., Shuster, J., Gold, P., Tahan, W. T., and Bastin, E. (1975). Dietary protection during radiation therapy. *Strahlentherapie* **149**, 476–483.

Brandsch, C., Friedl, P., Lange, K., Richter, T., and Mothes, T. (1998). Primary culture and transfection of epithelial cells of human small intestine. *Scand. J. Gastroenterol.* **33**, 833–838.

Brennan, P. C., Carr, K. E., Seed, T., and McCullough, J. S. (1998). Acute and protracted radiation effects on small intestinal morphological parameters. *Int. J. Radiat. Biol.* **73**, 691–698.

Brittingham, J., Phiel, C., Trzyna, W. C., Gabbeta, V., and McHugh, K. M. (1998). Identification of distinct molecular phenotypes in cultured gastrointestinal smooth muscle cells. *Gastroenterology* **115**, 605–617.

Buell, M. G., and Harding, R. K. (1989). Proinflammatory effects of local abdominal irradiation on rat gastrointestinal tract. *Dig. Dis. Sci.* **34**, 390–399.

Busch, D. B. (1990). Pathology of the radiation-damaged bowel. In “Radiation Enteritis” (R. B. Galland and J. Spencer, Eds.), pp. 66–87. Edward Arnold, a division of Hodder and Stoughton, London.

Cai, W. B., Roberts, S. A., Bowley, E., Hendry, J. H., and Potten, C. S. (1997a). Differential survival of murine small and large intestinal crypts following ionizing radiation. *Int. J. Radiat. Biol.* **71**, 145–155.

Cai, W. B., Roberts, S. A., and Potten, C. S. (1997b). The number of clonogenic cells in crypts in three regions of murine large intestine. *Int. J. Radiat. Biol.* **71**, 573–579.

Camilleri, M., Hasler, W. L., Parkman, H. P., Quigley, E. M. M., and Soffer, E. (1998). Measurement of gastrointestinal motility in the GI laboratory. *Gastroenterology* **115**, 747–762.

Campbell, F., Fuller, C. E., Williams, G. T., and Williams, E. D. (1994). Human colonic stem cell mutation frequency with and without irradiation. *J. Pathol.* **174**, 175–182.

Capps, G. W., Fulcher, A. S., Szuchs, R. A., and Turner, M. A. (1997). Imaging features of radiation-induced changes in the abdomen. *RadioGraphics* **17**, 1455–1473.

Carr, A. M. (2000). Piecing together the p53 puzzle. *Science* **287**, 1765–1766.

Carr, K. E., and Toner, P. G. (1972). Surface studies of acute radiation injury in the mouse intestine. *Virchows Arch. B* **11**, 201–210.

Carr, K. E., Hamlet, R., Nias, A. H. W., and Watt, C. (1979). Lack of correlation between villus and crypt damage in irradiated mouse intestine. *Br. J. Radiol.* **52**, 485–493.

Carr, K. E., Hamlet, R., Nias, A. H. W., and Watt, C. (1981). Multinucleate giant enterocytes in small intestinal villi after irradiation. *J. Microsc. (Oxford)* **123**, 169–176.

Carr, K. E., Hume, S. P., Marigold, J. C. L., and Michalowski, A. (1982). Scanning and transmission electron microscopy of the damage to small intestinal mucosa following X irradiation or hyperthermia. *Scanning Electron Microsc.* **1**, 393–402.

Carr, K. E., Hamlet, R., Nias, A. H. W., and Watt, C. (1983). Damage to the surface of the small intestinal villus: An objective scale of assessment of the effects of single and fractionated radiation doses. *Br. J. Radiol.* **56**, 467–475.

Carr, K. E., Hamlet, R., Nias, A. H. W., and Watt, C. (1984). Morphological differences in the response of mouse small intestine to radiobiologically equivalent doses of X- and neutron irradiation. *Scanning Electron Microsc.* **1**, 445–454.

Carr, K. E., Hamlet, R., Nias, A. H. W., Boyle, F. C., and Fife, M. G. (1985). Stromal damage in the mouse small intestine after  $^{60}\text{Co}$  gamma or D-T neutron irradiation. *Scanning Electron Microsc.* **4**, 1615–1621.

Carr, K. E., Ellis, S., and Michalowski, A. (1986). Surface studies of duodenal lesions induced by thoracic irradiation. *Scanning Electron Microsc.* **1**, 209–219.

Carr, K. E., Hayes, T. L., Indran, M., Bastacky, S. J., McAlinden, G., Ainsworth, E. J., and Ellis, S. (1987). Morphological criteria for comparing effects of X-rays and neon ions on mouse small intestine. *Scanning Microsc.* **1**, 799–809.

Carr, K. E., Hayes, T. L., Abbas, B., and Ainsworth, E. J. (1990). Collared crypts in irradiated small intestine. *J. Submicrosc. Cytol. Pathol.* **22**, 265–271.

Carr, K. E., Bullock, C., Ryan, S. S., McAlinden, M. G., and Boyle, F. C. (1991a). Radioprotectant effects of atropine on small intestinal villous shape. *J. Submicrosc. Cytol. Pathol.* **23**, 569–577.

Carr, K. E., McCullough, J. S., Nunn, S., Hume, S. P., and Nelson, A. C. (1991b). Neutron and X-ray effects on small intestine summarized by using a mathematical model or paradigm. *Proc. R. Soc. Lond. Ser. B* **243**, 187–194.

Carr, K. E., McCullough, J. S., Nelson, A. C., Hume, S. P., Nunn, S., and Kamel, H. H. M. (1992a). Relationship between villous shape and mural structure in neutron irradiated small intestine. *Scanning Microsc.* **6**, 561–572.

Carr, K. E., Nelson, A. C., Hume, S. P., and McCullough, J. S. (1992b). Characterisation through a data display of the different cellular responses in X-irradiated small intestine. *J. Radiat. Res.* **33**, 163–177.

Carr, K. E., McCullough, J. S., Gilmore, R. St. C., Abbas, B., Hume, S. P., Nelson, A. C., Hayes, T. L., and Ainsworth, E. J. (1993). Effects of neon ions, neutrons and X rays on small intestine. In “Biological Effects and Physics of Solar and Galactic Cosmic Radiation. Part A” (C. E. Swenberg, G. Horneck, and E. G. Stassinopoulos, Eds.), pp. 203–216. Plenum Press, New York.

Carr, K. E., McCullough, J. S., Brennan, P., Hayes, T. L., Ainsworth, E. J., and Nelson, A. C. (1994). Heavy ion induced changes in small intestinal parameters. *Adv. Space Res.* **14**, 521–530.

Carr, K. E., Hume, S. P., Nelson, A. C., O’Shea, O., Hazzard, R. A., and McCullough, J. S. (1996). Morphological profiles of neutron and X-irradiated small intestine. *J. Radiat. Res.* **37**, 38–48.

Carr, N. D., Pullen, B. R., Hasleton, P. S., and Schofield, P. F. (1984). Microvascular studies in human radiation bowel disease. *Gut* **25**, 448–454.

Carratu, R., Secondulfo, M., de Magistris, L., Daniele, B., Pignata, S., D’Agostino, L., Frezza, P., Elmo, M., Silvestro, G., and Sasso, F. S. (1998). Assessment of small intestinal damage in patients treated with pelvic radiotherapy. *Oncol. Rep.* **5**, 635–639.

Chen, D., Hoshi, H., Tanaka, K., and Murakami, G. (1995). Postnatal development of lymphoid follicles in rat Peyer’s patches, with special reference to increased follicle number. *Arch. Histol. Cytol.* **58**, 335–343.

Chomette, G., Daburon, F., Auriol, M., and Garnier, H. (1977). High-dose irradiation in the pig small intestine. Histoenzymology and electron microscopic study. *Virchows Arch. B* **23**, 237–256.

Chun, H., Sasaki, M., Fujiyama, Y., and Bamba, T. (1997). Effect of enteral glutamine on intestinal permeability and bacterial translocation after abdominal radiation injury in rats. *J. Gastroenterol.* **32**, 189–195.

Ciecura, L., Bartel, H., Kaczmarek, B., and Harazna, J. (1976). Radiation-induced histochemical and ultrastructural changes in the enterocytes in the rabbit. *Folia Histochem. Cytochem.* **14**, 83–90.

Classen, J., Belka, C., Paulsen, F., Budach, W., Hoffmann, W., and Bamberg, M. (1998). Radiation-induced gastrointestinal toxicity. Pathophysiology, approaches to treatment and prophylaxis. *Strahlenther. Onkol.* **174**(Suppl. 3), 82–84.

Cobb, R. A., and Galland, R. B. (1990). Early reports of radiation-damaged gut. In “Radiation Enteritis”

(R. B. Galland and J. Spencer, Eds.), pp. 1–6. Edward Arnold, a division of Hodder and Stoughton, London.

Coia, L. R., Myerson, R. J., and Tepper, J. E. (1995). Late effects of radiation therapy on the gastrointestinal tract. *Int. J. Radiat. Oncol. Biol. Phys.* **31**, 1213–1236.

Coleman, C. N. (2000). Review of “Biological Basis of Radiation Sensitivity.” Rosen, E. M., Fan, S., Goldberg, I. D., and Rockwell, S. *Oncology*, **14**, 757–761.

Coleman, C. N., and Harris, J. R. (1998). Current scientific issues related to clinical radiation oncology. *Radiat. Res.* **150**, 125–133.

Conklin, J. J., and Hagan, M. P. (1987). Research issues for radiation protection during prolonged space flight. In “Advances in Radiation Biology,” 13th ed. (J. T. Lett, U. K. Lehmann, and A. B. Cox, Eds.), pp. 235–284. Academic Press, London.

Coopersmith, C. M., and Gordon, J. I. (1997).  $\gamma$ -ray-induced apoptosis in transgenic mice with proliferative abnormalities in their intestinal epithelium: Re-entry of villus enterocytes into the cell cycle does not affect their radioresistance but enhances the radiosensitivity of the crypt by inducing p53. *Oncogene* **15**, 131–141.

Corring, T., Daburon, F., Remy, J., Guengeau, A. M., Roger, A., and Tricaud, Y. (1975). Effects of acute irradiation on exocrine pancreatic secretion in the pig. *Strahlentherapie* **149**, 417–425.

Coutinho, H. B., Robalinho, T., Coutinho, V. B., Amorin, A. M. S., Almeida, J. R., Filho, J. T. O., Walker, E., King, G., Sewell, H. F., and Wakelin, D. (1996). Immunocytochemical demonstration that human duodenal Brunner’s glands may participate in intestinal defence. *J. Anat.* **189**, 193–197.

Daniel, E. E., Wang, Y.-F., and Cayabyab, F. S. (1998). Role of gap junctions in structural arrangements of interstitial cells of Cajal and canine smooth muscle. *Am. J. Physiol.* **274**, G1125–G1141.

de Boer, J., and Hoeijmakers, J. H. J. (2000). Nucleotide excision repair and human syndromes. *Carcinogenesis* **21**, 453–460.

Delaney, J. P., Kimm, G. E., and Bonsack, M. E. (1992). The influence of luminal pH on the severity of acute radiation enteritis. *Int. J. Radiat. Biol.* **61**, 381–386.

Deore, S. M., Shrivastava, S. K., Supe, S. J., Viswanathan, P. S., and Dinshaw, K. A. (1993).  $\alpha/\beta$  value and importance of dose per fraction for the late rectal and recto-sigmoid complications. *Strahlenther. Onkol.* **169**, 521–526.

Der-Silaphet, T., Malysz, J., Hagel, S., Arsenault, A. L., and Huizinga, J. D. (1998). Interstitial cells of Cajal direct normal propulsive contractile activity in the mouse small intestine. *Gastroenterology* **114**, 724–736.

Dewey, W. C., Ling, C. C., and Meyn, R. E. (1995). Radiation-induced apoptosis: Relevance to radiotherapy. *Int. J. Radiat. Oncol. Biol. Phys.* **33**, 781–796.

Dewit, L., and Oussoren, Y. (1987). Late effects in the mouse small intestine after a clinically relevant multifractionated radiation treatment. *Radiat. Res.* **110**, 372–384.

Diffley, J. F. X., and Evan, G. (2000). Oncogenes and cell proliferation. Cell cycle, genome integrity and cancer—a millennial view [editorial overview]. *Curr. Opin. Genet. Dev.* **10**, 13–16.

Duan, R.-D. (1998). Sphingomyelin hydrolysis in the gut and clinical implications in colorectal tumorigenesis and other gastrointestinal diseases [review]. *Scand. J. Gastroenterol.* **33**, 673–683.

Dublineau, I., Ksas, B., Aigueperse, J., Gourmelon, P., and Griffiths, N. M. (1998). *In vivo* alterations of fluid and electrolyte fluxes in rat colon by gamma irradiation. *Dig. Dis. Sci.* **43**, 652–662.

Dubois, A., King, G. L., and Livengood, D. R. (1995). “Radiation and the Gastrointestinal Tract.” CRC Press, Boca Raton, FL.

Dutta, S., Barber, B. J., and Parameswaran, S. (1995). Texture analysis of protein distribution images to find differences due to aging and superfusion. *Ann. Biomed. Eng.* **23**, 772–786.

Ebert, E. C. (1998). Interleukin 15 is a potent stimulant of intraepithelial lymphocytes. *Gastroenterology* **115**, 1439–1445.

Egawa, J., and Ishioka, K. (1978). Radiation effects on the fine blood vessels in abdominal organs of mice. *Acta Radiol. Oncol.* **17**, 414–422.

Erbil, Y., Dibekoglu, C., Turkoglu, U., Ademoglu, E., Berber, E., Kizir, A., Mercan, S., and Toker, G. (1998). Nitric oxide and radiation enteritis. *Eur. J. Surg.* **164**, 863–868.

Eriksson, B. (1982). Microangiographic pattern in the small intestine of the cat after irradiation. *Scand. J. Gastroenterol.* **17**, 887–895.

Eriksson, B., and Johnson, L. (1983). Capillary filtration in the small intestine after irradiation. An experimental study in the cat. *Scand. J. Gastroenterol.* **18**, 209–215.

Eriksson, B., Johnson, L., and Rubio, C. (1982). A semiquantitative histological method to estimate acute and chronic radiation injury in the small intestine of the cat. *Scand. J. Gastroenterol.* **17**, 1017–1024.

Eriksson, B., Johnson, L., and Lundqvist, P.-G. (1983). Ultrastructural aspects of capillary function in irradiated bowel. An experimental study in the cat. *Scand. J. Gastroenterol.* **18**, 473–480.

Esposito, V., Linard, C., Maubert, C., Aigueperse, J., and Gourmelon, P. (1996). Modulation of gut substance P after whole-body irradiation. *Dig. Dis. Sci.* **41**, 2070–2077.

Esposito, V., Linard, C., Wysocki, J., Griffiths, N. M., and Mathe, D. (1998). A substance P receptor antagonist (FK 888) modifies gut alterations induced by ionizing radiation. *Int. J. Radiat. Biol.* **74**, 625–632.

Ettarh, R. R., Hodges, G. M., and Carr, K. E. (2000). Radiation effects in the small bowel of the diabetic mouse. *Int. J. Radiat. Biol.* **76**, 241–248.

Fajardo, L. F., and Berthrong, M. (1988). Vascular lesions following radiation. *Pathol. Annu.* **23**, 297–330.

Farrell, C. L., Bready, J. V., Rex, K. L., Chen, J. N., DiPalma, C. R., Whitcomb, K. L., Yin, S., Hill, D. C., Wiemann, B., Starnes, C. O., Havill, A. M., Lu, Z. N., Aukerman, S. L., Pierce, G. F., Thomason, A., Potten, C. S., Ulich, T. R., and Lacey, D. L. (1998). Keratinocyte growth factor protects mice from chemotherapy and radiation-induced gastrointestinal injury and mortality. *Cancer Res.* **58**, 933–939.

Fatemi, S. H., Antosh, M., Cullan, G. M., and Sharp, J. G. (1985). Late ultrastructural effects of heavy ions and gamma irradiation in the gastrointestinal tract of the mouse. *Virchows Arch. B* **48**, 325–340.

Feldmeier, J. J., Heimbach, R. D., Davolt, D. A., Court, W. S., Stegmann, B. J., and Sheffield, P. J. (1996). Hyperbaric oxygen: an adjunctive treatment for delayed radiation injuries of the abdomen and pelvis. *Undersea Hyperbaric Med.* **23**, 205–213.

Felemonvicius, I., Bonsack, M. E., Baptista, M. L., and Delaney, J. P. (1995). Intestinal radioprotection by vitamin E (alpha-tocopherol). *Ann. Surg.* **222**, 504–508.

Finnon, P., Lloyd, D. C., and Edwards, A. A. (1995). Fluorescence *in situ* hybridization detection of chromosomal aberrations in human lymphocytes: Applicability to biological dosimetry. *Int. J. Radiat. Biol.* **68**, 429–435.

Fisk, S., and Sanderson, D. C. (1999). Chernobyl-derived radiocesium in heather honey and its dependence on deposition patterns. *Health Phys.* **77**, 431–435.

Flickinger, J. C., Bloomer, W. D., and Kinsella, T. J. (1990). Intestinal tolerance of radiation injury. In “Radiation Enteritis” (R. B. Galland and J. Spencer, Eds.), pp. 49–65. Edward Arnold, a division of Hodder and Stoughton, London.

Flynn, D. F., Mihalakis, I., Mauceri, T., and Pins, M. R. (1995). Gastrointestinal syndrome after accidental overexposure during radiotherapy. In “Radiation and the Gastrointestinal Tract” (A. Dubois, G. L. King, and D. R. Livengood, Eds.), pp. 225–234. CRC Press, Boca Raton, FL.

Forsberg, J. O., Jiborn, H., and Jung, B. (1979). Protective effect of hypoxia against radiation induced fibrosis in the rat gut. *Acta Radiol. Oncol.* **18**, 65–67.

Forsgren, S., Hockerfelt, U., Norrgard, O., Henriksson, R., and Franzen, L. (2000). Pronounced substance P innervation in irradiation-induced enteropathy—a study on human colon. *Regul. Pept.* **88**, 1–13.

Francois, A., Aigueperse, J., Gourmelon, P., MacNaughton, W. K., and Griffiths, N. M. (1998). Exposure to ionizing radiation modifies neurally-evoked electrolyte transport and some inflammatory responses in rat colon *in vitro*. *Int. J. Radiat. Biol.* **73**, 93–101.

Francois, A., Dublineau, I., Lebrun, F., Ksas, B., and Griffiths, N. M. (1999). Modified absorptive and secretory processes in the rat distal colon after neutron irradiation: *in vivo* and *in vitro* studies. *Radiat. Res.* **151**, 468–478.

Freeman, S. L., and MacNaughton, W. K. (2000). Ionizing radiation induces iNOS-mediated epithelial dysfunction in the absence of an inflammatory response. *Am. J. Physiol.* **278**, G243–G250.

Fukutsu, K., Kanai, T., Furusawa, Y., and Ando, K. (1997). Response of mouse intestine after single and fractionated irradiation with accelerated carbon ions with a spread-out Bragg peak. *Radiat. Res.* **148**, 168–174.

Gabe, S. M., Bjarnason, I., Tolou-Ghamari, Z., Tredger, J. M., Johnson, P. G., Barclay, G. R., Williams, R., and Silk, D. B. A. (1998). The effect of tacrolimus (FK506) on intestinal barrier function and cellular energy production in humans. *Gastroenterology* **115**, 67–74.

Galland, R. B., and Spencer, J. (1990). “Radiation Enteritis.” Edward Arnold, a division of Hodder and Stoughton, London.

Gamaley, I. A., and Klyubin, I. V. (1999). Roles of reactive oxygen species: signaling and regulation of cellular functions. *Int. Rev. Cytol.* **188**, 203–255.

Garabedian, E. M., Roberts, L. J. J., McNevin, M. S., and Gordon, J. I. (1997). Examining the role of Paneth cells in the small intestine by lineage ablation in transgenic mice. *J. Biolog. Chem.* **272**, 23,729–23,740.

Gard, P. R. (1998). “Human Endocrinology.” Taylor and Francis Ltd., London.

Geisinger, K. R., Scobey, M. W., Northway, M. G., Cassidy, K. T., and Castell, D. O. (1990). Radiation-induced proctitis cystica profunda in the rat. *Dig. Dis. Sci.* **35**, 833–839.

Gerard, J. P., Coquard, R., Romestaing, P., Ardiel, J. M., Rocher, F. P., Trillet Lenoir, V., and Sentenac, I. (1995). Prevention of radiation related complications in the treatment of rectal adenocarcinoma. The importance of the dose volume relationship. *Tumori* **81**(3 Suppl.), 114–116.

Giussani, A., Cantone, M. C., de Bartolo, D., Roth, P., and Werner, E. (1998). A revised model of molybdenum biokinetics in humans for application in radiation protection. *Health Phys.* **75**, 479–486.

Gordon, A. T., and McMillan, T. J. (1997). A role for molecular radiobiology in radiotherapy? *Clin. Oncol.* **9**, 70–78.

Grasl, M. C., Kornfehl, J., Neuchrist, C., Ehrenberger, K., Piza, H., Roka, R., Braun, O., and Stanek, C. (1991). Histological study of the influence of postoperative irradiation of free transplanted jejunal grafts. *Laryngo-Rhino-Otol.* **70**, 375–379.

Grider, J. R., Foxx-Orenstein, A. E., and Jin, J.-G. (1998). 5-hydroxytryptamine<sub>4</sub> receptor agonists initiate the peristaltic reflex in human, rat, and guinea pig intestine. *Gastroenterology* **115**, 370–380.

Griffin, C. S., Marsden, S. J., Stevens, D. L., Simpson, P., and Savage, J. R. (1995). Frequencies of complex chromosome exchange aberrations induced by <sup>238</sup>Pu alpha-particles and detected by *in situ* hybridization using single chromosome-specific probes. *Int. J. Radiat. Biol.* **67**, 431–439.

Griffiths, N. M., Francois, A., Dublineau, I., Lebrun, F., Joubert, C., Aigueperse, J., and Gourmelen, P. (1996). Exposure to either gamma or a mixed neutron/gamma field irradiation modifies vasoactive intestinal peptide receptor characteristics in membranes isolated from pig jejunum. *Int. J. Radiat. Biol.* **70**, 361–370.

Griffiths, N. M., Linard, C., Dublineau, I., Francois, A., Esposito, V., Niemer-Tucker, M. M. B., van der Hage, M., Broerse, J. J., and Wagemaker, G. (1999). Long-term effects of X-irradiation on gastrointestinal function and regulatory peptides in monkeys. *Int. J. Radiat. Biol.* **75**, 183–191.

Grosovsky, A. (1999). Radiation-induced mutations in unirradiated DNA. *Proc. Natl. Acad. Sci. USA* **96**, 5346–5347.

Gunter-Smith, P. J. (1989). Gamma radiation affects active electrolyte transport by rabbit ileum. II. Correlation of alanine and theophylline response with morphology. *Radiat. Res.* **117**, 419–432.

Gunter-Smith, P. J. (1995). The effect of radiation on intestinal electrolyte transport. In “Radiation and the Gastrointestinal Tract” (A. Dubois, G. L. King, and D. R. Livengood, Eds.), pp. 149–160. CRC Press, Boca Raton, FL.

Gurbuz, A. T., Kunzelman, J., and Ratzer, E. E. (1998). Supplemental dietary arginine accelerates intestinal mucosal regeneration and enhances bacterial clearance following radiation enteritis in rats. *J. Surg. Res.* **74**, 149–154.

Haboubi, N. Y., Schofield, P. F., and Rowland, P. L. (1988). The light and electron microscopic features of early and late phase radiation-induced proctitis. *Am. J. Gastroenterol.* **83**, 1140–1144.

Hale, M. L., and McCarthy, K. F. (1984). Effect of sublethal ionizing radiation on rat Peyer's patch lymphocytes. *Radiat. Res.* **99**, 151–164.

Hamlet, R., Carr, K. E., Toner, P. G., and Nias, A. H. W. (1976). Scanning electron microscopy of mouse intestinal mucosa after cobalt-60 and D-T neutron irradiation. *Br. J. Radiol.* **49**, 624–629.

Hamlet, R., Carr, K. E., Nias, A. H. W., and Watt, C. (1981). Surface damage in the small intestine of the mouse after X- or neutron irradiation. *Scanning Electron Microsc.* **4**, 73–78.

Hampton, J. C. (1966). Effects of ionizing radiation on the fine structure of Paneth cells of the mouse. *Radiat. Res.* **28**, 71–83.

Hampton, J. C., and Rosario, B. (1972). The fine structure of intestine and liver in irradiated mice during fat absorption. *Radiat. Res.* **52**, 152–167.

Hanson, W. R. (1995). Modification of radiation injury to the intestine by eicosinoids and thiol radio-protectors. In "Radiation and the Gastrointestinal Tract" (A. Dubois, G. L. King, D. R. Livengood, Eds.), pp. 171–181. CRC Press, Boca Raton, FL.

Harrison, J. D. (1995). Ingested radionuclides. In "Radiation and Gut" (C. S. Potten and J. H. Hendry, Eds.), pp. 253–289. Elsevier Science, Amsterdam.

Harrison, J. D. (1998). Gut transfer and doses from environmental plutonium and americium. *J. Radiol. Prot.* **18**, 73–76.

Harrison, J. D., and Stather, J. W. (1996). The assessment of doses and effects from intakes of radioactive particles. *J. Anat.* **189**, 521–530.

Hasleton, P. S., Carr, N., and Schofield, P. F. (1985). Vascular changes in radiation bowel disease. *Histopathology* **9**, 517–534.

Hauer-Jensen, M. (1990). Late radiation injury of the small intestine. Clinical, pathophysiologic and radiobiologic aspects. A review. *Acta Oncol.* **29**, 401–415.

Hauer-Jensen, M., Sauer, T., Devik, F., and Nygaard, K. (1983a). Late changes following single dose Roentgen irradiation of rat small intestine. *Acta Radiol. Oncol.* **22**, 299–303.

Hauer-Jensen, M., Sauer, T., Devik, F., and Nygaard, K. (1983b). Effects of dose fractionation on late Roentgen radiation damage of rat small intestine. *Acta Radiol. Oncol.* **22**, 381–384.

Hauer-Jensen, M., Sauer, T., Berstad, T., and Nygaard, K. (1985). Influence of pancreatic secretion on late radiation enteropathy in the rat. *Acta Radiol. Oncol.* **24**, 555–560.

Hauer-Jensen, M., Poulakos, L., and Osborne, J. W. (1988). Effects of accelerated fractionation on radiation injury of the small intestine: A new rat model. *Int. J. Radiat. Oncol. Biol. Phys.* **14**, 1205–1212.

Hauer-Jensen, M., Richter, K. K., Wang, J., Abe, E., Sung, C.-C., and Hardin, J. W. (1998). Changes in transforming growth factor  $\beta$ 1 gene expression and immunoreactivity levels during development of chronic radiation enteropathy. *Radiat. Res.* **150**, 673–680.

Hauer-Jensen, M., Zheng, H., and Wang, J. (2000). Pharmacologic induction of transforming growth factor- $\beta$  enhances intestinal radiation toxicity. *Radiat. Res. Soc.* **47**, 143.

Hecht, G., and Savkovic, S. D. (1997). Effector role of epithelia in inflammation—interaction with bacteria [review]. *Aliment. Pharmacol. Ther.* **11**(Suppl. 3), 64–69.

Hendry, J. H., Cai, W. B., Roberts, S. A., and Potten, C. S. (1997). p53 deficiency sensitizes clonogenic cells to irradiation in the large but not the small intestine. *Radiat. Res.* **148**, 254–259.

Hirschowitz, L., and Rode, J. (1991). Changes in neurons, neuroendocrine cells and nerve fibres in the lamina propria of irradiated bowel. *Virchows Arch. A: Pathol. Anat. Histopathol.* **418**, 163–168.

Hockerfelt, U., Henriksson, R., Franzen, L., Norrgard, O., and Forsgren, S. (1999). Irradiation induces marked immunohistochemical expression of vasoactive intestinal peptide in colonic mucosa of man. *Dig. Dis. Sci.* **44**, 393–401.

Hockerfelt, U., Franzen, L., Kjorell, U., and Forsgren, S. (2000). Parallel increase in substance P and VIP in rat duodenum in response to irradiation. *Peptides* **21**, 271–281.

Huang, J., Padbury, R. T. A., Schloithe, A. C., Cox, M. R., Simula, M. E., Harvey, J. R., Baker, R. A., Toouli, J., and Saccone, G. T. P. (1998). Somatostatin stimulates the brush-tailed possum sphincter of Oddi *in vitro* and *in vivo*. *Gastroenterology* **115**, 672–679.

Huizinga, J. D., Thuneberg, L., Vanderwinden, J.-M., and Rumessen, J. J. (1997). Interstitial cells of Cajal as targets for pharmacological intervention in gastrointestinal motor disorders. *Trends Pharmacol. Sci.* **18**, 393–403.

Humble, C. A. (1995). Lymphedema: Incidence, pathophysiology, management, and nursing care. *Oncol. Nurs. Forum* **22**, 1503–1509.

Hunt, G. J. (1998). Transfer across the human gut of environmental plutonium, americium, cobalt, caesium and technetium: Studies with cockles (*Cerastoderma edule*) from the Irish sea. *J. Radiol. Prot.* **18**, 101–109.

Husebye, E., Hauer-Jensen, M., Kjorstad, K., and Skar, V. (1994). Severe late radiation enteropathy is characterised by impaired motility of proximal small intestine. *Dig. Dis. Sci.* **39**, 2341–2349.

Indran, M., Carr, K. E., and Boyle, F. C. (1988). Radiation-induced changes in mouse duodenal papilla. *Br. J. Radiol.* **61**, 1039–1042.

Indran, M., Carr, K. E., Gilmore, R. St. C., and Boyle, F. C. (1991). Mucosal changes in mouse duodenum after gamma-irradiation or reserpine treatment. *J. Submicrosc. Cytol. Pathol.* **23**, 267–278.

Izzo, A. A., Mascolo, N., and Capasso, F. (1998). Nitric oxide as a modulator of intestinal water and electrolyte transport. *Dig. Dis. Sci.* **43**, 1605–1620.

Jahnson, S., Graf, W., Rikner, G., and Gerdin, B. (1995). Anastomotic breaking strength and healing of anastomoses in rat intestine with and without chronic radiation damage. *Eur. J. Surg.* **161**, 425–430.

Jahnson, S., Christofferson, R. H., and Gerdin, B. (1998). Reduced mucosal perianastomotic capillary density in rat small intestine with chronic radiation damage. *Radiat. Res.* **150**, 542–548.

Johnson, R. J. R., Schemann, M., Santer, R. M., and Cowen, T. (1998). The effects of age on the overall population and on subpopulations of myenteric neurons in the rat small intestine. *J. Anat.* **192**, 479–488.

Joubert, C., Meslin, J. C., Forlac, D., and Strup, C. (1999). Effects of mixed field neutron irradiation on rat colonic insoluble mucin pattern expression. Paper presented at 11th International Congress of Radiation Research, Dublin.

Kallfass, E., Kramling, H.-J., and Schultz-Hector, S. (1996). Early inflammatory reaction of the rabbit coeliac artery wall after combined intraoperative (IORT) and external (ERT) irradiation. *Radiat. Oncol.* **39**, 167–178.

Kalman, D. R., Barnard, G. F., Massimi, G. J., and Swanson, R. S. (1995). Primary aortoduodenal fistula after radiotherapy. *Am. J. Gastroent.* **90**, 1148–1150.

Kandasamy, S. B. (1995). Neurochemical changes in the irradiated brain-gut axis. In “Radiation and the Gastrointestinal Tract” (A. Dubois, G. L. King, and D. R. Livengood, Eds.), pp. 101–110. CRC Press, Boca Raton, FL.

Kandasamy, S. B. (1998). Effect of ionizing radiation on the release of cholecystokinin in the hypothalamus of the rat. *Radiat. Res.* **150**, 298–303.

Kasai, K., Matsuura, A., Kikuchi, K., Hashimoto, Y., and Ichimiya, S. (1997). Localisation of rat CD1 transcripts and protein in rat tissues—an analysis of rat CD1 expression by *in situ* hybridisation and immunohistochemistry. *Clin. Exp. Immunol.* **109**, 317–322.

Kaur, A., Dubey, D. P., and Gupta, G. S. (1975). Radiation effects on alkaline phosphatase and glucose-6-phosphatase in anatomically different regions of mouse intestine. *Strahlentherapie* **150**, 427–432.

Kawabata, S., Boyaka, P. N., Coste, M., Fujihashi, K., Yamamoto, M., McGhee, J. R., and Kiyono, H. (1998). Intraepithelial lymphocytes from villus tip and crypt portions of the murine small intestine show distinct characteristics. *Gastroenterology* **115**, 866–873.

Keast, J. R. (1999). Unusual autonomic ganglia: Connections, chemistry, and plasticity of pelvic ganglia. *Int. Rev. Cytol.* **193**, 1–69.

Keelan, M., Cheeseman, C., Walker, K., and Thomson, A. B. R. (1986). Effect of external abdominal irradiation on intestinal morphology and brush border membrane enzyme and lipid composition. *Radiat. Res.* **105**, 84–96.

Keelan, M., Thomson, A. B. R., Clandinin, M. T., Tavernini, M., Walker, K., and Cheeseman, C. I. (1989). Effect of oral enprostil, a synthetic prostaglandin E<sub>2</sub>, on intestinal brush border membrane lipid composition following abdominal irradiation in the rat. *Clin. Invest. Med.* **12**, 350–356.

Khan, W. B., Shui, C., Ning, S., and Know, S. J. (1997). Enhancement of murine intestinal stem cell survival after irradiation by keratinocyte growth factor. *Radiat. Res.* **148**, 248–253.

Kim, G. E., Lim, J. J., Park, W., Park, H. C., Chung, E. J., Seong, J., Suh, C. O., Lee, Y. C., and Park, H. J. (1998). Sensory and motor dysfunction assessed by anorectal manometry in uterine cervical carcinoma patients with radiation-induced late rectal complication. *Int. J. Radiat. Oncol. Biol. Phys.* **41**, 835–841.

Klimberg, V. S., Souba, W. W., Dolson, D. J., Salloum, R. M., Hautamaki, R. D., Plumley, D. A., Mendenhall, W. M., Bova, F. J., Khan, S. R., Hackett, R. L., Bland, K. I., and Copeland, E. M., III (1990). Prophylactic glutamine protects the intestinal mucosa from radiation injury. *Cancer (N.Y.)* **66**, 62–68.

Klurfeld, D. M. (1999). Nutritional regulation of gastrointestinal growth. *Front. Biosci.* **4**, D299–D302.

Kozakova, H., Mandel, L., Trebichavsky, I., Kolinska, J., and Barot-Ciorbaru, R. (1994). Protective effects of Nocardia delipidated cell mitogen on the mucosa of the small intestine after irradiation of germ-free piglets. *Cell Biol. Int.* **18**, 237–243.

Krantis, A., Rana, K., and Harding, R. K. (1996). The effects of  $\gamma$ -radiation on intestinal motor activity and faecal pellet expulsion in the guinea pig. *Dig. Dis. Sci.* **41**, 2307–2316.

Kucharzik, Y., Lugering, N., Schmid, K. W., Schmidt, M. A., Stoll, R., and Domsche, W. (1998). Human intestinal M cells exhibit enterocyte-like intermediate filaments. *Gut* **42**, 54–62.

Kvetnoy, I. M., Yuzhakov, V. V., Molotkov, A. O., Bandurko, L. N., Brodsky, R. A., and Yakovleva, N. D. (1996). Diffuse neuroendocrine system: structural and functional effects of radiation injury to amine precursor uptake and decarboxylation (APUD) cells. *Scanning Microsc.* **10**, 261–278.

Lang, S., and Raunemaa, T. (1991). Behavior of neutro-activated uranium dioxide dust particles in the gastrointestinal tract of the rat. *Radiat. Res.* **126**, 273–279.

Langberg, C. W., Sauer, T., Reitan, J. B., and Hauer-Jensen, M. (1996). Relationship between intestinal fibrosis and histopathologic and morphometric changes in consequential and late radiation enteropathy. *Acta Oncol.* **35**, 81–87.

Lange, K. (1999). Microvillar Ca<sup>2+</sup> signalling: A new view of an old problem. *J. Cell. Physiol.* **180**, 19–34.

Lantz, B., and Einhorn, N. (1984). Intestinal damage and malabsorption after treatment for cervical carcinoma. *Acta Radiol. Oncol.* **23**, 33–36.

Leborgne, J., Bourret, J.-F., Heloury, Y., Paineau, J., and Le Neel, J.-C. (1984). Massive hemorrhage of colorectal origin. Exploratory procedures and therapeutic difficulties. *J. Chir. (Paris)* **121**, 39–49.

Lebrun, F., Francois, A., Vergnet, M., Lebaron-Jacobs, L., Gourmelon, P., and Griffiths, N. M. (1998). Ionizing radiation stimulates muscarinic regulation of rat intestinal mucosal function. *Am. J. Physiol.* **275**, G1333–G1340.

Lehy, T., Dessirier, V., Attoub, S., Bado, A., Griffiths, N. M., and Linard, C. (1998). Exposure to ionizing radiation modifies circulating gastrin levels and gastrointestinal endocrine cell densities in the rat. *Int. J. Radiat. Biol.* **73**, 331–340.

Lencer, W. I. (1998). Paneth cells: On the front line or in the backfield? *Gastroenterology* **114**, 1343–1345.

Lencer, W. I., and Alper, S. L. (1999). The potassium channel and how it works. *Gastroenterology* **116**, 216–217.

Lesher, J., and Lesher, S. (1970). Effects of single-dose, whole body,  $^{60}\text{Co}$  gamma irradiation on number of cells in DNA synthesis and mitosis in the mouse duodenal epithelium. *Radiat. Res.* **43**, 429–438.

Letschert, J. G. (1995). The prevention of radiation-induced small bowel complications. *Eur. J. Cancer* **31A**(7–8) 1361–1365.

Lewicki, Z., Figurski, R., and Sulikowska, A. (1975). Histological studies on the regeneration of small intestine epithelium of rats irradiated with sublethal doses of X-rays. *Pol. Med. Sci. Hist. Bull.* **15**, 539–549.

Libotte, F., Autier, P., Delmelle, M., Gozy, M., Pector, J. C., Van Houtte, P., and Gerard, A. (1995). Survival of patients with radiation enteritis of the small and the large intestine. *Acta Chir. Belg.* **95**(4 Suppl.) 190–194.

Linard, C., Griffiths, N. M., Esposito, V., Aigueperse, J., and Gourmelon, P. (1997). Changes in gut neurotensin and modified colonic motility following whole-body irradiation in rat. *Int. J. Radiat. Biol.* **71**, 581–588.

Lindqvist, S. M., Sharp, P., Johnson, I. T., Satoh, Y., and Williams, M. R. (1998). Acetylcholine-induced calcium signaling along the rat colonic crypt axis. *Gastroenterology* **115**, 1131–1143.

Little, J. B. (2000). Radiation carcinogenesis. *Carcinogenesis* **21**, 397–404.

Lorimore, S. A., Kadhim, M. A., Pocock, D. A., Papworth, D., Stevens, D. L., Goodhead, D. T., and Wright, E. G. (1998). Chromosomal instability in the descendants of unirradiated surviving cells after  $\alpha$ -particle irradiation. *Proc. Natl. Acad. Sci. USA* **95**, 5730–5733.

Lowe, S. W., and Lin, A. W. (2000). Apoptosis in cancer. *Carcinogenesis* **21**, 485–495.

Lowndes, N. F., and Murguia, J. R. (2000). Sensing and responding to DNA damage. *Curr. Opin. Genet. Dev.* **10**, 17–25.

Macleod, K. (2000). Tumor suppressor genes. *Curr. Opin. Genet. Dev.* **10**, 81–93.

MacNaughton, W. K., Leach, K. E., Prud'homme-Lalonde, L., Ho, W., and Sharkey, K. A. (1994). Ionizing radiation reduces neurally evoked electrolyte transport in rat ileum through a mast cell-dependent mechanism. *Gastroenterology* **106**, 324–335.

MacNaughton, W. K., Leach, K. E., Prud'homme-Lalonde, L., and Harding, R. K. (1997). Exposure to ionizing radiation increases responsiveness to neural secretory stimuli in the ferret jejunum *in vitro*. *Int. J. Radiat. Biol.* **72**, 219–226.

MacNaughton, W. K., Aurora, A. R., Bhamra, J., Sharkey, K. A., and Miller, M. J. S. (1998). Expression, activity and cellular localization of inducible nitric oxide synthase in rat ileum and colon post-irradiation. *Int. J. Radiat. Biol.* **74**, 255–264.

Marnett, L. J. (2000). Oxylradicals and DNA damage. *Carcinogenesis* **21**, 361–370.

Mason, K. A., Withers, H. R., McBride, W. H., Davis, C. A., and Smathers, J. B. (1989). Comparison of the gastrointestinal syndrome after total-body or total-abdominal irradiation. *Radiat. Res.* **117**, 480–488.

McArdle, A. H. (1994). Protection from radiation injury by elemental diet: does added glutamine change the effect? *Gut* **35**, S60–S64.

McArdle, A. H., Wittnich, C., Freeman, C. R., and Duguid, W. P. (1985). Elemental diet as prophylaxis against radiation injury. Histological and ultrastructural studies. *Arch. Surg.* **120**, 1026–1032.

McCue, J. L., Sheffield, J. P., and Phillips, R. K. S. (1995). Adjuvant radiotherapy and anastomosis in rectal cancer—disturbing evidence from animal studies. *Dis. Colon Rectum* **38**, 152–158.

McNiven, M. A., and Marlowe, K. J. (1999). Contributions of molecular motor enzymes to vesicle-based protein transport in gastrointestinal epithelial cells. *Gastroenterology* **116**, 438–451.

Michael, B. D., and O'Neill, P. (2000). A sting in the tail of electron tracks. *Science* **287**, 1603–1604.

Michailova, K., Wassilev, W., and Wedel, T. (1999). Scanning and transmission electron microscopic study of visceral and parietal peritoneal regions in the rat. *Anat. Anz.* **181**, 253–260.

Michałowski, A., Uehara, S., Yin, W.-B., Burgin, J., and Silvester, J. A. (1983). Alternative types of duodenal ulcer induced in mice by partial body irradiation of the thorax. *Radiat. Res.* **95**, 78–86.

Miller, S. M., Farrugia, G., Schmalz, P. F., Ermilov, L. G., Maines, M. D., and Szurszewski, J. H. (1998). Heme oxygenase 2 is present in interstitial cell networks of the mouse small intestine. *Gastroenterology* **114**, 239–244.

Minami, K., Matsuzaki, S., Hayashi, N., Mokarim, A., Ito, M., and Sekine, I. (1998). Immunohistochemical study of p53 overexpression in radiation-induced colon cancers. *J. Radiat. Res.* **39**, 1–10.

Ming, S.-C., and Goldman, H. (1998). "Pathology of the Gastrointestinal Tract," 2nd ed. Williams and Wilkins, Baltimore, MD.

Moghaddami, M., Cummins, A., and Mayrhofer, G. (1998). Lymphocyte-filled villi: comparison with other lymphoid aggregations in the mucosa of the human small intestine. *Gastroenterology* **115**, 1414–1425.

Mohiuddin, M., and Kramer, S. (1978). Therapeutic effect of an elemental diet on proline absorption across the irradiated rat small intestine. *Radiat. Res.* **75**, 660–663.

Mohiuddin, M., Tamura, K., and DeMare, P. (1978). Changes in absorption of glucose and proline following irradiation to the exteriorised ileum. *Radiat. Res.* **74**, 186–190.

Montgomery, R. K., Mulberg, A. E., and Grand, R. J. (1999). Development of the human gastrointestinal tract: Twenty years of progress. *Gastroenterology* **116**, 702–731.

Morris, M. M., and Powell, S. N. (1997). Irradiation in the setting of collagen vascular disease: acute and late complications. *J. Clin. Oncol.* **15**, 2728–2735.

Moser, A. R., Pitot, H. C., and Dove, W. F. (1990). A dominant mutation that predisposes to multiple intestinal neoplasia in the mouse. *Science* **247**, 322–324.

Mulholland, M. W., Levitt, S. H., Song, C. W., Potish, R. A., and Delaney, J. P. (1984). The role of luminal contents in radiation enteritis. *Cancer (N.Y.)* **54**, 2396–2402.

Muraoka, M., Mine, K., and Kubo, C. (1998). A study of intestinal dysfunction induced by restraint stress in rats. *Scand. J. Gastroenterol.* **33**, 806–810.

Naylor, G. P., Haines, J. W., Whysall, K., Bonas, H. E., and Harrison, J. D. (1993). Measurements of the gastrointestinal absorption and tissue distribution of plutonium, americium and polonium in experimental animals. *Sci. Total Environ.* **130–131**, 429–435.

Nenot, J. C. (1998). Radiation accidents: Lessons learnt for future radiological protection. *Int. J. Radiat. Biol.* **73**, 435–442.

Nias, A. H. W. (1998). "An Introduction to Radiobiology," 2nd ed. Wiley, Chichester, England.

Nieuwenhuijzen, G. A. P., Deitch, E. A., and Goris, R. J. A. (1996). The relationship between gut-derived bacteria and the development of the multiple organ dysfunction syndrome. *J. Anat.* **189**, 537–548.

Nikjoo, H., Uehara, S., Wilson, W. E., Hoshi, M., and Goodhead, D. T. (1998). Track structure in radiation biology: Theory and applications. *Int. J. Radiat. Biol.* **73**, 355–364.

Oberhausen, H. (1975). Effect of O-(beta-hydroxyethyl)rutoside on intestinal tract cells following partial body irradiation. *Arzneim.-Forsch.* **25**, 101–105.

Ogino, I., Kitamura, T., Okamoto, N., Yamasita, K., Aikawa, Y., Okajima, H., and Matsubara, S. (1995). Late rectal complication following high dose rate intracavitary brachytherapy in cancer of the cervix. *Int. J. Radiat. Oncol. Biol. Phys.* **31**, 725–734.

Orian-Rousseau, V., Aberdam, D., Fontao, L., Chevalier, L., Meneguzzi, G., Kedinger, M., and Simon-Assmann, P. (1996). Developmental expression of laminin-5 and HD1 in the intestine: Epithelial to mesenchymal shift for the laminin gamma-2 chain subunit deposition. *Dev. Dyn.* **206**, 12–23.

Osborne, J. W., Nicholson, D. P., and Prasad, K. N. (1963). Induction of intestinal carcinoma in the rat by X-irradiation of the small intestine. *Radiat. Res.* **18**, 76–85.

Osborne, J. W., Prasad, K. N., and Zimmerman, G. R. (1970). Changes in the rat intestine after X-irradiation of exteriorized short segments of ileum. *Radiat. Res.* **43**, 131–142.

Osman, N. E., Westrom, B., and Karlsson, B. (1998). Serosal but not mucosal endotoxin exposure increases intestinal permeability *in vitro* in the rat. *Scand. J. Gastroenterol.* **33**, 1170–1174.

Otterson, M. F., and Summers, R. W. (1995). Postirradiation alterations in small and large bowel

motility. In "Radiation and the Gastrointestinal Tract" (A. Dubois, G. L. King, and D. R. Livengood, Eds.), pp. 77–88. CRC Press, Boca Raton, FL.

Otterson, M. F., Sarna, S. K., Leming, S. C., Moulder, J. E., and Fink, J. G. (1992). Effects of fractionated doses of ionizing radiation on colonic motor activity. *Am. J. Physiol.* **263**, G518–G526.

Otterson, M. F., Koch, T. R., Zhang, Z., Leming, S. C., and Moulder, J. E. (1995). Fractionated irradiation alters enteric neuroendocrine products. *Dig. Dis. Sci.* **40**, 1691–1702.

Panés, J., and Granger, D. N. (1996). Neutrophils generate oxygen free radicals in rat mesenteric microcirculation after abdominal irradiation. *Gastroenterology* **111**, 981–989.

Panés, J., and Granger, D. N. (1998). Leucocyte–endothelial cell interactions: Molecular mechanisms and implications in gastrointestinal disease. *Gastroenterology* **114**, 1066–1090.

Panés, J., Anderson, D. C., Miyasaka, M., and Granger, D. N. (1995). Role of leukocyte–endothelial cell adhesion in radiation-induced microvascular dysfunction in rats. *Gastroenterology* **108**, 1761–1769.

Park, H. S., Goodlad, R. A., and Wright, N. A. (1995). Crypt fission in the small intestine and colon. A mechanism for the emergence of G6PD locus-mutated crypts after treatment with mutagens. *Am. J. Pathol.* **147**, 1416–1427.

Park, H. S., Goodlad, R. A., Ahnen, D. J., Winnett, A., Sasieni, P., Lee, C. Y., and Wright, N. A. (1997). Effects of epidermal growth factor and dimethylhydrazine on crypt size, cell proliferation, and crypt fission in the rat colon. Cell proliferation and crypt fission are controlled independently. *Am. J. Pathol.* **151**, 843–852.

Parks, D. A., Bulkley, G. B., and Granger, D. N. (1983). Role of oxygen-derived free radicals in digestive tract diseases. *Surgery* **94**, 415–422.

Peacock, J. H., Nahum, A. E., and Steel, G. G. (1998). Normal-tissue effects in radiotherapy: Physics meets biology. Report on a workshop held at Hartsfield Manor, Betchworth, Surrey, U.K., 14–16 July, 1997. *Int. J. Radiat. Biol.* **73**, 341–344.

Penttila, A., Kormano, M., and Ahonen, A. (1975). Effects of 400R whole-body X-irradiation on 5-hydroxytryptamine content of the rat gastrointestinal tract. *Strahlentherapie* **149**, 426–437.

Phillips, S. F., and Wingate, D. L. (1998). "Functional Disorders of the Gut." Churchill Livingstone, London.

Pietroletti, R., Blaauwgeers, J. L., Taat, C. W., Simi, M., Brummelkamp, W. H., and Becker, A. E. (1989). Intestinal endocrine cells in radiation enteritis. *Surg. Gynecol. Obstet.* **169**, 127–130.

Porvaznik, M. (1979). Tight junction disruption and recovery after sublethal gamma-irradiation. *Radiat. Res.* **78**, 233–250.

Porvaznik, M., Walker, R. I., and Gillmore, J. D. (1979). Reduction of the indigenous filamentous microorganisms in rat ilea following  $\gamma$ -radiation. *Scanning Electron Microsc.* **3**, 15–21.

Potten, C. S. (1990). A comprehensive study of the radiobiological response of the murine (BDF1) small intestine [review]. *Int. J. Radiat. Biol.* **58**, 925–973.

Potten, C. S. (1997). Epithelial cell growth and differentiation. II. Intestinal apoptosis. *Am. J. Physiol.* **273**, G253–G257.

Potten, C. S., and Hendry, J. H. (1995). "Radiation and Gut." Elsevier, Amsterdam.

Potten, C. S., Rezvani, M., Hendry, J. H., Moore, J. V., and Major, D. (1981). The correction of intestinal microcolony counts for variation in size. *Int. J. Radiat. Biol.* **40**, 321–326.

Potten, C. S., Booth, C., and Pritchard, D. M. (1997a). The intestinal stem cell: the mucosal governor. *Int. J. Exp. Pathol.* **78**, 219–243.

Potten, C. S., Wilson, J. W., and Booth, C. (1997b). Regulation and significance of apoptosis in the stem cells of the gastrointestinal epithelium. *Stem Cells* **15**, 82–93.

Preedy, V. R., and Watson, R. R., Eds. (1998). "Methods in Disease: Investigating the Gastrointestinal Tract." Greenwich Medical Media Ltd., London.

Prieto, I., Gomez de Segura, I. A., Garcia Grande, A., Guerra, A., Pozo, F., Garcia, P., and de Miguel, E. (1998). Growth hormone reduces bacterial translocation in radiation enteritis in the rat. *Rev. Esp. Enferm. Dig.* **90**, 357–360.

Prives, C., and Hall, P. A. (1999). The p53 pathway [review]. *J. Pathol.* **187**, 112–126.

Quastler, H. (1956). The nature of intestinal radiation death. *Radiat. Res.* **4**, 303–320.

Raja, K. B., Simpson, R. J., Watson, R. R., and Preedy, V. T. (1998). Attention to methodology. Fundamental criteria for studies in gastroenterology. In “Methods in Disease: investigating the gastrointestinal tract” (V. R. Preedy and R. R. Watson, Eds.), pp. 1–4. Greenwich Medical Media Ltd., London.

Rang, H. P., Dale, M. M., and Ritter, J. M. (1999). “Pharmacology,” 4th ed. Churchill Livingstone, Edinburgh.

Rao, K. R., and Fritz-Niggli, H. (1988). Alterations in the length of jejunal villi in mice irradiated with graded doses of X-rays. *Br. J. Radiol.* **61**, 839–842.

Richter, K. K., Langberg, C. W., Sung, C.-C., and Hauer-Jensen, M. (1996). Association of transforming growth factor  $\beta$  (TGF- $\beta$ ) immunoreactivity with specific histopathologic lesions in subacute and chronic experimental radiation enteropathy. *Radiother. Oncol.* **39**, 243–251.

Richter, K. K., Fagerhol, M. K., Carr, J. C., Winkler, J. M., Sung, C.-C., and Hauer-Jensen, M. (1997a). Association of granulocyte transmigration with structural and cellular parameters of injury in experimental radiation enteropathy. *Radiat. Oncol. Invest.* **5**, 275–282.

Richter, K. K., Fink, L. M., Hughes, B. M., Sung, C.-C., and Hauer-Jensen, M. (1997b). Is the loss of endothelial thrombomodulin involved in the mechanism of chronicity in late radiation enteropathy? *Radiother. Oncol.* **44**, 65–71.

Richter, K. K., Langberg, C. W., Sung, C.-C., and Hauer-Jensen, M. (1997c). Increased transforming growth factor  $\beta$  (TGF- $\beta$ ) immunoreactivity is independently associated with chronic injury in both consequential and primary radiation therapy. *Int. J. Radiat. Oncol. Biol. Phys.* **39**, 187–195.

Richter, K. K., Fink, L. M., Hughes, B. M., Shmaysami, H. M., Sung, C.-C., and Hauer-Jensen, M. (1998). Differential effect of radiation on endothelial cell function in rectal cancer and normal rectum. *Am. J. Surg.* **176**, 642–647.

Risica, S., Rogani, A., Grisanti, G., and Tancredi, F. (1999). A new study on radionuclide contamination of maternal milk. *Int. J. Radiat. Med.* **1**, 71–77.

Ropolo, R., and Cesana, P. (1997).  $^{137}\text{Cs}$  urinary excretion by northwestern Italians ten years after the Chernobyl accident. *Health Phys.* **73**, 498–501.

Rubio, C. A., and Jahnas, M. (1996). Dose-time-dependent histological changes following irradiation of the small intestine of rats. *Dig. Dis. Sci.* **41**, 392–401.

Rubio, C. A., Eriksson, B., and Johnsson, L. (1983). Ectopic intestinal glands after segmental small bowel irradiation in the cat. *Acta Radiol. Oncol.* **22**, 473–475.

Ruifrock, A. C. C., Mason, K. A., Lozano, G., and Thames, H. D. (1997). Spatial and temporal patterns of expression of epidermal growth factor, transforming growth factor alpha and transforming growth factor beta 1-3 and their receptors in mouse jejunum after radiation treatment. *Radiat. Res.* **147**, 1–12.

Ruifrock, A. C. C., Weil, M. M., Mason, K. A., and Thames, H. D. (1998a). Induction of transforming growth factor alpha in irradiated mouse jejunum. *Int. J. Radiat. Oncol. Biol. Phys.* **42**, 1137–1146.

Ruifrock, A. C. C., Weil, M. M., Thames, H. D., and Mason, K. A. (1998b). Diurnal variations in the expression of radiation-induced apoptosis. *Radiat. Res.* **149**, 360–365.

Sanchez, A. L., Walters, C. B., Singleton, D. L., Wood, N. H., and Mondon, K. (1999). Food ingestion doses from artificial radionuclides in Cumbrian diets, ten years post-Chernobyl. *J. Environ. Radioactiv.* **43**, 301–317.

Santos, J., Saperas, E., Nogueiras, C., Mourelle, M., Antolin, M., Cadahia, A., and Malagelada, J.-R. (1998). Release of mast cell mediators into the jejunum by cold pain stress in humans. *Gastroenterology* **114**, 640–648.

Saxena, S. K., Thompson, J. S., Crouse, D. A., and Sharp, J. G. (1991). Epithelial cell proliferation and uptake of radiolabeled urogastrone in the intestinal tissues following abdominal irradiation in the mouse. *Radiat. Res.* **128**, 37–42.

Scanff, P., Grison, S., Monti, P., Joubert, C., Griffiths, N. M., and Gourmelon, P. (1997). Whole-body gamma irradiation modifies bile composition in the pig. *Radiat. Res.* **148**, 175–180.

Scanff, P., Monti, P., Joubert, C., Grison, S., Gourmelon, P., and Griffiths, N. M. (1999). Modified bile acid profiles in mixed neutron and  $\gamma$ -irradiated pigs. *Int. J. Radiat. Biol.* **75**, 209–216.

Schleicher, E. D., Wagner, E., and Nerlich, A. G. (1997). Increased accumulation of the glycoxidation product N ( $\varepsilon$ )-(carboxymethyl)lysine in human tissues in diabetes and aging. *J. Clin. Invest.* **99**, 457–468.

Schmidt-Ullrich, R. K., Dent, P., Grant, S., Mikkelsen, R. B., and Valerie, K. (2000). Signal transduction and cellular radiation responses. *Radiat. Res.* **153**, 245–257.

Schmitz, H., Barmeyer, C., Fromm, M., Runkel, N., Foss, H.-D., Bentzell, C. J., Riecken, E.-O., and Schulzke, J.-D. (1999). Altered tight junction structure contributes to the impaired epithelial barrier function in ulcerative colitis. *Gastroenterology* **116**, 301–309.

Scott, B. R., Langberg, C. W., and Hauer-Jensen, M. (1995). Models for estimating the risk of ulcers in the small intestine after localized single or fractionated irradiation. *Br. J. Radiol.* **68**, 49–57.

Sebes, J. I., Zaldivar, R., and Vogel, H. H., Jr. (1975). Histopathologic changes induced in rats by localized X-irradiation of an exteriorised segment of the small intestine. *Strahlentherapie* **150**, 403–410.

Sedgwick, D. M., and Ferguson, A. (1994). Dose-response studies of depletion and repopulation of rat intestinal mucosal mast cells after irradiation. *Int. J. Radiat. Biol.* **65**, 483–495.

Seibold, F., Seibold-Schmid, B., Cong, Y., Yu Shu, F., McCabe, R. P., Weaver, C., and Elson, C. O. (1998). Regional differences in L-selectin expression in murine intestinal lymphocytes. *Gastroenterology* **114**, 965–974.

Seifert, W. F., Wobbes, T., Hoogenhout, J., de Man, B. M., Huyben, K. M. L. C., and Hendriks, T. (1995). Intra-operative irradiation delays anastomotic repair in rat colon. *Am. J. Surg.* **170**, 256–261.

Seifert, W. F., Wobbes, T., Hoogenhout, J., de Man, B. M., and Hendriks, T. (1997). Intraoperative irradiation prolongs the presence of matrix metalloproteinase activity in large bowel anastomoses of the rat. *Radiat. Res.* **147**, 354–361.

Sharma, N., Hess, C. T., and Thrall, K. D. (1997). A compartmental model of water radon contamination in the human body. *Health Phys.* **72**, 261–268.

Shimoda, H., Kato, S., and Kudo, T. (1997). Enzyme-histochemical demonstration of the intramural lymphatic network in the monkey jejunum. *Arch. Histol. Cytol.* **60**, 215–224.

Shiraga, T., Miyamoto, K.-I., Tanaka, H., Yamamoto, H., Taketani, Y., Morita, K., Tamai, I., Tsji, A., and Takeda, E. (1999). Cellular and molecular mechanisms of dietary regulation on rat intestinal H<sup>+</sup>/peptide transporter PepT1. *Gastroenterology* **116**, 354–362.

Sindelar, W. F., Tepper, J. E., Kinsella, T. J., Barnes, M., DeLuca, A. M., Terrill, R., Matthews, D., Anderson, W. J., Bollinger, B. K., and Johnstone, P. A. (1994). Late effects of intraoperative radiation therapy on retroperitoneal tissues, intestine, and bile duct in a large animal model. *Int. J. Radiat. Oncol. Biol. Phys.* **29**, 781–788.

Singh, S. K., Binder, H. J., Boron, W. F., and Geibel, J. P. (1995). Fluid absorption in isolated perfused colonic crypts. *J. Clin. Invest.* **96**, 2373–2379.

Skwarchuk, M. W., and Travis, E. L. (1998). Volume effects and epithelial regeneration in irradiated mouse colorectum. *Radiat. Res.* **149**, 1–10.

Solheim, K. E., Laerum, F., Stordahl, A., and Aase, S. (1991). Urinary excretion of iohexol after enteral administration in rats with radiation injury of the small intestine. *Scand. J. Gastroenterol.* **26**, 1097–1106.

Somosy, Z., Kovacs, J., Siklos, L., and Koteles, G. J. (1993). Morphological and histochemical changes in intercellular junctional complexes in epithelial cells of mouse small intestine upon X-irradiation: Changes of ruthenium red permeability and calcium content. *Scanning Microsc.* **7**, 961–971.

Somosy, Z., Thuroczy, G., Koteles, G. J., and Kovacs, J. (1994). Effects of modulated microwave and X-ray irradiation on the activity and distribution of Ca<sup>2+</sup>-ATPase in small intestine epithelial cells. *Scanning Microsc.* **8**, 613–620.

Sosula, L., Nicholls, E. M., and Skeen, M. (1988). Ultrastructure of *Campylobacter jejuni* in gamma-irradiated mouse jejunum. *Am. J. Pathol.* **131**, 125–131.

Spitzer, T. R. (1995). Clinical aspects of irradiation-induced alimentary tract injury. In "Radiation and the Gastrointestinal Tract" (A. Dubois, G. L. King, and D. R. Livengood, Eds.), pp. 3–19. CRC Press, Boca Raton, FL.

Sprugel, W., Schubert, E., Mitznegg, P., Heim, F., Hasl, G., and Pauly, H. (1977). Immediate X-radiation induced contractions of the isolated guinea pig terminal ileum: the localization of the effect by drugs. *Radiat. Environ. Biophys.* **14**, 31–37.

Srinivasan, V., and Dubois, A. (1995). Nutritional support of irradiated intestine. In "Radiation and the Gastrointestinal Tract" (A. Dubois, G. L. King, and D. R. Livengood, Eds.), pp. 201–213. CRC Press, Boca Raton, FL.

St Clair, W. H., and Osborne, J. W. (1985). Crypt fission and crypt number in the small and large bowel of post-natal rats. *Cell Tissue Kinet.* **18**, 255–262.

Steel-Goodwin, L., and Carmichael, A. J. (1995). Nitric oxide and smooth muscle relaxation in the intestine. Chemical and radiation effects measured by EPR/spin trapping. In "Radiation and the Gastrointestinal Tract" (A. Dubois, G. L. King, and D. R. Livengood, Eds.), pp. 89–100. CRC Press, Boca Raton, FL.

Stone, H. B., Dewey, W. C., Wallace, S. S., and Coleman, C. N. (1998). Molecular biology to radiation oncology: A model for translational research? Opportunities in basic and translational research. *Radiat. Res.* **150**, 134–147.

Sullivan, M. F., Cross, F. T., and Dagle, G. E. (1987). Dosimetry of the gastrointestinal tract. In "Age-Related Factors in Radionuclide Metabolism and Dosimetry" (G. B. Gerber, H. Metivier, and H. Smith, Eds.), pp. 49–66. Martinus Nijhoff Publishers, Kluwer Academic Publishers Group, Dordrecht, Netherlands.

Summers, R. W., and Hayek, B. I. (1993). Changes in colonic motility following abdominal irradiation in dogs. *Am. J. Physiol.* **264**, G1024–G1030.

Summers, R. W., Flatt, A. J., Prihoda, M. J., and Mitros, F. A. (1987). Effect of irradiation on morphology and motility of canine small intestine. *Dig. Dis. Sci.* **32**, 1402–1410.

Summers, R. W., Maves, B. V., Reeves, R. D., Arjes, L. J., and Oberley, L. W. (1989). Irradiation increases superoxide dismutase in rat intestinal smooth muscle. *Free Radical Biol. Med.* **6**, 261–270.

Summers, R. W., Glenn, C. E., Flatt, A. J., and Elahmady, A. (1991). Radiation and indomethacin effects on morphology, prostaglandins and motility in dog jejunum. *Am. J. Physiol.* **261**, G145–G151.

Summers, R. W., Glenn, C. E., Flatt, A. J., and Elahmady, A. (1992). Does irradiation produce irreversible changes in canine jejunal myoelectric activity? *Dig. Dis. Sci.* **37**, 716–722.

Sun, Z., Wang, X., Wallen, R., Deng, X., Du, X., Hallberg, E., and Andersson, R. (1998). The influence of apoptosis on intestinal barrier integrity in rats. *Scand. J. Gastroenterol.* **33**, 415–422.

Takahashi, T., and Owyang, C. (1998). Regional differences in the niteric innervation between the proximal and the distal colon in rats. *Gastroenterology* **115**, 1504–1512.

Tamou, S., and Trott, K. R. (1995). The effects of local X-irradiation on the distensibility of the rectum in rats. *Br. J. Radiol.* **68**, 64–69.

Taverner, D., Talbot, I. C., Carr-Locke, D. L., and Wicks, A. C. B. (1982). Massive bleeding from the ileum: A late complication of pelvic radiotherapy. *Am. J. Gastroenterol.* **77**, 29–31.

Taylor, D. M., and Taylor, S. K. (1997). Environmental uranium and human health. *Rev. Environ. Health* **12**, 147–157.

Tepper, J. E., Sindelar, W., Travis, E. L., Terrill, R., and Padikal, T. (1983). Tolerance of canine anastomoses to intraoperative radiation therapy. *Int. J. Radiat. Oncol. Biol. Phys.* **9**, 987–992.

Thacker, J. (1999). Repair of ionizing radiation damage in mammalian cells. Alternative pathways and their fidelity. *C. R. Acad. Sci. Paris Life Sciences* **322**, 103–108.

Thomson, A. B. R., and Wild, G. (1997). Small bowel review: Part II. *Can. J. Gastroenterol.* **11**, 607–618.

Thomson, A. B. R., Cheesman, C. I., and Walker, K. (1984). Effect of external abdominal irradiation on the dimensions and characteristics of the barriers to passive transport in the rat intestine. *Lipids* **19**, 405–418.

Thomson, A. B. R., Keelan, M., Cheeseman, C. I., Walker, K., and Clandinin, M. T. (1989a). Saturated fatty acid diet prevents radiation-associated decline in intestinal uptake. *Am. J. Physiol.* **256**, G178–G187.

Thomson, A. B. R., Keelan, M., Clandinin, M. T., Tavernini, M., Lam, K., Walker, K., and Cheeseman, C. I. (1989b). Lack of protective effect of oral enprostil, a synthetic prostaglandin E<sub>2</sub>, on intestinal transport and morphology following abdominal irradiation in the rat. *Can. J. Physiol. Pharmacol.* **67**, 1351–1356.

Thomson, J. S., Crouse, D. A., Mann, S. L., Saxena, S. K., and Sharp, J. G. (1988). Intestinal glucose uptake is increased in aged mice. *Mech. Aging Dev.* **46**, 135–143.

Thornton, F. J., and Barbul, A. (1997). Healing in the gastrointestinal tract. *Surg. Clin. North Am.* **77**, 549–573.

Totafurno, J., Bjerknes, M., and Cheng, H. (1987). The crypt cycle. Crypt and villus production in the adult intestinal epithelium. *Biophys. J.* **52**, 279–294.

Touboul, E., Balosso, J., Schlienger, M., and Laugier, A. (1996). Small bowel radiation injury: Radio-biological and radiopathological aspects, risk factors and prevention. *Ann. Chir.* **50**, 58–71.

Toyoda, H., Ina, K., Kitamura, H., Tsuda, T., and Shimada, T. (1997). Organisation of the lamina propria mucosae of rat intestinal mucosa, with special reference to the subepithelial connective tissue. *Acta Anat.* **158**, 172–184.

Trott, K.-R. (1984). Chronic damage after radiation therapy: Challenge to radiation biology. *Int. J. Radiat. Oncol. Biol. Phys.* **10**, 907–913.

Trott, K.-R., Breiter, N., and Spiethoff, A. (1986). Experimental studies on the pathogenesis of the chronic radiation ulcer of the large bowel in rats. *Int. J. Radiat. Oncol. Biol. Phys.* **12**, 1637–1643.

Trott, K.-R., Tamou, S., Sassy, T., and Kiszel, Z. (1995). The effect of irradiated volume on the chronic radiation damage of the rat large bowel. *Strahlenther. Onkol.* **171**, 326–331.

Tucker, J. D., Ramsey, M. J., Lee, D. A., and Minkler, J. L. (1993). Validation of chromosome painting as a biodosimeter in human peripheral lymphocytes following acute exposure to ionizing radiation *in vitro*. *Int. J. Radiat. Biol.* **64**, 27–37.

Ueno, Y., Sugimoto, C., Onoyama, Y., Imura, T., Yoshida, Y., and Nakajima, N. (1976). Rectal injuries following radiation therapy for cervical cancer. *Radiol. Clin.* **45**, 435–442.

van Nagell, J. R., Jr., Kielar, R., Donaldson, E. S., Gay, E. C., Powell, D. F., Maruyama, Y., and Yoneda, J. (1979). Correlation between retinal and pelvic vascular status: a determinant factor in patients undergoing pelvic irradiation for gynecologic malignancy. *Am. J. Obstet. Gynecol.* **134**, 551–556.

Vigneulle, R. M. (1995). Nearby shielding influences survival of the irradiated intestine. In “Radiation and the Gastrointestinal Tract” (A. Dubois, G. L. King, and D. R. Livengood, Eds.), pp. 161–170. CRC Press, Boca Raton, FL.

Vigneulle, R. M., Vriesendorp, H. M., Taylor, P., Burns, W., and Pelkey, T. (1989). Survival after total-body irradiation. I. Effects of partial small bowel shielding. *Radiat. Res.* **119**, 313–324.

Vigneulle, R. M., Herrera, J., Gage, T., MacVittie, T. J., Taylor, P., Zeman, G., Nold, J. B., and Dubois, A. (1990). Nonuniform irradiation of the canine intestine. I. Effects. *Radiat. Res.* **121**, 46–53.

Vriesendorp, H. M., Vigneulle, R. M., Kitto, G., Pelky, T., Taylor, P., and Smith, J. (1992). Survival after total body irradiation: Effects of irradiation of exteriorized small intestine. *Radiother. Oncol.* **23**, 160–169.

Wagner, H. N., Jr. (1996). The future. *Semin. Nucl. Med.* **26**, 194–200.

Walker, R. I., Brook, I., Costerton, J. W., MacVittie, T., and Myhal, M. L. (1985). Possible association of mucous blanket integrity with postirradiation colonization resistance. *Radiat. Res.* **104**, 346–357.

Wallace, H. J., 3rd, Willett, C. G., Shellito, P. C., Coen, J. J., and Hoover, H. C., Jr. (1995). Intraoperative radiation therapy for locally advanced recurrent rectal or rectosigmoid cancer. *J. Surg. Oncol.* **60**, 122–127.

Walsh, D. (1897). Deep traumatism from Roentgen ray exposure. *Br. Med. J.* **2**, 272–273.

Wang, J., Zheng, H., Sung, C.-C., Richter, K. K., and Hauer-Jensen, M. (1998). Cellular sources of transforming growth factor- $\beta$  isoforms in early and chronic radiation enteropathy. *Am. J. Pathol.* **153**, 1531–1540.

Wang, J., Richter, K. K., Sung, C.-C., and Hauer-Jensen, M. (1999a). Upregulation and spatial shift in the localization of the mannose 6-phosphate/insulin-like growth factor II receptor during radiation enteropathy development in the rat. *Radiother. Oncol.* **50**, 205–213.

Wang, J., Zheng, H., Sung, C.-C., and Hauer-Jensen, M. (1999b). The synthetic somatostatin analogue, octreotide, ameliorates acute and delayed intestinal radiation injury. *Int. J. Radiat. Oncol. Biol. Phys.* **45**, 1289–1296.

Wang, J., Albertson, C. M., Zheng, H., Fink, L. M., Herbert, J.-M., and Hauer-Jensen, M. (2000a). Inhibition of ADP-induced platelet aggregation ameliorates delayed radiation toxicity. *Radiat. Res. Soc.* **47**, 144.

Wang, J., Zheng, H., Mao, J., Hollenberg, M. D., and Hauer-Jensen, M. (2000b). Upregulation and spatial shift in protease activated receptor-2 in irradiated rat intestine. *Radiat. Res. Soc.* **47**, 144.

Wang, J. Y., and Huang, D. S. (1998). Evaluation of cytokine profile in the gastrointestinal tract. In “Methods in Disease: Investigating the Gastrointestinal Tract” (V. R. Preedy and R. R. Watson, Eds.), pp. 87–97. Greenwich Medical Media Ltd., London.

Ward, S. M., Morris, G., Reese, L., Wang, X.-Y., and Sanders, K. M. (1998). Interstitial cells of Cajal mediate enteric inhibitory neurotransmission in the lower esophageal and pyloric sphincters. *Gastroenterology* **115**, 314–329.

Wartiovaara, J., and Tarpila, S. (1977). Cell contacts and polysomes in irradiated human jejunal mucosa at onset of epithelial repair. *Lab. Invest.* **36**, 660–665.

Wasan, H. S., Park, H. S., Liu, K. C., Mandir, N. K., Winnett, A., Sasieni, P., Bodmer, W. F., Goodlad, R. A., and Wright, N. A. (1998). APC in the regulation of intestinal crypt fission. *J. Pathol.* **185**, 246–255.

Watanabe, H. (1978). Experimentally induced intestinal metaplasia in Wistar rats by X-ray irradiation. *Gastroenterology* **75**, 796–799.

Watanabe, H., Nakagawa, Y., and Ito, A. (1987). Induction of gastric tumor and intestinal metaplasia in rats exposed to localised X-irradiation of the gastric region. *Gann* **78**, 27–31.

Wei, W. I., Lam, L. K., Yuen, P. W., Kwong, D., and Chan, K. W. (1998). Mucosal changes of the free jejunal graft in response to radiotherapy. *Am. J. Surg.* **175**, 44–46.

Weiss, J. F., Landauer, M. R., Gunter-Smith, P. J., and Hanson, W. R. (1995). Effect of radioprotective agents on survival after acute intestinal radiation injury. In “Radiation and the Gastrointestinal Tract” (A. Dubois, G. L. King, and D. R. Livengood, Eds.), pp. 183–199. CRC Press, Boca Raton, FL.

Wicke, C., Gottwald, T., and Becker, H.-D. (1996). Brief clinical report: glutamine-enriched total parenteral nutrition in a patient with radiation-induced renal and intestinal fibrosis. *Nutrition* **12** (11–12 Suppl.), S85–S86.

Wiernik, G., and Plant, M. (1971). The origin and kinetics of goblet cells in the human jejunum during irradiation. *Br. J. Radiol.* **44**, 348–356.

Wingate, D. L., and Phillips, S. F. (1998). Functional anatomy and physiology. In “Functional Disorders of the Gut” (S. F. Phillips and D. L. Wingate, Eds.), pp. 3–18. Churchill Livingstone, London.

Wiseman, J. S., Senagore, A. J., and Chaudry, I. H. (1996). Relationship of pelvic radiation to intestinal blood flow. *J. Surg. Res.* **60**, 239–244.

Withers, H. R., and Elkind, M. M. (1970). Microcolony survival assay for cells of mouse intestinal mucosa exposed to radiation. *Int. J. Radiat. Biol.* **17**, 261–267.

Withers, H. R., Taylor, J. M. G., and Maciejewski, B. (1988). Treatment volume and tissue tolerance. *Int. J. Radiat. Oncol. Biol. Phys.* **14**, 751–759.

Wong, M. H., Stappenbeck, T. S., and Gordon, M. J. I. (1999). Living and commuting in intestinal crypts. *Gastroenterology* **116**, 208–215.

Wood, J. D. (1998). Enteric neuropathobiology. In “Functional Disorders of the Gut” (S. F. Phillips and D. L. Wingate, Eds.), pp. 19–42. Churchill Livingstone, London.

Wright, E. G. (1999). Inherited and inducible chromosomal instability: A fragile bridge between genome integrity mechanisms and tumourigenesis. *J. Pathol.* **187**, 19–27.

Wyatt, M. G., Hume, S. P., Carr, K. E., and Marigold, J. C. L. (1987). A preliminary study of the role of gastrointestinal endocrine cells in the maintenance of villous structure following X-irradiation. *Scanning Microsc.* **1**, 291–300.

Yamamoto, Y., Kubota, T., Atoji, Y., and Suzuki, Y. (1996). Distribution of  $\alpha$ -vascular smooth muscle actin in the smooth muscle cells of the gastrointestinal tract of the chicken. *J. Anat.* **189**, 623–630.

Yazdani, A., Takahashi, T., Bagnol, D., Watson, S. J., and Owyang, C. (1999). Functional significance of a newly discovered neuropeptide, orphanin FQ, in rat gastrointestinal motility. *Gastroenterology* **116**, 108–117.

Yoon, S. C., Park, J. M., Jang, H. S., Shinn, K. S., and Bahk, Y. W. (1994). Radioprotective effect of captopril on the mouse jejunal mucosa. *Int. J. Radiat. Oncol. Biol. Phys.* **30**, 873–878.

Yuan, X., Zheng, X., Lu, D., Rubin, D. C., Pung, C. Y., and Sadler, J. E. (1998). Structure of murine enterokinase (enteropeptidase) and expression in small intestine during development. *Am. J. Physiol.* **274**, G342–349.

Zamolodchikova, T. S., Sokolova, E. A., Alexandrov, S. L., Mikhaleva, I. I., Prudchenko, I. A., Morozov, I. A., Kononenko, N. V., Mirgorodskaya, O. A., Da, U., Larionova, N. I., Pozdnev, V. F., Ghosh, D., Duax, W. L., and Vorotyntseva, T. I. (1997). Subcellular localisation, substrate specificity and crystallization of duodenase, a potential activator of enteropeptidase. *Eur. J. Biochem.* **249**, 612–621.

Zhang, C., Cai, W., Li, Y., Huang, W., and Su, H. (1998). Quantitative analysis of calcitonin gene-related peptide- and neuropeptide Y-immunoreactive nerve fibers in mesenteric blood vessels of rats irradiated with cobalt-60 gamma rays. *Radiat. Res.* **149**, 19–26.

Zheng, H., Wang, J., and Hauer-Jensen, M. (2000a). Role of mast cells in early and delayed radiation injury in rat intestine. *Radiat. Res.* **153**, 533–539.

Zheng, H., Wang, J., Koteliansky, V. E., Gotwals, P. J., and Hauer-Jensen, M. (2000b). Recombinant soluble transforming growth factor- $\beta$  type II receptor ameliorates radiation-induced fibrosis in mouse intestine. *Gastroenterology* **119**, 1286–1296.

Zook, B. C., Bradley, E. W., Casarett, G. W., and Rogers, C. C. (1983). Pathologic effects of fractionated fast neutrons or photons on the pancreas, pylorus and duodenum of dogs. *Int. J. Radiat. Oncol. Biol. Phys.* **9**, 1493–1504.

This Page Intentionally Left Blank

# Nonneuronal Cellular Prion Protein

Jean-Guy Fournier

Service de Neurovirologie, CEA-DSV/DRM, 92265 Fontenay aux Roses Cedex, France

---

The normal cellular prion protein ( $\text{PrP}^{\text{C}}$ ) is a membrane sialoglycoprotein of unknown function having the unique property of adopting an abnormal tertiary conformation. The pathological conformer  $\text{PrP}^{\text{sc}}$  would be the agent of transmissible spongiform encephalopathies or prion diseases. They include scrapie and bovine spongiform encephalopathy in animals and Creutzfeldt-Jakob disease in humans. The conversion of  $\text{PrP}^{\text{C}}$  into  $\text{PrP}^{\text{sc}}$  in the brain governs the clinical phenotype of the disease. However, the three-dimensional structure change of  $\text{PrP}^{\text{C}}$  can also take place outside the central nervous system, in nonneuronal cells particularly of lymphoid tissue where the agent replicates. In natural infection,  $\text{PrP}^{\text{C}}$  in nonneuronal cells of peripheral extracerebral organs may play a key role as the receptor required to enable the entry of the infectious agent into the host. In the present review we have undertaken a first evaluation of compelling data concerning the  $\text{PrP}^{\text{C}}$ -expressing cells of nonneuronal origin present in cerebral and extracerebral tissues. The analysis of tissue, cellular, and subcellular localization of  $\text{PrP}^{\text{C}}$  may help us better understand the biological function of  $\text{PrP}^{\text{C}}$  and provide some information on physiopathological processes underlying prion diseases.

**KEY WORDS:** Extracerebral tissues,  $\text{PrP}^{\text{C}}$ , Metalloprotein, Laminin, Prion diseases, Pathogenesis. © 2001 Academic Press.

---

## I. Introduction

The cellular origin of an infectious particle, exemplified by the discovery of the prion (an acronym for proteinaceous infectious particle, introduced by S. Prusiner), remains one of the most fascinating aspects of microbiology and cell biology. This situation is based on the prion concept, which considers a cellular protein (called a cellular prion protein or  $\text{PrP}^{\text{C}}$ ) to be able to modify its tertiary conformational structure to give a pathological isoform (called a prion protein of scrapie type or

TABLE I  
Prion Diseases

Disease <sup>a</sup>	Host	Origin	Onset age	Clinical features	Duration
Kuru	Humans	Infectious; contamination through ritual cannibalism	Children/adult females	Slowly progressive cerebellar ataxia	3–9 months
sCJD	Humans	Mutations or spontaneous conversion?	50–75	Myoclonus, ataxia, motor signs	1–30 months
iCJD	Humans	Infectious; transmission by dura mater graft, corneal graft, electroencephalogram electrodes, growth hormone, and gonadotrophin therapy		Myoclonus, ataxia, motor signs	
fCJD	Humans	Mutations	31–58	Dementia, ataxia	3 months–15 years
nCJD	Humans	Infectious; transmission by BSE contaminated foods	16–41	Behavioral changes, ataxia, progressive dementia	8–22 months
FFI	Humans	Mutations	40–60	Progressive insomnia, ataxia, motor signs	7–18 months
GSS	Humans	Mutations	35–55	Predominance of cerebellar dysfunction	2–17 years
Scrapie	Sheep, goat	Infectious	2–5	Tremor, pruritus, cachexia	2–12 months
BSE	Cattle	Infectious	3–7	Locomotor signs, hyperesthesia	1–6 months
FSE	Cats	Infectious			
TME	Mink	Infectious			
CWD	Mule deer, elk	Unknown			

<sup>a</sup>iCJD, iatrogenic Creutzfeldt-Jakob disease; sCJD, sporadic CJD; fCJD, familial CJD; nCJD, new variant CJD; FFI, fatal familial insomnia; GSS, Gerstmann-Sträussler-Sheinker disease; BSE, bovine spongiform encephalopathy; FSE, feline spongiform encephalopathy; TME, transmissible mink encephalopathy; CWD, chronic wasting disease.

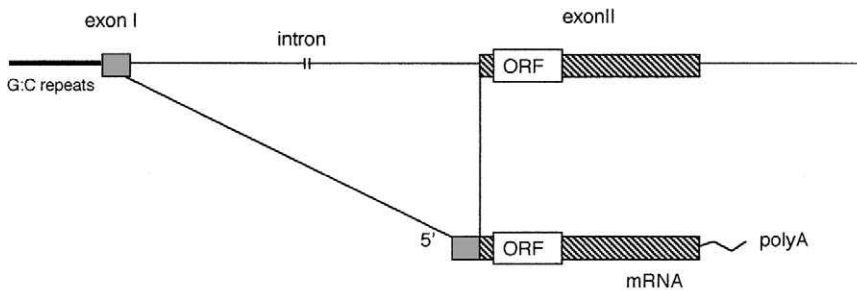
PrP<sup>Sc</sup>) with the unique property of being infectious (Prusiner *et al.*, 1998). The conformational interconversion process implies a structure rich in  $\alpha$  helices into a structure with high  $\beta$ -sheet content (Pan *et al.*, 1993). Cofactors designated “protein X” (Telling *et al.*, 1995) are required for the alpha-beta conversion leading to the formation of the infectivity-associated isoform of prion protein (PrP). This atypical pathogen would be the cause of a group of neurodegenerative disorders called transmissible spongiform encephalopathies (TSE) or prion diseases (Gajdusek, 1977; Prusiner, 1998) (see Table I). In animals, these diseases include scrapie in goat and sheep and a recent bovine spongiform encephalopathy (BSE) in cattle. In humans, a new variant of Creutzfeldt-Jakob disease (CJD) has recently emerged in the United Kingdom and France (Will *et al.*, 1996; Chazot *et al.*, 1996) resulting from the possibility of the BSE agent transmission to humans by contaminated beef consumption (Lasmézas *et al.*, 1996; Collinge *et al.*, 1996; Bruce *et al.*, 1997). TSE declares clinically in humans as dementia and ataxia, which can have various origins (sporadic, infectious, iatrogenic, and genetic). The neuropathology highlights several abnormalities including spongiform changes, glial reaction, neuronal loss, and amyloid plaques. All of these modifications are not prion disease specific and vary largely in intensity. In contrast, the abnormal isoform of prion protein PrP<sup>Sc</sup> is always specifically found accumulated in the brain.

Because the clinical phenotype corresponds to neurodegeneration in brain tissue, interest in the cell biology of prions is legitimately focused on neuronal cells. First considered to be a protein essentially found in the neuron (Kretzschmar *et al.*, 1986), several subsequent observations have shown that PrP<sup>c</sup> could be expressed in relative abundance in extraneuronal tissues. Since the pioneer works by Cashman *et al.* (1990) and Bendheim *et al.* (1992), the list of contributions is growing and it is now well established that PrP<sup>c</sup> is a cellular protein widely distributed in the organism. Although data are still lacking, we think that a first evaluation on the nonneuronal aspect of the normal cellular prion protein (PrP<sup>c</sup>) will be appreciated. Enlightenment regarding the tissue, cellular, and possibly subcellular localization of PrP<sup>c</sup> can be helpful in gaining further insight into its biological function and in the understanding of the pathogenesis including the conversion process that leads to the formation of its pathological counterpart.

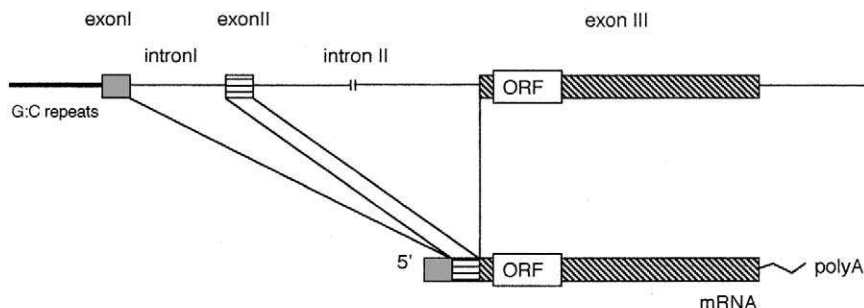
## II. The Prion Protein Gene and Protein Isoforms

### A. Gene Organization and Expression

The *PrP* gene is a single gene composed of 2 (in human and hamster) or 3 exons (sheep, bovine, and mouse) with only one open reading frame (ORF), meaning that alternative RNA splicing does not occur (Fig. 1). The 3' coding exon of 2 kb



### A) HUMAN



### B) SHEEP

FIG. 1 Organization and expression of the mammalian *PrP* gene. Structure of the human *PrP* gene (A) and the sheep *PrP* gene (B). G:C repeats in the *PrP* promoter regions are reminiscent of “housekeeping” genes. Exon I and exon II in A and exon III in B are separated by a large intron of 10–14 kb. Small exons have a length of 50–82 nucleotides, whereas the large exons have a length of about 2300 nucleotides in A, and 4000 nucleotides in B. ORF, open reading frame. Untranslated regions of the mRNA are represented by hatched boxes.

is separated from the 5' exon by a 10- to 14-kb intron. By use of somatic cell hybrids, the *PrP* gene has been assigned to human chromosome 20 and to mouse chromosome 2 (Prusiner, 1991).

The structure of the gene is highly conserved in mammals, and candidate *PrP* genes have been detected by hybridization in genomes of chicken (Harris *et al.*, 1993) turtle (Simonic *et al.*, 2000), salmon (Gibbs and Bolis, 1997), and certain invertebrates such as nematode, *Drosophila*, and yeast (Prusiner, 1991). However, attempts to demonstrate the existence of *PrP*-like proteins in the lower organisms have failed. The evolutionary conservation of the *PrP* gene argues that the translation product fulfills an important function.

## 1. PrP Gene Promoter

The promoter region has no TATA box, but contains three (hamster) or four (human) repeats of the sequence CCGCCC similarly observed in “housekeeping” genes. The transcription factor SP1 is a binding protein with specificity for GC-rich elements and a consensus sequence can be detected in the hamster PrP promoter region (nucleotides 285–293) (Puckett *et al.*, 1991). In mice, the first intron contains two promoter regions associated with a suppressor region. The deletion of this intron dramatically diminishes the PrP expression level (Baybutt and Manson, 1997).

## 2. The ORF Exon

The length of the ORF exon is about 85% of the total mRNA length. Human (2350 bp) (Puckett *et al.*, 1991) and rodent ORF exon (2000 bp) (Oesch *et al.*, 1985) are of similar size whereas ruminants possess a much larger ORF exon (about 4000 bp) (Puckett *et al.*, 1991). The ORF start codon AUG is 10 bp downstream of the intron–exon border. The ORF length varies between 759 (in humans) and 792 bp (in bovines). The signal of polyadenylation is localized 1200 bp after the stop codon. Exons might have evolved as units that can be modified to generate new proteins. That is not the case for the PrP ORF exon, which consequently explains why PrP shows little if any homology with other proteins of the mammalian genome (Bamforth *et al.*, 1996). The role of other exons is not known.

## 3. RNA Expression

*PrP* coding gene transcription provides a mRNA of 2.1–2.5 kb (Oesch *et al.*, 1985; Chesebro *et al.*, 1985). At the cellular level, *in situ* hybridization studies have specified that in brain, neurons constitute the main source of *PrP* transcript (Kretzschmar *et al.*, 1986; Brown *et al.*, 1990). However PrP<sup>c</sup> translation is regulated. The mRNA distribution indicates that 70% of total mRNA is found in active polyribosomes while 30% remains sequestered in inactive ribosomes (Denman *et al.*, 1991).

One odd aspect of the experimental scrapie is that the rate of *PrP* gene transcription is not modified, even though PrP<sup>c</sup> isoform is normally synthesized in the brain and the amount of PrP<sup>Sc</sup> increases exponentially throughout the course of the disease (Prusiner, 1991). In contrast, *PrP* mRNA expression in developing hamster brain is elevated by nerve growth factor (NGF), as well as the mRNA of amyloid precursor protein. This increase coincides with that of choline acetyl transferase activity (Mobley *et al.*, 1988). In addition the level of mRNA is regulated in a circadian manner (Cagampang *et al.*, 1999). In extracerebral tissues, various physiological and pathological situations can also increase the *PrP* mRNA expression as described below.

## B. Prion Protein Isoforms

### 1. Structure of the Protein

**a. Primary Structure** The amino acid sequence of the *PrP* polypeptide chain has been deduced from genomic and cDNA sequences (Oesch *et al.*, 1985; Locht *et al.*, 1986) and was found to be the same after protein sequencing (Turk *et al.*, 1988; Stahl *et al.*, 1993). The polypeptide has a length that varies only slightly between 253 (human) and 265 (bovine) residues and presents a very high homology in mammals (85–95%).

The sequence shows several peculiarities (Fig. 2). The amino terminus displays a segment of 22 residues, which is typical of signal peptides required for translocation in the membrane of the endoplasmic reticulum and is next cleaved to generate

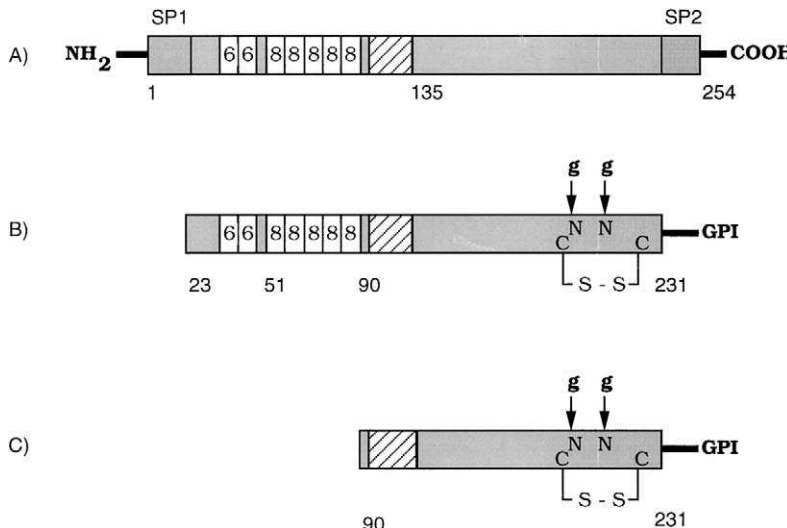


FIG. 2 Prion protein elements. (A) Precursor molecule. The protein contains two signal peptides, SP1 and SP2. The first routes the protein to the cellular membrane; the second is for the attachment of a GPI group. From residue 25 there is a short stretch of basic amino acids rich in proline and glycine (KKP/GRPKPGG). This sequence is regarded as a nuclear localization signal. The two hexapeptides and the five octapeptides have the sequence (GGS/NRYP) and (PHGGGGWGGQ), respectively. The following sequence is rich in hydrophobic amino acids alanine and glycine and contains a transmembrane insertion site between residues 110 and 135 (Lopez *et al.*, 1990). (B) Structure of the mature protein of 33–35 kDa. The N-terminal region starts at residues 23 after cleavage of the SP1 fragment. At the C-terminal region the GPI group is anchored at serine 231 after cleavage of the SP2 fragment. Two polysaccharide chains are generated at the N terminal of residues Asn 181 and Asn 187. A disulfide bond is established between Cys 179 and Cys 214. (C) Structure of the protease-resistant form of the *PrP<sup>c</sup>* abnormal isoform. The initial molecule similar to *PrP<sup>c</sup>* is cleaved at residue 90 by proteinase K enzyme to yield the 27- to 30-kDa polypeptide. This truncated protein is typically detected in prion-infected tissues.

the N-terminal sequence Lys-Lys-Arg of mature PrP. In the subsequent region, between residues 23 and 91, we find a highly conserved sequence rich in prolin and glycine that could be a nuclear localization signal (Oesch, 1994). This region is followed by two repeats of hexapeptides, and by a longer set of five (six in bovine) repeats of octapeptides. This N-terminal domain is a potential site for interaction with structures of the membrane glycosaminoglycan type and shows specific properties to bind copper (Hornshaw *et al.*, 1995; Miura *et al.*, 1996). When PrP<sup>sc</sup> is treated with proteinase K, this region is cleaved to generate PrP 27–30 kDa. Finally, there are two hydrophobic regions: (111 to 134) and (231 to 253). The polypeptide chain shows several phosphorylation consensus sequences. Recently the possibility of phosphorylating the recombinant bovine PrP (25–242) with PKC, CK2, and two tyrosine kinases, Lyn and c-Fgr, has been demonstrated. With regard to CK2, phosphorylation occurs at Ser 154, which might modulate PrP biological activity (Negro *et al.*, 2000).

**b. Posttranslational Modifications of Prion Protein** At the two N-glycosylation sites of the type Asn-Ile-Thr at codon 181 and Asn-Phe-Thr at codon 197, N-linked oligosaccharides are added during transit in the endoplasmic reticulum and Golgi apparatus providing a mature protein of 33–35 kDa. The two oligosaccharides with high-mannose cores differ in their sugar sequence. The PrP molecule is not O-glycosylated although it contains several potential sites on serine and threonine residues. PrP contains an intramolecular disulfide bound at Cys residues 177 and 212 (in hamster), which creates a loop of 36 amino acids containing the two Asn-linked oligosaccharides (Turk *et al.*, 1988). The C terminus is a hydrophobic region containing a sequence of 23 amino acids that is cleaved when the glyco-phosphatidylinositol group is attached to serine 231. The GPI anchor of PrP contains 30% sialic acid, constituting a unique example for a GPI-anchor protein (Stahl *et al.*, 1992).

**c. Secondary and Tertiary Structures** Cloning sequences and mass spectrometry did not show differences between PrP<sup>c</sup> and PrP<sup>sc</sup>. However, structural studies using Fourier transform infrared (FTIR) and circular dichroism (CD) spectroscopy indicated that PrP<sup>c</sup> and PrP<sup>sc</sup> differ from each other in their conformation (Caughey *et al.*, 1991; Safar *et al.*, 1993). PrP<sup>c</sup> has a secondary structure that contains approximately 43% of  $\alpha$  helix and very few  $\beta$  sheets (3%), while PrP<sup>sc</sup> has a  $\beta$ -sheet content of 43% and an  $\alpha$ -helix content of 30% (Pan *et al.*, 1993) (Fig. 3). PrP<sup>c</sup> displays a high plasticity depending on physicochemical conditions. The solubilization of native PrP<sup>c</sup> in solvent such as octadecylglucoside increases the proportion of  $\beta$ -sheet structure (Zhang *et al.*, 1997). From these data and computational procedures to predict the three-dimensional structures, four helix regions were identified: H1 (109–122), H2 (129–141), H3 (178–191), and H4 (202–218). During the process of conversion the first two helices would be transformed in  $\beta$  sheet. However, the refined analysis of murine recombinant PrP (produced in *Escherichia coli*) by nuclear magnetic resonance spectroscopy (NMR) (Riek *et al.*, 1996; Zahn *et al.*,

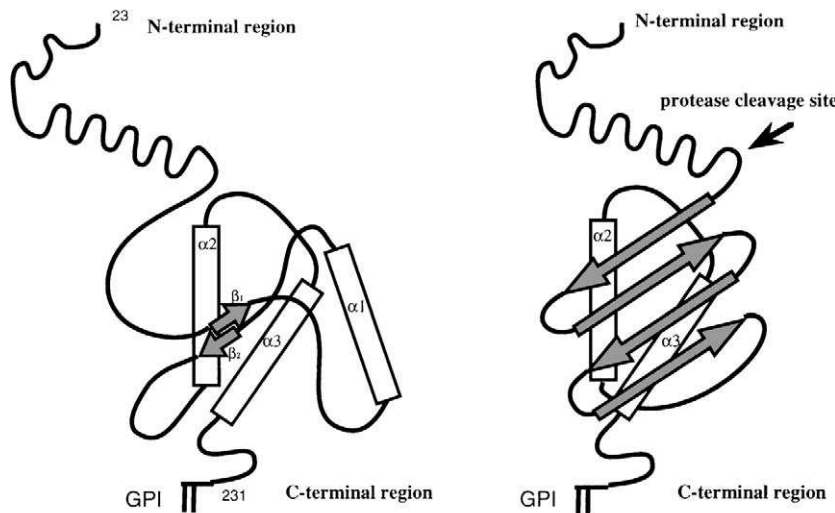


FIG. 3 Schematic representation of the three-dimensional structures of  $\text{PrP}^c$  and  $\text{PrP}^{sc}$ . Nuclear magnetic resonance (NMR) studies of recombinant murine prion protein indicate that the normal cellular protein is composed of two distinct regions: a flexible N-terminal segment (residues 23–125) and a globular domain (residues 126–231), which contains three  $\alpha$  helices (alpha 1: residues 144–154; alpha 2: residues 175–195; alpha 3: residues 200–219) and two antiparallel stranded  $\beta$  sheets (beta 1: residues 128–131; beta 2: residues 161–164). The transconformation of  $\text{PrP}^c$  into  $\text{PrP}^{sc}$  involves a change with decrease in  $\alpha$ -helix structures (43% to 30%) and increase in  $\beta$ -sheet content (3% to 43%). These structural modifications are accompanied by new physico chemical features (see Table II). The arrow indicates the cleavage site of proteinase K at residue 90.

2000) have brought more information on the globular domain of  $\text{PrP}^c$ , which shows in fact three helices comprising residues 144–154, 175–193 (173–195 in human), and 200–219 (200–228 in human) and a short antiparallel-sheet comprising residues 128–131 and 161–164. They also indicate that the N-terminal tail is a flexible, disordered structure that can be stabilized in  $\alpha$  helix by chelation with copper (Riek *et al.*, 1997; Zhang, *et al.*, 1997; Donne *et al.*, 1997; Liu *et al.*, 1999).

## 2. Metabolism of the Prion Protein

Metabolic labeling studies have shown that  $\text{PrP}^c$  is synthesized and degraded rapidly (Caughey *et al.*, 1989; Caughey and Raymond, 1991; Borchelt *et al.*, 1992). In less than 1 hr after the initiation of its biosynthesis,  $\text{PrP}^c$  reaches the cell surface (Fig. 4). Once on the plasma membrane,  $\text{PrP}^c$  normally has a half-life of 3–6 hr. The intracellular degradation process is not clear.

TABLE II

Properties of Normal (PrP<sup>c</sup>) and Abnormal (PrP<sup>sc</sup>) Forms of Prion Protein

PrP <sup>c</sup>	PrP <sup>sc</sup>
Sensitive to proteinase K	Resistant to proteinase K
Soluble in detergents	Insoluble in detergents
Membrane-bound	Membrane-bound and amyloid fibrils
Function unclear	Prion disease specific
Widely distributed in the organism	Accumulated in brain and lymphoid tissue

As a membrane glycoprotein, PrP<sup>c</sup> begins its metabolic cycle in the endoplasmic reticulum where a glycosphingolipid anchor and high-mannose glycans are rapidly attached. During the transit in the Golgi apparatus, the high-mannose moieties are converted to complex or hybrid glycans containing sialic acid and are resistant to endonuclease H (Caughey *et al.*, 1989). They account for up to 30% of

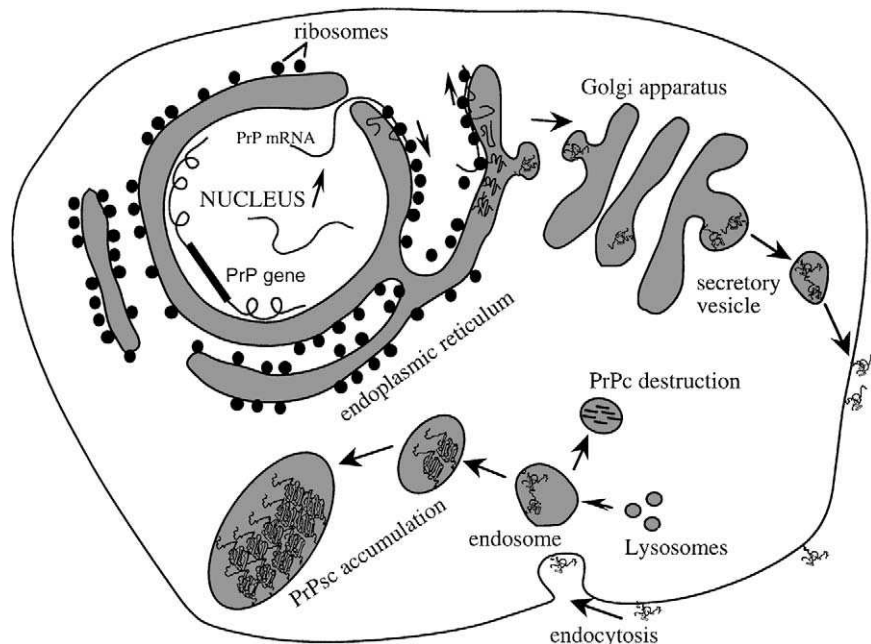


FIG. 4 Prion protein cellular cycle. The biosynthetic pathway of PrP<sup>c</sup> involves the endoplasmic reticulum, the Golgi apparatus where the protein is glycosylated, and secretory vesicles to reach the plasma membrane. After endocytosis PrP<sup>c</sup> is degraded by an unclear mechanism. The conversion of PrP<sup>c</sup> into PrP<sup>sc</sup> probably takes place in the endocytic pathway to lysosomes where PrP<sup>sc</sup> accumulates.

the mass of the protein (Bolton *et al.*, 1985). Chemical analysis of PrP<sup>sc</sup> derived from hamster brain tissue revealed about 400 different glycoforms (Endo *et al.*, 1989) suggesting that highly diverse glycan moieties are also produced during the biosynthesis of PrPc. While in brain tissue generally only three mature species of PrP (unglycosylated, monoglycosylated, and diglycosylated) can be observed, in cell cultures there is a predominance of several intermediate forms appearing between the three usual bands (Harris, 1999). Alterations in N-Asn glycosylation modify the biosynthetic transport of PrP<sup>c</sup>, which accumulates in a compartment proximal to the mid-Golgi stack (Lehmann and Harris, 1997; Rogers *et al.*, 1990). However some PrP<sup>c</sup> molecules can still be expressed at the cell surface in the presence of the glycosylation inhibitor tunicamycin (Lehmann and Harris, 1997). At the same time the disulfide bond is created, which influences the N glycosylation (Capellari *et al.*, 1999). Then via the secretory vesicles, PrP<sup>c</sup> is transported to the plasma membrane where it is anchored by the GPI moiety. This group can be digested by phosphoinositol-phospholipase C (PIPLC) and proteinase treatments removing PrP<sup>c</sup> from the cell surface (Stahl *et al.*, 1990).

Using transfected cell lines, complementary information has been obtained on the posttranslational cleavage of PrP<sup>c</sup> and its behavior at the plasma membrane. PrP<sup>c</sup> undergoes two cleavages as part of its normal metabolism. One occurs in the GPI, which releases PrP<sup>c</sup> in the extracellular space. It has been speculated that, as for other GPI-anchored proteins, a cell surface phospholipase is responsible for the cleavage (Harris, 1999). The second cleavage occurs in the peptide chain within a segment of 16 hydrophobic amino acids near position 110 and concerns 1–5% of the molecules. The cleavage can take place either within the endocytic compartment (Harris, 1999) or in the cholesterol-rich domain of the plasma membrane (Taraboulos *et al.*, 1995). The physiological significance of the cleavage is not known. The 10-kDa N-terminal fragment could serve as a biologically active ligand by analogy to polypeptide growth factors that are released by cleavage of membrane-bound precursors (Harris, 1999). At the cell surface PrP<sup>c</sup> undergoes continuous recycling between the plasma membrane and an endocytic compartment (Shyng *et al.*, 1993). Sulfated glycans stimulate endocytosis of PrP<sup>c</sup>, directing some of the molecules to late endosomes and/or lysosomes (Shyng *et al.*, 1995a).

Endocytosis is a general phenomenon used by a number of cell surface receptors involving a specialized structure named clathrin-coated pits. They are formed by invagination of plasma membrane to form vesicles that subsequently fuse with other intracellular organelles. Based on electron microscopy and PrP<sup>c</sup> detection in coated vesicle preparations purified from brain tissue, it has been shown that PrP<sup>c</sup> is internalized through these morphological structures (Shyng *et al.*, 1994); to be efficient, this process requires the N-terminal PrP<sup>c</sup> sequence (Shyng *et al.*, 1995b). However, clathrin-mediated endocytosis requires specialized amino acids in the cytoplasmic domain of transmembrane receptors that is lacking for GPI-anchored proteins such as PrP<sup>c</sup>. To explain the association of PrP<sup>c</sup> with coated pits, the existence of

a PrP<sup>c</sup> receptor having the properties to be endocytosed by coated pits and establishing binding with the N-terminal portion of PrP<sup>c</sup> has been postulated (Harris *et al.*, 1996). Among putative receptors many glycosaminoglycan molecules have shown affinity for the N-terminal half of the PrP sequence (Shyng *et al.*, 1995a). Alternatively, PrP<sup>c</sup> could be endocytosed by a process adapted for GPI-anchored proteins, implying other surface invagination called caveolae, which are coated on their surface with a protein named caveolin (Anderson, 1993). Interaction of PrP<sup>c</sup> and caveolin has been established in neuroblastoma cell lines where a physical association between the two proteins exists (Harmey *et al.*, 1995), and caveola-like membranous domains have been recognized as subcellular localization of PrP<sup>c</sup> in cultured cells and in Syrian hamster brain (Vey *et al.*, 1996). Although these possibilities remain under discussion (Shyng *et al.*, 1994; Gorodinsky and Harris, 1995), the caveolae-mediated membrane trafficking appears to be a process of primary importance for the conversion of PrP<sup>c</sup> into PrP<sup>sc</sup> (Vey *et al.*, 1996; Kaneko *et al.*, 1997).

### **III. Production and Subcellular Localization of Prion Proteins**

#### **A. Synthesis of PrP<sup>c</sup> of Nonneuronal Origin**

##### **1. Cerebral Tissues**

**a. Glial Cells** In addition to neuronal cells, several studies have shown that glial cell population of the central nervous system (CNS) had the potential to produce PrP<sup>sc</sup>. The first evidence was brought by Diedrich *et al.* (1991a) describing the immunodetection of PrP<sup>sc</sup> in astrocytes. Interestingly PrP accumulation occurs early in the course of the disease prior to the cardinal neuropathological changes, suggesting that these cells participate actively in PrP<sup>sc</sup> production. This appears to be correlated with increased expression of glial-specific genes such as apo E and cathepsin (Diedrich *et al.*, 1991b). Recently, the involvement of astrocytes has been confirmed in a scrapie-infected hamster model, where astrocytes localized mostly in the section area of the hippocampus disclosed accumulation of PrP<sup>sc</sup> in the cytoplasm (Ye *et al.*, 1998).

These observations strongly suggest that these cells synthesize the normal form though it has not been directly detected. Nevertheless, *in situ* hybridization studies strengthen this assumption. Indeed, previous observations report *PrP* mRNA localization in these cells in normal animals (Brown *et al.*, 1990; Moser *et al.*, 1995). *In vitro*, the expression of astroglial *PrP* mRNA is not modified by cytokines IGF-1 and growth hormone (GH) (Castelnau *et al.*, 1994), while it seems to increase after infection with the HIV-1 virus (Müller *et al.*, 1992). This is explained by the fact that the *PrP* mRNA contains loop regions that can be activated by a cofactor

(Schröder *et al.*, 1994). Finally, several subsequent experiments, have evidenced PrP<sup>c</sup> in astrocytes. In neuron-astrocyte cocultures, only PrP<sup>c</sup>-expressing astrocytes are able to protect neurons from glutamate-mediated toxicity (Brown, 1999). The use of pure cultures of astrocytes from mice has allowed researchers to examine the properties of PrP<sup>c</sup> to bind cation metals. The results showed that only the double glycosylated form found in astroglial cells (D. R. Brown *et al.*, 2000) is capable of incorporating manganese or nickel as a replacement for copper. The incorporation of manganese into PrP<sup>c</sup> abrogates almost completely its superoxide dismutase (SOD)-like enzymatic activity in aged cultures, and surprisingly makes it resistant to proteinase K, reminiscent of the PrP<sup>sc</sup> scrapie isoform property. These results suggest a mechanism to generate a resistant form of PrP that can initiate a conversion process in the absence of exogenous infectious particles as is thought to be the case in sporadic prion disease (D. R. Brown *et al.*, 2000).

These observations, in conjunction with transgenic experiments showing that the expression of the *PrP* gene in astrocytes alone is sufficient to induce scrapie disease (Raeber *et al.*, 1997), indicate that the astrocyte is presumably a good candidate for PrP<sup>sc</sup> production in brain tissue. In human, PrP<sup>sc</sup> in glial cells has been rarely mentioned (Kretzschmar *et al.*, 1991). An accurate understanding of brain pathology should take into account the fact that astrocytes express PrP<sup>c</sup> and replicate the agent, which can thus diffuse through these cells in the brain tissue. To date, no data are available on the implication of oligodendrocytes in PrP<sup>sc</sup> production even though the *PrP* gene is active in these cells (Moser *et al.*, 1995). Microglia at least in culture seem to express PrP mRNA (Merz *et al.*, 1986; Brown *et al.*, 1990) as well as the protein that appears to be important for its normal activation function (D. R. Brown *et al.*, 1998a). It has been suggested that in certain circumstances microglia could participate in the formation of PrP amyloid plaques (Wisniewski *et al.*, 1990). Nevertheless, the involvement of microglia in PrP<sup>sc</sup> formation is not clear. Immunoelectron microscopy studies have shown that PrP is detected in microglial lysosomal organelles that would suggest rather a role in degradation (Jeffrey *et al.*, 1994).

**b. Vessels** In the course of TSE pathogenesis, it is assumed that the agent progresses from the peripheral site of infection to the CNS via the peripheral nervous system through peripheral nerves and spinal cord. However, we cannot completely exclude the possibility that blood borne CNS contamination occurs (Foster *et al.*, 2000). This implies that the blood-brain barrier is disrupted or that cells sensitive to the agent (that is to say, expressing PrP<sup>c</sup> at the cell surface) are present in blood vessels. Molecular *in situ* hybridization experiments have shown that in fact endothelial cells of blood vessels are positive for *PrP* mRNA (Brown *et al.*, 1990) and consequently are capable of expressing PrP<sup>c</sup> at their surface, permitting access by the agent to the brain parenchyma.

**c. Other** By histoautoradiography, PrP mRNA has been reported to be localized in ependymal cells (H. R. Brown *et al.*, 1990; De Armond *et al.*, 1992), choroid

plexus epithelium, pericytes, and meningeal cells (Brown *et al.*, 1990). This expression provides a level of PrP<sup>c</sup> that is not detected by immunohistochemical methods. However, it is interesting to note that PrP<sup>sc</sup> can be detected in subpial and subependymal regions (DeArmond and Prusiner, 1993; Fournier *et al.*, 1996).

## 2. Extracerebral Tissues

**a. Lymphoreticular System** The lymphoreticular system has long been known to play a pivotal role in the pathogenesis of scrapie following peripheral infection (Mabbott *et al.*, 1998). Indeed, the spleen is the primary target for the replication of the agent before its propagation to the CNS (Fraser and Dickinson, 1978; Kimberlin and Walker, 1989), and the abnormal isoform of PrP has been detected in the spleen as well as in the lymph nodes (Rubenstein *et al.*, 1986; Shinagawa *et al.*, 1986; Doi *et al.*, 1988). Subsequent studies have specified in spleen fractions that the infectivity is associated with nonlymphoid cells (Clarke and Kimberlin, 1984). Finally immunocytochemical approaches have revealed that the cell candidate for replication is the follicular dendritic cell (FDC) (Kitamoto *et al.*, 1992; McBride *et al.*, 1992; Muramoto *et al.*, 1993). A positive signal is found in FDCs from spleen, lymph node, and intestine Peyer's patches (van Keulen *et al.*, 1999). Although the detection of PrP<sup>sc</sup> associated with FDCs suggests that the cells express PrP<sup>c</sup>, the expression level appears to be very low in noninfected animals (McBride *et al.*, 1992), and new immunohistochemical approaches have been necessary to demonstrate the presence of PrP<sup>c</sup> on FDCs by double immunofluorescence using cell markers (Ritchie *et al.*, 1999; K. L. Brown *et al.*, 1999, 2000). Although several lymphoid cell populations in the spleen express PrP<sup>c</sup> (Cashman *et al.*, 1990; Mabott *et al.*, 1997; and see below), it seems that FDCs are the privileged target for the prion disease agent (Mabbott *et al.*, 2000). In the lymphoid follicle, FDCs are also known to be the preferential site for replication of some conventional viruses (Burton *et al.*, 1997) such as HIV (Tenner-Racz and Racz, 1995) and Aleutian mink disease parvovirus (van Rooijen, 1992). In the thymus, which contains infectivity during scrapie (Fraser and Dickinson, 1978), FDCs are not present and PrP<sup>sc</sup> has been found to be associated with cells having rather an epithelial aspect (McBride *et al.*, 1992). Recently, in genetically modified mice, a reporter gene under the bovine PrP promoter has been visualized in thymus epithelial cells and Hassal's corpuscles, indicating the potential of these cells to express PrP<sup>c</sup> and therefore replicate the infectious agent (Lemaire-Vieille *et al.*, 2000).

### b. Circulating Blood Elements

*i. Mononuclear Cells* The analysis of human blood cells by immunoblot and cytofluorometry has established that PrP<sup>c</sup> is expressed on the membrane of all resting lymphocytes and monocytes, while erythrocytes and granulocytes do not express detectable levels (Cashman *et al.*, 1990). The PrP<sup>c</sup> expression is increased

after concanavalin A (Con A) lectin stimulation. The inhibition of lymphocyte mitogenesis is obtained by polyclonal antibodies to PrP in a concentration-dependent manner. The effect is lower when mitogenesis is induced by phytohemagglutinin. More recent experiments have confirmed these data and specified that T cells and monocytes have a similar PrP<sup>c</sup> expression level, while B cells displayed a lower level (Durig *et al.*, 2000). Cultured CD14<sup>+</sup> monocytes stimulated by interferon-gamma express PrP<sup>c</sup> at a higher level. This activation is inhibited by cycloheximide, indicating the implication of protein synthesis in the process. In mice the involvement of PrP<sup>c</sup> in lymphocyte activation by Con A lectin has also been demonstrated where a 50–80% reduction is observed in lymphocytes from genetically engineered mice with the inactive *PrP<sup>c</sup>* gene (*PrP* null mice) (Mabbott *et al.*, 1997). In human, researchers have described the B and T lymphocytes from tonsil as expressing PrP<sup>c</sup> at a lower level than the corresponding circulating cells and that the level is not affected after mitogenic stimulation *in vitro* (Antoine *et al.*, 2000). PrP<sup>c</sup> is also observed on normal hamster spleen cells and a variety of human hematologic cell lines including CEM T lymphoblasts, Raji and JY B lymphoblasts, and the U-937 histiocytic lymphoma (Cashman *et al.*, 1990). If granulocytes are PrP<sup>c</sup> negative, in contrast, PrP<sup>c</sup> is found in CD34<sup>+</sup> stem cells of bone marrow indicating that PrP<sup>c</sup> is suppressed in the course of the granulocyte differentiation. Experimentally, the suppression of PrP<sup>c</sup> in the differentiation process has been observed in the PrP<sup>c</sup>-positive premyeloid line HL-60 in which the retinoic acid induces differentiation, leading to PrP<sup>c</sup>-negative granulocyte-like cells (Dodelet and Cashman, 1998).

*ii. Platelets* The first description of PrP<sup>c</sup> in circulating platelets was made from human blood (Perini *et al.*, 1996a). The protein was detected by immunoblot after release from the plasma membrane by physiological stimulation using collagen or by enzymatic treatment with PIPLC. In addition, it appears that in resting and agonist-stimulated platelets a soluble N-terminal truncated PrP<sup>c</sup> isoform starting at position 90 (reminiscent of the cleavage of PrP<sup>Sc</sup>) is secreted (Perini *et al.*, 1996b). Subsequently, flow cytometry studies have specified that the activation causes an increase in the number of molecules at the cell surface from 1500–1800 to 4300–4800 (Holada *et al.*, 1998; Barclay *et al.*, 1999). Also, it has been observed that during activation, PrP<sup>c</sup>-like P selectin is translocated from internal granules to the plasma membrane (Holada *et al.*, 1998). In these experiments, it appears that PrP<sup>c</sup> is degraded by proteinase K, but contradictory results have been found about its resistance (Holada *et al.*, 1998) or not (Barclay *et al.*, 1999) to PIPLC treatment. In a recent study, a quantification of PrP<sup>c</sup> in human blood was done using a new method, time-resolved dissociation-enhanced fluoroimmunoassay (McGregor *et al.*, 1999). The results show that the majority of blood PrP<sup>c</sup> is found in the platelets (26.5%) and plasma compartments (68.5%). In future experiments it will be interesting to explore the presence of PrP<sup>c</sup> in precursor megacaryocytes. The presence of PrP<sup>c</sup> in platelets is potentially very attractive because these cells contain intracellular vesicular organelles having large similarities with vesicular synaptic function and platelets are considered as a model to examine biochemical and

pharmacological properties of synapsomes and nerve endings (Chatterjee and Anderson, 1993). They could be a useful model (Da Prada *et al.*, 1988; Bahler *et al.*, 1990; Lemons *et al.*, 1997) for exploring the function of PrP<sup>c</sup>, the morphological data of which have pointed out that it is mainly sublocalized in presynaptic vesicular organelles (Fournier *et al.*, 1995, 2000; Sales *et al.*, 1998; Moya *et al.*, 2000; Haerbelé *et al.*, 2000).

**c. Macrophages** As noted above, blood monocytes express PrP<sup>c</sup>; the differentiated cells in tissues or histiocytes such as microglial cells in brain are also capable of synthesizing PrP<sup>c</sup>. In skin, in addition to epithelial cell, PrP<sup>c</sup> is detected in mononuclear cells presumed to be lymphocytes and macrophages (Pammer *et al.*, 1998). Macrophages infiltrating muscle tissue during various neuromuscular disorders, such as polymyositis and sporadic inclusion-body myositis, show a high expression of *PrP* mRNA, which is translated in the corresponding protein (Sarkosi *et al.*, 1994). The inframicroscopic observations after immunoelectron microscopy indicated the presence of PrP<sup>c</sup> on membranous and fibrillar structures but without other information in the absence of a good morphological preservation. The expression of PrP<sup>c</sup> is accompanied by that of the  $\beta$ -amyloid precursor protein, suggesting that these proteins play a role in the biology of muscle macrophages, including those involved in human muscle immune/inflammatory responses (Askanas *et al.*, 1993b).

**d. Gastrointestinal Tract** Western blot analysis of the gastrointestinal tract has revealed the presence of PrP<sup>c</sup> in hamster (Bendheim *et al.*, 1992) and sheep tissues (Horiuchi *et al.*, 1995). One can suppose that although the enteric nervous system contains PrP<sup>c</sup> (Beekes and McBride, 2000), the intensity of the signal observed on the blot is generated by nonneuronal gastrointestinal cells. Several observations confirm this point.

*i. Stomach* Immunohistochemistry methods have shed some light on the identity of the cells that express PrP<sup>c</sup>. The first evidence came from studies of Bendheim *et al.* (1992) showing that parietal cells in mucosa disclosed intense immunofluorescence labeling. The identification of the PrP<sup>c</sup>-positive cells at the ultrastructural level on human material has revealed that parietal (Fig. 5) but also vessel endothelial cells express PrP<sup>c</sup> strongly at the cell membrane (Fournier *et al.*, 1996, 1998, 2000). In these studies, using two anti-PrP antibodies, mucous cells of the epithelial border were also found harboring PrP<sup>c</sup> in their secretory granules and at the plasma membrane (Fig. 6) both in human and hamster tissues. In human and mice, epithelial cells lining the gastrointestinal tract have been found expressing PrP<sup>c</sup> (Liu *et al.*, unpublished data, cited in Sy and Gambetti, 1999).

Recently, the digestive tract of lemurs fed with BSE-contaminated food has been analyzed by immunocytochemistry (Bons *et al.*, 1999). The abnormal prion protein (PrP<sup>Sc</sup>) has been detected in cells of the stomach, the esophagus, and the intestine. Although the immunocytochemical approach was restricted to the detection of

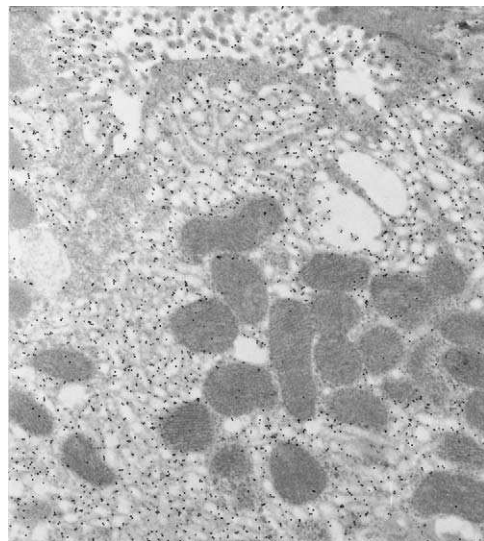


FIG. 5 Human stomach parietal cell showing PrP<sup>c</sup>-immunogold labeling on microvilli (20,000 $\times$ ).

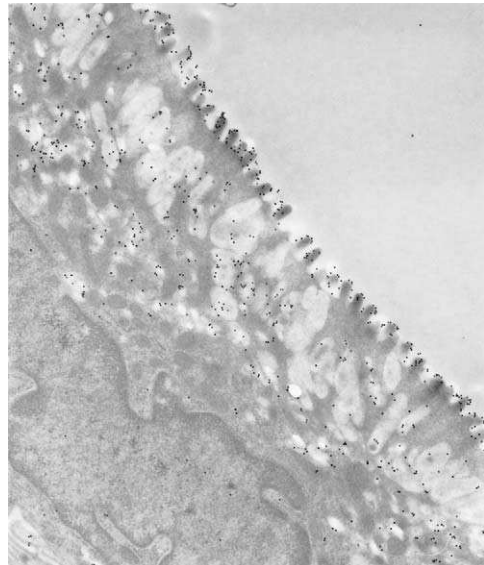


FIG. 6 Ultrastructural immunogold-labeling specific for PrP<sup>c</sup> on hamster stomach secretory granules and plasma membrane (20,000 $\times$ ).

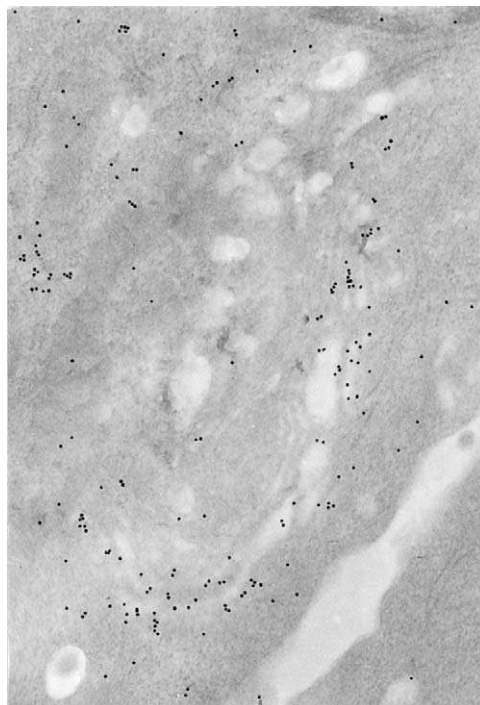


FIG. 7 Ultrastructural immunogold-labeling specific for PrP<sup>c</sup> on hamster intestine Golgi apparatus. (25,000 $\times$ ).

PrP<sup>sc</sup>, one can suppose that cells also express PrP<sup>c</sup>, since PrP<sup>sc</sup> cannot be formed in the absence of PrP<sup>c</sup>.

*i. Intestine* Immunoelectron microscopy studies have revealed in hamster intestine an accumulation of PrP<sup>c</sup> essentially in the secretory granules and the Golgi apparatus of goblet mucous cells (Fig. 7) (Fournier *et al.*, 1998). In contrast, in mouse intestine we observed a PrP<sup>c</sup> labeling localized on microvilli of enteric cells (unpublished data). The difference might be explained by a species-specific regulation of the *PrP* gene.

**e. Skin** Epidemiological and experimental data suggest that the skin could serve as a portal of entry for the TSE agent in the organism (Gajdusek, 1996; Taylor *et al.*, 1996). This implies that some categories of skin cells should express PrP<sup>c</sup>. To reveal such cells, an immunocytochemistry study has been performed on human skin in normal and pathological situations including inflammatory diseases, psoriasis, and contact dermatitis as well as squamous cell carcinomas and viral warts (Pammer *et al.*, 1998). In normal epidermis, keratinocytes in the basal layer express PrP<sup>c</sup> at

a low level, whereas in disease situations (eczema, psoriasis, and common warts), one can note a PrP up-regulation in these cells. A similar study undertaken with cow material demonstrated that PrP<sup>c</sup> is expressed in normal basal keratinocytes, while in acanthotis epidermis adjacent to skin ulcers PrP<sup>c</sup> is up-regulated in these cells (Pammer *et al.*, 1999). These experiments provide evidence that *in vivo*, the *PrP* gene is specifically regulated according to the physiopathological state of the cells. In both cases, primary cultured bovine and human keratinocytes express constitutively PrP<sup>c</sup> having a molecular weight ranging between 30 and 43 kDa. The melanoma cell line SkMEL28 also expresses PrP<sup>c</sup>, but no expression is detected in HaCaT and A431 epithelial cell lines. The expression is up-regulated by TGF- $\alpha$  and IFN- $\gamma$  in keratinocyte primary cultures. While the cytokines are without effect on the epidermoid carcinoma cell line A431, they strongly stimulate PrP<sup>c</sup> expression on HaCaT cells. Interestingly, in cytokine-stimulated cells an additional band of approximately 23 kDa appears corresponding to the nonglycosylated form of PrP<sup>c</sup>. Skin contains antigen-presenting dendritic cells called Langerhan's cells. In the future, it will be interesting to determine whether these cells express PrP<sup>c</sup> (like follicular dendritic cells) and therefore could have the potential to replicate the infectious agent.

**f. Liver** Between the endothelial cells and the hepatocytes, there is a zone of rapid intercellular exchange containing perisinusoidal stellate or Ito cells. These cells are modified resting fibroblasts that can store fat and vitamin A (Schirmacher *et al.*, 1992) and they appear to play a significant role in liver fibrogenesis. To examine the activation and proliferation of hepatic stellate cells during injury, the expression of different gene in rat has been analyzed using suppression subtractive hybridization. Surprisingly it has been observed that the *PrP* gene is included among 13 genes expressed in activated stellate cells (Ikeda *et al.*, 1998). The *PrP* mRNA increases in cultured stellate cells from rat and hamster in a time-dependent manner, similar to smooth-muscle  $\alpha$ -actine mRNA expression. In fibrotic liver tissue induced by carbon tetrachloride, stellate cells localized in and around the fibrous septa display expression of *PrP* mRNA and the corresponding protein detected by histohybridization and immunohistochemistry, respectively. In contrast, in untreated liver a negligible *PrP* mRNA is noted and no immunoreactivity is present. These results are in agreement with previous studies indicating that in normal liver, PrP<sup>c</sup> is not detected by Western blot (Bendheim *et al.*, 1992). PrP<sup>c</sup> has also been examined in cultured freshly isolated stellate cells with a very low expression of *PrP* mRNA at day 0 after culture that increases in a time-dependent manner up to day 14, concomitant with  $\alpha$ -actin mRNA. Further exploring the subcellular site of stellate cell PrP<sup>c</sup> by immunoelectron microscopy, the authors have demonstrated that PrP<sup>c</sup> is preferentially located along the plasma membrane (Ikeda *et al.*, 1998). The overexpression of PrP<sup>c</sup> might be correlated to oxidative stress (Lee *et al.*, 1995) and could be involved in the development of liver fibrosis. It has been demonstrated that hepatocytes do not support the propagation of the

prion agent even though they expressed PrP<sup>c</sup>. In *PrP* knockout mice, when the *PrP* gene is introduced under the control of the albumin promoter to give rise to hepatocyte-specific expression of PrP<sup>c</sup>, the inoculation of TSE agent does not induce scrapie (Raeber *et al.*, 1999).

**g. Lung** In the normal hamster lung tissue, PrP<sup>c</sup> detection by immunocytochemistry is predominantly observed in bronchiolar cells. At the electron microscopy level, submicroscopic immunodetection of PrP<sup>c</sup> is revealed in secretory granules of nonciliated Clara cells (Bendheim *et al.*, 1992). We have confirmed this observation (Fournier *et al.*, 1998) showing for the first time the morphological aspect of the *in vivo* secretory function of PrP<sup>c</sup> (Hay *et al.*, 1987). Nevertheless, it appears that other cells in the lung can potentially express PrP<sup>c</sup> since a DNA probe specific for *PrP* reacts on histological sections containing alveolar lining and septal interstitial pulmonary cells (Brown *et al.*, 1990). From the pathogenesis point of view, these results suggest that contamination is possible by the respiratory tract. Indeed, the lung is able to replicate the agent, signifying that a proportion of permissive cells are present in this tissue (Bolton, 1998).

**h. Muscle** In muscle, immunohistofluorescence studies conducted on human material have shown that a fluorescent signal specific for PrP<sup>c</sup> was generated at the neuromuscular junction (NMJ) (Askanas *et al.*, 1993a). In this structure, PrP<sup>c</sup> is localized in the postsynaptic domain identified with alpha-bungaratoxin ( $\alpha$ -BT), which reacts with the receptor of acetyl-choline bound to the postsynaptic plasma membrane. These observations indicate that the PrP<sup>c</sup> signal is generated by the nonneuronal part of the junction constituted by skeletal muscle cell. We have confirmed and extended these data to mammalian muscle tissues. In human, hamster, and mouse, the NMJ is positive after incubation with two specific anti-PrP antibodies (Gohel *et al.*, 1999). The signal colocalizes with the  $\alpha$ -BT one. However, the two fluorescence signals observed with a confocal microscope remain distinct, implying that the two molecules are not strictly colocalized. To specify this point, we have conducted experiments at the ultrastructural level using a postembedding immunogold electron microscopy method (Fournier and Escaig-Haye 1999). The result clearly indicates that PrP<sup>c</sup> is not sublocalized at the plasma membrane but concentrated in the subsynaptic sarcoplasm of the NMJ. The PrP<sup>c</sup>-gold signal is distributed from near the plasma membrane of the synaptic folds to the myofibril domain. At that place, PrP<sup>c</sup> is presumed to be associated with the membrane of endosomal organelles. *In vitro* experiments have shown that heparan sulfate proteoglycans induce internalization of PrP<sup>c</sup> (Shyng *et al.*, 1995a). The presence of such biomolecules in abundance in the basal lamina of the synaptic cleft might explain the internalized form of PrP<sup>c</sup> that is seen in the subsynaptic region (Fig. 8).

Several data indicate that PrP<sup>c</sup> is constitutively synthesized by muscle cell and does not come from the neuronal part, because *PrP* mRNA detected by *in situ*

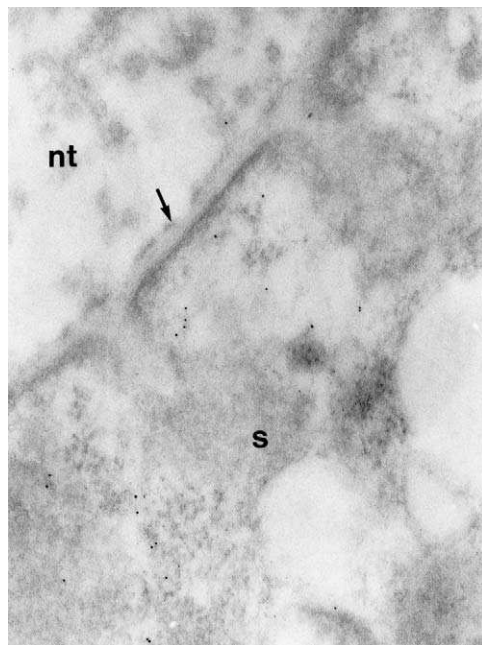


FIG. 8 Neuromuscular junction of mouse skeletal muscle. The 5-nm gold particle-labeling specific for PrP<sup>c</sup> is distributed over the subsynaptic sarcoplasm (S). nt, nerve terminal; basal lamina, arrow (80,000 $\times$ ).

hybridization accumulates at the NMJ (Sarkozi *et al.*, 1994) and cultured muscle-dissected mouse cells express PrP<sup>c</sup> (Brown *et al.*, 1998b). In this *in vitro* system, it has been established that an up-regulation of PrP<sup>c</sup> expression occurs in the course of the differentiation from myoblasts to myotubes. However, the *in vivo* localization of PrP<sup>c</sup> at the subsynaptic compartment of the NMJ and its appearance 7 days postnatally (Fournier *et al.*, 2000) would imply PrP<sup>c</sup> during NMJ maturation rather than formation. This localization is not sufficient in itself to differentiate between a physiologic function of PrP<sup>c</sup> in relation to the activity of the NMJ, or a role in the maintenance of the morphological integrity of the structure (Nguyen and Lichtman, 1996).

**i. Sperm Cells** It has been previously demonstrated that testes contain PrP<sup>c</sup> (Bendheim *et al.*, 1992), and *PrP* mRNA has been subsequently revealed in seminiferous tubules (Tanji *et al.*, 1995). A recent study has specified the presence of PrP<sup>c</sup> in mature sperm cells from cattle and human and in epididymis cells from cattle and rodents (Shaked *et al.*, 1999). Interestingly, it is noted that during the process of sperm maturation, PrP<sup>c</sup> loses the GPI group, after a C-terminal region

truncation, and remains at the membrane even with PIPLC treatment. This unique situation prevents the conversion process into a PrP<sup>sc</sup> isoform, which requires an intact GPI anchor (Taraboulos *et al.*, 1995). Nevertheless, this truncated molecule keeps its copper-binding properties and the authors suggest a putative role in protection against stress situations. Given that sperm cells have a reduced metabolism, the authors propose to use these cells as a model to elucidate the function of PrP<sup>c</sup> (Shaked *et al.*, 1999).

**j. Pancreas** In the pancreas, PrP<sup>c</sup> is synthesized in islet of Langerhans (McBride *et al.*, 1992; K. L. Brown *et al.*, 2000). In fetal rat islet primary cultures and in various cell lines producing insulin-( $\beta$ ) (RINm5F, INS-1,  $\beta$ TC-1, and  $\beta$ TC-3) and glucagon-( $\alpha$ ) ( $\alpha$ -TC), expression of *PrP* mRNA similar to neuronal cells has been shown (Atouf *et al.*, 1994). This expression appears to be regulated by hormones such as growth hormone and dexamethasone, two factors implicated in  $\beta$ -cell (INS-1) maturation, which increased the *PrP* mRNA steady-state level. Although PrP<sup>c</sup> is expressed in rodent tissue (Bendheim *et al.*, 1992), it would seem that in sheep, this expression is absent or very low (Horiuchi *et al.*, 1995). No information is available on the identity of the cells responsible for the appearance of PrP<sup>sc</sup> in scrapie-infected hamster pancreas showing deep morphological alterations within islets of Langerhans (Ye and Carp, 1995). The knowledge of the precise role of PrP<sup>c</sup> in  $\beta$  cells is of great importance because  $\beta$  and neuronal cells share a large number of similarities, such as synthesis of catecholamine enzymes (Teitelman and Lee, 1987), synaptophysin (Kalina *et al.*, 1991; Brudzynski and Martinez, 1993), and neuronal cell adhesion (Langley *et al.*, 1989). These cells also resemble neurons, being electrically excitable and responding to stimuli by depolarization and exocytosis in a process similar to that of neurotransmitter from synaptic vesicles (De Camilli and Jahn, 1990). They could also be implicated in the replication of the agent to explain the infectivity that is found in pancreas after peripheral infection (Farquhar *et al.*, 1994).

**k. Eyes** The observation that the Alzheimer precursor protein (APP) and the pathological form of  $\beta$  amyloid are overexpressed in organ culture mammalian lenses exposed to UV radiation and hydrogen peroxide (Frederikse *et al.*, 1996) led the authors to examine another amyloidogenic protein represented by the prion protein (Frederikse *et al.*, 1999). By reverse transcriptase–polymerase chain reaction (RT-PCR) they revealed mRNA coding for PrP<sup>c</sup> in guinea pig and rhesus monkey lenses. In subsequent experiments, a similar approach was used to measure the relative level of PrP<sup>c</sup> mRNA expression from epithelial and fiber cells of guinea pig lenses. In normal mammalian lens development, epithelial cells migrate to evolve into elongated fiber cells, which lose their cellular organelles and debase their DNA. The results show that *PrP* gene expression is approximately 8- to 10-fold greater in the fiber cells compared to epithelial cells, signifying that the expression increases in the course of the differentiation. The increase is also

significantly observed in the cultured human lens epithelial cell line SRA 01-04 exposed to oxidative stress induced by  $200\text{-}\mu\text{M}$  hydrogen peroxide for 3 hr. In human lenses, immunoblotting confirms the presence of 28–30 kDa specific to PrP<sup>c</sup> revealed with a 3F4 monoclonal antibody. The analysis of human lenses with cortical cataracts by immunocytochemistry identifies the regions of lens fiber cell disorganization and degeneration as accumulating PrP<sup>c</sup> similar to APP,  $\beta$  amyloid, and presenilin proteins. These experiments demonstrate the implication of Alzheimer's disease and prion proteins in lens pathology (Frederikse *et al.*, 1999).

***l. Other*** Adrenal, kidney, heart, and salivary glands also express the normal isoform of prion protein (Bendheim *et al.*, 1992; McBride *et al.*, 1992; Horiuchi *et al.*, 1995; K. L. Brown *et al.*, 2000). In salivary glands, PrP<sup>c</sup> is found in mucous-secreting cells, whereas in the adrenal, it is the zona fasciculata that is the most prominent structure involved in immunohistodetection (K. L. Brown *et al.*, 2000). In kidney, cuboidal epithelium cells of proximal and distal tubules are positive (K. L. Brown *et al.*, 2000) for PrP<sup>c</sup> and seem to be sublocalized at the plasma membrane (Fournier *et al.*, 1998). By immunoelectron microscopy, the plasma membranes of some collector tube cells have also been observed to be PrP positive (Fournier *et al.*, 1998). In hamster heart, the cells involved could be myocardial cells, which express *PrP* mRNA (Brown *et al.*, 1990). In rat, histohybridization experiments have also localized expression of *PrP* mRNA in placenta (subpopulation of decidua cells and in the amnion and mesodermal layer of the yolk sac) and in the myometrium of the uterus (Tanji *et al.*, 1995). Similar data were obtained for mouse tissues (Manson *et al.*, 1992).

## B. Subcellular Localization

Biochemical experiments have demonstrated the cellular secretory pathway of PrP<sup>c</sup> from the endoplasmic reticulum to the plasma membrane using the neuroblastoma cell line. Some distinct locations of PrP<sup>c</sup> along its biosynthesis process have been morphologically visualized in nonneuronal cells.

### 1. Plasma Membrane

The plasma membrane is considered to be the final destination of PrP<sup>c</sup>. Although evidenced *in vitro*, the PrP<sup>c</sup> plasma membrane localization has not yet been documented in neurons of cerebral tissue. In contrast, several studies have shown this location in nonneuronal cells. The PrP<sup>c</sup> cell surface has been identified by cytofluorometry approaches, in lymphoid cells and platelets from circulating blood (Cashman *et al.*, 1990; Perini *et al.*, 1996a). The network pattern of immunofluorescence labeling obtained with FDCs in spleen sections suggests very strongly that the cell

surface is involved (K. L. Brown *et al.*, 1999). In liver, immunoelectron microscopy studies have demonstrated this localization on stellate cells (Pammer *et al.*, 1998). Similarly, in hamster and human stomach the epithelial cell border expresses PrP<sup>c</sup> at the plasma membrane, in addition to human stomach parietal and endothelial cells. Hamster kidney tubule cells and human collector tubule cells also express PrP<sup>c</sup> at the cell surface (Fournier *et al.*, 1998).

## 2. Secretory Vesicles and Granules

While PrP<sup>c</sup> is expressed at the cell surface of kidney, stomach, and intestine cells, it is also found in the vesicles and granules of secretion. In lung nonciliated Clara cells, the expression seems to occur only in secretory granules (Bendheim *et al.*, 1992; Fournier *et al.*, 1998). At the neuromuscular junction, PrP<sup>c</sup>-gold labeling is observed in the subplasmalemma regions, likely in vesicular organelles of the subsynaptic sarcoplasm (Gohel *et al.*, 1999).

## 3. Golgi Apparatus

Ultrastructural studies have also shown that the Golgi apparatus is a step in the pathway of the protein in nonneuronal cells. In human stomach and hamster intestine, gold labeling specific for PrP<sup>c</sup> has been seen on this cellular organelle (Fournier *et al.*, 1998). Similar PrP<sup>c</sup> labeling has also been recently reported in a human neuroblastoma cell line (Zanusso *et al.*, 1998).

## 4. Nucleus

In the mouse scrapie-infected neuroblastoma cell line (ScN2a), immunocytochemical studies have revealed epitopes from prion proteins sequestered in the nuclear compartment particularly the nucleolus (Pfeifer *et al.*, 1993). On the basis of the N-terminal extremity which contains the sequence KKRPKP, Oesch (1994) proposed that the prion protein could have a nuclear localization. This short stretch of basic amino acid is indeed reminiscent of the classical nuclear localization signal of some viruses such as the simian virus 40 large T antigen (Kalderon *et al.*, 1984). Although this PrP sequence appears not to be efficient in targeting the protein in the nuclear compartment in Hela cells (Jaegly *et al.*, 1998), an association of PrP with a ribonucleoprotein complex containing the nuclear lectin CBP35 has been reported (Schröder *et al.*, 1994). The presence of PrP<sup>c</sup> in the nucleus and particularly in the nucleolus has been examined in the human promyelocytic leukemia cell line, where PrP<sup>c</sup> is a partner to another nuclear specific lectin CBP70 (A. P. Sève, personal communication). The exact role of PrP<sup>c</sup> in this nuclear environment remains to be determined but it might be in relation to the regulation of its own mRNA (Schröder *et al.*, 1994).

## 5. Mitochondria

Two sets of experiments have evidenced an intriguing relation between prion proteins and mitochondria. Purified mitochondria from scrapie-infected brain have been shown to contain infectivity, particularly in the mitoplasm (Aiken *et al.*, 1989). In the SAF fraction, which contains infectivity and PrP<sup>sc</sup>, a fragment of the mitochondrial DNA loop has been revealed using PCR (Aiken *et al.*, 1990). Even though PrP<sup>sc</sup> has not been found in the mitochondrial fraction, these observations suggest a possible location of PrP<sup>sc</sup> within mitochondria. The facts that PrP<sup>c</sup> is a metalloprotein with an affinity for copper and manganese and has a SOD-like enzymatic activity (D. R. Brown *et al.*, 1999, 2000) also suggest a possible PrP<sup>c</sup> mitochondrial site. The existence of a PrP<sup>c</sup>-bcl2 interaction (Kurschner and Morgan, 1995) and given that bcl2 is partially mitochondrial (Hockenberry *et al.*, 1990; Zhu *et al.*, 1996) reinforce such an assumption. We have sometimes observed a mitochondrial localization of PrP<sup>c</sup> in some extracerebral tissues. Because it is conceivable that PrP<sup>c</sup> has several subcellular locations, all of these fragmented data might justify further exploration of the mitochondrial location.

## IV. Functions of Cellular Prion Proteins

Studies of PrP<sup>c</sup> are undertaken for two main reasons: first for a better understanding of the pathogenesis process, since this molecule plays a central role in the replication of the infectious agent not only in the central nervous system but also elsewhere particularly in the lymphoreticular system. The second reason is to elucidate the PrP<sup>c</sup> function in the organism. Given the widespread presence of PrP<sup>c</sup>, the question is to determine if this function is unique to all PrP<sup>c</sup>-expressing cells or if it is cell specific. From the data available so far neither hypothesis can be confirmed.

### A. Cell-Specific Physiological Roles

#### 1. Central Nervous System

In animals with a defective *PrP* gene, the phenotype is various: either the animals look healthy (Büeler *et al.*, 1992; Manson *et al.*, 1994) or present neurological abnormalities, ataxia, (Sakaguchi *et al.*, 1996) and sleep disorders (Tobler *et al.*, 1996). These differences could be linked to the construction of genetically engineered mice (Weissmann, 1996). However, no abnormalities have ever been observed outside the CNS, indicating that even though PrP<sup>c</sup> is widely distributed in the organism the physiologic role of the PrP<sup>c</sup> seems to be more crucial for nerve cells, particularly neurons. In fact, it has been shown that this particular

vulnerability is related to the ectopic expression of the prion-like protein gene (Doppel) in the brain (Moore *et al.*, 1999; Silverman *et al.*, 2000). In healthy animals, with only the deletion of the PrP coding sequence, electrophysiologic abnormalities have been reported (Collinge *et al.*, 1994). However, for others (Herms *et al.*, 1995; Lledo *et al.*, 1996) a deficiency in PrP<sup>c</sup> seems to have no effect on neuron physiology. A similar situation is observed in mutant mice lacking synaptophysin, where the absence of the protein does not modify the synaptic transmission and plasticity (McMahon *et al.*, 1996). Interestingly, a PrP<sup>c</sup>-synaptophysin colocalization has been observed in the central synapse (Fournier *et al.*, 1995) and several data are convergent to assign PrP<sup>c</sup> to the presynaptic compartment (Kitamoto *et al.*, 1992; Fournier *et al.*, 1997; Sales *et al.*, 1998; Herms *et al.*, 1999; Fournier, 2000) where it could be connected with vesicular synaptic organelles (Fournier *et al.*, 2000; Haeberlé *et al.*, 2000; Moya *et al.*, 2000). Further studies will be necessary to specify to which category of presynaptic vesicular organelles PrP<sup>c</sup> is located and the role played by PrP<sup>c</sup> in neurotransmission.

## 2. Outside the Nervous System

In lymphocytes, PrP<sup>c</sup> participates in the activation process and can interact with blastogenic lectine molecules (Cashman *et al.*, 1990; Mabbott *et al.*, 1999; Durig *et al.*, 2000). During activation, PrP<sup>c</sup> expression is similarly up-regulated to Thy-1, Qa-2, CD14, LFA-3, FcR-III, and Blast-1. So PrP<sup>c</sup>, like other glycosyl-phosphatidylinositol-linked lymphoid proteins, may act as cell-cell adhesion molecules (LFA3 binding to CD2), a membrane receptor-transducer (FCR-III binding immune complexes), or an activation released soluble signal (Thy-1, Qa-2, and CD14) (Cashman *et al.*, 1990). The presence of PrP<sup>c</sup> in mucous-secreting cells of the salivary gland (K. L. Brown *et al.*, 2000) and in secretory granules of lung, stomach, and intestine cells suggests a role in the secretory process (Bendheim *et al.*, 1992; Fournier *et al.*, 1998) in which PrP<sup>c</sup> could also be a secretory product. It has been observed that in cerebrospinal fluid, normal PrP<sup>c</sup> is present in soluble form (Tagliavini *et al.*, 1992), indicating that the release by cell is a natural phenomenon for PrP<sup>c</sup>, which is known to have a secretory form (Hay *et al.*, 1987).

### B. Nonspecific Cellular Functions

The data available concerning the putative role of PrP<sup>c</sup> have so far been essentially obtained using cells of neuronal origin. If the PrP<sup>c</sup> function is universal in the cellular physiology, one would think that it would be the same in all nonneuronal cells of the organism expressing PrP<sup>c</sup>. Nevertheless, this should be confirmed in future experiments.

## 1. Metalloprotein and Oxidative Stress

The discovery that PrP<sup>c</sup> is a metalloprotein with an affinity for copper has provided elements of an argument to suggest a universal role in all cells coupled to the copper metabolism (Hornshaw *et al.*, 1995; Miura *et al.*, 1996; Brown *et al.*, 1998a; Viles *et al.*, 1999). It is worth noting that copper is implicated in neurodegenerative disorders and cuprizone is a copper-chelating molecule that can reproduce neuropathological lesions observed in scrapie (Kimberlin *et al.*, 1974). As noted above, a specific domain of the protein sequence is able to bind copper, which stabilizes the PrP molecule in the N-terminal region (Donne *et al.*, 1997; Riek *et al.*, 1997) and restores the proteinase resistance and infectivity after denaturation with guanidine (McKenzie *et al.*, 1998).

The content of copper in membrane preparations (measured with radioactive copper-67) from *PrP* null mouse brain is markedly reduced as compared to that of wild-type mice (Brown *et al.*, 1997c). In the N2a neuroblastoma cell, the addition of Cu<sup>2+</sup> to the medium stimulates the internalization of PrP<sup>c</sup>, reducing the amount at the cell surface while subsequent removal of Cu<sup>2+</sup> restores the cell surface PrP<sup>c</sup> expression. The authors propose that PrP<sup>c</sup> could serve as an endocytic receptor for the uptake of copper from the extracellular milieu (Pauly and Harris, 1998). A similar role of removal of Cu<sup>2+</sup> has been observed in a variant of PC12 cells selected for resistance to copper toxicity and oxidative stress and that expresses elevated levels of PrP<sup>c</sup> (D. R. Brown *et al.*, 1997a). These results indicate that PrP<sup>c</sup> and copper metabolism can be linked to oxidative stress.

Several data have shown a link between PrP<sup>c</sup> and cellular resistance to oxidative stress (Brown *et al.*, 1996, 1997b; White *et al.*, 1999). Cultures of cerebellar cells from mice deficient in the *PrP* gene are more sensitive to oxidative stress (induced by treatment with superoxide radicals) and undergo cell death more readily than wild-type cells. This effect is reversible by treatment with vitamin E (Brown *et al.*, 1997b). The reduced resistance to oxidative stress is associated with lower activity of the Cu/Zn superoxide dismutase (SOD). The reduction of SOD activity is also noted *in vivo* in the brain from *PrP* gene-ablated mice (Brown *et al.*, 1997b). PrP<sup>c</sup> would regulate SOD activity by influencing copper incorporation into the molecule (Brown and Besinger, 1998). Moreover, recombinant *PrP* from chicken and mouse and brain-derived PrP<sup>c</sup> have a unexpected copper-dependent SOD activity (D. R. Brown *et al.*, 1999). This activity is abolished by deletion of the binding copper octapeptide-repeat region or by addition of the copper chelator diethyldithiocarbamate.

Taken together, these data support the hypothesis that the normal cellular isoform of the prion protein plays a role as an antioxidant factor in the copper cellular metabolism, promoting the delivery of copper to cuproenzymes and having itself such an enzymatic activity. Recent data, however require a reevaluation of this view (Waggoner *et al.*, 2000). It has been found that, first, there is no direct

relationship between the level of PrP<sup>c</sup> expression and the amount of copper (measured by mass spectrometry and atomic absorption) in brain fractions from *PrP* null, wild-type, and *PrP*-overexpressing mice; second, the enzymatic activity of Cu/Zn SOD and cytochrome *c* oxidase is similar in these groups of animals. Based on these observations, the authors propose that the role of PrP<sup>c</sup> in the copper metabolism be reconsidered, suggesting a function in the copper trafficking and its possible intracellular sequestration (Waggoner *et al.*, 2000). The capacity of PrP<sup>c</sup> to accumulate copper in intracytoplasmic vesicular organelles might explain the predominant internalized form of PrP<sup>c</sup> we have observed at the nerve–nerve and nerve–muscle synapses (Fournier *et al.*, 1995; Gohel *et al.*, 1999). The PrP<sup>c</sup> molecule also shows properties of participation in the redox balance, because PrP<sup>c</sup> can achieve its antioxidative function by being itself oxidized on reactive chemical groups such as methionine residues (Wong *et al.*, 1999).

The analysis of the role of PrP<sup>c</sup> in oxidative stress through copper metabolism should now be extended to PrP<sup>c</sup>-expressing nonneuronal cells. A first example is provided by human lens cultures, which respond to peroxide treatment by increasing the *PrP* gene expression level (Frederikse *et al.*, 1999). Otherwise, further experiments are necessary to clarify the relationship between copper metabolism and other metal ions with which PrP<sup>c</sup> is connected such as manganese (D. R. Brown *et al.*, 2000) and calcium (Whatley *et al.*, 1995).

## 2. Receptors for PrP<sup>c</sup>

A number of studies have been conducted to analyze molecules that can interact with PrP<sup>c</sup>. The knowledge of such a ligand is useful, first, to characterize proteins collectively designated “protein X,” which play a key role in the conversion of PrP<sup>c</sup> into PrP<sup>Sc</sup>; second, to help in the understanding of the PrP<sup>c</sup> cellular function. Several proteins have been identified such as Hsp104, GroEL, Hsp60, Bcl-2, and Nrf-2 (DebBurmann *et al.*, 1997; Edenhofer *et al.*, 1996; Kurschner and Morgan, 1995; Yehiely *et al.*, 1997). The interaction with heat-shock proteins evoked the affiliation of PrP<sup>c</sup> with heat-shock stress conditions (Tatzelt *et al.*, 1995, 1998). However, the molecular mechanism of the PrP<sup>c</sup> implication is not clear. While the absence of PrP<sup>c</sup> in cultured skin fibroblasts isolated from *PrP* null mice does not modify the major heat-shock proteins in response to cellular stress (Satoh *et al.*, 1998), the same conditions increase the *PrP* mRNA and protein expression in human neuronal NT-2 cells (Shyu *et al.*, 2000). Recently, the involvement of the 37-kDa laminin receptor precursor (LRP) has been evidenced (Rieger *et al.*, 1997) using a yeast two-hybrid system. This approach is known to be a powerful tool in divulging a high intermolecular affinity between two proteins. The LRP–PrP interaction was confirmed by coinfection and cotransfection studies in insect and mammalian cells, respectively. Interestingly the expression of LRP in mice brain, spleen, and pancreas is increased in scrapie-infected animal regions where PrP<sup>Sc</sup> is found.

LRP expression has also been observed to be increased twofold in scrapie-infected N2a cells compared with uninfected N2a cells in which immunofluorescence microscopy showed that LRP is located on the cell surface (Rieger *et al.*, 1999). It is worth noting that the LRP is a transmembrane protein that interacts with PrP<sup>c</sup> in the 161- to 180-amino-acid sequence, a domain localized in the extracellular space. The molecule could thus be a good candidate to help the internalization of PrP<sup>c</sup> in clathrin-coated pits (Harris, 1999). The LRP is the precursor of the 67-kDa laminin receptor and it is interesting to note that an unidentified 66-kDa protein has also been shown to be a ligand for PrP (Martins *et al.*, 1997). In addition a recent study has demonstrated the molecular interaction of PrP<sup>c</sup> with the laminin gamma-1 chain influencing neuritogenesis from cultured primary neuronal rat cells or PC-12 cells treated with NGP (Graner *et al.*, 2000). Laminin is a 900-kDa glycoprotein forming a molecule family that differs in the three peptide chains alpha, beta, and gamma (Beck *et al.*, 1990). This protein constitutes an essential component of the extracellular matrix and basement membranes, which play a role in cell attachment, differentiation, movement, and growth (Patton *et al.*, 1997). The discovery of the LRP-PrP interaction, revealing a relationship between PrP<sup>c</sup> and the extracellular matrix, opens perspectives on the role of PrP<sup>c</sup> in cell adhesion and signalling. It would be interesting to explore the PrP<sup>c</sup>-laminin interaction in nonneuronal experimental models such as fibroblasts from cultured periodontal ligament cells in which a correlation exists between PrP<sup>c</sup> mRNA expression and cell growth arrest and differentiation (Kniazeva *et al.*, 1997).

### C. Possible Role in the Pathogenesis of Prion Diseases

The expression of PrP<sup>c</sup> is necessary for replication of the infectious agent but not sufficient. As reported in the present review, a large number of cells in the organism express PrP<sup>c</sup>; however, among them, only a few are able to replicate the agent, namely, neurons and glial and follicular dendritic cells, and only the infected nerve cells induce a specific disease in brain. Indeed no physiologic abnormalities are observed outside the CNS. The idea that the PrP<sup>sc</sup> abnormal isoform is sufficient to promote pathological events in contact with PrP<sup>c</sup>-expressing cells seems not to be satisfactory for the lymphoreticular system where PrP<sup>sc</sup> accumulates in the germinal center in the absence of injuries of the FDC and lymphoid tissue. This situation is reminiscent of slow virus infection in brain where the virus is present outside the CNS, particularly in lymphoid organs, without giving rise to noticeable physiologic abnormalities (Brown *et al.*, 1989). PrP<sup>c</sup> in nonneuronal cells has an important consequence for the pathogenesis of prion disease. In natural infection, several peripheral organs have been suspected to be the site of entry used by the TSE agent. PrP<sup>c</sup> expression in skin, lung, and digestive tract reinforces this assumption. The episode of BSE and nCJD has at least demonstrated the involvement of the gastrointestinal system. The presence of PrP<sup>c</sup> at the cell surface may constitute a receptor

for the infectious agent, which can then be conveyed to reach vital locations required to enable its replication. Therefore, three actors play a major role in prion diseases: the infectious transmissible agent, the neuronal cell, and the FDC. But several secondary actors are involved, represented by nonneuronal cells in which the expression of PrP<sup>c</sup> is crucial in permitting the entrance and diffusion of the agent into the host. These sensitive nonneuronal cells are not capable of replicating the agent because they probably lack several cellular factors such as “protein X.”

## **V. Concluding Remarks**

PrP<sup>c</sup> plays a central role in TSE because it constitutes the fundamental substratum of the infectious agent required for its replication. The expression of the protein in the CNS governs the manifestation of the disease. Elsewhere, PrP<sup>c</sup> expression is necessary for penetration diffusion and primary replication of the agent in lymphoid tissue.

From the pathogenesis point of view, two extracerebral sites appear important enough to be taken into consideration during future investigations: First, the gastrointestinal tract, which is in direct contact with the agent in the course of oral infection. The exact localization of PrP<sup>c</sup> in different categories of cells along the digestive pathway should be examined and particularly the involvement of M cells, which are specialized in the ingestion of microbial agents. The second site concerns the lymphoreticular system and the expression of PrP<sup>c</sup> in various cells present in the germinal center such as macrophages, which can store the pathological isoform PrP<sup>sc</sup>. New avenues of research are opening by exploring the interface between the immune and nervous systems and the conditions of agent transfer from the nonneuronal to the neuronal cell.

A better understanding of these mechanisms would be useful to develop new therapeutic strategies that could specifically prevent the replication of the infectious agent in lymphoid tissue and/or the passage to the CNS. It would also be interesting to specify the subcellular localization of PrP<sup>c</sup> in tissues where infectivity can be found such as the pancreas and salivary glands. We noted that in some tissues (lens, skin, liver, and muscle), PrP<sup>c</sup> expression increases in the course of pathological processes. Knowledge of the behavior of PrP<sup>c</sup> in nonneuronal cells could be useful in the framework of general pathology. It would be interesting to explore further its implication in physiopathologic mechanisms, which could in turn also be fruitful in highlighting aspects of its normal physiologic function.

The ubiquitous localization of PrP<sup>c</sup> in the organism raises the question of such a function. Although a cell-specific function is not entirely excluded in certain cases, the idea of a universal role has opened two directions of research. The first is concerned with the analysis of the connection of PrP<sup>c</sup> with copper metabolism in relation to oxidative stress. The second consists of further exploring the role

of PrP<sup>c</sup> in cell adhesion, differentiation and signaling through its interaction with components of the extracellular matrix such as laminin. These studies should be undertaken with cells of nonneuronal origin to substantiate the hypothesis of a common role for PrP<sup>c</sup> in all cells expressing PrP<sup>c</sup>. Currently, this role seems to distinguish two categories of cells in the organism according to the two putative roles assigned to PrP<sub>c</sub>.

## Acknowledgments

The author wishes to thank Steve Simoneau and Corinne Lasmézas for helpful discussions and readings of the manuscript. This work was supported by grants from Ministère de la Recherche et de la Technologie. Philippe Bozin is thanked for illustrations.

## References

Aiken, J. M., Williamson, J. L., and Marsh, R. F. (1989). Evidence of mitochondrial involvement in scrapie infection. *J. Virol.* **63**, 1686–1694.

Aiken, J. M., Williamson, J. L., Borchardt, L. M., and Marsh, R. F. (1990). Presence of mitochondrial D-loop DNA in scrapie-infected brain preparations enriched for the prion protein. *J. Virol.* **64**, 3265–3268.

Anderson, R. G. (1993). Caveolae: Where incoming and outgoing messengers meet. *Proc. Natl. Acad. Sci. USA* **90**, 10909–10913.

Antoine, N., Cesbron, J. Y., Coumans, B., Jolais, O., Zorzi, W., and Heinen, E. (2000). Differential expression of cellular prion protein on human blood and tonsil lymphocytes. *Haematologica* **5**, 475–480.

Askanas, V., Bilak, M., King Engel, W., Leclerc, A., and Tomé, F. (1993a). Prion protein is strongly immunolocalized at the postsynaptic domain of human normal neuromuscular junctions. *Neurosci. Lett.* **159**, 111–114.

Askanas, V., Bilak, M., King Engel, W., Alvarez, R. B., Tomé, F., and Leclerc, A. (1993b). Prion protein is abnormally accumulated in inclusion-body myositis. *Neuroreport* **5**, 25–28.

Atouf, F., Scharfmann, R., Lasmezas, C., and Czernichow, P. (1994). Tight hormonal control of *PrP* gene expression in endocrine pancreatic cells. *Biochem. Biophys. Res. Commun.* **201**, 1220–1226.

Bahler, M., Cesura, A. M., Fischer, G., Kuhn, H., Klein, R. L., and Da Prada, M. (1990). Serotonin organelles of rabbit platelets contain synaptophysin. *Eur. J. Biochem.* **194**, 825–829.

Bamborough, P., Wille, H., Telling, G. C., Yehiely, F., Prusiner, S. B., and Cohen, F. E. (1996). Prion protein structure and scrapie replication: Theoretical, spectroscopic, and genetic investigations. *Cold Springs Harb. Symp. Quant. Biol.* **61**, 495–509.

Barclay, G. R., Hope, J., Birkett, C. R., and Turner, M. L. (1999). Distribution of cell-associated prion protein in normal adult blood determined by flow cytometry. *Br. J. Haematol.* **107**, 804–814.

Baybutt, H., and Manson, J. (1997). Characterisation of two promoters for prion protein (*PrP*) gene expression in neuronal cells. *Gene* **184**, 125–131.

Beck, K., Hunter, I., and Engel, J. (1990). Structure and function of laminin: Anatomy of a multidomain glycoprotein. *FASEB J.* **4**, 148–160.

Beekes, M., and McBride, P. A. (2000). Early accumulation of pathological PrP in the enteric nervous system and gut-associated lymphoid tissue of hamsters orally infected with scrapie. *Neurosci. Lett.* **278**, 181–184.

Bendheim, P. E., Brown, H. R., Rudelli, R. D., Scala, J., Goller, N. L., Wen, G. Y., Kascsak, R. J., Cashman, N. R., and Bolton, D. C. (1992). Nearly ubiquitous tissue distribution of the scrapie agent precursor protein. *Neurology* **42**, 149–156.

Bolton, D. C. (1998). Prion distribution in hamster lung and brain following intraperitoneal inoculation. *J. Gen. Virol.* **79**, 2557–2562.

Bolton, D. C., Meyer, R. K., and Prusiner, S. B. (1985). Scrapie PrP 27–30 is a sialoglycoprotein. *J. Virol.* **53**, 596–606.

Bons, N., Mestre-France, N., Belli, P., Cathala, F., Gajdusek, D. C., and Brown, P. (1999). Natural and experimental oral infection of nonhuman primates by bovine spongiform encephalopathy agents. *Proc. Natl. Acad. Sci. USA* **96**, 4046–4051.

Borchelt, D. R., Taraboulos, A., and Prusiner, S. B. (1992). Evidence for synthesis of scrapie prion protein in the endocytic pathway. *J. Biol. Chem.* **267**, 16188–16199.

Brown, D. R., and Besinger, A. (1998). Prion protein expression and superoxide dismutase activity. *Biochem. J.* **334**, 423–429.

Brown, D. R. (1999). Prion protein peptide neurotoxicity can be mediated by astrocytes. *J. Neurochem.* **73**, 1105–13.

Brown, D. R., Schmidt, B., and Kretzschmar, H. A. (1996). Role of microglia and host prion protein in neurotoxicity of a prion protein fragment. *Nature (Lond.)* **380**, 345–347.

Brown, D. R., Schmidt, B., and Kretzschmar, H. A. (1997a). Effects of oxidative stress on prion protein expression in PC12 cells. *Int. J. Dev. Neurosci.* **15**, 961–972.

Brown, D. R., Schulz-Schaeffer, W. J., Schmidt, B., and Kretzschmar, H. A. (1997b). Prion protein-deficient cells show altered response to oxidative stress due to decreased SOD-1 activity. *Exp. Neurol.* **146**, 104–112.

Brown, D. R., Qin, K., Herms, J. W., Madlung, A., Manson, J., Strome, R., Fraser, P. E., Kruck, T., von Bohlen, A., Schulz-Schaeffer, W., Giese, A., Westaway, D., and Kretzschmar, H. (1997c). The cellular prion protein binds copper *in vivo*. *Nature (Lond.)* **390**, 684–687.

Brown, D. R., Besinger, A., Herms, J. W., and Kretzschmar, H. A. (1998a). Microglial expression of the prion protein. *Neuroreport* **9**, 1425–1429.

Brown, D. R., Schmidt, B., Groschup, M. H., and Kretzschmar, H. A. (1998b). Prion protein expression in muscle cells and toxicity of a prion protein fragment. *Eur. J. Cell Biol.* **75**, 29–37.

Brown, D. R., Wong, B. S., Hafiz, F., Clive, C., Haswell, S. J., and Jones, I. M. (1999). Normal prion protein has an activity like that of superoxide dismutase. *Biochem. J.* **344**, 1–5.

Brown, D. R., Hafiz, F., Glasssmith, L. L., Wong, B. S., Jones, I. M., Clive, C., and Haswell, S. J. (2000). Consequences of manganese replacement of copper for prion protein function and proteinase resistance. *EMBO J.* **19**, 1180–1186.

Brown, H. R., Goller, N. L., Rudelli, R. D., Dymecki, J., and Wisniewski, H. M. (1989). Postmortem detection of measles virus in non-neuronal tissues in subacute sclerosing panencephalitis. *Ann. Neurol.* **26**, 263–268.

Brown, H. R., Goller, N., Rudelli, G., Wolfe, G. C., Wisniewski, H. M., and Robakis, N. K. (1990). The mRNA encoding the scrapie agent protein is present in a variety of non neuronal cells. *Acta Neuropath.* **80**, 1–6.

Brown, K. L., Stewart, K., Ritchie, D. L., Mabbott, N. A., Williams, A., Fraser, H., Morrison, W. I., and Bruce, M. E. (1999). Scrapie replication in lymphoid tissues depends on prion protein-expressing follicular dendritic cells. *Nat. Med.* **5**, 1308–1312.

Brown, K. L., Ritchie, D. L., McBride, P. A., and Bruce, M. E. (2000). Detection of PrP in extraneuronal tissues. *Microsc. Res. Tech.* **50**, 40–45.

Bruce, M. E., Will, R. G., Ironside, J. W., McConnell, I., Drummond, D., Suttie, A., McCurdle, L., Chree, A., Hope, J., Birkett, C., Cousens, S., Fraser, H., and Bostock, C. J. (1997). Transmissions to mice indicate that “new variant” CJD is caused by the BSE agent. *Nature (Lond.)* **389**, 498–501.

Brudzynski, K., and Martinez, V. (1993). Synaptophysin-containing microvesicles transport heat-shock protein hsp60 in insulin-secreting beta cells. *Cytotechnology* **11**, 23–33.

Büeler, H., Aguzzi, A., Saile, A., Greiner, R. A., Autenried, P., Aguet, M., and Weissmann, C. (1992). Normal development and behaviour of mice lacking the neuronal cell-surface PrP protein. *Cell* **73**, 1339–1347.

Burton, G. F., Masuda, A., Heath, S. L., Smith, B. A., Tew, J. G., and Szakal, A. K. (1997). Follicular dendritic cells (FDC) in retroviral infection: Host/pathogen perspectives. *Immunol. Rev.* **156**, 185–197.

Cagampang, F. R., Whatley, S. A., Mitchell, A. L., Powell, J. F., Campbell, I. C., and Coen, C. W. (1999). Circadian regulation of prion protein messenger RNA in the rat forebrain: A widespread and synchronous rhythm. *Neuroscience* **91**, 1201–1204.

Capellari, S., Zaidi, S. I., Uriel, C. B., Perry, G., Smith, M. A., and Petersen, R. B. (1999). Prion protein glycosylation is sensitive to redox change. *J. Biol. Chem.* **274**, 34846–34850.

Cashman, N. R., Lortscher, R., Nallbantoglu, J., Shaw, I., Kascak, R. J., Bolton, D. C., and Bendheim, P. E. (1990). Cellular isoform of the scrapie agent protein participates in lymphocyte activation. *Cell* **61**, 185–192.

Castelnau, P., Lazarin, F., Deslys, J. P., and Dormont, D. (1994). Prion protein gene expression in cultured astrocytes treated by recombinant growth hormone and insulin-like growth factor. *Exp. Neurol.* **130**, 407–410.

Caughey, B., and Raymond, G. J. (1991). The scrapie-associated form of PrP is made from a cell surface precursor that is both protease and phospholipase sensitive. *J. Biol. Chem.* **266**, 18217–18223.

Caughey, B., Race, R. E., Ernst, D., Buchmeier, M. J., and Chesebro, B. (1989). Prion protein (PrP) biosynthesis in scrapie infected and uninfected neuroblastoma cells. *J. Virol.* **63**, 175–181.

Caughey, B., Dong, A., Bhat, K. S., Ernst, D., Hayes, S. F., and Caughey, W. S. (1991). Secondary structure analysis of the scrapie-associated protein PrP 27–30 in water by infrared spectroscopy. *Biochemistry* **30**, 7672–7680.

Chatterjee, D., and Anderson, G. M. (1993). The human platelet dense granule, serotonin uptake, tetra-benazine binding, phospholipid and ganglioside profiles. *Arch. Biochem. Biophys.* **302**, 4339–4346.

Chazot, G., Broussolle, E., Lapras, C. L., Blattler, T., Aguzzi, A., and Kopp, N. (1996). New variant of Creutzfeldt-Jakob disease in a 26-year-old French man. *Lancet* **347**, 1181.

Chesebro, B., Race, R., Wehrly, K., Nishio, J., Bloom, M., Lechner, D., Bergstrom, S., Robbins, K., Mayer, L., Keith, J. M., Garon, C., and Haase, A. (1985). Identification of scrapie prion protein-specific mRNA in scrapie-infected and uninfected brain. *Nature (Lond.)* **315**, 331–333.

Clarke, M. C., and Kimberlin, R. H. (1984). Multiplication of scrapie agent in mouse spleen. *Res. Vet. Sci.* **9**, 215–225.

Collinge, J., Whittington, M., Sidle, K., Smith, C., Palmer, M., Clarke, A., and Jefferys, J. (1994). Prion protein is necessary for normal synaptic function. *Nature (Lond.)* **370**, 295–297.

Collinge, J., Sidle, K. C., Meads, J., Ironside, J., and Hill, A. F. (1996). Molecular analysis of prion strain variation and the aetiology of “new variant” CJD. *Nature (Lond.)* **383**, 685–590.

Da Prada, M., Cesura, A. M., Launay, J. M., and Richards, J. G. (1988). Platelets as a model for neurones? *Experientia* **44**, 115–126.

De Armond, S. J., Jendoska, K., Yang, S. L., Taraboulos, A., Hecker, R., Hsiao, K., Stowring, L., Scott, M., and Prusiner, S. B. (1992). Scrapie prion protein accumulation correlates with neuropathology and incubation times in hamsters and transgenic mice. In “Prion Diseases of Humans and Animals” (S. B. Prusiner, J. Collinge, J. Powell, and B. Anderton, Eds.), pp. 481–496. Ellis Horwood Limited, Chichester, England.

DeArmond, S. J., and Prusiner, S. B. (1993). The neurochemistry of prion diseases. *J. Neurochem.* **61**, 1589–1601.

DeBurman, S. K., Raymond, G. J., Caughey, B., and Lindquist, S. (1997). Chaperone-supervised conversion of prion protein to its protease-resistant form. *Proc. Natl. Acad. Sci. USA* **94**, 13938–13943.

De Camilli, P., and Jahn, R. (1990). Pathways to regulated exocytosis in neurons. *Annu. Rev. Physiol.* **52**, 625–645.

Denman, R., Potempaska, A., Wolfe, G., Ramakrishna, N., and Miller, D. L. (1991). Distribution and activity of alternatively spliced Alzheimer amyloid peptide precursor and scrapie PrP mRNAs on rat brain polysomes. *Arch. Biochem. Biophys.* **288**, 29–38.

Diedrich, J. F., Bendheim, P. E., Kim, Y. S., Carp, R. I., and Haase, H. T. (1991a). Scrapie-associated prion protein accumulates in astrocytes during scrapie infection. *Proc. Natl. Acad. Sci. USA* **88**, 375–379.

Diedrich, J. F., Minnigan, H., Carp, R. I., Whitaker, J. N., Race, R., Frey, W., and Haase, A. T. (1991b). Neuropathological changes in scrapie and Alzheimer's disease are associated with increased expression of apolipoprotein E and cathepsin D in astrocytes. *J. Virol.* **65**, 4759–4768.

Dodelet, V. C., and Cashman, N. R. (1998). Prion protein expression in human leukocyte differentiation. *Blood* **91**, 1556–1561.

Doi, S., Ito, M., Shinagawa, M., Sato, G., Isomura, H., and Goto, H. (1988). Western blot detection of scrapie-associated fibril protein in tissues outside the central nervous system from preclinical scrapie-infected mice. *J. Gen. Virol.* **69**, 955–960.

Donne, D. G., Viles, J. H., Groth, D., Mehlhorn, I., James, T. L., Cohen, F. E., Prusiner, S. B., Wright, P. E., and Dyson, H. J. (1997). Structure of the recombinant full-length hamster prion protein PrP(29–231): The N terminus is highly flexible. *Proc. Natl. Acad. Sci. USA* **94**, 13452–13457.

Durig, J., Giese, A., Schulz-Schaeffer, W., Rosenthal, C., Schmucker, U., Bieschke, J., Duhrsen, U., and Kretzschmar, H. A. (2000). Differential constitutive and activation-dependent expression of prion protein in human peripheral blood leucocytes. *Br. J. Haematol.* **108**, 488–495.

Edenhofer, F., Rieger, R., Famulok, M., Wendler, W., Weiss, S., and Winnacker, E. L. (1996). Prion protein PrP<sup>c</sup> interacts with molecular chaperones of the Hsp60 family. *J. Virol.* **70**, 4724–4728.

Endo, T., Groth, D., Prusiner, S. B., and Kobata, A. (1989). Diversity of oligosaccharide structures linked to asparagines of the scrapie prion protein. *Biochemistry* **28**, 8380–8338.

Farquhar, C. F., Dornan, J., Somerville, R. A., Tunstall, A. M., and Hope, J. (1994). Effect of Sinc genotype, agent isolate and route of infection on the accumulation of protease-resistant PrP in non-central nervous system tissues during the development of murine. *J. Gen. Virol.* **75**, 495–504.

Foster, P. R., Welch, A. G., McLean, C., Griffin, B. D., Hardy, J. C., Bartley, A., MacDonald, S., and Bailey, A. C. (2000). Studies on the removal of abnormal prion protein by processes used in the manufacture of human plasma products. *Vox Sang.* **78**, 86–95.

Fournier, J. G. (2000). Introduction to histological localization of prion proteins. *Microsc. Res. Tech.* **50**, 1.

Fournier, J. G., and Escaig-Haye, F. (1999). In situ molecular hybridization techniques for ultra-thin sections. In "Electron Microscopy, Methods and Protocols. Methods in Molecular Biology" (M. A. Hajibagheri, Ed.), pp. 167–182. Humana Press, Ottawa.

Fournier, J. G., Escaig-Haye, F., Billette de Villemeur, T., and Robain, O. (1995). Ultrastructural localization of cellular prion protein (PrP<sup>c</sup>) in synaptic boutons of normal hamster hippocampus. *C. R. Acad. Sci. Paris* **318**, 339–344.

Fournier, J. G., Escaig-Haye, F., Billette de Villemeur, T., and Robain, O. (1996). Distinct subcellular localization of PrP<sup>c</sup> detected by immunoelectron microscopy: Functional implications. In "Transmissible Subacute Spongiform Encephalopathies: Prion Diseases" (L. Court and B. Dodet, Eds.), pp. 121–128. Elsevier, Paris.

Fournier, J. G., Escaig-Haye, F., Billette de Villemeur, T., and Robain, O. (1997). Synaptic aspects of cellular prion protein. In "Advances in Organ Biology" (B. Festoff, D. Hantai, and B. A. Citron, Eds.), Vol. 2, pp. 99–111. JAI Press Inc., Greenwich, CT.

Fournier, J. G., Escaig-Haye, F., Billette de Villemeur, T., Robain, O., Lasmezas, C. I., Deslys, J. P., Dormont, D., and Brown, P. (1998). Distribution and submicroscopic immunogold localization of cellular prion protein (PrP<sup>c</sup>) in extracerebral tissues. *Cell Tiss. Res.* **22**, 77–84.

Fournier, J. G., Escaig-Haye, F., and Grigoriev, V. (2000). Ultrastructural localization of prion proteins: Physiological and pathological implications. *Microsc. Res. Tech.* **50**, 76–88.

Fraser, H., and Dickinson, A. G. (1978). Studies of the lymphoreticular system in the pathogenesis of scrapie: the role of spleen and thymus. *J. Comp. Pathol.* **88**, 563–573.

Frederikse, P. H., Garland, D., Zigler, J. S., Jr., and Piatigorsky, J. (1996). Oxidative stress increases production of beta-amyloid precursor protein and beta-amyloid (Abeta) in mammalian lenses, and Abeta has toxic effects on lens epithelial cells. *J. Biol. Chem.* **271**, 10169–10174.

Frederikse, P. H., Zigler, S. J., Jr., Farnsworth, N., and Carper, D. A. (1999). Prion protein expression in mammalian lenses. *Curr. Eye Res.* **20**, 137–143.

Gajdusek, D. C. (1977). Unconventional viruses and the origin and disappearance of kuru. *Science* **197**, 943–960.

Gajdusek, D. C. (1996). Infectious amyloids. In “Fields Virology” (B. N. Fields, D. M. Knipe, and P. M. Howley, Eds.), pp. 2851–2900. Lippincott-Raven, Philadelphia, PA.

Gibbs, C. J., Jr., and Bolis, C. L. (1997). Normal isoform of amyloid protein (PrP) in brains of spawning salmon. *Mol. Psychiatry* **2**, 146–147.

Gohel, C., Grigoriev, V., Escaig-Haye, F., Lesmezas, C. I., Deslys, J. P., Langeveld, J., Akaaboune, M., Hantai, D., and Fournier, J. G. (1999). Ultrastructural localization of cellular prion protein (PrP<sup>C</sup>) at the neuromuscular junction. *J. Neurosci. Res.* **55**, 261–267.

Gorodinsky, A., and Harris, D. A. (1995). Glycolipid-anchored proteins in neuroblastoma cells form detergent-resistant complexes without caveolin. *J. Cell Biol.* **129**, 619–627.

Graner, E., Mercadante, A. F., Zanata, S. M., Forlenza, O. V., Cabral, A. L., Veiga, S. S., Juliano, M. A., Roessler, R., Walz, R., Minetti, A., Izquierdo, I., Martins, V. R., and Brentani, R. R. (2000). Cellular prion protein binds laminin and mediates neuritogenesis. *Brain Res. Mol. Brain Res.* **76**, 85–92.

Haeberlé, A., Ribaut-Barassin, C., Bombarde, G., Mariani, J., Hunsmann, G., Grassi, J., and Bailly, Y. (2000). Synaptic prion protein immuno-reactivity in the rodent cerebellum. *Microsc. Res. Tech.* **50**, 66–75.

Harmey, J. H., Doyle, D., Brown, V., and Rogers, M. S. (1995). The cellular isoform of the prion protein, PrP<sup>C</sup>, is associated with caveolae in mouse neuroblastoma (N2a) cells. *Biochem. Biophys. Res. Commun.* **210**, 753–759.

Harris, D. (1999). Cellular biology of prion diseases. *Clin. Microbiol. Rev.* **12**, 429–444.

Harris, D. A., Lele, P., and Snider, W. D. (1993). Localization of the mRNA for a chicken prion protein by *in situ* hybridization. *Proc. Natl. Acad. Sci. USA* **90**, 4309–4313.

Harris, D. A., Gorodinsky, A., Lehmann, S., Moulder, K., and Shyng, S. L. (1996). Cell biology of the prion protein. *Curr. Topics Microbiol. Immunol.* **207**, 77–93.

Hay, B., Prusiner, S. B., and Lingappa, V. R. (1987). Evidence for a secretory form of the cellular prion protein. *Biochemistry* **26**, 8110–8115.

Herms, J., Kretzschmar, H., Titz, S., and Keller, B. (1995). Patch-clamp analysis of synaptic transmission to cerebellar Purkinje cells of prion protein knockout mice. *Eur. J. Neurosci.* **7**, 2508–2512.

Herms, J., Tings, T., Gall, S., Madlung, A., Giese, A., Siebert, H., Schurmann, P., Windl, O., Brose, N., and Kretzschmar, H. (1999). Evidence of presynaptic localization and function of the prion protein. *J. Neurosci.* **19**, 8866–8875.

Hockenberry, D., Nunez, G., Milliman, C., Schreiber, R. D., and Korsmeyer, S. J. (1990). Bcl-2 is an inner mitochondrial membrane protein that blocks programmed cell death. *Nature (Lond.)* **348**, 334–336.

Holada, K., Mondoro, T. H., Muller, J., and Vostal, J. G. (1998). Increased expression of phosphatidylinositol-specific phospholipase C resistant prion proteins on the surface of activated platelets. *Br. J. Haematol.* **3**, 276–282.

Horiuchi, M., Yamazaki, N., Ikeda, T., Ishiguro, N., and Shinagawa, M. (1995). A cellular form of prion protein PrP<sup>C</sup> exists in many non-neuronal tissues of sheep. *J. Gen. Virol.* **76**, 2583–2587.

Hornshaw, M. P., McDermott, J. R., Candy, J. M., and Lakey, J. H. (1995). Copper binding to the N-terminal tandem repeat regions of mammalian and avian prion protein. *Biochem. Biophys. Res. Commun.* **207**, 621–629.

Ikeda, K., Kawada, N., Wang, Y. Q., Kadoya, H., Nakatani, K., Sato, M., and Kandea, K. (1998). Expression of cellular prion protein in activated hepatic stellate cells. *Am. J. Pathol.* **153**, 1695–1700.

Jaegly, A., Mounthon, F., Peyrin, J. M., Camugli, B., Deslys, J. P., and Dormont, D. (1998). Search for nuclear localization signal in the prion protein. *Mol. Cell. Neurosci.* **11**, 127–133.

Jeffrey, M., Goodsir, C. M., Bruce, M., McBride, P. A., Scott, J. R., and Halliday, W. G. (1994). Correlative light and electron microscopy studies of PrP localisation in 87V scrapie. *Brain Res.* **656**, 329–343.

Kalderon, D., Richardson, W. D., Markam, A. T., and Smith, A. E. (1984). Sequence requirements for nuclear location of simian virus 40 large T antigen. *Nature (Lond.)* **311**, 33–38.

Kalina, M., Lukinius, A., Grimalius, L., Hoog, A., and Falkmer, S. (1991). Ultrastructural localization of synaptophysin to the secretory granules of normal glucagon and insulin cells in human islets of Langerhans. *Ultrastruct. Pathol.* **15**, 215–219.

Kaneko, K., Vey, M., Scott, M., Pilkuhn, S., Cohen, F. E., and Prusiner, S. B. (1997). COOH-terminal sequence of the cellular prion protein directs subcellular trafficking and controls conversion into the scrapie isoform. *Proc. Natl. Acad. Sci. USA* **94**, 2333–2338.

Kimberlin, R. H., Millson, G. C., Bountiff, L., and Collis, S. C. (1974). A comparison of the biochemical changes induced in mouse brain cuprizone toxicity and by scrapie infection. *J. Comp. Pathol.* **84**, 263–270.

Kimberlin, R. H., and Walker, C. A. (1989). The role of the spleen in the neuroinvasion of scrapie in mice. *Virus Res.* **12**, 201–211.

Kitamoto, T., Shin, R. W., Doh-ura, K., Tomokane, N., Miyazono, M., Muramoto, T., and Tateishi, J. (1992). Abnormal isoform of prion proteins accumulates in the synaptic structures of the central nervous system in patients with Creutzfeldt-Jakob disease. *Am. J. Pathol.* **140**, 1285–1294.

Kniazeva, M., Orman, R., and Terranova, V. P. (1997). Expression of *PrP* mRNA is regulated by a fragment of MRP8 in human fibroblasts. *Biochem. Biophys. Res. Commun.* **234**, 59–63.

Kretzschmar, H. A., Prusiner, S. B., Stowring, L. E., and DeArmond, S. J. (1986). Scrapie prion proteins are synthesized in neurons. *Am J. Pathol.* **122**, 1–5.

Kretzschmar, H. A., Kitamoto, T., Doerr-Schott, J., Mehraein, P., and Tateishi, J. (1991). Diffuse deposition of immunohistochemically labeled prion protein in the granular layer of the cerebellum in a patient with Creutzfeldt-Jakob disease. *Acta Neuropathol.* **82**, 536–540.

Kurschner, C., and Morgan, J. I. (1995). The cellular prion protein (PrP) selectively binds to Bcl-2 in the yeast two-hybrid system. *Brain Res. Mol. Brain Res.* **30**, 165–168.

Langley, O. K., Aletsee-Utrecht, M. C., Grant, N. J., and Gratzl, M. (1989). Expression of the neural cell adhesion molecule NCAM in endocrine cells. *J. Histochem. Cytochem.* **37**, 781–791.

Lasmézas, C. I., Deslys, J. P., Demaismay, R., Adjou, K. T., Lamoury, F., Dormont, D., Robain, O., Ironside, J., and Hauw, J. J. (1996). BSE transmission to macaques. *Nature (Lond.)* **381**, 743–744.

Lee, K. S., Buck, M., Hougum, K., and Chojkier, M. (1995). Activation of hepatic stellate cell by TGF $\alpha$  and collagen type I is mediated by oxidative stress through c-myc expression. *J. Clin. Invest.* **96**, 2461–2468.

Lehmann, S., and Harris, D. A. (1997). Blockage of glycosylation promotes acquisition of scrapie-like properties by the prion protein in cultured cells. *J. Biolog. Chem.* **272**, 21479–21487.

LeMaire-Vieille, C., Schulze, T., Podevin-Dimster, V., Follet, J., Bailly, Y., Blanquet-Grossard, F., Decavel, J. P., Heinen, E., and Cesbron, J. Y. (2000). Epithelial and endothelial expression of the green fluorescent protein reporter gene under the control of bovine prion protein (PrP) gene regulatory sequences in transgenic mice. *Proc. Natl. Acad. Sci. USA* **97**, 5422–5427.

Lemons, P. P., Chen, D., Bernstein, A. M., Bennet, M. K., and Whiteheart, S. W. (1997). Regulated secretion in platelets: Identification of elements of the platelet exocytosis machinery. *Blood* **90**, 1490–1500.

Liu, H., Farr-Jones, S., Ulyanov, N. B., Llinas, M., Marqusee, S., Groth, D., Cohen, F. E., Prusiner, S. B., and James, T. L. (1999). Solution structure of Syrian hamster prion protein rPrP(90–231). *Biochemistry* **38**, 5362–5377.

Lledo, P. M., Tremblay, P., DeArmond, S. J., Prusiner, S. B., and Nicoll, R. A. (1996). Mice deficient for prion protein exhibit normal neuronal excitability and synaptic transmission in the hippocampus. *Proc. Natl. Acad. Sci. USA* **93**, 2403–2407.

Locht, C., Chesebro, B., Race, R., and Keith, J. M. (1986). Molecular cloning and complete sequence of prion protein cDNA from mouse brain infected with the scrapie agent. *Proc. Natl. Acad. Sci. USA* **83**, 6372–6376.

Lopez, C. D., Yost, C. S., Prusiner, S. B., Myers, R. M., and Lingappa, V. R. (1990). Unusual topogenic sequence directs prion protein biogenesis. *Science* **248**, 226–229.

Mabbott, N. A., Brown, K. L., Manson, J., and Bruce, M. E. (1997). T-lymphocyte activation and the cellular form of the prion protein. *Immunology* **92**, 161–165.

Mabbott, N. A., Farquhar, C. F., Brown, K. L., and Bruce, M. E. (1998). Involvement of the immune system in TSE pathogenesis. *Immunol. Today* **19**, 201–203.

Mabbott, N. A., Williams, A., Farquhar, C. F., Pasparakis, M., Kollias, G., and Bruce, M. E. (2000). Tumor necrosis factor alpha-deficient, but not interleukin-6-deficient, mice resist peripheral infection with scrapie. *J. Virol.* **74**, 3338–3344.

Manson, J. C., West, J. D., Thomson, V., McBride, P., Kaufman, M. H., and Hope, J. (1992). The prion protein gene: A role in morphogenesis? *Development* **115**, 117–122.

Manson, J. C., Clarke, A. R., Hooper, M. L., Aitchison, L., McConnel, I., and Hope, J. (1994). 129/Ola mice carrying a null mutation in PrP that abolishes mRNA production are developmentally normal. *Mol. Neurobiol.* **8**, 121–127.

Martins, V. R., Graner, E., Garcia-Abreu, J., de Souza, S. J., Mercadante, A. F., Veiga, S. S., Zanata, S. M., Neto, V. M., and Brentani, R. R. (1997). Complementary hydrophathy identifies a cellular prion protein receptor. *Nat. Med.* **3**, 1376–1382.

McBride, P. A., Eikelenboom, P., Kraal, G., Fraser, H., and Bruce, M. E. (1992). PrP protein is associated with follicular dendritic cells of spleens and lymph nodes in uninfected and scrapie-infected mice. *J. Pathol.* **168**, 413–418.

McGregor, I., Hope, J., Barnard, G., Kirby, L., Drummond, O., Pepper, D., Hornsey, V., Barclay, R., Bessos, H., Turner, M., and Prowse, C. (1999). Application of a time-resolved fluoroimmunoassay for the analysis of normal prion protein in human blood and its components. *Vox Sang.* **77**, 88–96.

McKenzie, D., Bartz, J., Mirwald, J., Olander, D., Marsh, R., and Aiken, J. (1998). Reversibility of scrapie inactivation is enhanced by copper. *J. Biolog. Chem.* **273**, 25545–25557.

McMahon, H. T., Bolshakov, V. Y., Janz, R., Hammer, R. E., Siegelbaum, S. A., and Sudhof, T. C. (1996). Synaptophysin, a major synaptic vesicle protein, is not essential for neurotransmitter release. *Proc. Natl. Acad. Sci. USA* **93**, 4760–4764.

Merz, G. S., Schwenk, V., Brown, H., Robakis, N., Rubenstein, R., Goller, N., and Wisniewski, H. (1986). Scrapie specific protein and mRNA in microglia isolated from normal and scrapie infected mouse brain. In “Unconventional virus diseases of the central nervous system” (L. A. Court, D. Dormont, P. Brown, and D. T. Kingsbury, Eds.), pp. 461–476. CEA, Fontenay aux Roses, France.

Miura, T., Hori-i, A., and Takeuchi, H. (1996). Metal-dependent alpha-helix formation promoted by the glycine-rich octapeptide region of prion protein. *FEBS Lett.* **396**, 248–252.

Mobley, W. C., Neve, R. L., Prusiner, S. B., and McKinley, M. P. (1988). Nerve growth factor increases mRNA levels for the prion protein and the beta-amyloid protein precursor in developing hamster brain. *Proc. Natl. Acad. Sci. USA* **85**, 9811–9815.

Moore, R. C., Lee, I. Y., Silverman, G. L., Harrison, P. M., Stromer, R., Heinrich, C., Karunaratne, A., Pasternak, S. H., Chishti, M. A., Liang, Y., Mastrangelo, P., Wang, K., Smit, A. F., Katamine, S., Carlson, G. A., Cohen, F. E., Prusiner, S. B., Melton, D. W., Tremblay, P. (1999). Ataxia in prion protein (PrP)-deficient mice is associated with upregulation of the novel PrP-like protein doppel. *J. Mol. Biol.* **292**, 797–817.

Moser, M., Colello, R. J., Pott, U., and Oesch, B. (1995). Developmental expression of the prion protein gene in glial cells. *Neuron* **14**, 509–517.

Moya, K. L., Sales, N., Hassig, R., Creminon, C., Grassi, J., and Di Giambardino, L. (2000). Immunolocalization of the cellular prion protein in normal brain. *Microsc. Res. Tech.* **50**, 58–65.

Müller, W. E., Pfeifer, K., Forrest, J., Rytik, P. G., Eremin, V. F., Popov, S. A., and Schröder, H. C. (1992). Accumulation of transcripts coding for prion protein in human astrocytes during infection with human immunodeficiency virus. *Biochim. Biophys. Acta* **1139**, 32–40.

Muramoto, T., Kitamoto, T., Tateishi, J., and Goto, I. (1993). Accumulation of abnormal prion protein in mice infected with Creutzfeldt-Jakob disease via intraperitoneal route: A sequential study. *Am. J. Pathol.* **143**, 1470–1479.

Negro, A., Meggio, F., Bertoli, A., Battistutta, R., Sorgato, M., and Pinna, L. A. (2000). Susceptibility of the prion protein to enzymic phosphorylation. *Biochem. Biophys. Res. Commun.* **271**, 337–341.

Nguyen, Q. T., and Lichman, J. W. (1996). Mechanism of synapse disassembly at the developing neuromuscular junction. *Curr. Opin. Neurobiol.* **6**, 104–112.

Oesch, B. (1994). Characterization of PrP binding proteins. *Philos. Trans. R. Soc. Lond. B: Biol. Sci.* **343**, 443–445.

Oesch, B., Westaway, D., Walchli, M., McKinley, M. P., Kent, S. B., Aebersold, R., Barry, R. A., Tempst, P., Teplow, D. B., Hood, L. E., Prusiner, S. B., and Weissmann, C. (1985). A cellular gene encodes scrapie PrP 27-30 protein. *Cell* **40**, 735–746.

Pammer, J., Weninger, W., and Tschaehler, E. (1998). Human keratinocytes express cellular prion-related protein *in vitro* and during inflammatory skin disease. *Am. J. Pathol.* **153**, 1353–1358.

Pammer, J., Suchy, A., Rendl, M., and Tschaehler, E. (1999). Cellular prion protein expressed by bovine squamous epithelia of skin and upper gastrointestinal tract. *Lancet* **354**, 1702–1703.

Pan, K. M., Baldwin, M., Nguyen, J., Gasset, M., Serban, A., Groth, D., Mehlhorn, I., Huang, Z., Fletterick, R. J., Cohen, F. E., and Prusiner, S. B. (1993). Conversion of alpha-helices into beta-sheets features in the formation of the scrapie prion proteins. *Proc. Natl. Acad. Sci. USA* **90**, 10962–10966.

Patton, B. L., Miner, J. H., Chiu, A. Y., and Sanes, J. R. (1997). Distribution and function of laminins in the neuromuscular system of developing, adult, and mutant mice. *J. Cell Biol.* **139**, 507–521.

Pauly, P. C., and Harris, D. A. (1998). Copper stimulates endocytosis of the prion protein. *J. Biol. Chem.* **273**, 33107–33110.

Perini, F., Frangione, B., and Prelli, F. (1996a). Prion protein released by platelets. *Lancet* **347**, 1635–1636.

Perini, F., Vidal, R., Ghetti, B., Tagliavini, F., Frangione, B., and Prelli, F. (1996b). PrP27-30 is a normal soluble prion protein fragment released by human platelets. *Biochem. Biophys. Res. Commun.* **223**, 572–577.

Pfeifer, K., Bachmann, M., Schröder, H., Forrest, J., and Müller, W. E. G. (1993). Kinetics of expression of prion protein in uninfected and scrapie-infected N2a mouse neuroblastoma cells. *Cell Biochem. Funct.* **71**, 1–11.

Prusiner, S. B. (1991). Molecular biology of prion diseases. *Science* **252**, 1515–1522.

Prusiner, S. B. (1998). Prion diseases. *Brain Pathol.* **8**, 499–513.

Prusiner, S. B., Scott, M. R., DeArmond, S. J., and Cohen, F. E. (1998). Prion protein biology. *Cell* **93**, 337–348.

Puckett, C., Concannon, P., and Hood, L. (1991). Genomic structure of the human prion protein gene. *Am. J. Hum. Genet.* **49**, 320–329.

Raeber, A. J., Race, R. E., Brandne, S., Priola, S. A., Sailer, A., Bessen, R. A., Mucke, L., Manson, J., Aguzzi, A., Oldstone, M. B., Weissmann, C., and Chesebro, B. (1997). Astrocyte-specific expression of hamster prion protein (PrP) renders PrP knockout mice susceptible to hamster scrapie. *EMBO J.* **16**, 6057–6065.

Raeber, A. J., Sailer, A., Hegyi, I., Klein, M. A., Rulicke, T., Fischer, M., Brandner, S., Aguzzi, A., and Weissmann, C. (1999). Ectopic expression of prion protein (PrP) in T lymphocytes or hepatocytes of PrP knockout mice is insufficient to sustain prion replication. *Proc. Natl. Acad. Sci. USA* **96**, 3987–3992.

Rieger, R., Edenhofer, F., Lasmezas, C. I., and Weiss, S. (1997). The human 37-kDa laminin receptor precursor interacts with the prion protein in eukaryotic cells. *Nat. Med.* **3**, 1383–1388.

Rieger, R., Lasmezas, C. I., and Weiss, S. (1999). Role of the 37 kDa laminin receptor precursor in the life cycle of prions. *Transfus. Clin. Biol.* **6**, 7–16.

Riek, R., Hornemann, S., Wider, G., Billeter, M., Glockshuber, R., and Wüthrich, K. (1996). NMR structure of the mouse prion protein domain (121–231). *Nature (Lond.)* **382**, 180–182.

Riek, R., Hornemann, S., Wider, G., Glockshuber, R., and Wüthrich, K. (1997). NMR characterization of the full-length recombinant murine prion protein, mPrP(23–231). *FEBS Lett.* **413**, 282–288.

Ritchie, D. L., Brown, K. L., and Bruce, M. E. (1999). Visualisation of PrP protein and follicular dendritic cells in uninfected and scrapie infected spleen. *J. Cell. Pathol.* **1**, 3–10.

Rogers, M., Taraboulos, A., Scott, M., Groth, D., and Prusiner, S. B. (1990). Intracellular accumulation of the cellular prion protein after mutagenesis of its Asn-linked glycosylation sites. *Glycobiology* **1**, 101–109.

Rubenstein, R., Kascak, R. J., Merz, P. A., Papini, M. C., Carp, R. I., Robakis, N. K., and Wisniewski, H. M. (1986). Detection of scrapie-associated fibril (SAF) proteins using anti-SAF antibody in non-purified tissue preparations. *J. Gen. Virol.* **67**, 671–681.

Safar, J., Roller, P. P., Gajdusek, D. C., and Gibbs, C. J., Jr. (1993). Conformational transitions, dissociation, and unfolding of scrapie amyloid (prion) protein. *J. Biol. Chem.* **268**, 20276–20284.

Sakaguchi, S., Katamine, S., Nishida, N., Moriochi, R., Shigematsu, K., Sugimoto, T., Nakatani, A., Kataoka, Y., Houtani, T., Shirabe, S., Okada, H., Hasegawa, S., Miyamoto, T., and Noda, T. (1996). Loss of cerebellar Purkinje cells in aged mice homozygous for a disrupted *PrP* gene. *Nature (Lond.)* **380**, 528–531.

Sales, N., Rodolfo, K., Hassig, R., Faucheuex, B., Di Giamberardino, L., and Moya, K. L. (1998). Cellular prion protein localization in rodent and primate brain. *Eur. J. Neurosci.* **10**, 2464–2471.

Sarkozi, E., Askanas, V., and King Engel, W. (1994). Abnormal accumulation of prion protein mRNA in muscle fibers of patients with sporadic inclusion-body myositis and hereditary inclusion-body myopathy. *Am. J. Pathol.* **145**, 1280–1284.

Satoh, J., Yukitake, M., Kurohara, K., Nishida, N., Katamine, S., Miyamoto, T., and Kuroda, Y. (1998). Cultured skin fibroblasts isolated from mice devoid of the prion protein gene express major shock proteins in response to heat stress. *Exp. Neurol.* **15**, 1105–1115.

Schirmacher, P., Geerts, A., Pietrangelo, A., Dienes, H. P., and Rogler, C. E. (1992). Hepatocyte growth factor/hepatopoietin A is expressed in fat-storing cells from rat liver but not myofibroblast-like cells derived from fat-storing cells. *Hepatology* **15**, 5–11.

Schröder, H. C., Scheffer, U., Forrest, J. M. S., Sève, A. P., Rytil, P. G., and Müller, W. E. G. (1994). Association of scrapie prion protein and protein-RNA stem-loop with nuclear carbohydrate-binding proteins 35 and other RNA-binding proteins. *Neurodegeneration* **3**, 177–189.

Shaked, Y., Rosenmann, H., Talmor, G., and Gabizon, R. (1999). A C-terminal-truncated PrP isoform is present in mature sperm. *J. Biol. Chem.* **274**, 32153–32158.

Shinagawa, M., Munekata, E., Doi, S., Takahashi, K., Goto, H., and Sato, G. (1986). Immunoreactivity of a synthetic pentadecapeptide corresponding to the N-terminal region of the scrapie prion. *J. Gen. Virol.* **67**, 1745–1750.

Shyng, S. L., Hubert, M. T., and Harris, D. A. (1993). A prion protein cycles between the cell surface and an endocytic compartment in cultured neuroblastoma cells. *J. Biol. Chem.* **268**, 15922–15928.

Shyng, S. L., Heuser, J. E., and Harris, D. A. (1994). A glycolipid-anchored prion protein is endocytosed via clathrin-coated pits. *J. Cell Biol.* **125**, 1239–1250.

Shyng, S. L., Lehmann, S., Moulder, K. L., and Harris, D. A. (1995a). Sulfated glycans stimulate endocytosis of the cellular isoform prion protein PrP<sup>c</sup> in cultured cells. *J. Biol. Chem.* **270**, 30221–30229.

Shyng, S. L., Moulder, K. L., Lesko, A., and Harris, D. A. (1995b). The N-terminal domain of a glycolipid-anchored prion protein is essential for its endocytosis via clathrin-coated pits. *J. Biol. Chem.* **270**, 14793–14800.

Shyu, W. C., Kao, M. C., Chou, W. Y., Hsu, Y. D., and Soong, B. W. (2000). Heat shock modulates prion protein expression in human NT-2 cells. *Neuroreport* **11**, 771–774.

Silverman, G., Qin, K., Moore, R. C., Yang, Y., Mastrangelo, P., Tremblay, P., Prusiner, S. B., Cohen, F. E., and Westaway, D. (2000). Doppel is an N-glycosylated GPI-anchored protein: Expression in testis and ectopic production in the brains of Prnp<sup>{super0/0}</sup> mice predisposed to Purkinje cell loss. *J. Biol. Chem.* **275**, 26834–26841.

Simonic, T., Duga, S., Strumbo, B., Asselta, R., Ceciliani, F., and Ronchi, S. (2000). cDNA cloning of turtle prion protein. *FEBS Lett.* **469**, 33–38.

Stahl, N., Borchelt, D. R., and Prusiner, S. B. (1990). Differential release of cellular and scrapie prion protein from cellular membranes by phosphatidylinositol-specific phospholipase C. *Biochemistry* **29**, 5405–5412.

Stahl, N., Baldwin, M. A., Hecker, R., Pan, K. M., Burlingame, A. L., and Prusiner, S. B. (1992). Glycosylinositol phospholipid anchors of the scrapie and cellular prion proteins contain sialic acid. *Biochemistry* **31**, 5043–5053.

Stahl, N., Baldwin, M. A., Teplow, D. B., Hood, L., Gibson, B. W., Burlingame, A. L., and Prusiner, S. B. (1993). Structural studies of the scrapie prion protein using mass spectrometry and amino. *Biochemistry* **32**, 1991–2002.

Sy, M. S., and Gambetti, P. (1999). Prion replication—once again blaming the dendritic cell. *Nat. Med.* **11**, 1235–1237.

Tagliavini, F., Pirelli, F., Porro, M., Salmona, M., Bugiani, O., and Frangione, B. (1992). A soluble form of prion protein in human cerebrospinal fluid: Implications for prion-related encephalopathies. *Biochem. Biophys. Res. Commun.* **184**, 1398–1404.

Tanji, K., Saeki, K., Matsumoto, Y., Takeda, M., Hirasawa, K., Doi, K., Matsumoto, Y., and Onodera, T. (1995). Analysis of PrP<sup>c</sup> mRNA by in situ hybridization in brain, placenta, uterus and testis of rats. *Intervirology* **38**, 309–315.

Taraboulos, A., Scott, M., Semenov, A., Avrahami, D., Laszlo, L., Prusiner, S. B., and Avraham, D. (1995). Cholesterol depletion and modification of COOH-terminal targeting sequence of the prion protein inhibit formation of the scrapie form. *J. Cell Biol.* **129**, 121–132.

Tatzelt, J., Zuo, J., Voellmy, R., Scott, M., Hartl, U., Prusiner, S. B., and Welch, W. J. (1995). Scrapie prions selectively modify the stress response in neuroblastoma cells. *Proc. Natl. Acad. Sci. USA* **92**, 2944–2948.

Tatzelt, J., Voellmy, R., and Welch, W. J. (1998). Abnormalities in stress proteins in prion diseases. *Cell Mol. Neurobiol.* **18**, 721–729.

Taylor, D. M., McConnel, I., and Fraser, H. (1996). Scrapie infection can be established readily through skin scarification in immunocompetent but not immunodeficient mice. *J. Gen. Virol.* **77**, 1595–1599.

Teitelman, G., and Lee, J. K. (1987). Cell lineage analysis of pancreatic islet development: Glucagon and insulin cells arise from catecholaminergic precursors present in the pancreatic duct. *Dev. Biol.* **121**, 454–466.

Telling, G. C., Scott, M., Masrianni, J., Gabizon, R., Torchia, M., Cohen, F. E., DeArmond, S. J., and Prusiner, S. B. (1995). Prion propagation in mice expressing human and chimeric PrP transgenes implicates the interaction of cellular PrP with another protein. *Cell* **83**, 79–90.

Tenner-Racz, K., and Racz, P. (1995). Follicular dendritic cells initiate and maintain infection of the germinal centers by human immunodeficiency virus. *Curr. Topics Microbiol. Immunol.* **20**, 1141–1159.

Tobler, I., Gaus, S. E., Deboer, T., Achermann, P., Fischer, M., Rulicke, T., Moser, M., Oesch, B., McBride, P. A., and Manson, J. C. (1996). Altered circadian activity rhythms and sleep in mice devoid of prion protein. *Nature (Lond.)* **380**, 639–642.

Turk, E., Teplow, D. B., Hood, L. E., and Prusiner, S. B. (1998). Purification and properties of the cellular and scrapie hamster prion proteins. *Eur. J. Biochem.* **176**, 21–30.

van Keulen, L. J., Schreuder, B. E., Vromans, M. E., Langeveld, J. P., and Smits, M. A. (1999). Scrapie-associated prion protein in the gastrointestinal tract of sheep with natural scrapie. *J. Comp. Pathol.* **121**, 55–63.

van Rooijen, N. (1992). Follicular dendritic cell-B cell interactions in virus disease. Common localization but different cell damage caused by antibody immobilized virus? *Arch. Virol.* **122**, 215–218.

Vey, M., Pilkuhn, S., Wille, H., Nixon, R., DeArmond, S. J., Smart, E. J., Anderson, R. G., Taraboulos, A., and Prusiner, S. B. (1996). Subcellular colocalization of the cellular and scrapie prion proteins in caveolae-like membranous domains. *Proc. Natl. Acad. Sci. USA* **93**, 14945–14949.

Viles, J. H., Cohen, F. E., Prusiner, S. B., Goodin, D. B., Wright, P. E., and Dyson, H. J. (1999). Copper binding to the prion protein: Structural implications of four identical cooperative binding sites. *Proc. Natl. Acad. Sci. USA* **96**, 2042–2047.

Waggoner, D. J., Drisaldi, B., Bartnikas, T., Casareno, L., Prohaska, J., Gitlin, J., and Harris, D. (2000). Brain copper content and cuproenzyme activity do not vary with prion protein expression level. *J. Biol. Chem.* **275**, 7455–7458.

Weissmann, C. (1996). PrP effects clarified. *Curr. Biol.* **6**, 1359.

Whatley, S. A., Powell, J. F., Politopoulou, G., Campbell, I. C., Brammer, M. J., and Percy, N. S. (1995). Regulation of intracellular free calcium levels by the cellular prion protein. *Neuroreport* **6**, 2333–2337.

White, A. R., Collins, S. J., Maher, F., Jobling, M. F., Stewart, L. R., Thyer, J. M., Beyreuther, K., and Masters, C. L. (1999). Prion protein-deficient neurons reveal lower glutathione reductase activity and increased susceptibility to hydrogen peroxide toxicity. *Am. J. Pathol.* **155**, 1723–1730.

Will, R. G., Ironside, J. W., Zeidler, M., Cousens, S. N., Estibeiro, K., Alperovitch, A., Poser, S., Pocchiari, M., Hofman, A., and Smith, P. G. (1996). A new variant of Creutzfeldt-Jakob disease in the UK. *Lancet* **347**, 921–925.

Wisniewski, H. M., Vorbrodt, A. W., Weigel, J., Morys, J., and Lossinsky, A. S. (1990). Ultrastructure of the cells forming amyloid fibres in Alzheimer's disease and scrapie. *Am. J. Med. Gene* **7**, 287–297.

Wong, B. S., Wang, H., Brown, D. R., and Jones, I. M. (1999). Selective oxidation of methionine residues in prion proteins. *Biochem. Biophys. Res. Commun.* **259**, 352–355.

Ye, X., and Carp, R. I. (1995). The pathological changes in peripheral organs of scrapie-infected animals. *Histol. Histopathol.* **10**, 995–1021.

Ye, X., Scallet, A. C., Kacsak, R. J., and Carp, R. I. (1998). Astrocytosis and amyloid deposition in scrapie-infected hamsters. *Brain Res.* **809**, 277–287.

Yehiely, F., Bamborough, P., Da Costa, M., Perry, B. J., Thinakaran, G., Cohen, F. E., Carlson, G. A., and Prusiner, S. B. (1997). Identification of candidate proteins binding to prion protein. *Neurobiol. Dis.* **3**, 339–355.

Zahn, R., Liu, A., Luhrs, T., Riek, R., von Schroetter, C., Lopez Garcia, F., Billeter, M., Calzolai, L., Wider, G., and Wüthrich, K. (2000). NMR solution structure of the human prion protein. *Proc. Natl. Acad. Sci. USA* **97**, 145–150.

Zanusso, G., Lu, D., Ferrari, S., Hegyi, I., Yin, X., Aguzzi, A., Hornemann, S., Liemann, S., Glockshuber, R., Manson, J. C., Brown, P., Petersen, R. B., Gambetti, P., and Sy, M. S. (1998). Prion protein expression in different species: Analysis with a panel of new MAbs. *Proc. Natl. Acad. Sci. USA* **95**, 8812–8816.

Zhang, H., Stockel, J., Mehlhorn, I., Groth, D., Baldwin, M. A., Prusiner, S. B., James, T. L., and Cohen, F. E. (1997). Physical studies of the conformational plasticity in a recombinant prion protein. *Biochemistry* **36**, 3543–3553.

Zhu, W., Cowie, A., Wasfy, G. W., Penn, L. Z., Leber, B., and Andrews, D. W. (1996). Bcl-2 mutants with restricted subcellular location reveal spatially distinct pathways for apoptosis in different cell types. *EMBO J.* **15**, 4130–4141.

# Cellular Basis of Shoot Apical Meristem Development

Jan Traas\* and John H. Doonan<sup>†</sup>

\*Laboratoire de Biologie Cellulaire, Institut National de la Recherche Agronomique, 78026 Versailles Cedex, France, and <sup>†</sup>John Innes Centre, Norwich NR4 7UH, England

---

Shoot apical meristems are composed of proliferating, embryonic type cells, that generate tissues and organs throughout the life of the plant. This review covers the cell biology of the higher plant shoot apical meristem (SAM). The first section describes the molecular basis of plant cell growth and division. The genetic mechanisms, that operate in meristem function and the identification of several key regulators of meristem behavior are described in the second section, and intercellular communication and coordination of cellular behavior in the third part. Finally, we discuss some recent results that indicate interaction between the cellular regulators, such as the cell cycle control genes and developmental regulators.

**KEY WORDS:** Angiosperm, Shoot apical meristem, Cell division, Cell elongation, Signaling. © 2001 Academic Press.

---

## I. Introduction

Plants can alter their growth habit to suit local conditions. This is achieved, in part, by the behavior of groups of cells, called *meristems*. These are composed of embryonic-type cells that proliferate both to maintain the meristem and to generate tissues and organs throughout the life of the plant. As a consequence the organogenic phase extends far beyond embryogenesis. Because meristems are able to alter their activity in response to both internal and external cues, they provide the developmental flexibility that allows plants to modulate their development with respect to prevailing conditions.

A typical plant may contain distinct meristems that differ in terms of identity and activity (Fig. 1). Apical meristems, positioned at the extremity of the shoots and roots, initiate aerial and underground organs, respectively. More diffuse

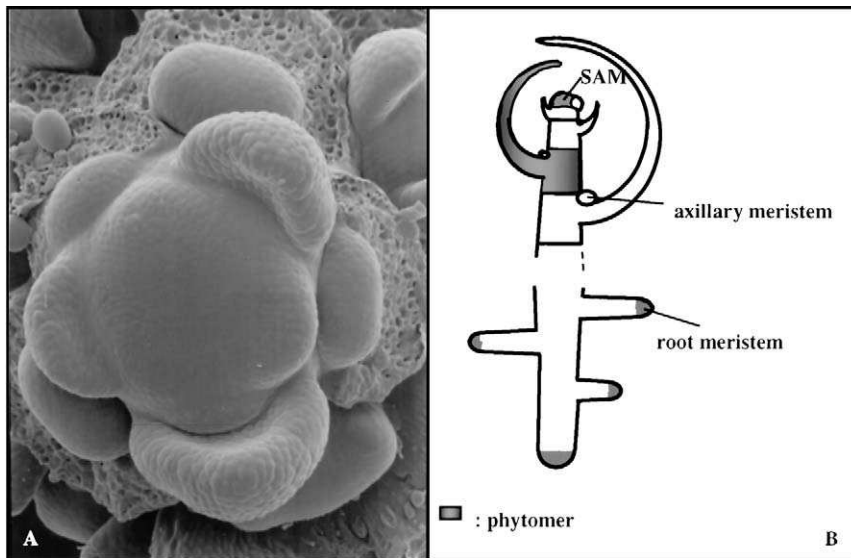


FIG. 1 Meristems and organization of the plant body plan. (A) Shoot apical inflorescence meristem of *Antirrhinum*, producing primordia at regular angles. (B) SAMs produce units or phytomers, comprising a stem segment, an axillary meristem, and usually a leaf.

secondary meristems exist within the stem and root and are responsible for secondary thickening of these structures. The activity of apical meristems determines the basic layout of the plant's architecture. For example, if the primary apical meristem (formed during embryogenesis) remains as the only active meristem, the resultant plant bodyform is linear. However, if the axillary apical meristems that arise in tissues behind the primary apical meristems are activated, then branching will occur, leading to a more complex body plan. The placement and activity of meristems can therefore have profound consequences for the overall growth and form of the plant.

In this review, we will focus on shoot apical meristems (SAMs), which initiate both stem tissues as well as organs (such as leaves or flowers) that usually extend laterally from the main stem. A scanning electron micrograph of a shoot meristem is shown in Fig. 1A. Typically, SAM development is reiterative; for example, sequential sets of leaves bearing new meristems in their axils (whose position is referred to as a node) are separated by a section of stem (the internode), thus forming a unit referred to as a phytomer (Fig. 1B). Another distinguishing feature of the SAM is the progressive identity changes that occur as the plant develops. In dicots, for example, the vegetative SAM, formed during embryogenesis, generates leaves. The properties of the organs produced by the vegetative meristem change as the plant grows; in many species there are distinct juvenile and adult

stages that can be recognized by the distinct leaf types generated and/or the organization of those leaves. The vegetative meristem may undergo a more profound identity change to give rise to an inflorescence meristem that generates modified leaves or bracts and flowers. Floral meristems, often produced *de novo* as a lateral meristem in the axils of bracts or as a result of a further identity change of the primary shoot apical meristem, are highly specialized and differ in a number of respects from their predecessors. First, they generate whorls (rings) of highly specialized floral organs such as sepals, petals, stamens, and carpels. Second, they are usually determinate structures with a defined developmental program, i.e., they generate a set number of organs and, after initiation, are largely independent of environmental influences. Nevertheless, floral meristems share a number of basic characteristics with other meristems and use many of the same genes to control organ initiation. Although the presence of a SAM is a universal feature of multicellular land plants its structure can differ significantly among species. Therefore, we will concentrate on the angiosperms that have been best characterized. In addition, because many insights into the apical meristem have come via studies of floral meristems, we will also cover selected aspects of floral development that seem relevant.

Several levels of organization can be recognized in the SAM. The first level is that of the individual cells (Fig. 1A): all higher plant apical meristems are multicellular. Yet, within the SAM, these cells are organized into different multicellular domains, allowing the meristem to act as a coordinated whole. In this review, we will start with the cellular perspective. First, we will discuss the molecules and cellular structures implicated in the regulation of two critically important aspects of meristem function and morphogenesis, i.e., cell expansion and cell division. An exhaustive review of the field would be beyond the scope of this article. We will, therefore, instead give a summary of the main conclusions coming from recent research, thus providing a basis for later sections where we will look at cell morphogenesis in a developmental context.

## II. Cellular Events during Morphogenesis

### A. Cell Expansion

#### 1. Cell Wall Synthesis as a Rate-Limiting Factor for Cell Growth

The cell wall is a semirigid, but highly dynamic, network of polysaccharides and proteins that surrounds and constrains almost all plant cells. The physical properties of the cell wall largely determine plant cell shape and form. The presence of neighboring cells also affects cell shape but this can be seen as an indirect effect of the walls of those neighboring cells. Turgor pressure provides an outward-acting hydrostatic force, which presses the plasma-membrane against the

cell wall and, as early as 1882, Sachs found that this is a prerequisite for cell growth (Sachs, 1882, reviewed in Kutschera, 1991). Turgor pressure is more or less constant during growth and can be thought of as the motor that drives cell elongation. In general, turgor is not limiting for growth, and it is widely accepted that the expansion rate and direction of growth are largely determined at the level of the wall, which irreversibly yields to the pressure inside the cell. Cell wall structure and synthesis have been discussed in a number of recent reviews (Cosgrove, 1997, 1999a, 1999b; Nicol and Höfte, 1998) and only a brief overview will be given here.

The primary wall, laid down in rapidly growing cells such as those found in meristems, typically consists of a network of rigid cellulose microfibrils, composed of crystalline bundles of 1,4- $\beta$ -D-glucan. The fibrils are surrounded by a hydrated matrix of hemicellulose and pectins. Cellulose, hemicellulose, and pectins each represent about 30–35% of the dry weight of the cell wall. Structural proteins make up 1–4%. The hemicelluloses, composed of short branched polysaccharide chains, are thought to link the cellulose microfibrils together in a dense network. A well-characterized example is xyloglucan, which is abundant in rapidly growing cells and which has a 1,4  $\beta$ -D-glucan backbone, with short side chains mainly composed of xylose and galactose. Pectins, a heterogeneous group of acidic polysaccharides, form an independent network or gel in the wall matrix in which the cellulose/hemicellulose fraction is embedded. The physical properties of the pectin network can be modified through different alterations such as esterification of the acidic residues with different groups and interactions with calcium.

Cell expansion requires both the incorporation of new polymers into the wall, and the rearrangement of the existing ones. Whereas hemicellulose and pectins are synthesized in the Golgi and then transported to the extracellular matrix, cellulose microfibrils are synthesized at the plasma-membrane most probably by hexameric terminal complexes. Only very recently have candidate genes, which could encode subunits of these complexes, been identified in *Arabidopsis*. These are members of a family showing homologies with bacterial cellulose synthases. Mutations in at least one member of this family, the *ROOTSWELLING 1 (RSW1)* locus, cause abnormal radial swelling of the cells and a reduction in cellulose synthesis (Arioli *et al.*, 1998). The mutant produces increased amounts of noncrystalline 1,4  $\beta$ -D-glucan indicating that the *RSW1* gene is necessary for assembling the cellulose microfibrils. Parallel to this work, other research has focused on the mechanisms that regulate incorporation of the new elements into the wall, allowing extension of the extracellular matrix. Extensive biochemical analysis has revealed a number of different mechanisms for cell expansion that require the presence of distinct enzymatic activities in the walls.

The first mechanism involves the rearrangement of the xyloglucan network by a family of conserved proteins called xyloglucan endo transglycosylase or XETs. At this moment the exact role of these enzymes is not fully elucidated. According to one model, which accounts for many observations, XET not only cuts the

xyloglucan chains that link the cellulose microfibrils, but could also ligate the newly formed ends to the ends of acceptor xyloglucans. In this way, XET would promote dynamic rearrangement and growth of the network allowing controlled turgor driven expansion to occur. Another class of proteins known to be involved in cell wall extension is the expansins. Expansins were originally identified as capable of inducing the loosening of purified cell walls under acidic conditions. Although their exact function has not been determined it has been proposed that they act on the non-covalent bonds between the cellulose microfibrils and the xyloglucan chains. By breaking these links, expansins loosen the walls and thus allow expansion to occur.

Other enzymes have also been associated with cell expansion and wall synthesis although their role has been less well characterized. Several glucanases are present in increased concentrations or show enhanced turnover during cell expansion. One class of membrane-bound endoglucanases could operate at the level of both cell wall synthesis and cell wall rearrangement. In *Arabidopsis*, KORRIGAN, a member of this family, is necessary for normal cell expansion (Nicol *et al.*, 1998). A loss-of-function mutation in the gene causes all differentiated cells to be smaller. It is not clear whether these enzymes function at the level of the plasma-membrane, where they could participate in the rearrangement of the cell wall polysaccharides, or whether they are associated with internal membranes, where they could participate in the synthesis of new polymers. Biochemical analysis on expansins and XETs and phenotypical analysis of cell wall mutants has been mainly carried out on differentiating cells that are no longer in the meristems. However, these enzymes are also necessary for growth in root and shoot meristems. This is very obvious in mutants such as *rsw1*, which show expansion defects in dividing cells and dramatically perturb meristem function.

## **2. The Orientation of Cell Expansion: Role of the Cytoskeleton and the Wall**

Cell wall synthesis and rearrangements of the polysaccharide network influence and limit the growth rate of the plant cell but morphogenesis also requires directional growth to obtain particular shapes of cells and organs. In plants, a major determinant of the orientation of cell expansion is, again, the cell wall. In particular the arrangement of the microfibrils, which largely determines the physical properties of the cell wall, appears to be an essential factor. What determines the orientation of the cell wall polysaccharides? Different models exist. According to one commonly accepted model, the cellulose microfibrils in the wall are oriented by cytoplasmic elements inside the cell. This hypothesis was originally based on studies by Ledbetter and Porter (1963) and extended by the simple but elegant microscopical observations of Green (1976). He found that the drug colchicine eliminated birefringence, an optical property of the wall, indicating the presence of highly ordered fibers oriented around the cell that acted like constraining hoops. He proposed a colchicine-sensitive cellulose template, probably based in the cytoplasm.

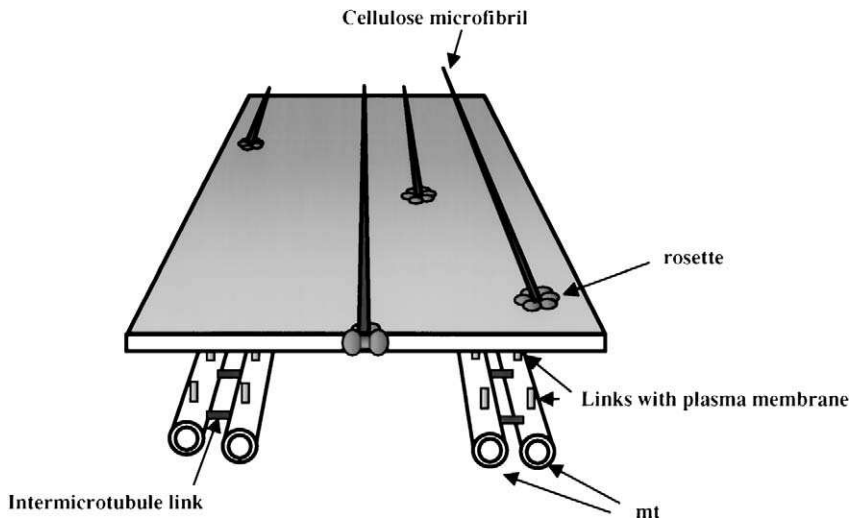


FIG. 2 A widely accepted model for the relation between the cytoskeleton and cell wall texture. Microtubules (mt), linked to each other via protein bridges, are attached to the plasma-membrane via links of an unknown nature. Thus channels are created in the plasma-membrane, which could guide the cellulose synthase complexes (arranged in rosettes).

Microtubules, previously observed in electron microscopic studies by Ledbetter and Porter (1963), are known to be sensitive to this group of drugs. The molecular mechanism(s) by which microtubules influence wall assembly is still hotly debated, but current views are that the relationship is probably indirect. Microtubules are tightly associated with the cell wall through transmembrane bridges. These aligned transmembrane bridges could create channels between adjacent microtubules, guiding the movements of the cellulose synthase complexes (Fig. 2; Lloyd, 1991). The biochemical isolation and analysis of functional guidance mechanisms have proven difficult. In addition, not all the evidence supports the idea that microtubules control cell wall texture. There are examples, such as root hairs in several species, where walls with distinct textures are produced without any obvious co-alignment between microtubules and cellulose microfibrils (Traas *et al.*, 1985). An important minority view even suggests mechanisms whereby wall textures can be generated by self-assembly of wall polymers. For instance, analogies were made with the spontaneous organization observed in liquid crystals (Satiat-Jeunemaître, 1987). Whereas such models are based mainly on the interactions between the wall molecules, other hypotheses, such as the one proposed by Emons and Kieft (1994), combine these interactions with other variables such as cell shape, space constraints, and the number of cellulose synthase complexes in the walls. New factors, identified by genetic dissection of cell expansion, should make it possible to differentiate between these hypotheses. The synthases have

been identified and immunological approaches or techniques using fusions with green fluorescent protein should make it possible to follow the cellulose synthases directly. In addition, a number of mutants are now available in *Arabidopsis* that show abnormal orientations of cell expansion. For instance, the meristematic cells of two mutants, *fass* (Torres-Ruiz and Jürgens, 1994; McClinton and Sung, 1997) and *tonneau1* (Traas *et al.*, 1995), show an incapacity to elongate in a particular direction. Although the *FASS* and *TONNEAU* genes have not yet been identified, immunofluorescence studies have revealed that in the root meristem cells the cortical microtubules are no longer organized into the highly ordered parallel arrays often observed (Traas *et al.*, 1995), implicating these genes in cytoskeletal organization. These mutants could also be very useful in studying the relation between the cytoskeleton and the cell wall.

## B. Cell Division

Another important characteristic of meristematic cells is their proliferative potential. All cells within the meristem can divide and the rate and position of divisions may influence growth. As in other eukaryotes, plant cells generally alternate between DNA replication (S phase) and DNA separation (mitosis or M phase) separated by two gaps of variable duration (Fig. 3). The gap between mitosis and S phase is referred to as G<sub>1</sub> and the gap between S phase and mitosis is G<sub>2</sub>. Progression through the cell division cycle is accompanied by changes in cell morphology and organization: cell growth occurs during G<sub>1</sub>, S, and G<sub>2</sub> phases; nuclear enlargement during S phase; and the most dramatic rearrangements of the cytoplasm and nucleus occur during mitosis and cytokinesis. While many of these changes are typical of other higher eukaryotes (e.g., nuclear envelope breakdown and chromatin condensation), the plant cell cycle has several characteristic features including a preprophase band that predicts the future plane of cell division; a spindle lacking discrete poles; and the phragmoplast, a cytokinetic apparatus that forms the cross wall between two daughter cells (Fig. 4) (see Lloyd, 1991, for reviews).

The future plane of cell division is marked before mitosis by a dense equatorial band of structural elements called the preprophase band. This band is positioned in the cortical cytoplasm adjacent to the plasma-membrane and contains diverse cytoskeletal elements, such as microtubules and actin as well as endoplasmic reticulum. The strict correlation between the preprophase band and the division plane suggests an important role in defining the site of division. In most plant cells, certainly in all apical meristem cells, mitosis is followed by cell division (or cytokinesis) and this event is also associated with another plant-specific structure, the phragmoplast. The phragmoplast contains short microtubules that are implicated in the movement of materials toward the forming cross wall. Like the preprophase band, the phragmoplast also contains other cytoskeletal elements and endoplasmic reticulum (Smith, 1999). In spite of these differences, the molecular

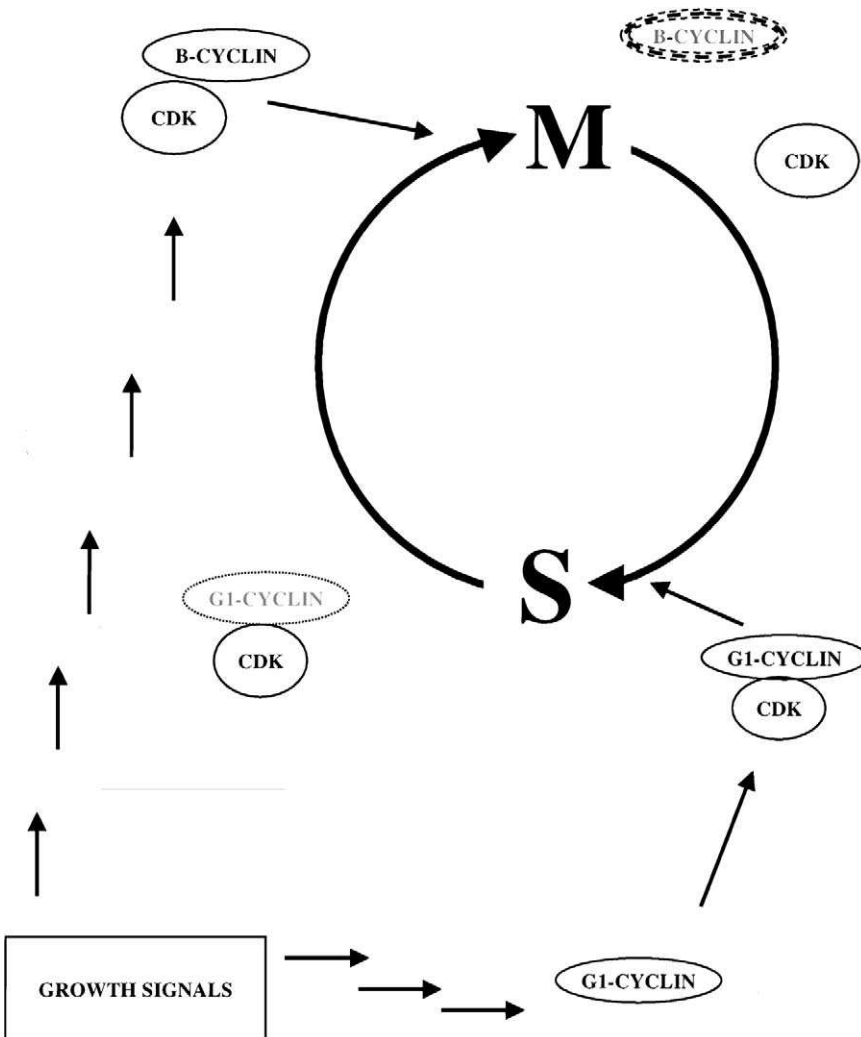


FIG. 3 Cell cycle controls. Schematic view of the cell cycle engine, driven by the cyclic activation and inactivation of CDK complexes. Synthesis and destruction of S phase and mitotic cyclins play an important role in the CDK activation/inactivation cycle, and known mechanisms that affect plant cyclin concentration are shown. A model of regulation of S-phase entry: the cyclin D-RB-E2F pathway. Cyclin D is synthesized in response to growth signals, and activates CDKs, which phosphorylate Rb and release E2F. Growth signals may include cytokinin and unknown signals generated by meristem regulators.

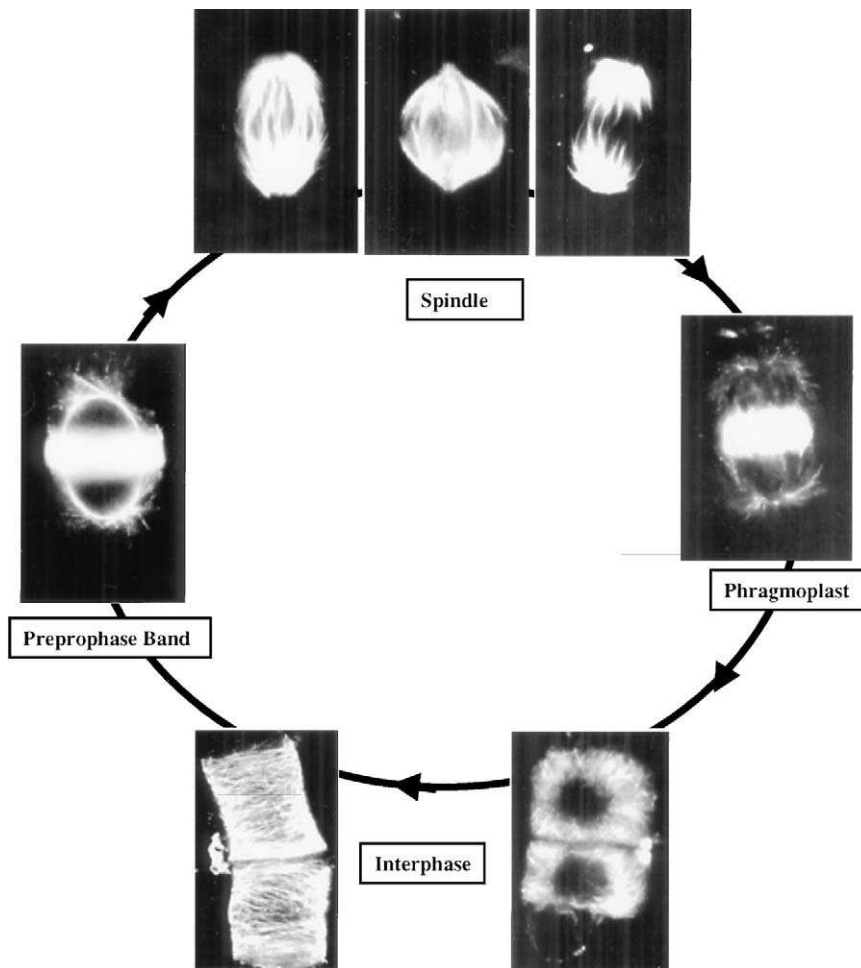


FIG. 4 Microtubular reorganization during the cell cycle of root cells. Microtubules are attached to the plasma-membrane during interphase (cortical microtubules), where they are often aligned perpendicular to the axis of expansion. During preprophase, the cortical array reorganizes into the preprophase band, which predicts the future site of division. This band disappears and a spindle with large poles forms. During cytokinesis the phragmoplast, composed of short microtubules and other cytoplasmic elements, synthesizes the new cross wall, which meets the existing wall at the site previously occupied by the preprophase band. New microtubules are then synthesized from the surface of the daughter nuclei and new cortical interphase arrays are formed.

mechanisms underlying plant cell cycle progression are generally similar to those found in microbes and animal cells (Fig. 3; Doonan and Fobert, 1997; John, 1996; Mironov *et al.*, 1997), as we will discuss in the next paragraphs.

## 1. CDKs and Cyclins: Key Regulators of Cell Cycle Progression

Key players in cell cycle progression are heteromeric protein complexes containing a catalytic kinase subunit called a cyclin-dependent kinase (CDK). CDKs are also known by the name given to the prototype gene from fission yeast, *cdc2*. As their name indicates, the activity of CDK complexes depends on the presence of a rate-limiting activating subunit called *cyclin* (so-called because their abundance often fluctuates in a cyclical manner). Although many questions still remain, it appears that these complexes initiate many of the important changes observed during the cell cycle by directly or indirectly phosphorylating a variety of targets, including nuclear envelope proteins, histones, and cytoskeletal elements (Tjandra *et al.*, 1998). In both budding yeast and fission yeast, a single CDK mediates more than one transition during the cell cycle but in mammals and plants, however, there are several CDKs. Most cells also express a multiplicity of cyclins, often at specific times during the cell cycle. The type of cyclin bound may alter the properties of the complex but this is not always the case; D and E cyclins appear to be interchangeable in mice (Geng *et al.*, 1999). A number of other proteins also bind stoichiometrically to the cyclin-CDK dimer and influence its activity. In plants, several of these proteins have been identified (Mironov and Inzé, 1999). These include CKS, a docking factor that could be involved in degradation of the complex, and different isoforms of the so-called CDK inhibitors (CKIs) (Wang *et al.*, 1998; Sherr and Roberts, 1999; Liu *et al.*, 2000). The CDK-cyclin complex is subject to multiple layers of regulation at the level of transcription, translation, protein stability and other posttranslational modifications. It therefore has the potential to integrate developmental or environmental signals and transduce these into effects on cell growth.

## 2. CDK Diversity and Role

Plants contain an extended *CDK* gene family that includes both cognate and variant CDK versions (Colasanti *et al.*, 1991; Ferreira *et al.*, 1991; Miao *et al.*, 1993; Fobert *et al.*, 1994, 1996; Magyar *et al.*, 1997). Plant CDKs have been organized in five subfamilies on the basis of primary sequence relationships (Joubes *et al.*, 2000). The first group, the CDK-a class, is most closely related to the yeast *CDK1* (*cdc2*). In alfalfa, protein complexes precipitated by antibodies against CDK-a produced high kinase activity at both  $G_1/S$  and  $G_2/M$  transitions, indicating a dual role for CDK-a during cell cycle progression (Magyar *et al.*, 1997). These cognate

orthologs encode proteins that contain a T-loop, a kinase catalytic domain, and a conserved cyclin interaction motif that consists of 16 amino acids generally referred to as the PSTAIR domain (from the single-letter code used for the amino acid residues in the central region of the motif). This domain determines the specificity of cyclin binding. The cognate CDK-a genes, when expressed in yeast, generally are capable of complementing at least some mutations in *cdc2* or its ortholog in *Saccharomyces cerevisiae*, CDC28.

In other eukaryotes, activation of the CDK complex requires changes in the phosphorylation status of key residues on the kinase subunit (Morgan, 1995). One critically important residue is Tyr15, whose phosphorylation status is essential for correct activation of the mitotic kinase. In several species, this residue is the target of signal transduction pathways that couple mitotic entry to processes such as cell size, DNA replication, and damage repair. Most CDKs contain a conserved Thr residue around position 158 within the T-loop and its phosphorylation is believed to enhance cyclin binding (Morgan, 1995). Cyclin binding is then thought to rotate the T-loop away from the catalytic site enabling substrate binding, P transfer, and inhibitory phosphorylation of Tyr15. Plant CDK-a proteins also have a conserved tyrosine residue at position 15, which, in at least some cell cultures, undergoes inhibitory phosphorylation. Application of the plant growth factor, cytokinin, which is required to allow these cells to progress into mitosis, is correlated with removal of this phosphate group (Zhang *et al.*, 1996). Mutant forms of CDK-a that lack this tyrosine residue are predicted to be resistant to checkpoint controls at the G<sub>2</sub>/M transition because they cannot be inactivated. However, overexpression of mutant CDK-a with substituted Thr14 and Tyr 15 residues in *Arabidopsis* has no phenotype under normal growth conditions (Hemerly *et al.*, 1995) raising a question as to the biological significance of the conserved tyrosine residue for plant development.

Although functional information mainly comes from complementation studies in yeast, ectopic expression of gain-of-function mutations has provided some intriguing insights in the possible role of CDK complexes in plant cell division. Expression of a dominant negative form of the *Arabidopsis* CDK-a, which had no kinase activity, is lethal in the same species and strongly inhibits cell division when expressed in tobacco (Hemerly *et al.*, 1995). Although the dominant construct may affect related CDK protein complexes by means of cyclin sequestration, the most appealing explanation is that it inhibits the CDK-a complex. These results indicate that the primary function of CDK-a is to promote plant cell division, as predicted from complementation experiments in yeast. Active CDK complexes have been implicated in promoting alterations in the microtubule cytoskeleton. Microinjection of an active plant CDK preparation into stamen hair cells causes a rapid breakdown of PPB microtubules, but not of other microtubule arrays (Hush *et al.*, 1996). It is not clear if this is due to differential sensitivity of various types of microtubules, or to differential stability/activity of the CDK preparation at other

stages of the cell cycle. Consistent with a role in premitotic and mitotic cells, a number of studies have shown that CDK-a proteins are located on the preprophase band and spindle (Stals *et al.*, 1997). The association with the PPB could point to a possible role in defining the division site, but an alternative role in regulating PPB assembly and disassembly seems more likely.

Noncognate or variant *cdc2*-like genes, CDK-b to CDK-e, have been identified in plants. These genes differ from CDK-a in the structure of their cyclin interaction domain and their ability to complement yeast CDK mutants (Fobert *et al.*, 1996; Porceddu *et al.*, 1999). The CDK family may have duplicated and diversified in plants since the plant-animal evolutionary divide. For example, animals do not contain genes structurally analogous to the CDK-b class. These have been found in genomic sequence surveys of primitive plants such as the moss *Physcomitrella patens* and algae. Of the noncognate forms, CDK-b genes are most closely related to CDK-a and are the best characterized of the noncognate CDKs. There are several indications that CDK-a and CDK-b functions have become specialized. First, transcription of the cognate and variant CDK-like genes appears to be regulated quite differently: the CDK-a genes are continuously expressed throughout all phases of the cell cycle but the CDK-b genes are expressed during limited periods of the cycle. In alfalfa, CDK-a and CDK-b proteins form distinct complexes with different substrate specificities and localize to different regions of the cell (Magyar *et al.*, 1997). Synchronized alfalfa cells were used to produce protein extracts from various points in the cell cycle. In one experiment, the proteins that were immunoprecipitated with CDK-a (Cdc2MsA/B) and CDK-b (Cdc2MsF) antibodies were analyzed for kinase activity. CDK-a antibodies can precipitate H1 kinase activity from cells at different parts of the cell cycle, including G<sub>1</sub>/S and G<sub>2</sub>/M. However, CDK-b antibodies produced a single peak of activity of G<sub>2</sub>/M. Detection of histone H1 phosphorylation activities in fractions immunoprecipitated with B-type cyclin (CyclinMs2) antibodies from G<sub>2</sub>-to-M phase cells indicated complex formation between this cyclin and a kinase partner in alfalfa, probably the noncognate CDK-b (Cdc2MsF). This indicates that while CDK-a may have several functions in cell cycle progression, CDK-b proteins may have a more specific function at G<sub>2</sub>/M. Other plant CDKs have been less well characterized, and their involvement in cell cycle control is still a matter of debate. These include CDK-c and CDK-d characterized by the presence of PITAIRE and N(I/F)TALRE sequences, respectively, and the highly divergent CDK-e with a SPTAIRE motif.

### 3. Plant Cyclins

Plant cyclins form a large superfamily of genes, in which several structurally related subclasses can be recognized (Renaudin *et al.*, 1998, Kouchi *et al.*, 1996). The nomenclature of the plant cyclin superfamily has been clarified by the detailed comparison of a large number of cyclin sequences from diverse plants (Renaudin *et al.*, 1996, 1998). These studies classified the plant cyclins into three groups

of so-called A-cyclins, two groups of B-cyclins, and three groups of D-cyclins. Although structurally related to mammalian cyclins, the degree of divergence between animal and plant cyclins makes it impossible to assign gene function on the basis of structural similarity with any degree of certainty. Cyclins may have diversified and acquired distinct functions prior to the plant–animal divide, but the evolutionary distance is too great to predict if given types of cyclins in plants have a functions similar to their animal namesakes.

Nevertheless, the B-cyclins are structurally analogous to animal B-cyclins and appear to function during late G<sub>2</sub> and M phase. Cyclin B1 transcripts (Fobert *et al.*, 1994; Hirt *et al.*, 1992; Ito *et al.*, 1997, 1998; Savoure *et al.*, 1995; and protein, Magyar *et al.*, 1997) accumulate during G<sub>2</sub> and disappear abruptly just after metaphase. Active kinase complexes containing cyclin B1 and one of the variant CDK proteins have been isolated from alfalfa cell suspension cultures, which can be synchronized in G<sub>2</sub> (Magyar *et al.*, 1997).

G1-cyclins are implicated in mediating the cellular response to extracellular proliferative signals in both mammalian cells, where they are called D-cyclins, and in yeast, where they are known as the CLN cyclins (Sherr, 1995). A number of plant cyclin genes have been isolated on the basis that they can complement yeast cells lacking CLN gene expression (Soni *et al.*, 1995; Dahl *et al.*, 1995) and these have been shown to respond to signals such as cytokinin and sucrose (Riou-Khamlichi *et al.*, 1999). In contrast to B-cyclins, the D-cyclins tested so far are expressed throughout the cell cycle. A number of cyclin D genes are expressed in a tissue-specific manner, a phenomenon that is not often encountered with the phase-specific cyclin genes (Gaudin *et al.*, 2000). This indicates that expression of these genes may respond to developmental signals.

The general model for cell cycle entry in mammalian cells involves the regulated transcription of D-cyclins in response to extracellular proliferative signals (Fig. 3). Enhanced levels of D-cyclins activate a CDK complex, which in turn phosphorylates and inactivates the Retinoblastoma (Rb) protein. Among its many proposed activities (Mulligan and Jacks, 1998), Rb can bind to and sequester the cell cycle transcription factor E2F. In the absence of available E2F, mammalian cells cannot enter S phase. Plant cells contain Rb homologs, which can bind D-cyclins through a well-conserved Rb–interaction motif (Ach *et al.*, 1997; Huntley *et al.*, 1998). The plant Rb proteins can be phosphorylated by cyclin D/CDK complexes (Nakagami *et al.*, 1999), but the functional significance of this event has yet to be demonstrated. When introduced in mammalian cells, plant Rb proteins have the capacity to modulate E2F-mediated gene expression (Huntley *et al.*, 1998). Plant homologs of E2F have been identified and are up-regulated in S phase (Ramirez-Parra *et al.*, 1999; Sekine *et al.*, 1999) when they may be involved in transcription of S-phase-specific genes.

The basic cellular processes that control cell morphogenesis have been relatively well characterized. Whereas the mechanisms that govern plant cell division are very similar to those in animals, the control of cell expansion is rather distinct, due

to the presence of the cell wall. In the next sections we will discuss the integration of cellular morphogenesis in the growing SAM.

### III. Meristem Organization

Looking at the meristem in a conventional scanning electron microscope, one intuitively tends to consider cells as the basic building blocks. However, the cells do not function autonomously in the SAM. Instead, they are organized into multicellular domains that are cytologically distinct and act as functional units (Fig. 5). Genetic

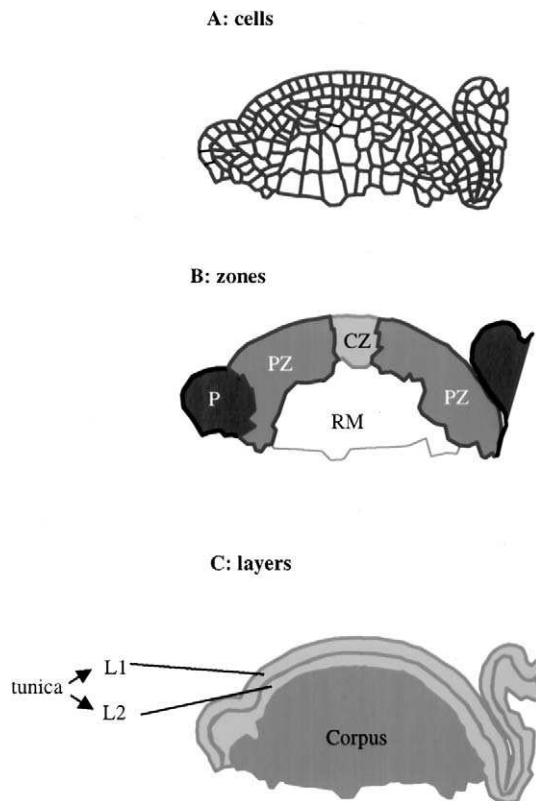


FIG. 5 The typical angiosperm meristem is composed of cells (A), which in turn are organized into zones (B) and layers (C), characterized by specific cytological features and gene expression patterns. The zonation model supposes the existence of a central zone of stem cells (CZ), surrounded by a peripheral zone (PZ) where the organs are initiated. The CZ and PZ are subtended by a rib meristem (RM), which generates the internal parts of the stem. Superimposed on this zonation is an organization into tunica and corpus. The tunica (which, depending on the species, can be composed of sublayers) is kept separated from the corpus by the strict orientation of the division planes in anticlinal orientations.

dissection has revealed the molecular mechanisms underlying organization of the SAM, providing a basis for understanding the integration of the cellular processes in the meristem.

### A. Layers and Zones

Microscopic examination of sections through the angiosperm SAM reveals the presence of distinct cell layers. The surface layer, or tunica, is formed and maintained by the strict anticlinal orientation of division planes during cell proliferation. The tunica surrounds an inner group of cells called corpus, which has no clearly defined stratification. In dicots, such as *Arabidopsis* or *Antirrhinum*, the tunica is composed of two layers, called L1 and L2, which surround a corpus. The latter often coincides with an internal layer, called L3 (Fig. 5). The L2 layer can be composed in turn of several sheets of cells, depending on the stage of development.

Superimposed on this partitioning into layers is a division into distinct domains that subdivide the meristem in an approximately radial fashion. Foster, in 1938, proposed a zonal model for the Gingko apical meristem (Fig. 5) that, with only minor modifications, seems to be common to all land plants with apical meristems. Extensive classical histological observations on numerous species define at least three zones: the central zone (CZ), the peripheral zone (PZ), and the rib zone (RZ). The CZ, a small group of cells at the meristem summit, spreads out over part of the tunica and corpus. The CZ is surrounded by the PZ where the primordia are initiated. Cells in the CZ usually proliferate at lower rates than in the periphery and in the primordia (Fig. 6). Differences in duration of the cell cycle can vary considerably among species. In rice, for instance, cells at the meristem flank have a doubling time that is about eight times higher than the cells at the summit, whereas in *pisum*, the ratio varies between 1.2 and 2.4 (Lyndon, 1999). Cells in the PZ are often smaller, slightly less vacuolated and have smaller nuclei than in the center. This is no general rule however. We could not, for instance, identify any major difference in cell size or nuclear size in the center or periphery of the *Arabidopsis* SAMs (Laufs *et al.*, 1998b). Inside the meristem, subtending the CZ and PZ is the RZ. This zone is characterized by the presence of cell files (hence, the name rib zone) that generate the internal parts of the stem. Within the last few years gene expression studies have shown that different regions are distinct at the molecular level and indeed demonstrate that meristem structure is even more complex than was previously suspected.

### B. Molecular Basis for the Layers and Zones

During the past 10 years the study of mutants with defective SAMs (Figs. 7 and 8) has produced a wealth of information regarding the molecular basis of meristem

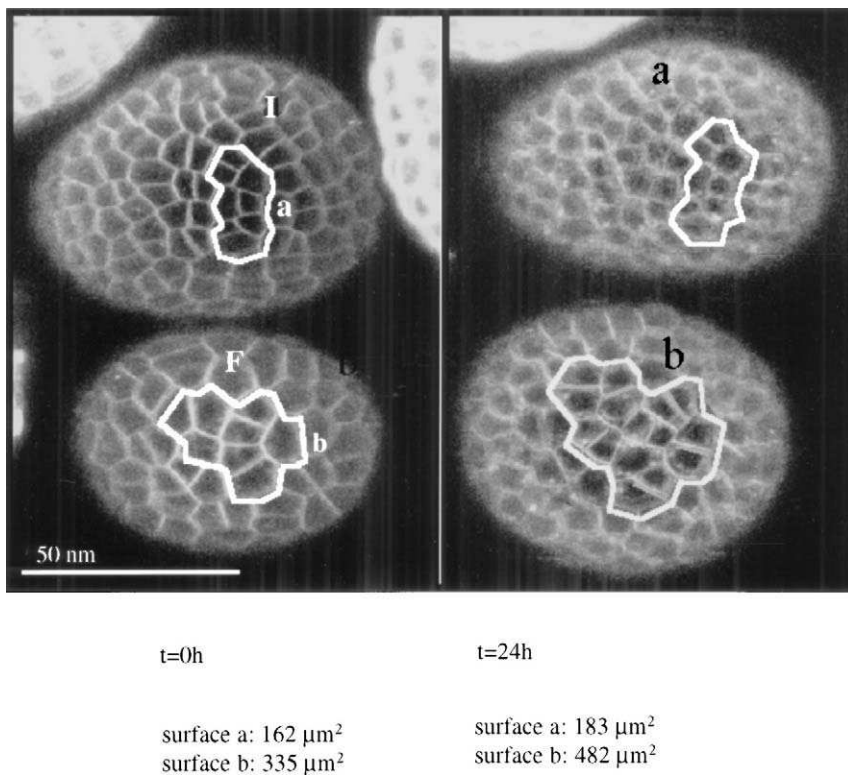


FIG. 6 Cell proliferation observed directly in a living inflorescence meristem of *Arabidopsis* using confocal microscopy and the membrane stain FM1-43 (Grandjean and Traas, unpublished). a and b represent groups of cells in an inflorescence meristem (I) and a floral meristem (F), respectively. During a 24-hr period the surface of group a shows an increase of 13%, whereas the surface of group b has increased with 44%. This demonstrates that cells in the primordia grow faster than the cells in the meristem proper.

function. This work has demonstrated that the cytological characteristics of different zones and layers have a molecular basis. A range of meristematic functions has been defined, including meristem maintenance, organ initiation, transcriptional control, and signal transduction.

### 1. Meristem Initiation and Maintenance: Involvement of the Homeobox Genes

Homeobox genes encode transcription factors that are involved in the specification and development of the body plan in many multicellular organisms (Kappen, 2000). Several classes of homeobox genes are implicated in SAM development.

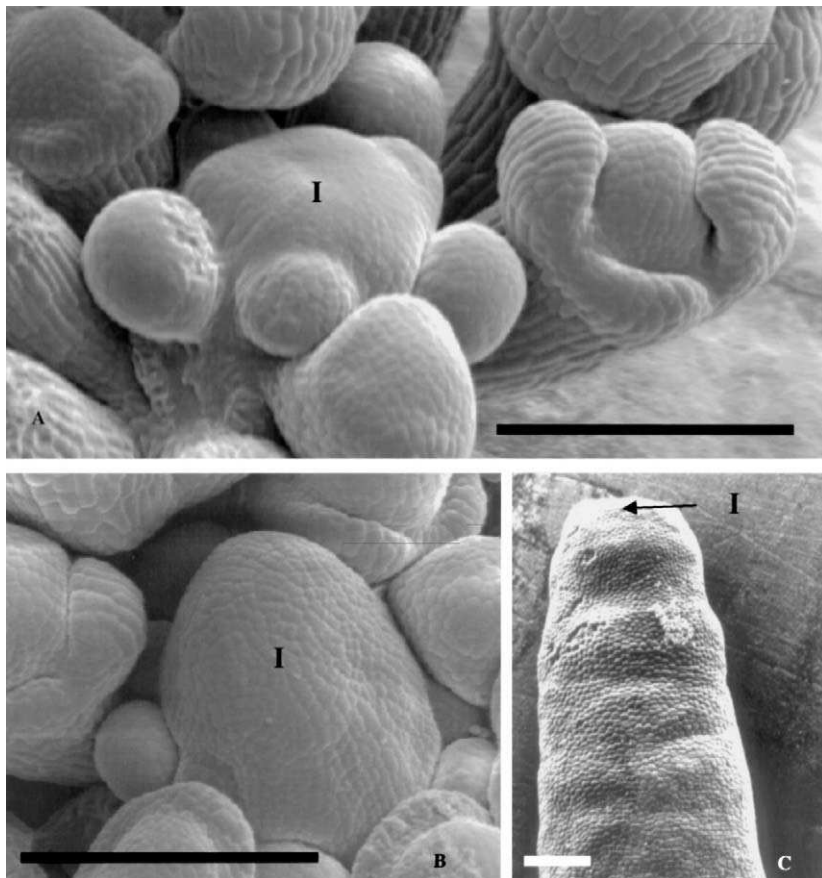


FIG. 7 Examples of meristem mutants. (A) The inflorescence meristem (I) of an *Arabidopsis* wild-type plant. (B) Enlarged meristem of the *clv3* mutant. (C) Naked apex of the *pin1-1* mutant, which usually does not initiate primordia at all (bar = 100 nm).

The *KNOTTED* gene family was initially identified in maize, where some of its members appear to play a role in meristem function and cell differentiation. KN1 was the first member to be discovered. It is expressed within the meristem and is down-regulated as cells enter the primordium. KN1 loss-of-function mutants have fewer branches and more determinate organs than wild type (Kerstetter *et al.*, 1997), supporting a role in meristem maintenance. The dominant KN1 mutants, which ectopically express the homeodomain protein in leaves, show a variety of defects in the leaf including knots of extra cells. This is consistent with the idea that the *KNOTTED* protein keeps cells in an undifferentiated proliferative state (Hake *et al.*, 1995).

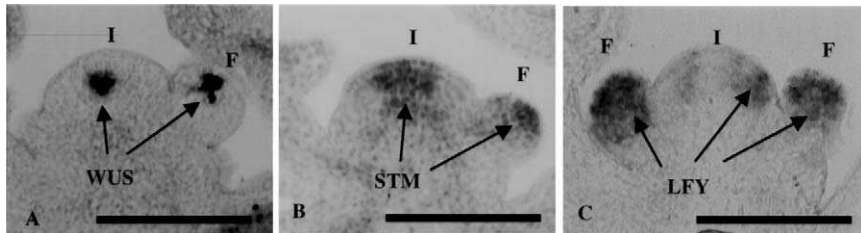


FIG. 8 Expression patterns of some meristem genes in inflorescence (I) and floral (F) meristems. (A) WUS is only expressed in some cells of the CZ. (B) STM is expressed in all inflorescence SAM cells, but is excluded from the young floral meristem primordia. Later on, STM expression is reestablished in the meristematic zone of the young flower. The organ identity gene LFY (C) is expressed in the young primordia only. Bar = 100 nm.

Mutants in *SHOOTMERISTEMLESS* (*STM*), a member of the *KNOTTED* family in *Arabidopsis*, are unable to develop or maintain a functional meristem during embryogenesis (Long and Barton, 1998; Long *et al.*, 1996). *STM* protein, like *KN1*, is present throughout the vegetative and inflorescence SAMs as well as in the floral meristems, but is excluded from the incipient primordia (Fig. 8). Interestingly, the *STM* gene is expressed from the very early stages of embryogenesis onward and can already be detected in a few cells at the top of the globular embryo but it is excluded from the incipient cotyledons (Long and Barton, 1998). The locations of *STM* transcript as well as the *stm* phenotype are consistent with a role in meristem formation. However, plants carrying strong loss-of-function *stm* alleles still have the capacity to initiate organs (i.e., cotyledons and leaves) and one could argue that they still have residual meristematic activity. An alternative hypothesis, therefore, is that *stm* mutants are able to initiate a meristem, but are incapable of maintaining it. In this scenario, *STM* would be necessary to keep the cells in a meristematic state. *Arabidopsis* has at least 7 *KNOTTED* class genes: *KNAT* (*Knotted Arabidopsis thaliana*) 1–5, *STM* (Granger *et al.*, 1996; Lincoln *et al.*, 1994), and at least 1 other is present in genomic databases. Of these genes, *KNAT1*, *KNAT2*, and *STM* are expressed in different but overlapping domains of the shoot meristem. *KNAT1* is expressed throughout the vegetative and inflorescence meristem in an area that largely overlaps with *STM*. *KNAT2* transcript has a more restricted pattern, as it can only be detected in the L3 layer in the young seedling and later on in vegetative development in the inner core of the apex within a domain that at least covers the rib meristem and possibly the entire corpus (Laufs *et al.*, 1998b). Later on, *KNAT2* is also expressed in basal parts of floral meristems and in part of the carpels (V. Pautot, J. Dockx, and J. Traas, unpublished, 2000). No loss-of-function mutants have been described for *KNAT1* and *KNAT2*. However, *KNAT1* overexpression induces the formation of lobes and leaf-like structures on leaves. It is also able to induce ectopic shoots and is therefore sufficient for meristem formation. This is

different for *KNAT2* overexpression, which causes the formation of lobed leaves but cannot induce ectopic meristems (V. Pautot, J. Dockx, and J. Traas, unpublished, 2000).

The *WUSCHEL* gene defines another homeobox gene family (Mayer *et al.*, 1998). Mutants lacking *WUSCHEL* are able to initiate a meristem, but, after having initiated several organs, the cells then fail to be incorporated into primordia (Laux *et al.*, 1996). New meristems continuously form but are defective and terminate prematurely in aberrant flat structures. Primordia initiation often occurs ectopically within the center. Flowers are eventually formed but these terminate prematurely in a central stamen. In the SAM, *WUS* transcript is present only in a few cells, probably forming the basal part of the central zone (Fig. 8). Based on the phenotype and the expression patterns, Mayer *et al.* (1998) proposed that cells expressing *WUS* could specify the identity of an overlying domain of stem cells in the central zone. One member of another class of homeobox genes, the *HD-GL2* family, has been implicated in meristem function, although no loss-of-function mutant has been characterized and its function is still unknown. *ATML1* (for *Arabidopsis thaliana* meristem L1) encodes a homeodomain protein that shares high sequence homology with both the *Phalaenopsis* O39 and the *Arabidopsis* *GLABRA2* (GL2) homeodomain proteins (Lu *et al.*, 1996). The *ATML1* gene is expressed generally in the apical part of the embryo until the 16-cell stage, whereupon its mRNA becomes restricted to the epidermal cells. Later, the transcript is found only in the L1 layer of the SAM in the mature embryo. After germination, this L1 layer-specific pattern of expression is maintained in the vegetative, inflorescence, and floral meristems and in young organ primordia.

## 2. Control of Meristem Size: The *CLAVATA* Genes

Loss-of-function mutations in any one of the three *CLV* genes (*CLV1-3*) cause an enlarged meristem from the embryo stage onward (Clark *et al.*, 1993; Kayes and Clark, 1998; Fig. 7). The meristem gradually increases in size throughout development, causing fasciation of the inflorescence stem and the production of flowers with increased floral organ numbers. Double mutants for *CLV1* and *CLV3* are indistinguishable from the single mutants, suggesting that these genes function in the same pathway. *clv2* mutants affect both meristem and lateral organs and genetic interactions with *clv1* and *clv3* suggest all three genes function in the same pathway controlling meristem behavior. However, *CLV2* has an additional role in lateral organ development (Kayes and Clark, 1998).

*CLV1* encodes a receptor kinase that is expressed in the corpus and possibly the L2 layers of the meristem (Clark *et al.*, 1997), in a domain that surrounds and covers the domain expressing *WUS*. *CLV3* encodes a small peptide which could be the extracellular ligand for *CLV1* (Fletcher *et al.*, 1999). *CLV3* is expressed in a zone that could correspond to the L1 and L2 layers of the classical CZ. *CLV2*, which has a more general expression pattern, encodes a receptor-like protein

(Jeong *et al.*, 1999). According to the current hypothesis, the *CLV* genes together with *WUS* regulate the size of the effective cell population within the CZ (see below).

### 3. Genes Involved in Organ Initiation and Separation

Meristems continuously produce cells, some of which are subsequently incorporated into the nascent lateral organs. Whereas *STM*, *WUS*, and *CLV* control meristem maintenance and size (and thus the number of cells that are produced by the meristem), another network of genes appears to partition these cells into organs (Fig. 4). A number of interrelated processes are necessary for organ formation and these include the attribution of cells to primordia, organ outgrowth, organ separation, and the determination of organ identity. Although we do not know the exact sequence of events, one of the first steps in the process is the isolation of groups of cells from the meristem. These cells subsequently lose their meristematic identity as is evidenced by the inactivation of *STM* expression. Different genes have been associated with these first steps in organ initiation. A very early event, the inactivation of *KN1/STM* in the organ primordia, is controlled by myb-like transcription factors encoded by the *ROUGH SHEATH 2 (RS2)* gene of maize, the *PHANTASTICA (PHAN)* gene of *Antirrhinum* and *ASYMMETRIC LEAVES 1* in *Arabidopsis* (Waines *et al.*, 1998; Byrne *et al.*, 2000). The *PHAN/AS1* genes are expressed in PZ cells, which will become part of the leaf primordia and are thought to be required to switch off expression of the KNOTTED-like meristem genes *STM*, *KNAT1*, *KNAT2*, *KN1* (Timmermans *et al.*, 1999; Sinha, 1999; Schneeberger *et al.*, 1998; Taylor, 1997; Byrne *et al.*, 2000). Mutations in *RS2/PHAN/AS1* perturb both leaf formation and meristem function, supporting the notion of a dynamic interaction between the lateral organs and the central meristem.

Subsequent to their isolation from the meristem (as evidenced by *RS2/PHAN/AS1* expression), the primordium initial cells start to grow more rapidly than the surrounding tissue. Another gene whose expression is associated with outgrowth is *AINTEGUMENTA (ANT)*. This is a very early marker for primordium initiation throughout development being expressed in nascent cotyledons, leaves, flowers, and floral organs (Long and Barton, 1998). *ANT* is a potential transcription factor, related to *APETALA2*, the latter being involved in the determination of floral organ identity; *ant* mutants have obvious defects only during floral and seed development where floral organs are reduced in size and number and integument outgrowth is perturbed (Elliott *et al.*, 1996; Klucher *et al.*, 1996; Mizukami and Fischer, 2000). If combined with *ap2*, the effects of losing *ANT* are intensified, suggesting that these two functions are partly redundant during floral morphogenesis. During vegetative development, the effect is more subtle, because leaf size is only slightly reduced. This is accompanied by a reduction in cell numbers.

The definition of an organ primordium also requires the establishment of its boundaries. Several genes have been implicated in this process. Mutations in the *Antirrhinum* gene, *FIMBRIATA* (Simon *et al.*, 1994) and in its ortholog, *UNUSUAL*

*FLOWER ORGANS (UFO)*, from *Arabidopsis* (Ingram *et al.*, 1995) have clear effects on organ separation. *ufo* mutants show fused and chimeric organs (Levin and Meyerowitz, 1995). The genes encode related F-box proteins and are expressed at the boundaries between floral organs. This would indicate a function in establishing organ boundaries but it must be noted that the genes are also expressed, at least transiently, in the inner parts of the vegetative and inflorescence meristems, and mutant phenotypes suggest other roles in meristem determinacy and organ identity. At least during early development, *UFO* expression depends on the presence of functional *STM*, because no *UFO* expression could be detected in *stm* mutants. Interestingly, *STM* and *UFO* expression overlap at the site of organ boundaries in the embryo (cotyledons) and in the flowers. This implies that *STM* could also be involved in organ separation.

Mutations of either of the two *CUP SHAPED COTYLEDON* genes have very mild phenotypes, but if both genes are inactivated, cotyledons fuse to produce a funnel-shaped structure (Aida *et al.*, 1997) surrounding the SAM, and later in development *cuc1/cuc2* mutants show fused organs. *CUC2* is homologous to *NO APICAL MERISTEM (NAM)*, originally identified in Petunia. In this species, *NAM* is absolutely required for the presence of an apical meristem (Souer *et al.*, 1996). In *Arabidopsis* several members of this family (termed the NAC family) have been identified and they may act as transcription factors. The *CUC2* gene is expressed in a zone between the cotyledons consistent with the idea that it acts as a local growth suppressor. Later on in development, the gene is expressed at all organ boundaries. *STM* interacts with the *CUC2* gene insofar as *STM* is required for the correct spatial expression of the *CUC2* gene and the *CUC* function is required for *STM* expression, at least in the postembryonic phase (Aida *et al.*, 1999).

#### 4. Other Elements of the Network

Two genes in *Arabidopsis*, *PIN-FORMED (PIN)* and *PINOID (PID)*, are necessary for both organ initiation and organ separation throughout development. During embryonic development and vegetative growth, loss of *PIN* activity causes the formation of reduced numbers of cotyledons and leaves, respectively. The effects of mutations in *PID* are less pronounced during the vegetative phase. Both mutations cause the formation, during the flowering phase, of a naked inflorescence stem (Fig. 7), which very infrequently initiates flowers with fused organs. *PIN-FORMED* was cloned and is predicted to be a transmembrane protein (Gälweiler *et al.*, 1998). The *PID* gene has recently been cloned and shown to be a serine/threonine kinase (Christensen *et al.*, 2000). Both *PIN* and *PID* are apparently up-regulated in the incipient organs throughout development, confirming a role outside the meristem in organ initiation. Both gene products have been associated with auxin action (see below).

Recessive mutations in the *mgoun1* and *mgoun2* genes cause fasciation (an asymmetric expansion of the meristem) and affect organ numbers (Laufs *et al.*,

1998a). Similar to *clv*, *mgo* displays an increased meristem size and this is correlated with an enlarged domain expressing *STM*. However *mgo* inflorescences show a characteristic type of fasciation distinct from that observed in *clv* mutants, in that there are multiple, juxtaposed meristems at the apex. Some meristems become independent from the main cluster, causing the formation of extra branches. Another major difference with *clv* mutants is that the number of organs is reduced. The combination of these two characteristics, enlarged meristem and reduced organ numbers, would suggest that the reduction of primordium initiation is not so much caused by a problem in the regulation of size or maintenance but by a defect in the transition of cells from the periphery to the primordia. The effects of both types of mutations is additive, supporting the idea that *CLV* and *MGO* function independently on the meristem.

The *fasciata1* and *fasciata2* mutants also have *mgo*-like phenotypes. Double mutants combining *fas* and *mgo* have a much more dramatic phenotype than can be expected from a simple addition of the single phenotypes, because the double mutants are almost incapable of initiating new organs. This suggests that *MGO* and *FAS* are partially redundant. Mutations in *MGO* also affect the layered structure of meristem, the layered organization being less obvious due to irregular division planes. Whether the effects of the *mgo* mutations on meristem structure are direct or indirect via their effect on organ initiation remains to be seen.

Besides the genes mentioned so far, a whole set of factors controls the identity of the organs produced (i.e., leaves, flowers, floral organs). These genes, which are expressed in the primordia, can be switched on very early in development in the incipient organs produced by all meristems. The *FLORICAULA* (*Antirrhinum*) and *LEAFY* (*Arabidopsis*) transcription factors, for instance, are the first identity genes switched on as soon as the cells leave the meristem. The organ identity issue is an extremely important and exciting field, which has given valuable information on the way differentiation patterns and domains within tissues are established. This topic will not be treated here in detail and the reader is referred to recent excellent reviews (Irish, 1999; Weigel, 1998; Ng and Yanofsky, 2000).

## 5. Meristem Structure and Gene Expression Patterns

Genetic analysis combined with expression studies not only confirms earlier histological studies, but also completes our view of meristem structure (Fig. 9). For example, whereas the expression patterns of *CLV3* and *ATML1* correspond to part of the *CZ* and *L1* respectively, *CLV1* and *CUC2* expression define domains that had not been identified previously using histochemical methods. Within each domain cells grow and divide in a characteristic manner: cells in the *L1* layer all divide in an anticlinal plane; cells in the *CZ* divide more slowly than at the periphery. How is this differential behavior controlled? In Sections IV and V we will discuss the potential links between cell morphogenesis and the factors controlling meristem organization.

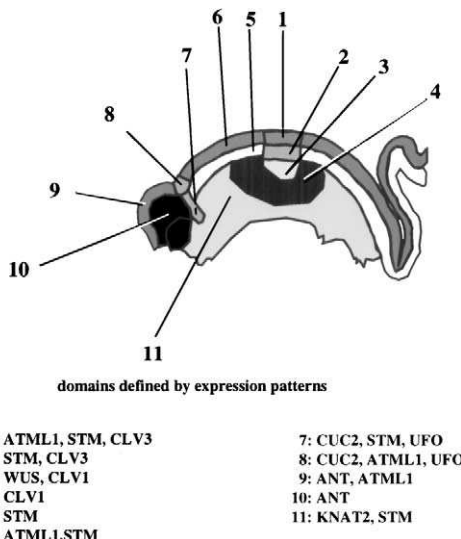


FIG. 9 The gene expression patterns define at least 11 distinct domains within the meristem.

#### IV. Integration of Cells within the Meristem

##### A. Dynamic Stability of the SAM

As we have seen, meristems are highly organized structures that can function for years or even centuries. At the same time, growing meristems are extremely dynamic with cell production being in equilibrium with cellular differentiation. How can the highly dynamic behavior of the cells be reconciled with the stability of the overall system?

Stability could be provided by detailed stereotypic programming of each cell's fate through its lineage. Is there any evidence that such a system exists in the meristem? Plant cells seem to align their division planes with precision; for example, cells in the L1 of the SAM divide systematically in anticalinal orientations, suggesting that daughter cells are already destined to become epidermal cells in the mature organs. However, careful clonal analyses have shown that the final developmental fate of a cell does *not* depend on cell lineage (Dawe and Freeling, 1991; Szymkowiak and Sussex, 1996). These studies have used chimeras in which the descendants of particular cells are marked, producing distinct sectors of cells. The analysis of these sectors has shown that L1 cells can leave descendants in different layers within the mature tissues of the plant. This means that cells in the L1 do not have a cell fate that is restricted to the epidermis, but that their offspring can readapt their differentiation program when an occasional change in division

plane alignment causes a daughter cell to occupy an unusual position. This is even more dramatically illustrated by the phenotype of the *tonneau* and *fass* mutants in *Arabidopsis* (Torres-Ruiz and Jürgens, 1994; Traas *et al.*, 1995). Both mutants, which grow as stunted dwarves, show highly perturbed patterns of cell division planes. This is correlated with an incapacity to form microtubular preprophase bands or to align division planes. In spite of this severe cellular phenotype, the plants are able to initiate organs at the apex, including flowers and floral organs in the correct position. Cell types, such as stomata, trichomes, and vascular tissues, also form at their correct relative positions. The current idea is that the maintenance of strict cell lineages is only of minor importance for generating the correct cell differentiation patterns. These experiments, therefore, support the idea outlined as early as in 1878 by Vochting (Holder, 1979) that plant cells adapt their developmental fate according to their position. This implies that the cells must somehow sense their position in the tissue via information coming from their immediate environment. Different sensing mechanisms have been proposed that rely either on physical signals such as tension within tissues or on signals of chemical nature.

Physical constraints put on meristems can modify growth patterns. Hernandez and Green (1993) forced sunflower SAMs to grow into ovals between fixed, parallel bars. This not only led to modifications in the position of organs, but also modified the identity of the organs produced. Although biophysical processes are likely to play an important role in the establishment of organized, patterned tissues, their interactions with molecular and cellular processes have not been characterized, and will not be discussed here in detail. Direct experimental proof for the importance of chemical signaling in the establishment of differentiation patterns in plants has come from work on *Arabidopsis* roots. Van den Berg and colleagues (1995) used confocal microscopy to ablate meristematic root cells in defined positions. They showed that the identity of recently divided initials requires the presence of more mature cells, and proposed that the latter generate signals that determine the behavior of their undifferentiated sisters. Questions remaining to be answered include these: What are the signals involved? How are these signals transported? How is the pattern established? We will first consider the different routes that signals can take in the SAM.

## B. Pathways for Chemical Signaling: Symplast and Apoplast

The two major local signaling routes for chemical signals are the symplast and the apoplast. In the symplast, molecules travel directly from cell to cell via cytoplasmic connections called plasmodesmata, whereas in the apoplast they travel through the cell wall or extracellular space. Signals can travel via the apoplast, but this is not a universal rule. An alternative is the symplast, and a variety of

molecules from hormones or sucrose to RNAs and proteins, can travel within the symplast. In this section we shall briefly review the salient features of these routes.

### 1. Apoplast

Different lines of evidence show that cell differentiation involves extracellular signals in plants that move through the apoplast. These signals can either be transported into the cells, as was suggested for auxin, or react with components of the cell surface, such as membrane receptors (see below). An example of apoplastic communication has been reported from algae: Bouget *et al.* (1998) combined laser ablation and microinjection to study cell–cell communication in the young embryo of the brown alga *Fucus* (Bouget *et al.*, 1998). The authors observed that rhizoid cells could inhibit the redifferentiation of thallus cells across an ablated zone, suggesting communication via the apoplast, although the exact nature of the signal is unknown. Likewise, the disruption of plasmodesmatal connections by plasmolysis in oat coleoptiles does not perturb auxin-induced curvature (Drake and Carr, 1978) indicating that this hormone travels via the apoplast. In particular, work on cultures of higher plant cells has also hinted at the existence of soluble extracellular signals. For example, the cell-free growth medium of an embryogenic suspension culture in carrot stimulates embryogenesis in a nonembryogenic suspension (McCabe *et al.*, 1997). There is evidence that arabinogalactan proteins, normally occurring in plasma membranes and cell walls, are involved in this stimulation.

### 2. Plasmodesmata and Direct Transfer of Molecules between Cells

Plasmodesmata are narrow tubes directly linking the cytosol and plasma membranes and usually the ER systems of neighboring cells to each other (Fig. 10; Ding *et al.*, 1999). The precise molecular structure of plasmodesmata has not been elucidated but a number of biochemical approaches have been developed to isolate and analyze their components. Ultrastructural studies show that besides ER and plasma membranes, they also contain structural spoke-like components, most probably proteinaceous in nature. Plasmodesmata can be formed directly during cytokinesis when the new plasma membrane and cell wall are laid down by the phragmoplast. Secondary plasmodesmata are formed between mature cells by a process that is not well understood but must involve the local degradation of the cell wall and the fusion of the neighboring plasma membranes and ER systems.

Molecules can travel through plasmodesmata via different ways. The small space created by the microspokes hold the ER and the plasma membrane apart and could allow for intercellular transport, but the membrane components as well as the ER lumen itself, could also be used for this purpose, although the latter

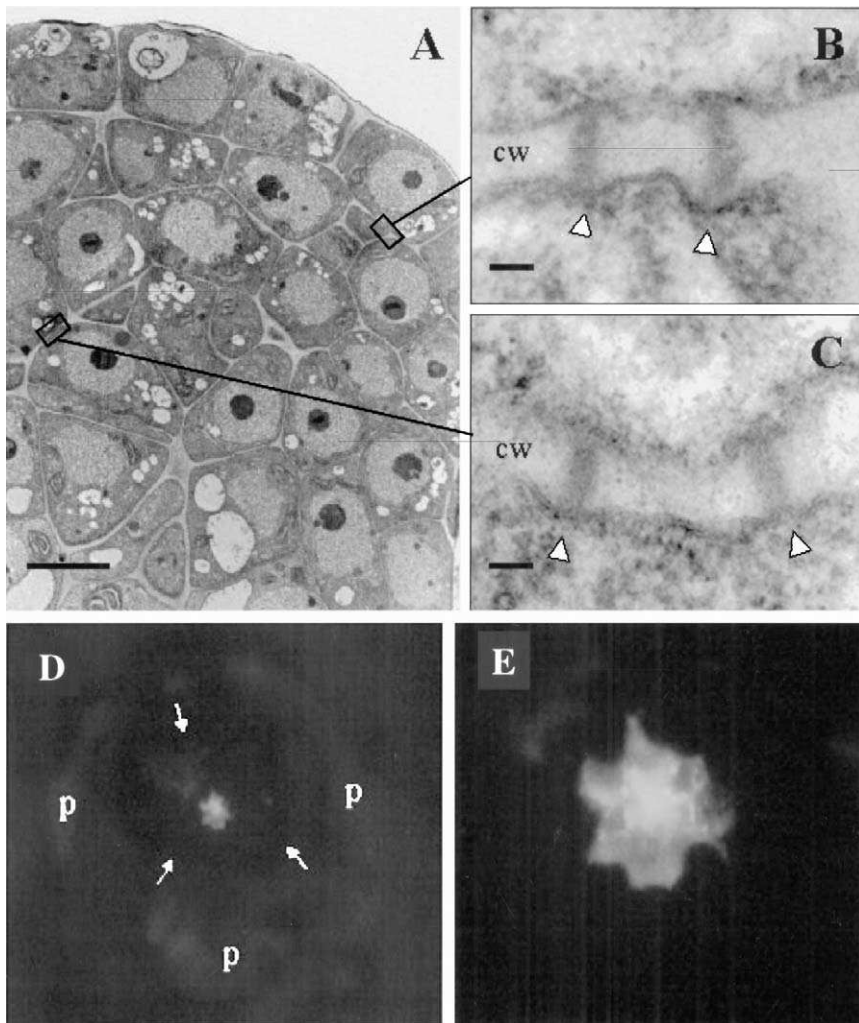


**FIG. 10** (A–C) Transmission electron micrographs showing position and morphology of plasmodesmata in the shoot apical meristem of *Arabidopsis thaliana*. (A) Overview showing a median-longitudinal section through the meristem with cells in L1, L2, and corpus. Linear plasmodesmata are present in all walls within the meristem. (B) Detail of a nondivision wall in the upper boxed area of part (A), showing two linear secondary plasmodesmata between an L1 cell and a divided L2 cell. (C) Detail of the wall in the lower boxed area in part (A). These plasmodesmata are either primary or secondary in nature, dependent on whether the wall is a division or nondivision wall, respectively. cw, cell wall. Arrowheads point at the plasmodesmata. Bars = 20  $\mu$ m (A) and 100 nm (B, C). (D, E) Centrally located symplasmic field within the tunica of the tobacco shoot apical meristem. After the impalement of a single central tunica cell a stable membrane potential was recorded ( $E_m = -41$  mV), and subsequently the fluorescent dye Lucifer Yellow was iontophoretically microinjected ( $I = -2$ –5 nA). LYCH was instantaneously diffusing from cell to cell via open plasmodesmata, thereby revealing the presence of a central symplasmically coupled cell group. (D) Overview of the tobacco meristem. P, primordia. Arrows, approximate boundary between the meristem proper and the leaf primordia. (E) Detail showing the central group (Fig. 10A–E courtesy of van der Schoot and Rinne, unpublished.)

possibility remains to be proven. Not all molecules can freely move through the symplasmic space. Plasmodesmata have a size exclusion limit (SEL), which appears to be variable as values between 1 and 10 kDa have been reported. Transport can also be actively promoted, as is the case for larger molecules such as RNAs or proteins. Although this process is not at all understood, it somehow must overcome the SEL, either by modifying plasmodesmatal structure or by unfolding larger molecules such as proteins or RNA. Symplasmic continuity between neighboring cells allows the generation of multicellular domains in which cell behavior is coordinated. A symplasmic field concept has been proposed to explain cell specification and behavior in the meristem (van der Schoot and Rinne, 1999). Cells in the L1 and L2 layers (i.e., the tunica) preferentially divide anticlinally forming sheets of cells that are rich in primary plasmodesmata. In contrast, the interfaces between the L1 and L2, and between the tunica and the corpus, contain mainly secondary plasmodesmata. Primary and secondary plasmodesmata may differ in their transfer capacity and specificity and could represent distinct subroutes for signaling. Because primary plasmodesmata are exclusively created during cytokinesis, division plane alignment has a clear effect on the structure of the plasmodesmatal network. Due to the strict alignment of the division sites, the tunica has no primary links with the corpus, which could be important for angiosperm SAM function. In this context, the *ton* and *fass* phenotypes are again of great interest. In these mutants the separation between primary and secondary plasmodesmatal circuits is probably not set up correctly, because division planes are not aligned properly. This in turn could perturb signaling in the meristem. Although this has no effect on the general spatial distribution of tissues and organs, the mutants do show some abnormal differentiation patterns (Traas *et al.*, 1995). The plants grow very slowly, and roots and leaves in *fass* and *ton* have extra cell layers, indicating problems in the specification of cell identity during the early phases of organ development. Further characterisation of developmental patterning in these mutants may provide insights into the interaction between division plane alignment and signalling mechanisms.

Although cell division patterns have an important impact on the plasmodesmatal network, the plant also has the possibility to modify existing connections. There is evidence that the plasmodesmata can be opened or closed, for instance, by the deposition or removal of callose plugs or the phosphorylation or dephosphorylation of plasmodesmal components (Ding *et al.*, 1999, for review). Evidence for the existence of symplasmic fields in the SAM, which overlap with the histological zones described in the previous section, came from microinjection studies. Rinne and van der Schoot (1998) injected Lucifer Yellow CH, a membrane impermeant probe, into birch SAMs and were able to show that cells at the periphery of the tunica are coupled to each other in a field that is separated from the central zone (see also van der Schoot and Rinne, 1999). In addition, the cells in the tunica from the central field, were separated from the central symplasmic domain of the corpus. The symplasmic fields are themselves dynamic and transient connections

can develop between fields. Thus the meristem can be seen as a number of distinct domains as defined by gene expression patterns, but this structure is overlaid by a partitioning into fields of cells linked by plasmodesmatal connections. Studying the interplay between these two phenomena should provide insight into the mechanisms underlying meristem organization.

### C. Apoplastic and Symplasmic Signals and Meristem Function

#### 1. Hormones

The “classical” hormones—gibberellin, auxin, cytokinin, abscissic acid—all seem to play distinct roles in meristem function, which have yet to be defined fully at the cellular and molecular level. So far, mainly auxin and cytokinin signaling pathways have been associated with a range of different aspects of meristem function. However, other hormones are also involved, such as gibberellins, which appear to play a major role in the transition to flowering or abscissic acid, which could regulate meristem dormancy and which could directly regulate cell division by interfering with the expression of cell cycle inhibitors such as CKIs (Wang *et al.*, 1998).

**a. Auxin Signals** Auxins are thought to be transported from cell to cell via the apoplastic space (Drake and Carr, 1978; Ding *et al.*, 1999). There is evidence that auxin plays a role in primordium initiation. When applied to young primordia, *N*-1-naphthyl-phtalamic acid (NPA), an inhibitor of auxin transport, induced their lateral extension (Meicenheimer, 1981). This could mean that the treatment prevented auxin to diffuse away, and that the increased amount of hormone subsequently increased the number of cells recruited into the primodium. This interpretation is consistent with the observation made by Pereira and Dale (1982) in *Phaseolus*, who induced an extension of primordia by local applications of the synthetic auxin 2,4-D. Several genes involved in auxin transport or signaling play important roles in organ initiation. In particular *PIN1* and *PID* have been studied in this context (see IIB4). The *PIN1* gene in *Arabidopsis*, encoding a 67-kDa transmembrane protein, has been associated with both auxin transport and organ initiation. *PIN1* may act as a catalytic auxin efflux carrier protein in auxin transport (Gälweiler *et al.*, 1998). The *pin1* phenotype, i.e., reduced organ numbers and the formation of fused primordia (Okada *et al.*, 1991), can be mimicked by treatment with inhibitors such as NPA, and it was shown that the *pin1* mutants have a reduced capacity to transport auxin in a polarized manner. When auxin is applied locally at the periphery of the naked *pin* meristems, flower primordia are induced at the site of application. This complementation of the phenotype by auxin indicates that *PIN1*, which is strongly expressed in the primordia, could permit primordium outgrowth via a local increase in auxin levels. Work on the *PID* gene also points at a role in auxin signaling. As

we have seen, *pid* mutants are very similar to *pin1*. *PID* overexpression leads to phenotypical alterations, which are reminiscent of auxin-resistant plants. 35S::*PID* plants, for instance, show reduced agravitropism of the roots and produce fewer lateral roots. This implies that *PID* is a negative regulator of auxin action. This is somewhat surprising because this means that both a positive regulator (PIN) and a negative regulator (*PID*) expressed in similar domains lead to identical mutant phenotypes. Therefore, although there is strong evidence that the distribution of auxin is involved in primordium initiation, the exact role of *PIN1* and *PID* remains to be established.

**b. Cytokinin Signaling and Meristem Function** Although cytokinins are clearly involved in meristem function, their precise mode of action at the meristem is not well defined. The mechanisms of cytokinin transport and perception are poorly understood. Cytokinins are found in the intercellular space and therefore travel via the apoplast. It cannot be excluded, however, that they are also transported via the symplasmic space. Genetic analyses of development in the moss *Physcomitrella patens* demonstrate that cytokinin is required to establish the SAM (Cove *et al.*, 1991) but, reminiscent of higher plants, excess exogenous or endogenous cytokinin perturbs its organization (Featherstone *et al.*, 1990). Classically, cytokinins have been thought of as positive regulators of cell proliferation within the meristem. The *abnormal meristem mutant 1* (*amp1*) in *Arabidopsis* (Conway and Poethig, 1997), which has abnormal levels of cytokinins, has an enlarged meristem that appears to produce extra primordia. These extra organs are also produced at a higher rate than normal, supporting the notion that cytokinin levels may be limiting for primordia initiation. Interestingly, the *amp* mutant has increased levels of D-cyclin transcript and exogenous cytokinins induce the expression of this cell cycle regulator (Riou-Khamlichi *et al.*, 1999).

STM/KNOTTED function may be linked with cytokinin action. Superficially, the ectopic expression of isopentenyl transferase (*ipt*) (a cytokinin biosynthetic gene) and KNOTTED have some similarities. General expression of *ipt* delays senescence, alters leaf shape, and promotes ectopic meristems (Estruch *et al.*, 1991; Li *et al.*, 1992; Williams-Carrier *et al.*, 1997). Overexpression of *KN1* and related genes can also induce the production of meristems on what would be differentiated tissues, such as leaves (Chuck *et al.*, 1996; Sinha *et al.*, 1993). If expressed from a senescence responsive promoter, *KN1* delays cell death in old leaves (Ori *et al.*, 1999). Analysis of such tissue demonstrates that cytokinin levels are increased, placing KNOTTED above cytokinin in the hierarchy of meristem regulation. Other KNOTTED-type homeodomain genes, when ectopically expressed, can also increase the levels of cytokinin without necessarily inducing meristem formation (Tamaoki *et al.*, 1997). However, other studies suggest that *KNOTTED/STM* transcript levels are regulated by cytokinin (Rupp *et al.*, 1999), which would place the hormone upstream of the homeobox genes. Therefore the hierarchy, if any, between cytokinins and the KNAT genes remains an open question.

Application of cytokinin to *Arabidopsis* inflorescences results in a number of developmental abnormalities including an increase in floral organ number, the formation of abnormal floral organs and induction of additional axillary meristems between floral organs. The authors suggest that these abnormalities resemble the phenotypes of mutants, *clv1* (increase in organ number), *ap1* (secondary floral buds in the axils of first-whorl organs, abnormal floral organs), *ap2*, *ap3* (abnormal floral organs), and propose that exogenous cytokinin suppresses floral meristem identity genes (Venglat and Sawhney, 1996).

## 2. Signaling in the Meristem: The CLAVATA Pathway

**a. The CLAVATA Complex** Evidence for the existence of signaling via the apoplast comes also from genetic and molecular studies on the 3 *clavata* mutants in *Arabidopsis*. As mentioned above, CLAVATA 3 together with CLAVATA1 and 2 regulate meristem size. The CLV3 gene encodes a small peptide that carries a secretion signal and potentially acts in the extracellular space (Fletcher *et al.*, 1999; Brand *et al.*, 2000; Trotochaud *et al.*, 2000). The cell autonomy of CLV3 function was determined using periclinal chimeras derived from unstable transposon-induced alleles (Fletcher *et al.*, 1999). This showed that CLV3 activity in one cell layer is sufficient to complement the absence of the peptide in other layers. It was hypothesized that the secreted CLV3 protein could move to underlying cell layers.

CLV1 encodes a receptor-like kinase (RLK) of about 105 kDa, with a putative extracellular domain of 21 tandem leucine-rich repeats (LRRs), a membrane-spanning sequence, and a presumed intracellular serine/threonine protein kinase domain. CLV3, which encodes a small predicted extracellular protein, could be a potential ligand for this receptor (see above). Trotochaud *et al.* (2000) showed that CLV3 is found in a multimeric 25-kDa complex. Several studies aimed at elucidating the biochemical events involved in this signaling pathway have revealed that CLV1 binds directly *in vitro* and *in vivo* to kinase associated phosphatase or KAPP (Stone *et al.*, 1998). This interaction requires the (auto)phosphorylation of CLV1. KAPP, a 65-kDa protein, is a potential effector in several kinase signaling pathways as it binds to multiple plant RLKs. Transgenics, in which the levels of KAPP transcript were reduced by means of cosuppression, partially repair the *clv1* mutant phenotype and the degree of repair seems to be correlated with the extent of cosuppression. Conversely, overexpression of KAPP mimics certain aspects of the *clv* phenotype, in particular the club-shaped siliques. These observations indicate that KAPP is a negative regulator of CLV whose role might be to modulate the signal strength needed to stimulate the CLV receptor complex.

Using cauliflower curds as a rich source of meristems, CLV complexes have been size fractionated, revealing that CLV1 is present in at least two different complexes: one of 185 kDa, another of 450 kDa. The 185-kDa complex is too small for a homodimer, therefore it must contain CLV1 linked to another protein, apparently via disulfide bridges. A probable suspect for this other protein is CLV2 (Kayes

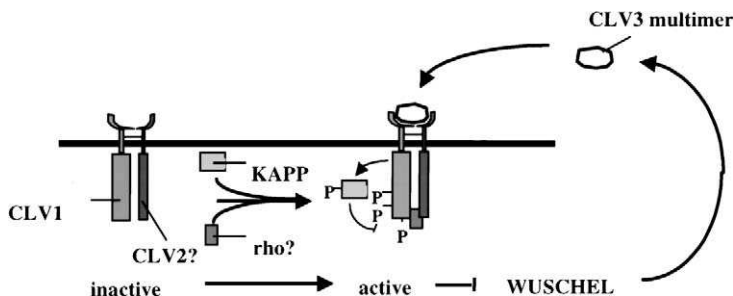


FIG. 11 The CLV/WUS feedback loop controlling meristem size. The CLV1 membrane-bound receptor kinase probably forms an inactive complex with the receptor-like CLV2. Activation of this complex requires phosphorylation of CLV1 and involves interaction with the CLV3 multimer. The active form of the CLV complex also interacts with the negative regulator KAPP and a Rho GTP-ase, which could relay a signal to downstream targets. The complex negatively regulates the transcription factor WUS. WUS in turn controls the expression of CLV3 in the CZ.

and Clark, 1998), which is a receptor-like protein, necessary for the assembly of the CLV1 complex (Jeong *et al.*, 1999; Trotochaud *et al.*, 2000). The 450-kDa complex contains a number of additional proteins including KAPP and a Rho GTPase-related protein (Trotochaud *et al.*, 1999). A number of mutations in CLV1 prevent the formation of the 450-kDa complex. The 450-kDa complex also requires CLV3 and Clark and colleagues have proposed a model whereby docking of the extracellular CLV3 ligand allows the CLV1/CLV2 heterodimer to interact with additional proteins such as KAPP and Rho (Stone *et al.*, 1998; Trotochaud *et al.*, 1999, Fig. 11). Hereby, the binding of CLV3 to CLV1 requires kinase activity of the latter (Trotochaud *et al.*, 2000). Signals would then be further relayed via the Rho-related protein toward downstream targets.

**b. The CLAVATA Pathway and the Regulation of Meristem Size** One of the targets of the CLAVATA complex is the WUS homeodomain protein, as indicated by genetic evidence. Indeed, *wus* is epistatic over *clv* mutants, suggesting that WUS functions downstream of CLV in the regulation of meristem size (Laux *et al.*, 1996). Interestingly, the ectopic expression of WUS, for instance under control of a primordium specific promoter, also ectopically induces CLV3 expression. This suggests that meristem maintenance involves a loop, in which WUS induces CLV3 in the CZ. CLV3 will then move to the CLV1 domain and activate the receptor kinase, which, in turn, will inhibit WUS. In other words, increased WUS activity will cause a larger CZ and increased CLV3 levels, which in turn will lead to a higher inhibitory capacity of CLV1 (Schoof *et al.*, 2000; see also Brand *et al.*, 2000). An interaction between CLV and STM was also investigated. In embryos that carry both *clv1* or *clv13* and *stm*, the latter is epistatic (Clark *et al.*, 1996). Thus CLV function depends on the presence of functional STM in

the embryo. However, STM is not required for *CLV* expression since the *CLV* gene is expressed in an *stm* background (Long and Barton, 1998). In addition, during postembryonic growth weak alleles of *clv* and *stm* act as mutual suppressors and an intermediate phenotype is observed. This would suggest that both genes act independently, but in an opposing way, on the same process.

### 3. Trafficking mRNA and Proteins between Cells

Some of the meristem regulators themselves can move from cell to cell and may be used as signals to instruct distant or neighboring cells. It was shown that several regulators travel via plasmodesmata. For example, the *KNOTTED1* homeobox gene from maize is only expressed in the corpus, whereas the protein is also detected in the tunica. Transport of the KN1 protein was analyzed using microinjection of fluorescent protein into young leaf mesophyll cells. This showed that KN1 was able to move into the surrounding bundle sheath and mesophyll cells. An increase in the plasmodesmatal SEL was associated with this movement, as KN1 also permitted the transport of certain coinjected molecules of 20 and 39 kDa (Lucas *et al.*, 1995). How KN1 interacts with the plasmodesmata to mediate its own transport, and what exactly the implications are for the meristem function remains to be established.

Non-cell autonomous action of DEFICIENS and GLOBOSA, two MADs box transcription factors in *Antirrhinum majus* involved in floral organ identity, could also involve transport through plasmodesmata. Perbal *et al.* (1996) used periclinal chimeras in which either the L1, L2, or L3 (corpus) layer lacked DEF or GLO. If the genes were expressed in the L2 and L3, protein could also be detected in the epidermal layer. At least for DEF, this movement is probably polar because in chimeras expressing DEF in the L1 only, the protein and mRNA remain confined to this layer (Perbal *et al.*, 1996). In addition, trafficking within one layer was limited. Likewise, Sessions *et al.* (2000) reported on the movement of the transcription factor LFY within the flower of *Arabidopsis*. These results confirm the hypothesis that the control of cell–cell signaling via symplasmic fields is an essential process in meristem function.

## V. Meristem Morphogenesis and Cellular Regulation

A combination of genetic, biochemical, and cellular analysis has given us a first insight into the regulation of meristem function (Fig. 12). Factors that act in specific domains of the meristem have been identified and some aspects of their interactions have been revealed. In addition, these studies point at the significance of cell interactions via symplast or apoplast, required for the organized development and maintenance of meristematic activity. The different elements of this network must interact with the processes involved in cellular morphogenesis, as cells in the

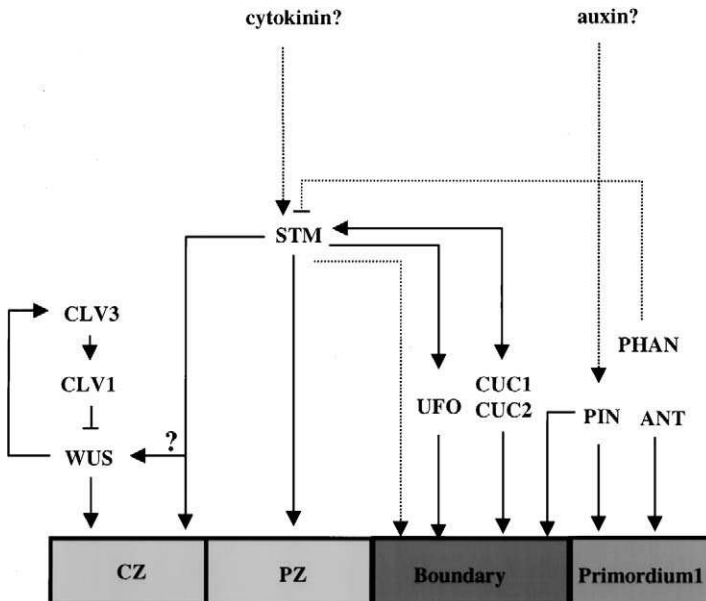


FIG. 12 Model of the regulatory network controlling meristem behavior, based on biochemical, genetic, and cellular analyses. The activity of certain factors, such as the CLV/WUS loop, is primarily restricted to subdomains. Other factors, such as STM play a role in different domains. STM is not only required for the activation of WUS, but also for the expression of UFO (Long and Barton, 1998) and CUC2 (Aida *et al.*, 1999), both involved in the definition of organ boundaries. At the periphery of the meristem; a PHAN homolog inactivates STM. ANT stimulates organ outgrowth. Several signals, including cytokinins and auxin, affect meristem function. Cytokinins are thought to interact with several homeobox genes of the KNOTTED family, whereas the putative auxin transporter PIN appears to regulate the establishment of primordia and primordium boundaries.

different parts of the meristem grow and proliferate at different rates. This interaction will be discussed in the next section.

How the behavior of cells impinges on the behavior of the meristem has been an area of active debate for a long time (Kaplan and Hagemann, 1991). One view is that development processes, such as shape and size control of whole organs, are regulated at a level above (and to some extent independently of) cellular behavior. According to the so-called organismal theory, multicellularity arises by the secondary “chambering” of the organism. In this view, cells play a passive role and do not represent a direct target for developmental regulation; cells grow and divide simply to fill the space provided by growth of the organism. The opposite model is the cellular theory, which puts cells at the center of morphogenesis, literally the building blocks that make up the whole organism. In between these extremes, compromise models can be proposed in which cells play an important role in development but are low in a regulatory hierarchy. In this scenario cellular

regulators are subservient to the developmental controls operating at the level of multicellular domains or whole organisms. In the next section, we will discuss a number of cases where the links between cellular morphogenesis and meristem regulators have been examined.

#### A. Links between Cell Morphogenesis and Meristem Regulators: Some Examples

##### **1. FIM and UFO: A Role in Cell Division?**

Mutations in both *ufo* and *fim* genes affect cell proliferation at organ boundaries. Both genes encode proteins with an F-box motif (Ingram *et al.*, 1995), which is implicated in protein degradation through the ubiquitination pathway. These data suggested a possible role in cell cycle control (Ingram *et al.*, 1995, 1997). Indeed Ingram *et al.* (1997) found that FIM interacted with a family of proteins, called FAPs, that are closely related to the human and yeast SKP1 protein. These are components of a complex that targets specific proteins for ubiquitin-mediated proteolysis. Because most of the proteins known at that time to be targeted by this complex were cell cycle regulators, it was proposed that FIM and UFO might negatively regulate the cell cycle machinery at organ boundaries. Ingram *et al.* (1997) suggested that these genes may provide a coupling between the pattern of cell proliferation rates and the pattern of cell identity. However, ubiquitin proteolysis is not specific for cell-cycle-related processes and since UFO and FIM do not simply affect separation between organs but also organ identity and gene expression, their function is probably much more complex than simply having a single role in cell cycle progression (Ingram *et al.*, 1997). Parcy and coworkers (1998) showed that the UFO gene also plays a role in meristem determination. Moreover, UFO seems to require other factors to have this effect: overexpression of UFO in *Arabidopsis* has no obvious phenotype (Lee *et al.*, 1997). However, when UFO is overexpressed in the presence of high levels of LEAFY, the meristem becomes determinate and organ primordia invade the CZ (Parcy *et al.*, 1998). This suggests that FIM/UFO help to establish determinate growth of the flower by inhibiting cell proliferation in the central zone of the meristem. In the *Antirrhinum* flower, FIM is expressed first in the central zone of the young flower before the first whorls of organs are initiated; it is only thereafter that the transcript becomes localized to the bases of the organ primordia. The mutant phenotype of *fim* deletions also supports this hypothesis in that floral meristems show loss of determinacy.

##### **2. STM and CLAVATA: Meristem Maintenance and Cell Proliferation**

A positive role in cell proliferation has been proposed for STM which is highly expressed in rapidly dividing cells (Meyerowitz, 1997; Traas and Laufs, 1998).

However, STM is also expressed at organ boundaries where mitotic activity is reduced. The phenotype of an STM loss-of-function mutant confirms this dual role. The SAM in the *stm* mutant is not maintained, which can be attributed to a lack of proliferative capacity. In contrast, the cotyledons are fused at their base, due to excess cell divisions at the organ boundaries (Long and Barton, 1998). Therefore the role of STM in cell division seems to depend on position within the meristem.

The *CLAVATA* genes have also been proposed to influence cell division. Since this class of mutants shows increased cell numbers within the meristem, the genes might negatively regulate cell proliferation. To test this hypothesis, Laufs and coworkers (1998b) analyzed proliferation patterns in wild-type and *clv* inflorescence meristems. As in other species, the wild-type *Arabidopsis* inflorescence meristem shows a significant difference in mitotic index between the CZ and the PZ. Thus, the meristem of the Ler ecotype has a central domain of five cells wide, where mitotic activity is reduced by 50% when compared to the periphery. In the *clv3* mutant, this central domain with a low proliferation rate is increased in size. This implies that the increased size of the meristem is not due to increased cell proliferation but supports the hypothesis that *clv* mutants have an extended CZ. The conclusion was that CLV proteins affect the size of the CZ. In the mutants, a gradually increasing population of cells is retained within the CZ and, despite that absolute proliferation rates are similar to wild type, the increased number of cells contributes to the enlarged meristem and attendant growth defects. Accordingly, it was shown that the expression domain of *CLV3*, a marker for the meristem center, is dramatically increased in *clv1* mutants.

### 3. The Cyclin D Pathway

As indicated above, the paradigm for cell cycle entry in mammalian cells involves the transcription of G<sub>1</sub> or D-type cyclins in response to extracellular proliferative signals. The availability of D-cyclins then allows the formation of a complex with CDK, which in turn phosphorylates and inactivates the Retinoblastoma (Rb) protein. In plants, the expression of D-cyclins is strongly influenced by growth regulators such as cytokinin, auxin, and sucrose (Soni *et al.*, 1995). For one gene, the cyclin D3 from *Arabidopsis*, cytokinin regulates its expression via a signal transduction chain not involving protein synthesis (Riou-Khamlichi *et al.*, 1999). Ectopic expression of cyclin D3 replaces the cytokinin requirement of leaf explants for cell proliferation. Taken together with the observation that cyclin D3 transcript levels are elevated in mutants that have high levels of cytokinin, it has been proposed that they mediate the growth effects of this hormone. Transgenic *Arabidopsis* calli overexpressing cyclin D3 failed to form shoots. To bypass this problem, the authors used a DNA *in vivo* recombination system that allowed them first to produce phenotypically normal plants on which they could induce sectors that overexpress D-cyclin. Seeds derived from such sectors had a number of

developmental aberrations such as extensive leaf curling, a disorganized SAM, increased leaf number, late flowering, and delayed senescence.

The idea that D-cyclins might mediate localized cell proliferation is further supported by the observation that cyclin D3b transcription in the dorsal anthers of *Antirrhinum* flowers is negatively regulated by the *CYCLOIDEA* gene (Gaudin *et al.*, 2000). *CYCLOIDEA* (*CYC*) is required for the morphogenesis of a bilaterally symmetrical flower (Luo *et al.*, 1996; Cubas *et al.*, 1999b). The *CYC* gene, expressed in the dorsal domain of the flower, is required to suppress cell proliferation in restricted locations. Although five stamen primordia are produced, only four mature; the dorsal anther is severely inhibited at an early stage in development and this is correlated with cessation of cell division and dramatically reduced cell cycle gene expression (Gaudin *et al.*, 2000). *CYC* is a member of the TCP family of proteins (Cubas *et al.*, 1999a). The TCP proteins are putative transcription factors and also include the *TEOSINTE BRANCHED* gene from maize (Doebley *et al.*, 1997) and the *PCF1* and *PCF2* genes from rice (Kosugi and Ohashi, 1997). *PCF1/2* were isolated on the basis that they could bind to *cis* elements in the rice *PCNA* gene, the latter being an auxiliary protein of DNA polymerase delta, strongly expressed during S phase. The *cis* elements are responsible for meristem specific expression demonstrating the potential of TCP proteins to bind to genetic elements with a demonstrated role in the expression of proliferative genes. More recently, another link between *cycD3* and a meristem regulator was uncovered in plants overexpressing *ANT* (Mizukami and Fischer, 2000; Krizek, 1999). In these plants the number of cells and organ size are increased, which is correlated with an ectopic production of *cycD3* transcript in mature leaves of *Arabidopsis*.

D-cyclins, therefore, seem to be an important target of developmental signals, perhaps acting to integrate a variety of such inputs into a local proliferative response. Thus a hierarchy of regulators that define the identity of a meristem or organ, along with environmental signals, could modulate spatial aspects of cell proliferation by controlling cyclin gene expression. In this model there is no direct regulation of the cell cycle phase-specific genes by the mechanisms that define the spatial aspects of cell proliferation within the meristem. Instead this occurs indirectly via the local transcription of cyclin D, which is rate limiting for entry into the cycle. That D-cyclins are rate limiting for growth has been demonstrated in transgenic tobacco where expression of the *Arabidopsis* cyclin D2 gene from a constitutive promoter significantly increases growth rate (Cockcroft *et al.*, 2000). Clearly, this model is simplistic and other controls including those impinging on the G<sub>2</sub>/M transition must also feed in and influence growth rate.

#### 4. Perturbing Cell Proliferation: Effects on Development

The importance of cells as a level of developmental control has been questioned by directly modifying the basic cellular machineries using transgenic and mutant approaches. Several mutants in cell cycle genes have been isolated, but, since they

have not been analyzed at the level of the shoot apical meristem, they will only be briefly discussed. A promoter trap strategy (Springer *et al.*, 1995) identified the *PROLIFERA* gene as essential and it is potentially involved in regulating entry into S phase. The corresponding mutant phenotype includes reduced fertility and embryo lethality, showing that the gene is essential for growth and development. Another example is *KNOLLE*, which is a cytokinesis-specific synthaxin, only expressed during specific phases of the cell cycle. *KNOLLE* is absolutely required for phragmoplast formation, and in its absence cytokinesis is perturbed. This in turn leads to incomplete cross walls and arrested growth of the embryos and seedlings.

The notion that the spatial control of cell proliferation does matter in development is also supported by observation of the phenotypes of cell cycle mutants such as *tousled*. *Tsl* mutants suffer from a random loss of floral organs (Roe *et al.*, 1997a, 1997b, 1993) and related genes in mammalian cells have been implicated in DNA replication (Sillje *et al.*, 1999). These results demonstrate that a gross perturbation of cell division arrests or perturbs growth and development, but they do not indicate the exact importance of the spatial control of cell division. In fact, development seems capable of coping with major changes in cell behavior: Hemerly and coworkers (1995) obtained substantial changes in cell proliferation patterns after overexpression of a mutant *Arabidopsis* CDK-a gene in tobacco. In this species the dominant negative version had reduced cell division at the shoot and root meristems, causing the formation of reduced cell numbers in the leaves. Interestingly, the overall architecture of the plant and the structure of the organs were not significantly altered, confirming that the patterns of tissue and cell differentiation do not depend on the strict regulation of cell proliferation. Earlier and cruder experiments already led to similar conclusions. Irradiation of *Triticum* seeds, for example, completely blocks cell proliferation, but the first primordia still grow out at their correct position (Foard, 1971).

These and other experiments appear to indicate that the patterns of differentiation can be uncoupled from cell proliferation control, at least within relatively broad limits. The relation between growth and cell proliferation is also controversial in animals where an increased cell division rate does not necessarily lead to extra growth. In *Drosophila*, for example, a combination of cyclin E and Cdc25stg overexpression increases cell proliferation in the wing, but does not increase the final size of the organ (Su and O'Farrell; 1998). Therefore, the size of the *Drosophila* wing is, within limits, independent of the number of cells, suggesting a level of control over organ development that is largely independent of cellular behavior. This might seem somewhat contradictory with the experiments using ectopic D-cyclin expression. As we have seen, D-cyclin has a negative effect on the capacity of calli to initiate meristems, indicating that it has an important role in establishing developmental patterns. We should bear in mind, however, that D-cyclin is believed to operate upstream of the basic cell cycle machinery and that it most probably affects transcription via the Rb pathway.

## 5. Perturbing Cell Expansion: Effects on Development

Growth, by definition, is an increase in size, and implies that cell expansion may be developmentally modulated. Surprisingly, the mechanisms underlying the control of cell expansion and their links with meristem regulators have not been investigated in any detail. Mutations affecting the cell expansion machinery also severely affect growth as illustrated by the *kor* or *rsw* phenotypes. Again, the available data on the phenotypes are not very informative about the regulatory mechanisms controlling growth at the meristem as they merely confirm the self-evident statement that cells have to expand in order to obtain plant growth. A more thorough analysis of cell differentiation patterns in these mutants using specific markers would be extremely important. There is now some indication that certain genes involved in cell expansion could be rate limiting for primordium development at the SAM. Using *in situ* hybridization, Reinhardt and coworkers (1998) showed that an expansin gene, *LeExp18*, was up-regulated at I1, the site of incipient leaf formation in tomato meristems. Thus, the expression pattern of this gene strongly indicates that expansins are important for normal leaf induction. This increase in transcription preceded the activation of a histone gene, suggesting that the cell expansion machinery is activated upstream of the cell cycle regulators. Evidence not only includes the observed up-regulation of expansin preceding rapid expansion in the incipient primordia, but Fleming *et al.* (1997) could also induce the formation of ectopic primordia at the meristem by applying expansin protein. Taken together, these results suggest a model, whereby primordium initiation depends on the up-regulation of cell expansion genes. At the same time, they also raise the question whether it is the cell expansion or cell division “machinery” that is limiting for growth.

### B. Cells and Domains in Meristem Function

Cellular morphogenesis appears to be strictly controlled during plant development: cells divide and grow slowly in the CZ, more rapidly at the periphery; division planes are strictly aligned in some cell layers but apparently not in others; and mutations in meristem control genes alter these phenomena as illustrated by many developmental mutants (Meyerowitz, 1997; Traas and Laufs, 1998; Laufs *et al.*, 1998b). Whereas these data could be interpreted as being in favor of the cellular hypothesis, or at least point to the importance of cells as a regulatory level, we cannot unequivocally reject the organismal theory. The uncoupling of cell numbers and organ size in plants overexpressing mutant CDK-a strongly supports the idea that cellular parameters do not need to be strictly coordinated in space. Likewise, STM or CLV seem to act at the multicellular level and their effects on cellular morphogenesis is apparently indirect. In addition, the link between other regulators such as FIM/UFO and cell proliferation remains unproven. Does this imply

that we should favor the organismal view? The connection between CYC, ANT, and D-cyclin expression indicates that cell proliferation may be actively regulated by factors operating at the level of multicellular domains. Overexpression of D-cyclins indicates that genes normally thought of as cellular regulators can affect developmental processes. Likewise, intervention at the level of cell expansion by the local application of expansin ectopically launches the developmental program of primordium initiation. Therefore, the evidence does not clearly discriminate between a hierarchical model in which global regulators act at the top and the cellular model where the organism is the sum of its cells. Indeed, meristem behavior seems to be regulated at a number of levels and bidirectional interactions between these levels are required for organized development.

## VI. Concluding Remarks

Components of the machinery controlling cell growth have been identified as have regulators controlling meristem function at the multicellular level. Although our knowledge has made spectacular progress during the last 10 years, a number of important questions need to be further addressed. These concern not only the molecular nature of the interactions between the cellular and multicellular level, but also the hierarchy, if any, between these two levels. In addition, available data point at the signaling mechanisms that integrate individual cells into the meristem and organize them into different functional domains. According to the current view, meristem function depends on a stable signaling network that is set up during embryogenesis and operates via plasmodesmata and the extracellular matrix. As soon as the network is established, signals between the different zones of the meristem seem to ensure stable reiterative development of sequential phytomers. A major challenge is therefore to further define the signaling mechanisms that govern meristem function.

## Acknowledgments

We thank Patrick Laufs, Clive Lloyd, Teva Vernoux, and Chris van der Schoot for helpful discussions and critical reading of the text. Chris van der Schoot and Päivi Rinne are thanked for sharing unpublished material.

## References

Ach, R. A., Durfee, T., Miller, A. B., Taranto, P., Hanley-Bowdoin, L., Zambryski, P. C., and Gruissem, W. (1997). RRB1 and RRB2 encode maize retinoblastoma-related proteins that interact with a plant D-type cyclin and geminivirus replication protein. *Mol. Cell Biol.* **17**, 5077–5086.

Aida, M., Ishida, T., Fukaki, H., Fujisawa, H., and Tasaka, M. (1997). Genes involved in organ separation in *Arabidopsis*: An analysis of the cup-shaped cotyledon mutant. *Plant Cell* **9**, 841–857.

Aida, M., Ishida, T., and Tasaka, M. (1999). Shoot apical meristem and cotyledon formation during *Arabidopsis* embryogenesis: Interaction among the *CUP-SHAPED COTYLEDON* and *SHOOT MERISTEMLESS* genes. *Development* **126**, 1563–1570.

Arioli, T., Peng, L., Betzner, A. S., Burn, J., Wittke, W., Herth, W., Camilleri, C., Hofte, H., Plazinski, J., Birch, R., Cork, A., Glover, J., Redmond, J., and Williamson, R. E. (1998). Molecular analysis of cellulose biosynthesis in *Arabidopsis*. *Science* **279**, 717–720.

Bouget, F. Y., Berger, F., and Brownlee, C. (1998). Position dependent control of cell fate in the *Fucus* embryo: Role of intercellular communication. *Development* **125**(11), 1999–2008.

Brand, U., Fletcher, J. C., Hobe, M., Meyerowitz, E. M., and Simon, R. (2000). Dependence of stem cell fate in *Arabidopsis* on a feedback loop regulated by CLV3 activity. *Science* **289**(5479), 617–619.

Christensen, S. K., Dagenais, N., Chory, J., and Weigel, D. (2000). Regulation of auxin response by the protein kinase PINOID. *Cell* **100**, 469–478.

Chuck, G., Lincoln, C., and Hake, S. (1996). KNAT1 induces lobed leaves with ectopic meristems when overexpressed in *Arabidopsis*. *Plant Cell* **8**, 1277–1289.

Clark, S. E., Running, M. P., and Meyerowitz, E. M. (1993). *CLAVATA1*, a regulator of meristem and flower development in *Arabidopsis*. *Development* **119**, 397–418.

Clark, S. E., Jacobsen, S. E., Levin, J. Z., and Meyerowitz, E. M. (1996). The *CLAVATA* and *SHOOT MERISTEMLESS* loci competitively regulate meristem activity in *Arabidopsis*. *Development* **122**, 1567–1575.

Clark, S. E., Williams, R. W., and Meyerowitz, E. M. (1997). The *CLAVATA1* gene encodes a putative receptor kinase that controls shoot and floral meristem size in *Arabidopsis*. *Cell* **89**, 575–585.

Cockcroft, C. E., den Boer, B. G., Healy, J. M., and Murray, J. A. (2000). Cyclin D control of growth rate in plants. *Nature* **405**, 575–9.

Colasanti, J., Tyers, M., and Sundaresan, V. (1991). Isolation and characterization of cDNA clones encoding a functional p34cdc2 homologue from *Zea mays*. *Proc. Natl. Acad. Sci. USA* **88**, 3377–3381.

Conway, L. J., and Poethig, R. S. (1997). Mutations of *Arabidopsis thaliana* that transform leaves into cotyledons. *Proc. Natl. Acad. Sci. USA* **94**, 10209–10214.

Cosgrove, D. J. (1997). Assembly and enlargement of the primary cell wall in plants. *Annu. Rev. Cell. Dev. Biol.* **13**, 171–201.

Cosgrove, D. (1999a). Enzymes and other agents that enhance cell wall extensibility. *Annu. Rev. Plant Phys. Plant Mol. Biol.* **5**, 391–417.

Cosgrove, D. (1999b). Relaxation in a high-stress environment: The molecular bases of extensible cell walls and cell enlargement. *Plant Cell* **9**, 1031–1041.

Cove, D. J., Kammerer, W., Knight, C. D., Leech, M. J., Martin, C. R., and Wang, T. L. (1991). Developmental genetic studies of the moss *Physcomitrella patens*. *Symp. Soc. Exp. Biol.* **45**, 31–43.

Cubas, P., Lauter, N., Doebley, J., and Coen, E. (1999a). The TCP domain: A motif found in proteins regulating plant growth and development. *Plant. J.* **18**, 215–222.

Cubas, P., Vincent, C., and Coen, E. (1999b). An epigenetic mutation responsible for natural variation in floral symmetry. *Nature (Lond.)* **401**, 157–161.

Dahl, M., Meskiene, I., Bogre, L., Ha, D. T., Swoboda, I., Hubmann, R., Hirt, H., and Heberle-Bors, E. (1995). The D-type alfalfa cyclin gene cycMs4 complements G<sub>1</sub> cyclin-deficient yeast and is induced in the G<sub>1</sub> phase of the cell cycle. *Plant Cell* **7**, 1847–1857.

Dawe, R., and Freeling, M. (1991). Cell lineage and its consequences in higher plants. *Plant J.* **1**, 3–8.

Ding, B., Itaya, A., and Woo, Y. (1999). Plasmodesmata and cell-to-cell communication in plants. *Int. Rev. Cytol.* **190**, 251–315.

Doebley, J., Stec, A., and Hubbard, L. (1997). The evolution of apical dominance in maize. *Nature (Lond.)* **386**, 485–488.

Doonan, J., and Robert, P. (1997). Conserved and novel regulators of the plant cell cycle. *Curr. Opin. Cell Biol.* **9**, 824–830.

Drake, G. A., and Carr, D. J. (1978). Plasmodesmata, tropisms and auxin transport. *J. Exp. Bot.* **29**, 1309–1318.

Elliott, R. C., Betzner, A. S., Huttner, E., Oakes, M. P., Tucker, W. Q., Gerentes, D., Perez, P., and Smyth, D. R. (1996). AINTEGUMENTA, an APETALA2-like gene of *Arabidopsis* with pleiotropic roles in ovule development and floral organ growth. *Plant Cell* **8**, 155–168.

Emons, A. M., and Kieft, H. (1994). Winding threads around plant cells. *Protoplasma* **180**, 59–69.

Estruch, J. J., Chiriqui, D., Grossmann, K., Schell, J., and Spena, A. (1991). The plant oncogene rolC is responsible for the release of cytokinins from glucoside conjugates. *EMBO J.* **10**(10), 2889–2895.

Featherstone, D. R., Cove, D. J., and Ashton, N. W. (1990). Genetic analysis by somatic hybridization of cytokinin overproducing developmental mutants of the moss *Physcomitrella patens*. *Mol. Gen. Genet.* **222**, 217–224.

Ferreira, P. C., Hemerly, A. S., Villarroel, R., Van Montagu, M., and Inze, D. (1991). The *Arabidopsis* functional homolog of the p34cdc2 protein kinase. *Plant Cell* **3**, 531–540.

Fleming, A. J., McQueen-Mason, S., Mandel, T., and Kuhlemeier, C. (1997). Induction of leaf primordia by the cell wall protein expansin. *Science* **276**, 1415–1418.

Fletcher, J. C., Brand, U., Running, M. P., Simon, R., and Meyerowitz, E. M. (1999). Signaling of cell fate decisions by CLAVATA3 in *Arabidopsis* shoot meristems. *Science* **283**, 1911–1914.

Foard, D. E. (1971). The initial protrusion of a leaf primordium can form without concurrent periclinal cell divisions. *Can. J. Bot.* **49**, 694–702.

Robert, P. R., Coen, E. S., Murphy, G. J., and Doonan, J. H. (1994). Patterns of cell division revealed by transcriptional regulation of genes during the cell cycle in plants. *EMBO J.* **13**, 616–624.

Robert, P. R., Gaudin, V., Lunness, P., Coen, E. S., and Doonan, J. H. (1996). Distinct classes of cdc2-related genes are differentially expressed during the cell division cycle in plants. *Plant Cell* **8**, 1465–1476.

Foster, A. S. (1938). Structure and growth of the shoot apex in *Ginkgo biloba*. *Bull. Torrey Botan. Club* **65**, 531–566.

Gälweiler, L., Guan, C., Wisman, E., Mendgen, K., Yephremov, A., and Palme, K. (1998). Regulation of polar auxin transport by AtPIN1 in *Arabidopsis* vascular tissue. *Science* **282**, 2226–2230.

Gaudin, V., Lumess, P., Robert, P., Towers, M., Riou-Khamlichi, C., Murray, J., Coen, E., and Doonan, J. (2000). The expression of D-cyclin genes define distinct developmental zones in *Antirrhinum* apical meristems and is locally regulated by the cyclin D1 gene. *Plant Physiol.* **122**, 1137–1148.

Geng, Y., Whoriskey, W., Park, M. Y., Bronson, R. T., Medema, R. H., Li, T., Weinberg, R. A., and Sicinski, P. (1999). Rescue of cyclin D1 deficiency by cyclin E. *Cell* **97**, 767–777.

Granger, C. L., Callos, J. D., and Medford, J. I. (1996). Isolation of an *Arabidopsis* homologue of the maize homeobox Knotted-1 gene. *Plant Mol. Biol.* **31**, 373–378.

Green, P. (1976). Growth and cell pattern formation on an axis-Critique of concepts, terminology and modes of study. *Bot. Gaz.* **137**, 187–202.

Hake, S., Char, B. R., Chuck, G., Foster, T., Long, J., and Jackson, D. (1995). Homeobox genes in the functioning of plant meristems. *Philos. Trans. R. Soc. Lond. B: Biol. Sci.* **350**, 45–51.

Hemerly, A., Engler, J. D. A., Bergounioux, C., Van Montagu, M., Engler, G., Inze, D., and Ferreira, P. (1995). Dominant negative mutants of the cdc2 kinase uncouple cell division from iterative plant development. *EMBO J.* **14**, 3925–3936.

Hernandez, L., and Green, P. (1993). Transductions for the expression of structural pattern: Analysis in sunflower. *Plant Cell* **5**, 1725–1738.

Hirt, H., Mink, M., Pfossner, M., Bogre, L., Gyorgyey, J., Jonak, C., Gartner, A., Dudits, D., and Heberle-Bors, E. (1992). Alfalfa cyclins: Differential expression during the cell cycle and in plant organs. *Plant Cell* **4**, 1531–1538.

Holder, N. (1979). Positional information and pattern formation in plant morphogenesis and a mechanism for the involvement of plant hormones. *J. Theor. Biol.* **77**, 195–212.

Huntley, R., Healy, S., Freeman, D., Lavender, P., de Jager, S., Greenwood, J., Makker, J., Walker, E., Jackman, M., Xie, Q., Bannister, A. J., Kouzarides, T., Gutierrez, C., Doonan, J. H., and Murray, J. A. (1998). The maize retinoblastoma protein homologue ZmRb-1 is regulated during leaf development and displays conserved interactions with G1/S regulators and plant cyclin D (CycD) proteins. *Plant Mol. Biol.* **37**, 155–169.

Hush, J., Wu, L., John, P. C., Hepler, L. H., and Hepler, P. K. (1996). Plant mitosis promoting factor disassembles the microtubule preprophase band and accelerates prophase progression in *Tradescantia*. *Cell Biol. Int.* **20**, 275–287.

Ingram, G. C., Goodrich, J., Wilkinson, M. D., Simon, R., Haughn, G. W., and Coen, E. S. (1995). Parallels between *UNUSUAL FLORAL ORGANS* and *FIMBRIATA*, genes controlling flower development in *Arabidopsis* and *Antirrhinum*. *Plant Cell* **7**, 1501–1510.

Ingram, G. C., Doyle, S., Carpenter, R., Schultz, E. A., Simon, R., and Coen, E. S. (1997). Dual role for fimbriata in regulating floral homeotic genes and cell division in *Antirrhinum*. *EMBO J.* **16**, 6521–6534.

Irish, V. F. (1999). Patterning the flower. *Dev. Biol.* **209**, 211–220.

Ito, M., Marie-Claire, C., Sakabe, M., Ohno, T., Hata, S., Kouchi, H., Hashimoto, J., Fukuda, H., Komamine, A., and Watanabe, A. (1997). Cell-cycle-regulated transcription of A- and B-type plant cyclin genes in synchronous cultures. *Plant J.* **11**, 983–992.

Ito, M., Iwase, M., Kodama, H., Lavisne, P., Komamine, A., Nishihama, R., Machida, Y., and Watanabe, A. (1998). A novel *cis*-acting element in promoters of plant B-type cyclin genes activates M phase-specific transcription. *Plant Cell* **10**, 331–341.

Jeong, S., Trotochaud, A., and Clark, S. (1999). The *Arabidopsis CLAVATA2* gene encodes a receptor-like protein required for the stability of the *CLAVATA1* receptor-like kinase. *Plant Cell* **11**, 1925–1934.

John, P. C. (1996). The plant cell cycle: Conserved and unique features in mitotic control. *Prog. Cell Cycle Res.* **2**, 59–72.

Joubes, J., Chevalier, C., Dudits, D., Heberle-Bors, E., Inzé, D., Umeda, M., and Renaudin, J. P. (2000). CDK-related protein-kinases in plants. *Plant Mol. Biol.* **43**, 607–620.

Kaplan, D. R., and Hagemann, W. (1991). The relationship of cell and organism in vascular plants: Are cells the building blocks of plant form? *Bioscience* **41**, 693–703.

Kappen, C. (2000). Analysis of a complete homeobox gene repertoire: Implications for the evolution of diversity. *Proc. Natl. Acad. Sci. USA* **97**, 4481–4486.

Kayes, J. M., and Clark, S. E. (1998). *CLAVATA2*, a regulator of meristem and organ development in *Arabidopsis*. *Development* **125**, 3843–3851.

Kerstetter, R. A., Laudencia-Chingcuanco, D., Smith, L. G., and Hake, S. (1997). Loss-of-function mutations in the maize homeobox gene, knotted1, are defective in shoot meristem maintenance. *Development* **124**, 3045–3054.

Klucher, K. M., Chow, H., Reiser, L., and Fischer, R. L. (1996). The *AINTEGUMENTA* gene of *Arabidopsis* required for ovule and female gametophyte development is related to the floral homeotic gene *APETALA2*. *Plant Cell* **8**, 137–153.

Kosugi, S., and Ohashi, Y. (1997). PCF1 and PCF2 specifically bind to *cis* elements in the rice proliferating cell nuclear antigen gene. *Plant Cell* **9**, 1607–1619.

Krizek, B. A. (1999). Ectopic expression of *AINTEGUMENTA* in *Arabidopsis* plants results in increased growth of floral organs. *Dev. Genet.* **25**, 224–236.

Kutschera, U. (1991). Regulation of cell expansion. In “The Cytoskeletal Basis of Plant Growth and Form,” (C. W. Lloyd, ed.), Academic Press, London.

Laufs, P., Dockx, J., Kronenberger, J., and Traas, J. (1998a). *MGOUN1* and *MGOUN2*: Two genes required for primordium initiation at the shoot apical and floral meristems in *Arabidopsis thaliana*. *Development* **125**, 1253–1260.

Laufs, P., Grandjean, O., Jonak, C., Kieu, K., and Traas, J. (1998b). Cellular parameters of the shoot apical meristem in *Arabidopsis*. *Plant Cell* **10**, 1375–1390.

Laux, T., Mayer, K. F., Berger, J., and Jurgens, G. (1996). The *WUSCHEL* gene is required for shoot and floral meristem integrity in *Arabidopsis*. *Development* **122**, 87–96.

Ledbetter, M. C., and Porter, K. (1963). A “microtubule” in plant cell fine structure. *J. Cell Biol.* **19**, 239–250.

Lee, I., Wolfe, D. S., Nilsson, O., and Weigel, D. (1997). A *LEAFY* co-regulator encoded by *UNUSUAL FLORAL ORGANS*. *Curr. Biol.* **7**, 95–104.

Levin, J. Z., and Meyerowitz, E. M. (1995). *UFO*: An *Arabidopsis* gene involved in both floral meristem and floral organ development. *Plant Cell* **7**, 529–548.

Li, Y., Hagen, G., and Guilfoyle, T. J. (1992). Altered morphology in transgenic tobacco plants that overproduce cytokinins in specific tissues and organs. *Dev. Biol.* **153**, 386–395.

Lincoln, C., Long, J., Yamaguchi, J., Serikawa, K., and Hake, S. (1994). A *knotted1*-like homeobox gene in *Arabidopsis* is expressed in the vegetative meristem and dramatically alters leaf morphology when overexpressed in transgenic plants. *Plant Cell* **6**, 1859–1876.

Lloyd, C. W. (1991). “The Cytoskeletal Basis of Plant Growth and Form.” Academic Press, London.

Long, J. A., and Barton, M. K. (1998). The development of apical embryonic pattern in *Arabidopsis*. *Development* **125**, 3027–3035.

Long, J. A., Moan, E. I., Medford, J. I., and Barton, M. K. (1996). A member of the *KNOTTED* class of homeodomain proteins encoded by the *STM* gene of *Arabidopsis*. *Nature (Lond.)* **379**, 66–69.

Lu, P., Porat, R., Nadeau, J. A., and O’Neill, S. D. (1996). Identification of a meristem L1 layer-specific gene in *Arabidopsis* that is expressed during embryonic pattern formation and defines a new class of homeobox genes. *Plant Cell* **8**, 2155–2168.

Lucas, W. J., Bouche-Pillon, S., Jackson, D. P., Nguyen, L., Baker, L., Ding, B., and Hake, S. (1995). Selective trafficking of *KNOTTED1* homeodomain protein and its mRNA through plasmodesmata. *Science* **270**, 1980–1983.

Liu, H., Wang, H., Delong, C., Fowke, L. C., Crosby, W. L., and Fobert, P. R. (2000). The *Arabidopsis* Cdc2a-interacting protein ICK2 is structurally related to ICK1 and is a potent inhibitor of cyclin-dependent kinase activity *in vitro*. *Plant J.* **21**, 379–385.

Luo, D., Carpenter, R., Vincent, C., Copsey, L., and Coen, E. (1996). Origin of floral asymmetry in *Antirrhinum*. *Nature (Lond.)* **383**, 794–799.

Lyndon, R. F. (1999). “The Shoot Apical Meristem.” Cambridge University Press, Cambridge.

Magyar, Z., Meszaros, T., Miskolczi, P., Deak, M., Feher, A., Brown, S., Kondorosi, E., Athanasiadis, A., Pongor, S., Bilgin, M., Bako, L., Koncz, C., and Dudits, D. (1997). Cell cycle phase specificity of putative cyclin-dependent kinase variants in synchronized alfalfa cells. *Plant Cell* **9**, 223–235.

Mayer, K. F., Schoof, H., Haecker, A., Lenhard, M., Jurgens, G., and Laux, T. (1998). Role of *WUSCHEL* in regulating stem cell fate in the *Arabidopsis* shoot meristem. *Cell* **95**, 805–815.

McCabe, P., Valentine, T., Forsberg, L., and Penell, R. (1997). Soluble signals from cells identified at the cell wall establish a developmental pathway in carrot. *Plant Cell* **9**, 2225–2231.

McClinton, R. S., and Sung, Z. R. (1997). Organization of cortical microtubules at the plasma membrane in *Arabidopsis*. *Planta* **201**, 252–260.

Meicenheimer, R. D. (1981). Changes in *Epilobium phyllotaxy* induced by N-1-naphthylphthalamic acid and alpha-4-chlorophenoxyisobutyric acid. *Am. J. Bot.* **68**, 1139–1154.

Meyerowitz, E. M. (1997). Control of cell division patterns in developing shoots and flowers of *Arabidopsis thaliana*. *Cold Spring Harb. Symp. Quant. Biol.* **62**, 369–375.

Miao, G. H., Hong, Z., and Verma, D. P. (1993). Two functional soybean genes encoding p34cdc2 protein kinases are regulated by different plant developmental pathways. *Proc. Natl. Acad. Sci. USA* **90**, 943–947.

Mironov, V., Van Montagu, M., and Inze, D. (1997). Regulation of cell division in plants: An *Arabidopsis* perspective. *Prog. Cell Cycle Res.* **3**, 29–41.

Mizukami, Y., and Fischer, R. L. (2000). Plant organ size control: *AINTEGUMENTA* regulates growth and cell numbers during organogenesis. *Proc. Natl. Acad. Sci. USA* **97**, 942–947.

Morgan, D. O. (1995). Principles of CDK regulation. *Nature (Lond.)* **374**, 131–134.

Mulligan, G., and Jacks, T. (1998). The retinoblastoma gene family—Cousins with overlapping interests. *Trends genet.* **14**, 223–229.

Nakagami, H., Sekine, M., Murakami, H., and Shinmyo, A. (1999). Tobacco retinoblastoma-related protein phosphorylated by a distinct cyclin-dependent kinase complex with Cdc2/cyclin D *in vitro*. *Plant J.* **18**, 243–252.

Ng, M., and Yanofsky, M. F. (2000). Three ways to learn the ABCs. *Curr. Opin. Plant Biol.* **3**, 47–52.

Nicol, F., and Höfte, H. (1998). Plant cell expansion: Scaling the wall. *Curr. Opin. Plant Biol.* **1**, 12–17.

Nicol, F., His, I., Jauneau, A., Vernhettes, S., Canut, H., and Höfte, H. (1998). A plasma membrane-bound putative endo-1,4- $\beta$ -D-glucanase is required for normal cell wall assembly and cell elongation in *Arabidopsis*. *EMBO J.* **17**, 5563–5576.

Okada, K., Ueda, J., Komaki, M. K., Bell, C. J., and Shimura, Y. (1991). Requirement of the auxin polar transport system in early stages of *Arabidopsis* floral bud formation. *Plant Cell* **3**, 677–684.

Ori, N., Juarez, M. T., Jackson, D., Yamaguchi, J., Banowetz, G. M., and Hake, S. (1999). Leaf senescence is delayed in tobacco plants expressing the maize homeobox gene knotted1 under the control of a senescence-activated promoter. *Plant Cell* **11**, 1073–1080.

Parcy, F., Nilsson, O., Busch, M. A., Lee, I., and Weigel, D. (1998). A genetic framework for floral patterning. *Nature (Lond.)* **395**, 561–566.

Perbal, M. C., Haughn, G., Saedler, H., and Schwarz-Sommer, Z. (1996). Non-cell-autonomous function of the *Antirrhinum* floral homeotic proteins DEFICIENS and GLOBOSA is exerted by their polar cell-to-cell trafficking. *Development* **122**, 3433–3441.

Pereira, M. F., and Dale, J. (1982). Effects of 2,4-dichlorophenoxyacetic acid on shoot apex development of *Phaseolus vulgaris*. *Z. Plantzenphysiol.* **107**, 169–177.

Porceddu, A., De Veylder, L., Hayles, J., Van Montagu, M., Inze, D., and Mironov, A. V. (1999). Mutational analysis of two *Arabidopsis thaliana* cyclin-dependent kinases in fission yeast. *FEBS Lett.* **446**, 182–188.

Ramirez-Parra, E., Xie, Q., Boniotti, M. B., and Gutierrez, C. (1999). The cloning of plant E2F, a retinoblastoma-binding protein, reveals unique and conserved features with animal G(1)/S regulators. *Nucleic Acids Res.* **27**, 3527–3533.

Reinhardt, D., Wittwer, F., Mandel, T., and Kuhlemeier, C. (1998). Localized upregulation of a new expansin gene predicts the site of leaf formation in the tomato meristem. *Plant Cell* **10**, 1427–1437.

Reinhardt, D., Mandel, T., and Kuhlemeier, C. (2000). Auxin regulates the initiation and radial position of plant lateral organs. *Plant Cell* **12**(4), 507–518.

Renaudin, J. P., Doonan, J., Freeman, D., Hashimoto, J., Hirt, H., Inzé, D., Jacobs, T., Kouchi, H., Rouzé, P., Sauter, M., Savoure, A., Sorrell, D., Sundaresan, V., and Murray, J. (1996). Plant cyclins: A unified nomenclature for plant A-, B- and D-Type cyclins based on sequence organisation. *Plant Mol. Biol.* **32**, 1003–1018.

Renaudin, J. P., Savouré, A., Philippe, H., Van Montagu, M., Inzé, D., and Rouzé, P. (1998). Characterization and classification of plant cyclin sequences related to A- and B-type cyclins. In “Plant Cell Division,” (D. Francis, D. Dudit, and D. Inzé, Eds.), Portland Press, London.

Rinne, P. L., and van der Schoot, C. (1998). Symplasmic fields in the tunica of the shoot apical meristem coordinate morphogenetic events. *Development* **125**, 1477–1485.

Riou-Khamlichi, C., Huntley, R., Jacqmar, A., and Murray, J. A. (1999). Cytokinin activation of *Arabidopsis* cell division through a D-type cyclin. *Science* **283**, 1541–1544.

Roe, J. L., Rivin, C. J., Sessions, R. A., Feldmann, K. A., and Zambryski, P. C. (1993). The *Tousled* gene in *A. thaliana* encodes a protein kinase homolog that is required for leaf and flower development. *Cell* **75**, 939–950.

Roe, J. L., Durfee, T., Zupan, J. R., Repetti, P. P., McLean, B. G., and Zambryski, P. C. (1997a). TOUSLED is a nuclear serine/threonine protein kinase that requires a coiled-coil region for oligomerization and catalytic activity. *J. Biolog. Chem.* **272**, 5838–5845.

Roe, J. L., Nemhauser, J. L., and Zambryski, P. C. (1997b). *TOUSLED* participates in apical tissue formation during gynoecium development in *Arabidopsis*. *Plant Cell* **9**, 335–353.

Rupp, H. M., Frank, M., Werner, T., Strnad, M., and Schmülling, T. (1999). Increased steady state mRNA levels of the *STM* and *KNAT1* homeobox genes in cytokinin overproducing *Arabidopsis thaliana* indicate a role for cytokinins in the shoot apical meristem [short communication]. *Plant J.* **18**, 557–563.

Sachs, J. von (1882). "Vorlesungen über Pflanzen-physiologie." Engelmann, Leipzig.

Satiat-Jeunemaître, B. (1987). Inhibition of the helicoidal assembly of the cellulose-hemicellulose complex by 2,6-dichlorobenzonitrile (DCB). *Biol. Cell* **59**, 89–96.

Savoure, A., Feher, A., Kalo, P., Petrovics, G., Csanadi, G., Szecsi, J., Kiss, G., Brown, S., Kondorosi, A., and Kondorosi, E. (1995). Isolation of a full-length mitotic cyclin cDNA clone CycIIIMs from *Medicago sativa*: Chromosomal mapping and expression. *Plant Mol. Biol.* **27**, 1059–1070.

Schneeberger, R., Tsiantis, M., Freeling, M., and Langdale, J. A. (1998). The rough *sheath2* gene negatively regulates homeobox gene expression during maize leaf development. *Development* **125**, 2857–2865.

Schoof, H., Lenhard, M., Haecker, A., Mayer, K. F., Jurgens, G., and Laux, T. (2000). The stem cell population of *Arabidopsis* shoot meristems is maintained by a regulatory loop between the *CLAVATA* and *WUSCHEL* genes. *Cell* **100**(6), 635–644.

Sekine, M., Ito, M., Uemukai, K., Maeda, Y., Nakagami, H., and Shinmyo, A. (1999). Isolation and characterization of the E2F-like gene in plants. *FEBS Lett.* **460**(1), 117–122.

Sessions, A., Yanofsky, M., and Weigel, D. (2000). Cell–cell signalling and movement by the floral transcription factors *LEAFY* and *APETALA1*. *Science* **289**, 779–782.

Sherr, C. J. (1995). Mammalian G<sub>1</sub> cyclins and cell cycle progression. *Proc. Assoc. Am. Physicians* **107**, 181–186.

Sherr, C. J., and Roberts, J. M. (1999). CDK inhibitors: Positive and negative regulators of G<sub>1</sub>-phase progression. *Genes Dev.* **13**, 1501–1512.

Sillje, H. H., Takahashi, K., Tanaka, K., Van Houwe, G., and Nigg, E. A. (1999). Mammalian homologues of the plant *Tousled* gene code for cell-cycle-regulated kinases with maximal activities linked to ongoing DNA replication. *EMBO J.* **18**, 5691–5702.

Simon, R., Carpenter, R., Doyle, S., and Coen, E. (1994). Fimbriata controls flower development by mediating between meristem and organ identity genes. *Cell* **78**, 99–107.

Sinha, N. (1999). Leaf development in Angiosperms. *Annu. Rev. Plant Physiol. Plant Mol. Biol.* **50**, 419–446.

Sinha, N. R., Williams, R. E., and Hake, S. (1993). Overexpression of the maize homeo box gene, *KNOTTED-1*, causes a switch from determinate to indeterminate cell fates. *Genes Dev.* **7**, 787–795.

Smith, L. G. (1999). Divide and conquer: Cytokinesis in plant cells. *Curr. Opin. Plant Biol.* **2**, 447–453.

Soni, R., Carmichael, J. P., Shah, Z. H., and Murray, J. A. (1995). A family of cyclin D homologs from plants differentially controlled by growth regulators and containing the conserved retinoblastoma protein interaction motif. *Plant Cell* **7**, 85–103.

Souer, E., van Houwelingen, A., Kloos, D., Mol, J., and Koes, R. (1996). The no apical meristem gene of *Petunia* is required for pattern formation in embryos and flowers and is expressed at meristem and primordia boundaries. *Cell* **85**, 159–170.

Springer, P. S., McCombie, W. R., Sundaresan, V., and Martienssen, R. A. (1995). Gene trap tagging of *PROLIFERA*, an essential MCM2-3-5-like gene in *Arabidopsis*. *Science* **268**, 877–880.

Stals, H., Bauwens, S., Traas, J., Van Montagu, M., Engler, G., and Inze, D. (1997). Plant CDC2 is not only targeted to the pre-prophase band, but also co-localizes with the spindle, phragmoplast, and chromosomes. *FEBS Lett.* **418**, 229–234.

Stone, J. M., Trotochaud, A. E., Walker, J. C., and Clark, S. E. (1998). Control of meristem development by *CLAVATA1* receptor kinase and kinase-associated protein phosphatase interactions. *Plant Physiol.* **117**, 1217–1225.

Su, T. T., and O'Farrell, P. (1998). Size control: Cell proliferation does not equal growth. *Curr. Biol.* **8**, R687–689.

Szymkowiak, E. J., and Sussex, I. M. (1996). What chimeras can tell us about plant development. *Annu. Rev. Plant Physiol. Plant Mol. Biol.* **47**, 351–376.

Tamaoki, M., Kusaba, S., Kano-Murakami, Y., and Matsuoka, M. (1997). Ectopic expression of a tobacco homeobox gene, *NTH15*, dramatically alters leaf morphology and hormone levels in transgenic tobacco. *Plant Cell Physiol.* **38**, 917–927.

Taylor, C. (1997). Knox-on effects on leaf development. *Plant Cell* **9**, 2101–2105.

Timmermans, M. C., Hudson, A., Becraft, P. W., and Nelson, T. (1999). ROUGH SHEATH2: A Myb protein that represses knox homeobox genes in maize lateral organ primordia. *Science* **284**, 151–153.

Tjandra, H., Compton, J., and Kellogg, D. (1998). Control of mitotic events by the Cdc42 GTPase, the Clb2 cyclin and a member of the PAK kinase family. *Curr. Biol.* **8**(18), 991–1000.

Torres-Ruiz, R. A., and Jürgens, G. (1994). Mutations in the FASS gene uncouple pattern formation and morphogenesis in *Arabidopsis* development. *Development* **120**, 2967–2978.

Traas, J., and Laufs, P. (1998). Cell cycle mutants in plants: A phenotypical overview. In "Plant cell division," (D. Francis, D. Dudit, and D. Inzé, Eds.). Portland Press, London.

Traas, J. A., Braat, P., Emons, A. M., Meekes, H., and Derkx, J. (1985). Microtubules in root hairs. *J. Cell Sci.* **76**, 303–320.

Traas, J., Bellini, C., Nacry, P., Kronenberger, J., Bouchez, D., and Caboche, M. (1995). Normal differentiation patterns in plant lacking microtubular preprophase bands. *Nature (Lond.)* **375**, 676–677.

Trottochaud, A. E., Hao, T., Wu, G., Yang, Z., and Clark, S. E. (1999). The CLAVATA1 receptor-like kinase requires CLAVATA3 for its assembly into a signaling complex that includes KAPP and a Rho-related protein. *Plant Cell* **11**, 393–406.

Trottochaud, A. E., Jeong, S., and Clark, S. E. (2000). CLAVATA3, a multimeric ligand for the CLAVATA1 receptor-kinase. *Science* **289**, 613–617.

Van den Berg, C., Willemsen, V., Hage, W., Weisbeek, P., and Scheres, B. (1995). Cell fate in the *Arabidopsis* root meristem determined by directional cell signalling. *Nature (Lond.)* **378**, 62–65.

Van den Schoot, C., and Rinne, P. (1999). Networks for shoot design. *Trends Plant Sci.* **4**, 31–37.

Venglat, S. P., and Sawhney, V. K. (1996). Benzylaminopurine induces phenocopies of floral meristem and organ identity mutants in wild-type *Arabidopsis* plants. *Planta* **198**, 480–487.

Waites, R., Selvadurai, H. R., Oliver, I. R., and Hudson, A. (1998). The *PHANTASTICA* gene encodes a MYB transcription factor involved in growth and dorsoventrality of lateral organs in *Antirrhinum*. *Cell* **93**, 779–789.

Wang, H., Qi, Q., Schorr, P., Cutler, A., Crosby, W. L., and Fowke, L. C. (1998). ICK1, a cyclin-dependent protein kinase inhibitor from *Arabidopsis* thaliana interacts with both Cdc2a and CycD3, and its expression is induced by abscisic acid. *Plant J.* **15**, 501–510.

Weigel, D. (1998). From floral induction to floral shape. *Curr. Opin. Plant. Biol.* **1**(1), 55–59.

Williams-Carrier, R. E., Lie, Y. S., Hake, S., and Lemaux, P. G. (1997). Ectopic expression of the maize *kn1* gene phenocopies the Hooded mutant of barley. *Development* **124**(19), 3737–3745.

Zhang, K., Letham, D. S., and John, P. C. (1996). Cytokinin controls the cell cycle at mitosis by stimulating the tyrosine dephosphorylation and activation of p34cdc2-like H1 histone kinase. *Planta* **200**, 2–12.

# Roles of Cytoskeletal and Junctional Plaque Proteins in Nuclear Signaling

Stefan Hübner,\* David A. Jans,<sup>†</sup> and Detler Drenckhahn\*

\*Institut für Anatomie, Universität Würzburg, D-97070 Würzburg, Germany, and

<sup>†</sup>Nuclear Signaling Laboratory, Division for Biochemistry and Molecular Biology, John Curtin School of Medical Research, Canberra, ACT 2601, Australia

---

Cytoplasmic junctional plaque proteins play an important role at intercellular junctions. They link transmembrane cell adhesion molecules to components of the cytoskeleton, thereby playing an important role in the control of many cellular processes. Recent studies on the subcellular distribution of some plaque proteins have revealed that a number of these proteins are able to localize in the nucleus. This dual location indicates that in addition to promoting adhesive interactions, plaque proteins may also play a direct role in nuclear processes, and in particular in the transfer of signals from the membrane to the nucleus. Therefore, translocation of plaque proteins into the nucleus in response to extracellular signals could represent a novel and direct mechanism by which signals can be transmitted from the plasma membrane to the nucleus. This could allow cells to respond to changing environmental conditions in a rapid and efficient way. In addition, conditional sequestration of karyophilic proteins at the sites of cell–cell and cell–substratum adhesion may represent a general mechanism for the regulation of nucleocytoplasmic transport.

**KEY WORDS:** Cell junctions, Plaque proteins, Cytoskeleton, Nuclear signaling, Nuclear protein import, Nuclear localization sequence. © 2001 Academic Press.

---

## I. Introduction

Specific interactions between neighboring cells and between cells and the extracellular matrix are the basis of multicellular organization whereby individual cells are assembled into three-dimensional tissues and organs to constitute an organism. This is brought about through interactions of the extracellular domains

of various transmembrane adhesion molecules, such as cadherins and integrins, with receptors on neighboring cells or with proteins of the extracellular matrix. Adhesion molecules may be clustered at focal sites of cell-to-cell contacts (adherens junctions, desmosomes) as well as at cell-to-extracellular matrix contacts (focal contacts, hemidesmosomes). Clustering at these adhesive junctions is accomplished by a variety of adapter molecules that are involved in the linkage of adhesion molecules to components of the cytoskeleton, namely, actin filaments (adherens junctions, focal contacts) or intermediate filaments (desmosomes or hemidesmosomes). Adaptor molecules are localized in cytoplasmic densities called junctional plaques that are situated on the cytoplasmic aspects of these junctions. In this review all proteins localized within these plaques will be collectively denoted as plaque proteins. Adhesive cellular junctions are ideally placed to mediate signal transfer between the extracellular and intracellular milieus. This is mirrored by the involvement of adhesive junctions in multiple cellular processes such as cell motility, cell locomotion, cell and tumor cell growth, metastasis, programmed cell death, cell shape determination, or paracellular trafficking. Extracellular binding of adhesion molecules must be reversible to allow dynamic cellular behavior to occur. This implies that adhesion molecules, which often consist of multiple domains, are able to change their cellular activities and to carry out different junctional roles in the same cell. During the past few years, it has become clear that adhesive interactions not only mediate mechanical linkages between neighboring cells or to the extracellular matrix, but also play a novel role in signal transduction, and in particular in translocating signals directly from the functional plaques into the nucleus. The nuclear pathway bypasses more conventional signaling routes, which generally constitute cascades of activation and interaction of multiple cytoplasmic components.

Because the functional relevance of nuclear translocation of only a small subset of such plaque proteins has been investigated in detail, this review aims to discuss the potential role of plaque proteins in nuclear signaling with particular emphasis on the problem of how nuclear translocation of such proteins can be regulated. With respect to the other function of plaque proteins the reader is directed to several recent reviews dealing with the molecular diversity of plaque proteins and their role in adhesive interactions (Schmidt *et al.*, 1994; Clark and Brugge, 1995; Craig and Johnson, 1996; Citi and Cordenonsi, 1998, 1999; Hemler, 1998; Howe *et al.*, 1998; Mitic and Anderson, 1998; Stevenson and Keon, 1998; Tsukita *et al.*, 1999; Critchley, 2000).

## **II. Rules and Players Involved in Nuclear Transport**

### **A. Rules of Nuclear Protein Transport**

The traffic of macromolecules between the nucleus and the cytoplasm serves many vital cellular functions such as export of mRNA and preribosomal particles to the

cytoplasmic space and import of nuclear proteins and proteins that regulate gene transcription into the nuclear compartment. An import mechanism for nuclear proteins is required because they are synthesized in the cytoplasmic space. All transport into and out of the nucleus proceeds through the nuclear pore complex (NPC; Feldherr *et al.*, 1984). Import of macromolecules greater than 50 kDa requires specific targeting signals called nuclear localization sequences (NLSs); analogously, proteins to be exported from the nucleus need signals conferring nuclear export, or nuclear export signals (NESs). That the NPC is the sole passageway of macromolecules into and out of the nucleus is demonstrated by the fact that the NPC-binding lectin wheat germ agglutinin (WGA; Finlay *et al.*, 1987; Dabauvalle *et al.*, 1988) or antibodies against components of the NPC block nuclear protein import (Baglia and Maul, 1983; Featherstone *et al.*, 1988), as well as the export of mRNA from the nucleus.

Conventional NLSs are generally short, modular sequences of predominantly positively charged amino acid residues, defined as being necessary and sufficient for entry into the nucleus of the proteins carrying them. The best characterized NLS is that of the simian virus SV40 large tumor antigen (T-ag) comprising a single stretch of basic amino acids PKKKRKV<sup>132</sup> (Kalderon *et al.*, 1984a, 1984b; Lanford and Butel, 1984). Similar sequences are being found in a number of proteins including transcription factors and nuclear structural proteins such as lamins and histones (Jans and Hübner, 1996; Jans *et al.*, 1998). A variant of the T-ag-like NLS (tNLS) is found in nucleoplasmin (Robbins *et al.*, 1991). This NLS consists of two clusters of basic amino acid residues separated by a 10- to 12-amino-acid spacer and is referred to as a bipartite NLS (bNLS). The third less well characterized class of NLS is made up of NLSs resembling those of the yeast homeodomain-containing protein Mata2 (Hall *et al.*, 1984, 1990), where charged/polar residues are interspersed with nonpolar residues. All three classes of NLS are specifically recognized by the  $\alpha/\beta$ -importin heterodimer during the first step of nuclear transport, as has been shown directly for the importins from several species (Hicks *et al.*, 1996; Efthymiadis *et al.*, 1997; Smith *et al.*, 1997; Hu and Jans, 1999; Hübner *et al.*, 1999).

Apart from conventional NLS-dependent nuclear import, nuclear translocation can also be achieved through distinct nuclear targeting sequences recognized by other members of the importin superfamily (Weis, 1998; Wozniak *et al.*, 1998; and see below). Nuclear import of the heterologous nuclear RNA binding protein (hnRNP A1), for example, is mediated by a 38-amino-acid-long sequence, M9, comprising mostly hydrophobic residues. This M9 sequence is recognized by transportin (importin  $\beta$ 2; Pollard *et al.*, 1996). Other nuclear import signals include the B1B domain of the ribosomal protein rpL23a (Jäkel and Görlich, 1998), which can be recognized by four different importin  $\beta$  homologs including importins  $\beta$ 1,  $\beta$ 2, and  $\beta$ 3 (Pse1p), and amino acids 1–41 of ribosomal protein rpL25 (Rout *et al.*, 1997; Schlenstedt *et al.*, 1997), which can be bound by either importin  $\beta$ 3 or  $\beta$ 4. Leucine-rich NESs are recognized by yet another importin  $\beta$  homolog called exportin (Crm1p; Fornerod *et al.*, 1997; Fukuda *et al.*, 1997; Stade *et al.*, 1997).

Lack of a nuclear transport signal does not necessarily preclude passage through the NPC even for proteins with a molecular weight above the NPC diffusion barrier (>50 kDa), whereby nuclear localization can occur through association with NLS-bearing proteins and cotransport into the nucleus (“piggyback” transport; Tsuneoka *et al.*, 1986; Zhao and Padmanabhan, 1988). This appears to be the case for the subunits of the mammalian pancreas-specific transcription factor PTF1, for example, which require a third 75-kDa glycoprotein for nuclear localization (Sommer *et al.*, 1991), and for the receptor subunits of interleukin-5 (IL-5), which can be cotargeted to the nucleus through association with IL-5 which contains a functional NLS (Jans *et al.*, 1997). Cotransport into the nucleus has also been shown for the plaque proteins  $\beta$ -catenin (Behrens *et al.*, 1996; Huber *et al.*, 1996) and vinculin (Simcha *et al.*, 1998).

## B. Players Mediating Nuclear Transport

Dissection of the individual steps of nuclear protein transport in mammalian cells was made possible through the reconstitution of NLS-dependent nuclear protein import *in vitro* using detergent-permeabilized cells (Adam *et al.*, 1990). It was found that protein import occurs in at least two discrete steps: energy independent docking of the NLS-bearing protein/translocation complex at the NPC, followed by energy- and temperature-dependent translocation into the nucleus. The first factor identified as being required for nuclear protein import was the monomeric guanine-nucleotide binding protein Ran (Melchior *et al.*, 1993; Moore and Blobel, 1993). The second import factor was the NLS-binding receptor importin  $\alpha$ , which was identified in 1994 (Görlich *et al.*, 1994). The role of importin  $\alpha$  to interact with importin  $\beta$  to dock NLS-containing transport substrates at the NPC was established shortly afterward (Chi *et al.*, 1995; Görlich *et al.*, 1995; Imamoto *et al.*, 1995). Both importin  $\alpha$  and  $\beta$  contain a series of structurally similar amino acid repeats. In the case of importin  $\alpha$ , it contains a central domain composed of 8 approximately 40-amino-acid armadillo-like (Arm) repeats (analogous to the *Drosophila*  $\beta$ -catenin homolog *Armadillo*), whereas importin  $\beta$  contains 14 tandemly arranged HEAT repeats (the acronym is based on proteins in which these repeats were originally identified). Both Arm repeats and HEAT motifs mediate protein–protein interactions, being responsible for NLS recognition in the case of importin  $\alpha$  (Conti *et al.*, 1998), and for binding to NPC components and Ran in the case of importin  $\beta$ . In addition to the central Arm repeats, importin  $\alpha$  possesses an approximately 50-amino-acid *N*-terminal domain (the importin  $\beta$  binding (IBB) domain; Görlich *et al.*, 1996a) responsible for interaction with importin  $\beta$ , and a carboxy-terminal domain involved in binding the importin  $\beta$  homolog CAS (cellular apoptosis susceptibility gene; Kutay *et al.*, 1997; Herold *et al.*, 1998).

The HEAT repeats of importin  $\beta$  represent a binding interface for a variety of different proteins, one of which is importin  $\alpha$  (via the IBB domain) (Cingolani *et al.*,

1999). Importin  $\beta$  plays a central role in nuclear import by mediating both docking (binds directly to the NPC) and translocation through the NPC (via indirect interaction with RanGDP). NTF2 (Moore and Blobel, 1994; Paschal and Gerace, 1995), a Ran interacting factor (which also mediates nuclear import of Ran; Ribbeck *et al.*, 1998; Smith *et al.*, 1998), and the Ran binding protein, RanBP1 (Bischoff and Ponstingl, 1991), appear to be important for stabilization of the importin  $\alpha/\beta$ -substrate complex during NPC translocation. RanGTP binding to importin  $\beta$  induces disassembly of the transport complex on the nucleoplasmic side of the NPC (Rexach and Blobel, 1995; Chi *et al.*, 1996; Görlich *et al.*, 1996b; Izaurrealde *et al.*, 1997). Both importin subunits are recycled back to the cytoplasm as individual subunits to be available for the next round of nuclear import. Importin  $\alpha$  is exported specifically by CAS acting cooperatively with RanGTP (Kutay *et al.*, 1997; Herold *et al.*, 1998). Importin  $\beta$  is presumed to exit the nucleus together with RanGTP, which, once in the cytoplasm, is converted to RanGDP and dissociates from importin  $\beta$ . The directionality of importin-dependent nuclear protein import is presumed to be determined by differences in the subcellular localization of the cytosolic Ran GTPase activating protein RanGAP1 (Hopper *et al.*, 1990; Matunis *et al.*, 1996; Mahajan *et al.*, 1997) and chromatin-bound nucleotide exchange factor RCC1 (Ohtsubo *et al.*, 1989; Bischoff and Ponstingl, 1991). The combined activities ensure a predominance of RanGDP in the cytoplasm and RanGTP in the nucleus.

As mentioned above, signal-mediated nuclear protein transport is not carried out exclusively by the  $\alpha/\beta$ -importin heterodimer, but is also mediated by a variety of importin  $\beta$  isoforms. Importin  $\beta$  itself, for example, appears to be able to function in the absence of importin  $\alpha$  to bind targeting sequences present in transport substrates such as the T-cell protein tyrosine phosphatase (TCPTP; Tiganis *et al.*, 1997), the human immunodeficiency virus (HIV-1) Rev protein (Truant and Cullen, 1999), and parathyroid hormone related protein (PTHrP; Lam *et al.*, 1999a), as well as dock them at the NPC, and interact with Ran to mediate translocation into the nucleus. In addition to importin  $\beta$  (importin  $\beta$ 1), there are at least 12 different importin  $\beta$  homologs in eukaryotic cells (Pemberton *et al.*, 1998; Wozniak *et al.*, 1998) with specific transport roles for particular classes of proteins. Importin  $\beta$ 4 (Yrb4p) mediates the import of ribosomal proteins into the nucleus (Schlenstedt *et al.*, 1997), for example, as can importin  $\beta$ 3 (Pse1p/RanBP5) (Yaseen and Blobel, 1997; Jäkel and Görlich, 1998), Sxm1p (Kap108p; Rosenblum *et al.*, 1997) and importin 7 (RanBP7; Jäkel and Görlich, 1998). The mitogen-activated protein kinase (MAPK) HOG1 (Ferrigno *et al.*, 1998) and TFIIs (Albertini *et al.*, 1998) appear to be transported to the nucleus through Nmd5p, and the transcription factor Pho4 by importin  $\beta$ 3 (Kaffman *et al.*, 1998b; Komeili and O'Shea, 1999). Importin  $\beta$ 2 (transportin) mediates the nuclear import and Mtr10p (Kap 111p) the nuclear export of mRNA-binding proteins (Bonifaci *et al.*, 1997; Siomi *et al.*, 1997). A heterodimer of importin  $\beta$ 1/importin 7 is purported to mediate nuclear import of linker histone H1 variants (Jäkel *et al.*, 1999). As already mentioned, exportin (Crm1p/Xpo1p) and CAS (Cse1p) mediate the nuclear export of leucine-rich

NES-containing proteins and importin  $\alpha$ , respectively, whereas exportin-t and Msn5p (Los1p) are responsible for the nuclear export of tRNA and Pho4, respectively (Kaffman *et al.*, 1998a).

### C. Regulation of Nuclear Transport

All nuclear proteins are translated in the cytoplasm. Several of these proteins are involved in gene regulation and transcription. One way to control the activity of these proteins is by tight regulation of their nuclear import. The regulation of NLS activity in response to activation of a signaling pathway can lead to precisely scheduled nuclear import of molecules such as kinases and transcription factors (Jans and Hübner, 1996). Specific mechanisms to regulate nuclear protein import involve the modulation of NLS accessibility to their importin binding partners (Jans *et al.*, 1998), these mechanisms thus constituting a step of nuclear transport additional to and prior to those of docking at the NPC and nuclear translocation (Jans and Hübner, 1996; Jans *et al.*, 1998).

One mechanism to modulate nuclear transport is to prevent the recognition of specific targeting sequences through masking by heterologous molecules. The best characterized NLS-masking protein is I- $\kappa$ B, which binds specifically to the NLS of the NF- $\kappa$ B p65 subunit (RELA). Recent crystal structural data for I- $\kappa$ B $\alpha$  complexed to NF- $\kappa$ B (Huxford *et al.*, 1998) support the idea that the NLS of the NF- $\kappa$ B p65 subunit is rendered inaccessible by I- $\kappa$ B $\alpha$ . Complex regulation including phosphorylation and proteolytic degradation (Jans and Hübner, 1996; Huxford *et al.*, 1998) is required to break the complex of p65/I- $\kappa$ B $\alpha$ , which is a prerequisite for the p65 NLS being recognized by the cellular nuclear import machinery. The myoD repressor inhibitory protein I-mf appears to function analogously to I- $\kappa$ B; it causes the cytoplasmic retention of myoD by masking the myoD NLS (Chen *et al.*, 1996).

Intramolecular NLS masking appears to be the mechanism by which nuclear import of the NF- $\kappa$ B p50 precursor, p105, is regulated, whereby the ankyrin repeat-containing p105 C terminus masks the NLS (Henkel *et al.*, 1992). Proteolysis of the p105 C terminus to generate NF- $\kappa$ B p50 unmasks the NLS and permits nuclear translocation, in a very similar fashion to unmasking of the NF- $\kappa$ B p65 NLS by dissociation from I- $\kappa$ B (see above). Other proteins for which specific proteolytic processing appears to be the mechanism of regulation of nuclear import include members of the family of Notch-1 ligand-activated transmembrane proteins (Lecourtois and Schweiguth, 1998; Schroeter *et al.*, 1998; Struhl and Adachi, 1998) and the sterol regulatory-element-binding protein SREBP, which in the unstimulated state is a membrane-docked transcription factor (Brown and Goldstein, 1997).

Ca<sup>2+</sup>/calcineurin-mediated dephosphorylation at multiple sites to unmask NLSs has been purported to be involved in nuclear import of the transcription factor NF-AT (Beals *et al.*, 1997a), whereas specific phosphorylation of NF-AT enhances

nuclear export mediated by Crm1p (Beals *et al.*, 1997b). Recent studies, however, indicate that rather than playing an NLS unmasking role through dephosphorylation, calcineurin's principal role in the case of NF-AT4 may be to mask NESs within the NF-AT4 N terminus (Zhu and McKeon, 1999). In particular, calcineurin binds NF-AT4 amino acids 100–126, thereby preventing binding of Crm1p (Zhu and McKeon, 1999). Thus, cellular signals triggering NF-AT4 nuclear translocation primarily appear to effect masking of the Crm1p-binding site on NF-AT4, which leads to nuclear accumulation by prevention of nuclear export.

Another way to regulate the nuclear transport process is to directly modulate target sequence recognition by phosphorylation. The best examples of this type of regulation are the NLSs of T-ag and the *Drosophila* morphogen Dorsal. Binding of these NLSs to importin  $\alpha/\beta$  is directly enhanced by phosphorylation sites for CK2 (protein kinase CK2) and dsDNA-PK (double-stranded DNA-dependent protein kinase), and PK-A (cAMP-dependent protein kinase), respectively (Hübner *et al.*, 1997; Xiao *et al.*, 1997; Briggs *et al.*, 1998). In the case of T-ag, the synergistically acting CK2/dsDNA-PK sites N terminal to the NLS combine to increase the affinity of NLS recognition by importin  $\alpha/\beta$  about 100-fold; that this is important with respect to the nuclear import efficiency is indicated by the fact that proteins lacking the CK2 site in particular accumulate in the nucleus at about a 50-fold slower rate. In the case of Dorsal (Briggs *et al.*, 1998), the presence or absence of a functional PK-A site 22 amino acids N terminal to the NLS corresponds to about a 7-fold difference in binding affinity and to a marked difference in transport efficiency. A lack of the PK-A site is lethal to development of *Drosophila* embryos.

In the case of the yeast transcription factor Pho4, which is required for phosphate starvation-specific gene expression, the precise regulation of subcellular localization is through phosphorylation at three different sites modulating recognition by either of the importin  $\beta$  homologs importin  $\beta$ 3 (Pse1p) and Msn5p, which are responsible for import and export, respectively (Kaffman *et al.*, 1998a, 1998b; Komeili and O'Shea, 1999). Phosphorylation at Ser<sup>152</sup> within the Pho4 NLS (SANKVTKNKSNSSPYLNKRKGKPGPDS<sup>166</sup>) prevents binding by importin  $\beta$ 3, whereas phosphorylation at Ser<sup>114</sup> and Ser<sup>128</sup> is absolutely essential for the binding of Msn5p in the presence of Ran in the GTP-bound form (Komeili and O'Shea, 1999). Pho4 thus has specific nuclear import and export targeting sequences, which are recognized by distinct importins, with the affinity of the respective interactions being regulated by differential phosphorylation in response to extracellular signals.

Another mechanism of regulation of signal-dependent nuclear transport (not related to masking of targeting sequences) is cytoplasmic retention, by anchorage of a nuclear localizing protein in the cytoplasm by binding to a "cytoplasmic retention factor." Examples include the glucocorticoid and dioxin (aryl hydrocarbon) receptors, both of which, in the absence of ligand, are retained in the cytoplasm by the 90-kDa heat shock protein HSP90 (McGuire *et al.*, 1995; Picard *et al.*, 1988). Cytoplasmic retention mediated by specific cytoplasmic retention domains has been described for cyclin B1 (Pines and Hunter, 1994), the *Xenopus* protein

xnf7 (*Xenopus* nuclear factor 7; Li *et al.*, 1994), and the yeast bZIP-containing TF yAP1 (Kuge *et al.*, 1997).

Another possibility to regulate nuclear protein transport is by inducing specific degradation, thereby down-regulating the level of the protein to be transported into the nucleus. This appears to be the case for nonjunctional, cytoplasmic  $\beta$ -catenin (see below). Alternative splicing is also a means through which subcellular localization can be effected. This has been shown for nuclear variants of members of the protein 4.1 family (De Cácer *et al.*, 1995; Krauss *et al.*, 1997; Lallena and Correas, 1997), the polypeptide ligands platelet derived growth factor and fibroblast growth factors (Jans and Jans, 1994; Jans and Hassan, 1998), nuclear isoforms of the multifunctional calmodulin-dependent protein kinase (CaMPK)  $\gamma$ B (Srinivasan *et al.*, 1994), and low molecular weight (LMW) isoforms of microtubule associated protein-2 (MAP2; Loveland *et al.*, 1999).

### **III. Roles of Plaque Proteins**

#### **A. Classical Role of Plaque at Adhesive Junctions**

The specificity of adhesive junctions is determined by the composition of transmembrane adhesion molecules. These are associated with a variety of different plaque proteins. In all cases, plaque proteins function as direct or indirect linker molecules anchoring the cytoplasmic domains of the adhesion molecules to the polymeric actin or intermediate filament system, thereby determining the overall cellular architecture. Cytoskeletal linkage is achieved through multidomain structure of most plaque proteins, which enables them to associate simultaneously with the cytoplasmic tail of adhesion molecules and with cytoskeletal filaments, either directly or via other plaque proteins. Adhesive intercellular junctions can be considered dynamic structures underlying continuous changes during the cellular life cycle.

#### **B. Roles of Plaque Proteins in Nuclear Signaling**

##### **1. Nuclear Signaling by Plaque Proteins of Adherens Junctions**

Adhesion at adherens junctions is mediated by  $\text{Ca}^{2+}$ -dependent adhesion molecules, the cadherins. Interaction of cadherins with members of the catenin family ( $\alpha$ -,  $\beta$ -catenin, plakoglobin, and p120<sup>ctn</sup>—formerly p120<sup>cas</sup>) occurs through the carboxy-terminal cytoplasmic domain of cadherins.  $\beta$ -Catenin and plakoglobin bind directly to the cytoplasmic domain of cadherins and form a complex with  $\alpha$ -catenin that binds directly or indirectly, via  $\alpha$ -actinin or vinculin, to actin

filaments.  $\beta$ -Catenin is associated with adherens junctions but may also occur in the cytosol and the nucleus.  $\beta$ -Catenin binds to transcription factors of the lymphoid enhancer binding factor (LEF)/T-cell specific factor (TCF) family, and is a substrate for several important tyrosine kinases. It is reasonable to assume therefore that its nuclear translocation may play an important role in certain aspects of signaling between the plasma membrane and the nucleus.  $\beta$ -Catenin is homologous to plakoglobin and p120<sup>ctn</sup>, all of which belong to the *Armadillo* protein family, whose members are distinguished by Arm repeats. Most of these members (see Table I) have also been found within the nucleus, suggesting a possible role for these proteins in nuclear signaling. However, although structurally homologous to each other they differ markedly with respect to interacting partners and their ability to translocate into the nucleus. Figure 1 (and see below) summarizes some of the pathways by which plaque proteins of adherens junctions can be translocated to the nucleus.

**a.  $\beta$ -Catenin**  $\beta$ -Catenin is the best studied example of a plaque protein that is found in different cellular compartments and exerts different functions related to the particular subcellular localization. On one hand, it mediates the physical link between the cytoplasmic domain of cadherins and actin filaments through the adaptor protein  $\alpha$ -catenin (Rimm *et al.*, 1995), the  $\alpha$ -catenin– $\alpha$ -actinin complex (Knudsen *et al.*, 1995) or the  $\alpha$ -catenin–vinculin complex (Hazan *et al.*, 1997; Weiss *et al.*, 1998). On the other hand, it transmits signals to the nucleus in response to certain developmental processes, e.g., as an integral part of the Wnt signaling pathway. This involves association of secreted Wnt growth factors with members of the family of Frizzled transmembrane receptors.

Cytosolic levels of  $\beta$ -catenin are normally down-regulated either through phosphorylation of  $\beta$ -catenin by glycogen synthase kinase 3 $\beta$  (GSK 3 $\beta$ ; Yost *et al.*, 1996) and subsequent degradation by the ubiquitin-proteasome system (Aberle *et al.*, 1997; Orford *et al.*, 1997), or through recruitment of  $\beta$ -catenin to adherens junctions. The proteins with which extrajunctional  $\beta$ -catenin associates and which prepare it for degradation are the adenomatous polyposis coli (APC; Rubinfeld *et al.*, 1993) protein, axin (Zeng *et al.*, 1997; Ikeda *et al.*, 1998; Kishida *et al.*, 1998), and the axin homolog conductin (Behrens *et al.*, 1998). APC is considered a tumor suppressor protein linked to predisposition of colon carcinoma. Axin stimulates GSK 3 $\beta$ -mediated phosphorylation of  $\beta$ -catenin. Mutations that abolish phosphorylation of  $\beta$ -catenin by GSK 3 $\beta$  (Munemitsu *et al.*, 1995; Yost *et al.*, 1996; Aberle *et al.*, 1997) or association with APC (Munemitsu *et al.*, 1996; Polakis, 1997) result in stabilization of  $\beta$ -catenin, which leads to an increase in the extrajunctional pool of  $\beta$ -catenin and its nuclear translocation. Activation of Disheveled (Dsh), a downstream target of the Wnt pathway, is a physiological mechanism that inhibits GSK 3 $\beta$ -mediated phosphorylation of  $\beta$ -catenin and thus its degradation. This appears to be the main signaling pathway with which Wnt-responsive genes become expressed, namely, by increasing the cytoplasmic pool or

TABLE I

Selected Examples of Cell–Cell and Cell–ECM Adhesion Junction-Associated Proteins and Cytoskeletal-Associated Proteins Exhibiting Nuclear Localization and the Targeting Signals/Mechanisms Responsible

Plaque protein	Localization <sup>a</sup>	NLS/NES <sup>b,c</sup>	Import/export mechanism
<b>A. Cell–cell and cell–ECM adhesion junction-associated proteins</b>			
β-Catenin	AJ, nucleus	Arm repeats?	Direct binding to NPC through Arm repeats Piggyback transport through association with tNLS bearing LEF-1/TCF <sup>e</sup>
Plakoglobin	AJ, DJ, nucleus	Arm repeats?	Piggyback transport through association with tNLS bearing LEF-1/TCF
Human p120 <sup>ctn</sup>	AJ, nucleus	Arm repeats? <i>QDEGQESLEEELDVVLVLDDEGGQVSYPSM</i> <sup>d</sup>	<i>Crm1-mediated? Nuclear export is blocked by Leptomycin</i>
Rat 1-afadin	AJ, nucleus, perinuclear	<sup>169</sup> KKKR, <sup>223</sup> KRRR, <sup>344</sup> KRRP, <sup>352</sup> PKKMKKH, <sup>1415</sup> RKKR, <sup>1438</sup> RKRR, <sup>158</sup> KRTLSKKEKKEKKREK, <sup>c</sup> <sup>353</sup> KKMKKHVEGKPLKGKDR, <sup>c</sup> <sup>1415</sup> RKKREEHQRWYEKEKAR, <sup>c</sup> <sup>1655</sup> RRQEEGYYYSRLEAERRR <sup>c</sup>	Importin-dependent nuclear import (?)
Vinculin	AJ, ECM-AJ, nucleus	nd	Piggyback transport through association with LEF-1/β-catenin or with β-catenin alone (?)
Human vinexin β <sup>f</sup>	AJ, ECM-AJ, cytoplasm, nucleus	<sup>38</sup> KKRK	Importin-dependent nuclear import (?)
Plakophilin 1a	DJ, nucleus	nd	Arm repeat-independent nuclear import
Plakophilin 1b	Nucleus	nd	nd
Plakophilin 2a,b	DJ, nucleus	nd	nd
Human plakophilin 3	DJ, nucleus	<sup>572</sup> PQSRLR, <sup>752</sup> KKKR	nd

Human ARVCF	AJ, nucleus	<sup>287</sup> RRRP, <sup>608</sup> RRRR, <sup>909</sup> RRPR, <sup>608</sup> RRRRDDASCFGGKKAKE <sup>c</sup>	nd
Human p0071	DJ, nucleus	Arm repeats? <sup>788</sup> KKKKKKKR, <sup>g</sup> <sup>868</sup> RPKRKGKP	Direct binding to NPC through Arm repeats (?) Importin-dependent nuclear import (?)
Mouse pinin	DJ, nucleus	<sup>283</sup> RPRR, <sup>652</sup> RKRR, <sup>660</sup> RKRR, <sup>693</sup> PDRKRSI, <sup>683</sup> RKGSKDKSSRPDRKRSI, <sup>c</sup> <sup>695</sup> RKRSIESSRSRGKRSSR, <sup>c</sup> <sup>707</sup> KRSSRSERDRKSDRKDK <sup>c</sup>	Importin-dependent nuclear import (?)
<i>Xenopus</i> DRS protein I/II	Nucleus	<sup>170</sup> KRRH, <sup>286</sup> RP RR <sup>618/649</sup> KRRR, <sup>625/656</sup> HKRR, <sup>127</sup> RDLIQDQNMDEKGKQR, <sup>c</sup> <sup>659/688</sup> RKRTTSEGSRSGKRPSR, <sup>c</sup> <sup>671/700</sup> KRPSRN/SERDRKSDRKDK <sup>c</sup>	Importin-dependent nuclear import (?)
Mouse ZO-1 $\alpha^{+h}$	TJ, nucleus	<sup>107</sup> RRKKK, <sup>i</sup> <sup>96</sup> RKSGKNAKITIRRKKKV, <sup>c,i</sup> <sup>748</sup> RKSARKLYERSHKLRLKN <sup>c</sup>	Importin-dependent nuclear import (?) Piggyback transport through association with the ZO-1-associated nucleic acid-binding protein (ZONAB)?
hDlg isoform 1/2	Cell-cell contact, nucleus	<sup>308</sup> KRRKP, <sup>i</sup> <sup>674</sup> KRKK, <sup>i</sup> <sup>748/770</sup> RPKR, <sup>642</sup> PSKRRVE	Importin-dependent nuclear import (?)
Dlg1	SJ, nucleus	<sup>4</sup> RKKKR, <sup>124</sup> KRKR, <sup>i</sup> <sup>661</sup> PSKRRWE, <sup>697</sup> RKKK, <sup>j</sup> <sup>804</sup> RPKR, <sup>113</sup> KKAGNVVKLHVKRKRGTC <sup>c,i</sup>	Importin-dependent nuclear import (?)
Human symplekin	TJ, nucleus	<sup>214</sup> RKRPR, <sup>385</sup> PQAKRRP, <sup>214</sup> RKPRPRDDSDSTLKKMKL <sup>c</sup>	Importin-dependent nuclear import (?)
<i>Xenopus</i> cingulin	TJ, nucleus	<sup>34</sup> PRGKRSK, <sup>132</sup> KRKP, <sup>965</sup> KRDLESKLDEAQRSLKR <sup>c</sup>	Importin-dependent nuclear import (?)
Rat b-/s-nexilin	ECM-AJ, nucleus	<sup>124/60</sup> RKRR, <sup>56/</sup> RRKEQYIREREWNRKQE, <sup>124/60</sup> RKRRRIEQDLLEKRKMQR, <sup>c</sup> <sup>301/251</sup> RREEEKRKAEEEARRRM <sup>c</sup>	nd

(continued)

TABLE I  
(continued)

Plaque protein	Localization <sup>a</sup>	NLS/NES <sup>b,c</sup>	Import/export mechanism
Chicken zyxin	ECM-AJ, nucleus	nd/ <sup>319</sup> LTMKEVEELELLTQKLM <sup>d</sup>	nd/CRM1-mediated nuclear export (?)
Mouse talin	ECM-AJ, nucleus	<sup>401</sup> KKKK <sup>k</sup>	Importin-dependent nuclear import (?)
Bovine supervillin	Vinculin-containing FA, AJ, nucleus	<sup>323</sup> PKRRSRN, <sup>748</sup> KKKR, <sup>931</sup> RPKRR, <sup>d</sup> <sup>765</sup> RKHLITVREDAWKTRGK <sup>c</sup>	Importin-dependent nuclear import (?)
<b>B. Cytoskeletal-associated proteins</b>			
$\alpha$ -Actinin 4	Cytoplasm (actin stress fibers), nucleus	nd	nd
Human protein 4.1H	Nucleus	<sup>247</sup> EED-spacer- <sup>615</sup> KKKR <sup>d,l</sup>	Importin-dependent nuclear import
Human protein 4.1E <sup>m</sup>	Nucleus	<sup>90</sup> KRPK	Importin-dependent nuclear import (?)
Mouse Mbh1-gCap39 <sup>n</sup>	Cytoplasm, nucleus	<sup>134</sup> PAAIRKLYQVKGKK <sup>c</sup>	nd
<i>S. cerev.</i> actin	Plasma membrane, cytoplasm, nucleus	nd/ <i>SLPHAILRIDLA</i> <sup>d</sup> , <i>DIKEKLCYVALD</i> <sup>d</sup>	nd/ <i>Crm1</i> -mediated nuclear export blocked by <i>Leptomycin B</i> .
LMW MAP2	Nucleus	RKVAKKEPSTVSRDEVRRK- KAVYKKAAELAKKSEVQAHSPSRK <sup>c,d</sup>	Importin-dependent nuclear import
Human ezrin	Cytoplasm, nucleolus <sup>o</sup>	<sup>293</sup> RRRKP, <sup>327</sup> KKRR, <sup>435</sup> RRRK	Importin-dependent nuclear import?

<sup>a</sup>AJ, adherens junction; DJ, desmosomal junction; IF-associated, intermediate filament-associated; ECM-AJ, extracellular matrix adherens junction; SJ, septate junction; nd, no data.

<sup>b</sup>Potential NLSs identified by the PSORT protein localization prediction program (Nakai and Kanehisa, 1992) and NESs.

<sup>c</sup>Bipartite nuclear localization signal (bNLS).

<sup>d</sup>Confirmed NLS and NES, respectively.

<sup>e</sup>Several possible mechanisms of nuclear translocation have been postulated for  $\beta$ -catenin (see text and Fig. 1A).

<sup>f</sup>Vinexin  $\alpha$  also contains the putative NLS but is not nuclear (see text).

<sup>g</sup><sup>788</sup>KKKKKKR is conserved in human neural plakophilin related Arm-repeat protein (NPRAP—<sup>811</sup>KKKKKKK) and various p120<sup>ctn</sup> isoforms (KKGKGKK). However, the NPRAP <sup>811</sup>KKKKKKK sequence alone did not show nuclear targeting activity in a transfection assay (see text).

<sup>h</sup>Nuclear accumulation of ZO-1 is not isoform specific (Gottardi *et al.*, 1996).

<sup>i</sup>Potential tNLS/bNLS within the PDZ1-2 interrepeat, which is conserved in ZO-1, Dlg, hDlg, and partly in PSD95 (not shown). The first 200 amino acids of ZO-1, containing this tNLS/bNLS, have been shown to be targeted into the nucleus (see text).

<sup>j</sup>Potential tNLS within IS3 of hDlg isoform 2 (not present in isoform 1), also conserved in Dlg and partly in PSD95 (not shown). Deletion of IS3 results in cytoplasmic localization of overexpressed hDlg (Lutchman *et al.*, 1997).

<sup>k</sup>Conserved in the amino terminus of talin from human (Ben-Yosef and Francomano, 1999), chicken (Hemmings *et al.*, 1996) and *C. elegans* (Moulder *et al.*, 1996).

<sup>l</sup>Nuclear accumulation of 4.1H isoform through joining exon 13 (...PTEAWK) with exon 16 (KKRERLDGENIYIR...), which creates a cluster of basic amino acids (Luque *et al.*, 1998). Efficient nuclear targeting of protein 4.1H additionally requires the acidic EED-motif encoded by exon 5 (Gascard *et al.*, 1999). Mutation of <sup>615</sup>KKKR to TNSG results in completely cytoplasmic localization (Luque *et al.*, 1998).

<sup>m</sup>Nuclear protein 4.1E lacks exon 16 [see footnote *l*; a potential NLS is localized at position 90 (KRPK) which is also conserved in isoform H]. But complete redistribution of nuclear isoform H to the cytoplasm through mutation of isoform H-NLS (KKKR to TNSG; Luque *et al.*, 1998), argues against the involvement of <sup>90</sup>KPRK in nuclear targeting of isoform E.

<sup>n</sup>The potential NLS of Mbh1 resembles that of nuclear oncoproteins (human c-myc: <sup>521</sup>PLKKIKQ; human N-myc: <sup>345</sup>PPQKKIKS; human p53: <sup>316</sup>PQPKKKP; and chicken c-erb-A: <sup>127</sup>SKRVAKRKL), containing helix-breaking amino acids followed by a cluster of positively charged amino acid residues (Dang and Lee, 1989).

<sup>o</sup>Anti-ezrin antibody nucleolar staining in normal and transformed human cells is attributable to a 55-kDa cleavage form of ezrin that lacks the C-terminal F-actin binding sequence (Kaul *et al.*, 1999).

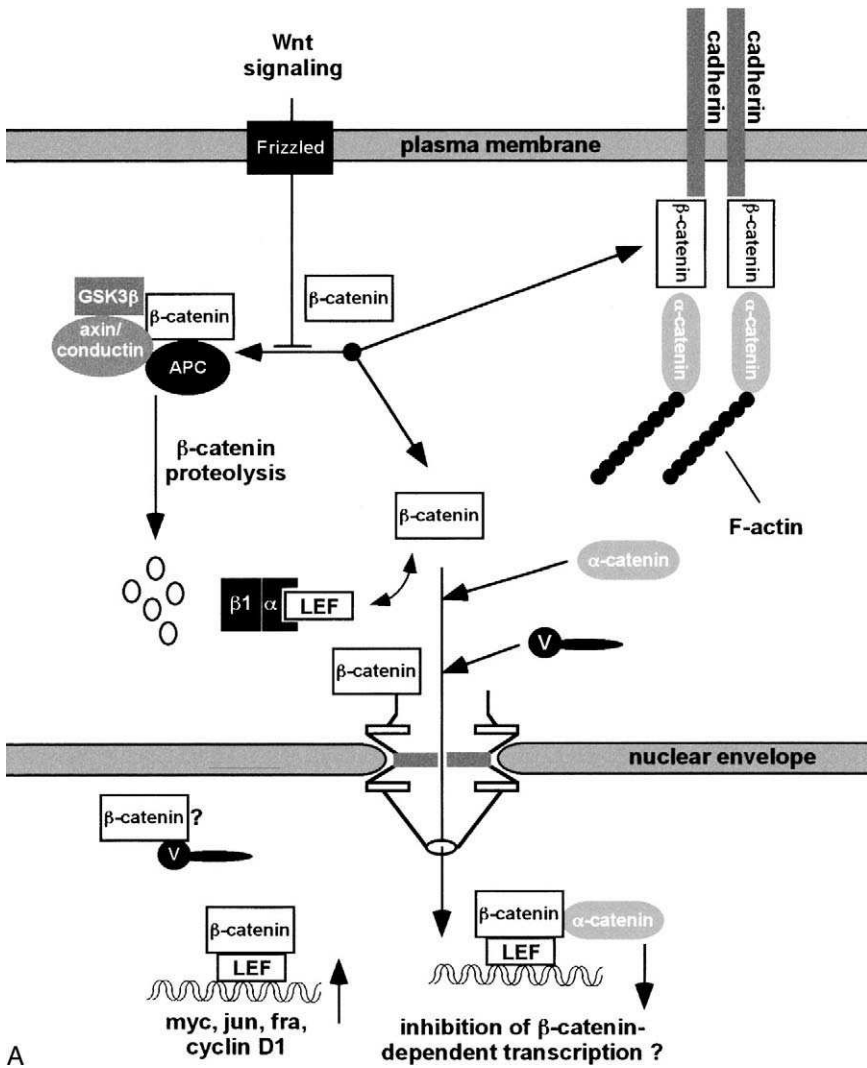
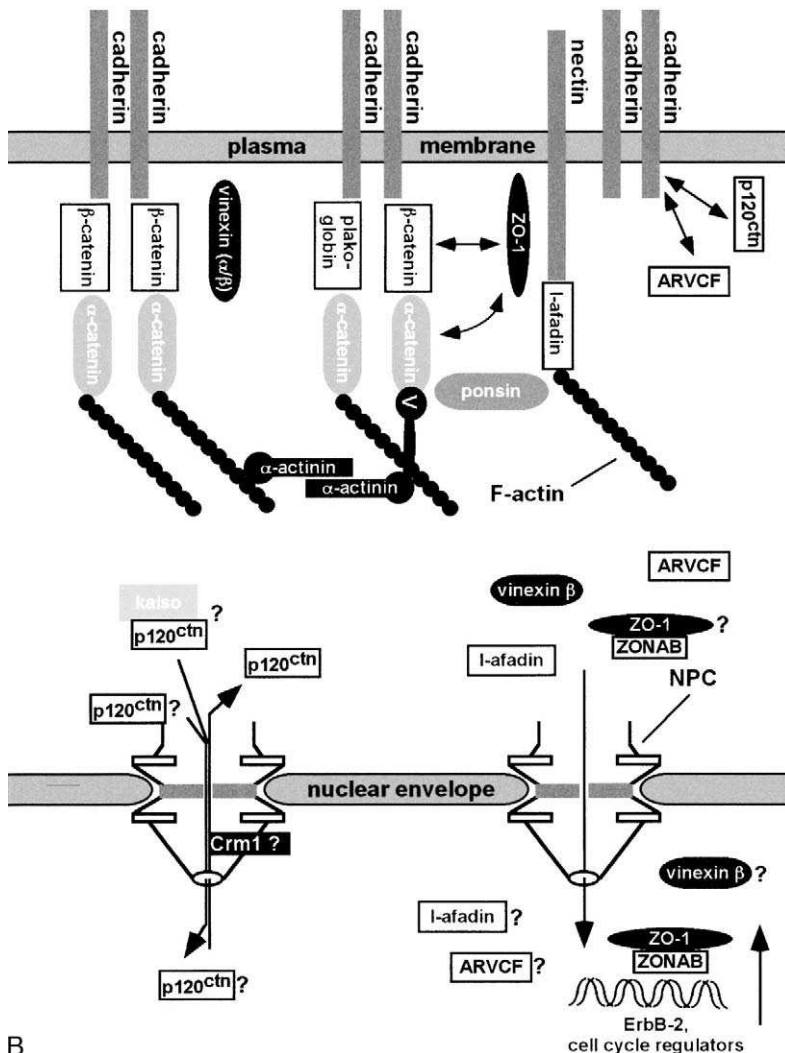


FIG. 1 Nuclear signaling by adherens junction-associated plaque proteins. Cadherins exhibit calcium-dependent homophilic binding to cadherins of opposing cells and display lateral dimerization. The cytoplasmic domain of cadherins interacts with  $\beta$ -catenin, plakoglobin, and p120<sup>ctr</sup>. Linkage of cadherins to the actin cytoskeleton via  $\beta$ -catenin or plakoglobin occurs via  $\alpha$ -catenin (Rimm *et al.*, 1995), which binds to actin, and the actin binding protein  $\alpha$ -actinin (Knudsen *et al.*, 1995) and vinculin (Weiss *et al.*, 1998).  $\alpha$ -Catenin and  $\beta$ -catenin also interact with ZO-1 (Rajasekaran *et al.*, 1996; Imamura *et al.*, 1999). Ponsin is also found at adherens junctions and binds to 1-afadin and vinculin (Mandai *et al.*, 1999).



Ponsin, 1-afadin, and vinculin are unable to form a ternary complex (Mandai *et al.*, 1999). Nectin is linked to F-actin through 1-afadin. Vinexin ( $\alpha/\beta$ ) is another vinculin binding protein that localizes to both adherens junctions and to focal adhesions (Kioka *et al.*, 1999).  $\beta$ -Catenin, plakoglobin, and p120<sup>ctn</sup> (all three are Arm-repeat proteins), as well as vinculin,  $\alpha$ -catenin, 1-afadin, vinexin  $\beta$ , and ZO-1, have been reported to localize to the nucleus. (A)  $\beta$ -Catenin seems to enter the nucleus either through binding to NLS-containing LEF/TCF transcription factors in the cytoplasm (Huber *et al.*, 1996; Molenaar *et al.*, 1996), involving  $\alpha/\beta$ , or independently (Fagotto *et al.*, 1998) through direct binding to the NPC. Inside the nucleus,  $\beta$ -catenin antagonizes negative regulators (such as Groucho; Cavallo *et al.*, 1998;

mainly by preventing phosphorylation and degradation of  $\beta$ -catenin and allowing its association with DNA-binding LEF/TCF family members.

Because no conventional NLS is evident in  $\beta$ -catenin's primary sequence, several mechanisms for its nuclear targeting have been postulated. The tNLS-bearing factors LEF/TCF, which are able to bind to  $\beta$ -catenin directly, have been proposed to mediate piggyback cotransport of  $\beta$ -catenin into the nucleus (Behrens *et al.*, 1996; Huber *et al.*, 1996). However, studies in *Drosophila* with an *Armadillo* mutant unable to complex with dTCF, which appears to be unaffected in nuclear translocation ability in response to Wingless signaling (Orsulic and Peifer, 1996; van de Wetering *et al.*, 1997), imply an additional TCF-independent pathway. Prieve and Waterman (1999) could also demonstrate nuclear translocation of  $\beta$ -catenin independently of LEF/TCF-binding. These observations are supported by the fact that *in vitro* nuclear transport assays demonstrate that  $\beta$ -catenin alone is able to translocate into the nucleus even in the absence of exogenously added cytosol and, in addition, to bind directly to the nuclear envelope. Interestingly, NPC-docking could be competed by importin  $\beta$ , implying that binding of  $\beta$ -catenin to nucleoporins of the NPC is at sites also used by importin  $\beta$ . Indeed,  $\beta$ -catenin is able to interact directly with specific amino acid repeat-containing nucleoporins (Fagotto *et al.*, 1998), which are known to provide binding sites for importin  $\beta$ , while the Arm repeats of  $\beta$ -catenin have been shown to be necessary and sufficient for its nuclear translocation (Funayama *et al.*, 1995; Giannini *et al.*, 2000). Since molecular phylogenetic analysis shows that the Arm repeats of importin  $\alpha$  and the HEAT repeats of importin  $\beta$  are similar in terms of secondary structure (Malik *et al.*, 1997), and the repeats of importin  $\beta$  and  $\beta$ -catenin confer NPC binding, it seems feasible that other Arm-repeat-containing junctional proteins such as plakophilins and p0071 (see below) may also be able to bind at the NPC.

Nuclear import of  $\beta$ -catenin *in vitro* has been reported to be inhibited by WGA (see above), underlining a role of nucleoporins in the pathway, as well as

---

Fisher and Caudy, 1998; Levanon *et al.*, 1998; Roose *et al.*, 1998) and CBP (Waltzer and Bienz, 1998) of LEF-1/TCF proteins. In the absence of a Wnt signal, cytoplasmic  $\beta$ -catenin is subjected to proteolysis stimulated by the APC/conductin/axin/GSK 3 $\beta$ -multiprotein complex. Vinculin localizes to the nucleus presumably through association with  $\beta$ -catenin (Simcha *et al.*, 1998). Overexpression of  $\beta$ -catenin and TCF-4 has been shown to result in nuclear localization of  $\alpha$ -catenin, which appears to repress  $\beta$ -catenin-dependent transcription (Giannini *et al.*, 2000). (B) Cytoplasmic localization of p120<sup>ctn</sup> exon B isoforms depends on a NES within exon B, with nuclear export presumably mediated by CRM1. Nuclear import of p120<sup>ctn</sup> may occur through association with the transcription factor Kaiso (Daniel and Reynolds, 1999) or through direct binding to the NPC, involving the Arm repeats. ARVCF, a novel Arm-repeat protein that associates with E-cadherin and competes with p120<sup>ctn</sup> for binding to the juxtamembrane domain of E-cadherin, also localizes to the nucleus (Mariner *et al.*, 2000). APC, adenomatous polyposis coli protein; V, vinculin; ZONAB, ZO-1-associated nucleic acid binding protein; NPC, nuclear pore complex; ARVCF, armadillo repeat gene deleted in velo-cardio-facial syndrome; GSK 3 $\beta$ , glycogen synthase kinase 3 $\beta$ ; CBP, cAMP-response-element binding protein;  $\alpha/\beta 1$ , importin  $\alpha/\beta 1$ .

nonhydrolyzable GTP analogs such as GTP $\gamma$ S, indicating the involvement of Ran (Fagotto *et al.*, 1998). A recent study (Yokoya *et al.*, 1999), however, shows that nuclear translocation of  $\beta$ -catenin can occur in a Ran-unassisted manner, similar to importin  $\beta$ , implying that nuclear transport may also be able to be mediated by a pathway involving components distinct from the conventional nuclear transport factors thus far characterized (see above).

Plakoglobin, which is more than 60% identical to  $\beta$ -catenin, is also part of the Wnt signaling pathway. However, although analogous to  $\beta$ -catenin, plakoglobin has been reported to show differences in terms of its dependence on LEF-1 for nuclear translocation, as well as in its ability to complex with vinculin and trans-activate LEF-1-responsive genes (Simcha *et al.*, 1998).

**b.  $p120^{ctn}$**   $p120^{ctn}$ , originally identified as a substrate of activated src kinase, differs from  $\beta$ -catenin and plakoglobin in that it does not interact with  $\alpha$ -catenin. This is probably the reason for the basis of the poor adhesive phenotype of  $p120^{ctn}$ -overexpressing cells and ras-transformed cells, in which  $p120^{ctn}$ -cadherin complexes predominate.  $p120^{ctn}$ , which belongs like  $\beta$ -catenin and plakoglobin to the family of *Armadillo*-related catenin proteins, localizes to adherens junctions (Golenhofen and Drenckhahn, 2000) and binds directly to E-cadherin. But  $p120^{ctn}$  does not bind APC and LEF-1, implying that  $p120^{ctn}$  may play a distinct role both at sites of cell–cell adhesion and in transmitting signals to the nucleus (see below). It has been reported that the human  $p120^{ctn}$  gene might encode up to 32 protein isoforms generated by alternative splicing (Keirsebilck *et al.*, 1998). Interestingly, subcellular localization of  $p120^{ctn}$  isoforms has been shown to be dependent on the inclusion of different exons (van Hengel *et al.*, 1999). The alternative exon B, for instance, has been shown to contain a functional NES, which results in cytoplasmic localization of exon B-containing isoforms, whereas treatment with leptomycin B, which inhibits exportin–NES interaction, induces a complete shift of such isoforms to the nucleus. However, exon B-lacking  $p120^{ctn}$  isoforms usually cannot be detected in the nucleus. This might be accounted for through inhibition of nuclear import due to sequestration of  $p120^{ctn}$  by E-cadherin. Consistent with this idea,  $p120^{ctn}$  lacking exon B is found in the nucleus in cells expressing low levels of E-cadherin, while overexpression of  $p120^{ctn}$  lacking exon B also leads to nuclear accumulation, possibly through a titration effect.

A two-hybrid screen recently identified a protein that binds to  $p120^{ctn}$ , which is a novel BTB/POZ (Broad complex, Tramta, Bric a brac/Pox virus and Zinc finger)-Zn finger protein named Kaiso (Daniel and Reynolds, 1999). It interacts specifically with  $p120^{ctn}$  but not with  $\beta$ -catenin or plakoglobin. Immunofluorescence studies revealed localization of Kaiso primarily in the nucleus but also at membrane/cell–cell junctions and in the cytoplasm.

Because Kaiso, like all other members of the BTB/POZ family of transcription factors, does not appear to possess a conventional NLS, its nuclear localization could occur through association with  $p120^{ctn}$ . The Arm repeats of  $p120^{ctn}$  may

allow NPC docking as shown for  $\beta$ -catenin (see above). Whether or not p120<sup>ctn</sup> alone or complexed to Kaiso is able to enter the nucleus independent of other factors remains to be investigated, but if so, it will be interesting to investigate the role of p120<sup>ctn</sup> in nuclear processes, which could be predicted to be quite different from those carried out by  $\beta$ -catenin.

**c. Afadin** Afadin is a novel ~205-kDa F-actin-binding protein that has recently been shown to localize to adherens junctions (Mandai *et al.*, 1997). l-Afadin contains one PDZ domain, initially identified as a 90-amino-acid repeat motif in the synaptic plaque proteins PSD-95 (postsynaptic density protein 95) and SAP 90 (synapse-associated protein 90; Cho *et al.*, 1992). This domain is also known as a PSD-95/Dlg/ZO-1 repeat domain. In l-afadin the PDZ domain is located in the midportion of the molecule and is followed by three carboxy-terminal proline-rich domains and an F-actin-binding domain. The small ~190-kDa splicing variant s-afadin lacks the C-terminal 166 amino acids, including the F-actin binding domain, as well as the third proline-rich region. So far, two l-afadin interacting proteins, ponsin and nectin, have been identified (Mandai *et al.*, 1999; Takahashi *et al.*, 1999). Ponsin, which is structurally related to vinexin, localizes to adherens junctions and cell–substrate contacts and interacts with l-afadin's third proline-rich region through two of its three src homology 3 (SH3) domains (Mandai *et al.*, 1999). s-Afadin, which lacks the third proline-rich region, does not bind ponsin. Interestingly, immunofluorescence studies show an additional nuclear localization of ponsin as well as of l-afadin (see below), although whether this is physiologically relevant or artifactual due to poor antibody specificity remains to be investigated. PDZ domains are known to mediate interactions with unique carboxy-terminal motifs of a large number of transmembrane proteins (Saras and Heldin, 1996), and may be directly involved in recruiting l-afadin to adherens junctions. With respect to this it has been found that the PDZ domain of l-afadin interacts with the cytoplasmic region of the recently identified l-afadin interacting protein, nectin, which is a member of the immunoglobulin superfamily (Takahashi *et al.*, 1999). While l-afadin is expressed ubiquitously, s-afadin is expressed abundantly in neural tissue. l-Afadin is the protein encoded by the *AF-6* gene, which was found to be fused to the *ALL-1* gene, identified as being involved in acute leukemia (Cimino *et al.*, 1991). Both afadin isoforms show differences in binding to junctional plaque proteins. l-Afadin does not directly bind  $\alpha$ -catenin,  $\beta$ -catenin, or ZO-1 (see below; Sakisaka *et al.*, 1999), whereas s-afadin has been shown to interact with ZO-1 (Yamamoto *et al.*, 1997). Immunofluorescence studies with an l-afadin antibody revealed perinuclear and also nuclear staining (Mandai *et al.*, 1997; Sakisaka *et al.*, 1999; Takahashi *et al.*, 1999) but the physiological role of nuclear l-afadin remains unclear. Analysis of the amino acid sequence reveals numerous positively charged clusters mostly within the amino-terminal domain which fit the consensus sequences for tNLSs and bNLSs (see Table I). However, NLS-masking through binding of ponsin to the third proline-rich domain of l-afadin (amino acids

1691–1713), which is immediately adjacent to the putative bNLS at position 1655, could also be a mechanism to regulate nuclear translocation of l-afadin. With respect to this, detailed domain analysis should confirm whether l-afadin is capable of NLS-dependent nuclear translocation, or rather is a plaque protein restricted to adherens junctions.

**d. Vinculin** Vinculin is a structural element of adherens junctions as well as focal cell–substrate contacts. It is known to bind to actin filaments (Menkel *et al.*, 1994; Johnson and Craig, 1995),  $\alpha$ -actinin (Belkin and Koteliansky, 1987; Wachstock *et al.*, 1987) and vinexin (Kioka *et al.*, 1999), as well as to the focal contact proteins talin (Otto, 1983; Burridge and Mangeat, 1984) and ponsin (Mandai *et al.*, 1999). Studies of nuclear translocation of  $\beta$ -catenin in overexpressing MDCK cells revealed nuclear structures containing LEF-1 and surprisingly vinculin (Simcha *et al.*, 1998). Because vinculin does not display any conventional NLS-like sequences, its nuclear translocation may be mediated through a LEF-1/ $\beta$ -catenin complex or through complexation with  $\beta$ -catenin alone. Consistent with the latter possibility is the observation that overexpression of LEF-1 alone does not result in nuclear accumulation of vinculin (Simcha *et al.*, 1998). These studies demonstrate a new interaction between  $\beta$ -catenin and vinculin and its possible role in nuclear targeting of vinculin, whose nuclear function is unknown.

Other proteins known to bind to  $\beta$ -catenin such as  $\alpha$ -catenin and APC (Neufeld and White, 1997) also localize to the nucleus. With respect to  $\alpha$ -catenin Giannini *et al.* (2000) have very recently observed that overexpression of  $\beta$ -catenin and Tcf-4 leads to nuclear localization of  $\alpha$ -catenin. In the nucleus,  $\alpha$ -catenin seems to repress  $\beta$ -catenin/Tcf-transcriptional activity (Giannini *et al.*, 2000).

**e. Vinexin** Vinexin is a novel vinculin binding, SH3 domain-containing protein that enhances actin cytoskeletal organization (Kioka *et al.*, 1999). Vinexin has two isoforms, vinexin  $\alpha$  (82 kDa) and vinexin  $\beta$  (37 kDa), the expression of which seems to be driven from alternative promoters, that give rise to an amino-terminally truncated vinexin  $\beta$ -isoform (starting at methionine 406). Both isoforms localize to adherens junctions and focal substrate contacts. Overexpression of vinexin  $\alpha$  increases the size of focal contacts and actin stress fiber formation. These effects were much more striking than those seen in response to vinexin  $\beta$ . Vinexin  $\beta$  was also found in the cytoplasm and sometimes in the nucleus. Both isoforms contain an NLS-like cluster of positively charged amino acids (see Table I), with conformational changes possibly accounting for the differences in subcellular localization of the two vinexin isoforms. The physiological significance of nuclear accumulation of vinexin  $\beta$  remains to be determined.

In summary,  $\beta$ -catenin, plakoglobin, l-afadin, vinculin,  $\alpha$ -catenin, and vinexin  $\beta$  represent examples of cell–cell adherens junction-associated plaque proteins that display functional diversity relating to their differential subcellular distribution. They can act as direct or indirect linker molecules between the actin cytoskeleton

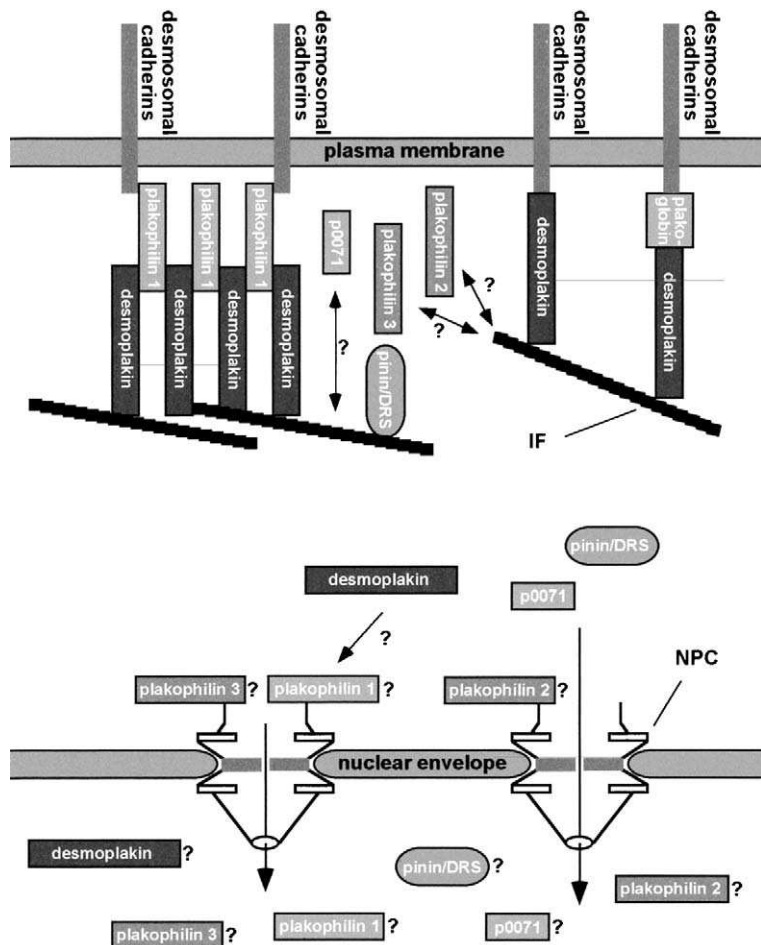


FIG. 2 Nuclear signaling by desmosome-associated plaque proteins. The desmosomal cadherins interact with plakoglobin (Troyanovsky *et al.*, 1994a, 1994b; Wahl *et al.*, 1996; Witcher *et al.*, 1996). The cadherin-plakoglobin complex is linked to the IF system via desmoplakin (Stappenbeck *et al.*, 1993, 1994; Kouklis *et al.*, 1994; Kowalczyk *et al.*, 1996, 1997; Meng *et al.*, 1997). Desmoplakin is also able to bind directly to the desmosomal cadherin Dsc1a (Smith and Fuchs, 1998). Plakophilin-1 (which is restricted to multilayered epithelia) is the other desmosomal plaque protein that binds directly to cytokeratin IFs (Kapprell *et al.*, 1988; Hatzfeld *et al.*, 1994, 2000; Heid *et al.*, 1994; Smith and Fuchs, 1998, to desmoplakin (Kowalczyk *et al.*, 1999a; Hatzfeld *et al.*, 2000), and to certain desmosomal cadherins (Mathur *et al.*, 1994; Smith and Fuchs, 1998; Kowalczyk *et al.*, 1999a; Hatzfeld *et al.*, 2000). It is proposed to play a role in lateral interactions with desmoplakin (Kowalczyk *et al.*, 1999b). The interactions of the plakophilin isoforms 2 (localized to plaques of desmosomes of simple and complex epithelia) and 3 with other desmosomal plaque proteins and the IF system have not yet been investigated.

and cadherin/integrin-type adhesion molecules and, in addition, are involved in crosstalk between the plasma membrane and the nucleus (Fig. 1).

## 2. Nuclear Signaling by Desmosomal Plaque Proteins

The intermediate filament-anchored desmosomes are prominent adhesive elements in epithelia and cardiac muscle (Schmidt *et al.*, 1994). Desmosomes resemble adherens junctions in so far that the desmosomal transmembrane adhesion molecules are members of the cadherin superfamily. The desmosomal cadherins are the desmogleins (Dsg1–3) and desmocollins (Dsc1a–3b). These cadherins do not occur in adherens junctions. Linkage of desmosomal cadherins to intermediate filaments (IFs) involves the plaque proteins desmoplakin I and II, plakoglobin, and plakophilin 1. Other cytoplasmic plaque proteins associated with desmosomes include the plakophilin 2 and 3, p0071, pinin, and further accessory cell-type-specific proteins such as desmocalmin, plectin, and IFAP300. Among the cytoplasmic plaque proteins, plakophilins, p0071, and pinin have attracted special attention because they display both desmosomal and nuclear localization (Fig. 2). Plakophilins and p0071 are like plakoglobin members of the *Armadillo* protein family, whereas pinin, a 140-kDa protein, is not related to other plaque proteins.

**a. Plakophilins 1–3** Plakophilins 1–3 are closely related desmosomal plaque proteins that belong to the *Armadillo* protein family (Franke *et al.*, 1983; Mueller and Franke, 1983; Kapprell *et al.*, 1988; Hatzfeld *et al.*, 1994; Heid *et al.*, 1994; Schmidt *et al.*, 1994; Bonné *et al.*, 1999). Plakophilin 1 and 2 each exist as at least two alternatively spliced isoforms, differing by short sequences of 21 (plakophilin 1a, 1b; Schmidt *et al.*, 1997) and 44 amino acids (plakophilin 2a, 2b; Mertens *et al.*, 1996). Plakophilins 1–3 are not only expressed in desmosome-forming cells but also occur in a variety of desmosome-free cells. Nuclear location of plakophilin 1 has been reported for both desmosome-forming and desmosome-free cells (such as skeletal muscle, lens epithelium, and lymph node cells). Plakophilin 1 thus appears to be an ubiquitous, constitutive nuclear protein of many vertebrate cells. In contrast to plakophilin 1b, which has been found exclusively in nuclei, plakophilin 1a can also be recruited to desmosomes of complex and stratified epithelia, implying a targeting role for the additional 21 amino acids of plakophilin 1b. Plakophilin 2 is associated with desmosomes but is also found

---

The role of the recently identified desmosomal plaque protein p0071 in desmosome assembly is also not known. Pinin/DRS, another desmosomal plaque protein, has been reported to directly interact with certain keratin IFs (Shi and Sugrue, 2000). Nuclear localization has been observed for plakophilin 1a, 1b (with plakophilin 1b being exclusively nuclear), 2a, 2b, and 3, pinin, and p0071. Desmoplakin has also been observed in the nucleus, but only after overexpression of plakophilin-1, presumably driven through the association of desmoplakin with plakophilin-1 (Hatzfeld *et al.*, 2000). However, the nuclear role of all of these desmosomal plaque proteins is still obscure. NPC, nuclear pore complex; IF, intermediate filament; DRS, domain rich in serines.

in the nucleus where it is spread throughout the interchromatinic karyoplasm but excluded from the nucleolus. Nuclear accumulation is independent of cellular proliferation and cell density, implying that plakophilin 2 is a constitutively nuclear protein. In addition to desmosomal localization, plakophilin 3 shows speckle-like nuclear distribution (Bonné *et al.*, 1999).

All members of the plakophilin family can thus be regarded as widespread basic nuclear proteins, which can also act, with the exception of plakophilin 1b, as desmosomal plaque proteins (see Fig. 2). Nuclear translocation of plakophilins seems likely to be independent of a classical importin  $\alpha/\beta$ -dependent pathway because the primary sequences are devoid of basic NLS-like sequences. However, because plakophilins are Arm-repeat-containing proteins, it is reasonable to assume that nuclear accumulation could be accomplished by specific binding to the Arm-repeat-binding nucleoporins of the NPC, as has been shown for  $\beta$ -catenin (see above). However, the subcellular localization of green fluorescent protein (GFP)-plakophilin 1 fusion proteins indicated that both the N-terminal head (lacking Arm repeats) and the Arm-repeat-containing C-terminal regions were capable of conferring nuclear entry (Klymkowsky, 1999). Clearly, sequence divergence within the Arm repeats may well account for differences in the nuclear import pathways and perhaps also in the function of plakophilins and related proteins.

**b. p0071** p0071 is a recently identified member of the *Armadillo* protein family. It is widely expressed and seems to localize at both desmosomal plaques (Hatzfeld and Nachtsheim, 1996) and within the nucleus (Hatzfeld, 1997). In contrast to other members of the *Armadillo* protein family, p0071 contains a stretch of 8 positively charged amino acids at the end of repeat 6 that might function as an NLS (see Table I). Of relevance in this context is the fact that neural plakophilin-related Arm-repeat protein (NPRAP) (Paffenholz and Franke, 1997), recently identified as being highly homologous to p0071, p120<sup>ctn</sup> and ARVCF (armadillo repeat gene deleted in velo-cardio-facial syndrome), also contains a stretch of positively charged amino acids at the end of repeat 6. In an attempt to address the question of whether this sequence can act as an NLS, it was fused to the N terminus of *Xenopus laevis* vimentin I, which is known to form IF bundles when shifted from the nonpermissive temperature (37° C) to the permissive temperature (28° C). Transfection of vimentin-negative cells with the cDNA encoding the vimentin chimera resulted in the appearance of IF-like structures that were exclusively cytoplasmic, whereas the nuclei were negative (Paffenholz and Franke, 1997). Based on these studies, which are not simple to interpret, Paffenholz and Franke (1997) concluded that this NLS-like motif alone from repeat 6 was not sufficient for nuclear targeting of vimentin. Nuclear translocation of p0071 may accordingly be mediated by other sequences. Just recently, it was observed that ARVCF can also localize to the nucleus (Mariner *et al.*, 2000). Sequences within the amino-terminal domain seem to be responsible for its nuclear localization (Mariner *et al.*, 2000).

**c. Pinin** Pinin is a newly described desmosomal phosphoprotein, related to proteins containing a domain rich in serines (DRS) (see below). DRS has been suggested to anchor intermediate-sized filaments to the desmosomal plaque. Pinin seems to be absent from developing desmosomes, but is associated with mature desmosomes, implying that pinin plays a role in stabilizing and maintaining desmosomal integrity (Ouyang and Sugrue, 1996). Transfection studies using pinin cDNA revealed enhanced cell–cell adhesion, reduction of the growth rate, and decreased anchorage-independent growth capability, implicating pinin in the negative regulation of growth or tumor suppression (Ouyang and Sugrue, 1996; Shi *et al.*, 1997). In this context, it is interesting that pinin is homologous to MEMA/hDRS, the mRNA of which is up-regulated in metastasizing melanoma cells (Degen *et al.*, 1999).

Pinin is not strictly confined to desmosomes. In migrating cells, pinin has been shown to redistribute to the cytoplasmic space (Shi *et al.*, 1997), and in transfected cells immunostaining for pinin was observed in the nucleus in discrete foci. Cell cycle synchronization experiments indicated that pinin redistributes to the nucleus during late S to G<sub>2</sub> phase (Shi *et al.*, 1997). Studies of GFP-pinin fusion proteins identified the C terminus of pinin as responsible for nuclear translocation and sub-nuclear compartmentalization (Simmons *et al.*, 1998). Pinin's C terminus contains a number of putative phosphorylation sites that might regulate its nuclear targeting. With respect to this we have demonstrated that phosphorylation is a widespread mechanism for regulating NLS-dependent nuclear protein transport (Jans *et al.*, 1998; Jans and Hübner, 1996).

Using a series of specific antibodies, Brandner *et al.* (1997) found pinin exclusively in the nucleus in both desmosome-containing and desmosome-free cells. Desmosomes were consistently negative for pinin, concluding that pinin is a widespread nuclear protein (Brandner *et al.*, 1997). However, the differences described for the localization of pinin and other DRS proteins (either desmosomal/nuclear or exclusively nuclear) could stem from differences in epitope accessibility of the antibodies used. Nuclear localization of DRS proteins has been investigated by Brandner *et al.* (1998), who found that DRS proteins exist within the cell nucleus as either diffusible 11–13 S protein complexes or are localized in speckles. Speckles are subnuclear structures known to contain components involved in mRNA splicing (Spector, 1993; Zhang *et al.*, 1994). All DRS proteins are highly homologous with respect to their N- and C-terminal domains and contain a region rich in arginine and glycine residues (RGG repeats/RGG Box). Such RGG motifs are found in a number of RNA-binding proteins and have been shown to be involved in RNA binding. DRS from *Xenopus* has indeed been shown to be able to bind to either mRNA or rRNA *in vitro* (Brandner *et al.*, 1998), implying that the role of DRS proteins in the nucleus may relate to RNA transport between nuclear and cytoplasmic compartments; this, however, needs to be confirmed experimentally.

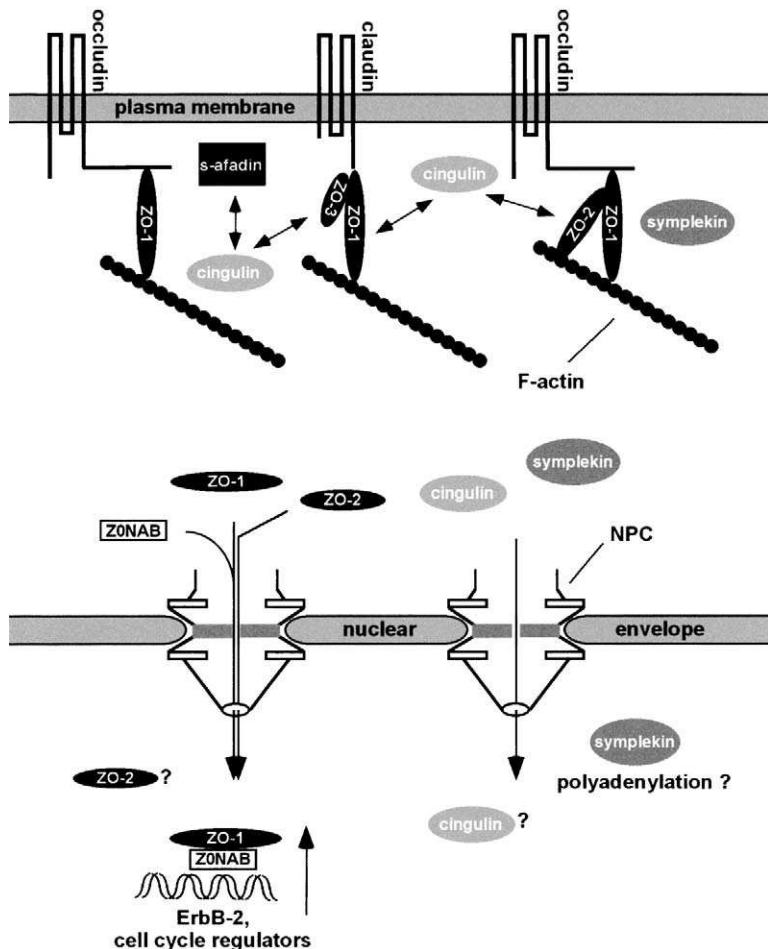


FIG. 3 Nuclear signaling by tight junction-associated plaque proteins. Only some of the possible interactions between TJ-specific transmembrane proteins and plaque proteins are shown. The TJ-specific transmembrane proteins occludin and claudin can bind to the MAGUK-protein family members ZO-1, ZO-2, and ZO-3 (Furuse *et al.*, 1994; Haskins *et al.*, 1998; Itoh *et al.*, 1999) and are linked via ZO-1 and ZO-2 to the actin filament system (Itoh *et al.*, 1997; Fanning *et al.*, 1998). An interaction between ZO-3 and actin filaments has not yet been examined. ZO-1 can bind to ZO-2 (Fanning *et al.*, 1998) and ZO-3 (Haskins *et al.*, 1998). Cingulin, symplekin, s-afadin, and others (e.g., 7H6, rab3B) are additional proteins recruited to the TJ plaque. Cingulin can interact with ZO-1, ZO-2, and ZO-3 and also binds the afadin splicing variant s-afadin (Cordenonsi *et al.*, 1999). s-Afadin can interact with ZO-1 (Yamamoto *et al.*, 1997). ZO-1, ZO-2, cingulin, and symplekin show additional translocation into the nucleus. Nuclear ZO-1 has very recently been reported to be involved in gene regulatory processes through association with a Y-box transcription factor, ZONAB protein (Balda and Matter, 2000). Inside the nucleus ZO-1 and ZONAB regulate expression of ErbB-2 and possibly

### 3. Nuclear Signaling by Tight-Junction-Associated Proteins

Occluding junctions [zonula occludens, tight junctions (TJs)] form a selective permeability barrier that regulates the transport of cells, macromolecules and ions through the paracellular space, thus ensuring the maintenance of compositionally distinct compartments within the body. TJs also serve as a barrier to diffusion within the plasma membrane. In polarized epithelial cells, TJs separate the apical from the basolateral membrane domain and are considered to be important for maintenance of compositional differences between both membrane domains and hence for cellular polarity. Actin filaments have been localized close to the cytoplasmic surface of TJs (Madara, 1987; Drenckhahn and Dermietzel, 1988) and occur in belt-like formations along the adherence junctions that are located immediately beneath TJs (Mooseker, 1985). Agents perturbing the actin-based cytoskeleton have been shown to modulate TJ barrier functions, suggesting a general role of actin and associated proteins in regulating TJ permeability. However, deciphering the molecular composition of the TJ is still in its infancy. Proteins involved in tissue-specific TJ formation include integral membrane proteins such as occludins (Furuse *et al.*, 1993), claudins (Furuse *et al.*, 1998), Jam (Martin-Padura *et al.*, 1998), the cytoplasmic plaque protein ZO-1 (Stevenson *et al.*, 1986; Balda and Anderson, 1993), ZO-2 (Jesaitis and Goodenough, 1994), ZO-3 (Haskins *et al.*, 1998), symplekin (Keon *et al.*, 1996), cingulin (Citi *et al.*, 1989), 7H6 antigen, and actin. ZO-1–3 are members of a family of membrane-associated-guanylate kinase (MAGUK) proteins. Members of this family possess multiple conserved structural motifs, including a variable number of PDZ domains, a region homologous to the guanylate kinase catalytic (GUK) domain (Fanning and Anderson, 1996), and an SH3 domain. So far only two TJ specific actin-binding proteins have been characterized, ZO-1, which shows both F-action (Itoh *et al.*, 1997) and spectrin binding activity (Itoh *et al.*, 1991), and afadin (see above). ZO-1 is not exclusively expressed in TJ-bearing cells, but can also be found at intercalated discs of cardiac muscle cells (Itoh *et al.*, 1993), as well as at cadherin-dependent adhesion sites in cells devoid of TJs (Howarth *et al.*, 1992), where it binds to  $\beta$ -catenin (Rajasekaran *et al.*, 1996). Cingulin interacts with ZO-1, ZO-2, ZO-3, and myosin and thus may play a role as an integrating component of the TJ plaque (Cordenonsi *et al.*, 1999). Interestingly, some of the TJ-associated plaque proteins, including ZO-1, ZO-2, afadin, symplekin, and cingulin, can also be found in the nucleoplasm (Fig. 3). This implies that TJ-associated plaque proteins, similar to those associated with adherens junctions and desmosomes

---

cell cycle regulatory proteins protein (Balda and Matter, 2000). Symplekin has been shown to interact with (StF-64, a protein involved in polyadenylation, and thus may function in the assembly of the polyadenylation machinery (Takagaki and Manley, 2000). The nuclear roles for ZO-2 (could play a similar role as ZO-1) and cingulin have not yet been determined. ZONAB, ZO-1-associated nucleic acid binding protein; NPC, nuclear pore complex.

(see above), may play a role in nuclear processes and possibly in transferring signals from the membrane to the nuclear compartment.

**a. ZO-1** ZO-1 is a 220-kDa membrane-associated protein which interacts with its cytoplasmic portion with occludins (Furuse *et al.*, 1998),  $\alpha$ -catenin (Itoh *et al.*, 1997),  $\beta$ -catenin (Rajasekaran *et al.*, 1996), spectrin (Itoh *et al.*, 1991), and F-actin (Itoh *et al.*, 1997). ZO-1 is also found in cells that lack TJs (Itoh *et al.*, 1991). As mentioned above, ZO-1 belongs to the family of MAKUG proteins, which are defined by a conserved multidomain structure (Willott *et al.*, 1993).

Besides MAKUG-specific domains, ZO-1 uniquely contains other motifs, including a leucine zipper motif, a variable 80-amino-acid motif ( $\alpha$ ) resulting from alternative splicing to generate the ZO-1 $\alpha^+$  isoform (as opposed to ZO-1 $\alpha^-$ ), and putative tNLSs and bNLSs (see Table I). The multidomain structure implies that ZO-1, in addition to serving as a cell junction-associated adaptor protein, may also be involved in signal transduction (see below). Studies on the subcellular localization of ZO-1 in cultured cells under subconfluent conditions indicated simultaneous junctional and nuclear localization of ZO-1 (Gottardi *et al.*, 1996). Moreover, nuclear localization of ZO-1 appeared to be dependent on the state of cell-cell contact formation: nuclear localization of ZO-1 was particularly prominent in migrating cells with a loosened state of cell-cell contacts and in cells in the process of locomotion at distinct regions within the intestinal crypt-villus axis. Nuclear accumulation does not seem to be unique to any particular ZO-1 isoform. Dependence of subcellular localization on cell density (extent of cell-cell contact formation) has also been described for the Hippel-Lindau tumor suppressor gene product (Lee *et al.*, 1996) and the influenza virus nucleoprotein (Whittaker *et al.*, 1998), both of which are either nuclear or cytoplasmic at low and high cell density, respectively. A truncated version of ZO-1 consisting of the first 200 amino acids, which contains a putative tNLS/bpNLS within the PDZ1-2 interrepeat sequence (see Table I), was found to be constitutively nuclear. The PDZ1-2 interrepeat sequences are conserved in a subset of MAKUG proteins (group I MAGUK proteins) that are known to localize to specific cytoplasmic domains of the plasma membrane. These include the *Drosophila* lethal(1) discs large-1 tumor suppressor gene product (Dlg; Woods and Bryant, 1991) its human homolog hDlg (Lue *et al.*, 1994), and PSD-95 (Cho *et al.*, 1992; Kistner *et al.*, 1993), that binds with its PDZ domain to the NMDA receptor and Shaker-K $^+$  channels (Kim *et al.*, 1995; Kornau *et al.*, 1995) All of these MAKUG proteins except for PSD-95 have been shown to be able to translocate into the nucleus (Lutchman *et al.*, 1997), implying that a conserved domain may be responsible for nuclear targeting of group I MAGUK proteins. The conserved tNLS/bNLS found within the PDZ1-2 interrepeat sequence seems a potential candidate (Table I).

On the other hand, it has been shown that a mutant hDlg isoform, which lacks the 34-amino-acid I3 insertion shows redistribution from the nucleus to the cytoplasm when overexpressed (Lutchman *et al.*, 1997). Interestingly, the I3 insertion harbors

a tNLS, which is also present in DIg, within a region 38% identical to hDIg I3, and partly in PSD-95. Studies on the subcellular targeting of hDIg have revealed that the PDZ1-2 interrepeat sequence and the I3 domain constitute protein 4.1 binding sites (Lue *et al.*, 1996). Thus, binding to protein 4.1 could result in NLS masking and submembranal retention of hDIg. Such a mechanism of regulating nuclear protein transport has been described for a number of proteins (Jans and Hübner, 1996). Whether the phenomenon of dual subcellular localization is a general property of types of MAKUG proteins remains to be determined, as does their role in nuclear processes.

With respect to the latter, ZO-1 has very recently been reported to be possibly involved in the modulation of the gene expression and in regulating cell cycle progression. This is achieved through association of ZO-1 via its SH3 domain with a newly described transcription factor, ZONAB (ZO-1-associated nucleic acid binding protein; Balda and Matter, 2000). ZONAB, which is homologous to a Y-box transcription factor, has been shown to bind to promotor sequences of genes encoding ErbB-2 and regulators involved in cell cycle progression (Balda and Matter, 2000). Nuclear staining of ZO-2 was also observed in the nucleus of MDCK cells (Gonzalez-Mariscal *et al.*, 1999) (and similar to ZO-1, nuclear appearance of ZO-2 was dependent on the confluence state of monolayer) and along the whole nephron (Gonzalez-Mariscal *et al.*, 2000). The significance of this feature remains to be determined, but like ZO-1, ZO-2 could also play a role in gene regulatory processes.

**b. Symplekin** Symplekin, a 126.5-kDa protein, is a recently identified cytosolic plaque protein of TJs that colocalizes with ZO-1 at the tight junction of epithelial but not endothelial cells (Keon *et al.*, 1996.) In a wide range of cells (e.g., cultured cells derived from polarized and nonpolarized and in cells completely devoid of cell-cell contacts) symplekin was found in the nucleoplasm, with exclusion from nucleoli. In contrast to ZO-1, nuclear localization of symplekin appears to be independent of proliferation. Potential NLSs located within the amino-terminal domain of symplekin (see Table I) could be involved in nuclear translocation. Investigating interactions between proteins of the polyadenylation machinery, Takagaki and Manley (2000) have just recently observed that one protein of this polyadenylation assembling machinery, CstF-64 (cleavage stimulating factor 64), interacts with symplekin. Moreover, symplekin was isolated from cells as part of large complex containing CstF and cleavage-polyadenylation specific factor. These observations imply that symplekin may function in the assembly of the polyadenylation machinery.

**c. Cingulin** Cingulin, a 140-kDa TJ-associated plaque protein (Citi *et al.*, 1989) appears to translocate into nuclei of subconfluent MDCK cells (Citi and Cordegnosi, 1999). The sequence of *Xenopus* cingulin contains a number of NLSs that are located near the amino and carboxy terminus (Table I). Overexpression of

an amino-terminal fragment of cingulin containing the amino-terminal NLS resulted in a predominant localization of this fragment in the nucleus, whereas the carboxy-terminal fragment was found to accumulate in the cytoplasm either in a diffuse pattern or in the form of aggregates (Cordenonsi *et al.*, 1999). Nuclear accumulation of the amino-terminal fragment could also result from passive diffusion through the NPC. However, whether nuclear translocation is a physiological property of cingulin *in vivo* remains to be investigated.

#### 4. Nuclear Signaling by Focal-Contact-Associated Plaque Proteins

The attachment of cells to the extracellular matrix (ECM) at focal contacts occurs through adhesion molecules of the integrin family. Integrins are heterodimeric transmembrane proteins consisting of an  $\alpha$  and  $\beta$  subunit. Several different  $\alpha$  subunits and  $\beta$  subunits have been identified giving rise to numerous combinatorial possibilities (Hynes, 1992), each of which differ with respect to the substrate specificity. Heterogeneity of integrins is further increased by alternatively spliced isoforms (Hynes, 1992). Integrins interact with many components of the ECM and serve as transmembrane bridges between the ECM and the actin-filaments of the cytoskeleton. Some integrins are also involved in cell-cell interaction. Integrin ligation results in the formation of specific complexes between integrins and cytoskeleton-associated proteins such as talin, vinculin,  $\alpha$ -actinin, tensin, and paxillin, which in turn are the basis of linking integrins to actin filaments. Ligation of integrins may also trigger a number of signaling events, including tyrosine phosphorylation, elevation of cytoplasmic calcium, and changes in lipid metabolism.

Because integrins do not possess intrinsic tyrosine kinase activity, intracellular signaling occurs through associating cytoplasmic kinases (e.g., FAK or members of the Src family) and signaling adaptor proteins (e.g., Shc, mSos, Grb2). Recruitment of the SH2-SH3 adapter proteins Grb2 and mSOS1 (the guanine nucleotide exchange factor for Ras-GDP) results in stimulation of GTPase activity of Ras and subsequent activation of MAPK. MAPK activation is known to be involved in phosphorylation, activation, and cellular translocation of transcription factors such as *c-Jun* and *c-Fos* and thereby modulation of gene expression (Hill and Treisman, 1995). This pathway of integrin-dependent signaling to the nucleus relies on a cascade of interacting focal adhesion-associated and cytosolic tyrosine kinases. Some focal contact-associated plaque proteins appear to have the ability to directly translocate into the nucleus, however, suggesting an additional role of these plaque proteins in transmitting signals to the nucleus. Such karyophilic focal contact-associated plaque proteins include vinculin (see above), nexilin, zyxin, and talin (Fig. 4).

**a. *Nexilin*** Nexilin is a novel F-actin binding protein that colocalizes specifically with focal contact-specific plaque proteins (Ohtsuka *et al.*, 1998). Two splice variants of nexilin were identified (b- and s-nexilin, respectively). Whereas b-nexilin

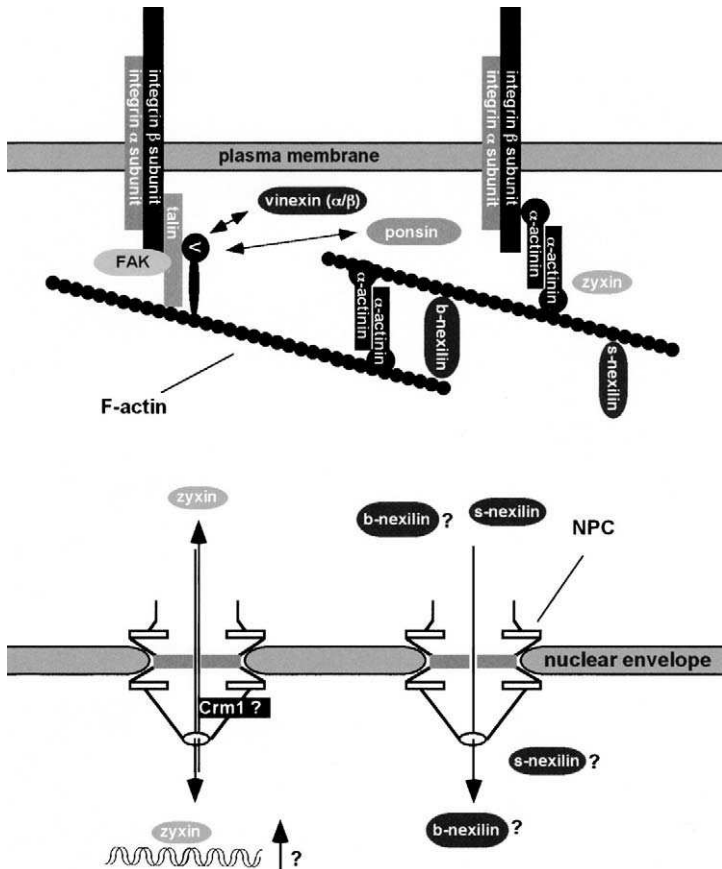


FIG. 4 Nuclear signaling by focal contact-associated plaque proteins. Some of the possible interactions between focal contact-associated plaque and transmembrane proteins are shown. Talin and  $\alpha$ -actinin bind to the cytoplasmic domain of the integrin  $\beta$  subunit (Horwitz *et al.*, 1986).  $\alpha$ -Actinin is an actin-binding and cross-linking protein. Talin has binding sites for vinculin and actin. Nexilin is a novel F-actin binding protein for which the splice variants b- and s-nexilin have been identified (Ohtsuka *et al.*, 1998). Whereas b-nexilin has two actin binding sites, and thus displays F-actin cross-linking activity, s-nexilin lacks one F-actin binding site (Ohtsuka *et al.*, 1998). Zyxin (which can interact with  $\alpha$ -actinin; Crawford *et al.*, 1992) as well as the vinculin-binding proteins ponsin (Mandai *et al.*, 1999) and vinexin (Kioka *et al.*, 1999), whose role in focal adhesion assembly is not yet known, all localize to focal adhesions. Both zyxin (Nix and Beckerle, 1997) and s-nexilin (Ohtsuka *et al.*, 1998) can localize to the nucleus. Zyxin is able to shuttle between the cytoplasm and nucleus. While the nuclear export factor CRM1 probably mediates nuclear export of zyxin, the factor involved in nuclear import of zyxin has not yet been identified. The significance of the nuclear localization of zyxin and s-nexilin is currently unknown. However, nuclear zyxin could play a role similar to that of the structurally related protein LPP (LIM-containing lipoma-preferred partner), which has been shown to display transcriptional activation activity (Petit *et al.*, 2000). NPC, nuclear pore complex; V, vinculin; FAK, focal adhesion kinase.

contains two F-actin binding sites, one within its amino terminus and the second in the middle of the protein, s-nexilin lacks the amino-terminal F-actin binding site due to two splicing regions within the amino terminus. Thus, b-nexilin but not s-nexilin shows F-actin cross-linking activity. Both proteins display tissue-specific expression with b-nexilin being expressed mainly in brain and testis while s-nexilin is expressed in testis, spleen, and fibroblasts. Both splice variants seem to be specifically expressed in nonepithelial cells. Studies on the subcellular localization of overexpressed nexilin and truncated mutants thereof show nuclear accumulation of s-nexilin and some b- and s-nexilin deletion mutants. Consistent with these findings is the fact that both splicing variants contain several tNLS/bNLSs (see Table I). The significance of nuclear accumulation of nexilin is still unknown.

**b. Zyxin** Zyxin, a low abundance phosphoprotein, colocalizes with integrin adhesion molecules at sites of cell-substratum attachment (Crawford and Beckerle, 1991; Crawford *et al.*, 1992; Sadler *et al.*, 1992). Like many other cytoplasmic plaque proteins, zyxin displays a multidomain structure, including a proline-rich region which enables zyxin to associate with proteins such as ENA/VASP,  $\alpha$ -actinin, and VAV (Pavalko and Burridge, 1991; Crawford *et al.*, 1992; Reinhard *et al.*, 1995; Hobert *et al.*, 1996) and three LIM motifs (cysteine- and histidine-rich zinc finger domains) known to be involved in protein–protein interaction and possibly DNA binding (Sadler *et al.*, 1992; Pérez-Alvardo *et al.*, 1994; Wu and Gill, 1994; Schmeichel and Beckerle, 1997, 1998). Interestingly, zyxins from different species display a conserved amino acid motif that includes a putative leucine-rich NES (see Table I). Transfection and microinjection studies (Nix and Beckerle, 1997) indicate that the NES of zyxin is functional in mediating the export of karyophilic proteins from the nucleus, whereas the deletion of the NES resulted in a prominent localization of NES-deleted zyxin within the nucleus. This indicates that zyxin also possesses a nuclear localization activity. Moreover, zyxin was shown to be able to shuttle between cytoplasm and the nucleus, implying that nuclear accumulation of zyxin may be accomplished either through a thus far unidentified nuclear import signal or by binding to a karyophilic carrier. The presence of an NES may allow the cell to regulate subcellular distribution of zyxin, possibly through NES masking. It is known that LIM domain-containing proteins are involved in transcriptional control (Sadler *et al.*, 1992; Sánchez-García and Rabbitts, 1994; Gill, 1995), with LIM domains being the principal determinant localizing certain LIM-containing proteins to the nucleus (Arber and Caroni, 1996). The possible role of zyxin in nuclear processes, however, has thus far not been addressed; molecular characterization of the domains involved in nucleocytoplasmic shuttling of zyxin and identification of binding partners should reveal the true functional importance of nuclear zyxin and its nucleocytoplasmic shuttling capability.

One clue as to a possible role of zyxin in the nucleus comes from studies on LPP (LIM-containing lipoma-preferred partner; Petit *et al.*, 2000) which is structurally related to zyxin (contains a proline-rich amino-terminal region and

three LIM-domains at the carboxy terminus) and localizes in focal contacts as well as adherens junctions. Like zyxin, LPP contains a functional NES mediating its CRMI-dependent nuclear export, and localizes in the nucleus of cells treated with leptomycin B. Because LPP does not contain an NLS, its nuclear transport of LPP may occur through its association with an NLS-bearing protein. Employing a GAL4-based transactivation assay, it was found that LPP displays transactivation activity, which requires the proline-rich region and the LIM domains. Although these regions are not well conserved in zyxin, the nuclear role of zyxin could be similar to that of LPP, which is in controlling gene transcription.

**c. Talin** Talin is a cytoskeleton-associated protein that specifically localizes at focal substrate contacts in several tissue cells (Drenckhahn *et al.*, 1988) and is thought to link the cytoplasmic domain of integrin receptors to the actin cytoskeleton. Talin has domains of  $\sim$ 200 and 47 kDa, which can be separated proteolytically by a variety of proteases, including the  $\text{Ca}^{2+}$ -activated protease calpain II, which is concentrated at points of cell–substratum contact. Although the physiological significance has not been determined, cleavage of talin has been shown to occur in platelets during aggregation and in focal contacts in CHO cells (Tranqui and Block, 1995). The 47-kDa domain, which contains a region with homology to the ERM (ezrin, radixin and moesin; see below) family of actin-binding proteins can bind to charged lipids (Niggli *et al.*, 1994), contains an actin binding site, and is important for targeting talin to cell–substrate junctions (Nuckolls *et al.*, 1990). However, a fusion protein containing the N-terminal actin binding site of talin alone showed significantly reduced resistance to Triton X-100 extraction, implying a less important role for this site in actin binding (Hemmings *et al.*, 1996). The  $\sim$ 200-kDa C terminus contains a binding site for the  $\beta 1$  integrin cytoplasmic domain (Horwitz *et al.*, 1986), as well as two actin- and three vinculin-binding domains. Microinjection of the fluorescently labeled 47-kDa domain of chicken and human talin into fibroblasts revealed significant nuclear staining in the case of the 47-kDa domain of human talin, in addition to diffuse cytoplasmic distribution and concentration at focal contacts (Nuckolls *et al.*, 1990). Interestingly, both chicken and human talin contain a potential tNLS approximately 30 amino acids upstream of the calpain II site, which is also conserved in mouse and *Caenorhabditis elegans* talin. Immobilization of talin at focal contacts through binding of the C-terminal domain to both F-actin and integrin  $\beta$  (Horwitz *et al.*, 1986) could be a way to regulate nuclear signaling of the 47-kDa fragment after it has been released by cleavage by membrane-bound calpain II/calpain II-like proteases. However, whether such a role exists for the small fragment in the nucleus remains to be investigated.

Examples of nuclear access of membrane-associated proteins has been shown for proteolytic fragments of members of the family of Notch-1 ligand-activated transmembrane proteins (Kidd *et al.*, 1998; Lecourtois and Schweigert, 1998; Schroeter *et al.*, 1998; Struhl and Adachi, 1998). Cytoplasmic nuclear signaling occurs through proteolytic release of the intracellular domain of Notch (NICD)

followed by transcriptional changes in the nucleus due to association of NICD with members of the *CSL* [where *CSL* stands for CBF1, Su(H), Lag-1] family of DNA-binding proteins. Ligand-induced proteolytic processing has also been shown for the sterol regulatory-element-binding protein, an integral membrane protein of the endoplasmic reticulum (Brown and Goldstein, 1997). Proteolysis occurs at low cholesterol and creates a fragment that translocates to the nucleus where it serves as a transcription factor. Nuclear localization of a C-terminal deleted form of ezrin seems also to be regulated through protease-dependent processing of full length ezrin (see below).

#### **IV. Nuclear Signaling by Nonjunctional Cytoskeletal Proteins**

##### **A. Actinin 4**

Actinin 4 belongs to a family of highly homologous proteins responsible for cross-linking actin filaments and connecting them to the plasma membrane. So far, three human  $\alpha$ -actinin isoforms have been found:  $\alpha$ -actinin 1 in smooth and nonmuscle (Millake *et al.*, 1989),  $\alpha$ -actinin 2 (expressed in skeletal and cardiac muscle),  $\alpha$ -actinin 3 (expressed only in skeletal muscle) (Youssoufian *et al.*, 1990; Beggs *et al.*, 1992). The smooth muscle  $\alpha$ -actinin isoform is localized at focal contact-like membrane-associated dense plaques and at cytoplasmic Z-line-like dense bodies (the latter are structures analogous to the muscle Z-line). In cardiac tissue  $\alpha$ -actinin is found in the fascia adherens of the intercalated discs as well as in association with Z-discs. In most other cells,  $\alpha$ -actinin is also localized at adherens-type cell-cell junctions (Knudsen *et al.*, 1995) and focal substrate contacts (Otey *et al.*, 1990).  $\alpha$ -Actinin also binds to the cytoskeletal proteins zyxin (Crawford *et al.*, 1992), vinculin (Wachsstock *et al.*, 1987) and  $\alpha$ -catenin (Nieset *et al.*, 1997). Despite high homology between members of this family,  $\alpha$ -actinin 4 has been found not to be localized at focal substrate contacts and adherens junctions, but mainly diffusively distributed throughout the cytoplasm, at the ends of actin stress fibers, and also within the nucleus. In a certain population of human cancer cells,  $\alpha$ -actinin 4 was found to be localized exclusively within the nucleus (Honda *et al.*, 1998). The physiological relevance of nuclear  $\alpha$ -actinin 4 is not clear. PIP2 (phosphatidylinositol 4,5-bisphosphate), a regulator of actin-binding proteins and a substrate for the phosphatidyl inositol 3 (PI3) kinase, seems to influence subcellular localization of  $\alpha$ -actinin 4, since treating cells with Wortmannin, a PI3 kinase inhibitor, results in nuclear translocation of  $\alpha$ -actinin 4 (Honda *et al.*, 1998). Loss of binding to the cytoskeleton also leads to nuclear translocation of  $\alpha$ -actinin 4 (Honda *et al.*, 1998). Because  $\alpha$ -actinin 4 does not appear to contain a conventional NLS, the pathway by which it enters the nucleus, whether direct or through an indirect mechanism (piggyback), remains unclear, as does its precise role in nuclear processes (Fig. 5).

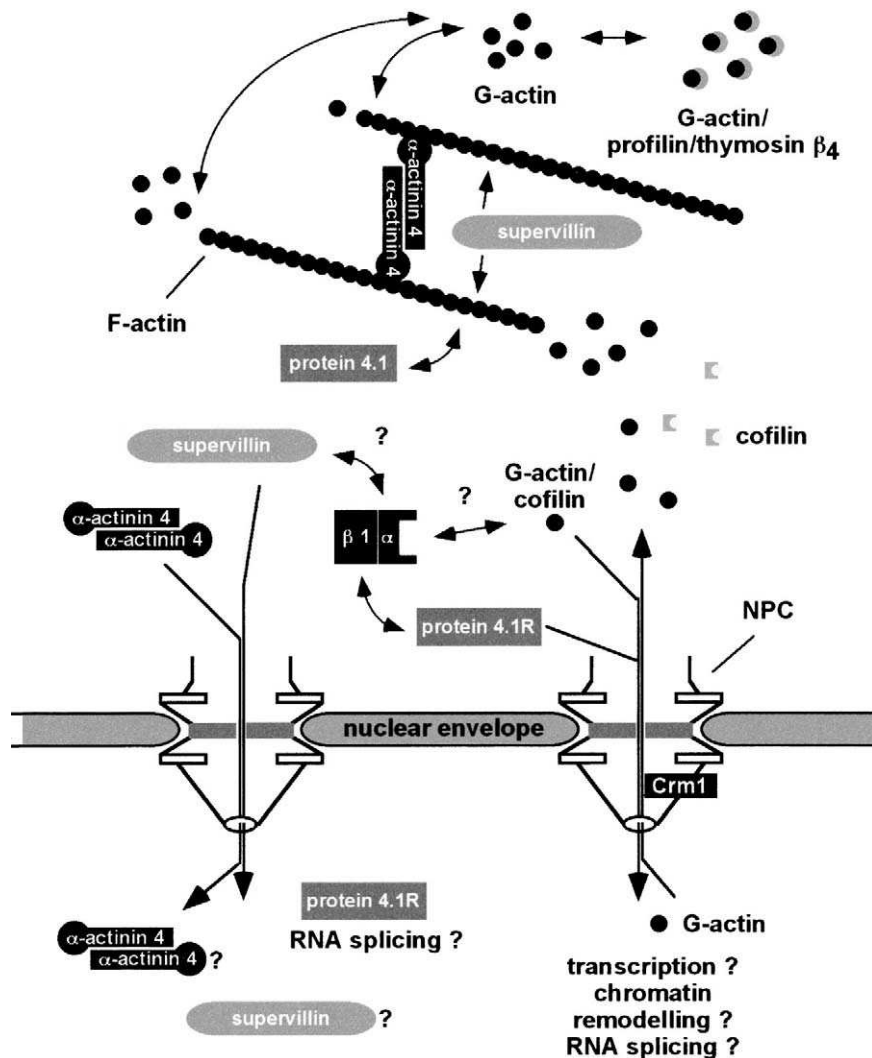


FIG. 5 Nuclear signaling by cytoskeletal proteins. Monomeric actin, G-actin, which is in a dynamic equilibrium with filamentous actin, F-actin, interacts with a number of low molecular weight proteins (e.g., profilin, thymosin  $\beta_4$ , cofilin), which regulate polymerization and depolymerization of F-actin. G-actin can enter the nucleus under certain circumstances (heat shock, DMSO treatment) in an NLS-dependent manner through association with cofilin (Ohta *et al.*, 1989; Nebl *et al.*, 1996) and may involve importin  $\alpha/\beta 1$ . Nuclear export is mediated through two NESs and can be blocked through LMB, indicating that nuclear export of G-actin involves Crm1 (Wada *et al.*, 1998). Inside the nucleus G-actin may participate in structural and dynamic nuclear processes. Supervillin, an F-actin bundling

## B. Protein 4.1

Structural proteins of the cytoskeleton involved in dynamic adhesive processes such as changes in cell morphology, stability, mobility, proliferation, etc., seem to play a novel role in nuclear signaling. Such duality with respect to subcellular distribution has been described for isoforms of the structural protein 4.1 of red blood cells (4.1R), a crucial molecular linker between the cytoskeleton and plasma membrane through interactions with several proteins including spectrin, actin, tubulin, glycophorin C, and anion exchanger 1 (AE1, band 3). The 4.1R isoforms are encoded by a single gene and have been found in erythroid as well as nonerythroid cells (Anderson *et al.*, 1988). The diversity of 4.1R isoforms is generated by complex alternative splicing and the use of at least two translation initiation sites (generating low and high molecular weight isoforms), as well as posttranslational modifications (Conboy, 1993). The roles of protein 4.1R isoforms outside the erythroid cell lineage have not yet been defined. In nucleated cells, protein 4.1R isoforms have been detected at subcellular sites such as cell–cell and cell–matrix contacts, and perinuclear regions (centrosomal and Golgi structures), as well as within the nuclear matrix (Krauss *et al.*, 1997). Nuclear protein 4.1R isoforms could play a structural role since known binding partners for protein 4.1R, including spectrin (Bachs *et al.*, 1990; Beck *et al.*, 1994), myosin (Berrios and Fisher, 1986; Hagen *et al.*, 1986; Milankov and DeBoni, 1993), and actin (see below), have also been identified in the nucleus. Rather than being associated with the nuclear envelope and the underlying lamin network, however, nuclear protein 4.1R isoforms appear to be distributed throughout the nucleoplasm and within nuclear speckles (Correas, 1991; De Cárcer *et al.*, 1995; Krauss *et al.*, 1997; Lallena and Correas; 1997) but are excluded from nucleoli. Nuclear protein 4.1 epitopes undergo dramatic rearrangements during cell division, being nucleoplasmic and centrosomal during interphase, in the mitotic spindle during mitosis, in perichromatin during telophase, and in the midbody of the cytoplasmic bridges during cytokinesis (Krauss *et al.*, 1997). Nuclear protein 4.1 epitopes also appear to colocalize with factors involved in pre-mRNA splicing (e.g., the non-snRNP splicing protein SC-35; see below) and DNA replication (e.g., the proliferating cell nuclear antigen PCNA, an accessory protein for the replicative DNA polymerase delta). Subnuclear distribution studies under various conditions such as heat shock and inhibition of transcription revealed tight colocalization of protein 4.1R isoforms

---

protein, enters the nucleus in an NLS-dependent manner. An NLS in the center of supervillin is the most dominant nuclear targeting signal (Wulffkuhle *et al.*, 1999). The sequences responsible for nuclear translocation of  $\alpha$ -actinin 4 are still unknown as well as the nuclear import factors involved. Isoforms of protein 4.1R can enter the nucleus in either an NLS-dependent (involving exon 5, 13, and 16) or NLS-independent (requiring the core region) manner. Nuclear protein 4.1R isoforms may play a role in RNA splicing. NPC, nuclear pore complex; DMSO, dimethylsulfoxide; G-actin, monomeric actin; F-actin, polymeric actin;  $\alpha/\beta 1$ , importin  $\alpha/\beta 1$ ; LMB, leptomycin B.

with SC35 (Lallena and Correas, 1997). Immunoprecipitation experiments with HeLa cell extracts additionally revealed binding of nuclear protein 4.1R isoforms to other factors that are directly involved in splicing (Lallena *et al.*, 1998). These findings suggest that nuclear protein 4.1R isoforms may play a role as nuclear structural elements to which splicing factors attach (Fig. 5).

Molecular cloning of two low molecular weight protein 4.1R isoforms (protein 4.1H and protein 4.1E) revealed differential nuclear targeting properties (Lallena *et al.*, 1998; Luque *et al.*, 1998), attributable to the fact that protein 4.1H contains a cluster of basic amino acids generated through joining the constitutive exon 13 with the alternative exon 16 (see Table I). Mutagenesis of this putative NLS abolished nuclear targeting by protein 4.1H (Luque *et al.*, 1998), although fusion of the protein 4.1H-NLS to the cytoplasmic reporter protein  $\beta$ -galactosidase failed to affect its nuclear localization. Further studies revealed that, additional to the 4.1H-NLS, an EED motif within exon 5 was necessary for efficient binding of nuclear protein 4.1R importin  $\alpha$  and nuclear translocation, even though both domains are separated by several hundred amino acids (Gascard *et al.*, 1999). The EED motif has been also shown to serve as a binding site to RRR motifs of AE1 (Jöns and Drenckhahn, 1992). The importance of sequence additional to the NLS in enhancing nuclear localization has been shown for the importin  $\alpha/\beta$ 1-recognized conventional NLSs of T-ag (Rihs *et al.*, 1991; Jans and Jans, 1994; Hübner *et al.*, 1997; Xiao *et al.*, 1997) and the *Drosophila* Rel family transcription factor Dorsal (Briggs *et al.*, 1998).

A high molecular weight isoform of protein 4.1R (135-kDa protein 4.1) has recently been found to interact with the nuclear mitotic apparatus (NuMA) protein (Matajagajasingh *et al.*, 1999), which is known to enhance organization and stability of the mitotic spindle. Both the 135-kDa 4.1R isoform and NuMA partially colocalize in the interphase nuclei of MDCK cells, and redistribute to the spindle pole early in mitosis, implying a role for the 135-kDa protein 4.1R isoform in cell division. In addition to the 135- and 80-kDa 4.1R isoforms generated through the alternatively used translation initiation sites, two novel  $\sim$ 68-kDa protein 4.1R isoforms generated from an initiation codon in exon 8 have been found to localize strongly in the nucleus (Gascard *et al.*, 1998). Both isoforms contain the alternative exon 16, which is critical for nuclear localization. Thus, the subcellular distribution of protein 4.1R isoforms appears to be regulated at least in part through the inclusion of exons affecting their nuclear localization. The NLS in exon 16, although not sufficient for efficient nuclear targeting on its own, plays a critical role.

However, other isoforms of protein 4.1R, lacking exon 5 and 16, are still able to localize to the nucleus, suggesting that sequences (comprising a region referred to as the core region) other than those encoded by exon 5 and 16 confer nuclear translocation to protein 4.1R (Luque and Correas, 2000). Interestingly, core region-containing isoforms lacking exon 16 showed cytoplasmic localization when exon 5 was expressed, implying that exon 5 reduces nuclear targeting but is necessary for nuclear targeting in the case of exon 16-containing isoforms (Luque and Correas, 2000).

### C. Supervillin and Mbh1

Two novel F-actin binding proteins, the 205-kDa protein supervillin, an F-actin bundling protein (Pestonjamas *et al.*, 1997), and the 45-kDa  $\text{Ca}^{2+}$ - and polyphosphoinositide-regulated actin-filament barbed-end capping protein, Mbh1 (myc basic motif homolog-1)/gCap39 (Yu *et al.*, 1990; Prendergast and Ziff, 1991), have recently been identified. Both share strong homology to members of the gelsolin family, which are involved in  $\text{Ca}^{2+}$ -dependent control of actin polymerization by monomer binding, filament capping, and severing. Originally characterized as a component of bovine neutrophil plasma membranes, supervillin has been found to colocalize with E-cadherin in confluent MDBK cells at sites of initial and established cell-cell contacts (Prendergast and Ziff, 1991). Supervillin was also found to concentrate at or near focal contacts sites (Wulffkuhle *et al.*, 1999), whereas in subconfluent cells lacking significant amounts of cell-cell contacts, supervillin was also found within the nucleus, in addition to a cytoplasmic- and membrane-associated pool. Supervillin contains a number of putative NLSs within its N-terminal half (see Table I). Studies of GFP fusion proteins revealed nuclear targeting of a protein including the amino-terminal domain of supervillin (amino acids 1–1009). Deletion of amino acids 831–1009 resulted in targeting of the corresponding fusion protein (amino acids 1–830) to cytoplasmic actin-containing structures rather than the nucleus, suggesting that a putative NLS at residues 931–935 (RPKRR) may play a role in nuclear targeting, whereas the basic sequences in the N terminus may mediate targeting to the cytoskeleton (Fig. 5; Wulffkuhle *et al.*, 1999). Because supervillin can be found in the cytoplasm as well as plasmalemmal and nuclear sites, it may play a role in transferring signals from the plasma membrane and the cytoplasm to the nucleus. In addition, the exclusion of supervillin from the nucleus in confluent cultures in contrast to its nuclear location in subconfluent cultures suggests that nuclear accumulation of supervillin may occur in an adhesion- or cell-cycle-dependent manner. Because supervillin contains several consensus phosphorylation sites, cell-cycle-dependent nuclear translocation of supervillin might be regulated through phosphorylation. Cell-cycle-dependent phosphorylation at sites close to NLSs has been shown to regulate the nuclear transport of many proteins (Jans and Hübner, 1996). However, whether nuclear signaling by supervillin is regulated through phosphorylation remains to be investigated, as does its possible role in nuclear processes.

The actin-binding protein Mbh1/gCap39 is distinguished by its homology to gelsolin (Yu *et al.*, 1990) and by a basic helix-loop-helix structural motif found in a variety of nuclear proteins such as *c*-Fos and *c*-Jun (Prendergast and Ziff, 1991). Like supervillin, Mbh1/gCap39 shows actin-binding activity and is structurally related to the amino-terminal domain of gelsolin (50% identity). Mbh1/gCap39 differs from the latter in that it caps and does not sever actin filaments. Within its amino terminus, Mbh1/gCap39 contains a motif that is similar to NLSs found in

a number of nuclear oncoproteins (see Table I) which consist of helix-breaking amino acids followed by a cluster of positively charged amino acid residues (Dang and Lee, 1989). Indeed, immunolocalization and overexpression studies identified Mbh1/gCap39 in the nucleus, whereas gelsolin was excluded (Prendergast and Ziff, 1991; Onoda *et al.*, 1993). Nuclear accumulation of this small protein seems to be modulated neither by proliferative signals nor by cell density. Because many actin-binding proteins can be found in the nucleus (e.g., cofilin, and see above), mbh1/pCap39 may play a structural role in the nucleus. That Mbh1/gCap39 enters the nucleus by diffusion cannot be ruled out, because its molecular weight is well below the exclusion limit for passive diffusion through the NPC.

#### D. Actin

Actin, involved in fundamental cellular processes such as cytokinesis, cell locomotion, cell morphology, cell motility, etc., exists in a dynamic equilibration between its monomeric (G-actin) and polymeric forms (F-actin). In addition to its localization in the cytoplasm, actin and actin-containing filaments have been reported to exist in interphase nuclei (Jockusch *et al.*, 1974; Milankov and De Boni, 1993; Sahlas *et al.*, 1993; Amankwah and De Boni, 1994; De Boni, 1994; Soyer-Gobillard *et al.*, 1996) as well as in the nuclei of amphibian oocytes (Clark and Merriam, 1977; Clark and Rosenbaum, 1979; Gounon and Karsenti, 1981; Parfenov *et al.*, 1995). Although nuclear actin has also been found in cells stressed with dimethylsulfoxide (DMSO) (Fukui and Katsumaru, 1979; Sanger *et al.*, 1980; Wehland *et al.*, 1980) or heat shock (Welch and Suhan, 1985; Iida and Yahara, 1986; Nishida *et al.*, 1987), the idea that actin may normally have a nuclear function is not widely accepted. Gonsior *et al.* (1999) recently showed unequivocally for the first time that nuclear actin can indeed occur in untreated cells in the form of discrete supramolecular structures, the occurrence of which appears to be differentiation dependent. Due to its small size (42 kDa), G-actin should be able to enter the nucleus by diffusion, but in many cases is found exclusively in the cytoplasm, implying that specific mechanisms may be preventing actin nuclear translocation. One possible mechanism by which nuclear translocation of G-actin may be prevented is through cytoplasmic sequestration of actin by actin-binding proteins such as profilin or thymosin  $\beta_4$ .

The mechanism by which actin reaches the nucleus may involve the actin-binding protein cofilin, which is known to translocate into the nucleus in a phosphorylation-regulated, NLS-dependent manner upon heat shock or DMSO treatment (Ohta *et al.*, 1989; Nebl *et al.*, 1996); other actin-binding proteins able to translocate to the nucleus could play a similar role. In contrast to its nuclear entry, nuclear exit of actin appears to be signal dependent, mediated by two functional NESs (Wada *et al.*, 1998). Export of nuclear actin can be blocked by leptomycin B (LMB), a specific inhibitor of Crm1/exportin-mediated nuclear export. The

subcellular distribution of actin under any given circumstance would thus appear to be the product of cofilin/actin-binding protein-mediated NLS-dependent nuclear import, and NES-dependent actin nuclear export or cytoplasmic retention by binding to cytoplasmic/cytoskeletal proteins. Because it is a major structural constituent of the cytoskeleton, actin may play a role in nuclear skeletal processes, especially in response to stress, and, consistent with this idea, overexpression of NES-mutated actin results in a decrease in the proliferative potential of the cells accompanied by a shrinkage of the nucleus (Wada *et al.*, 1998). Alternatively, it has also been variously proposed that actin may be involved in transcription (Scheer *et al.*, 1984), in the transport of RNA (Sahlas *et al.*, 1993), in chromatin remodeling (Rando *et al.*, 2000 and references therein), and/or in the function of a motor system important for chromatin dynamics (Milankov and De Boni, 1993). Figure 5 displays some of actin's features within different cellular compartments.

### E. Intermediate Filaments

Intermediate filaments, presumed to exert effects on cell shape, cell–cell interaction, adherence to the substratum, cell locomotion, cell division, etc., are widely distributed in eukaryotic cells. IFs share a common structural characteristic, comprising a central  $\alpha$ -helical rod domain flanked by variable non- $\alpha$ -helical head and tail domains. Among IFs, nuclear lamins, which are found exclusively in the cell nucleus, have been implicated as important structural determinants of nuclear size and shape. NLS-dependent nuclear localization of lamins is regulated by phosphorylation by protein kinase C (Hennekes *et al.*, 1993). It has also been suggested that nuclear lamins may also play a role in DNA replication and nuclear envelope formation, thus being integrally involved in key nuclear processes. Interestingly, all typical nonepithelial IF proteins (including vimentin, desmin, glial fibrillary acidic protein, neurofilament triplet proteins) have been shown to be nucleic acid-binding proteins (Traub and Nelson, 1983; Traub *et al.*, 1985; Vorgias and Traub, 1986; Shoeman *et al.*, 1988; Shoeman and Traub, 1990). In the case of vimentin, which is one of the most prominent phosphoproteins found in many nonepithelial cells and especially in mesenchyme-derived cells, proteolytic digestion identified the head domain to be the principal DNA-binding site (Shoeman *et al.*, 1988). In addition, the N terminus of vimentin is structurally related to certain prokaryotic ssDNA-binding proteins, nuclear matrix proteins, and transcription factors (Traub and Shoeman, 1994). It thus appears possible that IFs may play a role in DNA-linked nuclear processes. This is consistent with the occurrence of other cytoskeletal proteins in the interphase nucleus, such as actin (see above), actin-binding proteins (e.g., myosin, spectrin), and tubulin (Douvas *et al.*, 1975; Ankenbauer *et al.*, 1989; Bachs *et al.*, 1990; Milankov and De Boni, 1993; Pereira *et al.*, 1998). Although vimentin does not appear to possess a canonical NLS, it could gain nuclear entry

during mitosis or through a karyophilic carrier, taking the form of either an NLS-containing or DNA-containing carrier protein. With respect to the latter, it has recently been demonstrated that single-stranded oligonucleotides as well as superhelical, circular DNA can effect vimentin nuclear import (Hartig *et al.*, 1998a, 1998b), although the physiological significance of such observations is unclear. Once inside the nucleus, vimentin or other IF proteins could exert an important role in nuclear events.

An example of IF-associated proteins that exhibit nuclear localization through a functional importin  $\alpha/\beta 1$ -recognized bNLS are particular low molecular weight (LMW) isoforms of microtubule-associated protein-2 (MAP2) (Loveland *et al.*, 1999). Alternative splicing in tissues such as brain and testis leads to the generation of novel LMW MAP2 isoforms containing the bNLS-containing exon 10 of the MAP2 gene, which appear to be able to translocate into the nucleus (in testicular germ cells, in particular). The role of nuclear localized MAP2 is unclear, but because LMW MAP2 binds tubulin, calmodulin, and various isoforms of the PK-A RII subunit, a nuclear cotransport role for one or all of these would seem quite possible. In this context, it is significant that the regulated pattern of MAP2 mRNA expression in the testis coincides with the progression of the germ cells into their postmitotic phase of development, and that MAP2 protein is detected in the nucleus of germ cells in the later stages of meiosis and in the nuclei of round spermatids. This correlates with the time in development at which calmodulin is reported to move from the cytoplasm to the nucleus of germ cells. Hence, cell-cycle-regulated movement of the bNLS-containing LMW MAP2 into the nucleus may directly mediate accompanying calmodulin movements. A consensus cyclin-dependent kinase phosphorylation site close to the MAP2 NLS may be of significance in this context (Jans *et al.*, 1995; Jans and Hübner, 1996).

#### F. PEBP2 $\beta$ /CBF $\beta$

PEBP2 $\beta$ /CBF $\beta$  is a constituent of the heterodimeric transcription factor PEBP2/CBF, where the  $\beta$  subunit dimerizes with PEBP2 $\alpha$ /CBF $\alpha$  to increase its binding to the enhancers of murine polyomavirus and leukemia virus. Nuclear translocation of PEBP2 $\beta$ /CBF $\beta$  is a prerequisite for PEBP2/CBF function. Interestingly the  $\alpha$  subunit was found to be constitutively localized within the nucleus, whereas the  $\beta$  subunit was conditionally localized within the cytoplasm. Immunohistochemical studies showed differentiation-dependent localization of PEBP2 $\beta$ /CBF $\beta$ , i.e., cytoplasmic in skeletal myogenic cells of murine embryos and nuclear in multinucleated myotubes (Chiba *et al.*, 1997). In skeletal muscle fibers PEBP2 $\beta$ /CBF $\beta$  was found to colocalize with  $\alpha$ -actinin at the Z-lines (Chiba *et al.*, 1997). It was also shown that PEBP2 $\beta$ /CBF $\beta$  colocalizes with actin-filament stress fibers and vinculin (Tanaka *et al.*, 1997), implying an affinity of

PEBP2 $\beta$ /CBF $\beta$  for components of the actin filament cytoskeleton. These observations provide a further example for the idea that not only cytoplasmic retention factors, but also the cytoskeleton itself, may play a direct role in anchoring nuclear proteins in the cytoplasmic space to prevent their nuclear import.

### G. ERM

ERM proteins such as ezrin, radixin, and moesin constitute a family of closely related proteins involved in the attachment of actin filaments to the plasma membrane at specialized micro domains, such as microvilli, adherens junctions, and the cleavage furrow. They have a defined domain structure, whereby the N-terminal's  $\sim$ 300 residues constitute a protease-resistant domain with homology to erythrocyte protein 4.1 and talin. This domain harbors N-ERMAD (ERM-associated domain) activity and binding sites for PIP2 and a specific group of integral membrane proteins (see below); the C-terminal's  $\sim$ 100 residues contain C-ERMAD activity and the F-actin-binding site. Ezrin has been proposed to function as a membrane-associated protein linking actin filaments to various integral membrane proteins such as CD44, CD43, and ICAM-1, -2, and -3. Interestingly, it was recently found that both normal and transformed human cells, when immunostained for ezrin, revealed nucleolar staining that was attributable to an antigen that appears to represent a 55-kDa cleavage product of ezrin, lacking C-terminal residues (Kaul *et al.*, 1999). Full-length 81-kDa ezrin was not detected in nuclear lysates in this study, but was detected in another study (Gutmann *et al.*, 1999). Studies investigating the subcellular localization of GFP-ezrin fusion proteins showed nuclear fluorescence of a C-terminally deleted GFP-ezrin fusion protein, whereas full-length GFP-ezrin was mostly cytoplasmic (Kaul *et al.*, 1999). This implies that removal of the C-terminal domain, containing the C-ERMAD and F-actin binding activity, reduces the ability of ezrin to bind to the cortical cytoskeleton. The putative NLSs (see Table I) of ezrin are absent from the actin-binding C-terminal domain, implying that it is not directly involved in nuclear transport.

The cleavage mechanism is obscure but there is some evidence that the Ca<sup>2+</sup>-dependent protease calpain may be involved (Hanzel *et al.*, 1991; Yao *et al.*, 1993). Almost all putative NLSs within the sequence of ezrin are conserved in the related proteins radixin and moesin, but nuclear localization of these ERM family members has not been reported. Merlin, another ERM-related protein, has been reported to be able to localize to the nucleus (Hitotsumatsu *et al.*, 1997; Xu *et al.*, 1998). However, merlin lacks an actin-binding domain and shares only low homology with the C-terminal domain of ezrin. This is consistent with the idea that the C terminus of ezrin is responsible for binding to the cytoskeleton. As an adaptor molecule between integral membrane proteins and the cortical cytoskeleton, ezrin and possibly other related ERM proteins may have a role in relaying information from the plasma membrane to the nucleus.

## V. Concluding Remarks

The recent progress in the area of nucleocytoplasmic protein transport has contributed to our understanding of how communication between the cytoplasm and the nucleus takes place and how the regulation of nuclear protein transport influences cell function. As outlined above, a number of proteins have been recently identified that not only participate in the formation of cell-to-cell and cell-to-substratum contacts, or are structural constituents of the cytoskeleton, but also seem to be able to translocate to and reside within the nuclear compartment. The role of these proteins in nuclear processes is largely unclear, although the fact that plaque proteins play an important role in cellular stability and flexibility implies that they may, of course, exert such a structural role within the nucleus in response to various conditions such as stress or changes during development and growth. Studies investigating the role of plaque proteins or cytoskeletal proteins in nuclear processes such as apoptosis or mitosis have not yet been performed, although there are some examples of plaque proteins implicated directly in the processes of transcriptional regulation ( $\beta$ -catenin, ZO-1), polyadenylation (symplekin), and mRNA splicing (protein 4.1).  $\beta$ -Catenin appears to play an important role in activation of the transcription factor LEF, and ZO-1 which associates with ZONAB (a Y-box transcription factor) seems to regulate expression of genes encoding ErbB-2 and regulators involved in cell cycle progression. Symplekin, which has been found to bind to a protein of the polyadenylation machinery, seems to play a role in the assembly of the polyadenylation machinery, whereas protein 4.1, which colocalizes with spliceosome assembly factors in the nucleus, seems to be involved in the regulation of RNA splicing. Since the expression of nuclear protein 4.1 isoforms depends on tissue-specific and developmentally, regulated alternative splicing (Tang *et al.*, 1998; Conboy *et al.*, 1991; Chasis *et al.*, 1993), nuclear protein 4.1 isoforms may play a role in regulating cell maturation/differentiation or embryonic development through control of alternative splicing of various other proteins. Whether other plaque proteins will be shown to have comparable, apparently direct roles in nuclear processes remains to be determined.

In terms of other mechanisms by which plaque proteins may modulate transcription, one possibility is that, independent of their own nuclear translocatory properties, plaque proteins could sequester and immobilize nuclear signaling molecules at the membrane and prevent them from nuclear entry. Extracellular signals at the cell surface (e.g., receptor activation) could then trigger rapid dissociation and subsequent nuclear translocation of these signaling molecules to modulate transcriptional activity. In terms of their intrinsic ability to translocate into the nucleus, a role of plaque proteins may be to mediate cotransport of specifically bound signaling molecules or cytoskeletal components to the nucleus through a piggyback mechanism (e.g., actin in the case of cofilin). The fact that plaque proteins contain binding sites for a number of other proteins, including signaling molecules

such as kinases, calmodulin, etc. (see above), means that their redistribution to the nucleus may not only cotranslocate signaling molecules, but also create binding sites for them within the nucleus. This may be central to nuclear processes such as regulation of transcription, e.g., through the phosphorylation of nuclear transcription factors. Thus, although the transport of cytoskeletal components to the nucleus is clearly of great importance in nuclear reshaping during development or in response to stress, it may also play an important role in regulating gene expression.

Significantly, there is also a growing body of evidence that signal-mediated nuclear-cytoplasmic transport processes may involve the cytoskeleton as a dynamic component. Nucleocytoplasmic shuttling by the glucocorticoid receptor, for example, has been shown to require an intact cytoskeleton (Galigniana *et al.*, 1999). The conventional NLS-binding importin  $\alpha$  subunit has recently been shown to associate with microtubules and actin filaments in mammalian cells (Barsony *et al.*, 1997; Percipalle *et al.*, 1999) and tobacco protoplasts (Smith and Raikhel, 1998). Importin  $\alpha$  has also been reported to bind to microtubules *in vitro* in an NLS-dependent manner, whereas yeast importin  $\alpha$  has been reported to bind directly to the actin-related protein Act2p (Yan *et al.*, 1997). Using the technique of fluorescence recovery after photobleaching of intracellularly expressed GFP fusion protein constructs, it has recently become possible to visualize the dynamic transport along cytoskeletal elements from the cytoplasm to the nucleus of an importin  $\beta$ -recognized transport substrate, i.e., PTHrP (Lam *et al.*, 1999b). The microtubule-disrupting agent nocodazole inhibits transport of PTHrP, implying that its transport may occur directly along microtubules (Smith and Raikhel, 1999). These studies indicate, that cytoskeletal proteins may not only be involved in the communication between the nucleus, the cytoplasm and the plasma membrane in the ways indicated above, but also constitute part of the nuclear import machinery itself.

There seems little doubt that there are multiple modes by which signals are transduced from the membrane to the nucleus. The idea that the cytoskeleton and membrane-cytoskeletal connections are largely inert structural elements is clearly in question. In view of the mounting evidence that nuclear translocation of membrane-associated plaque proteins may constitute a direct nuclear signaling pathway, and that the cytoskeleton plays a dynamic role with respect to the nuclear transport process itself and its regulation, future research should unravel the specific role that plaque proteins play in the nuclear compartment and that cytoskeletal components may play in regulating nuclear protein transport.

## Acknowledgment

This review is related to research funded by the Deutsche Forschungsgemeinschaft (Hu 621/3-1 to S.H.).

## References

Aberle, H., Bauer, A., Stappert, J., Kispert, A., and Kemler, R. (1997). Beta-catenin is a target for the ubiquitin-proteasome pathway. *EMBO J.* **16**, 3797–3804.

Adam, S. A., Marr, R. S., and Gerace, L. (1990). Nuclear protein import in permeabilized mammalian cells requires soluble cytoplasmic factors. *J. Cell Biol.* **111**, 807–816.

Albertini, M., Pemberton, L. F., Rosenblum, J. S., and Blobel, G. (1998). A novel nuclear import pathway for the transcription factor TFIIS. *J. Cell Biol.* **143**, 1447–1455.

Amankwah, K. S., and De Boni, U. (1994). Ultrastructural localization of filamentous actin within neuronal interphase nuclei *in situ*. *Exp. Cell Res.* **210**, 315–325.

Anderson, R. A., Correas, I., Mazzucco, C., Castle, J. D., and Marchesi, V. T. (1988). Tissue-specific analogues of erythrocyte protein 4.1 retain functional domains. *J. Cell Biochem.* **37**, 269–284.

Ankenbauer, T., Kleinschmidt, J. A., Walsh, M. J., Weiner, O. H., and Franke, W. W. (1989). Identification of a widespread nuclear actin binding protein. *Nature (Lond.)* **342**, 822–825.

Arber, S., and Caroni, P. (1996). Specificity of single LIM motifs in targeting and LIM/LIM interactions *in situ*. *Genes Dev.* **10**, 289–300.

Bachs, O., Lanini, L., Serratosa, J., Coll, M. J., Bastos, R., Aligué, R., Rius, E., and Carafoli, E. (1990). Calmodulin-binding proteins in the nuclei of quiescent and proliferatively activated rat liver cells. *J. Biol. Chem.* **265**, 18595–18600.

Baglia, F. A., and Maul, G. G. (1983). Nuclear ribonucleoprotein release and nucleoside triphosphatase activity are inhibited by antibodies directed against one nuclear matrix glycoprotein. *Proc. Natl. Acad. Sci. USA* **80**, 2285–2289.

Balda, M. S., and Anderson, J. M. (1993). Two classes of tight junctions are revealed by ZO-1 isoforms. *Am. J. Physiol.* **264**, C918–C924.

Balda, M. S., and Matter, K. (2000). The tight junction protein ZO-1 and an interacting transcription factor regulate ErbB-2 expression. *EMBO J.* **19**, 2024–2033.

Barsony, J., Lenherr, S., Shih, K., Smith, C. L., and Sackett, D. L. (1997). Importin alpha mediates steroid receptor interaction with microtubules during translocation. *Mol. Biol. Cell* **8S**, 49a.

Beals, C. R., Clipstone, N. A., Ho, S. N., and Crabtree, G. R. (1997a). Nuclear localization of NF-ATc by a calcineurin-dependent, cyclosporin-sensitive intramolecular interaction. *Genes Dev.* **11**, 824–834.

Beals, C. R., Sheridan, C. M., Turck, C. W., Gardner, P., and Crabtree, G. R. (1997b). Nuclear export of NF-ATc enhanced by glycogen synthase kinase-3. *Science* **275**, 1930–1934.

Beck, K. A., Buchanan, J. A., Malhotra, V., and Nelson, W. J. (1994). Golgi spectrin: identification of an erythroid beta-spectrin homolog associated with the Golgi complex. *J. Cell Biol.* **127**, 707–723.

Beggs, A. H., Byers, T. J., Knoll, J. H., Boyce, F. M., Bruns, G. A., and Kunkel, L. M. (1992). Cloning and characterization of two human skeletal muscle alpha-actinin genes located on chromosomes 1 and 11. *J. Biol. Chem.* **267**, 9281–9288.

Behrens, J., von Kries, J. P., Kühl, M., Bruhn, L., Wedlich, D., Grosschedl, R., and Birchmeier, W. (1996). Functional interaction of beta-catenin with the transcription factor LEF-1. *Nature (Lond.)* **382**, 638–642.

Behrens, J., Jerchow, B. A., Würtele, M., Grimm, J., Asbrand, C., Wirtz, R., Kühl, M., Wedlich, D., and Birchmeier, W. (1998). Functional interaction of an axin homolog, conductin, with beta-catenin, APC, and GSK3beta. *Science* **280**, 596–599.

Belkin, A. M., and Koteliansky, V. E. (1987). Interaction of iodinated vinculin, metavinculin and alpha-actinin with cytoskeletal proteins. *FEBS Lett.* **220**, 291–294.

Ben-Yosef, T., and Francomano, C. A. (1999). Characterization of the human talin (TLN) gene: genomic structure, chromosomal localization, and expression pattern. *Genomics* **62**, 316–319.

Berrios, M., and Fisher, P. A. (1986). A myosin heavy-chain-like polypeptide is associated with the nuclear envelope in higher eukaryotic cells. *J. Cell Biol.* **103**, 711–724.

Bischoff, F. R., and Ponstingl, H. (1991). Catalysis of guanine nucleotide exchange on Ran by the mitotic regulator RCC1. *Nature (Lond.)* **354**, 80–82.

Bonifaci, N., Moroianu, J., Radu, A., and Blobel, G. (1997). Karyopherin beta2 mediates nuclear import of a mRNA binding protein. *Proc. Natl. Acad. Sci. USA* **94**, 5055–5060.

Bonné, S., van Hengel, J., Nollet, F., Kools, P., and van Roy, F. (1999). Plakophilin-3, a novel armadillo-like protein present in nuclei and desmosomes of epithelial cells. *J. Cell Sci.* **112**, 2265–2276.

Brandner, J. M., Reidenbach, S., and Franke, W. W. (1997). Evidence that pinin, reportedly a differentiation-specific desmosomal protein, is actually a widespread nuclear protein. *Differentiation* **62**, 119–127.

Brandner, J. M., Reidenbach, S., Kuhn, C., and Franke, W. W. (1998). Identification and characterization of a novel kind of nuclear protein occurring free in the nucleoplasm and in ribonucleoprotein structures of the speckle type. *Eur. J. Cell Biol.* **75**, 295–308.

Briggs, L. J., Stein, D., Goltz, J., Corrigan, V. C., Efthymiadis, A., Hübner, S., and Jans, D. A. (1998). The cAMP-dependent protein kinase site (Ser312) enhances dorsal nuclear import through facilitating nuclear localization sequence/importin interaction. *J. Biol. Chem.* **273**, 22745–22752.

Brown, M. S., and Goldstein, J. L. (1997). The SREBP pathway: regulation of cholesterol metabolism by proteolysis of a membrane-bound transcription factor. *Cell* **89**, 331–340.

Burridge, K., and Mangeat, P. (1984). An interaction between vinculin and talin. *Nature (Lond.)* **308**, 744–746.

Cavallo, R. A., Cox, R. T., Moline, M. M., Roose, J., Polevoy, G. A., Clevers, H., Peifer, M., and Bejsovec, A. (1998). *Drosophila* Tcf and Groucho interact to repress Wingless signalling activity. *Nature (Lond.)* **395**, 604–608.

Chasis, J. A., Coulombel, L., Conboy, J., McGee, S., Andrews, K., Kan, Y. W., and Mohandas, N. (1993). Differentiation-associated switches in protein 4.1 expression. Synthesis of multiple structural isoforms during normal human erythropoiesis. *J. Clin. Invest.* **91**, 329–338.

Chen, C. M., Kraut, N., Groudine, M., and Weintraub, H. (1996). I-mf, a novel myogenic repressor, interacts with members of the MyoD family. *Cell* **86**, 731–741.

Chi, N. C., Adam, E. J., and Adam, S. A. (1995). Sequence and characterization of cytoplasmic nuclear protein import factor p97. *J. Cell Biol.* **130**, 265–274.

Chi, N. C., Adam, E. J., Visser, G. D., and Adam, S. A. (1996). RanBP1 stabilizes the interaction of Ran with p97 nuclear protein import. *J. Cell Biol.* **135**, 559–569.

Chiba, N., Watanabe, T., Nomura, S., Tanaka, Y., Minowa, M., Niki, M., Kanamaru, R., and Satake, M. (1997). Differentiation dependent expression and distinct subcellular localization of the protooncogene product, PEBP2beta/CBFbeta, in muscle development. *Oncogene* **14**, 2543–2552.

Cho, K. O., Hunt, C. A., and Kennedy, M. B. (1992). The rat brain postsynaptic density fraction contains a homolog of the *Drosophila* discs-large tumor suppressor protein. *Neuron* **9**, 929–942.

Cimino, G., Moir, D. T., Canaani, O., Williams, K., Crist, W. M., Katzav, S., Cannizzaro, L., Lange, B., Nowell, P. C., and Croce, C. M. (1991). Cloning of ALL-1, the locus involved in leukemias with the t(4;11)(q21;q23), t(9;11)(p22;q23), and t(11;19)(q23;p13) chromosome translocations. *Cancer Res.* **51**, 6712–6714.

Cingolani, G., Petosa, C., Weis, K., and Müller, C. W. (1999). Structure of importin-beta bound to the IBB domain of importin-alpha. *Nature (Lond.)* **399**, 221–229.

Citi, S., and Cordenonsi, M. (1998). Tight junction proteins. *Biochim. Biophys. Acta* **1448**, 1–11.

Citi, S., and Cordenonsi, M. (1999). The molecular basis for the structure, function and regulation of tight junctions. In “Adhesive Interactions of Cells” (D. R. Garrod, A. J. North, and M. A. J. Chidgey, Eds.), Vol. 28, pp. 203–233. JAI Press, Inc., Greenwich, CT.

Citi, S., Sabanay, H., Kendrick-Jones, J., and Geiger, B. (1989). Cingulin: characterization and localization. *J. Cell Sci.* **93**, 107–122.

Clark, E. A., and Brugge, J. S. (1995). Integrins and signal transduction pathways: the road taken. *Science* **268**, 233–239.

Clark, T. G., and Merriam, R. W. (1977). Diffusible and bound actin nuclei of *Xenopus laevis* oocytes. *Cell* **12**, 883–891.

Clark, T. G., and Rosenbaum, J. L. (1979). An actin filament matrix in hand-isolated nuclei of *X. laevis* oocytes. *Cell* **18**, 1101–1108.

Conboy, J. G. (1993). Structure, function, and molecular genetics of erythroid membrane skeletal protein 4.1 in normal and abnormal red blood cells. *Semin. Hematol.* **30**, 58–73.

Conboy, J. G., Chan, J. Y., Chasis, J. A., Kan, Y. W., and Mohandas, N. (1991). Tissue- and development-specific alternative RNA splicing regulates expression of multiple isoforms of erythroid membrane protein 4.1. *J. Biol. Chem.* **266**, 8273–8280.

Conti, E., Uy, M., Leighton, L., Blobel, G., and Kuriyan, J. (1998). Crystallographic analysis of the recognition of a nuclear localization signal by the nuclear import factor karyopherin alpha. *Cell* **94**, 193–204.

Cordenonsi, M., D'Atri, F., Hammar, E., Parry, D. A., Kendrick-Jones, J., Shore, D., and Citi, S. (1999). Cingulin contains globular and coiled-coil domains and interacts with ZO-1, ZO-2, ZO-3, and myosin. *J. Cell Biol.* **147**, 1569–1582.

Correas, I. (1991). Characterization of isoforms of protein 4.1 present in the nucleus. *Biochem. J.* **279**, 581–585.

Craig, S. W., and Johnson, R. P. (1996). Assembly of focal adhesions: progress, paradigms, and portents. *Curr. Opin. Cell Biol.* **8**, 74–85.

Crawford, A. W., and Beckerle, M. C. (1991). Purification and characterization of zyxin, an 82,000-dalton component of adherens junctions. *J. Biol. Chem.* **266**, 5847–5853.

Crawford, A. W., Michelsen, J. W., and Beckerle, M. C. (1992). An interaction between zyxin and alpha-actinin. *J. Cell Biol.* **116**, 1381–1393.

Critchley, D. R. (2000). Focal adhesions—the cytoskeletal connection. *Curr. Opin. Cell Biol.* **12**, 133–139.

Dabauvalle, M. C., Schulz, B., Scheer, U., and Peters, R. (1988). Inhibition of nuclear accumulation of karyophilic proteins in living cells by microinjection of the lectin wheat germ agglutinin. *Exp. Cell Res.* **174**, 291–296.

Dang, C. V., and Lee, W. M. (1989). Nuclear and nucleolar targeting sequences of c-erb-A, c-myb, N-myc, p53, HSP70, and HIV tat proteins. *J. Biol. Chem.* **264**, 18019–18023.

Daniel, J. M., and Reynolds, A. B. (1999). The catenin p120(ctn) interacts with Kaiso, a novel BTB/POZ domain zinc finger transcription factor. *Mol. Cell Biol.* **19**, 3614–3623.

De Boni, U. (1994). The interphase nucleus as a dynamic structure. *Int. Rev. Cytol.* **150**, 149–171.

De Cácer, G., Lallena, M. J., and Correas, I. (1995). Protein 4.1 is a component of the nuclear matrix of mammalian cells. *Biochem. J.* **312**, 871–877.

Degen, W. G., Agterbos, M. A., Muyrers, J. P., Bloemers, H. P., and Swart, G. W. (1999). memA/DRS, a putative mediator of multiprotein complexes, is overexpressed in the metastasizing human melanoma cell lines BLM and MV3. *Biochim. Biophys. Acta* **1444**, 384–394.

Douvas, A. S., Harrington, C. A., and Bonner, J. (1975). Major nonhistone proteins of rat liver chromatin: preliminary identification of myosin, actin, tubulin, and tropomyosin. *Proc. Natl. Acad. Sci. USA* **72**, 3902–3906.

Drenckhahn, D., and Dermietzel, R. (1988). Organization of the actin filament cytoskeleton in the intestinal brush border: a quantitative and qualitative immunoelectron microscope study. *J. Cell Biol.* **107**, 1037–1048.

Drenckhahn, D., Beckerle, M., Burridge, K., and Otto, J. (1988). Identification and subcellular location of talin in various cell types and tissues by means of [<sup>125</sup>I]vinculin overlay, immunoblotting and immunocytochemistry. *Eur. J. Cell Biol.* **46**, 513–522.

Efthymiadis, A., Shao, H., Hübner, S., and Jans, D. A. (1997). Kinetic characterization of the human retinoblastoma protein bipartite nuclear localization sequence (NLS) *in vivo* and *in vitro*. A comparison with the SV40 large T-antigen NLS. *J. Biol. Chem.* **272**, 22134–22139.

Fagotto, F., Glück, U., and Gumbiner, B. M. (1998). Nuclear localization signal-independent and importin/karyopherin-independent nuclear import of beta-catenin. *Curr. Biol.* **8**, 181–190.

Fanning, A. S., and Anderson, J. M. (1996). Protein–protein interactions: PDZ domain networks. *Curr. Biol.* **6**, 1385–1388.

Fanning, A. S., Jameson, B. J., Jesaitis, L. A., and Anderson, J. M. (1998). The tight junction protein ZO-1 establishes a link between the transmembrane protein occludin and the actin cytoskeleton. *J. Biol. Chem.* **273**, 29745–29753.

Featherstone, C., Darby, M. K., and Gerace, L. (1988). A monoclonal antibody against the nuclear pore complex inhibits nucleocytoplasmic transport of protein and RNA *in vivo*. *J. Cell Biol.* **107**, 1289–1297.

Feldherr, C. M., Kallenbach, E., and Schultz, N. (1984). Movement of a karyophilic protein through the nuclear pores of oocytes. *J. Cell Biol.* **99**, 2216–2222.

Ferrigno, P., Posas, F., Koepf, D., Saito, H., and Silver, P. A. (1998). Regulated nucleo/cytoplasmic exchange of HOG1 MAPK requires the importin beta homologs NMD5 and XPO1. *EMBO J.* **17**, 5606–5614.

Finlay, D. R., Newmeyer, D. D., Price, T. M., and Forbes, D. J. (1987). Inhibition of *in vitro* nuclear transport by a lectin that binds to nuclear pores. *J. Cell Biol.* **104**, 189–200.

Fisher, A. L., and Caudy, M. (1998). Groucho proteins: transcriptional corepressors for specific subsets of DNA-binding transcription factors in vertebrates and invertebrates. *Genes Dev.* **12**, 1931–1940.

Fornerod, M., Ohno, M., Yoshida, M., and Mattaj, I. W. (1997). CRM1 is an export receptor for leucine-rich nuclear export signals. *Cell* **90**, 1051–1060.

Franke, W. W., Mueller, H., Mittnacht, S., Kapprell, H. P., and Jorcano, J. L. (1983). Significance of two desmosome plaque-associated polypeptides of molecular weights 75000 and 83000. *EMBO J.* **2**, 2211–2215.

Fukuda, M., Asano, S., Nakamura, T., Adachi, M., Yoshida, M., Yanagida, M., and Nishida, E. (1997). CRM1 is responsible for intracellular transport mediated by the nuclear export signal. *Nature (Lond.)* **390**, 308–311.

Fukui, Y., and Katsumaru, H. (1979). Nuclear actin bundles in *Amoeba*, *Dictyostelium* and human HeLa cells induced by dimethyl sulfoxide. *Exp. Cell Res.* **120**, 451–455.

Funayama, N., Fagotto, F., McCrea, P., and Gumbiner, B. M. (1995). Embryonic axis induction by the *armadillo* repeat domain of beta-catenin: evidence for intracellular signaling. *J. Cell Biol.* **128**, 959–968.

Furuse, M., Hirase, T., Itoh, M., Nagafuchi, A., Yonemura, S., and Tsukita, S. (1993). Occludin: a novel integral membrane protein localizing at tight junctions. *J. Cell Biol.* **123**, 1777–1788.

Furuse, M., Itoh, M., Hirase, T., Nagafuchi, A., Yonemura, S., and Tsukita, S. (1994). Direct association of occludin with ZO-1 and its possible involvement in the localization of occludin at tight junctions. *J. Cell Biol.* **127**, 1617–1626.

Furuse, M., Fujita, K., Hiragi, T., Fujimoto, K., and Tsukita, S. (1998). Claudin-1 and -2: novel integral membrane proteins localizing at tight junctions with no sequence similarity to occludin. *J. Cell Biol.* **141**, 1539–1550.

Galigniana, M. D., Housley, P. R., DeFranco, D. B., and Pratt, W. B. (1999). Inhibition of glucocorticoid receptor nucleocytoplasmic shuttling by okadaic acid requires intact cytoskeleton. *J. Biol. Chem.* **274**, 16222–16227.

Gascard, P., Lee, G., Coulombe, L., Auffray, I., Lum, M., Parra, M., Conboy, J. G., Mohandas, N., and Chasis, J. A. (1998). Characterization of multiple isoforms of protein 4.1R expressed during erythroid terminal differentiation. *Blood* **92**, 4404–4414.

Gascard, P., Nunomura, W., Lee, G., Walensky, L. D., Krauss, S. W., Takakuwa, Y., Chasis, J. A., Mohandas, N., and Conboy, J. G. (1999). Deciphering the nuclear import pathway for the cytoskeletal red cell protein 4.1R. *Mol. Biol. Cell* **10**, 1783–1798.

Giannini, A. L., Vivanco, M. M., and Kypta, R. M. (2000). Analysis of  $\beta$ -catenin aggregation and

localization using GFP fusion proteins: nuclear import of  $\alpha$ -catenin by the  $\beta$ -catenin/Tcf complex. *Exp. Cell Res.* **255**, 207–220.

Gill, G. N. (1995). The enigma of LIM domains. *Structure* **3**, 1285–1289.

Golenhofen, N., and Drenckhahn, D. (2000). The catenin, p120<sup>ctn</sup>, is a common membrane-associated protein in various epithelial and non-epithelial cells and tissues. *Histochem. Cell Biol.* **114**, 147–155.

Gonsior, S. M., Platz, S., Buchmeier, S., Scheer, U., Jockusch, B. M., and Hinssen, H. (1999). Conformational difference between nuclear and cytoplasmic actin as detected by a monoclonal antibody. *J. Cell Sci.* **112**, 797–809.

Gonzalez-Mariscal, L., Islas, S., Gonzalez-Robles, A., and Ponce, L. (1999). Expression of the tight junction protein ZO-2 at the nuclei of subconfluent cells. *Mol. Biol. Cell* **10S**, 407a.

Gonzalez-Mariscal, L., Namorado, M. C., Martin, D., Luna, J., Alarcon, L., Islas, S., Valencia, L., Muriel, P., Ponce, L., and Reyes, J. L. (2000). Tight junction proteins ZO-1, ZO-2, and occludin along isolated renal tubules. *Kidney Int.* **57**, 2386–2402.

Görlich, D., Prehn, S., Laskey, R. A., and Hartmann, E. (1994). Isolation of a protein that is essential for the first step of nuclear protein import. *Cell* **79**, 767–778.

Görlich, D., Kostka, S., Kraft, R., Dingwall, C., Laskey, R. A., Hartmann, E., and Prehn, S. (1995). Two different subunits of importin cooperate to recognize nuclear localization signals and bind them to the nuclear envelope. *Curr. Biol.* **5**, 383–392.

Görlich, D., Henklein, P., Laskey, R. A., and Hartmann, E. (1996a). A 41 amino acid motif in importin-alpha confers binding to importin-beta and hence transit into the nucleus. *EMBO J.* **15**, 1810–1817.

Görlich, D., Panté, N., Kutay, U., Aeby, U., and Bischoff, F. R. (1996b). Identification of different roles for RanGDP and RanGTP in nuclear protein import. *EMBO J.* **15**, 5584–5594.

Gottardi, C. J., Arpin, M., Fanning, A. S., and Louvard, D. (1996). The junction-associated protein, zonula occludens-1, localizes to the nucleus before the maturation and during the remodeling of cell-cell contacts. *Proc. Natl. Acad. Sci. USA* **93**, 10779–10784.

Gounon, P., and Karsenti, E. (1981). Involvement of contractile proteins in the changes in consistency of oocyte nucleoplasm of the newt *Pleurodeles waltlii*. *J. Cell Biol.* **88**, 410–421.

Gutmann, D. H., Sherman, L., Seftor, L., Hairek, C., Hoang Lu, K., and Hendrix, M. (1999). Increased expression of the NF2 tumor suppressor gene product, merlin, impairs cell motility, adhesion and spreading. *Hum. Mol. Genet.* **8**, 267–275.

Hagen, S. J., Kiehart, D. P., Kaiser, D. A., and Pollard, T. D. (1986). Characterization of monoclonal antibodies to *Acanthamoeba* myosin-I that cross-react with both myosin-II and low molecular mass nuclear proteins. *J. Cell Biol.* **103**, 2121–2128.

Hall, M. N., Hereford, L., and Herskowitz, I. (1984). Targeting of *E. coli* beta-galactosidase to the nucleus in yeast. *Cell* **36**, 1057–1065.

Hall, M. N., Craik, C., and Hiraoka, Y. (1990). Homeodomain of yeast repressor alpha 2 contains a nuclear localization signal. *Proc. Natl. Acad. Sci. USA* **87**, 6954–6958.

Hanzel, D., Reggio, H., Bretscher, A., Forte, J. G., and Mangeat, P. (1991). The secretion-stimulated 80K phosphoprotein of parietal cells is ezrin, and has properties of a membrane cytoskeletal linker in the induced apical microvilli. *EMBO J.* **10**, 2363–2373.

Hartig, R., Shoeman, R. L., Janetzko, A., Grub, S., and Traub, P. (1998a). Active nuclear import of single-stranded oligonucleotides and their complexes with non-karyophilic macromolecules. *Biol. Cell* **90**, 407–426.

Hartig, R., Shoeman, R. L., Janetzko, A., Tolstonog, G., and Traub, P. (1998b). DNA-mediated transport of the intermediate filament protein vimentin into the nucleus of cultured cells. *J. Cell Sci.* **111**, 3573–3584.

Haskins, J., Gu, L., Wittchen, E. S., Hibbard, J., and Stevenson, B. R. (1998). ZO-3, a novel member of the MAGUK protein family found at the tight junction, interacts with ZO-1 and occludin. *J. Cell Biol.* **141**, 199–208.

Hatzfeld, M. (1997). Band 6 protein and cytoskeletal organization. In “Cytoskeletal–Membrane

Interactions and Signal Transduction" (P. Cowin and M. W. Klymkowsky, Eds.), pp. 49–59. Landes Company and Chapman Hall, Austin, TX.

Hatzfeld, M., and Nachtsheim, C. (1996). Cloning and characterization of a new *armadillo* family member, p0071, associated with the junctional plaque: evidence for a subfamily of closely related proteins. *J. Cell Sci.* **109**, 2767–2778.

Hatzfeld, M., Kristjansson, G. I., Plessmann, U., and Weber, K. (1994). Band 6 protein, a major constituent of desmosomes from stratified epithelia, is a novel member of the *armadillo* multigene family. *J. Cell Sci.* **107**, 2259–2270.

Hatzfeld, M., Haffner, C., Schulze, K., and Vinzens, U. (2000). The function of plakophilin 1 in desmosome assembly and actin filament organization. *J. Cell Biol.* **149**, 209–222.

Hazan, R. B., Kang, L., Roe, S., Borgen, P. I., and Rimm, D. L. (1997). Vinculin is associated with the E-cadherin adhesion complex. *J. Biol. Chem.* **272**, 32448–32453.

Heid, H. W., Schmidt, A., Zimbelmann, R., Schäfer, S., Winter-Simanowski, S., Stumpp, S., Keith, M., Figge, U., Schnölzer, M., and Franke, W. W. (1994). Cell type-specific desmosomal plaque proteins of the plakoglobin family: plakophilin 1 (band 6 protein). *Differentiation* **58**, 113–131.

Hemler, M. E. (1998). Integrin associated proteins. *Curr. Opin. Cell Biol.* **10**, 578–585.

Hemmings, L., Rees, D. J., Ohanian, V., Bolton, S. J., Gilmore, A. P., Patel, B., Priddle, H., Trevithick, J. E., Hynes, R. O., and Critchley, D. R. (1996). Talin contains three actin-binding sites each of which is adjacent to a vinculin-binding site. *J. Cell Sci.* **109**, 2715–2726.

Henkel, T., Zabel, U., van Zee, K., Müller, J. M., Fanning, E., and Baeuerle, P. A. (1992). Intramolecular masking of the nuclear location signal and dimerization domain in the precursor for the p50 NF- $\kappa$ B subunit. *Cell* **68**, 1121–1133.

Hennekes, H., Peter, M., Weber, K., and Nigg, E. A. (1993). Phosphorylation on protein kinase C sites inhibits nuclear import of lamin B2. *J. Cell Biol.* **120**, 1293–1304.

Herold, A., Truant, R., Wiegand, H., and Cullen, B. R. (1998). Determination of the functional domain organization of the importin alpha nuclear import factor. *J. Cell Biol.* **143**, 309–318.

Hicks, G. R., Smith, H. M., Lobreaux, S., and Raikhel, N. V. (1996). Nuclear import in permeabilized protoplasts from higher plants has unique features. *Plant Cell* **8**, 1337–1352.

Hill, C. S., and Treisman, R. (1995). Transcriptional regulation by extracellular signals: mechanisms and specificity. *Cell* **80**, 199–211.

Hitotsumatsu, T., Iwaki, T., Kitamoto, T., Mizoguchi, M., Suzuki, S. O., Hamada, Y., Fukui, M., and Tateishi, J. (1997). Expression of neurofibromatosis 2 protein in human brain tumors: an immunohistochemical study. *Acta Neuropathol.* **93**, 225–232.

Hobert, O., Schilling, J. W., Beckerle, M. C., Ullrich, A., and Jallal, B. (1996). SH3 domain-dependent interaction of the proto-oncogene product Vav with the focal contact protein zyxin. *Oncogene* **12**, 1577–1581.

Honda, K., Yamada, T., Endo, R., Ino, Y., Gotoh, M., Tsuda, H., Yamada, Y., Chiba, H., and Hirohashi, S. (1998). Actinin-4, a novel actin-bundling protein associated with cell motility and cancer invasion. *J. Cell Biol.* **140**, 1383–1393.

Hopper, A. K., Traglia, H. M., and Dunst, R. W. (1990). The yeast RNA1 gene product necessary for RNA processing is located in the cytosol and apparently excluded from the nucleus. *J. Cell Biol.* **111**, 309–321.

Horwitz, A., Duggan, K., Buck, C., Beckerle, M. C., and Burridge, K. (1986). Interaction of plasma membrane fibronectin receptor with talin—a transmembrane linkage. *Nature (Lond.)* **320**, 531–533.

Howarth, A. G., Hughes, M. R., and Stevenson, B. R. (1992). Detection of the tight junction-associated protein ZO-1 in astrocytes and other nonepithelial cell types. *Am. J. Physiol.* **262**, C461–C469.

Howe, A., Aplin, A. E., Alahari, S. K., and Julian, R. L. (1998). Integrin signaling and cell growth control. *Curr. Opin. Cell Biol.* **10**, 220–231.

Hu, W., and Jans, D. A. (1999). Efficiency of importin alpha/beta-mediated nuclear localization sequence recognition and nuclear import. Differential role of NTF2. *J. Biol. Chem.* **274**, 15820–15827.

Huber, O., Korn, R., McLaughlin, J., Ohsugi, M., Herrmann, B. G., and Kemler, R. (1996). Nuclear localization of beta-catenin by interaction with transcription factor LEF-1. *Mech. Dev.* **59**, 3–10.

Hübner, S., Xiao, C. Y., and Jans, D. A. (1997). The protein kinase CK2 site (Ser111/112) enhances recognition of the simian virus 40 large T-antigen nuclear localization sequence by importin. *J. Biol. Chem.* **272**, 17191–17195.

Hübner, S., Smith, H. M., Hu, W., Chan, C. K., Rihs, H. P., Paschal, B. M., Raikhel, N. V., and Jans, D. A. (1999). Plant importin alpha binds nuclear localization sequences with high affinity and can mediate nuclear import independent of importin beta. *J. Biol. Chem.* **274**, 22610–22617.

Huxford, T., Huang, D. B., Malek, S., and Ghosh, G. (1998). The crystal structure of the IkappaBalpha/NF-kappaB complex reveals mechanisms of NF-kappaB inactivation. *Cell* **95**, 759–770.

Hynes, R. O. (1992). Integrins: versatility, modulation, and signaling in cell adhesion. *Cell* **69**, 11–25.

Iida, K., and Yahara, I. (1986). Reversible induction of actin rods in mouse C3H-2K cells by incubation in salt buffers and by treatment with non-ionic detergents. *Exp. Cell Res.* **164**, 492–506.

Ikeda, S., Kishida, S., Yamamoto, H., Murai, H., Koyama, S., and Kikuchi, A. (1998). Axin, a negative regulator of the Wnt signaling pathway, forms a complex with GSK-3beta and beta-catenin and promotes GSK-3beta-dependent phosphorylation of beta-catenin. *EMBO J.* **17**, 1371–1384.

Imamoto, N., Shimamoto, T., Kose, S., Takao, T., Tachibana, T., Matsubae, M., Sekimoto, T., Shimonishi, Y., and Yoneda, Y. (1995). The nuclear pore-targeting complex binds to nuclear pores after association with a karyophile. *FEBS Lett.* **368**, 415–419.

Imamura, Y., Itoh, M., Maeno, Y., Tsukita, S., and Nagafuchi, A. (1999). Functional domains of alpha-catenin required for the strong state of cadherin-based cell adhesion. *J. Cell Biol.* **144**, 1311–1322.

Itoh, M., Yonemura, S., Nagafuchi, A., and Tsukita, S. (1991). A 220-kD undercoat-constitutive protein: its specific localization at cadherin-based cell–cell adhesion sites. *J. Cell Biol.* **115**, 1449–1462.

Itoh, M., Nagafuchi, A., Yonemura, S., Kitani-Yasuda, T., and Tsukita, S. (1993). The 220-kD protein colocalizing with cadherins in non-epithelial cells is identical to ZO-1, a tight junction-associated protein in epithelial cells: cDNA cloning and immunoelectron microscopy. *J. Cell Biol.* **121**, 491–502.

Itoh, M., Nagafuchi, A., Moroi, S., and Tsukita, S. (1997). Involvement of ZO-1 in cadherin-based cell adhesion through its direct binding to alpha catenin and actin filaments. *J. Cell Biol.* **138**, 181–192.

Itoh, M., Morita, K., and Tsukita, S. (1999). Characterization of ZO-2 as a MAGUK family member associated with tight as well as adherens junctions with a binding affinity to occludin and alpha catenin. *J. Biol. Chem.* **274**, 5981–5986.

Izaurralde, E., Kutay, U., von Kobbe, C., Mattaj, J. W., and Görlich, D. (1997). The asymmetric distribution of the constituents of the Ran system is essential for transport into and out of the nucleus. *EMBO J.* **16**, 6535–6547.

Jäkel, S., and Görlich, D. (1998). Importin beta, transportin, RanBP5 and RanBP7 mediate nuclear import of ribosomal proteins in mammalian cells. *EMBO J.* **17**, 4491–4502.

Jäkel, S., Albig, W., Kutay, U., Bischoff, F. R., Schwamborn, K., Doenecke, D., and Görlich, D. (1999). The importin beta/importin 7 heterodimer is a functional nuclear import receptor for histone H1. *EMBO J.* **18**, 2411–2423.

Jans, D. A., and Hassan, G. (1998). Nuclear targeting by growth factors, cytokines, and their receptors: a role in signaling? *Bioessays* **20**, 400–411.

Jans, D. A., and Hübner, S. (1996). Regulation of protein transport to the nucleus: central role of phosphorylation. *Physiol. Rev.* **76**, 651–685.

Jans, D. A., and Jans, P. (1994). Negative charge at the casein kinase II site flanking the nuclear localization signal of the SV40 large T-antigen is mechanistically important for enhanced nuclear import. *Oncogene* **9**, 2961–2968.

Jans, D. A., Moll, T., Nasmyth, K., and Jans, P. (1995). Cyclin-dependent kinase site-regulated signal-dependent nuclear localization of the SW15 yeast transcription factor in mammalian cells. *J. Biol. Chem.* **270**, 17064–17067.

Jans, D. A., Briggs, L. J., Gustin, S. E., Jans, P., Ford, S., and Young, I. G. (1997). The cytokine interleukin-5 (IL-5) effects cotransport of its receptor subunits to the nucleus in vitro. *FEBS Lett.* **410**, 368–372.

Jans, D. A., Chan, C. K., and Huebner, S. (1998). Signals mediating nuclear targeting and their regulation: application in drug delivery. *Med. Res. Rev.* **18**, 189–223.

Jesaitis, L. A., and Goodenough, D. A. (1994). Molecular characterization and tissue distribution of ZO-2, a tight junction protein homologous to ZO-1 and the *Drosophila* discs-large tumor suppressor protein. *J. Cell Biol.* **124**, 949–961.

Jockusch, B. M., Becker, M., Hindennach, I., and Jockusch, E. (1974). Slime mould actin: homology to vertebrate actin and presence in the nucleus. *Exp. Cell Res.* **89**, 241–246.

Jöns, T., and Drenckhahn, D. (1992). Identification of the binding interface involved in linkage of cytoskeletal protein 4.1 to the erythrocyte anion exchanger. *EMBO J.* **11**, 2863–2867.

Johnson, R. P., and Craig, S. W. (1995). F-actin binding site masked by the intramolecular association of vinculin head and tail domains. *Nature (Lond.)* **373**, 261–264.

Kaffman, A., Rank, N. M., O'Neill, E. M., Huang, L. S., and O'Shea, E. K. (1998a). The receptor Msn5 exports the phosphorylated transcription factor Pho4 out of the nucleus. *Nature (Lond.)* **396**, 482–486.

Kaffman, A., Rank, N. M., and O'Shea, E. K. (1998b). Phosphorylation regulates association of the transcription factor Pho4 with its import receptor Pse1/Kap121. *Genes Dev.* **12**, 2673–2683.

Kalderon, D., Richardson, W. D., Markham, A. F., and Smith, A. E. (1984a). Sequence requirements for nuclear location of simian virus 40 large-T antigen. *Nature (Lond.)* **311**, 33–38.

Kalderon, D., Roberts, B. L., Richardson, W. D., and Smith, A. E. (1984b). A short amino acid sequence able to specify nuclear location. *Cell* **39**, 499–509.

Kapprell, H. P., Owaribe, K., and Franke, W. W. (1988). Identification of a basic protein of Mr 75,000 as an accessory desmosomal plaque protein in stratified and complex epithelia. *J. Cell Biol.* **106**, 1679–1691.

Kaul, S. C., Kawai, R., Nomura, H., Mitsui, Y., Reddel, R. R., and Wadhwa, R. (1999). Identification of a 55-kDa ezrin-related protein that induces cytoskeletal changes and localizes to the nucleolus. *Exp. Cell Res.* **250**, 51–61.

Keirsebilck, A., Bonné, S., Staes, K., van Hengel, J., Nollet, F., Reynolds, A., and van Roy, F. (1998). Molecular cloning of the human p120ctn catenin gene (CTNND1): expression of multiple alternatively spliced isoforms. *Genomics* **50**, 129–146.

Keon, B. H., Schäfer, S., Kuhn, C., Grund, C., and Franke, W. W. (1996). Symplekin, a novel type of tight junction plaque protein. *J. Cell Biol.* **134**, 1003–1018.

Kidd, S., Lieber, T., and Young, M. W. (1998). Ligand-induced cleavage and regulation of nuclear entry of Notch in *Drosophila melanogaster* embryos. *Genes Dev.* **12**, 3728–3740.

Kim, E., Niethammer, M., Rothschild, A., Jan, Y. N., and Sheng, M. (1995). Clustering of Shaker-type K<sup>+</sup> channels by interaction with a family of membrane-associated guanylate kinases. *Nature (Lond.)* **378**, 85–88.

Kioka, N., Sakata, S., Kawauchi, T., Amachi, T., Akiyama, S. K., Okazaki, K., Yaen, C., Yamada, K. M., and Aota, S. (1999). Vinexin: a novel vinculin-binding protein with multiple SH3 domains enhances actin cytoskeletal organization. *J. Cell Biol.* **144**, 59–69.

Kishida, S., Yamamoto, H., Ikeda, S., Kishida, M., Sakamoto, I., Koyama, S., and Kikuchi, A. (1998). Axin, a negative regulator of the Wnt signaling pathway, directly interacts with adenomatous polyposis coli and regulates the stabilization of beta-catenin. *J. Biol. Chem.* **273**, 10823–10826.

Kistner, U., Wenzel, B. M., Veh, R. W., Cases-Langhoff, C., Garner, A. M., Appeltauer, U., Voss, B., Gundelfinger, E. D., and Garner, C. C. (1993). SAP90, a rat presynaptic protein related to the product of the *Drosophila* tumor suppressor gene dlg-A. *J. Biol. Chem.* **268**, 4580–4583.

Klymkowsky, M. W. (1999). Plakophilin, *armadillo* repeats, and nuclear localization. *Microsc. Res. Tech.* **45**, 43–54.

Knudsen, K. A., Soler, A. P., Johnson, K. R., and Wheelock, M. J. (1995). Interaction of alpha-actinin with the cadherin/catenin cell–cell adhesion complex via alpha-catenin. *J. Cell Biol.* **130**, 67–77.

Komeili, A., and O’Shea, E. K. (1999). Roles of phosphorylation sites in regulating activity of the transcription factor Pho4. *Science* **284**, 977–980.

Kornau, H. C., Schenker, L. T., Kennedy, M. B., and Seuberg, P. H. (1995). Domain interaction between NMDA receptor subunits and the postsynaptic density protein PSD-95. *Science* **269**, 1737–1740.

Kouklis, P. D., Hutton, E., and Fuchs, E. (1994). Making a connection: direct binding between keratin intermediate filaments and desmosomal proteins. *J. Cell Biol.* **127**, 1049–1060.

Kowalczyk, A. P., Borgwardt, J. E., and Green, K. J. (1996). Analysis of desmosomal cadherin-adhesive function and stoichiometry of desmosomal cadherin-plakoglobin complexes. *J. Invest. Dermatol.* **107**, 293–300.

Kowalczyk, A. P., Bornslaeger, E. A., Borgwardt, J. E., Palka, H. L., Dhaliwal, A. S., Corcoran, C. M., Denning, M. F., and Green, K. J. (1997). The amino-terminal domain of desmoplakin binds to plakoglobin and clusters desmosomal cadherin-plakoglobin complexes. *J. Cell Biol.* **139**, 773–784.

Kowalczyk, A. P., Bornslaeger, E. A., Norvell, S. M., Palka, H. L., and Green, K. J. (1999a). Desmosomes: intercellular adhesive junctions specialized for attachment of intermediate filaments. *Int. Rev. Cytol.* **185**, 237–302.

Kowalczyk, A. P., Hatzfeld, M., Bornslaeger, E. A., Kopp, D. S., Borgwardt, J. E., Corcoran, C. M., Settler, A., and Green, K. J. (1999b). The head domain of plakophilin-1 binds to desmoplakin and enhances its recruitment to desmosomes. Implications for cutaneous disease. *J. Biol. Chem.* **274**, 18145–18148.

Krauss, S. W., Larabell, C. A., Lockett, S., Gascard, P., Penman, S., Mohandas, N., and Chasis, J. A. (1997). Structural protein 4.1 in the nucleus of human cells: dynamic rearrangements during cell division. *J. Cell Biol.* **137**, 275–289.

Kuge, S., Jones, N., and Nomoto, A. (1997). Regulation of yAP-1 nuclear localization in response to oxidative stress. *EMBO J.* **16**, 1710–1720.

Kutay, U., Bischoff, F. R., Kostka, S., Kraft, R., and Görlich, D. (1997). Export of importin alpha from the nucleus is mediated by a specific nuclear transport factor. *Cell* **90**, 1061–1071.

Lallena, M. J., and Correas, I. (1997). Transcription-dependent redistribution of nuclear protein 4.1 to SC35-enriched nuclear domains. *J. Cell Sci.* **110**, 239–247.

Lallena, M. J., Martínez, C., Valcárcel, J., and Correas, I. (1998). Functional association of nuclear protein 4.1 with pre-mRNA splicing factors. *J. Cell Sci.* **111**, 1963–1971.

Lam, M. H., Briggs, L. J., Hu, W., Martin, T. J., Gillespie, M. T., and Jans, D. A. (1999a). Importin beta recognizes parathyroid hormone-related protein with high affinity and mediates its nuclear import in the absence of importin alpha. *J. Biol. Chem.* **274**, 7391–7398.

Lam, M. H. C., Thomas, R. J., Schilders, S. P., Gu, M., Martin, T. J., Gillespie, M. T., and Jans, D. A. (1999b). Dynamic visualization of nuclear import along microfilaments of the importin  $\beta$ 1-recognized transport substrate PTHrP. *submitted*

Lanford, R. E., and Butel, J. S. (1984). Construction and characterization of an SV40 mutant defective in nuclear transport of T antigen. *Cell* **37**, 801–813.

Lecourtois, M., and Schweigert, F. (1998). Indirect evidence for Delta-dependent intracellular processing of notch in *Drosophila* embryos. *Curr. Biol.* **8**, 771–774.

Lee, S., Chen, D. Y., Humphrey, J. S., Gnarra, J. R., Linehan, W. M., and Klausner, R. D. (1996). Nuclear/cytoplasmic localization of the von Hippel-Lindau tumor suppressor gene product is determined by cell density. *Proc. Natl. Acad. Sci. USA* **93**, 1770–1775.

Levanon, D., Goldstein, R. E., Bernstein, Y., Tang, H., Goldenberg, D., Stifani, S., Paroush, Z., and Groner, Y. (1998). Transcriptional repression by AML1 and LEF-1 is mediated by the TLE/Groucho corepressors. *Proc. Natl. Acad. Sci. USA* **95**, 11590–11595.

Li, X., Shou, W., Kloc, M., Reddy, B. A., and Etkin, L. D. (1994). Cytoplasmic retention of *Xenopus* nuclear factor 7 before the mid blastula transition uses a unique anchoring mechanism involving a retention domain and several phosphorylation sites. *J. Cell Biol.* **124**, 7–17.

Loveland, K. L., Hersfeld, D., Chu, B., Rames, E., Christy, E., Briggs, L. J., Shakri, R., de Kretser, D. M., and Jans, D. A. (1999). Novel low molecular weight microtubule-associated protein-2 isoforms contain a functional nuclear localization sequence. *J. Biol. Chem.* **274**, 19261–19268.

Lue, R. A., Marfatia, S. M., Branton, D., and Chishti, A. H. (1994). Cloning and characterization of hdlg: the human homologue of the *Drosophila* discs large tumor suppressor binds to protein 4.1. *Proc. Natl. Acad. Sci. USA* **91**, 9818–9822.

Lue, R. A., Brandin, E., Chan, E. P., and Branton, D. (1996). Two independent domains of hDlg are sufficient for subcellular targeting: the PDZ1-2 conformational unit and an alternatively spliced domain. *J. Cell Biol.* **135**, 1125–1137.

Luque, C. M., and Correas, I. (2000). A constitutive region is responsible for nuclear targeting of 4.1R: modulation by alternative sequences results in differential intracellular localization. *J. Cell Sci.* **113**, 2485–2495.

Luque, C. M., Lallena, M. J., Alonso, M. A., and Correas, I. (1998). An alternative domain determines nuclear localization in multifunctional protein 4.1. *J. Biol. Chem.* **273**, 11643–11649.

Lutchman, M., Peel, D., Kim, A. C., Bryant, P. J., and Chishti, A. H. (1997). Nuclear localization of protein 4.1 and the MAGUK family members p55 and hDlg. *Mol. Biol. Cell* **8**, 176a.

Madara, J. L. (1987). Intestinal absorptive cell tight junctions are linked to cytoskeleton. *Am. J. Physiol.* **253**, C171–C175.

Mahajan, R., Delphin, C., Guan, T., Gerace, L., and Melchior, F. (1997). A small ubiquitin-related polypeptide involved in targeting RanGAP1 to nuclear pore complex protein RanBP2. *Cell* **88**, 97–107.

Malik, H. S., Eickbush, T. H., and Goldfarb, D. S. (1997). Evolutionary specialization of the nuclear targeting apparatus. *Proc. Natl. Acad. Sci. USA* **94**, 13738–13742.

Mandai, K., Nakanishi, H., Satoh, A., Obaishi, H., Wada, M., Nishioka, H., Itoh, M., Mizoguchi, A., Aoki, T., Fujimoto, T., Matsuda, Y., Tsukita, S., and Takai, Y. (1997). Afadin: A novel actin filament-binding protein with one PDZ domain localized at cadherin-based cell-to-cell adherens junction. *J. Cell Biol.* **139**, 517–528.

Mandai, K., Nakanishi, H., Satoh, A., Takahashi, K., Satoh, K., Nishioka, H., Mizoguchi, A., and Takai, Y. (1999). Ponsin/SH3P12: an I-afadin- and vinculin-binding protein localized at cell–cell and cell–matrix adherens junctions. *J. Cell Biol.* **144**, 1001–1017.

Mariner, D. J., Wang, J., and Reynolds, A. B. (2000). ARVCF localizes to the nucleus and adherens junction and is mutually exclusive with p120(ctn) in E-cadherin complexes. *J. Cell Sci.* **113**, 1481–1490.

Martin-Padura, I., Lostaglio, S., Schneemann, M., Williams, L., Romano, M., Fruscella, P., Panzeri, C., Stoppacciaro, A., Ruco, L., Villa, A., Simmons, D., and Dejana, E. (1998). Junctional adhesion molecule, a novel member of the immunoglobulin superfamily that distributes at intercellular junctions and modulates monocyte transmigration. *J. Cell Biol.* **142**, 117–127.

Mathur, M., Goodwin, L., and Cowin, P. (1994). Interactions of the cytoplasmic domain of the desmosomal cadherin Dsg1 with plakoglobin. *J. Biol. Chem.* **269**, 14075–14080.

Mattagajasingh, S. N., Huang, S. C., Hartenstein, J. S., Snyder, M., Marchesi, V. T., and Benz, E. J. (1999). A nonerythroid isoform of protein 4.1R interacts with the nuclear mitotic apparatus (NuMA) protein. *J. Cell Biol.* **145**, 29–43.

Matunis, M. J., Coutavas, E., and Blobel, G. (1996). A novel ubiquitin-like modification modulates the partitioning of the Ran-GTPase-activating protein RanGAP1 between the cytosol and the nuclear pore complex. *J. Cell Biol.* **135**, 1457–1470.

McGuire, J., Coumailleau, P., Whitelaw, M. L., Gustafsson, J. A., and Poellinger, L. (1995). The basic helix-loop-helix/PAS factor Sim is associated with hsp90. Implications for regulation by interaction with partner factors. *J. Biol. Chem.* **270**, 31353–31357.

Melchior, F., Paschal, B., Evans, J., and Gerace, L. (1993). Inhibition of nuclear protein import by nonhydrolyzable analogues of GTP and identification of the small GTPase Ran/TC4 as an essential transport factor. *J. Cell Biol.* **123**, 1649–1659.

Meng, J. J., Bornslaeger, E. A., Green, K. J., Steinert, P. M., and Ip, W. (1997). Two-hybrid analysis reveals fundamental differences in direct interactions between desmoplakin and cell type-specific intermediate filaments. *J. Biol. Chem.* **272**, 21495–21503.

Menkel, A. R., Kroemker, M., Bubeck, P., Ronsiek, M., Nikolai, G., and Jockusch, B. M. (1994). Characterization of an F-actin-binding domain in the cytoskeletal protein vinculin. *J. Cell Biol.* **126**, 1231–1240.

Mertens, C., Kuhn, C., and Franke, W. W. (1996). Plakophilins 2a and 2b: constitutive proteins of dual location in the karyoplasm and the desmosomal plaque. *J. Cell Biol.* **135**, 1009–1025.

Milankov, K., and De Boni, U. (1993). Cytochemical localization of actin and myosin aggregates in interphase nuclei *in situ*. *Exp. Cell Res.* **209**, 189–199.

Millake, D. B., Blanchard, A. D., Patel, B., and Critchley, D. R. (1989). The cDNA sequence of a human placental alpha-actinin. *Nucleic Acids Res.* **17**, 6725.

Mitic, L. L., and Anderson, J. M. (1998). Molecular architecture of tight junctions. *Annu. Rev. Physiol.* **60**, 121–142.

Molenaar, M., van de Wetering, M., Oosterwegel, M., Peterson-Maduro, J., Godsave, S., Korinek, V., Roose, J., Destree, O., and Clevers, H. (1996). XTcf-3 transcription factor mediates beta-catenin-induced axis formation in *Xenopus* embryos. *Cell* **86**, 391–399.

Moore, M. S., and Blobel, G. (1993). The GTP-binding protein Ran/TC4 is required for protein import into the nucleus. *Nature (Lond.)* **365**, 661–663.

Moore, M. S., and Blobel, G. (1994). Purification of a Ran-interacting protein that is required for protein import into the nucleus. *Proc. Natl. Acad. Sci. USA* **91**, 10212–10216.

Mooseker, M. S. (1985). Organization, chemistry, and assembly of the cytoskeletal apparatus of the intestinal brush border. *Annu. Rev. Cell Biol.* **1**, 209–241.

Moulder, G. L., Huang, M. M., Waterston, R. H., and Barstead, R. J. (1996). Talin requires beta-integrin, but not vinculin, for its assembly into focal adhesion-like structures in the nematode *Caenorhabditis elegans*. *Mol. Biol. Cell* **7**, 1181–1193.

Mueller, H., and Franke, W. W. (1983). Biochemical and immunological characterization of desmoplakins I and II, the major polypeptides of the desmosomal plaque. *J. Mol. Biol.* **163**, 647–671.

Munemitsu, S., Albert, I., Souza, B., Rubinfeld, B., and Polakis, P. (1995). Regulation of intracellular beta-catenin levels by the adenomatous polyposis coli (APC) tumor-suppressor protein. *Proc. Natl. Acad. Sci. USA* **92**, 3046–3050.

Munemitsu, S., Albert, I., Rubinfeld, B., and Polakis, P. (1996). Deletion of an amino-terminal sequence beta-catenin *in vivo* and promotes hyperphosphorylation of the adenomatous polyposis coli tumor suppressor protein. *Mol. Cell Biol.* **16**, 4088–4094.

Nakai, K., and Kanehisa, M. (1992). A knowledge base for predicting protein localization sites in eukaryotic cells. *Genomics* **14**, 897–911.

Nebl, G., Meuer, S. C., and Samstag, Y. (1996). Dephosphorylation of serine 3 regulates nuclear translocation of cofilin. *J. Biol. Chem.* **271**, 26276–26280.

Neufeld, K. L., and White, R. L. (1997). Nuclear and cytoplasmic localizations of the adenomatous polyposis coli protein. *Proc. Natl. Acad. Sci. USA* **94**, 3034–3039.

Nieset, J. E., Redfield, A. R., Jin, F., Knudsen, K. A., Johnson, K. R., and Wheelock, M. J. (1997). Characterization of the interactions of alpha-catenin with alpha-actinin and beta-catenin/plakoglobin. *J. Cell Sci.* **110**, 1013–1022.

Niggli, V., Kaufmann, S., Goldmann, W. H., Weber, T., and Isenberg, G. (1994). Identification of functional domains in the cytoskeletal protein talin. *Eur. J. Biochem.* **224**, 951–957.

Nishida, E., Iida, K., Yonezawa, N., Koyasu, S., Yahara, I., and Sakai, H. (1987). Cofilin is a component of intranuclear and cytoplasmic actin rods induced in cultured cells. *Proc. Natl. Acad. Sci. USA* **84**, 5262–5266.

Nix, D. A., and Beckerle, M. C. (1997). Nuclear-cytoplasmic shuttling of the focal contact protein, zyxin: a potential mechanism for communication between sites of cell adhesion and the nucleus. *J. Cell Biol.* **138**, 1139–1147.

Nuckolls, G. H., Turner, C. E., and Burridge, K. (1990). Functional studies of the domains of talin. *J. Cell Biol.* **110**, 1635–1644.

Ohta, Y., Nishida, E., Sakai, H., and Miyamoto, E. (1989). Dephosphorylation of cofilin accompanies heat shock-induced nuclear accumulation of cofilin. *J. Biol. Chem.* **264**, 16143–16148.

Ohtsubo, M., Okazaki, H., and Nishimoto, T. (1989). The RCC1 protein, a regulator for the onset of chromosome condensation locates in the nucleus and binds to DNA. *J. Cell Biol.* **109**, 1389–1397.

Ohtsuka, T., Nakanishi, H., Ikeda, W., Satoh, A., Momose, Y., Nishioka, H., and Takai, Y. (1998). Nexilin: a novel actin filament-binding protein localized at cell–matrix adherens junction. *J. Cell Biol.* **143**, 1227–1238.

Onoda, K., Yu, F. X., and Yin, H. L. (1993). gCap39 is a nuclear and cytoplasmic protein. *Cell Motil. Cytoskeleton* **26**, 227–238.

Oxford, K., Crockett, C., Jensen, J. P., Weissman, A. M., and Byers, S. W. (1997). Serine phosphorylation-regulated ubiquitination and degradation of beta-catenin. *J. Biol. Chem.* **272**, 24735–24738.

Orsulic, S., and Peifer, M. (1996). An *in vivo* structure-function study of *armadillo*, the beta-catenin homologue, reveals both separate and overlapping regions of the protein required for cell adhesion and for wingless signaling. *J. Cell Biol.* **134**, 1283–1300.

Otey, C. A., Pavalko, F. M., and Burridge, K. (1990). An interaction between alpha actinin and the beta 1 integrin subunit *in vitro*. *J. Cell Biol.* **111**, 721–729.

Otto, J. J. (1983). Detection of vinculin-binding proteins with an  $^{125}\text{I}$ -vinculin gel overlay technique. *J. Cell Biol.* **97**, 1283–1287.

Ouyang, P., and Sugrue, S. P. (1996). Characterization of pinin, a novel protein associated with the desmosome-intermediate filament complex. *J. Cell Biol.* **135**, 1027–1042.

Paffenholz, R., and Franke, W. W. (1997). Identification and localization of a neurally expressed member of the plakoglobin/armadillo multigene family. *Differentiation* **61**, 293–304.

Parfenov, V. N., Davis, D. S., Pochukalina, G. N., Sample, C. E., Bugaeva, E. A., and Murti, K. G. (1995). Nuclear actin filaments and their topological changes in frog oocytes. *Exp. Cell Res.* **217**, 385–394.

Paschal, B. M., and Gerace, L. (1995). Identification of NTF2, a cytosolic factor for nuclear import that interacts with nuclear pore complex protein p62. *J. Cell Biol.* **129**, 925–937.

Pavalko, F. M., and Burridge, K. (1991). Disruption of the actin cytoskeleton after microinjection of proteolytic fragments of alpha-actinin. *J. Cell Biol.* **114**, 481–491.

Pemberton, L. F., Blobel, G., and Rosenblum, J. S. (1998). Transport routes through the nuclear pore complex. *Curr. Opin. Cell Biol.* **10**, 392–399.

Percipalle, P., Butler, P. J., Finch, J. T., Jans, D. A., and Rhodes, D. (1999). Nuclear localization signal recognition causes release of importin-alpha from aggregates in the cytosol. *J. Mol. Biol.* **292**, 263–273.

Pereira, G., Knop, M., and Schiebel, E. (1998). Spc98p directs the yeast gamma tubulin-complex into the nucleus and is subject to cell cycle-dependent phosphorylation on the nuclear side of the spindle pole body. *Mol. Biol. Cell* **9**, 775–793.

Pérez-Alvarado, G. C., Miles, C., Michelsen, J. W., Louis, H. A., Winge, D. R., Beckerle, M. C., and Summers, M. F. (1994). Structure of the carboxy-terminal LIM domain from the cysteine rich protein CRP. *Nat. Struct. Biol.* **1**, 388–398.

Pestonjamasp, K. N., Pope, R. K., Wulffkuhle, J. D., and Luna, E. J. (1997). Supervillin (p205): a novel membrane-associated, F-actin-binding protein in the villin/gelsolin superfamily. *J. Cell Biol.* **139**, 1255–1269.

Petit, M. M., Fradelizi, J., Golsteyn, R. M., Ayoubi, T. A., Menichi, B., Louvard, D., Van de Ven, W. J., and Friederich, E. (2000). LPP, an actin cytoskeleton protein related to zyxin, harbors a nuclear export signal and transcriptional activation capacity. *Mol. Biol. Cell* **11**, 117–129.

Picard, D., Salser, S. J., and Yamamoto, K. R. (1988). A movable and regulable inactivation function within the steroid binding domain of the glucocorticoid receptor. *Cell* **54**, 1073–1080.

Pines, J., and Hunter, T. (1994). The differential localization of human cyclins A and B is due to a cytoplasmic retention signal in cyclin B. *EMBO J.* **13**, 3772–3781.

Polakis, P. (1997). The adenomatous polyposis coli (APC) tumor suppressor. *Biochim. Biophys. Acta* **1332**, F127–F147.

Pollard, V. W., Michael, W. M., Nakielny, S., Siomi, M. C., Wang, F., and Dreyfuss, G. (1996). A novel receptor-mediated nuclear protein import pathway. *Cell* **86**, 985–994.

Prendergast, G. C., and Ziff, E. B. (1991). Mbh 1: a novel gelsolin/severin-related protein which binds actin *in vitro* and exhibits nuclear localization *in vivo*. *EMBO J.* **10**, 757–766.

Prieve, M. G., and Waterman, M. L. (1999). Nuclear localization and formation of beta-catenin-lymphoid enhancer factor 1 complexes are not sufficient for activation of gene expression. *Mol. Cell Biol.* **19**, 4503–4515.

Rajasekaran, A. K., Hojo, M., Huima, T., and Rodriguez-Boulan, E. (1996). Catenins and zonula occludens-1 form a complex during early stages in the assembly of tight junctions. *J. Cell Biol.* **132**, 451–463.

Rando, O. J., Zhao, K., and Crabtree, G. R. (2000). Searching for a function for nuclear actin. *Trends Cell Biol.* **10**, 92–97.

Reinhard, M., Jouvenal, K., Tripier, D., and Walter, U. (1995). Identification, purification, and characterization of a zyxin-related protein that binds the focal adhesion and microfilament protein VASP (vasodilator-stimulated phosphoprotein). *Proc. Natl. Acad. Sci. USA* **92**, 7956–7960.

Rexach, M., and Blobel, G. (1995). Protein import into nuclei: association and dissociation reactions involving transport substrate, transport factors, and nucleoporins. *Cell* **83**, 683–692.

Ribbeck, K., Lipowsky, G., Kent, H. M., Stewart, M., and Görlich, D. (1998). NTF2 mediates nuclear import of Ran. *EMBO J.* **17**, 6587–6598.

Rihs, H. P., Jans, D. A., Fan, H., and Peters, R. (1991). The rate of nuclear cytoplasmic protein transport is determined by the casein kinase II site flanking the nuclear localization sequence of the SV40 T-antigen. *EMBO J.* **10**, 633–639.

Rimm, D. L., Koslov, E. R., Kebriaei, P., Cianci, C. D., and Morrow, J. S. (1995). Alpha 1(E)-catenin is an actin-binding and -bundling protein mediating the attachment of F-actin to the membrane adhesion complex. *Proc. Natl. Acad. Sci. USA* **92**, 8813–8817.

Robbins, J., Dilworth, S. M., Laskey, R. A., and Dingwall, C. (1991). Two interdependent basic domains in nucleoplasmin nuclear targeting sequence: identification of a class of bipartite nuclear targeting sequence. *Cell* **64**, 615–623.

Roose, J., Molenaar, M., Peterson, J., Hurenkamp, J., Brantjes, H., Moerer, P., van de Wetering, M., Destree, O., and Clevers, H. (1998). The *Xenopus* Wnt effector XTcf-3 interacts with Groucho-related transcriptional repressors. *Nature (Lond.)* **395**, 608–612.

Rosenblum, J. S., Pemberton, L. F., and Blobel, G. (1997). A nuclear import pathway for a protein involved in tRNA maturation. *J. Cell Biol.* **139**, 1655–1661.

Rout, M. P., Blobel, G., and Aitchison, J. D. (1997). A distinct nuclear import pathway used by ribosomal proteins. *Cell* **89**, 715–725.

Rubinfeld, B., Souza, B., Albert, I., Muller, O., Chamberlain, S. H., Masiarz, F. R., Munemitsu, S., and Polakis, P. (1993). Association of the APC gene product with beta-catenin. *Science* **262**, 1731–1734.

Sadler, I., Crawford, A. W., Michelsen, J. W., and Beckerle, M. C. (1992). Zyxin and cCRP: two interactive LIM domain proteins associated with the cytoskeleton. *J. Cell Biol.* **119**, 1573–1587.

Sahlas, D. J., Milankov, K., Park, P. C., and De Boni, U. (1993). Distribution of snRNPs, splicing factor SC-35 and actin in interphase nuclei: immunocytochemical evidence for differential distribution during changes in functional states. *J. Cell Sci.* **105**, 347–357.

Sakisaka, T., Nakanishi, H., Takahashi, K., Mandai, K., Miyahara, M., Satoh, A., Takaishi, K., and Takai, Y. (1999). Different behavior of and neurabin-II during the formation and destruction of cell-cell adherens junction. *Oncogene* **18**, 1609–1617.

Sánchez-García, I., and Rabbits, T. H. (1994). The LIM domain: a new structural motif found in zinc-finger-like proteins. *Trends Genet.* **10**, 315–320.

Sanger, J. W., Sanger, J. M., Kreis, T. E., and Jockusch, B. M. (1980). Reversible translocation of cytoplasmic actin into the nucleus caused by dimethyl sulfoxide. *Proc. Natl. Acad. Sci. USA* **77**, 5268–5272.

Saras, J., and Heldin, C. H. (1996). PDZ domains bind carboxy-terminal sequences of target proteins. *Trends Biochem. Sci.* **21**, 455–458.

Scheer, U., Hinszen, H., Franke, W. W., and Jockusch, B. M. (1984). Microinjection of actin-binding proteins and actin antibodies demonstrates involvement of nuclear actin in transcription of lampbrush chromosomes. *Cell* **39**, 111–122.

Schlenschedt, G., Smirnova, E., Deane, R., Solsbacher, J., Kutay, U., Görlich, D., Ponstingl, H., and Bischoff, F. R. (1997). Yrb4p, a yeast ran-GTP-binding protein involved in import of ribosomal protein L25 into the nucleus. *EMBO J.* **16**, 6237–6249.

Schmeichel, K. L., and Beckerle, M. C. (1997). Molecular dissection of a LIM domain. *Mol. Biol. Cell* **8**, 219–230.

Schmeichel, K. L., and Beckerle, M. C. (1998). LIM domains of cysteine-rich protein 1 (CRP1) are essential for its zyxin-binding function. *Biochem. J.* **331**, 885–892.

Schmidt, A., Heid, H. W., Schäfer, S., Nuber, U. A., Zimbelmann, R., and Franke, W. W. (1994). Desmosomes and cytoskeletal architecture in epithelial differentiation: cell type-specific plaque components and intermediate filament anchorage. *Eur. J. Cell Biol.* **65**, 229–245.

Schmidt, A., Langbein, L., Rode, M., Prätzel, S., Zimbelmann, R., and Franke, W. W. (1997). Plakophilins 1a and 1b: widespread nuclear proteins recruited in specific epithelial cells as desmosomal plaque components. *Cell. Tissue Res.* **290**, 481–499.

Schroeter, E. H., Kisslinger, J. A., and Kopan, R. (1998). Notch-1 signalling requires ligand-induced proteolytic release of intracellular domain. *Nature (Lond.)* **393**, 382–386.

Shi, J., and Sugrue, S. P. (2000). Dissection of protein linkage between keratines and pinin, a protein with dual location at desmosome-intermediate filament complex and in the nucleus. *J. Biol. Chem.* **275**, 14910–14915.

Shi, Y., Tabesh, M., Shi, J., and Sugrue, S. P. (1997). Pinin, a desmosome-associated protein and a potential tumor suppressor. *Mol. Biol. Cell* **8S**, 418a.

Shoeman, R. L., and Traub, P. (1990). The *in vitro* DNA-binding properties of purified nuclear lamin proteins and vimentin. *J. Biol. Chem.* **265**, 9055–9061.

Shoeman, R. L., Wadle, S., Scherbarth, A., and Traub, P. (1988). The binding *in vitro* of the intermediate filament protein vimentin to synthetic oligonucleotides containing telomere sequences. *J. Biol. Chem.* **263**, 18744–18749.

Simcha, I., Shtutman, M., Salomon, D., Zhurinsky, J., Sadot, E., Geiger, B., and Ben-Ze'ev, A. (1998). Differential nuclear translocation and transactivation potential of beta-catenin and plakoglobin. *J. Cell Biol.* **141**, 1433–1448.

Simmons, M., Shi, Y., Shi, J., and Sugrue, S. P. (1998). Identification of nuclear and subnuclear localization domains in the desmosome-associated and nuclear protein pinin. *Mol. Biol. Cell* **9S**, 186a.

Siomi, M. C., Eder, P. S., Kataoka, N., Wan, L., Liu, Q., and Dreyfuss, G. (1997). Transportin-mediated nuclear import of heterogeneous nuclear RNP proteins. *J. Cell Biol.* **138**, 1181–1192.

Smith, A., Brownawell, A., and Macara, I. G. (1998). Nuclear import of Ran is mediated by the transport factor NTF2. *Curr. Biol.* **8**, 1403–1406.

Smith, E. A., and Fuchs, E. (1998). Defining the interactions between intermediate filaments and desmosomes. *J. Cell Biol.* **141**, 1229–1241.

Smith, H. M., and Raikhel, N. V. (1998). Nuclear localization signal receptor importin alpha associates with the cytoskeleton. *Plant Cell* **10**, 1791–1799.

Smith, H. M., and Raikhel, N. V. (1999). Protein targeting to the nuclear pore. What can we learn from plants? *Plant Physiol.* **119**, 1157–1164.

Smith, H. M., Hicks, G. R., and Raikhel, N. V. (1997). Importin alpha from *Arabidopsis thaliana* is a nuclear import receptor that recognizes three classes of import signals. *Plant Physiol.* **114**, 411–417.

Sommer, L., Hagenbüchle, O., Wellauer, P. K., and Strubin, M. (1991). Nuclear targeting of the transcription factor PTF1 is mediated by a protein subunit that does not bind to the PTF1 cognate sequence. *Cell* **67**, 987–994.

Soyer-Gobillard, M. O., Ausseil, J., and Géraud, M. L. (1996). Nuclear and cytoplasmic actin in dinoflagellates. *Biol. Cell* **87**, 17–35.

Spector, D. L. (1993). Macromolecular domains within the cell nucleus. *Annu. Rev. Cell Biol.* **9**, 265–315.

Srinivasan, M., Edman, C. F., and Schulman, H. (1994). Alternative splicing introduces a nuclear localization signal that targets multifunctional CaM kinase to the nucleus. *J. Cell Biol.* **126**, 839–852.

Stade, K., Ford, C. S., Guthrie, C., and Weis, K. (1997). Exportin 1 (Crm1p) is an essential nuclear export factor. *Cell* **90**, 1041–1050.

Stappenbeck, T. S., Bornslaeger, E. A., Corcoran, C. M., Luu, H. H., Virata, M. L., and Green, K. J. (1993). Functional analysis of desmoplakin domains: specification of the interaction with keratin versus vimentin intermediate filament networks. *J. Cell Biol.* **123**, 691–705.

Stappenbeck, T. S., Lamb, J. A., Corcoran, C. M., and Green, K. J. (1994). Phosphorylation of the desmoplakin COOH terminus negatively regulates its interaction with keratin intermediate filament networks. *J. Biol. Chem.* **269**, 29351–29354.

Stevenson, B. R., and Keon, B. H. (1998). The tight junction: morphology to molecules. *Annu. Rev. Cell Dev. Biol.* **14**, 89–109.

Stevenson, B. R., Siliciano, J. D., Mooseker, M. S., and Goodenough, D. A. (1986). Identification of ZO-1: a high molecular weight polypeptide associated with the tight junction (zonula occludens) in a variety of epithelia. *J. Cell Biol.* **103**, 755–766.

Struhl, G., and Adachi, A. (1998). Nuclear access and action of notch *in vivo*. *Cell* **93**, 649–660.

Takagaki, Y., and Manley, J. L. (2000). Complex protein interactions within the human polyadenylation machinery identify a novel component. *Mol. Cell Biol.* **20**, 1515–1525.

Takahashi, K., Nakanishi, H., Miyahara, M., Mandai, K., Satoh, K., Satoh, A., Nishioka, H., Aoki, J., Nomoto, A., Mizoguchi, A., and Takai, Y. (1999). Nectin/PRR: an immunoglobulin-like cell adhesion molecule recruited to cadherin-based adherens junctions through interaction with Afadin, a PDZ domain-containing protein. *J. Cell Biol.* **145**, 539–549.

Tanaka, Y., Watanabe, T., Chiba, N., Niki, M., Kuroiwa, Y., Nishihira, T., Satomi, S., Ito, Y., and Satake, M. (1997). The protooncogene product, PEBP2beta/CBFbeta, is mainly located in the cytoplasm and has an affinity with cytoskeletal structures. *Oncogene* **15**, 677–683.

Tang, T. K., Leto, T. L., Correas, I., Alonso, M. A., Marchesi, V. T., and Benz, E. J. J. (1988). Selective expression of an erythroid-specific isoform of protein 4.1. *Proc. Natl. Acad. Sci. USA* **85**, 3713–3717.

Tiganis, T., Flint, A. J., Adam, S. A., and Tonks, N. K. (1997). Association of the T-cell protein tyrosine phosphatase with nuclear import factor p97. *J. Biol. Chem.* **272**, 21548–21557.

Tranqui, L., and Block, M. R. (1995). Intracellular processing of talin occurs within focal adhesions. *Exp. Cell Res.* **217**, 149–156.

Traub, P., and Nelson, W. J. (1983). The interaction *in vitro* of the intermediate filament protein vimentin with synthetic polyribo- and polydeoxyribonucleotides. *Hoppe Seylers Z. Physiol. Chem.* **364**, 575–592.

Traub, P., and Shoeman, R. L. (1994). Intermediate filament proteins: cytoskeletal elements with gene-regulatory function? *Int. Rev. Cytol.* **154**, 1–103.

Traub, P., Vorgias, C. E., and Nelson, W. J. (1985). Interaction *in vitro* of the neurofilament triplet proteins from porcine spinal cord with natural RNA and DNA. *Mol. Biol. Rep.* **10**, 129–136.

Troyanovsky, S. M., Troyanovsky, R. B., Eshkind, L. G., Krutovskikh, V. A., Leube, R. E., and Franke, W. W. (1994a). Identification of the plakoglobin-binding domain in desmoglein and its role in plaque assembly and intermediate filament anchorage. *J. Cell Biol.* **127**, 151–160.

Troyanovsky, S. M., Troyanovsky, R. B., Eshkind, L. G., Leube, R. E., and Franke, W. W. (1994b).

Identification of amino acid sequence motifs in desmocollin, a desmosomal glycoprotein, that are required for plakoglobin binding and plaque formation. *Proc. Natl. Acad. Sci. USA* **91**, 10790–10794.

Truant, R., and Cullen, B. R. (1999). The arginine-rich domains present in human immunodeficiency virus type 1 Tat and Rev function as direct importin beta-dependent nuclear localization signals. *Mol. Cell Biol.* **19**, 1210–1217.

Tsukita, S., Furuse, M., and Itoh, M. (1999). Structural and signalling molecules come together at tight junctions. *Curr. Opin. Cell Biol.* **11**, 628–633.

Tsuneoka, M., Imamoto, N. S., and Uchida, T. (1986). Monoclonal antibody against non-histone chromosomal protein high mobility group 1 co-migrates with high mobility group 1 into the nucleus. *J. Biol. Chem.* **261**, 1829–1834.

van de Wetering, M., Cavallo, R., Dooijes, D., van Beest, M., van Es, J., Loureiro, J., Ypma, A., Hursh, D., Jones, T., Bejsovec, A., Peifer, M., Mortin, M., and Clevers, H. (1997). *Armadillo* coactivates transcription driven by the product of the *Drosophila* segment polarity gene dTCF. *Cell* **88**, 789–799.

van Hengel, J., Vanhoenacker, P., Staes, K., and van Roy, F. (1999). Nuclear localization of the p120(ctn) *Armadillo*-like catenin is counteracted by a nuclear export signal and by E-cadherin expression. *Proc. Natl. Acad. Sci. USA* **96**, 7980–7985.

Vorgias, C. E., and Traub, P. (1986). Nucleic acid-binding activities of the intermediate filament subunit proteins desmin and glial fibrillary acidic protein. *Z. Naturforsch.* **41**, 897–909.

Wachstock, D. H., Wilkins, J. A., and Lin, S. (1987). Specific interaction of vinculin with alpha-actinin. *Biochem. Biophys. Res. Commun.* **146**, 554–560.

Wada, A., Fukuda, M., Mishima, M., and Nishida, E. (1998). Nuclear export of actin: a novel mechanism regulating the subcellular localization of a major cytoskeletal protein. *EMBO J.* **17**, 1635–1641.

Wahl, J. K., Sacco, P. A., McGranahan-Sadler, T. M., Saupé, L. M., Wheelock, M. J., and Johnson, K. R. (1996). Plakoglobin domains that define its association with the desmosomal cadherins and the classical cadherins: identification of unique and shared domains. *J. Cell Sci.* **109**, 1143–1154.

Waltzer, L., and Bienz, M. (1998). *Drosophila* CBP represses the transcription factor TCF to antagonize Wingless signalling. *Nature (Lond.)* **395**, 521–525.

Wehland, J., Weber, K., and Osborn, M. (1980). Translocation of actin from the cytoplasm into the nucleus in mammalian cells exposed to demethylsulfoxide. *Biol. Cell* **39**, 109–111.

Weis, K. (1998). Importins and exportins: how to get in and out of the nucleus. *Trends Biochem. Sci.* **23**, 185–189.

Weiss, E. E., Kroemker, M., Rüdiger, A. H., Jockusch, B. M., and Rüdiger, M. (1998). Vinculin is part of the cadherin-catenin junctional complex: complex formation between alpha-catenin and vinculin. *J. Cell Biol.* **141**, 755–764.

Welch, W. J., and Suhar, J. P. (1985). Morphological study of the mammalian stress response: characterization of changes in cytoplasmic organelles, cytoskeleton, and nucleoli, and appearance of intranuclear actin filaments in rat fibroblasts after heat-shock treatment. *J. Cell Biol.* **101**, 1198–1211.

Whittaker, G. R., Myers, J., Bui, M., and Helenius, A. (1998). Nucleo-cytoplasmic localization of influenza virus nucleoprotein depends on cell density and phosphorylation. *Mol. Biol. Cell* **9S**, 187a.

Willott, E., Balda, M. S., Fanning, A. S., Jameson, B., Van Itallie, C., and Anderson, J. M. (1993). The tight junction protein ZO-1 is homologous to the *Drosophila* discs-large tumor suppressor protein of septate junctions. *Proc. Natl. Acad. Sci. USA* **90**, 7834–7838.

Witcher, L. L., Collins, R., Puttagunta, S., Mechanic, S. E., Munson, M., Gumbiner, B., and Cowin, P. (1996). Desmosomal cadherin binding domains of plakoglobin. *J. Biol. Chem.* **271**, 10904–10909.

Woods, D. F., and Bryant, P. J. (1991). The discs-large tumor suppressor gene of *Drosophila* encodes a guanylate kinase homolog localized at septate junctions. *Cell* **66**, 451–464.

Wozniak, R. W., Rout, M. P., and Aitchison, J. D. (1998). Karyopherins and kissing cousins. *Trends Cell Biol.* **8**, 184–188.

Wu, R. Y., and Gill, G. N. (1994). LIM domain recognition of a tyrosine-containing tight turn. *J. Biol. Chem.* **269**, 25085–25090.

Wulffkuhle, J. D., Donina, I. E., Stark, N. H., Pope, R. K., Pestonjamas, K. N., Niswonger, M. L., and Luna, E. J. (1999). Domain analysis of supervillin, an F-actin bundling plasma membrane protein with functional nuclear localization signals. *J. Cell Sci.* **112**, 2125–2136.

Xiao, C. Y., Hübner, S., and Jans, D. A. (1997). SV40 large tumor antigen nuclear import is regulated by the double-stranded DNA-dependent protein kinase site (serine 120) flanking the nuclear localization sequence. *J. Biol. Chem.* **272**, 22191–22198.

Xu, L., Gonzalez-Agosti, C., Beauchamp, R., Pinney, D., Sterner, C., and Ramesh, V. (1998). Analysis of molecular domains of epitope-tagged merlin isoforms in Cos-7 cells and primary rat Schwann cells. *Exp. Cell Res.* **238**, 231–240.

Yamamoto, T., Harada, N., Kano, K., Taya, S., Canaani, E., Matsuura, Y., Mizoguchi, A., Ide, C., and Kaibuchi, K. (1997). The Ras target AF-6 interacts with ZO-1 and serves as a peripheral component of tight junctions in epithelial cells. *J. Cell Biol.* **139**, 785–795.

Yan, C., Leibowitz, N., and Mélèse, T. (1997). A role for the divergent actin gene, ACT2, in nuclear pore structure and function. *EMBO J.* **16**, 3572–3586.

Yao, X., Thibodeau, A., and Forte, J. G. (1993). Ezrin-calpain I interactions in gastric parietal cells. *Am. J. Physiol.* **265**, C36–C46.

Yaseen, N. R., and Blobel, G. (1997). Cloning and characterization of human karyopherin beta3. *Proc. Natl. Acad. Sci. USA* **94**, 4451–4456.

Yokoya, F., Imamoto, N., Tachibana, T., and Yoneda, Y. (1999). beta-catenin can be transported into the nucleus in a Ran-unassisted manner. *Mol. Biol. Cell* **10**, 1119–1131.

Yost, C., Torres, M., Miller, J. R., Huang, E., Kimelman, D., and Moon, R. T. (1996). The axis-inducing activity, stability, and subcellular distribution of beta-catenin is regulated in *Xenopus* embryos by glycogen synthase kinase 3. *Genes Dev.* **10**, 1443–1454.

Youssoufian, H., McAfee, M., and Kwiatkowski, D. J. (1990). Cloning and chromosomal localization of the human cytoskeletal alpha-actinin gene reveals linkage to the beta-spectrin gene. *Am. J. Hum. Genet.* **47**, 62–71.

Yu, F. X., Johnston, P. A., Südhof, T. C., and Yin, H. L. (1990). gCap39, a calcium ion- and polyphosphoinositide-regulated actin capping protein. *Science* **250**, 1413–1415.

Zeng, L., Fagotto, F., Zhang, T., Hsu, W., Vasicek, T. J., Perry, W. L. 3rd, Lee, J. J., Tilghman, S. M., Gumbiner, B. M., and Costantini, F. (1997). The mouse Fused locus encodes Axin, an inhibitor of the Wnt signaling pathway that regulates embryonic axis formation. *Cell* **90**, 181–192.

Zhang, G., Taneja, K. L., Singer, R. H., and Green, M. R. (1994). Localization of pre-mRNA splicing in mammalian nuclei. *Nature (Lond.)* **372**, 809–812.

Zhao, L. J., and Padmanabhan, R. (1988). Nuclear transport of adenovirus DNA polymerase is facilitated by interaction with preterminal protein. *Cell* **55**, 1005–1015.

Zhu, J., and McKeon, F. (1999). NF-AT activation requires suppression of Crm1-dependent export by calcineurin. *Nature (Lond.)* **398**, 256–260.

This Page Intentionally Left Blank

# INDEX

## A

A-Actinin 4, 218  
Abdominal irradiation  
    side effects, 2  
A/ $\beta$  importin, 210–211  
    NLS, 213  
Abscisic acid  
    meristem, 188  
Absorptive cells  
    intestines, 7–8  
Acetylcholine, 10–11  
Acid  
    single dose unshielded low-LET  
        irradiation, 67  
Actin, 243–244  
    enterocytes, 7  
    *Saccharomyces cerevisiae*, 218  
Actinin-4, 238  
A-cyclins, 173  
Adenocarcinoma, 13, 39–41  
Adherens junctions  
    plaque proteins  
        nuclear signaling, 214–227  
Adhesive junctions  
    plaque proteins, 214  
Adrenal glands  
    PrPc, 142  
Adventitia  
    intestine, 6  
Afadin, 224–225  
Age  
    intestinal radiation, 92  
    intestines, 12  
    radiation enteropathy, 99  
AINTEGUMENTA (ANT), 180

Angiosperm meristem  
    organization, 174  
Anorectal manometry, 83  
ANT, 180  
*Antirrhinum*, 175, 180  
*Antirrhinum majus*, 192  
Apical meristem  
    Ginkgo  
        zonal model, 175  
    shoot, 161–163  
Apoplast, 185  
Apoptosis, 19  
    enterocytes, 7  
    intestinal epithelium, 3–4, 15  
    radiation, 13–14  
        time of day, 91–92  
*Arabidopsis*, 167, 171,  
    175, 181  
    meristem  
        cell proliferation, 176  
*Arabidopsis GLABRA2*,  
    179  
*Arabidopsis thaliana*  
    plasmodesmata  
        TEM, 186  
*Armadillo*, 226–227  
Arteriosclerosis  
    IORT, 79  
*AS1* genes, 180  
Astrocytes  
    PrPsc, 131–132  
ASYMMETRIC LEAVES 1, 180  
Atherosclerosis, 79  
*ATML1* gene, 179  
Auxin signals  
    meristem, 188–189

**B**

Background radiation, 87  
 Base excision repair (BER), 19  
 B-catenin, 214–224  
     homolog  
     *Drosophila*, 210  
     WGA, 222–223  
 B-cyclins, 173  
 Becquerel (Bq), 17  
 BER, 19  
 B-galactosidase, 42  
 B-glucuronidase, 42  
 B importin, 210–211  
     HEAT repeats, 210–211  
     NLS, 213  
 Books, 2  
 Bovine spongiform encephalopathy (BSE), 122, 123  
 Bovine supervillin, 218  
 Bq, 17  
 Brunner's glands  
     intestines, 8  
 Brush border enzymes, 42  
 BSE, 122, 123  
 Bursa of Fabricius  
     apoptosis, 65  
 Bystander effect, 100

**C**

Ca<sup>2+</sup>/calcineurin-mediated  
     dephosphorylation, 212–213  
 Cadherins  
     adherens junctions, 214–215  
     catenins, 214–215  
*Campylobacter jejuni*, 57–58  
 Carcinoma  
     large intestine, 74  
 Cat  
     single dose partial body low-LET  
         irradiation  
         cell growth disturbances, 39–41  
 Catenins  
     cadherins, 214–215  
 Cat intestines  
     intercellular separation, 41  
     irradiated, 43  
     TGF- $\beta$ , 49  
 CCK

intestine, 6–7  
 rat hypothalamus, 66  
 CDC28, 171  
 CDK, 170  
 CDK-b proteins, 172  
 Cell cycle checkpoints, 21  
 Cell division  
     meristematic cells, 167–174  
 Cell expansion  
     cell wall, 165–167  
 Cell growth  
     cell wall synthesis, 163–165  
     fractionated low-LET radiation, 74  
     single dose partial body low-LET  
         irradiation, 39–41  
 Cell injury  
     ROS, 18  
 Cellulobiose/mannitol, 74–75  
 Cell survival, 22  
 Cellular prion protein (PrP<sup>C</sup>), 121–122  
     adrenal glands, 142  
     central nervous system, 144–145  
     copper, 146–147  
     eyes, 141–142  
     functions, 144–150  
     gastrointestinal tract, 135–137  
     golgi apparatus, 137, 143  
     granules, 143  
     heart, 142  
     hepatocytes, 138–139  
     intestines, 137  
     islet of Langerhans, 141  
     Ito cells, 138  
     keratinocytes, 138  
     kidneys, 142  
     liver, 138–139  
     lung, 139  
     macrophages, 135  
     metalloprotein, 146–147  
     mitochondria, 144  
     mononuclear cells, 133–134  
     muscles, 139–140  
     NMJ, 139–140  
     nucleus, 143  
     oxidative stress, 146–147  
     pancreas, 141  
     parietal cells, 135–137  
     perisinusoidal stellate, 138  
     plasma membrane, 142–143  
     platelets, 134–135  
     posttranslational cleavage, 130

prion diseases, 148–149  
properties, 129  
receptors, 147–148  
salivary glands, 142  
secretory vesicles, 143  
sperm cells, 140–141  
stomach, 135–137  
three-dimensional structure, 128  
vessels, 132

Cell wall  
cell expansion, 165–167

Central nervous system  
PrPc, 144–145

Central zone  
meristem, 175

CGRP  
intestine, 7

Chemotherapy  
intestinal radiation, 92

Chernobyl accident, 90

Cholecystokinin (CCK)  
intestine, 6–7  
rat hypothalamus, 66

Choroid plexus epithelium  
PrP, 132–133

Chronic wasting disease (CWD), 122

Cingulin, 233–234

Circadian rhythm  
intestinal epithelial kinetics, 91

Circulating blood elements  
PrP, 133–135

CJD, 122, 123

CLAVATA genes  
meristem, 179–180, 194–195

CLAVATA pathway  
meristem, 190–192

Colonic familial adenomatous polyposis, 13

Colonic microvilli  
enterocytes, 7–8

Colonic mucosa  
stained, 76

Concanavalin A lectin, 134

Copper  
PrPc, 146–147

Corpus, 175

Creutzfeldt-Jakob disease (CJD), 122, 123

Crypt  
fission  
intestinal, 5

Cryptal enterocytes  
rat small intestines, 41

Crypts, 88  
Crypt squash cells  
DNA synthesis, 56

Crypt-villus axis, 3–5

Cultured cells  
radiation-induced proliferative changes, 22

CUP SHAPED COTYLEDON genes, 181

Cu-ZnSOD, 53

CWD, 122

Cyclin B1  
cytoplasmic retention, 213–214

Cyclin-dependent kinase (CDK), 170

Cyclin-dependent kinase (CDK)-b  
proteins, 172

Cyclin D pathway  
meristem, 195–196

Cyclins, 170  
plant, 172–174

CYLCOIDEA gene, 196

Cysteine, 19

Cytokines  
intestine, 6–7

Cytokinin  
meristem, 188  
signaling  
meristem, 189–200

Cytoplasmic retention factor, 213–214

Cytoskeleton  
cell expansion, 165–167

**D**

D-cyclins, 173

DEFICIENS, 192

Dephosphorylation  
 $\text{Ca}^{2+}$ /calcineurin-mediated, 212–213

Desmosome  
plaque proteins  
nuclear signaling, 226–230

Diabetes  
intestinal radiation, 93

Diet  
intestinal fibrosis, 95  
intestinal radiation, 12, 94–95, 99

Dietary supplements  
intestinal radiation, 94–95

Dioxin  
receptors, 213

Dlg, 217

DNA  
 damage, 19  
 endonuclease, 19  
 glycosylase, 19  
 ligase, 19  
 polymerase, 19

Dog intestines  
 cryptal necrosis, 41  
 fractionated low-LET radiation  
 endocrine system, 81

LET  
 neutrons, 85

single dose partial body low-LET  
 irradiation  
 cryptal changes, 35  
 fibrogenesis, 45–46  
 inflammatory system, 47–48

Dog large intestines  
 fractionated low-LET radiation  
 muscles, 82–83

Dog small intestines, 75  
 fractionated low-LET radiation  
 inflammatory system,  
 77–78

IORT  
 outcomes, 84

Dorsal  
 NLS, 213

Dose ranges  
 irradiated intestine, 23

*Drosophila*, 197  
 $\beta$ -catenin homolog, 210

Duodenal villous enterocytes, 7

**E**

Ectopic mucous glands  
 rat small intestines, 33

EGF, 8

Electromagnetic radiation, 16

Elemental diet  
 intestinal radiation, 94, 95

Emaciation  
 intestinal radiation, 92

Endocrine cells  
 intestines, 8  
 Paneth cells, 8  
 rat in  
 whole-body exposure, 68

single dose low-LET irradiation  
 partial body, 51  
 unshielded, 66–70

Endocrine system  
 fractionated low-LET radiation, 81–82

Endocytosis, 130–131

Endoplasmic reticulum, 19

ENS, 9–10  
 Enteric nervous system (ENS), 9–10  
 Enteric secretomotor innervation, 12

Enteritis  
 radiation, 93–96

Enterocytes  
 apoptosis, 7  
 colonic microvilli, 7–8  
 cryptal  
 rat small intestines, 41  
 duodenal villous, 7  
 intestines, 7–8  
 microvillous membranes, 7  
 mucosal barrier, 7  
 radiation-induced changes, 97  
 single dose low-LET irradiation  
 partial body, 41–42  
 unshielded, 57–58

Environmental radionuclides, 87

Eosinophils  
 fractionated low-LET radiation, 78  
 single dose unshielded low-LET  
 irradiation, 63–64

Ependymal cells  
 PrP, 132–133

Epidermal growth factor (EGF), 8

Epithelial basement membrane  
 intestine, 6

Epithelial regeneration  
 mouse colorectal fibrosis, 84

Epithelial TGF- $\beta$ 1, 43

Epithelium  
 fractionated low-LET radiation, 74–75  
 intestine, 3  
 single dose partial body low-LET  
 irradiation, 41–42

ERT, 22–23  
 rabbit celiac artery, 79  
 TGF- $\alpha$   
 rabbit intestines, 48–49

External radiotherapy (ERT), 22–23  
 rabbit celiac artery, 79  
 TGF- $\alpha$   
 rabbit intestines, 48–49

Extracellular matrix, 22

Eyes  
PrPc, 141–142

**F**

F-actin binding proteins, 242–243  
Familial CJD (fCJD), 122  
*Fasciata1* mutants, 182  
*Fasciata2* mutants, 182  
*Fass* mutants  
    meristematic cells, 167, 184  
Fatal familial insomnia (FFI), 122  
FCJD, 122  
FDC  
    scrapie, 133  
Feline spongiform encephalopathy (FSE), 122  
FFI, 122  
Fibers  
    fractionated low-LET radiation, 77  
    single dose low-LET irradiation  
        partial body, 45–46  
        unshielded, 62–63

Fibroblasts, 90  
Fibrogenesis  
    fractionated low-LET radiation, 77  
    single dose low-LET irradiation  
        partial body, 45–46  
        unshielded, 62–63  
Fibrosis  
    intestinal  
        diet, 95  
    M6P/IGF-II receptor positive cells, 46  
Field/volume irradiated  
    intestinal radiation, 84  
FIMBRIATA, 180  
*Fim* gene  
    meristem, 194  
Fistula  
    radiation, 79  
Floral meristem, 163  
FLORICAULA transcription factors, 182  
Focal contact  
    plaque proteins  
        nuclear signaling, 234–238  
Follicular dendritic cell (FDC)  
    scrapie, 133  
Food chain  
    radionuclides, 87

Fractionated doses, 90  
    diet, 94  
Fractionated low-LET radiation  
    cell growth, 74  
    compartments, 72–74  
    cryptal changes, 72–73  
    endocrine system, 81–82  
    epithelial cells, 74–77  
    immune system, 77–78  
    inflammatory system, 77–78  
    intestine, 70–83  
    muscles, 82–83  
    stroma/connective tissue, 77–81  
    tissue changes, 73–74  
    vascular components, 79–81  
    villous changes, 72–73  
FSE, 122

**G**

GALT, 63  
    intestines, 9  
Gastrin  
    single dose unshielded low-LET  
        irradiation, 67  
Gastrointestinal disease  
    classification, 13  
    developmental disorders, 13  
    inflammatory reaction, 13  
    metaplasia, 13  
Gastrointestinal tract  
    PrPc, 135–137  
G1-cyclins, 173  
Gene expression patterns  
    meristem, 182–183  
Gene-related peptide (CGRP)  
    intestine, 7  
Gerstmann-Straussler-Sheinker disease  
    (GSS), 122  
Ginkgo apical meristem  
    zonal model, 175  
Glands  
    single dose low-LET irradiation  
        partial body, 41–42  
        unshielded, 57–58  
Glial cells  
    PrPsc, 131–132  
GLOBOSA, 192  
Glucocorticoid  
    receptors, 213

Glucose, 43  
 Glutamine  
     intestinal radiation, 94, 95  
 Glutathione, 19  
 Glycoforms  
     PrPsc, 130  
 GMP, 28  
 Goblet cells  
     fractionated low-LET radiation, 75–77  
     intestines, 8  
     single dose low-LET irradiation  
         partial body, 43–44  
         unshielded, 61–62  
     time of day of irradiation, 91–92  
 Golgi apparatus  
     PrPc, 137, 143  
 Granules  
     PrPc, 143  
 Granulocyte marker protein (GMP), 28  
 Gray, 16–17  
 GSS, 122  
 Gut associated lymphoid tissue (GALT)  
     intestines, 9

## H

HDlg isoform 1/2, 217  
 Heart  
     PrPc, 142  
 Heavy ion beams  
     LET intestinal radiation, 86–87  
 Hepatocytes  
     PrPc, 138–139  
 Heterologous nuclear RNA binding protein  
     (hnRNP A1), 209  
 HnRNP A1, 209  
 Homeobox genes  
     meristem, 176–179  
 Homologous recombination repair (HRR), 19  
 Hormones  
     meristem, 188–190  
 HRR, 19  
 Hyperbaric oxygen, 93–94

## I

Iatrogenic Creutzfeldt-Jakob disease  
     (iCJD), 122  
 ICCs, 10–11

ICJD, 122  
 IELs, 9  
 IFs, 244–245  
 Immune responses  
     intestinal, 64  
 Immune status  
     intestinal radiation, 90  
 Immune system  
     fractionated low-LET radiation, 77–78  
     single dose low-LET irradiation  
         partial body, 46–48  
         unshielded, 63–64  
 Inflammatory system  
     fractionated low-LET radiation, 77–78  
     single dose low-LET irradiation  
         partial body, 46–48  
         unshielded, 63–64  
 Ingested radioactive material  
     intestinal radiation, 89–90  
 Injury score  
     irradiated rat small intestines, 28–29  
 Inner elastic membrane  
     microphotography, 78  
 iNOS immunoreactivity (iNOS-IR), 69  
     mouse colon, 60  
 iNOS-IR, 69  
     mouse colon, 60  
 Intermediate filaments (IFs), 244–245  
 Interstitial cells of Cajal (ICCs), 10–11  
 Intestinal epithelium  
     apoptosis, 3–4, 15  
 Intestinal fibrosis  
     diet, 95  
 Intestinal immune responses, 64  
 Intestinal radiation, 16–22, 43  
     bright-field micrograph, 37  
     diet, 94–95  
     dietary supplements, 94–95  
     dose ranges, 23  
     field/volume irradiated, 84  
     immune status, 90  
     ingested radioactive material, 89–90  
     injury score, 28–29  
     interparameter comparisons, 30  
     LET, 85–87  
     mechanistic experiments, 95–96  
     medical treatment, 93–96  
     morphology, 23–26  
         data classification, 24–26  
         data interpretation, 26  
         variables, 23

pathology, 92–93  
physical intervention, 90–91  
schedules, 87–88  
    changes, 96–100  
shielding, 84  
surgical status, 90–91  
time of day, 91–93  
time ranges, 24

**I**  
Intestines. *See also* Cat intestines; Dog intestines; Large intestines; Mouse intestines; Pig intestines; Rabbit intestines; Rat intestines; Small intestines  
    absorptive cells, 7–8  
    adventitia, 6  
    aging, 12  
    Brunner's glands, 8  
    CCK, 6–7  
    CGRP, 7  
    diet, 12  
    effector pathways, 9–11  
    endocrine cells, 8  
    enterocytes, 7–8  
    epithelial basement membrane, 6  
    epithelium, 3  
    fractionated low-LET radiation, 70–83  
    GALT, 9  
    goblet cells, 8  
    injury  
        epithelial response, 13–14  
    intercellular messengers, 6–7  
    irradiated  
        ratio score, 29–30  
        time ranges, 24  
    lamina propria, 3  
        superficial reticular sheet, 6  
    muscularis externa, 6  
    nerve supply, 9–11  
    pacemaker activity, 10–11  
    PrPc, 137  
    radiation-damaged  
        first reference to, 1  
    secretin, 6–7  
    serosa, 6  
    single dose partial body low-LET  
        irradiation, 26–53  
        multiparameter studies, 28–34  
    single dose unshielded low-LET  
        irradiation, 53–70  
        monkey, 61  
    stress, 12  
    TGF- $\beta$ , 36  
    tubular crypts, 3  
Intraepithelial lymphocytes (IELs), 9  
Intraoperative radiotherapy (IORT), 22–23  
    arteriosclerosis, 79  
    outcomes, 84  
    rabbit celiac artery, 79  
    rabbit intestines, 48–49

Invertase, 42  
Ionizing radiation, 16  
**IORT.** *See* Intraoperative radiotherapy  
Irradiated intestine  
    time ranges, 24  
Irradiated intestines  
    ratio score, 29–30  
Islet of Langerhans  
    PrPc, 141  
Isopentenyl transferase, 189  
Ito cells  
    PrPc, 138

**J**

Jejunum  
    villi, 4  
Journal articles, 2

**K**

Keratinocyte growth factor (KGF), 95  
Keratinocytes  
    PrPc, 138  
KGF, 95  
Kidneys  
    PrPc, 142  
KNAT (*Knotted Arabidopsis thaliana*), 178  
KN1 loss-of-function mutants, 177  
KNOLLE, 197  
*Knotted Arabidopsis thaliana*, 178  
KNOTTED gene family, 177  
KN1/STM, 180  
Kuru, 122

**L**

Lactase, 42  
Lamina propria

Lamina propria (*continued*)  
 intestine, 3  
 single dose partial body low-LET  
 irradiation, 48  
 superficial reticular sheet  
 intestine, 6

Laminin receptor precursor (LRP), 147–148

Large intestines. *See also* Rat large intestines  
 carcinoma, 74  
 dog  
 muscles, 82–83  
 epithelium, 3  
 fractionated low-LET radiation  
 compartments, 73–74  
 endocrine system, 82  
 muscles, 83  
 function, 3  
 goblet cells, 75  
 lamina propria, 3  
 mouse  
 goblet cells, 44  
 single dose partial body low-LET  
 irradiation, 27  
 vs. small intestine  
 radiosensitivity, 2  
 structure, 3–6  
 tumor risk, 2  
 tumors risk, 2

LEAFY transcription factors, 182

LEF/TCF, 215

Leucine-amino-peptidase, 42

Leukocytes  
 single dose partial body low-LET  
 irradiation  
 endothelial cells, 47–48

Linear energy transfer (LET), 17, 85–87  
 heavy ion beams, 86–87  
 neutrons, 85–86  
 single dose irradiation  
 partial body, 26–53  
 unshielded, 54–87

Lipids  
 radiation effects, 17

Liver  
 PrPc, 138–139

LRP, 147–148

Lung  
 PrPc, 139

Lymphocytes  
 intraepithelial, 9

Lymphoid enhancer binding factor (LEF), 215

Lymphoid follicles  
 neutron irradiation, 86

Lymphoreticular system  
 scrapie, 133

**M**

Macrophages  
 PrPc, 135

Malignant tumors, 13

Maltase, 42

Mammalian prion protein gene  
 organization and expression, 124  
 structure, 124

Manometry  
 anorectal, 83

Mast cells  
 single dose low-LET irradiation  
 partial body, 47  
 unshielded, 59, 63

Mbh1, 242–243

Mechanochemical enzymes  
 enterocytes, 7

Megacaryocytes, 134

Meningeal cells  
 PrP, 133

Meristem, 161–162  
 angiosperm  
 organization, 174  
 apical  
 zonal model, 175  
 apoplasmic signals, 188–192  
 cell expansion, 198  
 cell integration, 183–192  
 cell proliferation, 196–197  
 cellular regulation, 192–199  
 chemical signaling pathways, 184–188  
 CLAVATA genes, 179–180  
 domains, 198–199  
 floral, 163  
 gene expression patterns, 182–183  
 genes  
 expression patterns, 178  
 homeobox genes, 176–179  
 initiation and maintenance, 176–179  
 layers and zones, 175–183  
 mRNA, 192  
 mutants, 177  
 organ initiation and separation, 180–181  
 organization, 174–183

proteins, 192  
shoot apical, 161–163  
signaling  
  CLAVATA pathway, 190–192  
size control, 179–180  
symplasmic signals, 188–192  
vegetative, 163

Meristematic cells  
  cell cycle controls, 168  
  cell division, 167–174  
  cell expansion  
    cytoskeleton, 165–167  
    orientation, 165–167  
  cell wall  
    physical properties, 163–164  
    structure, 163–164  
  cell wall synthesis  
    cell growth, 163–165

Metalloprotein  
  PrPc, 146–147

Microenvironment, 22

Microvilli  
  colonic  
    enterocytes, 7–8

Mitochondria  
  PrPc, 144

MnSOD, 53

Monkey intestines  
  single dose unshielded low-LET  
    irradiation, 61

Mononuclear cells  
  PrPc, 133–134

Mouse colon  
  iNOS-IR, 60

Mouse colorectal fibrosis  
  epithelial regeneration, 84

Mouse intestines  
  radiation schedules, 87–88  
  single dose partial body low-LET  
    irradiation  
    cryptal changes, 35  
  single dose unshielded low-LET  
    irradiation  
    fibers, 63  
    luminal changes, 55  
    TEM, 58  
    villous changes, 55–56  
  villous enterocyte, 41

Mouse large intestines  
  goblet cells, 44

Mouse small intestines  
  goblet cells, 44  
  single dose unshielded low-LET  
    irradiation, 69  
    glands, 57–58  
    muscle, 70  
  Mouse talin, 218  
  M6P/IGF-II receptor immunoreactivity  
    localization, 37  
  M6P/IGF-II receptor positive cells  
    fibrosis, 46  
  mRNA  
    meristem, 192  
  Multiple intestinal neoplasia, 13  
  Multiple organ dysfunction syndrome, 14

Muscles  
  fractionated low-LET radiation, 82–83  
  neutron irradiation, 86  
  PrPc, 139–140  
    single dose low-LET irradiation  
      partial body, 52–53  
      unshielded, 70

Muscularis externa  
  intestine, 6

**N**

NAM, 181

NCJD, 122

Necrosis, 41

Nerve cells  
  single dose low-LET irradiation  
    partial body, 51–52  
    unshielded, 69–70

Nerves  
  neutron irradiation, 86

Neural plakophilin-related Arm-repeat protein (NPRAP), 228

Neuroendocrine cells, 26  
  radiation-induced changes, 97–98

Neuromuscular junction (NMJ)  
  PrPc, 139–140

Neurotensin cell  
  single dose unshielded low-LET  
    irradiation, 67

Neutrons  
  LET intestinal radiation, 85–86

New variant CJD (nCJD), 122

Nexilin, 234–236

NLSS, 209, 212  
  nuclear protein import, 210

## NMJ

- PrP<sub>c</sub>, 139–140
- NO APICAL MERISTEM (NAM), 181
- Nonjunctional cytoskeletal proteins
  - nuclear signaling, 238–247
- Nonneuronal cellular prion protein, 121–150
  - synthesis, 129–142
  - cerebral tissue, 129–133
  - extracerebral tissues, 133–142
- Noradrenalin, 10, 12
- NPRAP, 228
- Nuclear accidents, 87
- Nuclear localization sequences (NLSs), 209, 212
  - dependent nuclear protein import, 210

## Nuclear proteins, 212

- NLS, 210
  - transport
    - alternative splicing, 214
    - degradation, 214
    - rules, 208–210

## Nuclear signaling

- associated plaque proteins
  - adherens junction, 220–221
  - desmosome, 226–230
  - focal-contact, 234–238
  - tight junction, 230–233
- nonjunctional cytoskeletal proteins, 238–247
- plaque proteins, 214–227

## Nuclear transport

- cytoplasmic retention, 213–214
- mediation, 210–212
- phosphorylation, 213
- regulation, 212–214

## Nucleic acids

- radiation effects, 17

## Nucleus

- PrP<sub>c</sub>, 143
- radiation damage, 19

## O

## Obesity

- intestinal radiation, 92

## Occluding junctions, 230–233

## Oxidative stress

- PrP<sub>c</sub>, 146–147

## Oxygen, 18

## P

- P0071, 217, 228–229
- Pancreas
  - PrP<sub>c</sub>, 141
- Pancreatic duct occlusion
  - radioprotective effects, 90
- Paneth cells, 26
  - endocrine cells, 8
  - fractionated low-LET radiation, 77
  - metaplasia, 45
  - single dose low-LET irradiation
    - partial body, 44–45
    - unshielded, 62
  - small intestine, 3
  - submucosal ectopic glands, 45
- Parietal cells
  - PrP<sub>c</sub>, 135–137
- Partial body radiation, 22–23
- P120<sup>ctn</sup>, 214–216, 223–224
- PEB2 $\beta$ /CBF $\beta$ , 245–246
- Pericytes
  - PrP, 133
- Peripheral zone
  - meristem, 175
- Perisinusoidal stellate
  - PrP<sub>c</sub>, 138
- Phalaneopsis* O39, 179
- PHAN gene, 180
- PHANTASTICA (PHAN) gene, 180
- Phaseolus*, 188
- Phosphatidylinositol 4,5-biphosphate (PIP2), 238
- Phragmoplast, 167–169
- Physcomitrella patens*, 189
- Physical intervention
  - intestinal radiation, 90–91
- Phytohemagglutinin, 134
- PID gene, 181, 188
- Pig intestines
  - irradiation, 41
  - LET
    - neutrons, 85
- Pig small intestines
  - goblet cells, 44
    - single dose unshielded low-LET irradiation, 58–59, 67
- PIN-FORMED (PIN) gene, 181, 188
- Pinin, 217, 229
- PINOID (PID) gene, 181, 188
- PIP2, 238

Plakoglobin, 214–215, 216  
Plakophilin, 216, 226–227  
Plant cyclin-dependent kinase subfamilies, 170–172  
Plant cyclins, 172–174  
Plaque proteins, 214–238 adhesive junctions, 214 nuclear signaling, 214–227 adherens junctions, 214–227 desmosome, 226–230 focal contact, 234–238 tight junction, 230–233

Plasma membrane PrP<sub>c</sub>, 142–143

Plasmodesmata, 185–188

Platelets PrP<sub>c</sub>, 134–135

Polymorphonuclear leucocytes fractionated low-LET radiation, 78

Prion cellular origin, 121

Prion diseases, 122 PrP<sub>c</sub>, 148–149

Prion protein gene, 123–131 mammalian organization and expression, 124 structure, 124 meningeal cells, 133 ORF exon, 125 organization and expression, 123–131 promoter, 125 RNA expression, 125

Prion protein of scrapie type (PrP<sup>SC</sup>), 121–123 glycoforms, 130 properties, 129 three-dimensional structure, 128

Prion protein (PrP) cell cycle, 129 choroid plexus epithelium, 132–133 circulating blood elements, 133–135 ependymal cells, 132–133 histohybridization mRNA, 132–134 isoforms, 126–131 meningeal cells, 133 metabolism, 128–131 pericytes, 133 posttranslational modifications, 127 production, 131–142 structure, 126–128

Programmed cell death. *See* Apoptosis

PROLIFERA gene, 197

Proline, 43

Protein 4.1, 240–241

Proteinaceous infectious particle. *See* Prion

Protein X, 123, 147–148

PrP. *See* Prion protein

PrP<sup>C</sup>. *See* Cellular prion protein; Prion protein

PrP<sup>SC</sup>. *See* Prion protein of scrapie type

PSTAIR domain, 171

**R**

Rabbit celiac artery ERT, 79 IORT, 79

Rabbit intestines ERT TGF- $\alpha$ , 48–49 intraoperative radiotherapy (IORT), 48–49 TGF- $\alpha$ , 49

Rabbit small intestines single dose unshielded low-LET irradiation, 58–59

Radiation background, 87 biological damage, 20 cellular interaction, 19–21 characteristics, 16–17 delivery, 22–23 enteritis, 93–96 enteropathy aging, 99 thrombomodulin, 80 fistula, 79 intestinal. *See* Intestinal radiation ionizing, 16 physical and chemical interactions, 17–19 proliferative changes cultured cells, 22 tissue interactions, 22

Radiation biology translational research, 21

Radiation-damaged intestine first reference to, 1

Radiation injury score (RIS), 28, 31, 72

Radioactive material ingested intestinal radiation, 89–90

Radionuclides  
environmental, 87  
food chain, 87

Radiosensitivity  
small intestine  
vs. large intestine, 2  
Radiotherapy  
intraoperative, 22–23  
outcomes, 84  
rabbit celiac artery, 79

Rads, 17

Rat 1-afadin, 216

Rat duodenum  
VIP immunoreactive varicosity, 52

Rat hypothalamus  
CCK, 66

Rat intestines  
radiation schedules, 88  
single dose partial body low-LET  
irradiation

fibrogenesis, 45–46

single dose unshielded low-LET irradiation  
fibers, 62–63  
goblet cells, 61–62  
immune system, 63–64  
luminal changes, 54–55  
villous changes, 55–56

Ratio score  
irradiated intestines, 29–30

Rat large intestines  
irradiation, 87  
neutron irradiation, 86

Rat small intestines  
cryptal enterocytes, 41  
ectopic mucous glands, 33

enterocytes  
cryptal, 41  
fractionated low-LET radiation  
cell growth, 74  
fibrogenesis, 77

goblet cells, 43–44

intestinal radiation  
shielding, 84

single dose partial body low-LET  
irradiation, 27–28  
cell growth disturbances, 39–41  
cryptal changes, 35  
data variation, 32  
multiparameter results, 30, 34

single dose unshielded low-LET  
irradiation, 59, 69

endocrine cells, 66  
muscle, 70  
TGF- $\beta$ , 48  
ulcerations, 33, 49

Resin casting, 64

Rib zone  
meristem, 175

RIS, 28, 31, 72

Root cells  
cell cycle  
microtubular reorganization,  
169

ROUGH SHEATH 2 (RS2), 180

RS2, 180

RS2 genes, 180

## S

*Saccharomyces cerevisiae*, 171

actin, 218

Salivary glands

PrPc, 142

SAM, 161–163

dynamic stability, 183–184

Saturated fatty acids

intestinal radiation, 94

Scanning microscopy, 64

Schedules

intestinal radiation, 87–88

SCJD, 122

ScN2a

nucleolus, 143

Scoring methods

radiation injury, 96

Scrapie, 123, 132

lymphoreticular system, 133

Scrapie-infected neuroblastoma cell line  
(ScN2a)

nucleolus, 143

Secretin

intestine, 6–7

Secretory vesicles

PrPc, 143

Serosa

intestine, 6

Shielding

intestinal radiation, 84

Shoot apical meristem (SAM),  
161–163

dynamic stability, 183–184

SHOOTMERISTEMLESS (STM), 178  
meristem, 194–195

Signaling pathway, 19

Simian virus SV40 large tumor antigen  
NLS, 209

Single dose partial body low-LET irradiation  
intestines, 26–33  
cell growth disturbances, 39–41  
cryptal changes, 34–39  
endocrine cells, 51  
epithelial cell changes, 41–45  
goblet cells, 43–44  
intestinal compartments, 34–41  
multiparameter studies, 28–30  
stroma/connective tissue, 45–51  
tissue changes, 39  
vascular components, 49–51  
villous changes, 34–39

luminal changes, 34

muscles, 52–53

nerve cells, 51–52

rat small intestines  
data variation, 32  
multiparameter results, 30, 34

Single dose unshielded low-LET irradiation  
intestines, 53–70  
cryptal changes, 55–56  
endocrine cells, 66–70  
epithelial cells, 57–62  
goblet cells, 61–62  
immune system, 63–64  
inflammatory system, 63–64  
intestinal compartments, 54–57  
luminal changes, 54–55  
tissues, 56–57  
vascular components, 64–66  
villous changes, 55–56

mouse intestines  
TEM, 58

muscle, 70

nerve cells, 69–70

Paneth cells, 62

stroma/connective tissue, 62–63

Skin  
TSE, 137–138

Small intestines. *See also* Dog small  
intestines; Mouse small intestines; Pig  
small intestines; Rat small intestines  
fractionated low-LET radiation

compartments, 72–74  
endocrine system, 82  
muscles, 83  
vascular components, 80–81

function, 3

goblet cells, 75

lamina propria, 3

vs. large intestine  
radiosensitivity, 2

Paneth cells, 3

radiation-induced changes, 33

single dose unshielded low-LET irradiation  
rabbit, 58–59

stem cells, 3

structure, 3–6

tubular crypts, 3

villous protrusions, 3–4

Smooth muscle cells  
radiation-induced changes, 97  
TGF- $\beta$ 1, 53

Somatostatin, 12

Sperm cells  
PrPc, 140–141

Spleen  
scrapie, 133

Sporadic CJD (sCJD), 122

Stem cells  
small intestine, 3

STM, 178  
meristem, 194–195

STM/KNOTTED, 189

Stomach  
PrPc, 135–137

Stress  
intestines, 12  
radiation, 99

Stroma  
radiation-induced changes, 97

Sublethal damage cells, 22

Submucosal ectopic glands  
Paneth cells, 45

Supervillin, 242–243  
bovine, 218

Surface epithelium  
single dose unshielded low-LET  
irradiation, 57–58

Surgical status  
intestinal radiation, 90–91

Symplast, 184–188  
Symplekin, 217, 233

Tunica, 175  
Tyr15, 171

## T

Talin, 237  
T-cell specific factor (TCF) family, 215  
TGF- $\alpha$   
ERT  
    rabbit intestines, 48–49  
    rabbit intestines, 49  
TGF- $\beta$ , 75, 96  
    cat intestines, 49  
    intestinal radiation, 93  
    intestines, 36  
mRNA  
    irradiated intestines, 40  
    rabbit intestines, 48–49  
    rat small intestines, 48, 77  
single dose partial body low-LET  
    irradiation  
mRNA, 47  
TGF- $\beta$ 1  
    epithelial, 43  
    smooth muscle cells, 53  
Thiophosphate, 19  
Thrombomodulin (TM)  
    intestinal radiation, 93  
    radiation enteropathy, 80  
Tight junction  
    plaque proteins  
        nuclear signaling, 230–233  
Time of day  
    intestinal radiation, 91–93  
Time ranges  
    irradiated intestine, 24  
TM  
    intestinal radiation, 93  
    radiation enteropathy, 80  
TME, 122, 123  
*Tonneau* mutants  
    meristematic cells, 167, 184  
Transmissible mink encephalopathy (TME),  
    122, 123  
Tubular crypts  
    intestine, 3  
Tumors  
    malignant, 13  
    risk  
        large intestine, 2

## U

UFO, 180–181  
*Ufo* gene  
    meristem, 194  
UNUSUAL FLOWER ORGANS (UFO),  
    180–181  
UPA  
    intestinal radiation, 93  
Uranium, 87  
Urokinase plasminogen activator (uPA)  
    intestinal radiation, 93

## V

Vacuolization, 41  
Vascular sclerosis, 50–51  
Vasoactive intestinal peptide (VIP), 6–7,  
    11–12  
    single dose unshielded low-LET  
        irradiation, 67–68  
Vegetative meristem, 163  
Vessels  
    PrPc, 132  
Villi, 88  
    human jejunum, 4  
Villous enterocyte  
    mice intestines, 41  
Villous protrusions  
    small intestine, 3–4  
Vinculin, 216, 225  
Vinexin, 216, 225–227  
VIP, 6–7, 11–12  
    single dose unshielded low-LET  
        irradiation, 67–68  
Vitamin E  
    intestinal radiation, 94

## W

Whole-body schedules  
    diet, 94  
Wortmannin, 238  
Wound healing, 14, 18–19, 90  
WUSCHEL gene, 179

**X**

*Xenopus* cingulin, 217,  
233–234  
*Xenopus* DRS protein I/II, 217  
*Xenopus* protein xnf7  
cytoplasmic retention, 213–214  
XETs, 164–165

Xyloglucan endo transglycosylase (XETs),  
164–165

**Z**

ZO-1, 232–233  
Zyxin, 218, 236–237